

Materials Horizons: From Nature to Nanomaterials

Jince Thomas
Sabu Thomas
Zakiah Ahmad *Editors*

Crosslinkable Polyethylene

Manufacture, Properties, Recycling, and
Applications

 Springer

Materials Horizons: From Nature to Nanomaterials

Series Editor

Vijay Kumar Thakur, School of Aerospace, Transport and Manufacturing,
Cranfield University, Cranfield, UK

Materials are an indispensable part of human civilization since the inception of life on earth. With the passage of time, innumerable new materials have been explored as well as developed and the search for new innovative materials continues briskly. Keeping in mind the immense perspectives of various classes of materials, this series aims at providing a comprehensive collection of works across the breadth of materials research at cutting-edge interface of materials science with physics, chemistry, biology and engineering.

This series covers a galaxy of materials ranging from natural materials to nanomaterials. Some of the topics include but not limited to: biological materials, biomimetic materials, ceramics, composites, coatings, functional materials, glasses, inorganic materials, inorganic-organic hybrids, metals, membranes, magnetic materials, manufacturing of materials, nanomaterials, organic materials and pigments to name a few. The series provides most timely and comprehensive information on advanced synthesis, processing, characterization, manufacturing and applications in a broad range of interdisciplinary fields in science, engineering and technology.

This series accepts both authored and edited works, including textbooks, monographs, reference works, and professional books. The books in this series will provide a deep insight into the state-of-art of Materials Horizons and serve students, academic, government and industrial scientists involved in all aspects of materials research.

More information about this series at <http://www.springer.com/series/16122>

Jince Thomas · Sabu Thomas · Zakiah Ahmad
Editors

Crosslinkable Polyethylene

Manufacture, Properties, Recycling,
and Applications

 Springer

Editors

Jince Thomas
Research and Post Graduate Department
of Chemistry, St. Berchmans' College
Changanassery, Kerala, India

International and Inter University Center
for Nanoscience and Nanotechnology
Mahatma Gandhi University
Kottayam, Kerala, India

Zakiah Ahmad
Faculty of Civil Engineering
Universiti Teknologi Mara
Shah Alam, Malaysia

Sabu Thomas
School of Energy Materials and
International and Inter University Center
for Nanoscience and Nanotechnology
Mahatma Gandhi University
Kottayam, Kerala, India

ISSN 2524-5384

ISSN 2524-5392 (electronic)

Materials Horizons: From Nature to Nanomaterials

ISBN 978-981-16-0513-0

ISBN 978-981-16-0514-7 (eBook)

<https://doi.org/10.1007/978-981-16-0514-7>

© Springer Nature Singapore Pte Ltd. 2021

This work is subject to copyright. All rights are reserved by the Publisher, whether the whole or part of the material is concerned, specifically the rights of translation, reprinting, reuse of illustrations, recitation, broadcasting, reproduction on microfilms or in any other physical way, and transmission or information storage and retrieval, electronic adaptation, computer software, or by similar or dissimilar methodology now known or hereafter developed.

The use of general descriptive names, registered names, trademarks, service marks, etc. in this publication does not imply, even in the absence of a specific statement, that such names are exempt from the relevant protective laws and regulations and therefore free for general use.

The publisher, the authors and the editors are safe to assume that the advice and information in this book are believed to be true and accurate at the date of publication. Neither the publisher nor the authors or the editors give a warranty, expressed or implied, with respect to the material contained herein or for any errors or omissions that may have been made. The publisher remains neutral with regard to jurisdictional claims in published maps and institutional affiliations.

This Springer imprint is published by the registered company Springer Nature Singapore Pte Ltd.
The registered company address is: 152 Beach Road, #21-01/04 Gateway East, Singapore 189721, Singapore

Preface

The book titled *Crosslinked Polyethylene: Manufacture, Properties, Recycling and Applications* precises many of the recent technological and research accomplishments in the area of cross-linked polyethylene (XLPE). Comprised in the book are the presentations of historical and theoretical analysis of XLPE, intellectual property trends in XLPE, new challenges and opportunities. Also discussed are the crosslinking techniques and recycling process of XLPE and their general purposes and commercial significance. The other topics covered are the flame-retardant studies in XLPE and their morphological, mechanical and thermal property analyses. As the caption specifies, the book highlights the frequent facets on XLPE.

This innovative book serves as an up-to-date record on the key findings, observations and outcomes of XLPE to power cable insulation and automobile fields. It is intended to assist as a pioneer reference resource for all types insulation industry as well as in science fields. The various chapters in this book are contributed by the prominent researchers from academe, industry and government–private research laboratories across the world. This book is an essential reference source for university and college faculties, professionals, post-doctoral research fellows, senior graduate students and researchers (from R&D laboratories) who are working in the areas of automobiles, energy resources, aviations, etc.

Chapter 1 gives a brief outline and an overview of the state of art in the XLPE and presents the new challenges, opportunities and commercial significances of XLPE in the present world. Chapter 2 deals with the historical and theoretical analyses of XLPE. The authors explain the various methods of computational studies in XLPE matrix and their molecule parameterization and crosslinking reactions. Chapter 3 delivers the manufacturing process of XLPE. Chapter 4 discusses the general awareness to XLPE manufactures. Chemistry and process technology for making grafted and silanes based XLPE is also presented. Chapter 5 deals with the physicochemical properties of XLPE. Chapter 6 provides the comprehensive investigation requirement changes in the morphology, structural and properties of XLPE, and its applications such as cable insulation, hip arthroplasty, foam, pipes are also discussed. In Chap. 7, new methods for polyethylene (PE) crosslinking and recycling process of

XLPE are mounted. Click-chemistry crosslinking of PE and XLPE's recycling techniques like vitrimers, γ radiation, ultrasonic decross-linking, supercritical decross-linking extrusion are presented in this chapter. Chapter 8 highlights the effect of thermal and radiation aging on dielectric and structural properties on XLPE. Flame-retardant (FR) properties of XLPE are discussed in Chap. 9. The relevant combustion and FR mechanisms on XLPE are reviewed in this chapter. Chapter 10 describes the historical perspective of power cable materials development and their design considerations. The industry specifications guiding the technical material design choices are also presented in this chapter. The common failure mechanisms in XLPE based cables are discussed in Chap. 11. Chapter 12 talks about the practical uses of XLPE-based products and future prospects. Chapter 13 is the continuity of Chap. 12. Industrial- and business-related benefits of XLPE are discussed.

Finally, we thank God for the successful completion of this book, and we would like to express our honest gratitude to all the contributors of this book who provided excellent support for the fruitful completion of this endeavor. We appreciate them for their commitment and the genuineness for their contributions to this book. We would like to acknowledge all the reviewers who have taken their valuable time to make critical comments on each chapter. Especially, we thank Dr. Jeffrey M. Cogen, Dr. Notingher Petru, Dr. Saurav S. Sengupta, Dr. Kai Zhou for the review process of chapters. We thank and acknowledge support of 'Springer Nature Singapore Pvt Ltd.' who recognized the demand for this book.

Kottayam, India

Jince Thomas
Sabu Thomas

Contents

1	Crosslinked Polyethylene: State-of-the-Art and New Challenges	1
	Jince Thomas, Minu Elizabeth Thomas, and Sabu Thomas	
2	Historical and Theoretical Background of XLPE	17
	Minu Elizabeth Thomas, Rajamani Vidya, Jince Thomas, and Zakiah Ahmad	
3	XLPE Manufacturing Processes	41
	Saurav S. Sengupta	
4	General Awareness of XLPE Manufacturers	67
	Saurav S. Sengupta and Pieter Calon	
5	Physicochemical Properties of XLPE	89
	Kai Zhou and Yaping Wu	
6	Morphology, Structure, Properties and Applications of XLPE	125
	Khaled Aljoumaa and Abdul Wahab Allaf	
7	XLPE: Crosslinking Techniques and Recycling Process	167
	Nithin Chandran, Anjaly Sivadas, E. V. Anuja, Deepa K. Baby, and Ragin Ramdas	
8	Aging and Degradation Studies in Crosslinked Polyethylene (XLPE)	189
	Meera Balachandran	
9	Flame-Retardant Aspects of XLPE	211
	Jeffrey M. Cogen, Bharat I. Chaudhary, Abhijit Ghosh-Dastidar, Yabin Sun, and Scott H. Wasserman	
10	Structural Design and Performance of XLPE for Cable Insulation	247
	Timothy J. Person, Saurav S. Sengupta, and Paul J. Caronia	

11 Failure Mechanisms in XLPE Cables 271
Petru V. Noțingher, Cristina Stancu, and Ilona Pleșa

**12 Short Overview of Practical Application and Further
Prospects of Materials Based on Crosslinked Polyethylene** 349
Ter-Zakaryan Karapet Armenovich and Zhukov Aleksey Dmitrievich

13 Industrial and Commercial Importance of XLPE 379
Shah Mohammed Reduwan Billah and Waseem Ibrahim

About the Editors

Jince Thomas received his Master's degree in Polymer Chemistry in 2012 and M.Tech. in Polymer Science and Technology in 2014 from Mahatma Gandhi University (MGU), India. He conducted his doctoral research at MGU in the research group of Prof. Sabu Thomas, the present Vice Chancellor of MGU, and Prof. Bejoy Francis (Ph.D. Guide), Assistant Professor, St. Berchmans College, India. He was a visiting student at the University of Tennessee (Knoxville) in 2014 and a project trainee at the International and Inter University Centre for Nanoscience and Nanotechnology, MGU, during 2015–2016. He worked as a project assistant in an Indo-Malaysian Project during 2016–2017 in collaboration with University Technology Mara, Malaysia. He also worked as a visiting student in Ariel University, Israel. He has contributed to numerous publications, book chapters, and books. His research interest focuses on polymer and polymer nanocomposites.

Prof. Sabu Thomas is currently Vice Chancellor of Mahatma Gandhi University, Kerala, India. Professor Thomas is an outstanding leader with sustained international acclaims for his work in Nanoscience, Polymer Science and Engineering and Green Materials. Professor Thomas has received more than 30 national and international awards. He has published over 1200 peer reviewed research papers, reviews, and book chapters. He has co-edited 150 books, and is an inventor of 15 patents. The H index of Prof. Thomas is 108 and has more than 56,000 citations. Professor Thomas has delivered over 350 plenary/inaugural and invited lectures in national/international meetings over 40 countries. Professor Thomas has supervised 115 Ph.D. programmes and his students occupy leading positions in academia and industry in India and abroad.

Prof. Zakiah Ahmad is the Dean of Faculty of Civil Engineering at Universiti Teknologi Mara. She obtained her Bachelor's and Master's at the Memphis State University (USA), and pursued her Ph.D. in Timber Engineering at the University of Bath, United Kingdom. Professor Ahmad specialises in timber engineering and timber composites, and her other interest includes nano-polymer composites as well as cement composites. She serves as a consultant, committee member and advisor to numerous public agencies and institutions, and has been appointed as visiting

scientist at BRE Research Institute, University of Bath, UK, Centre for Nanoscience and Nanotechnology, School of Chemical Sciences, Mahatma Gandhi University India and Timber Research Institute, Kyoto University Japan. Professor Ahmad has published more than 300 papers in journals and proceedings, and plays an essential role in the Malaysian Standard committees as the Chairman and committee member and as Malaysian delegates/representative for ISO technical committee.

Chapter 1

Crosslinked Polyethylene: State-of-the-Art and New Challenges



Jince Thomas, Minu Elizabeth Thomas, and Sabu Thomas

1 Introduction

Polyethylene (PE) is the most common plastic used today, out of 70% of the global market of the plastic commodity [1]. PE was accidentally obtained during an investigation of diazomethane by Hans von Pechmann in 1898. Another interesting fact on the preparation of PE is that the first industrially prepared PE protocol is again an accidental discovery when Eric Fawcett and Reginald Gibson apply extremely high pressure to the ethylene and benzaldehyde mixture to form XLPE in 1933. However, until 1935, the industrial production of PE was not successful due to the reproducibility of that accidental reaction. Through, in 1935, Michael Perrin's success in the synthesis of low-density polyethylene (LDPE), industrial production was started in 1939.

Now, there are wide ranges of PE resins available today, including LDPE, linear low-density polyethylene (LLDPE), medium-density polyethylene (MDPE), high-density polyethylene (HDPE) and ultrahigh molecular weight polyethylene (UHMWPE), which are the most popular ones. The ethylene molecules may or may not add on regularly, but the irregular addition of ethylene molecules leads to form short branches of ethylene molecules from the main PE chain. This branching

J. Thomas

Research and Post Graduate Department of Chemistry, St. Berchmans' College, Changanassery, Kerala, India

e-mail: jincethomas25@gmail.com

J. Thomas · S. Thomas (✉)

International and Inter University Center for Nanoscience and Nanotechnology, Mahatma Gandhi University, Kottayam, Kerala, India

e-mail: sabuthomas@mgu.ac.in

M. E. Thomas · S. Thomas

School of Chemical Sciences, Mahatma Gandhi University, Kottayam, Kerala, India

e-mail: minuputhen@gmail.com

© Springer Nature Singapore Pte Ltd. 2021

J. Thomas et al. (eds.), *Crosslinkable Polyethylene*, Materials

Horizons: From Nature to Nanomaterials,

https://doi.org/10.1007/978-981-16-0514-7_1

out of PE from the main polymer chain leads to these above classifications. LDPE is a less compact molecular structure with excessive branching and lesser density ranging between 0.91 and 0.925 g cm⁻³; LLDPE has shot with a significant number of branches with density range between 0.91 and 0.94 g cm⁻³; MDPE is with medium branching with density range 0.926–0.94 g cm⁻³; HDPE has minimal branching with density range between 0.941 and 0.965 g cm⁻³; and UHMWPE has extremely long chains with a molecular weight of ten thousand to twenty-five thousand monomer units per molecule with 0.928–0.941 g cm⁻³. Even though all these varieties of PE have high impact strength, good electrical insulation and chemical resistance, the low thermal stability makes its commercial applicability to a limit.

The fundamental technique to strengthen the mechanical, chemical and thermal properties is through crosslinking the PE chains, and the association of polymers through intra- or intermolecular chemical bonding is termed as ‘crosslinking,’ which is mostly irreversible. Crosslinks between PE chains form a structure with a three-dimension network called crosslinked polyethylene (XLPE or PEX) (Fig. 1). In March 1963, Al Gilbert and Frank Precopio of GE Research Laboratory located in Niskayuna, New York [2], introduced crosslinks in PE chains. That was the starting moment of the milestone era of plastics, and from then, XLPE has taken over the main

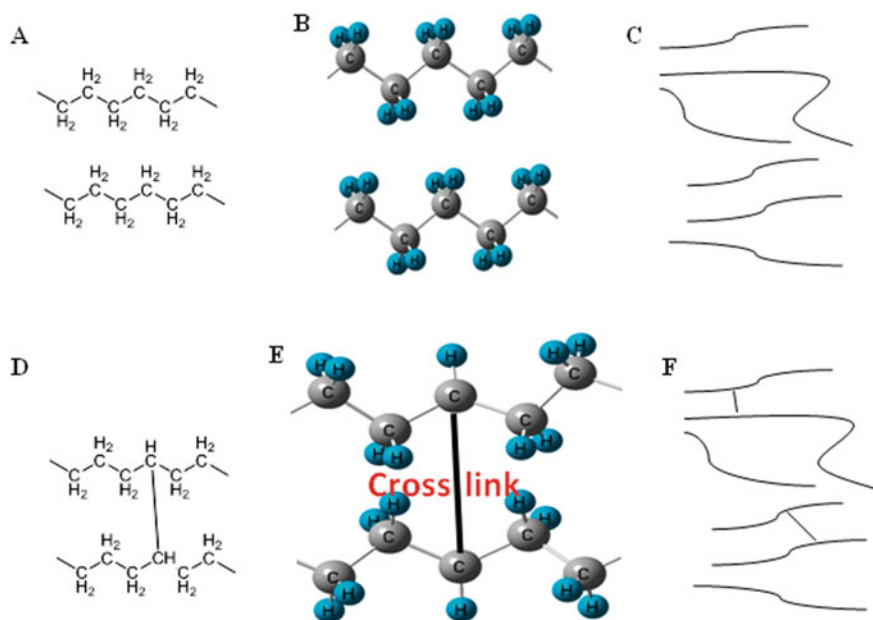


Fig. 1 Representation of PE and XLPE—**a** molecular structure **b** 3D molecular structure **c** schematic representation of PE and **d** molecular structure **e** 3D molecular structure **f** schematic representation of XLPE

share of the engineering plastic market due to its advanced properties compared with other plastics. The crosslinking is made by both physical and chemical processes; every crosslinking agent used in these methods ties carbon atoms of different PE chains together and transforms the viscous linear segments to insoluble gel with a three-dimensional network.

2 Crosslinking Methods of PE

The crosslinking process is classified based on two main factors, activator used for crosslinking and the state of the polymer throughout the crosslinking process. Hence, the crosslinking process is classified into two, physical and chemical, processes.

2.1 Physical Process

In the physical crosslinking process, PE is subjected to high-energy sources like microwave radiation, high-energy electron, etc. This process is also called radiation method. In **radiation method**, the radiation techniques (high-energy waves or particles) allow forming an active intermediate (free radical) in the PE chain. Ultraviolet (UV), X-ray, ultrahigh frequency, gamma (γ) and electron beam radiations are mainly used for radiation technique, in which γ and electron beam radiations are mostly used in industrial applications. The reaction mechanism involves the scission of the C–H bond of PE by absorbing high-energy radiation to form radicals of hydrogen and polymer, and these polymer radicals form C–C crosslinked bonds. During the reaction, hydrogen and some small aliphatic molecules are released out as gas. The radiation method is the cleaner process because, additives (other than some coagents for boosting the radiation efficiency) are not necessary to initiate the reaction. Forming of heterogeneous crosslinking network and risk in the process and installation cost of radiation equipment is the main drawback of radiation technique.

2.2 Chemical Process

Chemical crosslinking involves the addition of some crosslinking agents to produce free radicals which form and induce the chemical crosslinking process; they are peroxide method, silane method and azo method [3]. Different chemical crosslinking techniques are compared below.

- (a) **Peroxide method:** In this method, peroxide-based chemicals (tert-butyl cumyl peroxide, dicumyl peroxide, etc.) generate polymer-free radicals which form crosslinks. The reaction is carried out in the molten stage above peroxide

decomposition temperature, and hence, PE crosslinks are almost homogeneous. Tertiary carbon is more prone to peroxide attack (due to better-stabilized free radical); hence, peroxide crosslinking reactivity in LDPE is greater than HDPE. Mostly two peroxide methods are used, Engel and Pont-à-Mousson method. **Engel method** involves in a single step by mixing PE, mainly HDPE, with the peroxide molecule into an extruder and melted. However, **Pont-à-Mousson** method involves in two steps, putting the mixture of PE and peroxide molecules in an extruder and the extruded crosslinked PE treated in a salt bath under temperature above decomposition of peroxide. Low outputs, high investment capital and high scraps rate are some of the drawbacks of peroxide crosslinking method.

- (b) **Silane method:** Silane crosslinking involves the incorporation of silane coupling agents into the PE chains. The widely used silane coupling agent is vinyl silane with methoxy or ethoxy groups on Si due to their double bonds and ability of rapid crosslinking. Two important silane methods are Monosil® and Sioplas®. Monosil® is a one-step process and Sioplas® is a two-step process. In **Monosil®**, grafting and shaping are in a single step in special extrusion equipment. PE with lower density is suitable for this method. However, in **Sioplas®**, the first step is the peroxide-activated grafting of silane onto the PE in a compounding unit, giving a grafted granular product, which melted with a catalyst masterbatch followed by conventional extrusion to get products. Sioplas® is more convenient with low scraps and high yield. The heterogeneous crosslinking network is the main drawback of silane crosslinking method.
- (c) **Azo methods:** In azo method, azo compounds are used for the initiation of crosslinking. The azo compounds are thermally more stable than peroxides; hence, it is more suitable for crosslinking higher molecular weight PE. The incorporation of antioxidants is limited in azo method to avoid obstruction in the reaction. To avoid premature crosslinking, the processing temperature is adjusted below the critical temperature of azo compound reactivity. Due to the formation of low active primary radicals through transfer reactions, limited crosslinking rate is a drawback of this technique.

The introduction of crosslinks in both LDPE and HDPE is employing all crosslinking methods. Besides, the peroxide method is used predominantly in HDPE. By crosslinking, both LDPE and HDPE get many improved properties such as bad electric conductor, high dielectric strength and long-term resistance to corrosion and pressure. They became light and flexible and hence easy to transport and install; these qualities lead to the vast application in cables and pipes. The crosslinked UHMWPE is used in medical implants, because crosslinking improves the wear resistance in UHMWPE, which mainly undergoes crosslinking through radiation method. A new technique called **click chemistry** is used in the crosslinking process of PE copolymers [4, 5]. This method helps to get rid of the limitations associated with traditional crosslinking methods like the production of hazard by-products. A detailed description of all these crosslinking techniques is in the coming chapters.

3 Main Manufactures of XLPE

The largest market of XLPE is North American countries like USA, Canada, Mexico, etc., and the fast-growing consumers are from Asia–Pacific countries like China, India, Japan, etc. There are some key manufactures for fragmented XLPE:

- Dow,
- Nouryon,
- Borealis AG,
- LyondellBasell Industries Holdings B.V.,
- PolyOne Corporation.

Some of the important patents for the methods used for crosslink PE are listed in Table 1.

4 Advantages and Disadvantages of Crosslinking in PE

Crosslink in PE transforms thermoplastic to thermoset with better heat and dimension stability; superior shape memory, improved impact resistance, greater environmental stress crack resistance (ESCR), improved resistance of solvent and electricity, high tensile strength, superior dielectric properties, durability, etc., are some key benefits of crosslinking in PE. Even though the crosslinks in PE lead to excellent properties, still some challenges exist. The transformation of PE thermoplastic to thermoset due to crosslinking reduces the flow, crystalline nature, etc. [1]. To control the degree of crosslinking and selection of a suitable crosslinking agent is very tricky. Also, recycling is not easily probable due to thermoset properties of XLPE. Although XLPE has some disadvantages, due to its improved physicochemical properties, an immense range of applications is employed.

5 Scope and Application

XLPE is employed mostly in the field of electrical insulations, medical, civil engineering, automobiles and packaging. However, each product of specific application needs XLPE material with specific property requirements, which can fabricate mainly by crosslinking techniques. Besides, the physicochemical properties can tailor using the degree of crosslinking and selection of compound ingredients. The main applications of XLPE are focused here.

Table 1 Important patents for the crosslinking method for PE

Patent No	Assignee/inventors	Filed on	Title
WO 2017/112,642 A1	Dow Global Technologies LLC	20 December 2016	Partially crosslinked polyethylene formulations and methods of making same
US 2015/0259523A1	Christopher Ross et al	9 March 2015	Tin-free catalysts for crosslinked polyethylene pipe and wire
US9951190	Howmedica Osteonics Corp	22 July 2015	Surface crosslinked polyethylene
WO/2015/077061A1	Chaudhary B. I., et al	10 November 2014	Moisture and peroxide crosslinkable polymer compositions
WO/2014/075,726/A1	Ho Chau-Hon, et al	15 November 2012	Chemically crosslinked polyethylene used for electrical insulation
US 2013/0064711A1	Howmedica Osteonics Corp	20 September 2012	Polyethylene crosslinked with an anthocyanin
EP 2 384 774 B1	Howmedica Osteonics Corp	3 May 2011	Surface crosslinked polyethylene
US 7,923,121 B2	Peter Jackson, et al	14 May 2010	Photo-crosslinkable polyolefin compositions
US2011/0111153A1	Russel R G., et al	31 December 2010	Crosslinked polyethylene process
US2008/0133021A1	Shen, et al	31 October 2007	Crosslinking of polyethylene for low wear using radiation and thermal treatments
US8299166B2	Carlsoon R.	16 April 2007	Crosslinkable polyolefin composition comprising high molecular weight silanol condensation catalyst
WO/2005/056,620	Giacobbi E., et al	8 December 2004	Improved process for producing silane crosslinking polyethylene
US7517919B2	Wang, et al	4 October 2004	Sequentially crosslinked polyethylene
US7204947B2	Hubbard, et al	30 September 2004	Method of crosslinking polyolefins

(continued)

Table 1 (continued)

Patent No	Assignee/inventors	Filed on	Title
WO/2005/023,908	Sultan B., et al	28 August 2004	Crosslinkable high-pressure polyethylene composition, a process for the preparation thereof, a pipe and a cable thereof
US5756582	Tsunehars M., et al	20 September 1996	Process for producing silane crosslinked polyolefin
US4297310	Akutsu S., et al	13 November 1979	Process for producing electric conductors coated with crosslinked polyethylene resin
US4129531	Rauer K., et al	14 December 1977	Crosslinking of polymers with azo esters
US3646155	Scott H. G., et al	18 December 1969	Crosslinking of a polyolefin with a silane
US 3,214,422	Mageli O. L., et al	28 August 1959	Crosslinked polyethylene

5.1 In the Cable Industry

The vast development of electrical apparatus made the insulation material very indispensable but until 1925, only naturally occurring materials (cotton thread, rubber, mica, etc.) are used. Synthetic insulations like PE, PVC, etc., are used, but excellent physical and chemical properties make XLPE overrule all other polymer materials. XLPE has numerous applications, but they are well known as insulation material [6]. In Germany, in 1970, XLPE had been used as insulated power cables. The good mechanical, thermal and electrical properties in a large range of voltage and chemical resistance made the XLPE insulations superior to all other insulation materials known. The key reasons for the consideration of polymeric-insulated system worldwide by replacing the old insulation systems like the oil-impregnated paper system are:

- Reduce cost for installation and maintenance,
 - Low environmental pollution issues,
 - Weight reduction leads to ease of installation of longer cables,
 - Reduction in dielectric loss,
 - Reduce jeopardy due to fire in earthquakes, etc.
- **Importance of XLPE as insulation cable**

Benefits of XLPE in insulation material compared with other polymeric insulation systems include:

- Works at a broad voltage range,
- Provides good mechanical protection,
- Can bear up to extreme pressure,
- Resists underground damage, weather, etc.,
- Thermal resistance withstands above,
- Permits high conductor operating temperatures,
- Reduces short circuit and overload levels,
- Is extra cost-effective than other polymers,
- Flexible and moisture resistant.

• XLPE versus other polymer cable insulations

Due to the excellent physical and chemical properties, XLPE beats other insulation materials like ethylene propylene rubber (EPR), polyvinyl chloride (PVC), PE, silicone rubber, etc. The mechanical properties like tensile strength, elongation, impact resistance and suitable for a wide range of voltage make XLPE superior. The properties of XLPE cables remain unchanged at a large temperature range, which is another key factor. The comparison of physical and chemical properties of more popular insulation cables like EPR, PVC and PE [7] is given in Table 2.

Table 2 Comparison of insulation cables-XLPE, PE, PVC and EPR

Insulation material	XLPE	PE	PVC	EPR
Strength	<ul style="list-style-type: none"> • Resist at high temperature • Low dielectric loss • Not melts at thermal expansion 	<ul style="list-style-type: none"> • Low dielectric loss • High initial dielectric strength 	<ul style="list-style-type: none"> • Cheap • Durable • Widely available 	<ul style="list-style-type: none"> • Low sensitive to water treeing • Reduction in thermal expansion
Weakness	<ul style="list-style-type: none"> • A little sensitive toward water treeing 	<ul style="list-style-type: none"> • High sensitive toward water treeing • At high temperature material will breakdown 	<ul style="list-style-type: none"> • High dielectric loss, so not suitable for MV or HV cables • Melts at high temperature • Environmental pollution may cause due to the presence of halogen 	<ul style="list-style-type: none"> • High dielectric loss • Requires fillers or additives for better results

• **XLPE global cable market**

The global XLPE cable market can be classified based on the installation mode, the necessity of voltage, the applicability of the users, etc. Because of installation mode is depends upon the insulation type, i.e., terrain, subterranean and submarine cable, related to the voltage need classified into extra high, high, medium and low. Based on the consumer, i.e., the user of the XLPE cables like in power, oil, gas, chemical industry, in infrastructure, for manufactures, etc., the classification picture is depicted in Fig. 2.

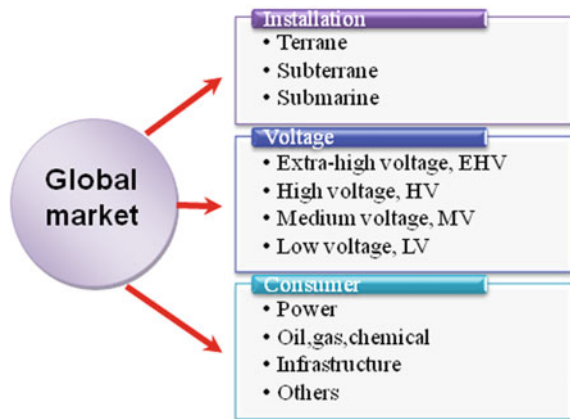
Increasing investments in renewable energy sectors, infrastructures and high power demand encourage the XLPE cable global market. (<https://www.fiormarkets.com>) It is expected to be an expected market of compound annual growth rate (CAGR) of 5.4%.

• **Main XLPE cable manufactures**

XLPE insulated cable consumption is very high in almost all countries due to the global electricity demand. Asia–Pacific is the main contributor to consumption. Some of the prominent manufactures of XLPE global cable market are:

- Prysmian Group, Italy,
- Brugg Kabel AG, Switzerland,
- General Cable Corporation, USA,
- Nexans, France,
- NKT A/S, Denmark,
- KEI Industries Ltd., India,
- Sumitomo Electric Industries, Japan,
- ABB Ltd., Switzerland.

Fig. 2 Classification of XLPE global insulation cable market



For improving the efficiency of insulation cables after many researches, the introduction of nanocomposites and blends of XLPE to the industry is well explained in volume 2 of this book series.

5.2 *XLPE Pipes*

Rather than the wide application of XLPE as insulation cable for power supply, it is also used to make pipes for plumbing in domestic and industries, for mining, radiant heating in residential houses, etc. [1]. The advantages of each application of XLPE pipes are explained below:

- (a) **Plumbing:** Industries utilize the XLPE tubes in plumbing by replacing the old copper piping. The flexibility of the material with a wide range temperature resistance (can use for both hot water and cold water) and high corrosion resistance makes XLPE pipes more popular. PVC pipes will burst on freeze but XLPE will be stable at both high and low temperatures. Color code for tubes is also applied in some industries, red for hot water and blue for cold water; hence, it can easily differentiate and make it more convenient. The other factor for the popularity of XLPE tubing is the low cost of XLPE insulation than copper.
- **Benefits of XLPE plumbing**

Some advantages for the XLPE plumbing compared with traditional plumbing schemes are as follows:

- (i) The flexibility of the material makes easy for installation,
 - (ii) Low material cost,
 - (iii) Due to less sharp turns in pipes provides high pressure,
 - (iv) Less corrosion compared with other plumbing systems,
 - (v) No need for welding which makes less risk of fire during installation,
 - (vi) Suitable for both hot and cold water,
 - (vii) Longevity.
- **Demerits of XLPE plumbing**

Some disadvantages for the XLPE plumbing compared with traditional plumbing schemes are as follows:

- (i) Degrade when exposed more to sunlight,
- (ii) Insects attack is found in XLPE pipes,
- (iii) Fewer options for XLPE adhesives make pipe installation a task,
- (iv) Odor and taste of chemical were found in some cases but no reports regarding public health issues.

- (b) **Radiant heating:** For radiant floor heating, XLPE tubing replaces the traditional heating option of residential housings. The ease of insulation, regulation of heat, a wide range of temperature resistance and low cost and less maintenance made XLPE very popular.
- (c) **Mining:** The ability to resist extreme pressure and temperature makes it popular in the mining industry. The ease of insulation is also another important reason for the popularity.

The aging strength of XLPE pipes can increase by the modification of dimension [8].

5.3 *In the Medical Field*

XLPE is used as artificial joints mainly in hip replacement and knee replacement because the wear resistance is high. XLPE component is firstly used in 1998 for total hip anthropology (THA) [9]. However, two-third of XLPE is used only from 2003, mostly in the USA. The vivo wear rate is considerably less for XLPE; hence, it is perfect for THA [10]. Knee joints made of crosslinked LDPE are not used due to less desired mechanical strength [11]; hence, crosslink UHMWPE with γ -radiation is used [12]. To sterilize, UHMWPE has to pass γ -radiation that leads to crosslink. Manning et al.'s studies confirm that XLPE increases wear resistance compared with all other polymers, and due to biological activity, it undergoes wear debris. Also, XLPE doped with antioxidant like vitamin E are also used for THA [13–15]. XLPE coated with poly(2-methacryloyloxyethyl phosphorylcholine) (PMPC) is a photo-induced grafted polymerization mimics articular cartilage [16, 17].

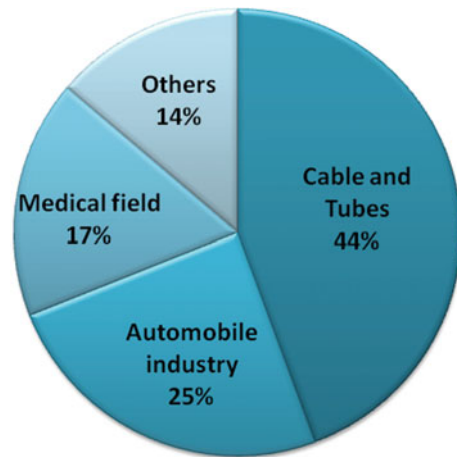
5.4 *Other Applications*

In addition to the above described applications, XLPE also used in, has also noticed the application in:

- Automobile industries: automotive ducts, headliner, dashboard padding, etc.,
- Sports goods, playground padding and protective packing,
- Dental applications: composite filling material for dental restoration,
- Making of watercraft products like canoes, kayaks,
- Chemical industry for chemical storage tank.

The demerits of the XLPE materials and its products are surmounted by its nanocomposites and blends [7] (see in volume 2).

Fig. 3 Pie-diagram representing the global XLPE market—field of application



6 The Commercial Significance of XLPE

The global market of XLPE if segmented according to its application cable and tubes for infrastructure is very large, next is for the automobile industry and third for the medical field, and a minor part is shared with other applications. A diagrammatic explanation for the global XLPE market according to the field of application is depicted in Fig. 3.

The need for XLPE is rising day to day and expecting the XLPE market to an increase of more than 6% in 2024 (<https://www.marketsandmarkets.com>). Hence, the commercial significance of XLPE is increasing exponentially.

7 Limitations and New Challenges of XLPE and Its Products

As discussed in the above section, XLPE has numerous applications out of which three are main applications: medical implants, cable insulations and pipes. The UHMWPE is crosslinked by radiation techniques, which are used as medical implants. The advantage of crosslinked UHMWPE is that the crosslinking improves the wear resistance but a high crosslinking may be possible which will reduce the mechanical strength. This high crosslinking is due to the presence of micro-voids or cracks and an increased amount of free radical than needed. The origin of the defects must be monitored throughout the process and hence reduced the high crosslinking rate. Both LDPE and HDPE are crosslinked through all methods, whose crosslinked products are mainly used in pipes and cables. Crosslinks in PE for the pipe materials cause high resistance in corrosion, low heat and electrical conductor, flexible and light weighted and hence easy to assemble. The slow crack growth (SCG) due

to the material defects or the presence of solid particles like the residual catalyst can be avoided by installing bimodal PE [18]. Like pipes, cable materials are also bad conductors of heat and electricity with high dielectric strength, but due to the presence of micro-cavities, gas particles and some conducting particles lead to water treeing. This water treeing will not lead to dielectric failure, but in some conditions, this will direct to electrical treeing [19]. The addition of hydrophilic clusters can avoid water treeing, but improper addition will decrease the dielectric strength. Hence, methods have to construct to decrease the water treeing without affecting the dielectric strength.

In addition, the increase of infrastructure and the advancements taken around the world increases the need for XLPE, so better advancements lead to more challenges to the XLPE products too—for the cable industry, the increase in the need for high power, defects like the space charge accumulation which leads to breakdown and distortion of an electric field with in the material. This space charge accumulation direct to aging and ultimately to breakdown [6, 20–22]. When an additive or fillers are added to the polymer matrix, which enhances the chemical properties and physical properties like mechanical, thermal, electrical, etc., restrict the breakdown. For this reason, in XLPE-based nanoparticles, nanoparticles in the polymer matrix trapped the charge and as a result reductions in the space charge accumulation. The resistance of moisture and the aggressive chemical is very challenging for both XLPE cable and pipes. Self-healing properties are introduced for cables and pipes because of the difficulty in detecting and repairing the damage [23].

Atomic-level understanding of XLPE leads to a better knowledge of chemical reactivity. Computational quantum mechanical studies are a good tool for such atomic- or molecular-level understanding [24, 25]. However, there are a handful of such studies in XLPE shadowing the better understanding at atomic-level of XLPE matrix [26–29]. Another challenge for XLPE and its products is the disposal of waste and recycling. Due to crosslinking, the recycling of XLPE is difficult, and this leads to environmental pollution. Lee et al., Hong et al. and Goto et al. studied on the recyclability of XLPE [30–33]. They point out some supercritical solvents that are capable of decross-linking, but more and more researches have to be done in this field. Various recycling techniques are discussed in the coming chapters.

8 Conclusion and Outlook

XLPE rules the major share of the plastic market due to its excellent desirable properties. All crosslinking methods have advantages and disadvantages, and XLPE material obtained through one method may be excellent for one application and may not good for another. Hence, it is important to choose the most appropriate method for specific needs with quality standards. XLPE as insulation material in the cable industry is one of the key applications of XLPE. However, the defects lead to water treeing and finally to electrical breakdown. Thus, to improve the efficiency of insulations, a new material is fabricated by the incorporation of nanocomposites or blends

in XLPE matrix. Advance research in XLPE is important, especially studies about the influence of crosslinking mechanical and thermal properties to obtain a potential XLPE material with high performances. Besides, the crosslink leads to limiting in recyclability that will adversely affect the environment. Researches have to focus not only on improving the efficiency of the material but concentrate to attain zero production wastes too. Fewer hazards, zero waste more efficient crosslinking method to obtain XLPE material with supreme properties for potential applications and efficient methods for its recyclability can make XLPE an ecofriendly product in the future.

References

1. Tamboli SM, Mhaske ST, Kale DD (2004) Crosslinked Polyethylene. *Indian J Chem Technol* 11:853–864. https://doi.org/10.1142/9781783267170_0006
2. Precopio F, Gilbert A (1999) The invention of chemically crosslinked polyethylene. *IEEE Electr Insul Mag* 15:23–25. <https://doi.org/10.1109/57.744587>
3. Lazar M, Rado R, Rychlý J (1990) Crosslinking of polyolefins. *Adv Polym Sci* 95:148–197. https://doi.org/10.1007/3-540-52159-3_8
4. Mauri M, Tran N, Prieto O et al (2017) Crosslinking of an ethylene-glycidyl methacrylate copolymer with amine click chemistry. *Polym (Guildf)* 111:27–35. <https://doi.org/10.1016/j.polymer.2017.01.010>
5. Mauri M, Hofmann AI, Gómez-Heincke D et al (2020) Click chemistry-type crosslinking of a low-conductivity polyethylene copolymer ternary blend for power cable insulation. *Polym Int* 69:404–412. <https://doi.org/10.1002/pi.5966>
6. Nishikawa S, Sasaki KI, Akita K et al (2017) XLPE cable for DC link. *SEI Tech Rev* 59–64
7. Thomas J, Joseph B, Jose JP et al (2019) Recent advances in cross-linked polyethylene-based nanocomposites for high voltage engineering applications: a critical review. *Ind Eng Chem Res* 58:20863–20879
8. Gedde UW, Ifwarson M (1990) Molecular structure and morphology of crosslinked polyethylene in an aged hot-water pipe. *Polym Eng Sci* 30:202–210. <https://doi.org/10.1002/pen.760300403>
9. Kurtz SM, Gawel HA, Patel JD (2011) History and systematic review of wear and osteolysis outcomes for first-generation highly crosslinked polyethylene. *Clinical orthopaedics and related research*. Springer, New York LLC, pp 2262–2277
10. Beksac B, Salas A, Della Valle AG, Salvati EA (2009) Wear is reduced in THA performed with highly cross-linked polyethylene. *Clin Orthop Relat Res* 467:1765–1772
11. Collier JP, Sutula LC, Currier BH, Currier JH, Wooding RE, Williams IR, Farber KB, Mayor MB (1996) Overview of polyethylene as a bearing material: comparison of sterilization methods. *Clin Orthop Relat Res* 333:76–86
12. Hodrick JT, Severson EP, McAlister DS, Dahl B, Hofmann AA (2008) Highly crosslinked polyethylene is safe for use in total knee arthroplasty. *Clin Orthop Relat Res* 466:2806–2812
13. Bracco P, Oral E (2011) Vitamin E-stabilized UHMWPE for total joint implants: a review. *Clinical orthopaedics and related research*. Springer, New York LLC, pp 2286–2293
14. Oral E, Muratoglu OK (2011) Vitamin E diffused, highly crosslinked UHMWPE: A review. *Int. Orthop.* 35:215–223
15. Dumbleton JH, D'Antonio JA, Manley MT et al (2006) The basis for a second-generation highly cross-linked UHMWPE. *Clin Orthop Relat Res* 453:265–271. <https://doi.org/10.1097/01.blo.0000238856.61862.7f>

16. Kyomoto M, Moro T, Konno T et al (2007) Enhanced wear resistance of modified cross-linked polyethylene by grafting with poly(2-methacryloyloxyethyl phosphorylcholine). *J Biomed Mater Res Part A* 82A:10–17. <https://doi.org/10.1002/jbm.a.31134>
17. Kyomoto M, Moro T, Iwasaki Y et al (2009) Superlubricious surface mimicking articular cartilage by grafting poly(2-methacryloyloxyethyl phosphorylcholine) on orthopaedic metal bearings. *J Biomed Mater Res Part A* 91A:730–741. <https://doi.org/10.1002/jbm.a.32280>
18. Hubert L, David L, Séguéla R et al (2002) Physical and mechanical properties of polyethylene for pipes in relation to molecular architecture. II. Short-term creep of isotropic and drawn materials. *J Appl Polym Sci* 84:2308–2317. <https://doi.org/10.1002/app.10538>
19. Sarathi R, Das S, Anil Kumar CR, Velmurugan R (2004) Analysis of failure of crosslinked polyethylene cables because of electrical treeing: a physicochemical approach. *J Appl Polym Sci* 92:2169–2178. <https://doi.org/10.1002/app.20200>
20. Salah Khalil M (1997) International research and development trends and problems of HVDC cables with polymeric insulation. *IEEE Electr Insul Mag* 13:35–47. <https://doi.org/10.1109/57.637152>
21. Khalil MS (1993) Effect of additive and polarization temperature on space charge formation in polyethylene. In: Annual report—conference on electrical insulation and dielectric phenomena. Publ by IEEE, pp 180–185
22. Terashima K, Suzuki H, Hara M, Watanabe K (1998) Research and development of ± 250 kV DC XLPE cables. *IEEE Trans Power Deliv* 13:7–16. <https://doi.org/10.1109/61.660837>
23. Zhou K, Zhao W, Tao W (2013) Self-healing phenomenon of water tree in the process of the accelerated aging of XLPE cables. In: Proceedings of IEEE international conference on solid dielectrics, ICSD, pp 824–827
24. Fried JR (2007) Computational parameters. *Phys Prop Polym Handb* 59–65. https://doi.org/10.1007/978-0-387-69002-5_4
25. Ramachandran KI, Deepa G, Namboori K (2008) Computational chemistry and molecular modeling: Principles and applications
26. Zhao H, Chen J, Zhang H (2017) Theoretical study on the reaction of triallyl isocyanurate in the UV radiation cross-linking of. *RSC Adv* 7:37095–37104. <https://doi.org/10.1039/C7RA05535H>
27. Zhang H, Shang Y, Zhao H et al (2017) Theoretical study on the reaction of maleic anhydride in the UV radiation cross-linking process of polyethylene. *Polym (Guildf)* 133:232–239. <https://doi.org/10.1016/j.polymer.2017.11.045>
28. Zhang H, Shang Y, Zhao H et al (2018) Theoretical study on the grafting reaction of maleimide to polyethylene in the UV radiation cross-linking process. *Polym (Basel)* 10:1033–1039. <https://doi.org/10.3390/POLYM10091044>
29. Process C, Zhang H, Shang Y et al (2018) Theoretical study on the grafting reaction of maleimide to polyethylene in the UV radiation. <https://doi.org/10.3390/polym10091044>
30. Goto T, Yamazaki T, Sugeta T et al (2003) Recycling of silane cross-linked polyethylene for insulation of cables by supercritical alcohol. In: Proceedings of the IEEE international conference on properties and applications of dielectric materials. pp 1218–1221
31. Ashihara S, Goto T, Yamazaki T et al (2008) Recycling of insulation of 600V XLPE cable using supercritical alcohol. In: Proceedings of the international symposium on electrical insulating materials, pp 522–525
32. Lee H-S, Jeong JH, Hong SM et al (2012) Recycling of crosslinked polypropylene and crosslinked polyethylene in supercritical methanol. *Korean Chem Eng Res* 50:88–92. <https://doi.org/10.9713/kcer.2012.50.1.088>
33. Goto T, Ashihara S, Yamazaki T et al (2011) Continuous process for recycling silane cross-linked polyethylene using supercritical alcohol and extruders. *Ind Eng Chem Res* 50:5661–5666. <https://doi.org/10.1021/ie101772x>

Chapter 2

Historical and Theoretical Background of XLPE



**Minu Elizabeth Thomas, Rajamani Vidya, Jince Thomas,
and Zakiah Ahmad**

1 Introduction

Crosslinked polyethylene (XLPE) is widely used as insulation for power cables, replace the paper insulated cables and contemporary thermoplastic insulated cables at the time when XLPE's invention in 1960. Due to many outstanding characteristics, mainly it can employ as an insulator in higher operation temperature makes XLPE more preferred in the insulation industry. XLPE also has many other applications rather than insulation. The first part of this chapter narrates the story of XLPE and its pathway to many applications, especially in insulation cables. However, to get a clear picture of XLPE olden times a detailed description of the account of insulation cables and the urgency of XLPE like material to the insulation industry must be strongly illustrated. Besides, a portrait of insulation until the time of XLPE invention is given because XLPE is first introduced as an insulator.

M. E. Thomas · R. Vidya
School of Chemical Sciences, Mahatma Gandhi University, Kottayam, Kerala, India
e-mail: minuputhen@gmail.com

R. Vidya
e-mail: vidyasree850@gmail.com

J. Thomas
Research and Post Graduate Department of Chemistry, St. Berchmans' College, Changanassery, Kerala, India

International and Inter University Center for Nanoscience and Nanotechnology, Mahatma Gandhi University, Kottayam, Kerala, India

J. Thomas
e-mail: jincethomas25@gmail.com

Z. Ahmad (✉)
Faculty of Civil Engineering, Universiti Teknologi Mara, Shah Alam, Selangor, Malaysia
e-mail: zakiah@uitm.edu.my

2 XLPE as Insulation: Behind the History

2.1 *Before the Introduction of XLPE*

It is believed that in Russia 1812 the first power cable is used. After the invention of the telegraph by Samuel Morse in 1837 and over 125 years ago, Thomas A Edison made an underground cable to connect his two famous invention generator and incandescent lamp. He named this as ‘street pipes’ [US Patent No. 251,552 dated December 27, 1881] [1]. This operated at DC 110 V. The structure of these pipes was consisting of copper bars wrapped with jute that are inserted into an iron tube, which is filled with (i.e., the gap between the wall of iron pipe and jute-wrapped copper rod), wax-like compound or bituminous.

In 1880s natural latex ‘gutta-percha’ was directly used as an insulator. In 1882, Edison used a rubber-insulated cables in New York City. Ferranti constructs a concentric cable model so that the structure of cables was appreciable and convenient. By the end of 1890 impregnated paper insulation was used to cables with high voltages up to 10 kV. Natural rubber as an insulation material is globally accepted only in 1900. After that armored cables with flexible sheathing and two cloth-covered, rubber insulation is practiced [2]. At Germany in 1903, Poly Vinyl Chloride (PVC) was invented but only after 30 years it is implemented as an insulator. By the end of the Second World War synthetic rubber [1933, IG Farben of Germany] and polyethylene (PE) were invented, but it takes much time to use as an insulator. In 1955 ethylene-propylene rubber (EPR) was developed and 1962 EPR insulation cables were commercially available. Before the accessibility of PE as insulator PVC was a well-accepted insulator. Due to low cost, excellent electrical properties good chemical resistance and temperature flexibility at low temperature make it as a ruled material throughout. However, its maximum operating temperature was 75 °C hence materials with high operating temperature and with chemical and electrical properties like PE want to invent. Crosslinked polyethylene (XLPE) was solved the problems faced by PE to some extent.

2.2 *After the Invention of XLPE*

In March 1963 in the GE Research Laboratory, located in Niskayuna, New York, Al Gilbert and Frank Precopio [3] invented XLPE, which is composed of low-density PE with dicumyl peroxide, a crosslinking agent. Long-chain PE ‘cross-link’ during the vulcanization process and get material with similar electrical character of thermoplastic PE but with improved mechanical properties at high temperature. Its paramount dielectric property and thermal stability making XLPE an excellent electrical insulator.

Only after 1968 XLPE has used for multi-volt (MV) cables with unjacketed and tape shielded. Cable manufactures are expected that XLPE insulation cable will

perform reliably for 20 or 30 years [4]. However, history has shown that the service life of such cables was far shorter than expected. But, the beginning of 1972 scientists and engineers identified defects in XLPE cables which leads to water treeing. Till then they were not aware that moisture, voltage stress, omitting jackets and imperfections within the cable structure accelerate the corrosion of cables which leads to water trees. These defects degraded the cable performance and XLPE cables fail to perform its best only till 10–15 years in service. The consequences of this lack of understanding were profound. It has been estimated that for every dollar that utilities spent installing the cable, they had to spend at least 10\$ to replace it. Engineers and scientists discovered that voids and contamination in the insulation, combined with ionic contamination in the semiconducting shields, as well as other design and manufacturing deficiencies, led to voltage stress concentrations within the cables. These increased voltage stresses, united with moisture way into the cable structure produced water trees. Today there are XLPE insulations that can be designed to inhibit the growth of water trees, allowing for even greater reliability for distribution class cables. Manufacture of such XLPE cables with water tree resisting and other improved qualities by adding nanoparticles and make XLPE-nanocomposites [5]. This chapter discusses only the pure XLPE and its properties which sets out to provide the foundations for this by identifying the critical developments and understanding. The developments in XLPE-nanocomposites are discussed in volume 2.

3 XLPE as Plumbing Pipes: Behind the History

In the midst of the twentieth century, the plumbing pipes were made of galvanized steel but rusting cause reduction rate in the volume of water flow. For this reason, copper tubes replace the galvanized steel. But some defects occur in copper tubes like leakages make them inferior. Later in 1970s plastic pipes, especially PVC pipes fitted with glue, were introduced but by the introduction of hydronic radiant heating the system, which circulates water from heater/boiler to household purposes. For this process of circulating of hot water XLPE pipes is chosen as a suitable material. Gradually XLPE became more popular not only for transporting hot water they used in all indoor plumbing purposes. In the 2000s copper pipes and PVC pipes are replaced with XLPE pipes. Now XLPE pipes used even for underground purposes. The aging strength of these pipes is increased by the tuning it dimension and thickness [6].

4 XLPE as Biomedical Equipment: Behind the History

The application of XLPE is mainly seen in the total hip arthroplasty (THA) [7]. The history of arthroplasty begins with the invention of metal on metal (MoM) bearings in 1965 [8] but it was declined by the medical field. When John Charnley in 1970

introduced a THA based on Metal on Polyethylene (MoP), whose long-term survival makes it well appreciable to use in younger and more active patients. A French surgeon, Pierre Boutin in 1970 [9], points out 'polyethylene disease' in MoP make an entry to Ceramic on Ceramic (CoC) hip implants and Ceramic on Polyethylene (CoP), these products are still in use.

Introduction of stainless steel [10] and alloys like cobalt–chromium alloys (Co–Cr), titanium alloys (Ti) [11] more used in stem and acetabular cementless in THA. These materials were used due to the high mechanical strength, low density, corrosion resistance, biocompatibility with bone, etc. But Ti alloys were not used for the manufacture of femoral heads due to poor wear resistance. Hence more surface modifications in alloys were considered to get rid of these difficulties. In 1962, when the introduction of ultrahigh molecular weight polyethylene (UHMWPE) in the Charnley hip prosthesis obtained a low friction material for arthroplasty [12]. But the main challenge is the wear debris mediated osteolysis and also the formation of crosslinks and free radicals when sterilized with γ -radiation [13]. However, in XLPE, the crosslinks can also accomplished by γ -radiation, which will increase the wear resistance for artificial joints. The in-vivo studies conducted by Manning et al. and Martell et al. show the wear rate reduction is very high compared with other materials. Biological activity of wear debris and osteolysis are also reduced by the use of XLPE [14–20].

The problem regarding the oxidation of free radical with γ -radiation makes an inferior trend in XLPE materials. These defects are replaced by doping with an antioxidant like Vitamin E [20–23] or by surface-treatment introduced by Kyomoto et al., a photo-induced grafted polymer which mimics articular cartilage used millions of people now [24, 25].

When we travel along with the history of XLPE, it can be noted that a long time interval is taken for the development of XLPE to its best outcome in the applications. To reduce the time consumption an alternate in-silico studies can be applied in the field of XLPE. Even though the experimental studies are rapidly growing around the world, a structure studies of XLPE are very less, i.e., the theoretical studies. To discuss the theoretical studies in XLPE one must know the theories behind the computational studies.

5 Classical and Quantum Mechanics Theories for Computational Studies

Theoretical chemistry is an emerging field, which has a lot of applications in studying the reactions with more efficiency. There is a close relationship between traditional theoretical chemistry and modern computational chemistry. It is really helpful to solve the problems via computerized calculations. But a newcomer will have to face

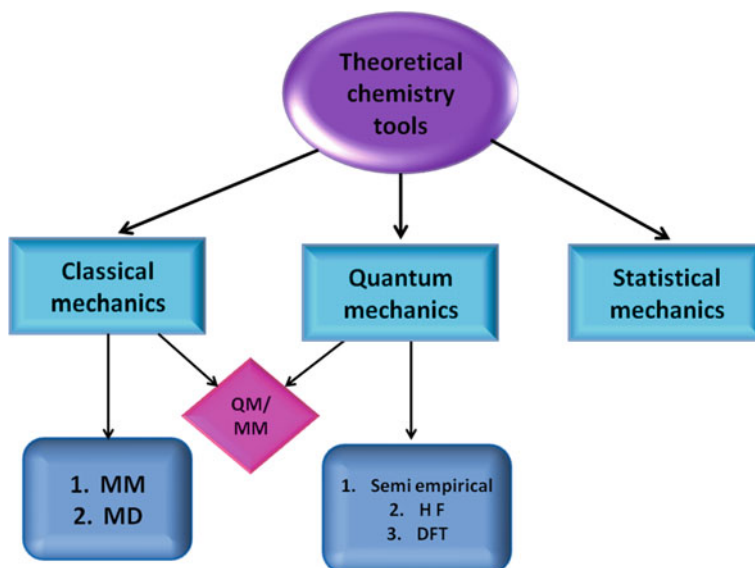


Fig. 1 Schematic representation of theoretical toolkit

some difficulties in this field, as he/she is not aware of the codes used for the programs, software and hardware used, the authenticity of the outputs, etc. Computer programs will make the user easier to handle a problem. For that, computational chemistry has its theoretical methods or techniques. In the following section, we will discuss briefly it. Figure 1 shows a schematic representation of the theoretical chemistry tools used for computations.

As from the above diagram, we can say that the theoretical chemistry has three major components known as classical mechanics, quantum mechanics and statistical mechanics. Classical mechanics deals with the mathematical study of the motion of objects in our everyday life and the corresponding forces. It is otherwise known as Newtonian mechanics. It has two disciplines: molecular mechanics (MM) and molecular dynamics (MD). Even though classical mechanics has its applications, it fails to explain several other factors such as black body radiation, wave-like nature of microscopic particles and also it is found to be inconsistent with Maxwell's electrodynamics. This leads to the birth of quantum mechanics.

Nowadays, we focus more on quantum mechanical aspects. It is a branch of science dealing with the wave-like nature of atomic and subatomic systems and its energy. With the help of modern computational techniques along with quantum mechanics, several studies can be conducted on micro to even large macromolecular systems. Most important methods of quantum mechanics include the semiempirical method, Hartree–Fock theory (HF) and Density Functional Theory (DFT). More theoretical studies on polymers were reported are based on these theories. There are not many

studies reported yet for pure crosslinked XLPE based on classical mechanics and statistical mechanics.

The theoretical investigation of pure XLPE is mostly dealing with quantum mechanical studies. It does not replace experiments, but give a proper idea about how the reaction works. This chapter provides an insight toward interpreting the nature of XLPE, its properties and reactions in a computational way. This section begins with a brief explanation of the fundamental aspects of quantum mechanics necessary to describe molecules.

5.1 Schrödinger Wave Equation

The Schrödinger wave equation [26–29] is a mathematical equation, that describes the changes over time of a physical system in which quantum effects, such as wave-particle duality, are significant. The equation is mainly used for studying quantum mechanical systems. The time-dependent Schrödinger wave equation can be written as:

$$i\hbar \frac{\partial}{\partial t} [\Psi(r, t)] = \hat{H}\Psi(r, t)$$

where ‘ i ’ imaginary unit, ‘ \hbar ’ reduced Planck’s constant ($\hbar = \frac{h}{2\pi}$), ‘ r ’ and ‘ t ’ are position and time vector, respectively, and ‘ \hat{H} ’ is Hamiltonian operator, which represents the total energy.

Hence, the time-independent Schrödinger wave equation can be written as:

$$\hat{H}\Psi = E\Psi$$

where

$$\hat{H} = \hat{H} - \frac{\hbar^2}{2m} \nabla^2 + V$$

$$\nabla^2 = \frac{\partial^2 \Psi}{\partial x^2} + \frac{\partial^2 \Psi}{\partial y^2} + \frac{\partial^2 \Psi}{\partial z^2}$$

‘ E ’ is the numerical value of total energy and ‘ Ψ ’ wave function.

Quantum chemistry requires the solution of the time-independent Schrödinger wave equation. But it cannot solve exactly. So, several approximations were used to perform mathematical calculations.

Approximations to the Schrödinger wave equation

5.2 Born–Oppenheimer Approximation

To solve the Schrodinger wave equation, certain approximations must be applied. The widely used approximation is the Born–Oppenheimer approximation. The total molecular wave function $\Psi(R, r)$ depends on both the positions of all of the nuclei and the positions of all of the electrons. Since electrons are much lighter than nuclei and therefore move much more rapidly, electrons can essentially instantaneously respond to any changes in the relative positions of the nuclei. This allows for the separation of the nuclear variables from the electron variables,

$$\Psi(R_1, R_2, \dots, R_N, r_1, r_2, \dots, r_n) = \varphi(R_1, R_2, \dots, R_N)\Psi(r_1, r_2, \dots, r_n)$$

This separation of the total wave function into an electronic wave function $\Psi(r)$ and a nuclear wave function $\varphi(R)$ means that the positions of the nuclei can be fixed and then one only has to solve the Schrödinger equation for the electronic part. This is Born–Oppenheimer approximation.

5.3 Hartree–Fock Method

The Hartree–Fock calculation is a simple ab-initio calculation. There was a problem with Hartree’s Self-Consistent Field method. It arises from the fact that, for any atom with more than one electron, an exact solution for the Schrödinger equation is not possible due to electron–electron repulsion. So HF theory was developed to solve the electronic wave equation which results from the time-independent Schrödinger wave equation after involving the Born–Oppenheimer approximation. The approximate energy in Hartree–Fock method is calculated using the equation:

$$E = \frac{\int \Psi^* \Psi d\tau}{\int \Psi^* \Psi d\tau}$$

Hartree’s method is used to write an approximate poly-electronic wave function for an atom as the product of one-electron wave function.

$$\Psi_0 = \Psi_0(1)\Psi_0(2)\Psi_0(3) \dots \Psi_0(n)$$

This function is called a Hartree Product. But the Hartree method did not respect the principle of antisymmetry of the wave function. Later, V. Fock overcome these limitations by modifying Hartree’s method by describing the many-electron wave function as an anti-symmetrized product of one-electron wave functions. For that, he used Slater orbitals or Slater determinants. Fock suggested the Hartree–Fock wave function using the Slater determinant as:

$$\Psi_i = \frac{1}{\sqrt{N!}} \begin{vmatrix} \Phi_1(1) & \Phi_2(1) & \dots & \Phi_N(1) \\ \Phi_2(2) & \Phi_2(2) & \dots & \Phi_N(2) \\ \vdots & \vdots & \ddots & \vdots \\ \Phi_1(N) & \Phi_2(N) & \dots & \Phi_N(N) \end{vmatrix}$$

which is anti-symmetric and satisfies Pauli exclusion principle. The columns represent single-electron wave function and the rows represent electron coordinates. Again, an effective potential is employed, and an iterative scheme provides the solution to the Hartree–Fock equations.

The solution of this Hartree–Fock model (Φ_i) is known as molecular orbitals (MO), which represents the entire molecule just like the atomic orbitals (AO) represents an atom. Since we consider the atomic properties within the molecule, it is sensible to construct molecular orbitals as an expansion of atomic orbitals,

$$\Phi_i = \sum_{\mu}^k C_{i\mu} \chi_{\mu}$$

where the index ‘ μ ’ represents all the ‘ k ’ AOs ‘ χ ’ of every atom in the molecule and ‘ $C_{i\mu}$ ’ is the expansion coefficient of AO ‘ χ_{μ} ’ in the MO ‘ Φ_i ’. This is defined as the linear combination of atomic orbitals (LCAO).

5.4 Hartree–Fock-Roothaan Method

The Hartree–Fock methods are not enough for the calculation of molecular orbitals, because they do not prescribe a mathematically favorable method for getting the initial guess for the MO wave function ‘ ψ_i ’, which is necessary to initiate the iterative procedure and the wave functions may be complicated so that it is not useful for the understanding the electron distribution qualitatively. Roothaan and Hall pointed out that these problems can be solved by taking MO as a linear combination of basis functions. It can be represented as:

$$\psi_i = \sum_{s=1}^m C_{si} \phi_s$$

where $i = 1, 2, 3, \dots, m$ (m MOs), ‘ C ’ is the coefficient of MOs, ‘ ϕ ’ represents the basis function.

Roothaan developed a procedure to obtain the self-consistent field solutions by taking the LCAO approximation for the MOs and combining it with the HF method. Roothaan equations are applied to closed-shell molecules or atoms where all molecular orbitals or atomic orbitals are doubly occupied, i.e., one electron is spin up and the other is spin down. These types of the wavefunction are known as a restricted

wavefunction because the paired electrons are restricted to the same spatial orbital which leads to the restricted Hartree–Fock (RHF) method. The open-shell case is a simple extension of these ideas. When the restriction is applied to the open-shell case, then it is known as restricted open-shell HF (ROHF). The matrix form of Hartree–Fock–Roothaan equation can be represented as:

$$FC = SC\varepsilon$$

where ‘ S ’ is the overlap matrix, ‘ C ’ is the coefficient matrix and ‘ ε ’ is the energy matrix and ‘ F ’ is the Fock matrix. This equation is similar to the matrix form of the secular equation along with Hückel’s MO formation. Here, the Fock matrix replaces the Hückel matrix.

Roothaan–Hall equations can also be applied to unrestricted wavefunctions. But in this case, the spin up and spin down electrons do not have the same spatial description. To handle this case, the Hartree–Fock–Roothaan procedure is slightly modified by forming different sets of the equation for both ‘ α ’ and ‘ β ’ electrons. The unrestricted Hartree–Fock (UHF) wavefunction is contaminated with higher spin states. It can be removed by using the spin projection procedure. Since the geometry optimization is quite difficult with this spin projection, great care must be needed when utilizing this unrestricted wavefunction.

5.5 Self-consistent Field Method

The self-consistent field method is an iterative method that involves selecting an approximate Hamiltonian, solving the Schrödinger equation to obtain a more accurate set of orbitals, and then solving the Schrödinger equation again with these until the results converge. The self-consistent field iterative procedure can be schematically represented in Fig. 2.

5.6 The Variation Principle

The variational principle is based on the variation theorem. It states that any wavefunction constructed as a linear combination of orthonormal functions, then its energy must be greater than or equal to the lowest energy, E_0 , of the system. It can be depicted as:

$$\frac{\langle \Phi | \hat{H} | \Phi \rangle}{\langle \Phi | \Phi \rangle} \geq E_0$$

if

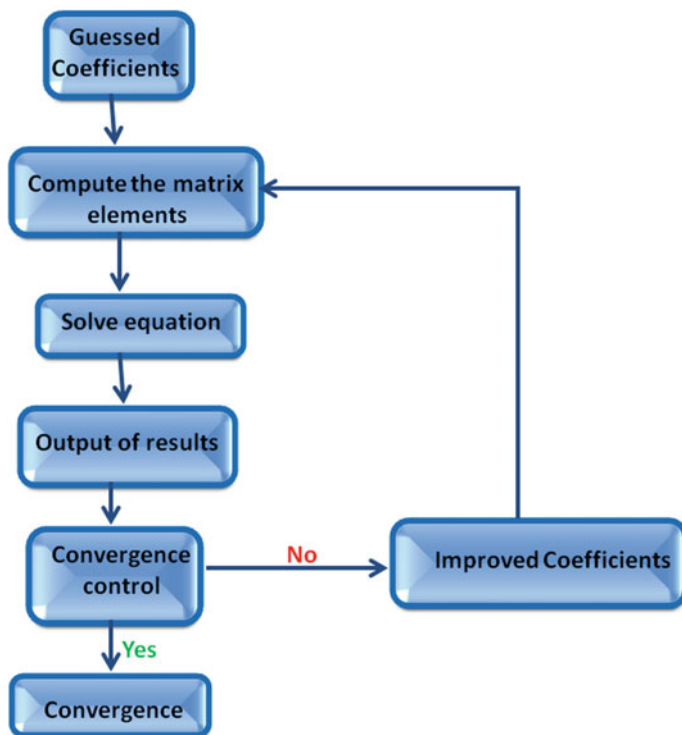


Fig. 2 Schematic representation of the self-consistent field iterative procedure

$$\Phi = \sum_i c_i \phi_i$$

The infinite set of functions ‘ ϕ_i ’ will produce the lowest energy for the particular Hamiltonian. But it is impossible to expand wavefunction using an infinite set of functions. The variational principle can be applied to predict the quality of various expansion; thus, it can save time. Variation principle, however, not an approximation method for solving the Schrödinger wave equation, somewhat, it provides a way to predict the effect of various approximation methods.

5.7 *Semiempirical Method*

The semiempirical method is a quantum chemical method based on the Schrödinger wave equation. To treat large molecules incomparably less cost, semiempirical methods can be used. Generally, it follows the HF method but it adopts many approximations as needed and depends on empirical data. While using this HF method,

some pieces of information have to be approximated or ignored. To overcome this loss, semiempirical methods are parametrized in such a way that the results can be produced which are in good agreement with the experimental data. Semiempirical methods often follow empirical methods known as the Hückel method (for π electrons) and extended Hückel method (for valence electrons). They are much faster than corresponding ab-initio calculations due to their zero differential overlap approximation.

Semiempirical calculations can be used to treat organic molecules as well as solids or nanostructures but, in each case, parametrization varies. To treat molecules in different categories (such as for π electrons and valence electron systems), different semiempirical methods can be applied. Pariser-Parr-Pople method (PPP), the first semiempirical method restricted to π electrons, can be used to perform the computations of electronically excited states of polyenes. It can provide the best results when parametrized well. The PPP method can also be used to calculate the ultra-violet (UV) spectra of conjugated compounds, especially dyes. Nowadays the PPP method has not much interest since it is limited to only π electrons and the development of Neglect of Differential Overlap (NDO) methods. They include Complete Neglect of Differential overlap (CNDO) method, Intermediate Neglect of Differential Overlap (INDO) method and Neglect of Diatomic Differential Overlap (NDDO) method. CNDO is the first self-consistent field (SCF) semiempirical method which treats molecules just beyond π electrons. It was a general geometry method which uses a minimal valence basis set of Slater-type orbitals, i.e., using just the valence electrons and the atomic orbitals of each atom. There are two variations, CNDO/1 and CNDO/2. INDO is also an SCF semiempirical method, which is just an extension of the CNDO method. It made use of zero differential overlap for the two-electron integrals but not for the integrals on the same atom. It is more accurate than the CNDO method and is used mostly for evaluating UV spectra. NDDO is another semiempirical method goes beyond INDO. It is the basis of currently popular successful semiempirical methods. It also uses zero differential overlap approximation. In this method, the overlap matrix S is replaced by unity.

5.8 *Density Functional Theory*

Generally, ab-initio methods and semiempirical methods are based on the Schrödinger wave equation. But Density Functional Theory (DFT) which is a quantum mechanical method is not based on the wave function. It is based on electron probability density function or electron density function commonly called the charge density and is designated as $\rho(x, y, z)$. Unlike wave functions, it is measurable.

DFT is based on two Hohenberg–Kohn theorems, which state that the ground-state properties of an atom or molecule are determined by its electron density function and that a trial electron density must give energy greater than or equal to true energy. The Hohenberg–Kohn existence theorem proves that there exists a unique functional such that:

$$E[\rho(r)] = E_{\text{elec}}$$

where E_{elec} is the ground-state energy. They also demonstrated that the electron density obeys the variational theorem. It means that the energy of the specific electron density will be greater than or equal to the exact energy. Here, the calculations of energy might be easier than that by ab-initio methods because of the variable dependence. Unlike HF and other post HF correlation methods, DFT provides an exact theory with an approximate solution. The general DFT energy expression can be written as:

$$E_{\text{DFT}}[\rho] = T_s[\rho] + E_{\text{ne}}[\rho] + J[\rho] + E_{\text{xc}}[\rho]$$

where

- E energy,
- T kinetic energy of electrons,
- E_{ne} nuclear-electron attraction energy,
- J electron–electron repulsion energy,
- E_{xc} electron–electron exchange–correlation energy.

By equating E_{DFT} to the exact energy, this expression defines E_{xc} , i.e., it is the part that remains after subtraction of the non-interacting kinetic energy, and the E_{ne} and J potential energy terms.

$$E_{\text{xc}}[\rho] = (T[\rho] - T_s[\rho]) + (E_{ee}[\rho] - J[\rho])$$

The first parenthesis may be considered as the kinetic correlation energy, while the last contains both potential correlation and exchange energy.

DFT can be classified in different ways based on the functional employed.

The commonly used functional are:

1. Local Density Approximation (LDA)—in LDA it is assumed that density locally can be treated as a uniform electron gas or density is a slowly varying function. In general, if α and β densities are not equal, LDA has been replaced by LSDA, Local Spin Density Approximation and it depends only on the up-spin and down-spin electron density.
2. Generalized Gradient Approximation (GGA)—in this method, the first derivative of the density is included as a variable. GGA methods are also sometimes referred to as non-local methods, although this is somewhat misleading since the functionals only depend on the density (and derivative) at a given point, not on a space volume as the Hartree–Fock exchange energy. It also depends on the magnitude of the gradient of the density.
3. Meta GGA—this functional includes the second derivative of the electron density (the laplacian). This is a natural development after GGA, that includes only the density and its first derivative in the exchange–correlation potential. It depends on kinetic energy density.

4. Hybrid GGA—these functions are a class of approximations to the exchange–correlation energy functional in DFT. It combines GGA with Hartree–Fock exchange and replaces the Kohn–Sham operators with hybrid Fock–Kohn–Sham operators. One of the most commonly used versions is B3LYP, which stands for Becke, 3-parameter, Lee–Yang–Parr.

5.9 Basis Set

To solve for the energy and wave function within the Hartree–Fock method, the atomic orbitals must be specified. According to the variational principle, if the set of atomic orbitals is infinite, then we obtain the lowest possible energy within the HF-SCF method. This is Hartree–Fock limit, E_{HF} . This is not the actual energy. Since an infinite set of atomic orbitals is impractical, a choice must be made. This choice defines a basis set, i.e., a set of the mathematical description of orbitals of a system, which is used for approximate theoretical calculation or modeling.

There are two types of basis function which are used for computational calculation:

- (i) Slater-type orbitals (STO),
- (ii) Gaussian type orbitals (GTO).

Mathematical functions which resemble the atomic orbitals of the hydrogen atom are known as Slater-type orbitals (STOs). Its mathematical form can be set as:

$$\chi = Nx^i y^j z^k e^{-\zeta(r-R)}$$

where ‘ N ’ is the normalization constant and ‘ R ’ is the position vector of the nucleus. The value of ‘ ζ ’ for each STOs are different and it can be found out by minimizing the atomic energy concerning ζ . Since the STOs mimics only the solution of single-electron atoms, it cannot be applied to non-hydrogenic systems. It can be possible only by using infinite series, which is not practical.

Later Boys and Pople decided to use a combination of Gaussian function which resembles the STOs. It can be represented as:

$$\chi = Nx^i y^j z^k e^{-\alpha(r-R)^2}$$

GTOs can be used to evaluate the integrals needed to generate the Fock matrix elements. STOs have proper radial shape but GTOs are different and it is continuously differentiable. So, more number of GTOs are needed to mimic STO, which increases the computational calculation time. Nevertheless, the most commonly used basis sets are comprised of GTOs. STOs are used in semiempirical methods and GTOs are used in modern molecular ab-initio methods.

There are several different basis sets with variations which are commonly used for computational calculations. The most popular and widely used basis sets are developed by Pople and co-workers. Here we consider, STO-1G, STO-3G, 3-21G,

6-31G, 6-31G* basis sets with variations obtained by adding polarization (*) and diffuse (+) functions. STO-1G basis functions are generally used for illustrative purposes but not for research calculations because of poor approximations.

For a particular quantum chemical calculation, the choice of the basis set depends on several factors such as the number of basis functions needed, size of the molecule. The basis set with the smallest number of basis functions per atomic orbital is known as a minimum basis set. For example, the STO-3G basis set. For second-row elements, it has 2 s-functions and p_x , p_y , p_z functions, i.e., a total of five basis functions. This type of basis sets is generally referred to as a single zeta basis set. As mentioned above, the term zeta symbolizes that each basis function mimics a single STO. It is easy to use and the main advantage is its speed compared to the higher ones.

Even though it is useful for time-saving, but gives only less accurate geometries and energies. Another disadvantage is it does not consider the core electrons. As a solution for this, the size of the basis set was doubled, thus created a double zeta (DZ) basis set. For carbon, the DZ basis set has four s-functions and two p-functions, i.e., a total of ten functions. Further improvement leads to the development of the next type, i.e., triple zeta (TZ) basis set which contains three times as many functions as the minimum basis set.

Later, Pople developed the split valence basis set, by minimizing the energy of the atom at the HF level for the contraction coefficients, which considers both core and valence electrons. It has a single zeta basis function in the core and DZ in the valence region. It is a type of DZ in which only the number of valence orbitals is doubled. A DZ split valence basis set for carbon consist of 3 s-functions and 2 p-functions constitute a total of nine basis functions. Similarly, a TZ split valence basis set contains four s-functions and three p-functions, a total of 13 basis functions and so on. The smallest split valence basis set is 3-21G basis set. It is made up of a group of Gaussian functions rather than a single one. The name itself specifies the scheme applied to develop this basis set. The dash separates the core electrons from the valence electrons. Here, each core basis function is comprised of three Gaussian functions and the valence area is split into two, commonly known as 'inner' and 'outer' functions. In this case, each inner basis function is composed of two Gaussians and the outer region is a single Gaussian. For carbon, the core region is a single s-basis function made up of three GTOs and its valence space has two s and two p basis functions. The inner basis function composed of 2 GTOs and the outer basis functions each composed of single Gaussian, i.e., one 's' and one 'p' basis function belong to inner basis function and the remaining belong to outer basis functions. Thus, the carbon 3-21G basis set has nine basis functions made up of 15 Gaussian functions. The other basis set 6-31G can also be explained similarly.

For molecules beyond Neon, the 3-21G basis set gives poor geometry optimizations and less accurate energies. To overcome this defect, the basis functions are provided with d functions and are known as polarization functions. Polarization functions allow the SCF procedure to develop a more anisotropic electron distribution. The polarization function can be represented by using an asterisk, *, i.e., 3-21G*, polarization only for molecules beyond neon. For hydrogen and helium, the 3-21G and 3-21G* are similar. This is for split valence basis set. In the case of higher

geometries, obtaining good relative energies with 3-21G* basis set is challenging. So, to obtain more accurate geometries another type of split valence basis set known as 6-31G* is used. It is the most commonly used basis set with polarization functions. It gives good geometries and relative energies and often much better than 3-21G*. But it takes almost five times more time for computational calculations than 3-21G*.

For multiple zeta basis sets, the polarization function is represented by the addition of polarization function using the +P symbol, i.e., DZ + P, which indicates the DZ basis set with one set of polarization function. For convenience, the addition of multiple sets of polarization can be indicated by using parenthesis. For example, 6-311G(2df, 2p), which indicates that there are two sets of d-functions and a set of functions are added to the non-hydrogen part and two sets of p- functions are added to the hydrogen atoms.

In case of molecules with anions or adjacent lone pairs, the basis set must be enlarged with diffuse functions so that the electron density can be expanded to a larger volume. For a split valence basis set, it can be represented by using + symbol as 6-31 + G(d), i.e., a full set of additional functions same as present in valence space are added.

6 Molecular Properties

From the solution of the Schrödinger equation not only we can obtain the wave function and its energy for a given geometry but also many other molecular properties. Mostly molecular property mainly based on the perturbation on wave function or energy using an operator rather than the Hamiltonian. These perturbations are mainly by external electrical field (F), external or internal magnetic field (B), change in nuclear geometry (R) and nuclear spin (I). The molecular properties analyzed here are optimization for the geometry and its harmonic vibrational frequency (IR frequency). The optimization of geometry means finding a minimum energy structure of given geometry. The optimization is the second derivative of the wave function for the position of nuclei. Molecular frequencies depend on the second derivative of energy concerning the position of nuclei.

This chapter discussed only on pure XLPE so the discussion of theories limited to molecular mechanics and quantum mechanics. The hybrid and multi-scale studies are mainly incorporate on XLPE-nanocomposites. Hence, the discussion about those theories is discussed in volume 2 of this book series. By keeping the knowledge of theories and software, we can now discuss the computational studies of XLPE. The reports show the studies mainly on the structural studies of XLPE and reaction of crosslinking of PE to XLPE.

7 Software Used for Computational Calculations

There is a wide range of software packages available to do the above-mentioned computational analysis. The choice of software is always important. Every software packages are different and have unique features. Generally, they vary in cost, functions, efficiency, easy to use features, automation and robustness. Analyzing these features can be used to select the most compatible software package for computational programs. Proper selection of software will be helpful to save time and money. There are different packages available to perform computational calculations using various tools. A brief discussion on the software packages are included below.

7.1 Integrated Packages

These include software packages which can perform computational calculations using various computational techniques. They are Alchemy, Chem3D, ChemSketch, HyperChem, NWChem, SPARTAN, UniChem, etc.

Alchemy 2000 is a graphic interface software program package, which is used for running both molecular mechanics and semiempirical calculations and is done by using built-in Tripos force field. It has several features such as creating 3D geometry and it can convert 2D input into 3D one. It can be used to build proteins and data of organic functional groups are available. Its output data can be printed or exported to a spreadsheet and it allows user to create a database of structures. Alchemy is designed by Tripos and sold by SciVision.

Chem3D is another software package for molecular modeling used in PC and Macintosh versions. It acts as a graphic interface for MOPAC and Gaussian and also performs computations using MM2 and extended Hückel methods. It has both graphic and text-based geometry building modes.

ChemSketch is a 2D structure drawing software designed for organic molecules. Similar to the above, this is also a graphic interface program package. It is found that the ChemSketch is convenient to use.

HyperChem is also an integrated graphic interface program which can be used for computational calculation as well as a visualization tool. It can be used for performing *ab-initio*, molecular mechanics and semiempirical programs.

NWChem is another software used in Linux systems. It is useful for computing *ab-initio*, band-structure, molecular mechanics and molecular dynamics programs. Input can be given in either geometric form or Z-matrix or cartesian coordinates.

SPARTAN is a well-known program which can be used to perform *ab-initio*, DFT, semiempirical and molecular mechanics integrated with a graphic interface. The attractive features of this software include its ease of use and robustness.

UniChem is another software package including graphic interface which is used for performing computations on remote machines.

7.2 *Ab-Initio and DFT Software*

This section discusses some of the software packages primarily used for performing *ab-initio* or DFT calculations. They include Amsterdam density functional (ADF), Crystal, GAMESS, Gaussian, Jaguar, Molpro, Q-Chem, etc.

ADF is a DFT program package which can perform relativistic DFT calculations and it can also include STO basis sets. Crystal is a program used to perform *ab-initio* and band-structure calculations. LoptCG script is available to perform optimizations. Both HF and DFT calculations can also be performed.

GAMESS stands for general atomic and molecular electronic structure system, which is used to perform *ab-initio* and semiempirical calculations. It is free, high-quality software.

Another software for performing *ab-initio* calculations is Gaussian. It includes a few molecular mechanics and semiempirical methods. Input can be given in both *z*-matrix or cartesian coordinates. It is user-friendly software.

Jaguar is another software designed for performing *ab-initio* calculations and the speciality is it can run computations on larger molecules efficiently. Molpro is also a software for *ab-initio* calculations which is specially designed to run complex calculations. Similarly, Q-chem is also designed to perform mainly *ab-initio* calculations on large molecules and is much faster compared to others.

7.3 *Graphics Packages*

This section includes the software packages used to building input files or viewing results. Some of them are GaussView, Molden and WebLab Viewer.

GaussView is a graphic interface program which can be used with the Gaussian program package. It can be used to view and construct molecules, run input files and display results. Molden is another program which is used to display molecular structure. It can also read from a molecular file format. WebLab Viewer is a molecular graphics program. It is capable of describing molecular structures with surfaces and labels.

8 Computational Studies in XLPE

The theoretical investigation in XLPE is carried out in two categories first regarding the study of the inhibition of electrical treeing, electric breakdown strength, etc. using aromatic/aliphatic molecules. The second investigations focus on the involvement of certain molecules in the UV radiation of PE during crosslinking to form XLPE.

8.1 *Studies on the Mechanism Behind Electrical Treeing and Electrical Breakdown*

One of the major failures of XLPE-cable manufacture is the efficiency breakdown due to the electrical treeing in the XLPE insulation materials. The researcher was working hard in both wet and dry lab to find the reason for treeing and factors to get rid of such failures, hence improve the electrical breakdown strength. Electrical treeing is a significant problem of XLPE cables whose mechanism was theoretically investigated by Zhang et al. through keto-enol tautomerism. Zhang et al. [30] investigated the inhibition initiation and propagation of polyethylene through keto-enol tautomerism of acetophenone. They use B3LYP/6-31G(d,p) level of theory for the optimization of structures in Gaussian 09 program package. They conducted the geometrical optimization of possible transition states of acetophenone and its analogues and confirm all structures are transition states by conducting the frequency analysis with an imaginary frequency.

According to the analysis, all transition states energy barriers are high, which need some more energy to overcome the energy barrier of keto-enol tautomerism but it is noted that alkyl group linked with para and meta substituted acetophenone with can only decrease the energy barrier of keto-enol tautomerism to some extent. Also, the presence of electron-withdrawing groups like—NH₂, -OH, -OR, etc. in para or meta position can also reduce the energy barrier. From the analysis of the energy barrier of keto-enol tautomerism of all 42 transition states is less than that of the breaking of the C—C bond of the XLPE.

The outcome of these studies proves that the energy barriers of keto-enol tautomerism of acetophenone and its analogues are lesser than the C—C bond energy of PE. The acetophenone and its analogues poisoned in XLPE can recover the strength of AC penetrate that PE can tolerate as well as inhibit electrical tree from initiation and propagation. Hence, in XLPE the electrical treeing is inhibition of electrical treeing is strong due to the presence of acetophenone by crosslinking. These results prove the statement of Yamono et al. [31] in 2009 that the addition of aromatic hydrocarbons can inhibit the electrical treeing in XLPE. Zhang et al. concluded by giving a micro-mechanism of keto-enol tautomerism of acetone and stated that the acetophenone either as doped in acetophenone/XLPE composites or as linked with XLPE chain can inhibit the electrical treeing.

Another study conducted a theoretical study by Zhang et al. [32] on the mechanism of electrical breakdown strength increment using acetophenone and its analogues. Here also the optimizations and analysis steps are same as that of the above studies and some of the transition states are also similar. According to their analysis, on singlet state (S_0) energy barrier is higher than compared with the triplet state (T_1). The energy barrier for the forward and backward reaction is the same for T_1 state. Hence, a decrease in the decrease in the electrical treeing can lead to the improved alternate breakdown strength of XLPE.

In 2014 Zhang et al. [33] studied the mechanism behind the electrical breakdown strength by the addition of voltage stabilizers. They studied more than 15 voltage

stabilizer molecules. The optimization of molecules is considered the isomerization reactions both in S_0 and T_1 state. From the frontier orbital analysis, they obtain the highest occupied MO–lowest occupied MO gap (HOMO–LUMO gap, E_g), electron affinities (EA) and ionization potentials (IP) of the molecules are calculated. The analysis of the electron-accepting ability of molecules has a high ability to trap the ‘hot-electron’ and dissipate through isomerization reaction. The energy barrier of isomerization reactions is less than C–C bond breakdown in XLPE. These voltage stabilizers can prevent the hot electrons bombarding to C–C bond of XLPE. 4,4'-didodecyloxybenzil has less E_g and excellent compatibility with the PE matrix leads to the electrical breakdown strength effectively, which has good agreement with experimental findings.

8.2 *Studies on the Mechanism of the UV Radiation Crosslinking Process*

Crosslinking using peroxides is a traditional way for crosslinking PE. UV radiation is a perfect candidate for the crosslinking of PE to form XLPE. Experimental investigation reveals that it is not the efficiency of the UV radiation but the presence of photoinitiator and crosslinker leads to an increase in the rate of crosslinking. Hence, a theoretical study gives an effortless investigation for choosing efficient photoinitiator and crosslinker.

Zhang et al. [34] conducted an atomic and molecular level systematic theoretical study on the benzophenone-initiated reaction mechanisms in the PE -UV radiation crosslinking process. The optimization of molecules and the reactions are carried out in B3LYP/6–311 + G(d,p) in Gaussian 09 program package. The by-products, photoinitiator, antioxidant and voltage stabilizer can improve the electrical breakdown strength. These antioxidant and voltage stabilizers can easily be grafted to the polymer chain at the course of UV radiation crosslinking and have better compatibility with XLPE matrix. They suggested that when 2,6-di-*t*-butyl-4-*n*-butylphenol (Bp) is used as an oxidizer and valerophenone(Vp) (Fig. 3) as voltage stabilizer gain better results.

When the ‘hot electrons’ will strike to those conjugated aromatic molecules which have strong capability of trapping the electron than the aliphatic chain of PE, hence prevent from the degradation of the polymer matrix and reduce electrical treeing and increase the electrical break down strength. These theoretical studies give the confidence to operate such materials as cables in high voltage 500 kV.

The reaction channels represented in Scheme 1 are more exothermic than other antioxidant and voltage stabilizers. The reaction channel with Vp is more thermodynamically favorable with temperature up to 180 °C. From this analysis, they conclude the best photoinitiator-benzophenone, and antioxidant Bp to design for a perfect voltage stabilizer.

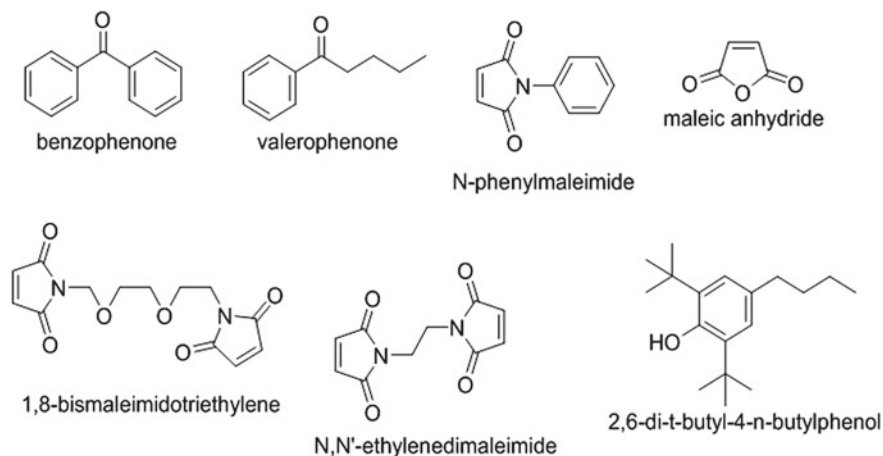
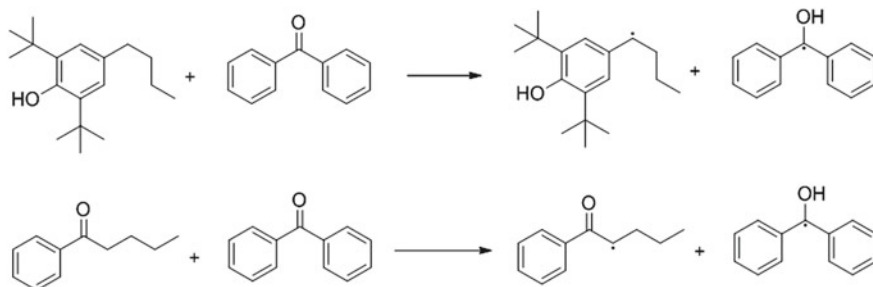


Fig. 3 Molecules used for effective UV radiation crosslinking process of PE



Scheme 1 Suggested mechanism T_1 transition state formation of 2,6-di-t-butyl-4-n-butylphenol(antioxidant) and valerophenone (voltage stabilizer)

Similarly, Zhang et al. [35] investigated maleic anhydride (MAH) is added along with benzophenone and investigated the theoretical reaction channels as above mentioned using B3LYP/6-311 + G(d,p) in Gaussian 09 package. Here also the antioxidant and voltage stabilizers are same and mechanism only has a minor difference. The potential barrier of MAH with PE is 0.10 eV lesser than that of benzophenone with PE (0.20 eV), hence MAH of grafting onto PE forms space lattice and inhibit space charge accumulation effectively. Therefore, the electrical breakdown strength will improve more compared with the reaction without MAH.

Zhang et al. [36] conducted the theoretical investigation with graft maleimide to PE in the UV radiation crosslinking reaction using Gaussian 09 software package with B3LYP/6-311 + G(d,p) level of theory. They conducted lots of derivatives of maleimide and obtained N,N'-ethylenedimaleimide as a better candidate. Another advantage is that N,N'-ethylenedimaleimide itself act as the crosslinking agent and also provide a charge trap. Hence, the system has a high degree of simplicity and

less byproduct. Besides, by analyzing the potential barrier of forming PE radical by maleimide is higher than MAH. The experimental results are conducted by Sun et al. [37] confirms that the MAH-grafted XLPE has better candidate for the development of HVDC cable materials, their results are well tune with the quantum chemical calculations by different groups. Hence, they concluded that suggest a prospective strategy for UV initiation for modification of XLPE grafted with polar molecule for obtaining an HVDC cables.

Wang et al. [38] conducted a theoretical investigation in grafting reaction of maleimide and its derivatives to polyethylene in the UV radiation crosslinking using B3LYP/6-311 + G(d,p) level of theory in Gaussian 09 software package. They predict that during the investigation the maleimide and its derivatives are grafted to PE. They also stated that the reaction barrier of N-phenylmaleimide grafted to PE is higher than that of 1,8-bismaleimidotriethylene glycol grafted to PE. Also, 1,8-bismaleimidotriethylene glycol can act as the crosslinking agent and also when it grafted to PE can be used as a space charge inhibitor. The dual function makes 1,8-bismaleimidoethylene glycol makes good information for the development of UV radiation crosslinking of PE high voltage cables.

Zhao et al. [39] theoretical investigation on the reaction of triallyl isocyanurate (TAIC) in the UV radiation crosslinking process of PE in Gaussian 09 with B3LYP/6-311 + G(d,p) level. Here, from the analysis of the reaction mechanism of the crosslinking is initiated by benzophenone and TAIC is very important for the crosslinking process. All the theoretical analysis of UV radiation crosslinking process gives reliable information about the optimization and measurements taken for such reactions.

There are limited computational studies are done in pristine XLPE out of which most of the research group adopted the DFT-based analysis with various hybrid theories especially B3LYP with variety of basis sets. The UV radiation analysis through computational studies show the way for new molecules incorporation in the radiation reactions and also new voltage stabilizer to improve the strength and efficacy of XLPE. Due to limited number of researches in computational simulations in XLPE, the combination of computational data with experiment is not reported. But it is sure that taking benefit of computational analysis can improve the experimental studies in XLPE. There are lot of such researches, i.e., computational analysis with experimental proof or vice versa, in various scientific fields hence, expecting this will also crop up in XLPE researches too.

9 Conclusion

To put on a revelation of future we need to consider the long history of XLPE. Here we discussed the path of XLPE emerges as a promising material for various applications especially as an insulator, hip arthroplasty, etc. This travelogue of XLPE history gives us an idea about the urgency and efficiency of XLPE materials. The theoretical investigation in XLPE involves mainly in the illustration of a mechanism

for the crosslinking process of PE to XLPE using UV radiation and also suggests the efficient oxidizer and voltage stabilizer to gain better electrical breakdown strength by reducing the electrical treeing. Another important investigation using theory is based on the mechanism of the inhibition of electrical treeing in XLPE. By these theoretical investigations, we can plan the steps taken for reducing the electric treeing and increase the electrical breakdown strength. Theoretical studies on XLPE are limited, but the approach to combine computational and experimental methods would significantly promote the innovations and improvement in XLPE research and its applications.

References

- Orton H (2013) History of underground power cables. *IEEE Electr Insul Mag* 29:52–57. <https://doi.org/10.1109/MEI.2013.6545260>
- Zuidema C, Kegerise W, Fleming R et al (2011) A short history of rubber cables. *IEEE Electr Insul Mag* 27:45–50. <https://doi.org/10.1109/MEI.2011.5954068>
- Precopio F, Gilbert A (1999) The invention of chemically crosslinked polyethylene. *IEEE Electr Insul Mag* 15:23–25. <https://doi.org/10.1109/57.744587>
- Mathes KN (1991) A brief history of development in electrical insulation. *Proc Electr Insul Conf* 147–150. <https://doi.org/10.1109/eEIC.1991.162590>
- Thomas J, Joseph B, Jose JP et al (2019) recent advances in cross-linked polyethylene-based nanocomposites for high voltage engineering applications: a critical review. *Ind Eng. Chem Res* 58:20863–20879
- Gedde UW, Ifwarson M (1990) Molecular structure and morphology of crosslinked polyethylene in an aged hot-water pipe. *Polym Eng Sci* 30:202–210. <https://doi.org/10.1002/pen.760300403>
- Callary SA, Solomon LB, Holubowycz OT et al (2015) Wear of highly crosslinked polyethylene acetabular components: a review of RSA studies. *Acta Orthop* 86:159–168. <https://doi.org/10.3109/17453674.2014.972890>
- Triclot P, Triclot P (2011) Metal-on-metal: history, state of the art (2010). *Int Orthop* 35:201–206. <https://doi.org/10.1007/s00264-010-1180-8>
- Boutin P (2014) Total arthroplasty of the hip by fritted alumina prosthesis. Experimental study and 1st clinical applications. *Orthop Traumatol Surg Res* 100:15–21
- Hu CY, Yoon TR (2018) Recent updates for biomaterials used in total hip arthroplasty. *Biomater. Res.* 22:1–12
- Head WC, Bauk DJ, Emerson RH (1995) Titanium as the material of choice for cementless femoral components in total hip arthroplasty. *Clinical orthopaedics and related research*. Springer, New York LLC, pp 85–90
- Charnley J (1961) Arthroplasty of the hip. a New Operation. *Lancet* 277:1129–1132. [https://doi.org/10.1016/S0140-6736\(61\)92063-3](https://doi.org/10.1016/S0140-6736(61)92063-3)
- Medel FJ, Kurtz SM, Hozack WJ et al (2009) Gamma inert sterilization: a solution to polyethylene oxidation? *J Bone Jt Surg Ser A* 91:839–849. <https://doi.org/10.2106/JBJS.H.00538>
- Manning DW, Chiang PP, Martell JM et al (2005) In vivo comparative wear study of traditional and highly cross-linked polyethylene in total hip arthroplasty. *J Arthroplasty* 20:880–886. <https://doi.org/10.1016/j.arth.2005.03.033>
- Martell JM, Verner JJ, Incavo SJ (2003) Clinical performance of a highly cross-linked polyethylene at two years in total hip arthroplasty: a randomized prospective trial. In: *Journal of Arthroplasty*. Churchill Livingstone Inc., pp 55–59

16. Collier JP, Currier BH, Kennedy FE et al (2003) Comparison of cross-linked polyethylene materials for orthopaedic applications. *Clin Orthop Relat Res* 414:289–304. <https://doi.org/10.1097/01.blo.0000073343.50837.03>
17. Muratoglu OK, Bragdon CR, O'Connor DO et al (1999) Unified wear model for highly crosslinked ultra-high molecular weight polyethylenes (UHMWPE). *Biomaterials* 20:1463–1470. [https://doi.org/10.1016/S0142-9612\(99\)00039-3](https://doi.org/10.1016/S0142-9612(99)00039-3)
18. Kurtz SM, Muratoglu OK, Evans M, Edidin AA (1999) Advances in the processing, sterilization, and crosslinking of ultra-high molecular weight polyethylene for total joint arthroplasty. *Biomaterials* 20:1659–1688. [https://doi.org/10.1016/S0142-9612\(99\)00053-8](https://doi.org/10.1016/S0142-9612(99)00053-8)
19. Chiesa R, Tanzi MC, Alfonsi S et al (2000) Enhanced wear performance of highly crosslinked UHMWPE for artificial joints. *J Biomed Mater Res* 50:381–387. [https://doi.org/10.1002/\(SICI\)1097-4636\(20000605\)50:3%3c381::AID-JBM12%3e3.0.CO;2-P](https://doi.org/10.1002/(SICI)1097-4636(20000605)50:3%3c381::AID-JBM12%3e3.0.CO;2-P)
20. Oral E, Muratoglu OK (2011) Vitamin E diffused, highly crosslinked UHMWPE: a review. *Int Orthop* 35:215–223
21. Dumbleton JH, D'Antonio JA, Manley MT et al (2006) The basis for a second-generation highly cross-linked UHMWPE. *Clin Orthop Relat Res* 453:265–271. <https://doi.org/10.1097/01.blo.0000238856.61862.7d>
22. Bracco P, Oral E (2011) Vitamin E-stabilized UHMWPE for total joint implants: a review. *Clinical orthopaedics and related research*. Springer, New York LLC, pp 2286–2293
23. Oral E, Christensen SD, Malhi AS et al (2006) Wear resistance and mechanical properties of highly cross-linked, ultrahigh-molecular weight polyethylene doped with Vitamin E. *J Arthroplasty* 21:580–591. <https://doi.org/10.1016/j.arth.2005.07.009>
24. Kyomoto M, Moro T, Konno T et al (2007) Enhanced wear resistance of modified cross-linked polyethylene by grafting with poly(2-methacryloyloxyethyl phosphorylcholine). *J Biomed Mater Res Part A* 82A:10–17. <https://doi.org/10.1002/jbm.a.31134>
25. Kyomoto M, Moro T, Iwasaki Y et al (2009) Superlubricious surface mimicking articular cartilage by grafting poly(2-methacryloyloxyethyl phosphorylcholine) on orthopaedic metal bearings. *J Biomed Mater Res Part A* 91A:730–741. <https://doi.org/10.1002/jbm.a.32280>
26. Lowe JP, Peterson KA (2006) *Quantum chemistry*. Elsevier Academic Press
27. Jensen F (2002) *Introduction to computational chemistry*, 3rd edn, Wiley, West Sussex, England
28. Bachrach SM (2006) *Computational organic chemistry*. Wiley, Hoboken, NJ, USA
29. Lewars EG, Lewars EG (2011) *An outline of what computational chemistry Is All About. Computational Chemistry*. Springer, Netherlands, pp 1–7
30. Zhang H, Shang Y, Zhao H, Han B (2013) Mechanisms on inhibition of polyethylene electrical tree aging : a theoretical study. 3035–3044. <https://doi.org/10.1007/s00894-013-1814-z>
31. Yamano Y, Iizuka M (2009) Suppression of electrical tree initiation in LDPE by additives of polycyclic compound. *IEEE Trans Dielectr Electr Insul* 16(1):189–198. <https://doi.org/10.1109/TDEI.2009.4784567>
32. Zhang H, Shang Y, Zhao H, Han B (2013) Mechanisms on electrical breakdown strength increment of polyethylene by acetophenone and its analogues addition: a theoretical study. 1:4477–4485. <https://doi.org/10.1007/s00894-013-1946-1>
33. Zhang H, Zhao H, Wang X, Shang Y (2014). Theoretical study on the mechanisms of polyethylene electrical breakdown strength increment by the addition of voltage stabilizers. <https://doi.org/10.1007/s00894-014-2211-y>
34. Zhang H, Shang Y, Zhao H et al (2017) Theoretical study on the reaction of maleic anhydride in the UV radiation cross-linking process of polyethylene. *Polymer (Guildf)* 133:232–239. <https://doi.org/10.1016/j.polymer.2017.11.045>
35. Zhang H, Shang Y, Zhao H et al (2017) Theoretical study on the reaction of maleic anhydride in the UV radiation cross-linking process of polyethylene. *Polymer (Guildf)*. <https://doi.org/10.1016/j.polymer.2017.11.045>
36. Zhang H, Shang Y, Zhao H et al (2018) Theoretical study on the grafting reaction of maleimide to polyethylene in the UV radiation cross-linking process. *Polymers (Basel)* 10:1033–1039. <https://doi.org/10.3390/POLYM10091044>

37. Zhao X-D, Zhao H, Sun W-F (2020) Significantly improved electrical properties of crosslinked polyethylene modified by UV-initiated grafting MAH. *mdpi.com* 12: <https://doi.org/10.3390/polym12010062>
38. Wang Y, Zhang H, Zhao H, et al (2018) Theoretical study on the grafting reaction of maleimide and its derivatives to polyethylene in the UV radiation cross-linking process
39. Zhao H, Chen J, Zhang H (2017) Theoretical study on the reaction of triallyl isocyanurate in the UV radiation cross-linking of. *RSC Adv* 7:37095–37104. <https://doi.org/10.1039/C7RA05535H>

Chapter 3

XLPE Manufacturing Processes



Saurav S. Sengupta

1 Introduction

Polyethylene (PE), which comprises low-density (LDPE), high-density (HDPE), and linear low-density (LLDPE) grades, represents the single largest category of the world's major thermoplastics, representing 37% of the 282 million metric ton global thermoplastic market in 2019. PE remains a relatively low-cost and versatile polymer used in a wide range of molded and extruded applications, including household and food containers, toys, food and nonfood packaging film and sheet, retail bags, trash bags, geomembranes, pipe, house wrap, pails, totes, crates, caps, closures, and bottles. Like other polymers, PE also typically competes against other traditional materials such as aluminum, steel, wood, cardboard, and glass. PE continues to be used in applications where it can deliver a cost advantage or performance enhancement. Despite growing environmental pressures associated with retail bags and plastic packaging, and the desire for more sustainable solutions, conventional PE polymers continue to have opportunities to replace traditional materials in numerous applications.

For a variety of purposes, the usefulness of polyolefins can be extended by crosslinking. Crosslinking is generally understood to be a process for covalently bonding polymer chains together leading to a three-dimensional network. Crosslinking of polyethylene has been shown to lead to improvements in chemical resistance, high temperature strength, toughness, resistance to stress cracking, weathering properties at a reasonable cost.

The first crosslinked polyethylene was reported by Charlesby in 1952 utilizing radiation process [1]. It was reported that the polyethylene was converted to a material with higher melting point, greater form stability and viscosity, lower solubility in solvents. This invention coupled with advances in radiation technologies leads to first

S. S. Sengupta (✉)
The Dow Chemical Company, Collegeville, PA, USA
e-mail: SSSengupta@dow.com

commercial crosslinked products being made in the mid-1950s. Initially, crosslinked polyethylene found its way into cables and films as the applications of choice [2].

The evolution of vulcanization chemistry using peroxides led to this technology being developed for polyethylenes [3]. The first work for peroxide crosslinked polyethylene was reported in 1948 by Du Pont whereby a dispersion-based process was explored [4]. 15 years later, General Electric Co. patented the peroxide cure through a melt process [5]. This expanded the application space of crosslinked polyethylene and filled and unfilled compositions began to be produced widely.

While crosslinkable polyolefins are superior to standard thermoplastic products in many properties this is achieved at some sacrifice in fabricability. The forming temperature of the crosslinked product must be kept well below the crosslinking temperature and these led issues related to the useful processing window for these materials. This coupled with the high investment cost of the above-mentioned process provided motivation for further improvements in the field. A breakthrough happened when in 1968 Midland Silicones (Dow Inc) patented a two-step crosslinking process based on covalently bonding alkoxy silane molecules to polyethylene in the first step followed by the silane coupling reaction in the second [6]. This is what is currently referred to as a SIOPLAS process. Shortly thereafter, a single-step process based on new screw design BICC was commercialized [6, 7]. This came to popularly be referred to as the MONOSIL process. Later in the 1980s, Union Carbide (Dow Inc) and Mitsubishi Petrochemical developed and commercialized the manufacture of ethylene and silane copolymers in high-pressure reactors [8].

This chapter covers the different aspects of the above-mentioned crosslinking processes. Chemistry considerations and related unit operations are discussed for the three crosslinking methods. A pragmatic comparison of all the crosslinking processes is also discussed.

2 Radiation Crosslinking

2.1 Reaction Chemistry

The chemistry of crosslinking involves the combination of two separate long chain polymer molecules to form a single molecule of increased molecular weight. The radiation chemistry begins with the energy absorption steps. In the case of the electron beam radiation, this is due to the interaction of the high energy electrons with the atoms and molecules of the polymer. In other forms of radiation, exposure leads to high energy electrons in the polymer molecules. The interaction of these high energy electrons with the polymer molecules results in a reduction of the energy, coupled with an elevation of the energy of the molecule to either a super-excited state (energy greater than ionization potential) or an excited state plus ion pairs. The excited state molecule can decompose into free radical species [9].

Ionization is accompanied by super-excitation, which reduces the ion yield due to other energy dissipative mechanisms. Low energy electrons are lost via attachment to positive ions, or via thermal electron capture by groups with low-lying anti-bonding orbitals, such as aromatics or carbonyl groups. In the case of high energy electrons, considerable scattering and even reflection occur during radiation. This further reduces penetration and energy transfer into the interior of the sample.

The effects of PE structure on the energy absorption process are not as broadly discussed in the literature. However, an examination of the fundamentals would suggest that since electron density (on unit volume basis) is important one would expect that the density variation between crystalline and amorphous regions will affect the rate of energy transfer. Variation in density, lamellae thickness and spherulite size resulting from specific quenching procedures used in thick parts could be expected to produce an inherent energy absorption gradient. All these variations are, of course, influenced by the architecture of the polymer molecules themselves.

Subsequent to energy absorption, a large number of reactions can occur [10]. Some of the possible reactions are listed in Table 1. These reactions result in generation of alkyl radicals, hydrogen gas evolution, trans-vinylene formation, crosslinking and potentially scission depending on the architecture of the molecules. In addition, decay of vinyl and vinylidene groups is observed.

Before considering the role of functionalities in radiation crosslinking, the role of crystallinity in the steps subsequent to energy absorption should be discussed. Polyethylene is semicrystalline at room temperature consisting of crystalline lamellae, interfacial and amorphous regions. The specific morphology is dependent on the thermal history of a particular sample. In addition to the lamellae, further structural order in the form of spherulites can occur upon slow cooling.

Table 1 Steps in radiation assisted crosslinking

Reaction	Event
$\text{PH} \rightarrow \text{PH}^*$	Excitation
$\text{PH}^* \rightarrow \text{P}^+ + \text{e}^- \rightarrow \text{P} \cdot + \text{H}$	Ionization
$2 \text{H} \cdot \rightarrow \text{H}_2$	Hydrogen gas evolution
$2 \text{P} \cdot \rightarrow \text{P-P}$	Crosslinking
$\text{P}^+ + \text{P} \cdot \rightarrow \text{P-P}$	Crosslinking
$\text{P}^+ + \text{PH} \rightarrow \text{P} \cdot + \text{P}^+$	
$\text{P} \cdot + \text{O}_2 \rightarrow \text{POO}$	Oxidation
$2 \text{PH} \cdot \rightarrow \text{P} + \text{P-CH=CHP}$	Disproportionation
$2 \text{PH} \cdot \rightarrow \text{P} \cdot + \text{P-CH=CH}_2$	Scission
$\text{P}_1\text{-CH-CH}_2\text{-P}_2 \rightarrow \text{P}_1\text{-CH}_2\text{-CH-P}_2$	Intramolecular hydrogen abstraction
$\text{P}_1 + \text{P}_2\text{H} \rightarrow \text{P}_2 + \text{P}_1\text{H}$	Intermolecular hydrogen abstraction

Table 2 Thermal properties of polyethylenes

Grades	T _g (°C)	T _m (°C)
LDPE	-118.1	110
LLDPE	-120	125
HDPE	-100	134

Motion in the amorphous region occurs above the glass transition temperature of the polymer. Above the melting temperature, the polymer is completely amorphous. Table 2 lists the typical glass transition (T_g) and melting temperatures (T_m) of different grades of polyethylene.

Chain ends, functionalities, methyl groups, side chains and branches are believed to be restricted to the amorphous region. Additives which may be present tend to agglomerate in the amorphous region as well. These characteristics have a profound effect on the radiation chemistry of polyethylene [10]. Besides the effect on the energy absorption process noted earlier crystallinity affects the subsequent reaction steps. At very low temperatures, radical pairs (R. and H.) are formed. These pairs are trapped by the immobility of the polymer matrix at low temperatures. Radical formation is slightly lower in the crystalline region due to cage recombination of the radical pairs. Radicals which do escape from the cage are much more mobile in the amorphous phase than in the crystalline phase. Practically all the alkyl radical decay occurs in the non-crystalline phases. It has been shown that at normal doses of radiation, crosslinking is restricted to the non-crystalline region. Crosslinking within the crystal structure requires energy prohibitive lattice distortions.

The structural changes occurring during irradiation of polyethylene are mostly summarized by Ungar [10]. Hydrogen gas evolution accompanies formation of trans-vinylene groups. Extent of chain scission and significance particularly for polyethylenes is an evolving topic and conclusions are dependent on characterization methods employed. The most important reaction from a commercial standpoint is the crosslinking reaction. This occurs non-randomly and concentration is highest in the amorphous regions. There may be tendency for some intramolecular crosslinking if radicals are trapped at the chain folds. Crosslinking efficiency is improved by radiation under pressure. This may be attributed to improved interlamellar contact, resulting in less intramolecular crosslinking.

In the presence of air, oxidation occurs during radiation. This is limited to the rate of diffusion of oxygen into the sample and is therefore limited to the amorphous regions. This can be eliminated by irradiating under vacuum or inert atmosphere.

It is also worthwhile to mention the role of vinyl and vinylidene groups during the crosslinking process. Based on the decay of vinyl and vinylidene groups at high temperatures, in 1958 Dole et al. [11] postulated a mechanism involving direct excitation of olefin groups by radiation, followed by crosslinking. This mechanism was later contradicted by Crook and Lyons who postulated direct addition of the alkyl radicals to the double bonds [12]. In the 1970s, further development of the model proposed by Lyons took place via the application of sol-gel theory and improved characterization techniques such as GPC [13]. In the 1980s, the first direct evidence

for the reaction of vinyls was obtained by the application of C13 NMR [14]. Toward the late 1980s, further evidence was obtained pointing toward the involvement of vinylidenes in the crosslinking process [15].

Summarizing the chemistry of radiation crosslinking, it is clear that the various effects are complex and inter-related. Molecular weight and molecular weight distribution affect the sol–gel partitioning or rate of formation of crosslinked network. Fractionation during crystallization can alter the effective molecular weight distribution. Branching affects the crystallization behavior and thus in part determines all the effects of crystallization discussed previously. Unsaturation in the form of vinyl and vinylidene is implicated in crosslinking and radical reactions.

2.2 Process

The basic steps in the radiation crosslinking involve fabrication of article using polyethylene followed by exposure of this fabricated material to radiation and finishing stages. A variety of equipment and instruments are used depending on the application. Following the manufacturing step, quality control measurements are performed to ensure consistency of desired material properties.

The processes and equipment used during the fabrication step of articles depend on nature and complexity of the article produced. For articles such as pipes or cables, an extrusion coating process is used, while for articles like films film extrusion processes are employed. Raw materials are usually received in bulk shipments in railcars or boxes and conveyed to these unit operations (Fig. 1).

The radiations for modifying polymers can cover a wide range of particulate and non-particulate radiations. The first observed form of crosslinking in polyethylene were obtained with a 60 eV electron beam used in electron diffraction. In irradiation work, energies are usually expressed in eV or electron volts. One eV per molecule being equal to 23 kcal/ mole. From the standpoint of practical application, it is possible to limit the usable radiation to those listed in Table 3. As an example, the bond energy between atoms of organic molecules usually lies in the range 30–200 kcal/mol which translate to 1.5–8.5 eV per bond.

High energy radiation like X-rays, γ -rays and electron beams are capable of penetrating specimens and creating excited and ionized atoms and molecules. This

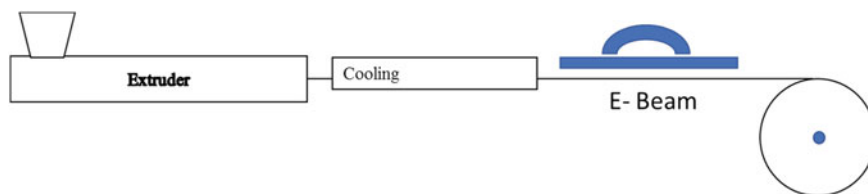


Fig. 1 Simplified manufacturing process from E-beam crosslinked wires

Table 3 Radiant energy of interest to processing

Radiation	Type	Approximate energy per particle
Infrared	Electromagnetic	0.01–1.6 eV
Visible light	Electromagnetic	1.6–3.3 eV
Ultraviolet	Electromagnetic	3.3–6.32 eV
Vacuum ultraviolet	Electromagnetic	6.2–310 eV
X-rays	Electromagnetic	0.0003- 1.5 meV
γ -rays	Electromagnetic	0.008- 9 meV
α -rays	Particulate	1–10 meV
β -rays	Particulate	0.02–13
Accelerated electrons	Particulate	0.25–15
Neutrons	Particulate	

in turn leads to formation of free radicals which participate in crosslinking. The implementation of any radiation-initiated process requires a convenient, efficient and economic source of radiation energy. While in principle a broad series of alternatives exist, the actual available practical sources are much more limited. In the area of ionizing radiation practical choices lies between an electron beam or gamma rays.

Cobalt-60 is presently the major radioisotope source for radiation processing via gamma rays. It is produced in nuclear reactors by addition of a neutron to naturally occurring cobalt-59. The physical form of the target cobalt is usually small pellets, wafers or wires. After irradiation these various forms are encapsulated to prevent accidental leakage. The major advantage of the cobalt-60 as an isotope source is its ready availability, reasonable cost and the ability to assemble easily into a variety of geometric shapes. As the atoms of the radioisotope disintegrate, and thus give off ionizing particles, the total number of them in a fixed source must necessarily decrease with time. The output of energy of the source thus diminishes and is called radioactive decay. Mathematically, the decay is first-order process, meaning that the rate of decay is directly proportional to the concentration or amount of radioactive material present in the source.

Thus,

$$\frac{-dC}{dt} = \lambda C$$

where λ is the decay constant, C is a measure of the amount of radioactivity for a given source and t is a measurement of time. Integration of this expression with respect to time is useful in determining the strength of a source after a given period of decay:

$$\log \frac{C_0}{C_t} = \frac{\lambda t}{2.303}$$

where C_0 is the initial source strength and C_t is the strength after the passage of time, t .

One of the characteristics of a first-order process is that a certain time is required for the decay of exactly one half of the material in any given system. This is referred to as the half-life. The decay constant can easily be calculated in terms of its half-life using the following expression:

$$\lambda = \frac{0.693}{t^{\frac{1}{2}}}$$

In the case of the sources of gamma radiation from isotopes, there are two major maintenance factors. One of these is the periodic replacement or augmentation of the radiation source to make up for decrease in energy brought about by the radioactive decay. The other relates to tasks directed at ensuring that there is no loose radioactive matter. Other associated tasks related to safety involve maintenance of the shielding environments.

There are a number of available types of electron accelerators all of which have the common elements of a high voltage field established by different techniques an evacuated accelerator tube and a source of electrons. One simple differentiation among the various machines is on the basis of electron energy. Low voltage machines in the range of 0.25–0.5 meV are excellent for surface treatment while a higher range of machines from 0.75 to 10 meV are useful where various degrees of penetration are required. The principal variables are beam current, beam energy, uniformity of energy, continuous or pulsed. Among these variables, the most important is the beam energy since it governs the depth of penetration in the target material. Several techniques such as irradiation for multiple sides are employed to facilitate penetration in thick articles [16].

This key step of the process consists of the following basic stages: a power supply, an electron source, an acceleration section, a vacuum across the accelerator, a beam sweep system if required, an opening through which accelerated electrons can pass to impinge and penetrate the product, air or inert atmosphere of the curing zone, and the shielding necessary to contain particles generated by the electrons.

The final step of the radiation process includes recovery of the crosslinked article in its useable form. Immediately after crosslinking, the article may be heated and expanded before it is cooled into its final shape. These articles are then collected and packaged for commercial distribution. A few samples are checked for several key properties to ensure consistency of quality.

Finally, the radiation crosslinking process offers a few advantages over the other alternatives. These are briefly enumerated as follows:

1. Since the free radicals necessary in crosslinking are formed in a manner that is relatively insensitive to temperature, this process is applicable industrially at ambient as well as elevated temperatures.
2. This also facilitates the use of heat-sensitive additives such as metal hydrates.

3. An attractive feature of this process is the fact that it is a relatively clean process requiring no additives, initiators thus leading to no harmful by-products.
4. The modular nature of this process offers advantages from the standpoint of improved quality control and also reduced scrap production.
5. Compared to conventional thermal processes which are limited by heat diffusion, radiation process offers a faster rate of crosslinking thus offering higher throughput.

There are also a few opposing points of view which needs to be mentioned when considering this process.

1. The relatively high capital cost associated with setting up a commercial manufacturing facility is a barrier for a lot of industries at all scales.
2. Extreme precautions need to be taken to protect operators from radiation.
3. The social aspects of setting up a large-scale facility utilizing radiation cannot be ignored due to the negative psychology associated.

When polymers are exposed to energetic radiation, they generally undergo a variety of crosslinking and chain scission reactions, which increase and decrease, respectively, the molecular weight of the affected chains. If crosslinking predominates over scission, such irradiation ultimately causes the formation of insoluble gel, a main goal of this investigation. Charlesby and Pinner [17] obtained a simple expression relating the sol fraction s to the irradiation dose D for a polymer.

$$s + \sqrt{s} = \frac{p_0}{q_0} + \frac{2}{q_0MD}$$

and

$$s = 1 - \text{gel fraction}$$

Where p_0 is average number of chain scission per monomer and q_0 is average number of crosslinks per monomer and M is the initial weight average molecular weight for polymers having a Flory molecular weight distribution. This approach is widely used analysis of the kinetics of irradiation crosslinking in the melt and solid state. Sol-gel data after polymer irradiation can then be analyzed by plotting $s + s^{1/2}$ versus $1/D$, which should produce a straight line, whose intercept gives the ratio p_0/q_0 , while the slope is $1/q_0M$. Since values for the sol fraction are restricted to the range from 0 to 1, the expression above is similarly bounded by 0 and 2. At the limiting case of $s + s^{1/2} = 2$, where insoluble gel (polymer network) just begins and gel formation can only occur if $p_0 > 2q_0$.

The process of gelation can be divided into three regions: (a) induction period during which the seed of the gel is formed, (b) gel growth where rapid gel evolution occurs and (c) plateau stage where a decrease in gelation rate is observed. This is quite often represented by the 'S-curve' for crosslinking. While the ratio p_0/q_0 dictates the crosslinking kinetics, dependence of the gel content with radiation dose is often used for process optimization purposes (Fig. 2).

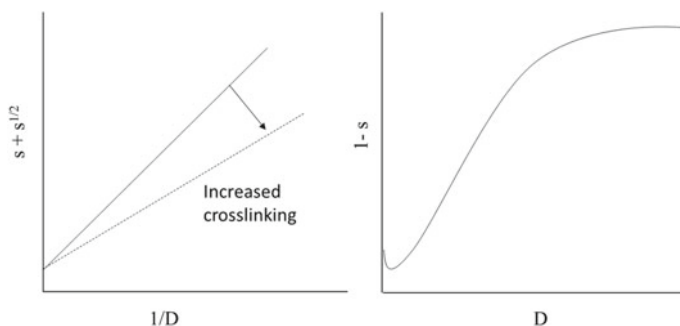


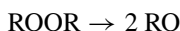
Fig. 2 Kinetics of radiation crosslinking

3 Peroxide Crosslinking

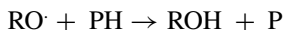
3.1 Reaction Chemistry

Thermal activation of peroxide is commonly used as a radical precursor for crosslinking of olefinic polymers like polyethylene. Similar to the vulcanization of rubber, crosslinking of polyethylene is accomplished by reacting polyethylene with an organic peroxide. Hercules, Cabot and General Electric each claim the early patent rights in this area. The first materials made by the Cabot process were carbon black filled compounds. Early patents from Du Pont Chemical Company (Dow Inc.) also cover the use of benzoyl peroxide as the crosslinking agent for polyethylene.

The first step is the initiation of the radical formation process which is achieved through the thermolytic decomposition of the peroxide. The O–O bond of peroxides (~150 kJ/mol) is preferentially cleaved as opposed to the much stronger carbon–hydrogen (~415 kJ/mol) or carbon–carbon (~350 kJ/mol).



The alkoxy radicals (RO·) formed abstracts hydrogen from the polyethylene substrate leading to the formation of the polymer bound radicals. These polymeric radicals are slightly electrophilic by nature and are principally secondary carbon-centered $-\text{CH}_2\cdot$ radicals.



This step is exothermic with activation energy being close to 25 kJ/mol and thus the hydrogen abstraction process occurs readily at elevated temperatures.

There are competing side-reactions of the alkoxy radicals that decrease the efficiency of the initiation reaction. Important among these is the β -scission of the alkoxy radicals themselves to yield a much lower energy hydrocarbon radical and a

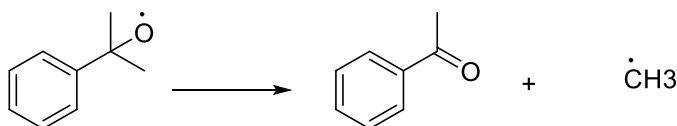


Fig. 3 Alkoxy radical fragmentation

carbonyl-containing species. The propensity of the side reactions to happen depends on the structure of the radical itself. At low temperatures, this event is reported to be slow. However, at high temperatures more than a quarter of the alkoxy radicals are not available for hydrogen abstraction reactions and are lost to this side reaction. This step does have a higher activation energy (~ 40 kJ/mol) than the hydrogen abstraction step and hence higher the temperature higher proportion of the alkoxy radicals are lost to this event (Fig. 3).

Branch points in olefinic polymers are common. These present unique structural (entanglement points) as well as functional features (tertiary $-\text{CH}-$ sites). The carbon-hydrogen bond dissociation energy for these sites is low (~ 400 kJ/mol) and tertiary radical formed as a result of hydrogen abstraction from these sites are quite stable. They quite often undergo β -scission reactions resulting in reduction of molecular weight. The degradation rate is controlled by peroxide decomposition kinetics and has a first-order dependence on the concentration of radicals (Fig. 4).

Termination reactions of radicals can happen by two ways, namely combination and disproportionation. During combination, radicals in close proximity terminate by coupling to each other leading to a large increase in molecular weight and form a point of covalent crosslink (Fig. 5).

During disproportionation, radicals containing a β -hydrogen undergo a hydrogen atom exchange leading to non-reactive species and no increase in molecular weight (Fig. 6).

Termination occurs at the diffusion limit of radical-radical encounters. Being bimolecular in nature, these processes are more sensitive to radical concentrations

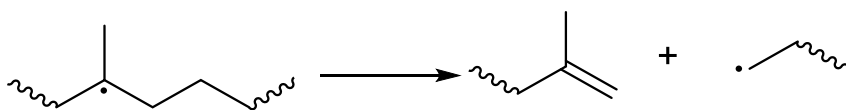


Fig. 4 β -scission of polymers

Fig. 5 Combination of polymer radicals

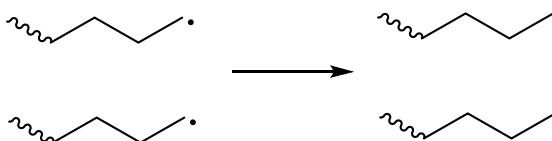
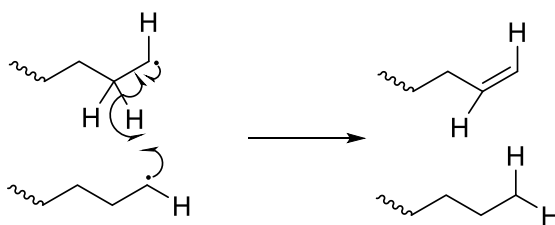


Fig. 6 Disproportionation of polymer radical



than previously discussed reactions, whose rates depend on radical concentration to the first order. An important factor is relative frequency of the two modes of termination-combination and disproportionation. Only radical-radical combination has a direct effect on molecular weight, acting to increase the melt viscosity of a polymer. The ratio of the rate constants for disproportionation to combination varies with alkyl radical structure, with primary radicals preferring combination, secondary radicals exhibiting a more balanced ratio, and tertiary radicals terminating mostly through disproportionation.

3.2 Process

The crosslinking process, developed over time is optimized to maximize desired reaction yields, minimize side reactions and provide a consistent end product. All comments made previously regarding process discussed in the previous section on radiation applies for peroxides as well.

Various factors are taken into consideration during selection of the organic peroxide. These include but are not limited to:

1. Appropriate half-life time, $t_{1/2}$,
2. Initiator efficiency,
3. Reactivity or selectivity,
4. Ease of handling,
5. Low toxicity,
6. Fit with process window.

The half-life time, $t_{1/2}$ is the measure of the activity of commercial organic peroxide initiators at a given condition. Under ideal conditions, the rate of homolytic cleavage follows first-order kinetics and half-life can be calculated from the kinetic data:

$$I \rightarrow 2RO$$

$$\frac{d[I]}{dt} = -k_d[I]$$

$$t_{1/2} = \frac{0.693}{k_d}$$

where I is the peroxide initiator, $RO\cdot$ is the alkoxy radicals, t is time and $k_d(s^{-1})$ is the peroxide decomposition rate constant.

The activity of commercial organic peroxide initiators at any given temperature is related by three factors:

1. The relative stability of the radicals formed,
2. Steric effects,
3. Electronic/polar effects.

These factors are manifested in the pre-exponential factor (A) and activation energies (ΔE) for the first-order reaction at a given temperature T :

$$k_d = A \exp\left(\frac{\Delta E}{RT}\right)$$

$$t_{1/2} = \frac{0.693}{A} \exp\left(\frac{\Delta E}{RT}\right)$$

If we consider ideal reactions and terminations, it stands to reason that steady-state approximations will apply and rate of formation of polymer radicals ($P\cdot$) will equal to the rate of consumption of radicals. This gives:

$$\frac{dP\cdot}{dt} = 2k_1[I] - 2k_{tc}[P\cdot]^2$$

where k_1 is a combined rate constant for the rate of polymer radical formation and k_{tc} is a rate constant for termination.

At steady state

$$\frac{dP\cdot}{dt} = 0$$

$$[P\cdot] = \left(\frac{k_1[I]}{k_{tc}}\right)^{1/2}$$

This provides a very simplistic kinetic framework to analyze and understand the crosslinking process.

The role of small amounts of unsaturation which are present in polyethylenes (LDPE) acts as points of reaction. Given the varying kinds of unsaturation present in polyethylene a number of reactions can follow. In an oversimplified framework we can hypothesize that the sterically unhindered unsaturation sites serve as points of polymer radical attack leading to a crosslink (Fig. 7).

This reaction yields a crosslink and also gives rise to another polymer radical. This lends 'chain character' to the crosslinking process and the above step can be visualized as a 'propagation' reaction leading to desired crosslinks. The ratio of the rate constant for propagation to that of termination is referred to as the kinetic chain length of the process. This reflective of the number of crosslinks formed per radical

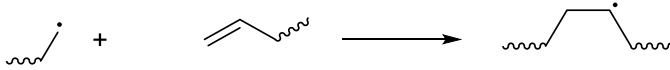


Fig. 7 Vinyl group consumption during crosslinking

before it terminates. As is evident from the reaction, the propagation rate is first order in radical concentration, while the termination events are second order. Hence kinetic chain length is proportional to the inverse of radical concentration.

The peroxide crosslinking process is a first-order reaction that is initiated with the thermally driven homolytic cleavage of the peroxide bond. The rate-determining step is the peroxide cleavage. The crosslinking reaction results from the combination of two radical bearing polymer chains resulting in increased molecular weights. This is typically studied by monitoring the increase in torque over time when a composition is held in a heated cone-and-plate geometry under an applied oscillatory strain (Fig. 8). Although, the crosslinking reaction is intended to occur during the cure process rather than during fabrication, some crosslinking, otherwise known as scorch, will happen inevitably via thermal initiation of the peroxide bond cleavage in the molten polymer (Fig. 9). Any stagnant spots, areas of low flow, or hot spots in an extruder may experience even higher levels of scorch, which could lead to shorter cable production runs before an unacceptable level of cable defects is encountered. The overall kinetics of scorch is controlled by the amount and type of peroxide, antioxidants and polymer architecture.

The unit operations involved depend on the article being fabricated and complexity thereof. Typically, polyethylenes are extruded and shaped into articles for end use such as pipes, wire coating and films. The facility would typically include an extruder, a plasticating screw, a die, a curing zone followed by downstream cooling operations.

Fig. 8 Crosslinking kinetics during cure of LDPE at 182 °C

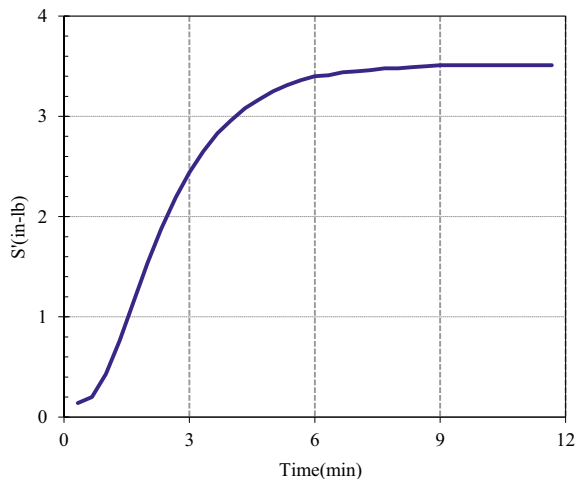
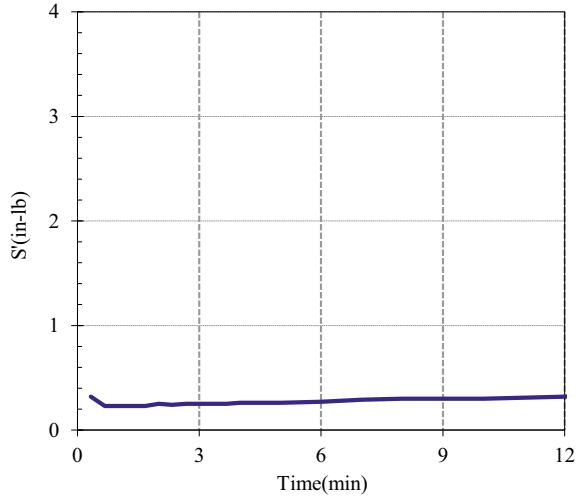


Fig. 9 Viscosity change during fabrication of LDPE at 140 °C



The extruders are equipped with a number of barrel heating zones, a water-cooled throat and other normal extruder machinery. Typical screw length varies from 24 to 32 *L/D* and from 60 to 150 mm. Most extruders today have either general purpose screw. Dies design is a very important parameter in determining the quality of the finished articles. The important considerations are proper streamlining, a good land to gap opening and good drawdown. By the time the polymer exits the die, the article is already shaped and ready to be cured.

The curing process involves the application of high temperature and pressure thus activating the crosslinking process. Finally, the finished articles are cooled down to room temperature. The cooling lengths are usually long and engineered to fit the needs of the dimensions of the article and heat diffusion. Given below is an example of a typical XLPE cable manufacturing process (Fig. 10).

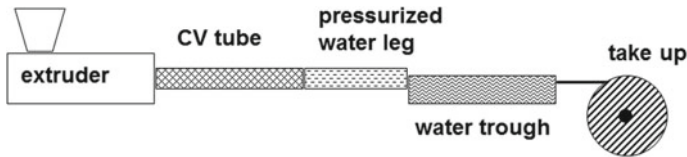


Fig. 10 Simplified peroxide cure continuous vulcanization process

4 Silane Crosslinking

Reaction Chemistry

Moisture cure of silane copolymers (grafted or copolymerized) is a very popular technology for manufacturing crosslinkable polyethylene articles. The curing step involves exposure of the silane copolymer to water (or moisture) in a water bath, sauna or just ambient humidity. It is no surprise that the rate of cure depends on the type of catalyst used, the temperature of cure and the amount of water or moisture available. The dependency on using high-temperature water baths for cure is reduced by introducing ambient curing catalysts like Brønsted acids and other selected organometallic catalysts.

Silane crosslinking kinetics has been studied and documented well in the literature in the context of ‘sol–gel’ [18], adhesives [19] and modifiers [20]. A lot of information is available in terms of experimental [21] and computational [22] data for silane hydrolysis and condensation in alkoxy silane systems. Significant fundamental work on alkoxy silane cure in polymer systems is also available [23].

It is not within the scope of this discussion to deduce and report on the complexity of structures possible through silane crosslinking and characterize them individually. However, for the purposes of this discussion, it is possible to hypothesize a variety of structures based on the degree of hydrolysis (Fig. 11). It is acknowledged that a mixture of linear and cyclic siloxane units is possible through this mechanism (Fig. 12). The structural evolution can be followed by studying small molecule as model systems.

Figures 13 and 14 shows the temporal change of ATR-FT-IR spectra observed from octyl triethoxysilane with different catalysts undergoing a water-crosslink reaction. It is shown that the intense absorbances of ethoxysilane moiety at 1074, and 1101 cm^{-1} decrease with time, while new bands appear at 1000 and 1020 cm^{-1} and grow in intensity with time. Gazel et al. assigned new shoulder bands at 1048 and 1120 cm^{-1} to single siloxane and multi-siloxane linkages, respectively [24]. For the purposes of quantitative analysis, the height of the siloxane peak was used as a measure of concentration relative to a baseline 1616–593 cm^{-1} . The extent of alkoxy silane consumed during this reaction was measured through the reduction in height of the silane peak at 1074 cm^{-1} relative to the same baseline [25].

Trialkoxy silanes undergo hydrolysis in dilute aqueous solution via a series of consecutive reactions producing hydrolyzed monomers (Fig. 11). The kinetics of ethoxysilane hydrolysis could be expressed as the decrease in concentration of

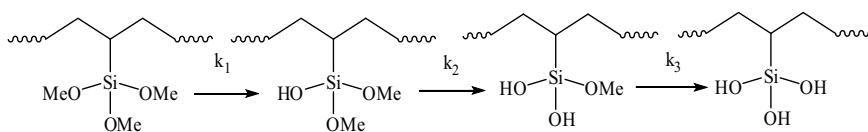


Fig. 11 Possible hydrolysis products during silane crosslinking

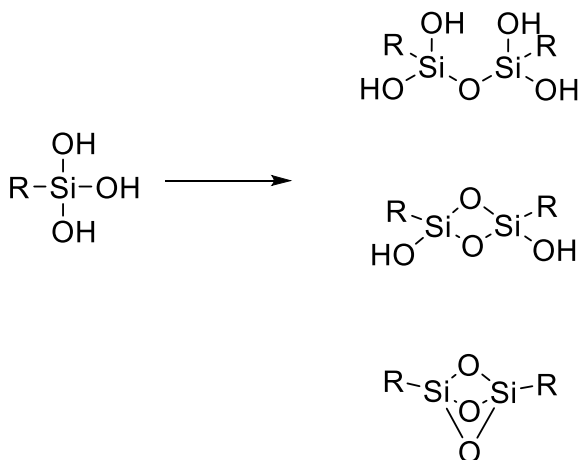


Fig. 12 Possible siloxane structures during alkoxy silane crosslinking

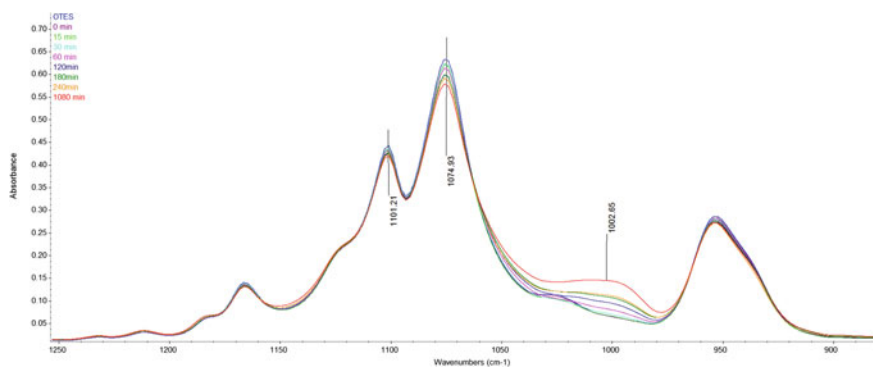


Fig. 13 Spectra evolution with time in the presence of DBTDL and H₂O

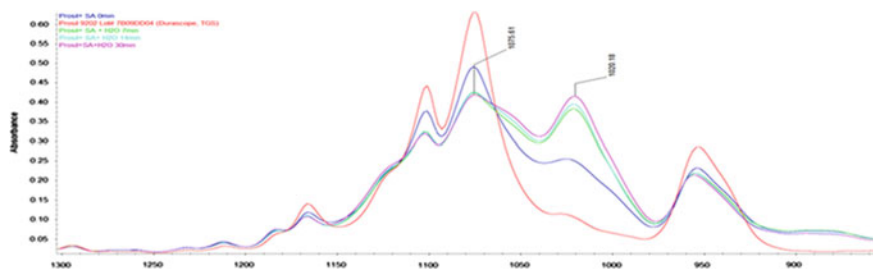


Fig. 14 Spectra evolution with time in the presence of sulfonic acid (SA) and H₂O

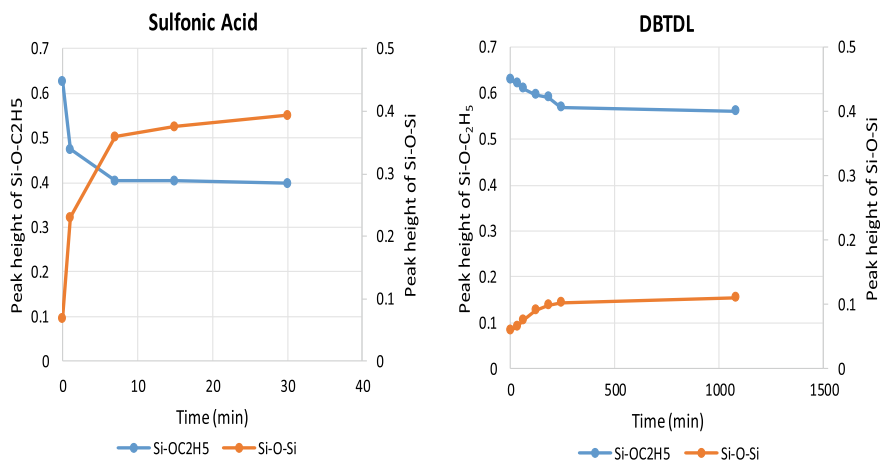


Fig. 15 Evolution of Si-O-Si peak and reduction of Si-O-C₂H₅ peak with time using different catalysts

monomer in the reaction mixture as a function of time. In the system at 50°C, the change of ethoxysilane concentration exhibited a typical exponential decay, which suggested that the reaction followed the first-order law assuming enough water availability. Figure 15 depicts the consumption of alkoxy silane and formation of siloxanes with time for two popular catalyst systems.

The rate expression for hydrolysis and hence alkoxy silane consumption can be described as follows:

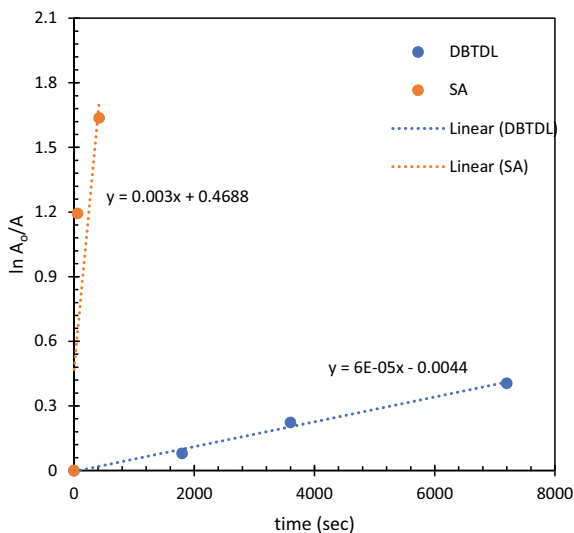
$$\frac{d[M]}{dt} = -K_h[M].$$

In the above equation, $[M]$ is the molar concentration of alkoxy silane and K_h denotes the hydrolysis rate constant. Integration of the above equation gives:

$$\ln \frac{M_0}{M} = \ln \frac{A_0}{A} = K_h t$$

The above equation, t denotes the reaction time, $[M]_0$ and $[A]_0$ refer to the initial concentration and initial absorption intensity of alkoxy silane, respectively. Therefore, the initial slope of the $\ln [A_0/A]$ versus time curve can be used to predict the magnitude of K_h . Linear regression fitting was performed (Fig. 16) and based on all measured data in Fig. 15. The acid-catalyzed systems have a higher value and are consistent with ranges reported in the literature [26]. Organotin are slower than acid catalyzed systems and are in the 10^{-5} s^{-1} range. This is consistent with the data reported in the literature for methoxy systems [19].

Fig. 16 Linear regression fit to evaluate rate constants for hydrolysis by different catalyst systems



The cure rate of the silane copolymers and the resulting physical properties of articles fabricated from it depend on the kinetics of the reactions involving the alkoxy silane. These two reactions involved, hydrolysis and condensation, have been widely studied in the context of silicone polymerization and related work. There is abundant literature on the kinetics and thermodynamics of these reactions in dilute aqueous solutions [27, 28].

The selectivity of the reactions depends on the catalyst being used and cure conditions. The sulfonic acids are very efficient proton donors and crosslink alkoxy silanes under ambient conditions. The reaction involves protonation at the oxygen atom followed by S_N2 type displacement at the silicon atom by water to produce the silanol. The silanol (or alkoxy silane) is again protonated and a similar nucleophilic displacement by another silanol gives rise to a siloxane and results in crosslinking. The rate-limiting step is the condensation step to form the siloxane [28] (Fig. 17).

The other class of catalyst is the Lewis acid like alkyl tin-organic acid salts (e.g., dibutyltin dilaurate). These are slower catalysts when compared to proton donors and are used to cure alkoxy silane functionalized polymers at higher temperatures in water bath or in saunas, but are cheap and do not need inexpensive stabilizers. The mode of reaction for this system involves hydrolysis of the tin salt to the hydroxytin derivative which is the active catalyst. Once the active catalyst is formed, a two-step S_N2 displacement reaction involving water attack on the silicon atom in a Sn–O–Si bond produces the silanol. Further reaction leads to crosslinking through a siloxane bond. The rate-limiting step for systems with this catalyst is the hydrolysis of alkoxy silane to form the silanol (Fig. 18) [29, 30].

Figure 19 best describes the process of progression of crosslinking in the bulk matrix. Chemically the crosslinking process can be monitored by measuring the signal intensity of siloxane at 1026 cm^{-1} with respect to an internal reference at

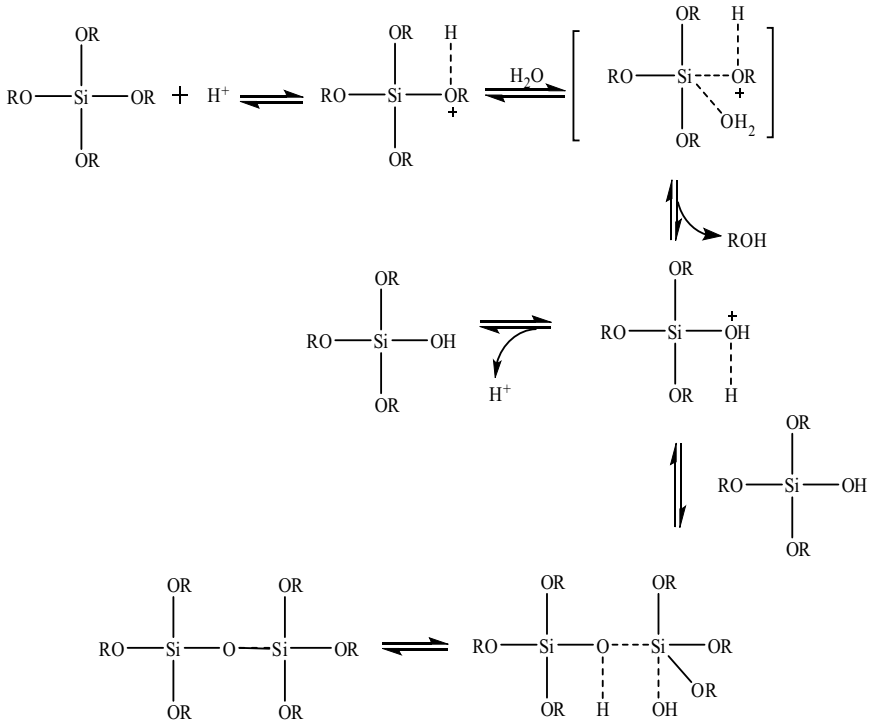


Fig. 17 Brønsted acid-catalyzed crosslinking of alkoxy silanes

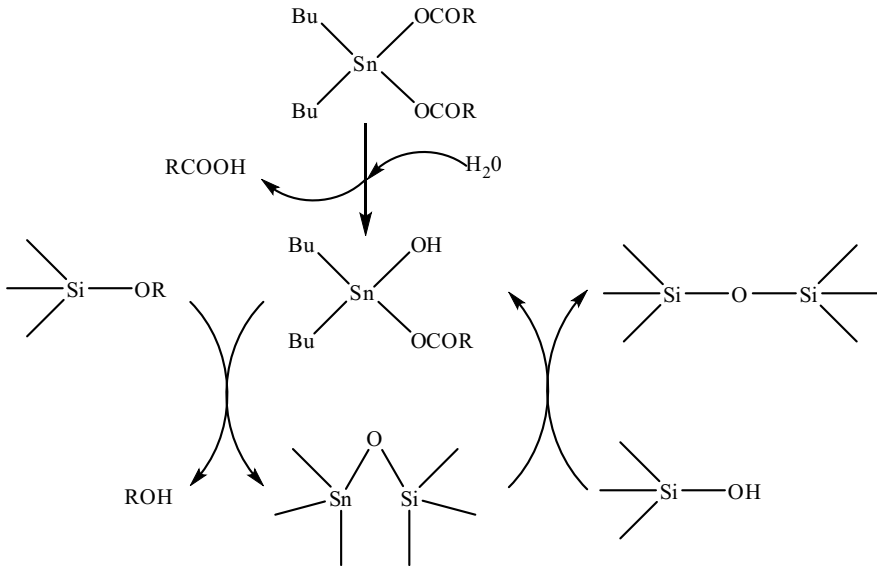


Fig. 18 Dibutyltin dilaurate catalyzed crosslinking of alkoxy silanes

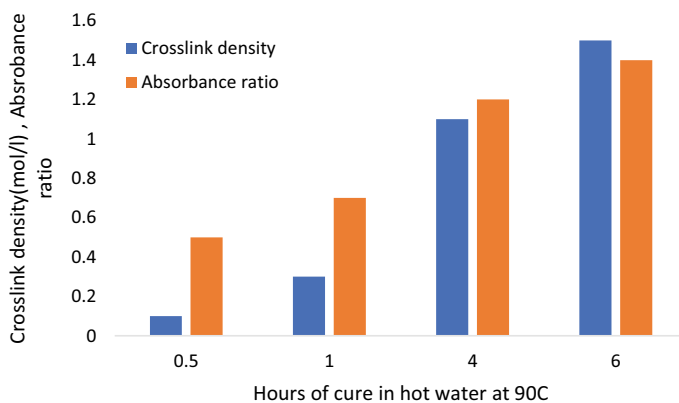


Fig. 19 Evolution of network structure in silane polymer [31]

2021 cm^{-1} . The progress in crosslinking is characterized by an increase in the concentration of the siloxane groups as indicated in Fig. 19. In tandem, the crosslink density (ν) also increases as more and more crosslinkable groups start participating in the network structure.

The evolution of the siloxane network is also characterized by gel formation. The gel content is measured as the insoluble fraction of the matrix. It should be borne in mind that all crosslinking events may not lead to gel. So, siloxane networks may be formed that give rise to oligomers and do not form gel of infinite molecular weight [31].

Process

Silane-containing grades of polyethylene have been produced commercially for decades by the radical copolymerization of ethylene and vinyltrialkoxysilanes and by the post-polymerization modification of ethylene-based materials through radical-mediated vinyl alkoxy silane grafting. Typically, the catalyst and antioxidant are added directly (Monosil) or via a masterbatch (Reactor copolymer & Sioplas) to the silane functionalized polymer to initiate the crosslinking reaction. Additional masterbatches are also added to meet other critical performance requirements such as flame retardant or weatherability specifications. This differs from peroxide cure compounds which typically have all the additives compounded into one product.

The extrude thermoplastic blend onto wire at optimal line speed based on extruder capacity and ancillary equipment. The crosslinking of insulation in high temperature/high humidity conditions found in a sauna or water bath or under ambient conditions. Moisture cure differs from traditional peroxide cure process by decoupling the curing process from the extrusion process. In most cases, the silane crosslinking process starts by drying the ingredients. Typically, the moisture content is targeted to be below 100 ppm. Otherwise, the moisture initiates premature crosslinking in the extruder. The crosslinking of the fabricated articles happens in warehouses equipped with saunas or under ambient conditions. The rate of crosslinking will depend on the

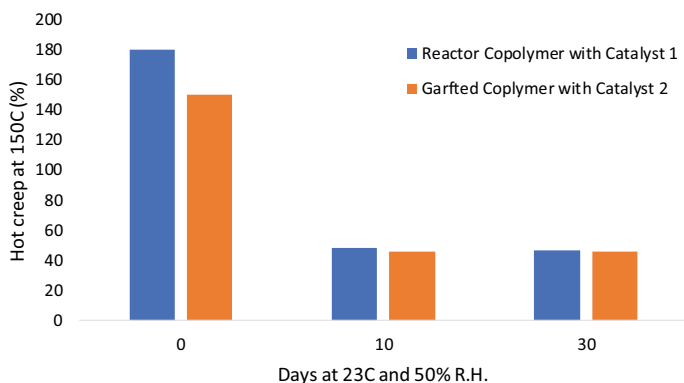


Fig. 20 Ambient cure rate of silane copolymer and grafted silanes systems [32]

diffusion of moisture from outside toward the inner parts of the fabricated article. It is important to note that the formulation of these systems is very specialized and specific to the application. Depending on the type of alkoxy silane functionalized resin technology utilized, various silanol condensation catalysts are available to achieve desirably similar crosslinking times after article fabrication at given conditions of temperature and humidity. This is depicted in Fig. 20 where the crosslinking rate of copolymer and grafted silanes is compared with each other using different catalysts that are compatible with them [32] (Fig. 21).

5 Current Trends and Concluding Remarks

Utilization of Coagents for Peroxide Crosslinking

Peroxide cure offers a lot of advantages, but a key trend is to formulate of increased efficiency of crosslinking to either consume less peroxide or to get higher crosslink density at the same concentration of peroxide. This accomplished through the use of coagents [33]. Fundamentally, there are two classes of these coagents: (a) addition (b) addition-fragmentation. The addition coagents follow the same mechanisms discussed earlier. The difference is brought about by increase in available unsaturation levels in the system. Alpha methyl styrene dimer (AMSD) is a popular addition-fragmentation type coagent used in polyethylene crosslinking. These addition-fragmentation coagents provide an excellent balance of scorch suppression and cure-boost. This is in line with the mechanistic studies using ESR where crosslinking at 145 °C was suppressed and alkyl radicals added to the unsaturation in AMSD instead of termination through combination. The resulting adduct radical has a heightened propensity to fragment at cure temperatures, due to high activation energy of fragmentation, to leave a pendant reactive double bond on the main chains. This resulted in cure boost or enhanced rate of cure at 180 °C [34].

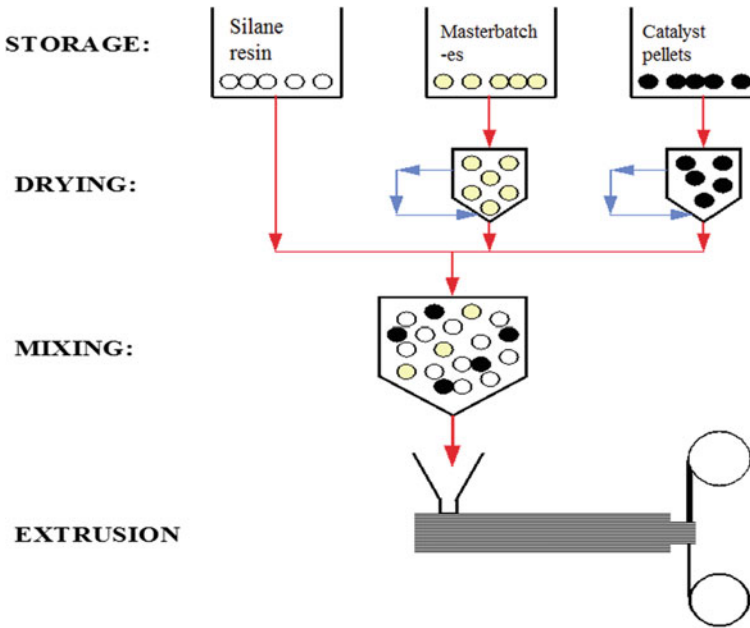


Fig. 21 Typical process for coating of cables with silane curable polyethylene

The overall kinetics of crosslinking is controlled by the amount of initiator, antioxidant, AMSD and other additives that may interact with alkyl radicals generated on the main chain. The initiating species is the cumyloxy radical; derived from the homolysis of dicumyl peroxide (Fig. 22). Although other pathways exist for consumption of the cumyloxy radical, the most favored direction is hydrogen atom abstraction from the polymer resulting in polymer radicals ($M_1\cdot$). Steric and polar effects influence the addition of polymer radicals ($M_1\cdot$) to the unsaturation in AMSD resulting in the intermediate adduct radical ($M_2\cdot$). Fragmentation of this adduct radical is preferred over bimolecular termination, leading to a structure that resembles an activated pendant olefin (M_3) on a PE backbone. The cure-boost effect is dependent on the kinetic chain length of the ensuing process. This involves addition of polymer radical ($M_1\cdot$) to the pendant olefin (M_3) to form an intermediate adduct radical ($PE_{XL}\cdot$). This radical can be quenched by abstracting hydrogen from the surrounding polymer chains to form crosslinks (XLPE). The number of times these abstraction events take place before termination via combination or disproportionation per radical is defined as the kinetic chain length. This means more crosslinks are derived on a per radical basis versus a conventional non-cure boosted systems where it is only because of termination events of two radicals. The result of this mechanism is a crosslinking process which provides scorch suppression by engaging early radicals in the addition-fragmentation process and then creating a cure boost effect via the favored addition to olefin pathway.

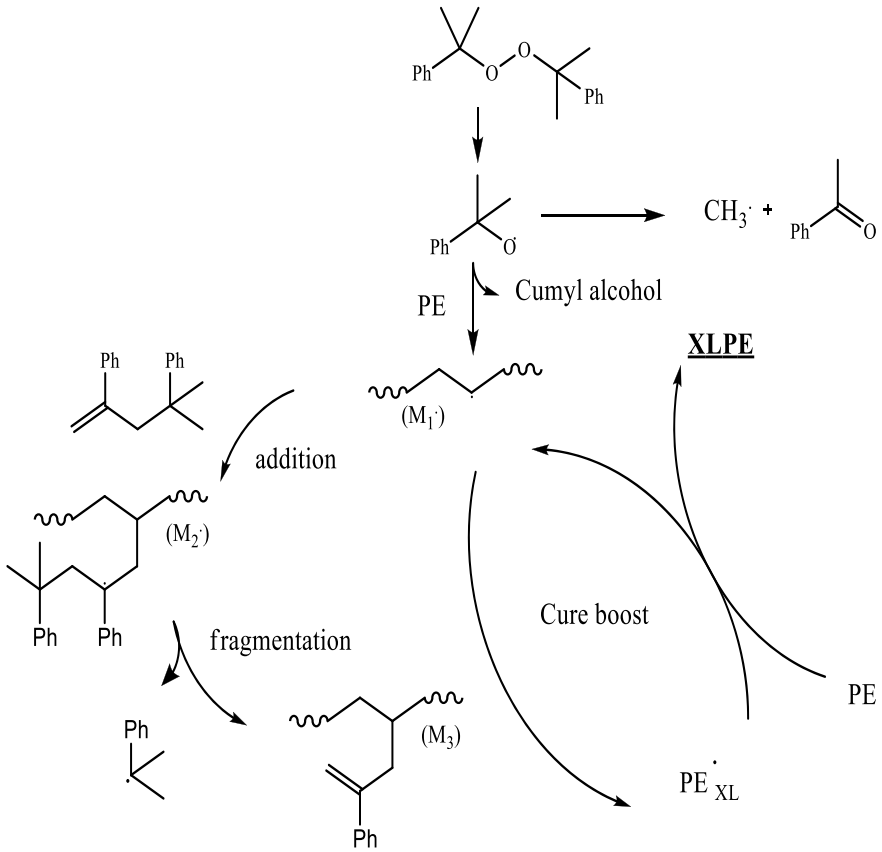


Fig. 22 Coagent assisted cure for XLPE

Comparison of different crosslinking processes

There are multiple crosslinking technologies that have evolved based on material needs and continue to add value by bringing along unique thermomechanical properties. They are formulated based on the specific application needs. The processes employed are dictated by the article being fabricated. All these technologies are adequate and have their own advantages and disadvantages. Table 4 summarizes these technologies from the perspective of end user. There have been significant advances in peroxide crosslinking and silane crosslinking. While polymer chain architecture offers significant opportunities to improve crosslinking efficiency, new coagent technology continues to evolve and improve efficiency of cure in peroxide crosslinking.

Table 4 Summary of the crosslinking processes for polyethylene

	SI-LINK® PE (reaction copolymer)	Monosil type (grafted)	Sioplas type (grafted)	Irradiation	Peroxide
Customer Purchases	<ul style="list-style-type: none"> • Reaction copolymer • Catalyst MB 	<ul style="list-style-type: none"> • Base resin • Silane • Peroxide • A/O • Catalyst 	<ul style="list-style-type: none"> • Grafted resin • Catalyst MB 	<ul style="list-style-type: none"> • PL resin 	<ul style="list-style-type: none"> • Resin with peroxide • Mold resin if mold cure
Process used	Mix reaction copolymer and catalyst MB in PR extruder	Mix all components in 30:1 extruder	Mix grafted resin and catalyst MB in PR extruder.	Extrude resin onto conductor.	CV tube: extrude resin slowly
Reactions	XL in water bath or sauna	Graft in extruder. XL in water bath/sauna	XL in water bath or sauna	XL using e-beam radiation	XL in CV tube OR XL in oven and remove and recycle mold material
Advantages	<ul style="list-style-type: none"> • Only resin to handle, no CV tube • Low initial cost. Shelf stable • Clean insulation • Requires conventional equipment • last extrusion rates • Minimal scorch • Safety: no CV or silane, peroxide and catalyst to handle 	<ul style="list-style-type: none"> • Cures rapidly • Flexibility in base resin selection 	<ul style="list-style-type: none"> • Requires conventional equipment • Cures rapidly • Flexibility in base resin selection • Safety: no CV or silane, peroxide and catalyst to handle 	<ul style="list-style-type: none"> • Requires conventional equipment • Flexibility in base resin selection • Fast extrusion rates 	<p>Well-established technology</p> <ul style="list-style-type: none"> • Shelf stable • Clean insulation • Mold cure: faster extrusion than CV tube

(continued)

Table 4 (continued)

Disadvantages	<ul style="list-style-type: none"> • Slightly slower XL than Monosil or Sioplas • Requires dryer and cure facility 	<ul style="list-style-type: none"> • Complicated technology • Requires special extruder • Material can scorch easily • Slow line speed • Safety: Must handle silane, peroxide and catalyst • Requires cure facility • Residual silane in insulation • Unsuitable for complicated additive packages like FR 	<ul style="list-style-type: none"> • Material can scorch easily • Shelf life less than 6 months • Requires dryer and cure facility • Residual silane in insulation 	<ul style="list-style-type: none"> • Complicated technology • Non-uniform XL of thick sections • Often requires cure accelerators in formulation 	<ul style="list-style-type: none"> • Initial investment is high • Slow line speed • Higher scrap rates than moisture cure • Safety: high temperatures and pressures in CV tube • Extra steps of applying, removing and recycling mold material
---------------	--	--	--	---	---

References

1. Charlesby A (1952) Cross-linking of polythene by pile radiation. *Proc R Soc Lond Ser A Math Phys Sci* 215(1121):187–214
2. Dole M (1986) The history of the crosslinking of polyolefins. In: Seymour RB, Cheng T (eds) *History of polyolefins: the world's most widely used polymers*. Springer Netherlands, Dordrecht, pp 71–86
3. Alliger G, Sjothun IJ (1964) *Vulcanization of elastomers: principles and practice of vulcanization of commercial rubbers*. Reinhold Pub. Corp.
4. Eugene KR (1950) Process for extruding and insolubilizing polymers of ethylene. US Patent 2,528,523
5. Precopio FM, Gilbert AR (1963) Peroxide cured polyethylene. Google Patents
6. Scott HG (1972) Cross-linking of a polyolefin with a silane. Google Patents
7. Swarbrick P, Green WJ, Maillefer C (1978) Manufacture of extruded products. US Patent 4,117,195
8. Isaka T et al (1983) Crosslinkable polyethylene resin compositions. Google Patents
9. Mark HF, Kroschwitz JI (1985) *Encyclopedia of polymer science and engineering*
10. Ungar G (1981) Radiation effects in polyethylene and n-alkanes. *J Mater Sci* 16(10):2635–2656
11. Dole M, Milner D, Williams TF (1958) Irradiation of polyethylene. II. Kinetics of unsaturation effects. *J Am Chem Soc* 80(7):1580–1588
12. Lyons B, Crook M (1963) Role of unsaturation in the radiation chemistry of polymers. Part I—polyethylene. *Trans Faraday Soc* 59:2334

13. Lyons BJ, Fox AS (1968) Unsaturation changes and other radiolytic reactions in polyethylene. II. An examination of crosslinking with gel permeation chromatography. *J Polym Sci Part C Polym Symp*
14. Randall J, Zoepfl FJ, Silverman J (1983) A ¹³C NMR study of radiation-induced long-chain branching in polyethylene. *Makromol. Chem* 4:149–157
15. Milinchuk V, Klinshpont E, Kiryukhin V (1986) Radiation effects in polymers at high pressure. *Int J Radiat Appl Instrument Part C Radiat Phys Chem* 28(3):331–334
16. Chmielewski A (2006) Worldwide developments in the field of radiation processing of materials in the down of 21st century. *Nukleonika* 51:3–9
17. Charlesby A, Pinner S (1959) Analysis of the solubility behaviour of irradiated polyethylene and other polymers. *Proc R Soc Lond Ser A Math Phys Sci* 249(1258):367–386
18. Tan B, Rankin SE (2006) Study of the effects of progressive changes in alkoxy silane structure on sol–gel reactivity. *J Phys Chem B* 110(45):22353–22364
19. Huber MP, Kelch S, Berke H (2016) FTIR investigations on hydrolysis and condensation reactions of alkoxy silane terminated polymers for use in adhesives and sealants. *Int J Adhes Adhes* 64:153–162
20. Paquet O et al (2012) Hydrolysis-condensation kinetics of 3-(2-amino-ethylamino) propyl-trimethoxysilane. *Mater Sci Eng C* 32(3):487–493
21. Oostendorp DJ, Bertrand GL, Stoffer JO (1992) Kinetics and mechanism of the hydrolysis and alcoholysis of alkoxy silanes. *J Adhes Sci Technol* 6(1):171–191
22. Okumoto S, Fujita N, Yamabe S (1998) Theoretical study of hydrolysis and condensation of silicon alkoxides. *J Phys Chem A* 102(22):3991–3998
23. PalmÖf M, Hjertberg T (1999) Catalysis of the crosslinking reactions of ethylene vinyl silane copolymers using carboxylic acids and DBTDL. *J Appl Polym Sci* 72(4):521–528
24. Gazel A et al (1985) Photooxidation of silane crosslinked polyethylene. *Die Makromolekulare Chemie, Rapid Commun* 6(4):235–240
25. Tejedor-Tejedor MI, Paredes L, Anderson MA (1998) Evaluation of ATR– FTIR Spectroscopy as an “in Situ” tool for following the hydrolysis and condensation of alkoxy silanes under rich H₂O conditions. *Chem Mater* 10(11):3410–3421
26. Jiang H, Zheng Z, Wang X (2008) Kinetic study of methyltriethoxysilane (MTES) hydrolysis by FTIR spectroscopy under different temperatures and solvents. *Vib Spectrosc* 46(1):1–7
27. Osterholtz F, Pohl E (1992) Kinetics of the hydrolysis and condensation of organofunctional alkoxy silanes: a review. *J Adhes Sci Technol* 6(1):127–149
28. Schmidt H, Scholze H, Kaiser A (1984) Principles of hydrolysis and condensation reaction of alkoxy silanes. *J Non-Cryst Solids* 63(1–2):1–11
29. van Der Weij FW (1980) The action of tin compounds in condensation-type RTV silicone rubbers. *Die Makromolekulare Chemie* 181(12):2541–2548
30. Smith K (1986) A study of the hydrolysis of methoxy silanes in a two-phase system. *J Org Chem* 51(20):3827–3830
31. Sengupta S et al (2008) Evolution of crosslinks during moisture cure of ethylene-vinylalkoxy silane copolymers in power cables. *Int Wire Cable Symp*
32. Chaudhary BIEA (2019) Effect of polyethylene structure on silane grafting and properties of associated moisture-crosslinked compositions and cable constructions. ANTEC 2019, SPE Detroit
33. Yabin S (2015) Recent developments in cure control for crosslinkable polyethylene (XLpe) power cable insulation. In: 9th international conference on insulated power cables, Jicable
34. Yamazaki T, Seguchi T (2001) Electron spin resonance study on chemical-crosslinking reaction mechanisms of polyethylene using a chemical agent. VI. Effect of α -methyl styrene dimer. *J Polym Sci Part A Polym Chem* 39(13):2151–2156

Chapter 4

General Awareness of XLPE Manufacturers



Saurav S. Sengupta and Pieter Calon

1 Structure of the Industry and Trends

The crosslinking business consists of four major segments:

1. Raw material producers supply the different grades of polyethylenes, initiators, antioxidants, etc. required to make a fully formulated product. Several companies are also upstream integrated because they also produce the intermediate product that is crosslinkable; they include Dow Inc, Borealis AG, Lyondell Basell among others.
2. Formulators or crosslinkable compound manufacturers primarily purchase the raw materials and formulate the crosslinkable compound for use in various types of applications. Formulators are a key step in the value-added chain, because they are in direct contact with end users and are often very secretive about their specialties. On an average three or more years of development work are often required to develop suitable compounds for a specific application. Formulators are key to improving final products and are instrumental in advising customers on product selection. Several companies like the ones mentioned above are also downstream integrated in that they also make the raw materials for use in the applications.
3. Manufacturers of curing equipment, application equipment, and processes play an integral role in ensuring quality of articles made. These include different extruder, die and continuous vulcanization equipment manufacturers such as Maillefer, Troester.

S. S. Sengupta (✉)
The Dow Chemical Company, Collegeville, PA, USA
e-mail: SSSengupta@dow.com

P. Calon
The Dow Chemical Company, Seadrift, TX, USA

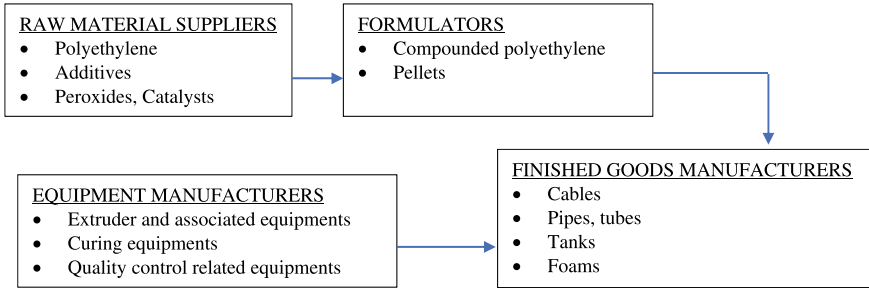


Fig. 1 Value chain of XLPE industry

4. Finished article manufacturers purchase the crosslinkable materials and fabricate them for the end-use industries. These include industries such as wire and cable, foams, tank, tubing (Fig. 1).

The evolution of intellectual property in this space is consistent with an active field. Figure 2 depicts the number of filings from WIPO on a yearly basis for crosslinked polyethylene over the last 10 years. The analysis of assignees shows a mix of finished goods manufacturers and formulated compound suppliers. Figure 3 depicts the IP owners with the most patent counts. The fact that the material continues to be used in multiple applications is borne out in the different IPC classes that are covered by the patents for crosslinked polyethylene.

It is interesting to note that number of patents related to wire and cable applications (H01B) is comparatively more than the others such as pipes (F16L). It is also interesting that compounds and formulations (C08L) as well as processes of making them (C08J) are also being patented. Post-compounding fabrication techniques such as molding, extrusion, joining (B29C) are also being pursued. The design of finished articles made using crosslinked materials are also being patented (B32B). Figures 4 and 5 illustrate the evolution of the number of patents over time in this space.

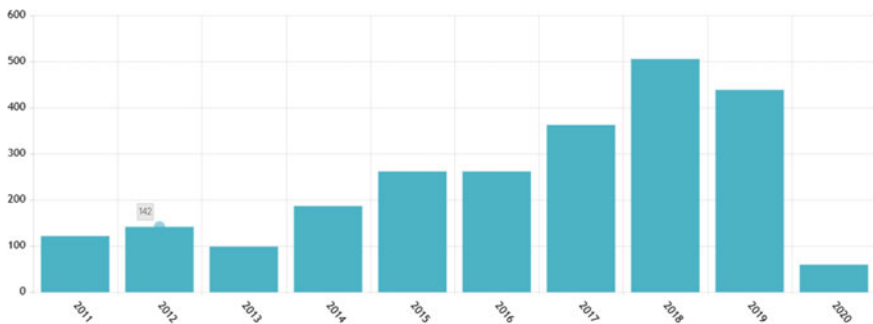


Fig. 2 Crosslinked polyethylene patent count by year for time period 2011–2020

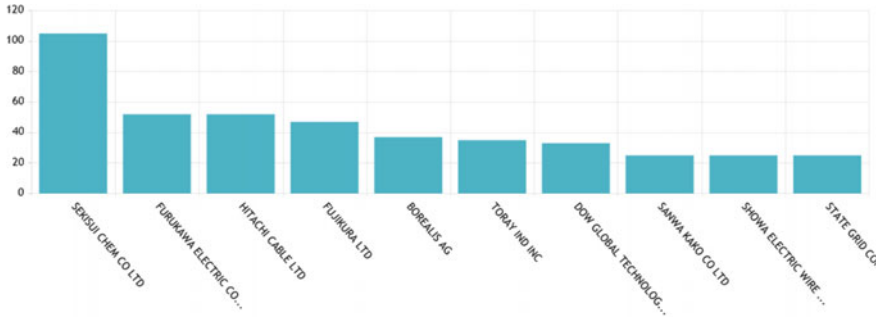


Fig. 3 Crosslinked polyethylene patent count by assignees for time period 2011–2020

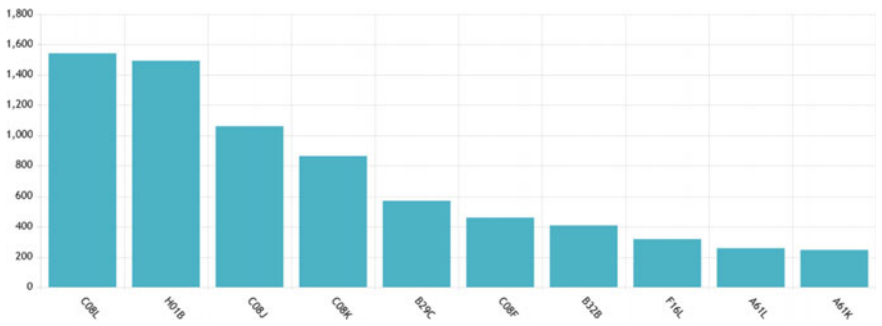


Fig. 4 Crosslinked polyethylene patent count by IPC class for time period 2011–2020

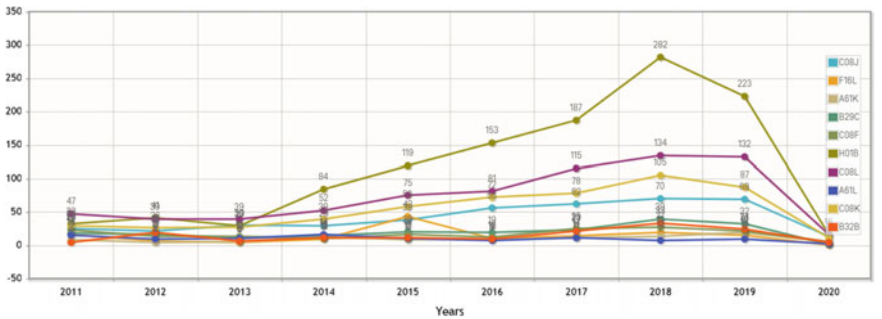


Fig. 5 Crosslinked polyethylene patent count evolution of IPC class over time period 2011–2020

2 XLPE Compound Manufacturing

The process for making polyethylene compounds depends on the method of cure and formulation to be used. As discussed earlier there are three major types of cure, i.e., irradiation, peroxide and silane. It is important to realize that crosslinkable

polyethylene is fully formulated materials and the process of making them will depend on the formulation components. Based on the individual components and process used, these materials also come specified with their own shelf lives and unique packaging requirements.

2.1 Manufacture of Peroxide Crosslinkable Compounds

In practice, peroxide-containing polyethylenes consist of peroxides, stabilizers/antioxidants, other additives along with the polyethylene [1]. The antioxidants and stabilizers are compounded into molten polyethylene [2]. These compounders are chosen based on throughput required and the state of dispersion needed.

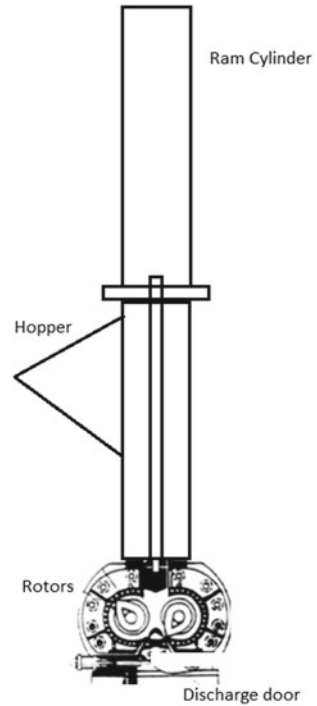
In small-scale operations, the components are frequently blended by tumbling them together [3]. The simplest apparatus is a drum which is approximately half filled with the components and rotated end over end at specified revolutions per minute. This method will generally give a satisfactory distribution of a small percentage of dry powders with polyethylene for producing compounds by one stage process. Mini mixing machines will tend to segregate one component if it varies in density, shape, surface finish or size from another in other words such mixers will only mix things which are physically similar it is difficult to achieve with continuous planting machines the accuracy of control required particularly with those which attempt to control the rate of feed volumetrically (Fig. 6).

Typically, the mixer/compounder is configured so as to raise the temperature of the polymer/additives mixture to a temperature in the range of about 250 to about 360 °C. This is done through work added to the mixture through viscous energy dissipation during mixing and homogenization of the entering feed stream components.

Very early on in the 1950s for large-scale compounding the most widely used and versatile equipment was the internal mixer, two examples of which were the Bolling and the Banbury [4]. They consist of a jacketed chamber whose cross-section is in the shape of a horizontal figure eight in which two cored specially shaped rotors counter rotate at slightly different speeds. This induces a kneading action between the rotors and a shearing action between the rotors and chamber. The chamber is closed below by a sliding door and above by a compressed air operated ram which is also cored for cooling and moves vertically in the hopper down which the polyethylene is charged to the chamber of the mixer. These internal mixers are produced in a range of sizes.

In making the compound, half is placed in the chamber then the additives and finally the remainder of the polyethylene is charged. If that additives are in liquid form it is preferable to have them added slowly when the polyethylene has just melted. The severity of the compounding process is varied by controlling the quantity of cooling water passing through the jacket and cored moving parts. The material in the internal mixer is heated entirely by the frictional work done on it. The shearing forces are high and therefore the compounding is quite effective. Since the viscosity of the melt decreases with increasing temperature the effectiveness of compounding is increased by lowering the rate of rise of temperature by the external application

Fig. 6 Banbury internal batch mixer



of cooling. The internal mixer is discharged by withdrawing the sliding door when the contents fall out leaving the chamber and rotors clean. The compounded material is either deposited onto a mill after which it can be removed as a continuous strip and fed to a granulator or is fed to an extruder which produces strand for subsequent cutting into pellets.

In some cases, good dispersion may be achieved in a orthodox single screw extruder by doing a considerable amount of work on the polyethylene [5]. The basic functions for this kind of an equipment are solids conveying, melting and pumping. Secondary functions constitute mixing and shear refining [6]. The single screw extruder broadly consists of 3 zones:

- a. Solids conveying section whose preliminary function is to prevent starving the forward zones and conveyer pellets. (Fig. 7).
- b. Melting section is where the primary melting of all components occurs. Usually, the process of melting progresses down the length of the melting section and occurs in both the thickness and cross-channel direction [7]. A very high-level mixing may occur during the melting phase (Fig. 8).
- c. Metering section controls the rate of the extruder and is always fully filled. Stagnant regions should be avoided at all costs.

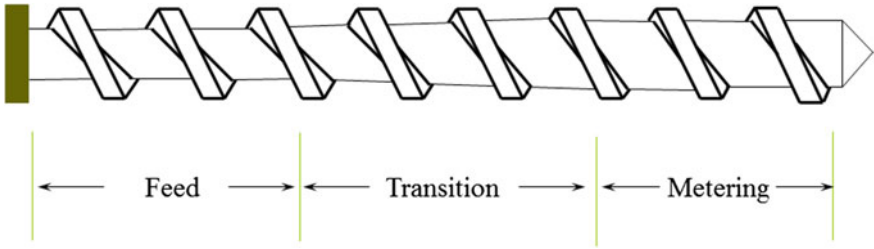


Fig. 7 Single screw extruder operation

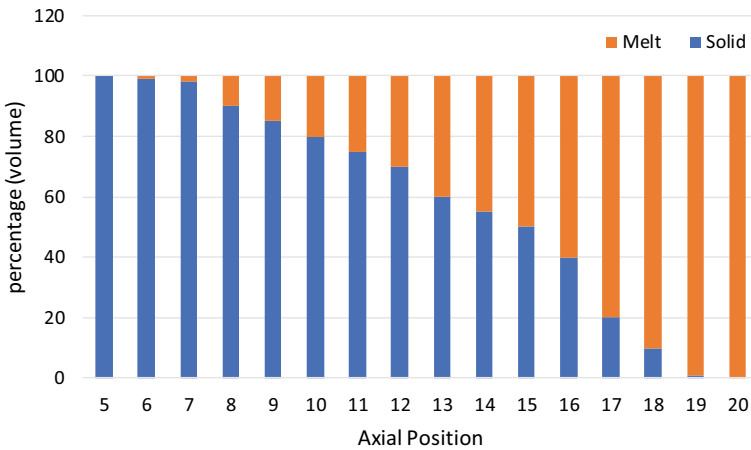


Fig. 8 Progression of melting in a single screw extruder at different axial position diameters [7]

In some cases, dispersive mixing elements are employed (Fig. 9). For all practical purposes the screw length to diameter ratios should be at least 15:1. A minimum compression ratio of 2.5:1 should be used depending on the type of solid feed. It is recognized that a single screw provides an excellent means of feeding granules, raising them above their melt point and pumping them under pressure. Very little mixing occurs on the microscopic scale unless mixing elements are employed [8].

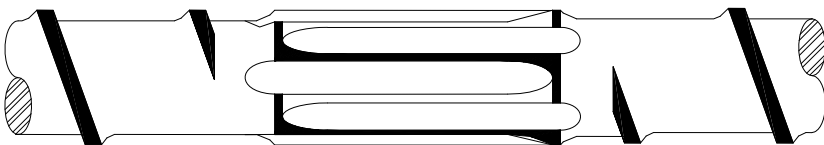


Fig. 9 Mixing elements in a single screw extruder [7]

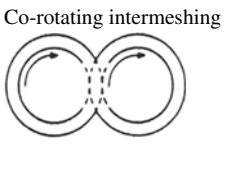
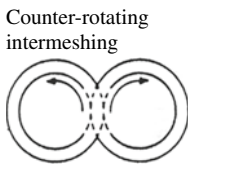
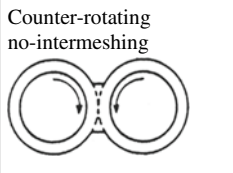
Twin-screw extruders are the most common compounding systems providing high output rates and excellent mixing performance at favorable economics and good versatility [9, 10]. They are classified as co-rotating and counter rotating systems. Both have different processing and mixing principles (Table 1). Co-rotating twin-screw extruders provide good process control at intensive mixing and shearing. The initial development of this self-wiping profile within a twin bore geometry was described by Meskat and Erdmenger with the objective of mixing high viscosity fluids which were already in the melt state [11]. Closely intermeshing and self-cleaning conveyor and kneading elements are combined on screw shafts which allow to address the process needs with an adapted screw design. From masterbatch and compound production to reactive and direct extrusion various concepts and systems of co-rotating twin-screw extruders are offered today. High shear rates and broad shear rate spectrum are the big disadvantages of co-rotating twin-screws extruders [6].

Counter rotating and intermeshing twin-screw extruders move the material in closed cells along the extruder screws like a nut on a thread. The melting of the polymers is generated by heat transfer and limited friction with the cylinder walls. There is little shear involved and the residence times are relatively short within a narrow spectrum [12–14].

The process control parameters for a twin-screw compounding operation would involve the following:

- a. Throughput,

Table 1 Considerations for different twin-screw designs [9, 10]

	Co-rotating intermeshing	Counter-rotating intermeshing	Counter-rotating no-intermeshing
			
Practical residence time	0.3–3 min	0.3–3 min	0.5–8 min
Residence time distribution	Variable	Variable/tighter	Variable
Dispersion	High	High	Good
Distributive mixing	Good	Good	Excellent
Heat transfer	Excellent	Excellent	Excellent
Venting	Excellent	Excellent	Excellent
Pumping	Good	Excellent	Fair
Self wiping	Excellent	Good	Fair
Zoning	Excellent	Excellent	Good
Output rate	High	Moderate	High

- b. Screw Speed,
- c. Barrel Temperature,
- d. Discharge Pressure,
- e. Screw Configuration,
- f. Throttle Position,
- g. Formulation/Order of Addition.

Typically, polymers and additives are added to the gravimetric feeders which transfer the required dosage of materials to the feed port of the extruder. Materials are then conveyed and mixed through the length of the extruder (Fig. 10). The state of the components and level of mixing depends on the screw design. The design of the screw configuration for a twin-screw extruder is complex and consists of a modular assembly built of various individual screw elements. The nature of the materials and the desired state of mixing dictates the choices of screw elements used, such as conveying elements (forward and reverse), kneading elements for dispersive mixing and mixing elements for distributive mixing (Fig. 11).

The melt is then forced through a die and pelletizers [16]. The usable form of the product from the compounding step is obtained in pellet form. There are various pelletizing technologies available for use based on production requirements [17].

The next step is the mixing of peroxide with the compounded polyethylene. In practice, the peroxide is typically added to polymer compositions as a liquid. The peroxide is typically sprayed onto the pellets although alternative forms of application can be employed, e.g., immersion, splashing, etc. Once the peroxide and any additives are absorbed into the pellet, the pellet is ready for packaging. This step involves heating the thermoplastic intermediate to about 55 to about 85 °C;

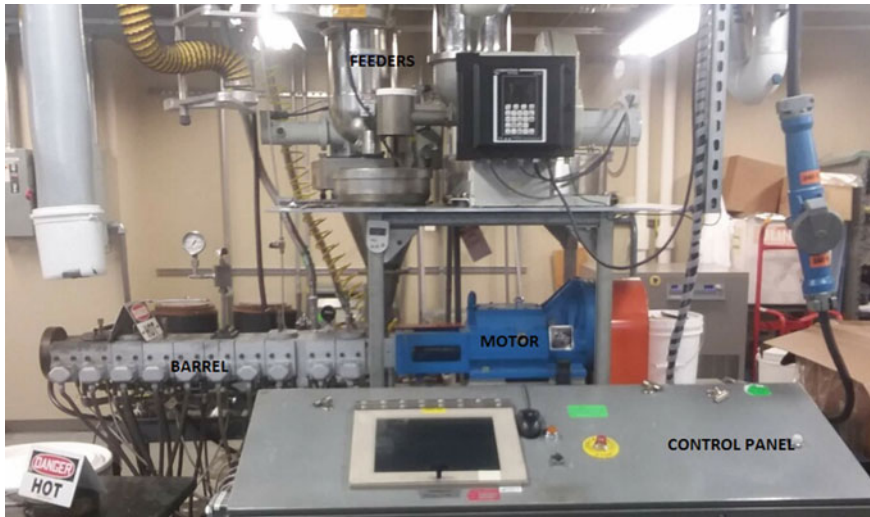


Fig. 10 Simple layout of a twin-screw extruder

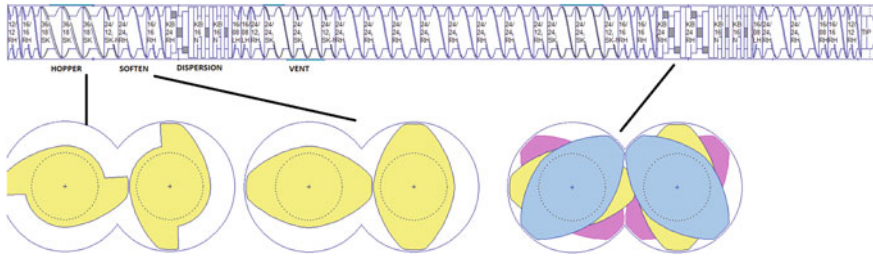


Fig. 11 Components and functions of a twin-screw extruder [15]

after which the pellets are introduced into a spraying chamber where blending, and coating is affected. The moving pellets, some partially coated with the crosslinking formulation and other still dry pellets gravity flow inside the blending system. Pellets are then stored to homogenize the composition of peroxide through the pellets [18, 19]. Mixing of peroxides can also be achieved through other processes. A turbo-mixer (such as a LICO type device) can be used, to distribute liquids quickly over the surface of the polyethylene granules [20]. The pellets are then cooled after which they are ready for use, shipping or storage.

2.2 Silane Crosslinkable Copolymer

Vinylalkoxysilane homopolymers made via radical polymerization was accomplished in the liquid state with high purity monomers [21]. But the chemistry has not been scaled up and the process is far from being commercialized. Currently ‘in-reactor’ copolymers of alkoxy silanes and ethylene are made through radical initiated high-pressure reactor process. This yields a low-density silane functionalized polyethylene product.

The basic principles underlying the polymerization by high-pressure technique are simple to outline but their operation is complicated, and a considerable amount of ‘know-how’ is attached to any successful plant [22]. Research in polymerization of polyethylene at high pressure (up to 2000 bar) was pioneered by ICI as early as 1930s and 1940s. During development, ICI licensed the process to DuPont and Union Carbide. By the late 1950s, ICI’s process had been licensed widely. Since then, however, most of the original ICI licensees have developed their own proprietary technology, either independently or jointly with ICI. Ethylene gas is polymerized by subjecting the pure gas to high pressure and relatively high temperatures. In order to attain suitable rates, suitable initiators are used.

The ethylene is first compressed in multistage compressors and initiators are introduced. The gas is in highly concentrated form when the reaction takes place permitting a relatively high rate of polymer production per unit reaction volume. The operating conditions currently employed are high pressure >300 bar and high

temperatures $>100\text{ }^{\circ}\text{C}$. Polymer product properties are controlled by reactor pressure and temperature profile across the reactor. Reactor control based on monomer feeds and peroxide injection schemes [23]. The product is finally recovered in a pellet or granule form. This kind of process limits the copolymerized silanes to LDPE architectures only.

During the process of making articles of use such as cable and pipes, the silane copolymers, catalyst masterbatches and additives are dried to ensure minimal moisture in the system. This is done to ensure minimal crosslinking during fabrication referred to as scorch (Fig. 12). Thus, conditions to avoid are as follows:

- Moisture,
- High Extrusion Temperatures ($>210\text{ }^{\circ}\text{C}$),
- Low rpm—Gives Long Residence Time,
- Equipment Dead Spots.

Typical formulations include $\sim 80\%$ silane copolymer and the rest being catalyst and additive masterbatches. Depending on the masterbatch and system used water content can be as high as 5000 ppm, e.g., color concentrates (Fig. 13). This is a very important variable to control for silane crosslinking processes. As such, the catalyst and carbon black masterbatches should be dried in a dehumidified ($-40\text{ }^{\circ}\text{C}$ Dewpoint) air dryer at $60\text{--}70\text{ }^{\circ}\text{C}$ for four to six hours. Good distribution of the hot air throughout the mass of the masterbatch is important to ensure thorough drying of the entire batch. After the masterbatches are dried, they should be mixed with the silane copolymer just prior to extrusion.

Conventional thermoplastic extrusion equipment may be used for processing the silane copolymer. Dead zones in the extruder, breaker plate, head, and die should be avoided. General guidelines include:

- Use a well streamlined extruder/head assembly,
- Operate at as low a temperature as possible,
- Minimize residence time in extruder,
- Avoid stagnant and no-flow situations,
- Avoid stopping the extruder during processing.

In general, for such a process the following is needed:

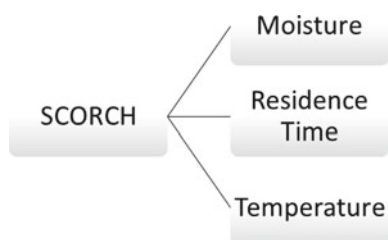


Fig. 12 Factors controlling scorch

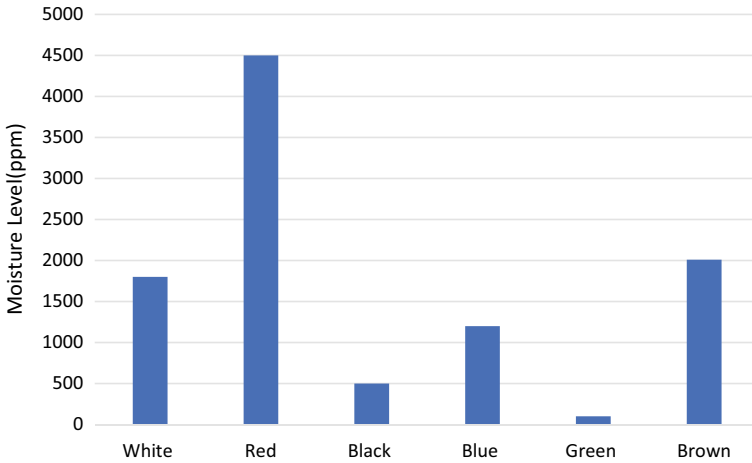


Fig. 13 Estimates of moisture coming into silane cure systems

- Extruder L/D 20-24/1,
- PE Screw recommended,
 - Recommended Compression Ratio 3/1,
 - Maddock Mixing Section recommended to promote dispersive mixing,
 - Screw Cooling is possible but not needed (Fig. 14).

These copolymers bring some unique features of practical importance to fabricators and manufacturers of finished goods. Shelf-life and storage stability is a very important parameter for the silane crosslinkable materials. The outstanding shelf-life stability of reactor copolymers is depicted in Fig. 15. This is well documented and is a improved feature that current grafted materials cannot provide [24]. This also enables the delivery of silane copolymer materials in bulk railcars, etc. [25].

The other feature is the stability of the compounding process related to the fabrication step over a period of time. Typically, the copolymer technology is quite robust and offers a very long process window compared to the grafted resins [24, 25].

Silane Copolymer, catalyst and additives

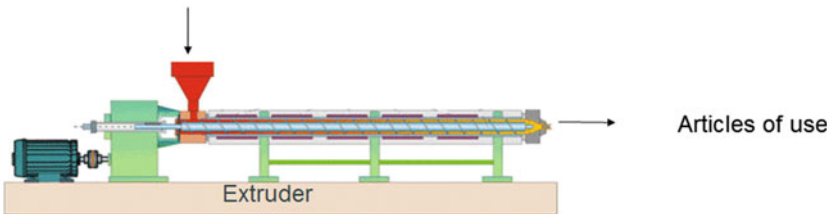


Fig. 14 Silane copolymer process

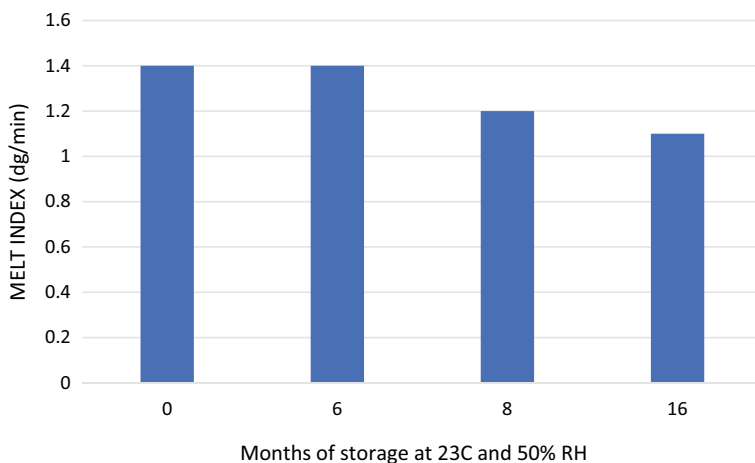


Fig. 15 Demonstration of storage stability of reactor copolymer [26]

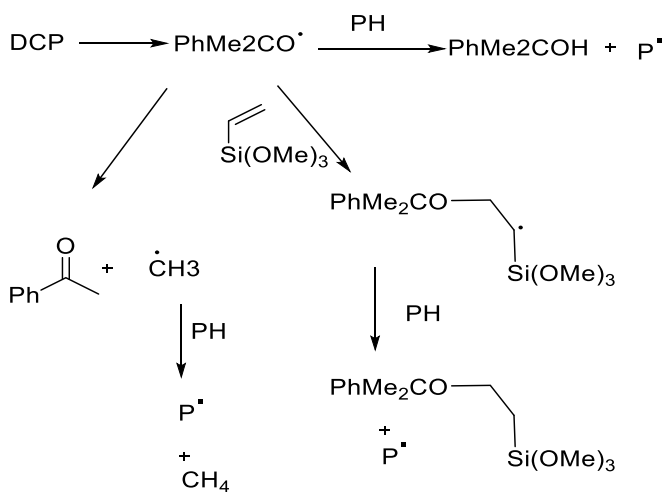
2.3 Silane Crosslinkable Grafted Polymer

Of the wide range of chemistry that may be brought to bear on functionalizing polyolefins, radical-mediated graft modification is most widely practiced technology. The process is robust and relatively inexpensive reagents are used. Furthermore, the chemistry is readily adapted for use in conventional polymer processing equipment. The chemistry and engineering principles that support these reactions have been reviewed recently by Moad [27] and by Russell [28]. The main disadvantage of radical-based modifications is the molecular weight change that accompanies graft addition. Functionalization requires polymer macroradicals to be produced in relatively low yields, and while radical-radical combination is of little consequence in small molecule systems, the coupling of polymer chains can compromise processing characteristics by increasing melt viscosity. This is a serious issue for ethylene-rich polyolefins [29].

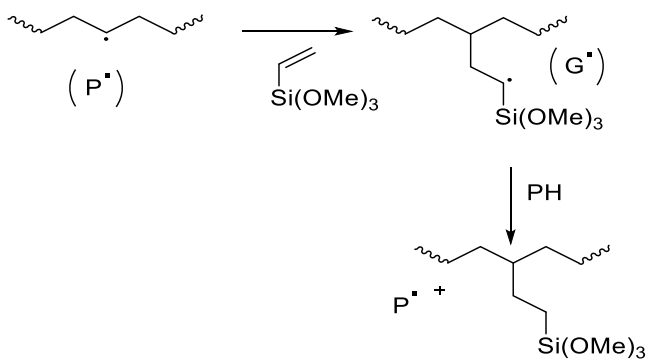
The main reactions that underlie peroxide-initiated polyolefin modifications are illustrated in Fig. 16. As with all chain processes, process designers are concerned with initiation of radical intermediates, propagation that leads to graft addition, and termination leading to non-radical products. The general objective is to maximize kinetic chain lengths by establishing conditions that favor propagation over radical-radical termination. In doing so, the number of required radicals is minimized along with the yield of undesirable crosslinking and/or chain scission reactions [30].

Industrial reactive extrusion processes must be carried out above the melting point of the polymer. This establishes a minimum operating temperature of 130 °C for polyethylene. Given its close relationship to radical concentrations, the half-life of an initiator at the processing temperature is a key reaction parameter. Long half-lives adversely affect throughput, while very short half-lives give rise to high

Initiation



Propagation



Termination

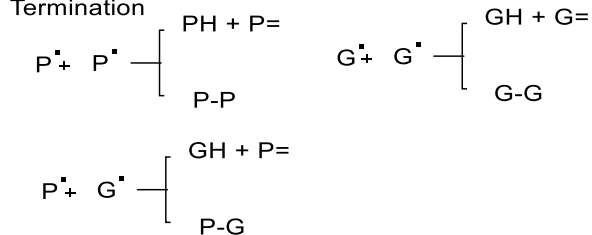


Fig. 16 Principal reactions of a conventional grafting process [30]

instantaneous radical concentrations, which increase the frequency of radical–radical termination and reduce the kinetic chain length of graft propagation. Given that reactive extrusion processes typically operate with residence times of at most a few minutes, commercially relevant half-lives are of the order of 1 min.

Graft propagation involves a closed sequence of macro-radical attack on monomers, and hydrogen atom transfer from the polymer to the resulting adduct. The addition of a carbon-centered radical to an olefin is usually energetically favorable as a new C–C σ bond (~ 370 kJ/mol) is formed at the expense of a weaker C = C π bond (~ 235 kJ/mol). In the case of vinyl silanes, attack occurs at the unsubstituted carbon due to steric effects. The hydrogen atom transfer component of propagation occurs both intermolecularly and intramolecularly, thereby affecting the distribution of grafts among polymer chains. Whereas inter-molecular transfer will introduce functionality to a different polymer chain, 1,5-intramolecular hydrogen abstraction promotes the repeated functionalization of a single molecule by placing grafts in close proximity. Since a linear transition state is preferred for these abstraction reactions only six- or seven-membered transition state allows such geometry.

Studies on polyethylene [31] indicated multiple single chain graft with graft content increasing linearly with the amount of silane charged in the system. Wong and Varral [32] performed grafting of vinyltrimethoxysilane onto different grades of polyethylene using DCP (0.1 wt%). LLDPE exhibited a much larger increase in free-radical-induced chain extension than LDPE or HDPE. Highly chain-extended LLDPE could be turned into a high crosslink density network without requiring much silane crosslinking. On the other hand, the less chain-extended HDPE or LDPE required much more silane crosslinking, and therefore longer crosslinking times, to achieve a satisfactory network structure. The relatively low level of silane grafting and free-radical-induced chain extension together with the tightly packed lamellar structure of HDPE rendered the resin difficult to crosslink rapidly to form a highly crosslinked structure. In 1974 BICC and Maillefer [33] jointly patented the Monosil process, where peroxide, silane and catalyst are directly injected into a single screw extruder thus combining the grafting and compounding steps. It has the advantage of bringing flexibility for resin architecture but increasing the process complexity overall. This results in increased time to stable steady state operation and increased scrap-rate during article fabrication [25]. Critical elements appear to be a 30/1 L/D extruder to which silane/peroxide/catalyst solution is metered in and a barrier screw which keeps solids pellets out of the grafting zone until melted (Fig. 17).

In 1968 Midland silicones patented the Sioplas process for crosslinking polyethylene [34]. This two-step process (Fig. 18) involves the grafting of vinyl silane onto polyethylene using an organic peroxide (n.b. peroxide concentrations are around twenty times less than that used in the peroxide crosslinking of polyethylene). In the second step, the grafted resin is re-extruded or fabricated with catalyst and other additives into a finished article. In the first step, longer grafting extruders and considerations discussed above are pertinent. In the second step standard PE extruders with length to diameter ratio (L/D) of at least 20:1 and a compression ratio of about 3:1 is used.

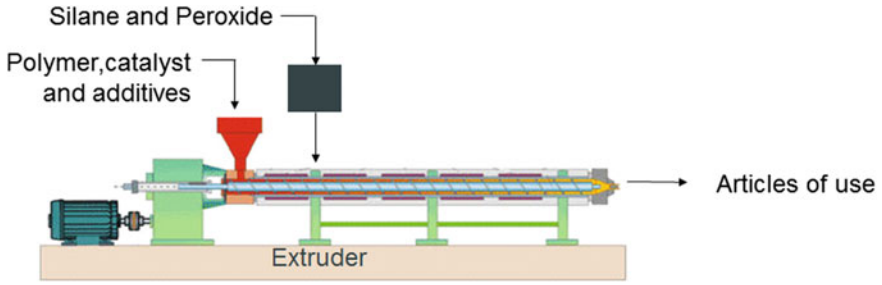
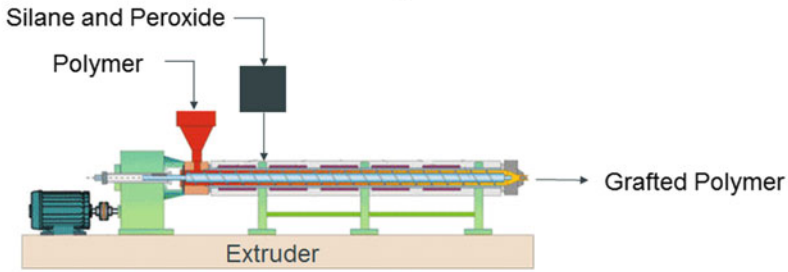


Fig. 17 Monosil process for silane functionalization

Step 1: Grafted Polymer manufacturing



Step 2: Fabrication and Curing

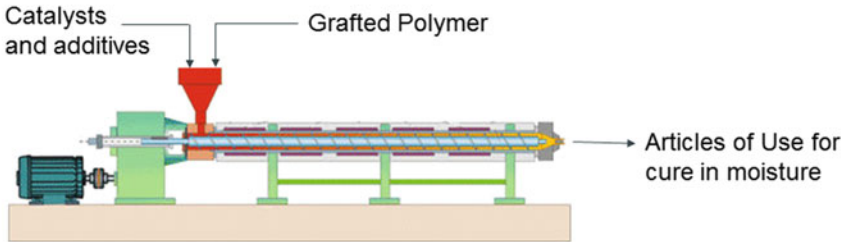


Fig. 18 Sioplas process for silane functionalization

3 Major Applications of XLPE and Related Processes

The following section discussed some of the considerations for use of XLPE in applications. The section will describe briefly process and fabrication basics for a few popular applications.

XLPE for electrical cables (peroxide cure)

LDPE is ideally suited to wire and cable insulation due to its outstanding electrical properties and processability. It has a low dielectric constant, a low tan delta dissipation factor and a high resistivity. Being a semicrystalline thermoplastic, polyethylene

softens and eventually flows at elevated temperature, rapidly losing its mechanical performance and severely restricting its' effective temperature of operation. This disadvantage is overcome by crosslinking the polymer chains. Medium and higher voltage power cable cores are typically composed of a stranded conductor (aluminum or copper), semi-conductive conductor shield, crosslinked polyethylene (XLPE) insulation, and a bonded or strippable semi-conductive insulation shield. A typical peroxide cured cable is produced by the 'triple-extrusion' process. Here, the cable is produced in a single pass and the layers are applied one after another in a specialized die. Several configurations of the die are available, and the key consideration is to minimize the exposure of extruded layers to the environment. The production speed is controlled by the extruder outputs, the continuous vulcanization operation and cooling. The continuous vulcanization (CV) curing process for manufacturing of such peroxide crosslinked cable cores is well known.

Figure 19 shows a schematic of a catenary continuous vulcanization line. Of key importance for the curing process is the CV tube, including both heating and cooling sections. Key process parameters determining the temperature development along the cable are: CV tube layout (length, diameter), heating zone-temperatures, atmosphere and pressure, cooling medium and temperature, cable dimensions, line speed (residence time), CV tube entry temperatures (i.e., conductor temperature, polymer melt temperatures), assumptions on the energy transmission from the tube heating and cooling into the cable (radiation, convection), and material parameters (heat capacity, conductivity, density) including those of the conductor. The cure kinetic data of the peroxide-containing materials are required to calculate the development of crosslinking along the CV tube, based on the temperature calculations.

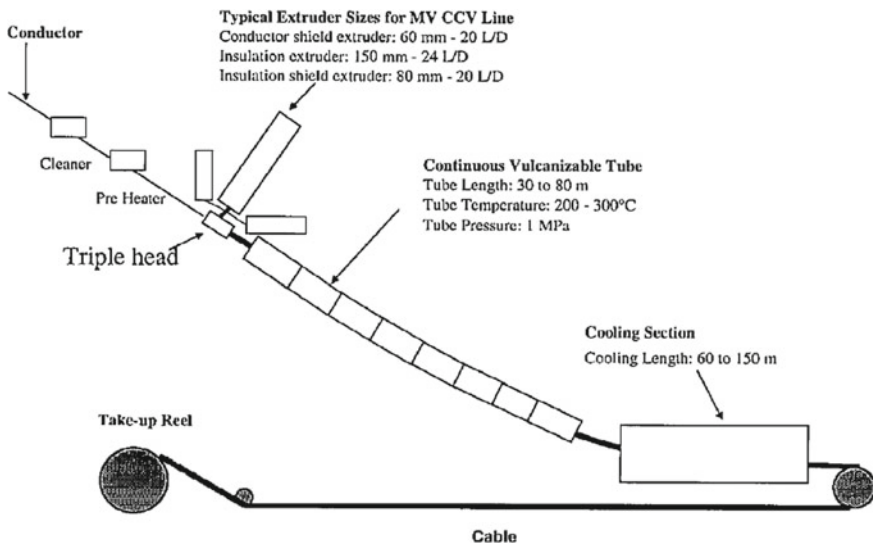


Fig. 19 Schematic of typical CCV line

As the cable core enters the CV tube, the temperature distribution within the polymer mass is affected by heat flow into the polymer mass from the outside of the cable, but also by interaction with the conductor.

- Transfer of heat from the heated tube surface to the cable core will depend on radiation and convection through the medium (steam or nitrogen). The radiation efficiency can be significantly affected by the emissivity factor of the tube inner surface and of the cable (black body radiation at a certain efficiency, expressed by the emissivity factor). The effective heat transfer will be affected by the surface area, hence diameter of the tube and of the cable core. The latter is affected by thermal expansion, thus density as a function of temperature. When cooling in water, this will occur by convection mainly. When cooling in nitrogen, radiation will also play a role.
- The conductor can be cold or pre-heated. The heat capacity of the conductor, being either aluminum or copper, will be important. Conduction of heat in axial direction will be relatively high through the metal conductor and can be an important factor in the heat balance.
- The conduction of heat within the polymer mass will depend on its thermal conductivity, but also on its heat capacity. The values of these parameters are a function of temperature. When the peroxide in the polymer mass decomposes, this results in some additional heat release.

XLPE for silane cure cable

In the production of low-voltage cables, the conductor is fed into the process by a pay-off reel. Before passing into the crosshead and die, it can be straightened, pre-heated and cleaned. After the coated wire leaves the crosshead, it passes through cooling troughs. Water is normally used as the cooling medium. The cooling length and water temperature are designed to prevent deformation of the coated wire in the wind-up operation (Fig. 20).

Other operations after cooling may include air wipe, diameter and thickness measurement, spark testing, capacitance testing and printing to mark cables. The coated wire passes next through a capstan or belt puller to pull it through the line and moves into a take up station [35, 36].

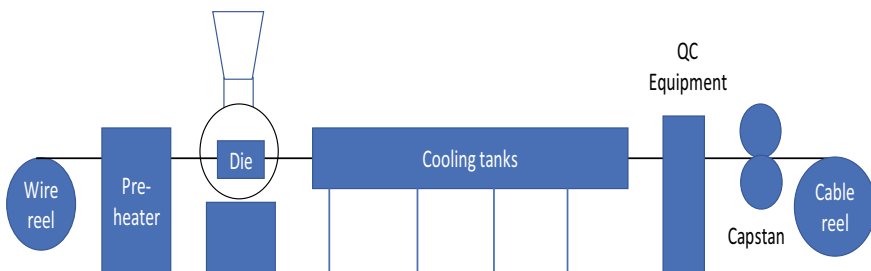


Fig. 20 Typical wire extrusion line

The majority of the extruders are 24 L/D and the most common diameter ranges from 60 to 150 mm. Compounds are fed through the feed hopper into temperature-controlled extruder. Four heating/cooling zones on the barrel are typical. In the cable process selection of proper screw design is paramount. A typical extruder screw may consist of a single flight square pitch screw with three sections feed, transition and metering as discussed earlier for single screw extruders. Many screws may also have a Maddock mixing head at the end. A typical compression ratio of 3 is used. The wire coating process often runs with a screen pack which is supported by a breaker plate. It provides a mechanical seal between the crosshead assembly and extruder. It also changes the pattern of flow from rotational to longitudinal along the screw axis (Fig. 21).

In the crosshead the wire passes through a mandrel and guider tip into the forming die. The melt enters from the side wraps around the mandrel and rejoins on the far side thereby coating the conductor or cable core. There is a weld line which may be visible where the melt rejoins. The weld line can show up as a defect on the extruded cable if the crosshead is not properly designed. To achieve bonding between the polymeric layer and conductor the melt is applied over the wire by a pressure die. In a pressure die the guider tip ends inside the die. In this set up the melt under pressure is in direct contact with the conductor inside the die and moves through the die around the conductor. In jacket or sheath coating where the core is much larger it is difficult to prevent leakage of the melt into the guider tip under pressure. To control this problem the tip is extended to the face of the die. This is the principle of a tube die in which the melt exits the die as a concentric tube around the core coming out through the center of the guider tip. A vacuum between the extruded tube and the core can be applied to help the drawdown process. The tube die is used on cores of irregular shapes to obtain a fairly uniform wall thickness and a smooth final cable [37].

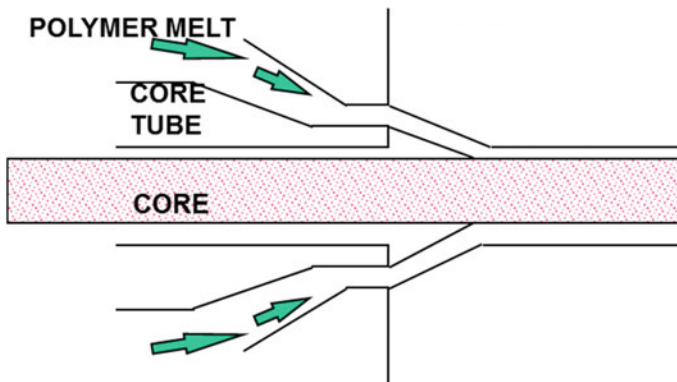


Fig. 21 Crosshead assembly from cable extrusion

XLPE for pipes

In the early 1960s polyethylene pipe has been introduced in water and gas pipe applications. Since the mid-1970s the use of polyethylenes in piping applications has been increasing. The use of polyethylene in these and other subsequent applications such as drip irrigation tubing, large diameter sewer and slurry pipe as well as electrical conduits can attribute it to the favorable advantages of polyethylene pipe or other piping materials such as cast-iron, steel. These favorable advantages are the following.

- Lighter weight,
- Ease of installation,
- Flexibility,
- Chemical resistance
- Corrosion resistance
- Non-electrolytic
- Low coefficient of friction
- Abrasion resistance
- Long service life
- Toughness and weatherability.

Some limitations may include its low use temperature, lower pressure ratings and susceptibility to mechanical damage. This is where crosslinked polyethylene closes the gap and finds expanded use [38]. They offer benefits such as

- Extension of maximum service temperature,
- Improved chemical resistance against organic solvents or oils,
- Better abrasion resistance,
- Improved impact properties,
- Improved creep and stress rupture performance.

Generally, these improved properties seem to be drastically increased at high gel contents. Moisture crosslinking with vinyl silane has a lot of advantages, higher line speed and low energy costs, number of process alternatives, less initial investment, formulation flexibility, lower overall operating costs, uniform crosslinking, applicable to a wide range of polymers, better mechanical flexibility [39]. The general principles of extrusion described earlier in this chapter are relevant to the extruded pipe fabrication process as well [40] 41.

The Pont A'Mousson process of making peroxide crosslinkable pipes follows the cable process and crosslinking is achieved in a salt bath at elevated temperatures. In the Engel process, the fabricated tubes are passed through heated dies for crosslinking.

Other Applications

The crosslinkable formulations intended for molding applications are not too different from those used for extruded products. These compositions are fabricated using injection, compression or transfer molding. A good example is the use of

crosslinked polyethylene in making tanks varying in sizes from a few to thousands of gallons are being used in agriculture and industrial applications [42]. Heat shrink tubing is also an area of XLPE applications owing to the elastic memory effect after crosslinking [43]. XLPE is also popular in foams made through thermoforming process for applications in automotive, sports and leisure markets. The science and technology of polyethylene foams based on crosslinked PE has been reviewed recently by Rodriguez-Pérez [44].

4 Concluding Remarks

Crosslinked polyethylene continues to be a popular item of choice in selected applications and a ripe area for innovation in academia and industries. The material combines good chemical resistance with excellent thermomechanical properties for a variety of applications. Compounding of formulation components through a variety of technologies have evolved with time and a range of options are practiced. For peroxide crosslinkable polyethylenes the incorporation of peroxide is a key step in the process. For silane crosslinkable polymer, both copolymers and grafted resins are used. The fabricators of application and articles employ a variety of methods depending on end-use, e.g., extrusion, molding, etc. The curing process for the fabricated articles are thermally activated or moisture activated depending on the technology used.

A key feature of differentiation between the process lies in the physical state that crosslinking happens. For peroxide cured processes most of the crosslinking happens in the melt state and it can be safely assumed that the crosslinking events are random. As the melt cools down to the solid state at the end of a fabrication process the polymer chains start to crystallize. Crosslinked polymer chains or segments have a much larger radius of gyration and tend to avoid being part of crystalline domains. This results in disruption of crystallinity and reordering of the structure. Hence, it is often reported that density decreases with increasing crosslink density for these systems [45]. So the physical properties are largely dictated by the crosslink densities for the peroxide crosslinked system. However, for silane cure systems the crosslinking largely happens in the solid state after fabrication of the article. Beyond the first shift there is not much change in the thermal properties, and it can be independent of the level of cure [46]. Thus the physical properties tend to be largely dominated by the properties of the starting material itself. As research in this area progresses newer methods and strategies will develop to bridge differences between current processes and increase industry efficiencies.

References

1. Gustafsson B, Boström JO, Dammert R (1998) Stabilization of peroxide crosslinked polyethylene. *Die Angewandte Makromolekulare Chemie* 261(1):93–99

2. Gross LH, Bartlett TM (1989) Process for grafting diacid anhydrides. US Patent 4,857,600
3. Toshio T, Hideaki T (1977) Polyethylene composition. US Patent 4,010,127
4. Clark CF, Hill RW (1963) Polyethylene compositions. US Patent 3,108,981
5. Thompson M, Donoian G, Christiano J (2000) Melting mechanism of a starved-fed single-screw extruder for calcium carbonate filled polyethylene. *Polym Eng Sci* 40(9):2014–2026
6. Spalding MA, Chatterjee A (2017) *Handbook of industrial polyethylene and technology: definitive guide to manufacturing, properties, processing, applications and markets* set. Wiley
7. Campbell GA, Spalding MA (2013) *Analyzing and troubleshooting single-screw extruders*. Carl Hanser Verlag GmbH Co KG
8. Spalding MA, Hyun K (2003) Troubleshooting mixing problems in single-screw extruders. In: ANTEC-conference proceedings
9. Caronia PJ, Cogen JM (2003) Polyethylene crosslinkable composition. US Patent 6,656,986
10. Cogen JM (2002) Polyethylene crosslinkable composition. US Patent 6,455,616
11. Meskat W, Erdmenger R (1944) DBP 872 732 Gleichdrall-Dreifachschnecke mit Dichtprofil zum Abpressen. Priorität
12. Sorcinelli GJ (1997) Continuous mixing, in the mixing of rubber. Springer, pp 211–220
13. Canedo E, Valsamis L (1994) Selecting continuous compounding equipment based on process considerations. *Int Polym Proc* 9(3):225–232
14. White JL (1991) Twin screw extrusion: technology and principles
15. <https://www.gem-chem.net/machinerytse.html>
16. Palmer WH, Hannon BM (1963) Internally heated die plate for polyethylene extruder. US Patent 3,114,169
17. Wiley VCH 9.2.3 Pelletizing, in *Ullmann's polymers and plastics—products and processes*, 4 volume set. Wiley
18. Kharazi A, Dunchus NW (1999) Process for the production of a thermosetting composition. US Patent 5,972,267
19. Talreja M et al (2020) Peroxide-crosslinkable compositions and processes for their manufacture. US Patent 10,577,482
20. Albizzati GP (2001) Process for producing an electrical cable, particularly for high voltage direct current transmission or distribution, U.P. Office, Editor. 2001, Prysmian Cavi e Sistemi Energia SRL: US
21. Bailey DL, Mixer RY (1957) Polymerization of vinylalkoxysilanes. US Patent 2,777,869
22. Ehrlich P, Mortimer G (1970) Fundamentals of the free-radical polymerization of ethylene. *Fortschritte der Hochpolymeren-Forschung*, pp 386–448
23. Patel RM et al (2008) *Polyethylene: an account of scientific discovery and industrial innovations*. ACS Publications
24. Sultan B-A, Palmlöf M (1994) Advances in crosslinking technology. *Plast Rubber Compos Process Appl* 21(2):65–73
25. Munteanu D (1997) Moisture cross-linkable silane-modified polyolefins. In *Reactive modifiers for polymers*. Springer, pp 196–265
26. Chaudhary BIEA (2019) Effect of polyethylene structure on silane grafting and properties of associated moisture-crosslinked compositions and cable constructions. In: ANTEC 2019. SPE Detroit
27. Moad G (1999) The synthesis of polyolefin graft copolymers by reactive extrusion. *Prog Polym Sci* 24(1):81–142
28. Russell K (2002) Free radical graft polymerization and copolymerization at higher temperatures. *Prog Polym Sci* 27(6):1007–1038
29. Suwanda D, Balks ST (1993) The reactive modification of polyethylene. I: the effect of low initiator concentrations on molecular properties. *Polym Eng Sci* 33(24):1585–1591
30. Parent JS, Parodi R, Wu W (2006) Radical mediated graft modification of polyolefins: Vinyltriethoxysilane addition dynamics and yields. *Polym Eng Sci* 46(12):1754–1761
31. Spencer M, Parent JS, Whitney RA (2003) Composition distribution in poly (ethylene-graft-vinyltrimethoxysilane). *Polymer* 44(7):2015–2023

32. Wong W, Varrall D (1994) Role of molecular structure on the silane crosslinking of polyethylene: the importance of resin molecular structure change during silane grafting. *Polymer* 35(25):5447–5452
33. Swarbrick P, Green WJ, Maillefer C (1978) Manufacture of extruded products. US Patent 4,117,195
34. Scott HG (1972) Cross-linking of a polyolefin with a silane, U.P. Office, Editor. Midland Silicones
35. Richardson PN (1974) Introduction to extrusion. Society of Plastics Engineers Brookfield Center, Conn
36. Levy S, Carley JF (1989) *Plastics extrusion technology handbook*. Industrial Press Inc.
37. Hopmann C, Michaeli W (2016) *Extrusion dies for plastics and rubber: design and engineering computations*. Carl Hanser Verlag GmbH Co KG
38. Kutz M 32.4.1 cross-linking technologies, 2nd edn. In: *Applied plastics engineering handbook—processing, materials, and applications*. Elsevier
39. Gedde U, Ifwarson M (1990) Molecular structure and morphology of crosslinked polyethylene in an aged hot-water pipe. *Polym Eng Sci* 30(4):202–210
40. Morshedian J, Mohammad HP (2009) Polyethylene cross-linking by two-step silane method: a review
41. Sultan B-Å et al (2011) Crosslinkable high pressure polyethylene composition, a process for the preparation thereof, a pipe and a cable prepared thereof. US Patent 8,017,710
42. Dodiuk H, Goodman SH 17.9.2 rotational molding, 3rd edn. In *Handbook of thermoset plastics*. Elsevier
43. Dodiuk H, Goodman SH 17.9.3 heat-shrinkable tubing, 3rd edn. In *Handbook of thermoset plastics*. Elsevier
44. Rodríguez-Pérez M (2005) Crosslinked polyolefin foams: production, structure, properties, and applications. *Crosslink Mater Sci*:55–56
45. Manley TR, Qayyum MM (1971) The effects of varying peroxide concentration in crosslinked linear polyethylene. *Polymer*:176–188
46. Sengupta S et al (2008) Evolution of crosslinks during moisture cure of ethylene-vinylalkoxysilane copolymers in power cables. *Int Wire Cable Symp*

Chapter 5

Physicochemical Properties of XLPE



Kai Zhou and Yaping Wu

1 Structure of XLPE

1.1 *Overviews of Polymer Structure*

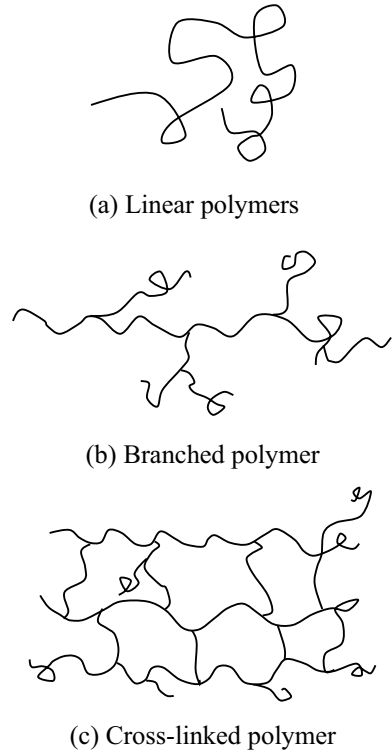
Macromolecule polymers refer to the compounds that are formed by a large number of atoms or atomic groups and have a molecular weight of more than 10,000; meanwhile, all the atoms and the atomic groups are mainly combined by covalent bonds [1]. Macromolecule polymers have repeating structural units and large molecular weight, and they can be divided into two types: inorganic polymers and organic polymers. The repeating structural units are called monomers and the basic structure of the polymer chain unit is called the structural unit.

According to the geometry of polymers, polymers can be divided into two categories, namely linear polymers, branched polymers, crosslinked polymers, star-like polymers, ladder-like polymers, etc., as shown in Fig. 1.

Linear polymers have more flexibility and are usually thermoplastic, and they can be melted by heating and dissolved in a specific solvent. The processing technology of linear polymers is relatively easy. Branched polymers are derived from some branch chains of linear polymer so they have the same structural units as the main chain,

K. Zhou (✉) · Y. Wu
College of Electrical Engineering, Sichuan University, Chengdu, Sichuan, China
e-mail: zhoukai_scu@163.com

Fig. 1 Geometry of the polymer chain. (a) Linear polymers. (b) Branched polymer. (c) Crosslinked polymer



and they are also soluble and fusible. Due to the existence of the branch chain, the distance between the molecules is increased, and the intermolecular force is reduced to improve the elasticity and plasticity of the polymer. The branched polymers have many properties similar to the linear polymers, while its physical and mechanical properties are significantly different from the linear polymers. Crosslinked polymers have a three-dimensional reticular structure [1], as shown in Fig. 1c. As for high-density polyethylene, linear low-density polyethylene and crosslinked polyethylene, although they have the same main chains, their physical properties are quite different due to the different condensed structures [1].

The solid structure of a polymer is an aggregated structure, which is also known as the higher-order structure. The higher-order structure of the polymer directly affects the performance of the material. The aggregated structure of the polymer can be divided into two basic forms: crystalline form and amorphous forms. Polymers that are predominantly amorphous or dominantly amorphous are called amorphous polymer materials, and polymers with a crystalline structure are called crystalline polymers.

Amorphous polymers have three different physical states: glassy state, rubbery state and viscous flow state. These three physical states can be transformed each other as the temperature changes. At the same time, the performance of the material

will also change. For example, rubber is linear amorphous phase polymer with better elasticity, while polyvinyl chloride (PVC) plastic is a semicrystalline polymer with better hardness. That is because their physical states are different at room temperature. Since the glass transition temperature (T_g) of PVC is at the range of 77–90 °C, it is at glassy state at room temperature, while rubber is at rubbery state at room temperature. When heated to a certain temperature, the plastic will transform from glassy state to rubbery state and lose the original physical properties. When the temperature continues to rise to a certain level, it will further transform from the rubbery state to the viscous flow state. For the rubber, if the temperature is reduced to a sufficiently low level, it will transform from the rubbery state to the glassy state. The elasticity of rubber will be lost and the rubber will become as hard as plastic [1]. Therefore, when applying polymer synthetic materials, the temperature range must be considered in order to exert its material properties.

Crystalline polymers have very regular internal molecular arrangement, and they present large intermolecular forces, so their heat resistance and mechanical strength are higher than those of amorphous polymers, while their melting enthalpies are relatively low. Crystalline polymers (such as polyvinyl chloride and isotactic propylene) at melting state can be also considered as the most disordered amorphous state, and this state can be also called as the amorphous state. To study the crystallization behavior of crystalline polymers often starts from their melting state. Quenching a crystalline polymer from its melting state to a certain temperature, such as the glassy transition temperature T_g , may let the polymer transform into amorphous glassy state, or it may lead to a partially crystalline polymer with relatively low crystallinity. The disordered state of the amorphous part will be different from the amorphous state at this time, and then the crystallization behavior can be studied from the amorphous glassy state or the partially crystalline state.

In summary, to understand the basic properties of polymers (high elasticity, plasticity and mechanical strength, hardness, etc.), we need to analyze the polymer composition, molecular weight, molecular structure, aggregation state and other several aspects. The reason why plastic is difficult to deform and has good mechanical strength is because of its linear or bulk structure, and its molecular chain and chain segment cannot move at room temperature. The reason why rubber has good elasticity is because it is a highly linear polymer with low crosslinking degree, which makes the molecular chain harder to move at room temperature, while its movement in segment is relatively easy.

1.2 Structure of XLPE and Water Tree Retardant

Polyethylene, which is solid at room temperature, has linear macromolecular structure, but as the temperature rises to the softening point, relative displacement will occur between the molecular chains, so its service temperature is limited. To improve the temperature resistance grade of polyethylene, crosslinking methods are adopted [2]. As each polyethylene molecular chain is independent to varying degrees, through

the crosslinking, different polyethylene molecules can be aggregated together. In other words, the polyethylene molecular chains are connected by branching connection after the cross linking, which makes the macromolecular structure become a three-dimensional network from linear structure, and transforms the material from thermoplastic polymer to thermosetting polymer, as shown in Fig. 2. After crosslinking, polyethylene not only improves its mechanical strength, heat resistance, anti-creep and anti-cracking performance, but also maintains its original low dielectric loss and other good electrical properties.

Compared with polyethylene (PE), crosslinked polyethylene (XLPE) has the following advantages [3, 4]:

1. XLPE inherits the high breakdown strength, low dielectric loss, moisture resistance, aging resistance and other properties of PE;
2. XLPE has better heat resistance: as the polyethylene molecule changes from linear structure to network structure during the crosslinking process, its heat resistance has been significantly improved. The long-term allowable working temperature of polyethylene before crosslinking is only 70 °C, while this value reaches 90 °C after crosslinking, and working current capacity of XLPE has been significantly improved;
3. XLPE has better environmental stress crack resistance and cold flow resistance, and it also improves chemical stability, heat aging and solvent resistance;
4. Air bubbles are eliminated during the production process of XLPE, which makes the insulation resistance of the cable be improved.

Crosslinked polyethylene is formed by physical or chemical changes of polyethylene. This kind of change is called crosslinking. There are a variety of crosslinking methods. Common crosslinking methods are mainly peroxide crosslinking, radiation crosslinking and silane crosslinking. Crosslinking methods can be also divided into the wet-type crosslinking and the dry-type crosslinking. The wet-type crosslinking results in higher water content and large microporous size. For this reason, the wet-type crosslinking method is mainly used for low-voltage cables. In the dry-type crosslinking, nitrogen and molten salt are always used as the pressure medium for chemical reactions, the reaction is under electric heating or heating with silicone oil,

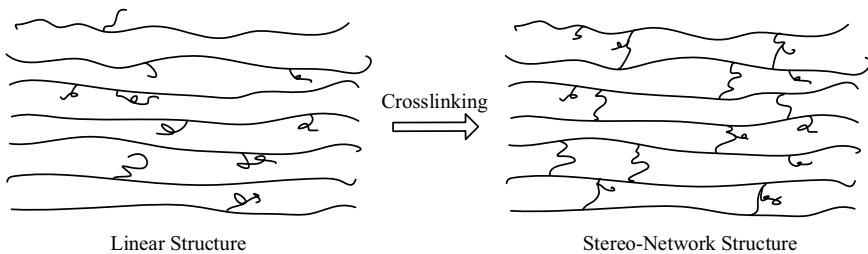


Fig. 2 Crosslinking of polyethylene molecules

molten salt, etc. The water tree retardancy of cable was greatly improved after the application of the dry-type crosslinking procedure.

Originally, the cable insulation is consisted of non-crosslinked polyethylene. However, the mechanical properties of the polyethylene are poor and it is prone to initiating water trees, which results in the remarkable reduction of their service lives. In order to improve the ability of resisting water trees [5–7], the industry adopts the crosslinked polyethylene for cable insulation which is known as XLPE. After crosslinking, the mechanical properties of the cables are significantly improved. The probability of water tree initiation and the propagation rate of water trees are reduced [8–10]. Later, a new water tree retardant cable is produced, which is further improved by changing the molecular structure of polyethylene or adding some additives into XLPE. In order to water tree initiation of XLPE, the following principles are considered [11]:

1. Polar additives or molecular chains with strong polarity which can absorb and prevent the migration of water under high electric fields to inhibit the growth of water trees.
2. Inhibit water tree by adding low molecular weight additives.
3. Mix other polymers which can increase the plasticity of the material.

1.3 Molecular Chain Movement in XLPE

Structure of material is the basis of the physical and mechanical properties. Different materials have different structures, and their properties are different. Even if the materials with the same structure also can show different physical and mechanical properties due to different molecular chain movement. Therefore, it is necessary to understand the molecular chain movement of polymers in order to establish the relationship between structure and performance. Molecular movements have three characteristics: the multiplicity of motion units, the time dependence of molecular movements and the temperature dependence of molecular dependence.

1. The multiplicity of motion units

Due to the long-chain structure of the polymer, the molecular chain not only has large molecular weight, but also has polydisperse. In addition, it also has different side groups, plus branching, crosslinking, crystallization, orientation, copolymerization and so on, which make the motion units have multiple properties. The motion units of a polymer can be polymer chains, a side group, branched chains, chain elements, chain segments, etc. The movement modes include vibration, rotation, and translation.

The overall movement of the polymer chains: the polymer chain as a whole has a mass center, and the movement of mass center needs to be completed through the coordinated movement of the segments. The macro-feature of this movement is the circulation or the solution of the polymer melt or the permanent deformation of the polymer material.

Segment movement: while the polymer chain maintains its mass center, part of the segments moves by single bond rotations. The movement of the polymer segments can cause macromolecules to stretch or to curl, and these kinds of conformational changes have an important impact on the material. The macro-feature is the transition of the polymer from the glassy state to the rubbery state, such as the stretching and retraction of the rubber.

Movement of chain elements, branched chains, side groups, etc.: the movement of small units requires less energy than the movement of chain segments, which can occur at the glassy transition temperature.

Crystal zone movement includes: crystal form transformation, crystal wafer slip, accordion movement of folding chain in crystal zone, etc. Customarily, the movements of polymer molecules are divided by two units with different size, which are, the movements of the entire macromolecular chain called large Brownian motion, and the movements of the chain segments or the movements of some smaller units below chain segments' size called micro-Brownian motion.

2. Time dependence of molecular motion

Small molecular substances will immediately respond after receiving external effects, while the polymer chain has a large structure and responds relatively slowly to external effects. Under external effects, the material transforms from a balanced state through molecular motion to adapt to the outside world, and the process is called the relaxation process, which makes the equilibrium state from old to new, and the time required to complete the relaxation process is called the relaxation time. For polymers, the relaxation process can be very long, from a few days to years. Different motion units have different degrees of time dependence. The larger the motor unit, the longer the relaxation time will be.

3. Temperature dependence of molecular motion

Temperature has two effects on the movements of polymer molecules: the first one is that the kinetic energy of the movement unit increases and make it active. The second is that the temperature will increase and the volume will be expanded, and this kind of change will provide free space for the movement unit to move, which accelerates the relaxation process and shortens relaxation time.

In general, the relationship between relaxation time and temperature is consistent with the chemical rate process theory (Arrhenius formula):

$$\tau = \tau_0 e^{\Delta E/RT} \quad (1)$$

where:

- τ_0 constant,
- ΔE the activation energy required for the relaxation process,
- R constant

Amorphous polymers exhibit three different physical states as temperature changes: glassy state, rubbery state, and viscous flow state. Three physical changes correspond to three mechanical states. At the glassy state, the material is rigid and solid, and only small deformation occurs under the external forces. In other word, material has larger module value at this state; the deformation capacity of rubbery state materials increases significantly, and the material becomes a soft elastomer; the viscous flow state materials have larger deformation, and irreversible viscous flow will occur. When the crosslinking density is not high, the motion of the segments will not be affected, and there will be a large range of elastic deformation. When the crosslinking density is high, as the crosslinking degree increases, the movement of the chain segments becomes more and more difficult, and the glass transition temperature becomes higher.

Without applying external forces, the polymer's macromolecular chains are always entangled each other and appear as random clusters, as shown in Fig. 3a. When subjected to external forces such as shear stress or tensile stress, the polymer's macromolecular chains, segments or crystallites will be ordered along the direction of the external force, resulting in different degrees of orientation and forming an oriented state structure, as shown in Fig. 3b. The orientation state of the polymer is thermodynamically non-equilibrium. When the external force is removed, the thermal motion of the molecules always makes the ordered structure tend to be disordered, which we call de-orientation. As a result, the orientation degree depends on the external force (should be below the fracture stress) and the thermal movement of macromolecules. Therefore, if the orientation needs to be maintained, the temperature must be quickly reduced below the glass transition temperature after orientation to freeze the movement of macromolecules and segments.

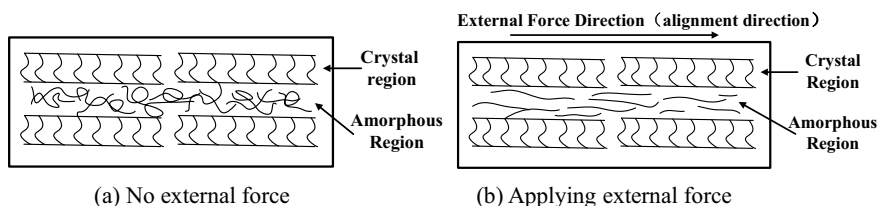


Fig. 3 Orientation of polymer under external force. (a) No external force. (b) Applying external force

2 Physical Properties of XLPE

2.1 Electrical Properties

The electrical behaviors of dielectrics mainly reflect their conductivity properties, dielectric properties, and electrical strength under the operation. They are represented by four main parameters, which are electrical conductivity (insulation resistivity), dielectric constant, dielectric loss factor $\tan \delta$ and breakdown strength.

Dielectrics will appear electrophysical phenomena such as polarization, conductance, and dielectric loss under the electric field. However, the polarization, conductance, and dielectric loss of gas media are very small and generally can be ignored. Therefore, those characteristics are only need to be noted in liquid and solid media.

1. Polarization

Dielectric polarization is the phenomenon in which the charge of molecules and atoms inside the dielectric is elastically deformed and the orientation of the dipoles corresponds to the direction of the electric field. At this time, the displacement of the charge is mostly microscopic and within the range of atoms or molecules, and an electrical moment (dipole moment) is generated. The most basic types of polarization are electron polarization, atomic polarization, and dipole polarization [12].

Electron polarization: under the external electric field, the orbit of the electrons in the atoms of the medium will be elastically displaced relative to the nucleus.

Atomic polarization: each nucleus in a molecule or group is displaced relative to each other under the action of an external electric field.

Dipole polarization: under the electric field, the intrinsic dipole moments of the molecules in the medium will be aligned along the direction of the electric field. The vector sum of all dipole moments is not zero, and the medium will generate macroscopic polarization intensity.

2. Conductance

No dielectric can be an ideal insulator, and they always have more or less charged particles (carriers) inside them, such as movable positive and negative ions, as well as electrons, holes, and charged molecular groups. Conductivity is a parameter describing the movement difficulty of charge in a substance. The standard unit of conductivity σ is Siemens/meter (abbreviated as S/m), which is the inverse of resistivity ρ , that is, $\sigma = 1/\rho$.

The factors that affect conductivity are: temperature, degree of impurity, anisotropy and so on. Conductivity has a great correlation with temperature. The conductivity of metal decreases with the increase in temperature, whereas the conductivity of semiconductor increases with the increase in temperature. At a certain range of temperature, the electrical conductivity can be considered approximately proportional to the temperature. In order to compare the electrical conductivity of a substance at different temperature conditions, a common reference temperature

Table 1 Dielectric loss factors and dielectric constant of common cables at 50 Hz [13]

The dielectric	$\tan \delta (10^{-3})$	ϵ_r
Impregnated paper	2–3	3.5
Polyethylene	0.2–0.4	2.2–2.3
XLPE	0.3–0.5	2.3–2.4
EPR	1.8–3	2.6–2.7

must be set. The correlation between electrical conductivity and temperature can often be expressed as the slope of the conductivity versus the temperature line graph. The doping level of the solid-state semiconductor will cause a large difference in the conductivity. Increasing doping level will cause the conductivity to increase. The conductivity of the aqueous solution depends on the concentration of its solute salt content or other chemical impurities that will decompose into electrolytes. The electrical conductivity of water sample is an important indicator for measuring the salt, ionic, and impurity components of water. The purer the water is, the lower the electrical conductivity it will be (Higher resistivity).

3. Dielectric Loss

There is no ideal dielectric without energy loss under electric field. In fact, there will always be a certain amount of energy loss while a dielectric is under electric field, those energy losses include losses caused by conductance and losses caused by some certain loss polarizations (such as dipole polarization, interface polarization, etc.), they are collectively called dielectric loss. Dielectric losses of some cable material are shown in Table 1, and their losses are generally low and are made of unipolar material.

Dielectric loss refers to the energy that is converted into thermal energy under the alternating electric field. Dielectric loss can be mainly divided into relaxation loss, resonance loss and conductivity loss according to the formation mechanism. The relaxation loss and the resonance loss are related to relaxation polarization and resonance polarization, while conductance loss is related to the conductance of the dielectric. The relaxation loss refers to the change in the degree and direction of the dielectric polarization as the alternating field E changes its strength and direction. If the dielectric is composed of polar molecules (polar dielectric) or contains weakly bound ions (such dipole polarization and ionic polarization are caused by thermal motion, which are called dipole and thermionic respectively) and it takes a certain time (relaxation time) for orientation polarization or displacement polarization, the phase difference between the dielectric polarization and the electric field will occur, which can generate the dielectric relaxation loss W_g . If the relaxation time τ of the polar molecules and thermionic that make up the dielectric is much larger than the period T of the alternating electric field, these particles will have no time to establish polarization, and the dielectric relaxation polarization will be very small. At low-frequency electric fields, the relaxation time of particles is much shorter than T , but the dielectric relaxation loss is also very small because the number of changes in

direction per unit time is very small. When the relaxation time is equal to the period T of the alternating electric field, the dielectric loss has a maximum value.

Relaxation polarization occurs in liquid and solid dielectric with polar molecules and weakly bound ions. For polymers with polar groups, relaxation polarization in the form of orientation polarization can also be produced by polar groups or chains with a certain length. The relaxation loss of liquid dielectrics is related to viscosity. For polar dielectrics with very low viscosity, such as water and alcohol, the relaxation loss occurs at the range of the centimeter band. The relaxation loss is related to temperature and electric field frequency.

The resonance loss and the conductance loss refer to the elastic displacement polarization of electrons and ions. The dielectric can be regarded as a collection of many oscillators, which are forced to vibrate under the action of electric field and finally consume the energy in the form of heat energy. When the electric field frequency is much higher or much lower than the oscillators' resonance frequency, little energy is consumed. Only when the electric field frequency is equal to the natural frequency of the oscillators (resonance), the loss of energy is the largest, so it is called dielectric resonance loss. For the electron elastic displacement polarization, it is in the ultraviolet frequency band. While for the ion displacement polarization, it is in the infrared frequency band.

4. **Breakdown strength**

Under a high electric field, the current passing through the polymer increases non-linearly with the electric field. When the electric field continues to increase, the current surges, and the polymer changes from an insulated state to a non-insulated state, which is called insulation breakdown. Insulation breakdown is an irreversible phenomenon of insulation failure. Polymer breakdown is divided into electrical breakdown, thermal breakdown and electrochemical breakdown.

(a) **Electrical breakdown**

In the low electric field, the carriers in the polymer get energy from the electric field. These energies are consumed in the collision of carriers with other carriers, molecules and atoms around them. When the carriers get energy from the electric field again, they can continue to move. Therefore, the polymer has stable conductance. But when the electric field strength reaches the critical value, the carriers gain enough energy from the electric field, and the carriers collide with polymers to produce electrons or ions. These new carriers get enough energy to collide with polymer and generate new carriers. This process is repeated periodically, and the number of carriers increases rapidly, the current rises sharply. Eventually, polymer breakdown will happen, which is called electrical breakdown.

The breakdown strength of the polymer under uniform electric field is only related to the chemical composition and properties of the polymer, which is often referred to as electrical strength or electrical intensity.

(b) Thermal breakdown

Under the action of strong electric field, the polymer will undergo dipole polarization. At the same time, the energy generated by overcoming the viscous resistance will be dissipated in the form of heat. If the polymer does not conduct heat quickly enough, the temperature inside the polymer gradually increases. With the increase in temperature, the internal conductivity in the polymer increases gradually, the dielectric loss is larger, more heat is released, and the temperature increases further. As a result, the polymer is oxidized, melted and coked, resulting in breakdown. The thermal breakdown occurs in the places where the heat dissipation is the worst and has the following characteristics:

1. Thermal breakdown usually occurs in high-temperature areas.
2. The breakdown voltage decreases rapidly with the rise of ambient temperature.
3. The breakdown voltage is related to the waveform, frequency, pressure time and boost speed of the applied voltage.
4. Thermal breakdown has nothing to do with the electrical properties of the material.
5. With the increase in sample thickness, the heat dissipation is difficult and the breakdown field strength decreases.

Thermal breakdown is different from electric breakdown. Thermal breakdown usually occurs in the high temperature region, while electrical breakdown usually occurs in the low temperature region. Moreover, electrical breakdown voltage has a short acting time and is less affected by the ambient temperature.

(c) Electrochemical breakdown

Electrochemical breakdown occurs when the polymer is subjected to high voltage over a long period of time. During operation, due to thermal, chemical and mechanical effects, the insulation performance gradually deteriorates and the insulation ages. Under the high electric field, ionization of local air gap occurs on polymer surface or in defects, which produce ozone or nitrogen oxides, etc. The ozone and nitrogen oxides make the polymer age and increase the conductance, resulting in the breakdown of the insulation. There are many factors influencing cable breakdown, including voltage action time, electric field uniformity, temperature, moisture and cumulative effect.

Voltage action time: if the voltage action time is very short, such as less than 0.1 s, electrical breakdown usually occurs at this time, and the breakdown voltage is of course also very high. With the increase in the time of voltage application, the breakdown voltage will drop. If the applied voltage is low, the cable will break down after several minutes to several hours. At this time, the effect is usually thermal breakdown. However, it is difficult to distinguish between thermal breakdown and electrical breakdown, and it is often a dual role of thermal and electrical breakdown. After the voltage is applied for a period of several years, the cable breaks down. At this time, the electrochemical breakdown usually occurs.

Electric field uniformity: the breakdown voltage of the solid medium in the uniform electric field is generally higher, and the breakdown voltage increases

linearly with the increase in the thickness of the solid medium. In an uneven electric field, the breakdown usually occurs at the points with field distortion.

Temperature: the breakdown of solid medium in a certain temperature range is electrical breakdown. When the temperature exceeds a certain temperature, the higher the temperature is, the lower the breakdown voltage is. For this situation, it is thermal breakdown. Therefore, the solid medium works in the local high temperature, under the working voltage, and there will be the risk of thermal breakdown.

Moisture: after solid media is moistened, conductivity and dielectric loss greatly increased, and breakdown voltage can be sharply reduced. Therefore, it is necessary to pay attention to moisture-proof during the operation of the cables.

Cumulative effect: under a non-uniform electric field or a low amplitude over-voltage, though the medium does not break down, but some traces such as local carbonization inside the solid medium will be left. After multiple effects of voltage, the local damages gradually accumulate, which lead to a decrease in the breakdown voltage of the solid medium.

2.2 *Mechanical Properties*

Mechanical properties are the basis for the excellent physical properties of polymers. The mechanical properties of materials represent the ability of materials to undergo reversible or irreversible deformation under stress and to resist damage. It is required that the polymer used as cable insulation material has certain strength and toughness. The most important mechanical properties of polymers are their high elasticity and viscoelasticity [1].

1. **High elasticity**

High elasticity refers to the large reversible deformation under the action of stress, which is caused by the change of internal conformational entropy, also known as entropy elasticity. The reason for the high elasticity of the polymer is the flexibility caused by the conformational change of the polymer chain, as shown in Fig. 4. A polymer material with high elasticity is called elastomer or rubber.

The difference between high elasticity and ordinary elasticity is: its elastic deformation is large for the high elastomer, and the high-elastic deformation can reach 1000%, whereas ordinary deformation is not more than 1%. The elastic modulus is very low, and the elastic modulus of high elasticity is only 10^5 N/m², and the elastic modulus of metal is as high as 10^{10} – 10^{11} N/m². Rubber materials get hot when they are stretched quickly, while metal materials absorb heat when they are stretched quickly.

The characteristics of high elasticity are related to the flexibility of polymer molecular chains. The macromolecules of high polymer have long chain structure, and the

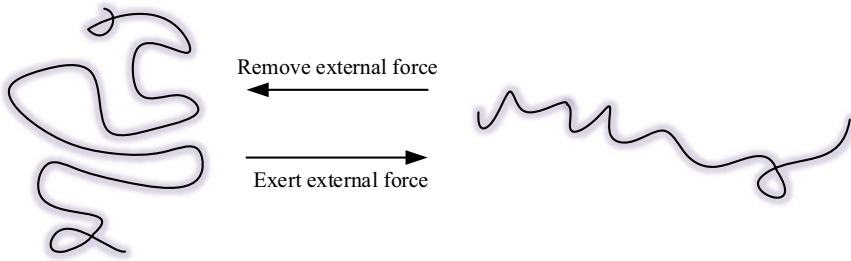


Fig. 4 High-elastic deformation of polymer molecules

molecular chains have great activity, which can stretch or curl rapidly. Thus, it can be seen that amorphous polymers have high elasticity only when the temperature is higher than the glass transition temperature.

The factors that affect the flexibility of the polymer chain will affect the high elasticity of the polymer: the higher the molecular weight of the polymer, the longer the molecular chain, the more the conformation of the molecular chain, and the more flexible the molecular chain. The greater the force is between the chain and the chain, the more difficult it is to slip between the macromolecules, so the higher the elasticity of the material is. The better the flexibility of macromolecules, the better the elasticity of rubber and the better the cold endurance. The appropriate crosslinking degree widens the material's high-elastic temperature and increases its strength to prevent the flow creep in use. Reducing the crystallinity of the polymer and the arrangement of the molecules is beneficial to improve the high elasticity of the material.

2. Viscoelasticity

High elasticity means that the deformation and the external force act at the same speed, that is, the stress and strain reach a balance in an instant. For example, if an external force is applied to the rubber band, the rubber band is stretched instantly. When the external force is removed, the rubber band rebounds immediately, which is called 'balanced high elasticity,' as shown in Fig. 5a. Unlike the balanced high elasticity, some high-elastic deformations lag behind the force, as shown in Fig. 5b. The reason for the delay of high elastic deformation is the difficulty of chain movement. The stiffer the segment, the lower the temperature, and the more serious the deformation delay. The viscoelastic features of polymers are creep, stress relaxation, hysteresis and internal friction.

Creep: the phenomenon that an object deforms under the action of external forces and the deformation continues to develop slowly with time is called creep.

Stress relaxation: it makes the polymer deform rapidly and produces a stress inside the material. The phenomenon that the stress gradually weakens with time is called stress relaxation.

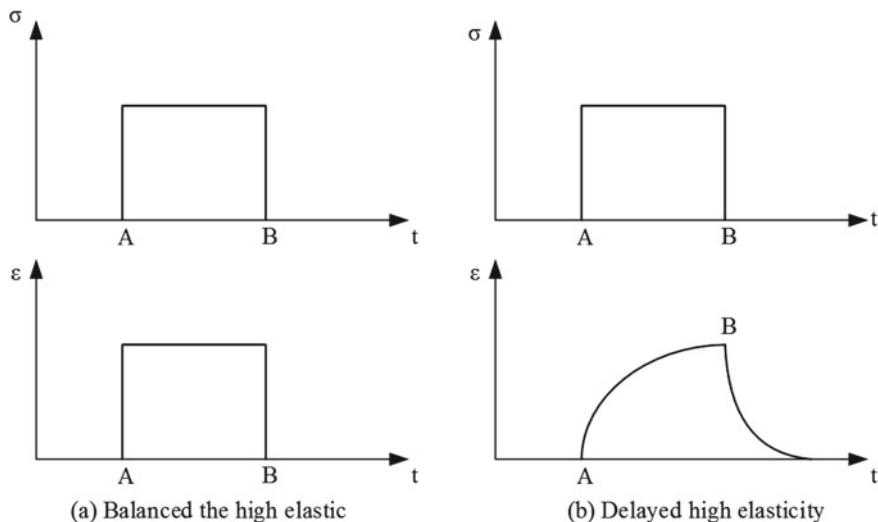
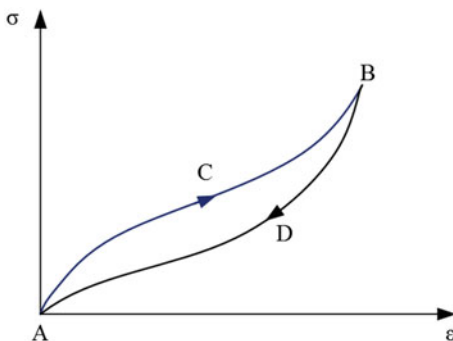


Fig. 5 Relationship between stress-strain and time of two high elastic bodies [14]

Hysteresis: the hysteresis is internal friction. When the change speed of macro-molecule conformation lags behind the change speed of profit, the deformation will lag. This phenomenon is called lag. As shown in Fig. 6, the stress-strain curve of rubber is shown during the process of shrinkage after one-time tensile.

The stress-strain curve changes along ACB during stretching and along BDA during retracting, and the deformation during retracting is larger than that during stretching. Since the stretch and the retraction are not same way along the same stress-strain curve, the absorption and release of energy in the material during a stretch and retraction cannot be offset. The area enclosed by ACBDA is called the hysteresis ring, and the hysteresis ring area represents the net absorbed energy of rubber during a stretch retraction. This energy is converted into heat, called internal friction, which causes the rubber to age.

Fig. 6 Stress-strain curve of rubber during one-time stretch and retraction [2]



2.3 Other Properties

1. Heat resistance

During the operation of cables and electrical equipment, the polymer material is always working at a certain temperature. If the temperature changes, the polymer will soften, deform or decompose. The processing process of the plastic or rubber will also be affected by the heat, so the heat resistance of polymer material is very important. Therefore, it is of great significance to increase the working temperature of the polymer dielectric for improving the capacity of electrical products, prolonging their service lives and reduce the production investment (Tables 2 and 3).

The changes of polymers after being heated can be divided into physical change and chemical change. The physical change refers to whether the material appears softening, deformation, melting and other phenomena under high temperature, or the change of the performance of the material under hot state. The chemical change is cyclization, crosslinking, degradation decomposition, oxidation, hydrolysis, etc. Due to the different uses of polymers, the indicators of these changes are different. There are many kinds of heat-resistant indicators of polymers, such as softening temperature, decomposition temperature, working temperature and heat-resistant grade.

2. Flame resistance

Most of the materials used in power cables are flammable materials, such as polyethylene, polypropylene, polystyrene and so on. Only a few polymers (such as fluoroplastics and fluororubber) have high flame resistance. When the polymer is heated, chemical destruction and the generation of volatiles will occur and leave porous residues. For this reason, the oxygen in the air is easy to

Table 2 Glass transition temperature T_g and melting temperature T_m of some polymers [2]

Polymer	T_g (glass transition temperature)/°C	T_m (melting temperature)/°C
Linear polyethylene	-80	137
Polypropylene	-18	176
Polyvinyl chloride	87	212
Polystyrene	100	112
Polymathic methacrylate	105	-
Teflon	126	-
Nylon 6	50	215

Table 3 Heat resistance grades (International) [2]

Heat resistance grades	Y	A	E	B	F	H	C
Working temperature/°C	90	105	120	130	155	180	>180

penetrate and cause further oxidation reactions in the solid matrix. The residues are usually composed of carbon residues, which increase the absorption of heat from the surrounding radiation and further the accelerate pyrolysis of the material. In this way, the accumulated temperature rises, and finally the volatiles ignite to form a flame. The ignition can be caused by an external flame or spontaneously. If the heat produced by the combustion can continuously provide the necessary heat for the thermal cracking of the matrix to maintain the combustion, such materials are called combustible materials; on the other hand, if the heat generated by the combustion is not enough to provide heat to cause the continuing combustion of the material, and not enough to produce volatiles at a sufficient rate to ignite, the flame will extinguish, such a material is called a self-extinguishing material.

The combustion characteristics of polymers can be characterized by the following parameters:

Specific heat capacity: it refers to the heat required for every 1 °C rise of unit mass substance, and the unit is J/kg K. If the specific heat capacity is larger, more heat will be absorbed in the heating stage. **Combustion heat:** it refers to the heat generated when 1 kg polymer is fully burned. The decomposition reactions of polymers are exothermic reactions, and the combustion heat is an important factor to maintain combustion and delayed combustion. **Flash point and spontaneous combustion point:** when the polymer is decomposed by heat to release combustible gas, which can just be ignited by a small flame outside, then the minimum temperature of the air around the sample is called the flash temperature of the material, and it is called flash point for short. When the polymer is heated to a certain temperature, it will burn or explode without external ignition source. At this time, the lowest temperature of the surrounding air is called the spontaneous combustion temperature of the material, which is referred to as the spontaneous combustion point for short. **Decomposition temperature:** the combustion of polymer is decomposition combustion, which is only possible above the decomposition temperature. If the decomposition temperature is low, the possibility of combustion is high. **Oxygen index:** the minimum amount of oxygen required to keep a candle-like specimen burning at a temperature in a mixture of oxygen and nitrogen. The higher the oxygen index, the more difficult the material is to burn.

The combustion characteristics of polymer are also characterized by thermal conductivity, combustion rate, etc. For different polymers, different standard parameters can be selected according to the actual situation.

3 Chemical Properties

Crosslinked polyethylene (XLPE) has become the insulating material of power cable because of its excellent dielectric, physical and chemical properties. The cable will be affected by various factors such as electricity, heat and mechanical stress for a

long-time during operation, which will lead to accelerated aging of the cable insulation material. In order to increase the service life of XLPE insulation material, its performance needs to be further improved. Generally, the methods to improve the performance of XLPE insulation materials mainly include copolymerization, blending and using additives, among which method of using additives are widely used, such as adding antioxidant, light stabilizer and voltage stabilizer. Additives have a long history, dating back to the 1960s. The main function of additives is to improve the performance of insulating materials by inhibiting thermal oxygen degradation, photooxidative degradation and electrical aging. According to the survey report of American Electric Power Research Institute, 83.33% of companies that make cable materials in the USA use additives. Most additives are derived from various additives in the plastics industry and are widely used because of their low cost and the need to introduce insulating materials without additional processes and equipment. This section will introduce the effect of additives on XLPE insulation from two aspects: polymer degradation mechanism and additive action mechanism.

3.1 Thermal Oxidation Resistance

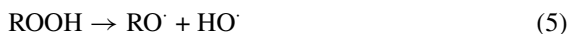
XLPE will contact with air during processing, storage and application. At a certain temperature, XLPE reacts with oxygen in the air and degrades, which is called thermo-oxidative degradation. In the thermal oxygen degradation process of XLPE, automatic oxidation reaction is the core reaction of thermal oxygen degradation. When XLPE is subjected to heat or light, free radicals will first be triggered on the molecular weaknesses. Free radicals react with the polymer to form ROOH, which is the main cause of automatic oxidation. Thermo-oxygen degradation is divided into three stages: initiation reaction, propagation reaction and termination reaction.

In the initiation reaction, free radicals are triggered on the weakness of XLPE molecule at a certain temperature, which react with oxygen quickly to form peroxide radicals.



In the propagation reaction, ROO^{\cdot} will capture the hydrogen atom in the polymer to generate ROOH. When enough ROOH is available, it will decompose into new free radicals and participate in the chain reaction. In XLPE, ROOH will form irregularly on the chain. Therefore, in the early stage of auto-oxidation, single-molecule decomposition is mainly, and single molecules will split to produce RO^{\cdot} and HO^{\cdot} radicals. As the concentration of ROOH increases, bimolecular decomposition begins to occupy a dominant position. Bimolecular will split to produce RO^{\cdot} , ROO^{\cdot} and HO^{\cdot} free radicals. These free radicals continue to interact with XLPE molecules to

generate more free radicals to accelerate the oxidation process.



In the termination reaction, after the free radical collides with each other, the double base coupling terminates and the free radical disappears.

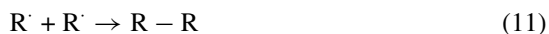
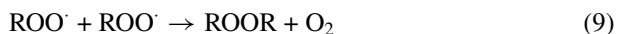


Figure 7 shows the automatic oxidation chain reaction process of thermal oxygen degradation. It can be seen from the figure that each time the thermal oxygen cycle

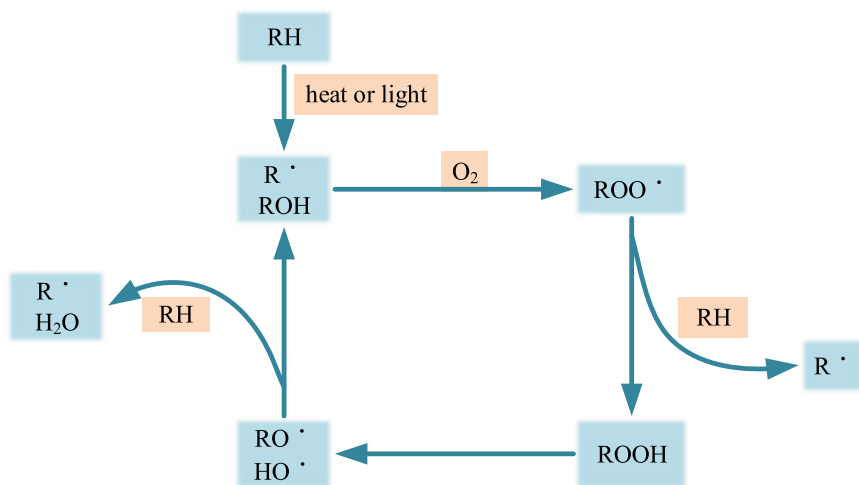


Fig. 7 Automatic oxidation chain reaction [15]

is carried out, an initial alkyl radical will generate at least three $R\cdot$, which will lead to higher and higher concentration of alkyl radicals in XLPE, and the thermal oxygen reaction speed will be accelerated. Finally, the automatic oxidation reaction will be formed, and XLPE will accelerate the degradation.

The above analysis describes the mechanism of thermal oxygen degradation in XLPE. For the polymer, its saturated degree, branched structure, substituent, crosslinking bond and crystallinity will affect its thermal oxygen stability, that is, changing the structure of the polymer can change the thermal oxygen stability of the polymer. However, for XLPE, the method to change its structure is obviously not feasible. Therefore, in order to improve the thermo-oxygen stability of XLPE, the method widely used at home and abroad is to add thermo-oxygen stabilizer, namely antioxidant, to improve its thermo-oxygen stability. The selection and use of antioxidants depend on the properties of the polymer, the conditions of manufacture, storage and application.

Antioxidants can be divided into two categories according to their different interventions in the process of automatic oxidation chain reaction. One is the main antioxidant, also known as free radical catching agent (mainly phenolic antioxidants), whose role is to stop the free radical chain reaction, i.e., to stop $R\cdot$ and $ROO\cdot$. This kind of antioxidant forms stable free radical compounds by providing hydrogen atom, which reacts with $ROO\cdot$ to form hydroperoxides $ROOH$. The other class is main antioxidant, which can also be called preventive antioxidant (mainly sulfur antioxidant). This kind of antioxidant can decompose hydroperoxides into stable product ROH in a non-free radical way, thus eliminating the main initiation point of chain reaction. The mechanism of action of the two antioxidants is shown in Fig. 8.

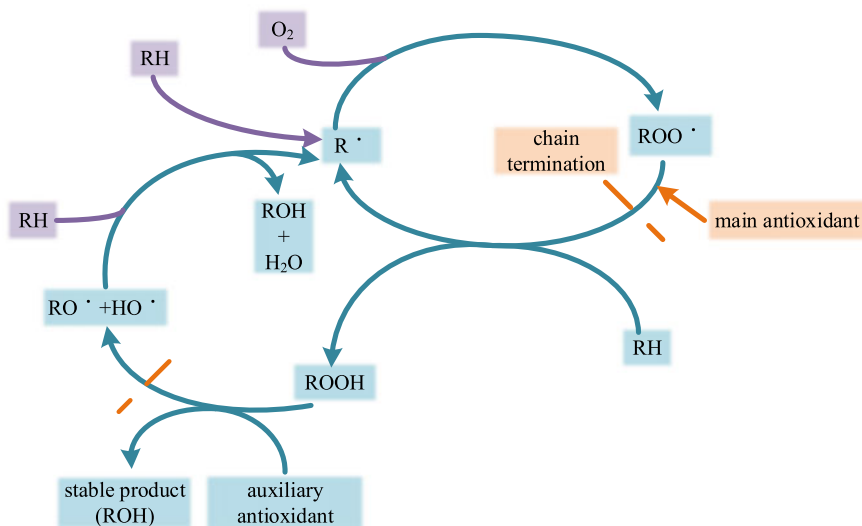


Fig. 8 Action principle of antioxidant [15]

3.2 Photo Oxidation Resistance

The mechanism of photooxidative degradation of polymers is very similar to that of thermo-oxidative degradation. The reaction process is also carried out in three stages: initiation reaction, growth reaction and termination reaction. It is different from thermo-oxidative degradation in that the initiator of photooxidative degradation is more than thermo-oxidative degradation. During the laying and operation of the cable, due to the limitations of the existing technology, micro-defects will inevitably be left in the XLPE insulation, and electrical branches may be caused during the operation during the defect to cause insulation breakdown. C. Laurent and S. S. Bamji proposed the theory of photodegradation induced by electric dendrite by studying the electroluminescence phenomenon of electric dendrite during the incubation period [16]. The theory is that under the action of AC voltage, electrons will be trapped by traps in the polymer during the negative half cycle as the polarity of the AC voltage is reversed, when it is in the positive half cycle of the AC voltage, the electrons in the deep trap will be difficult to fall off due to the different depths of traps in the polymer. Electrons that cannot be trapped will emit photons after recombining with the injected holes, and the emitted photons can generate visible light and ultraviolet light. With the increase in the applied voltage, some local states will change from trap states to composite centers, which will produce shorter wavelength light, that is, the intensity and energy of ultraviolet rays generated by higher voltages will be greater.

Generally, polymers containing only single bonds do not absorb or hardly absorb ultraviolet rays in principle and are relatively stable. However, materials such as catalysts and additives are added during the manufacturing and processing of XLPE insulation materials. These materials contain chromophore groups. The chromophore is easily excited by absorbing ultraviolet light. These excited substances will become photo-initiators and cause the C–C bond in XLPE to break to generate alkyl radicals $R\cdot$. These free radicals $R\cdot$ react with oxygen to produce $ROO\cdot$, $ROO\cdot$ capture the hydrogen atom in the XLPE molecular chain to generate the hydroperoxide $ROOH$, and the photooxidation reaction begins. The hydroperoxide $ROOH$ can absorb ultraviolet light and cause a photochemical reaction to break the O–O bond, and the hydroperoxide $ROOH$ all splits into alkoxy radicals $RO\cdot$ with $HO\cdot$, alkoxy radicals can take hydrogen atoms from XLPE to generate alkyl radicals $R\cdot$ alkyl radical $R\cdot$ reacts with oxygen to produce peroxide radicals $ROO\cdot$. The photooxidative degradation chain reaction starts, which will accelerate the degradation of XLPE. It is worth noting that in the initial stage of photodegradation, in addition to generating hydroperoxide, carbonyl group $C=O$ is also generated. The carbonyl group can also be used as a photo-initiated source of photooxidation to generate alkyl radicals. The mechanism of photo-oxygen degradation is shown in Fig. 9.

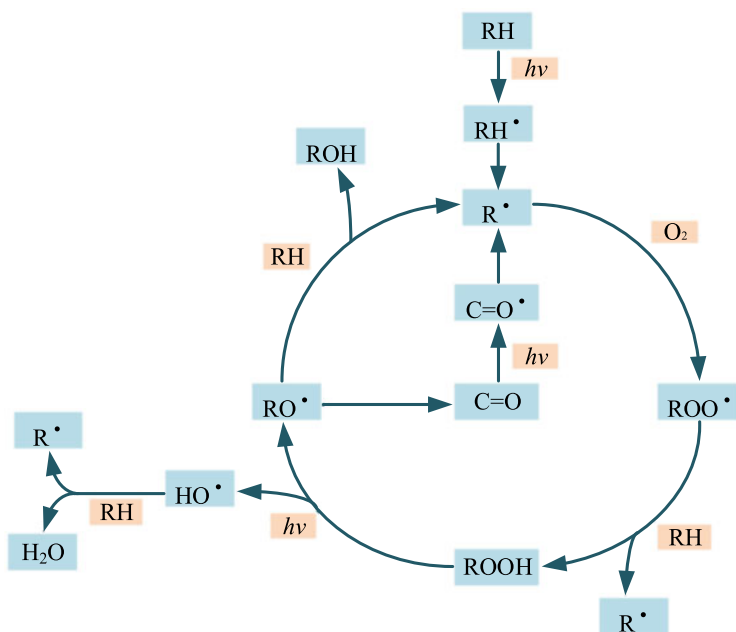


Fig. 9 Mechanism of photooxidative degradation [16]

Light stabilizers are a general term for a class of substances that can inhibit or eliminate photochemical processes in polymers. According to the mechanism of photooxidative degradation of polymers, radiation shielding, absorption and conversion of radiation, quenching processes, and elimination of free radicals and decomposition of hydroperoxides make the polymer have light stability. Therefore, according to these methods, light stabilizers can be classified into light-shielding agents, ultraviolet light absorbers, excited state quenchers, radical scavengers and hydrogen peroxide. Light-shielding agent is a substance that is opaque to ultraviolet light. It can prevent ultraviolet light from entering the polymer material. There are mainly inorganic and organic pigments, including carbon black, zinc oxide and so on. Ultraviolet light absorbers can absorb harmful substances. The ultraviolet light converts the energy of ultraviolet light into fluorescence or phosphorescence that is not harmful to the polymer or heat energy that is not harmful to the polymer, including salicylates, benzophenones, benzotriazoles, etc. The excited state quencher can accept the energy of the excited state of the chromophore and emit it in a form that is not harmful to the polymer. It can avoid the reaction of the polymer's molecular chain break, mainly the organic complex of nickel.

Light-shielding agents, ultraviolet light absorbers and excited-state quenchers are all three types of light stabilizers that provide stability to the polymer from the perspective of preventing photo-initiation. Free radical scavengers are different from these three in that they are free from scavenging. The method of radical and

cut-off automatic oxidation chain reaction achieves the stability of the polymer. The radical scavenger has the same effect as the antioxidant in Sect. 3.1, that is, the radical scavenger is actually an antioxidant under photooxidation conditions. Hindered amine light stabilizer (HALS) is currently recognized as a highly effective light stabilizer at home and abroad. From the perspective of chemical structure, HALS light stabilizers are mainly piperidine derivatives with steric hindrance, so this type of stabilizer is also called hindered amine or hindered piperidine. This type of stabilizer was created and produced by Japan's Sankyo Company in the 1970s and has received widespread attention and attention since its inception. According to the stabilization mechanism of HALS, it can be known that HALS is oxidized to nitroso radicals, which is extremely stable. It can capture alkyl radicals to form alkoxy hindered amine compounds, which continue to react with peroxy radicals to form an unstable hindered quaternary ammonium salt compound, which will produce stable ketone and alcohol products after decomposition, and finally generate stable nitroso free radicals.

4 Test Methods of Electrical Properties

4.1 Polarization and Depolarization Current Method (PDC)

The principle of the polarization-depolarization current method is to apply a DC voltage to a dielectric and the polarization current is measured. After a period of time, the polarization voltage is removed and the depolarization current is measured [17–19]. By measuring, recording and analyzing the polarization current and depolarization current in this process, the dielectric characteristics are analyzed. When an external electric field is applied, the positive and negative charge centers within the dielectric are shifted and no longer coincide, and they move in opposite directions along the direction of the electric field, breaking the original equilibrium state and appearing as a polarization phenomenon on a macro-scale. The particles contribute to macroscopic polarization due to: the distorted polarization of the electron cloud outside the nucleus, which is the electron displacement polarization; the relative displacement polarization of the positive and negative ions in the molecule, which is the ion displacement polarization; the orientation polarization (or dipole) of the molecule's inherent electrical moment; interlayer polarization occurring at the interface of the medium, and space charge polarization caused by charge movement. The schematic diagram of polar media polarization is shown in Fig. 10.

When the external electric field is no longer applied to the dielectric, the electric dipole moments of positive and negative charges tend to cancel each other out under the action of thermal movement, return to the equilibrium position, and appear to be weakened or even completely eliminated in the macroscopic view. For the

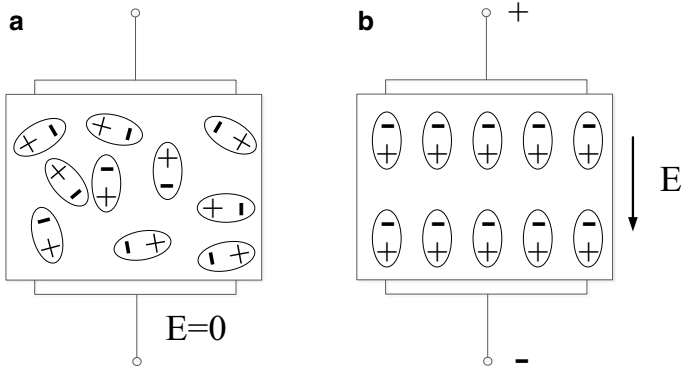


Fig. 10 Schematic diagram of polar dielectric polarization. **a** When no electric field is applied **b** When an electric field is applied

depolarization process, it can be seen that depolarization is a completely opposite phenomenon to polarization.

It can be seen from the above that the polarization-depolarization process is a change process in which the dielectric responds under the action of an applied electric field. Different dielectrics have different internal structures and different molecular structures. During the polarization-depolarization process, the positive and negative charges move differently, and the displayed macro-characteristics are naturally different. When there are impurities, moisture or aging in it, XLPE insulation's structure must be different from the new XLPE insulation of good quality. Under DC voltage, there will be different degrees of orientation polarization, sandwich polarization and space charge polarization, but different poles. The types of settling time and energy loss are different, so the polarization-depolarization process will have corresponding differences. By measuring the polarization-depolarization current, the current data during the entire polarization and depolarization process are recorded, processed and analyzed, and parameters can be extracted and identified.

The basic circuit principle of polarization-depolarization current method for power cable insulation detection is shown in Fig. 11, and the PDC device is shown in Fig. 12.

The two resistors in Fig. 11 are current-limiting protection resistors, which limit the circuit current and protect the electronic device in the circuit. At the same time, they can reduce the current value and extend the polarization-depolarization time, which is convenient for measuring and recording experimental data. At $t_0 = 0$, switch the switch to the polarization loop, apply voltage to the cable through the DC power supply, enter the polarization phase, and the polarization current is $i_{\text{pol}}(t)$. After a certain polarization time t_1 , switch the switch to the depolarization loop, discharge through the current-limiting resistor, and enter the depolarization phase, and the depolarization current is $i_{\text{depol}}(t)$. Measure the polarization-depolarization current through a picoammeter located at the low voltage end, and send it to the upper

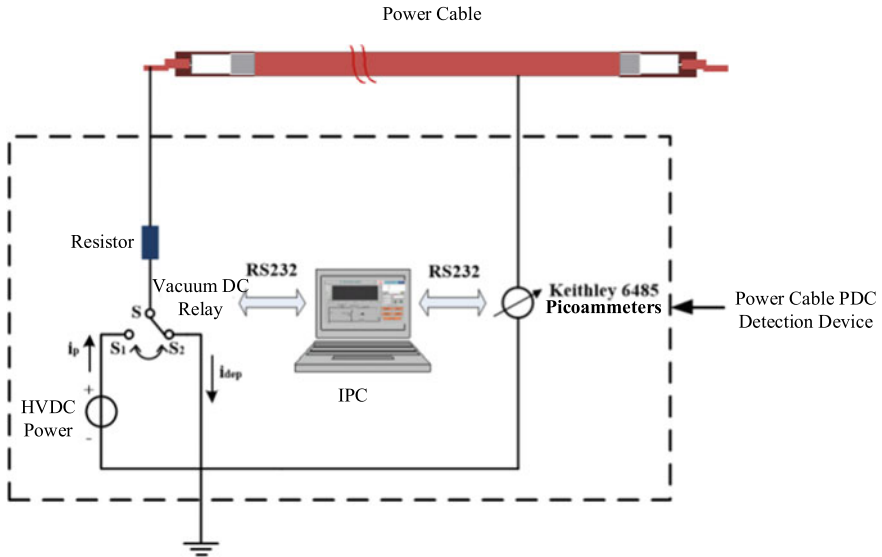


Fig. 11 Basic circuit schematic

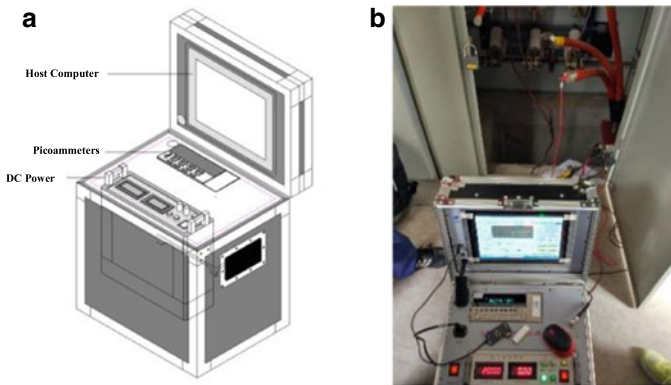


Fig. 12 PDC test device. a Schematic diagram. b Physical diagram of device

computer is used for analysis. It should be noted that in order to avoid the impact caused by the switching, a small piece of data at the beginning of the depolarization current should be ignored.

For an ideal capacitor model, both the charging current and the discharge current follow an exponential relationship. If U_0 is the initial voltage, R is the current-limiting resistor, and t is the time, the polarization current i_{pol} and depolarization current i_{depol} of the ideal capacitance, as shown in Eqs. 12 and 13:

$$i_{pol} = U_0 e^{-t/RC} / R = i_0 e^{-t/RC} \tag{12}$$

$$i_{\text{depol}} = -U_0 e^{-t/RC} / R = i_0 e^{-t/RC} \tag{13}$$

Logarithmic transformation of Eqs. 12 and 13 gives the result:

$$\ln i = -\frac{t}{RC} + \ln\left(\frac{U_0}{R}\right) \tag{14}$$

It can be seen from the formula that the natural logarithm of the polarization or depolarization current of an ideal capacitor is a linear function about time t with a slope of $-1/RC$. Where R is the resistance of the current-limiting resistor and C is the ideal capacitor. The value of $-1/RC$ determines the rate of the polarization or depolarization process. The larger the value of R times C , the slower the polarization-depolarization process.

The above is the polarization-depolarization process for the ideal capacitor. However, the polarization-depolarization process of the actual XLPE dielectric is not exactly the same as the ideal capacitor, as shown in Fig. 13.

Where i_{pol} is the polarization current, i_{depol} is the depolarization current, i_{dc} is the DC leakage current. It can be seen from the above figure that even after a long enough time of polarization, the polarization current i_{pol} does not tend to 0, but there is a DC component, that is, the DC leakage current i_{dc} .

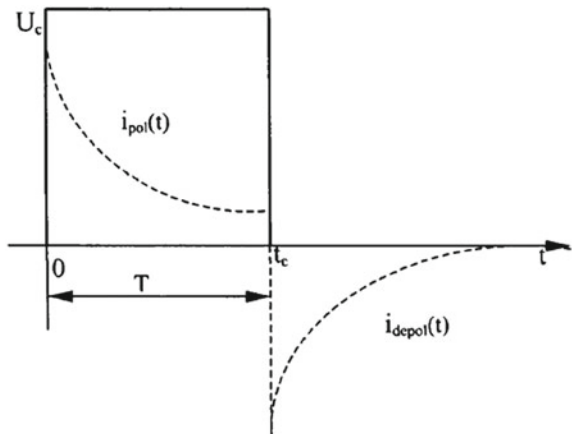
Assume that the XLPE dielectric is isotropic and its dielectric constant is ϵ . When an electric field \mathbf{E} is applied, the electrical displacement is:

$$\mathbf{D} = \epsilon_0 \mathbf{E} + \mathbf{P} \tag{15}$$

where \mathbf{P} is the polarization intensity.

According to Maxwell's equation, the full current density in an ideal XLPE insulation satisfies:

Fig. 13
Polarization-depolarization current curve of an actual cable



$$\mathbf{J} = \sigma_0 \mathbf{E} + \frac{\partial \mathbf{D}}{\partial t} = \sigma_0 \mathbf{E} + \varepsilon_0 \frac{\partial \mathbf{E}}{\partial t} + \frac{\partial \mathbf{P}}{\partial t} \quad (16)$$

where ε_0 is the vacuum dielectric constant ($\varepsilon_0 = 8.842 \times 10E-12$ F/m), σ_0 is the DC conductivity of the XLPE insulation layer. The first term on the right side of Eq. (16) is an electrically conductive current, the second term is a vacuum displacement current, and the third term is a polarization current that includes fast polarization and slow polarization processes. At the same time, the polarization intensity can be expressed as:

$$\mathbf{P} = \varepsilon_0(\varepsilon_\infty - 1)\mathbf{E} + \varepsilon_0 \int_{-\infty}^t f(t)\mathbf{E}(t - \tau)d\tau \quad (17)$$

where ε_∞ is the high-frequency component of the dielectric constant of the XLPE insulation, and its value is equal to the square of the optical refractive index of the XLPE material. The first term on the right side of the equation is the instantaneous displacement part, and the second term is the relaxed polarization part. $f(t)$ is a response function that reflects the slow polarization behavior of the insulating dielectric.

Since the insulating medium is $f(t) = 0(t < 0)$, therefore:

$$\mathbf{P} = \varepsilon_0(\varepsilon_\infty - 1)\mathbf{E} + \varepsilon_0 \int_0^t f(t)\mathbf{E}(t - \tau)d\tau \quad (18)$$

Substituting Eqs. (18) into (16), we can get the full-current expression:

$$\mathbf{J} = \sigma_0 \mathbf{E} + \varepsilon_0 \varepsilon_\infty \frac{d\mathbf{E}}{dt} + \varepsilon_0 \frac{d}{dt} \int_0^t f(t)\mathbf{E}(t - \tau)d\tau \quad (19)$$

When the applied voltage is $U(t)$, full current $i(t)$ can be expressed as:

$$i(t) = C_0 \left[\frac{\sigma_0}{\varepsilon_0} U(t) + \varepsilon_\infty \frac{dU(t)}{dt} + \frac{d}{dt} \int_{-\infty}^t f(t)U(t - \tau)d\tau \right] \quad (20)$$

Applied voltage $U(t) = d \cdot E(t)$, d is the XLPE insulation thickness.

If the XLPE material is completely discharged before charging, $t = 0$ external DC power at all times U_c . At this time, the polarization current passing through the test object can be expressed as:

$$i_{\text{pol}} = C_0 U_0 \left[\frac{\sigma_0}{\varepsilon_0} + \varepsilon_\infty \delta(t) + f(t) \right] \quad (21)$$

In the formula, $\delta(t)$ is the impact function. Because the impact change of the current amplitude during the fast polarization of the insulation is difficult to accurately measure in practice, it is generally not considered, and then formula (21) can be expressed as:

$$i_{\text{pol}} = C_0 U_0 \left[\frac{\sigma_0}{\varepsilon_0} + f(t) \right] \quad (22)$$

When $t = t_c$ (t_c : Charging time), the XLPE material is shorted to ground, and the current flowing through the insulation layer is the depolarization (relaxation) current. According to the superposition theorem, it can be equivalent to $t = t_c$ apply voltage to XLPE insulation from moment to moment $-U_c$, and the depolarization current expression can be obtained:

$$i_{\text{depol}} = -C_0 U_0 [f(t) - f(t + t_c)] \quad (23)$$

Due to $f(t)$ is a monotonically decreasing function, when t_c is larger, the second term on the right side of the above formula (23) can be ignored. At this time, it is approximately considered that the relaxation current of the cable is proportional to the dielectric response function of the insulation, that is:

$$f(t) \approx \frac{-i_{\text{depol}}(t)}{C_0 U_0} \quad (24)$$

From Eqs. (22) and (24), it can be known that the polarization current can be considered as the sum of the depolarization current and the conduction current. If the DC conductance part of the polarization current is small relative to the dielectric response function $f(t)$, the polarization current can also be expressed in the form of (24).

When the test time is long enough, (22) and (24) can calculate the DC conductivity of XLPE insulation:

$$\sigma_0 \approx \frac{\varepsilon_0}{C_0 U_0} [i_{\text{pol}}(t) + i_{\text{depol}}(t)] \quad (25)$$

where C_0 is insulated vacuum capacitor (or geometric capacitor), ε_0 is a constant, for a specific type of test object PDC experiment, the polarization voltage U_0 can be set to a fixed value. Therefore, the DC conductivity of XLPE σ_0 only with the average value and capacitance of the polarization depolarization current C_0 relevant. For a particular test subject, due to ε_0 , U_0 , C_0 it is a fixed value, so the difference between the DC conductivity and the average value of the polarization depolarization current is directly proportional. The difference of the average value of the polarization depolarization current will directly determine the magnitude of the conductivity, which can reflect the insulation performance, and the difference. The larger or the greater the conductivity, the more severe the insulation aging.

XLPE material is widely used in the insulation layer of power cables. Similar to polyethylene material, XLPE is easy to initiate water trees under the action of electric field, moisture and internal defects of the material, causing the reduction in insulation performance of the material. The non-linear conductivity characteristic is analogous to the absorption ratio of the insulation resistance, so a non-linear coefficient (DONL) is introduced to evaluate the degree of non-linearity of the cable insulation. The definition of DONL is shown in Eq. (26):

$$\text{DONL} = \frac{\sigma_0(U_2 = 2 \text{ kV})}{\sigma_0(U_2 = 1 \text{ kV})} \quad (26)$$

In the formula: DONL is the non-linear coefficient of the DC conductivity of the cable insulation, and its value is equal to the ratio of the DC conductivity with a polarization voltage of 2 kV to the DC conductivity with a polarization voltage of 1 kV. The polarization can be appropriately increased in engineering applications voltage to obtain more obvious non-linear characteristics. Under normal circumstances, the non-linear coefficient should be equal to about 1. The non-linear coefficient can intuitively reflect the degree of non-linearity of the cable insulation. At the same time, the non-linear coefficient can be used to detect some non-linearities such as micro-holes and water trees in the cable insulation.

Through the PDC test results, the low-frequency dielectric loss (0.1 Hz dielectric loss factor) of the material can also be extracted. When the dielectric response function $f(t)$ of the XLPE insulating dielectric obeys the ‘Curie-von Schweidler’ model, the Fourier transform can be used to perform simple conversion from time domain to frequency domain. Whether the dielectric response function $f(t)$ is an analytical function or a two-dimensional array expressed numerically, it can be Fourier transformed. Existing research shows that this conversion method is ideal for calculation in the low-frequency band. Then, performing Fourier transform on Eq. (20) can obtain the current expression in the frequency domain:

$$\begin{aligned} \dot{I}(\omega) &= C_0 \left[\frac{\sigma_0}{\varepsilon_0} \dot{U}(\omega) + j\omega\varepsilon_\infty \dot{U}(\omega) + j\omega\dot{F}(\omega)\dot{U}(\omega) \right] \\ &= \dot{U}(\omega) \left[\frac{\sigma_0}{\varepsilon_0} C_0 + j\omega C_0(\varepsilon_\infty + \dot{F}(\omega)) \right] \end{aligned} \quad (27)$$

Due to $\dot{F}(\omega)$ is the dielectric response function $f(t)$ Fourier transform, the repolarization rate is:

$$\chi(\omega) = \dot{F}(\omega) = \chi'(\omega) - j\chi''(\omega) = \int_0^\infty f(t)e^{-j\omega t} dt \quad (28)$$

Therefore, Eq. (27) can be rewritten as:

$$\dot{I}(\omega) = \dot{U}(\omega) \left[\frac{\sigma_0}{\varepsilon_0} C_0 + j\omega C_0 (\varepsilon_\infty + \chi'(\omega) - j\chi''(\omega)) \right] \quad (29)$$

The frequency domain expression of full current is:

$$\dot{I}(\omega) = j\omega C_0 \dot{U}(\omega) \left[\varepsilon_0 + \chi'(\omega) - j \left(\frac{\sigma_0}{\varepsilon_0 \omega} + \chi''(\omega) \right) \right] = j\omega C_0 \dot{U}(\omega) \quad (30)$$

Therefore, the relationship between the total loss factor of the cable insulation medium and the frequency can be obtained:

$$\tan \delta(\omega) = \frac{\varepsilon''(\omega)}{\varepsilon'(\omega)} = \frac{\frac{\sigma_0}{\varepsilon_0 \omega} + \chi''(\omega)}{\varepsilon_\infty + \chi'(\omega)} = \frac{\frac{\sigma_0}{\varepsilon_0 \omega}}{\varepsilon_\infty + \chi'(\omega)} + \frac{\chi''(\omega)}{\varepsilon_\infty + \chi'(\omega)} \quad (31)$$

In the formula, the first term on the right side of the equation is the conductivity loss, and the second term is the polarization loss, and the sum of the two is the total dielectric loss. σ_0 can be solved by Eq. (25), and $\chi'(\omega)$ and $\chi''(\omega)$ are the real and imaginary parts of the polarizability, respectively, so the depolarization current can be solved by using Eqs. (24) and (27).

If the DC conductance part of the polarization current is small compared to the dielectric response function $f(t)$, the time domain to frequency domain conversion can also be performed by using the polarization current, so as to obtain the relationship between the dielectric loss factor of the cable insulation and the frequency as formula (31).

Because dipole polarization and interface polarization inevitably accompany energy loss, and the process is relatively slow, it usually takes seconds or minutes, or even longer, so the ultra-low-frequency dielectric loss can more effectively reflect the overall aging of the dielectric insulation. And it is more sensitive to cable insulation moisture or water tree aging. Figure 14 shows the relationship between the low-frequency dielectric loss and the frequency of the aging sample of a laboratory long cable. According to Eq. (31) and Fig. 14, it can be known that the dielectric loss factor consists of two parts, which are the conductivity loss and polarization loss, respectively. At low frequencies (such as 0.1 Hz), the order of $\varepsilon_0 \omega$ at $10\text{E}-11$ is much larger than σ_0 (good XLPE insulation material is at the order of $10\text{E}-15$ S/m). At this time, the dielectric loss of the insulating medium is mainly polarization loss, almost negligible conductance loss. When the frequency is lower than 0.1 Hz, as the frequency decreases, the polarization loss increases because the dipole steering can keep up with the frequency change. Referring to the IEEE Std 400™-2001 standard, at $0.5-1.5U_0$, when the dielectric loss factor is less than 0.6×10^{-3} at ultra-low frequency 0.1 Hz, it indicates that the cable is well insulated; it is greater than 0.6×10^{-3} and less than 1×10^{-3} indicates that the cable insulation may have a slight aging phenomenon, which needs further follow-up and diagnosis; when it is greater than 1×10^{-3} , it indicates that the cable insulation has deteriorated severely. Judging from the results in Fig. 14, it shows that the water tree has developed more severely

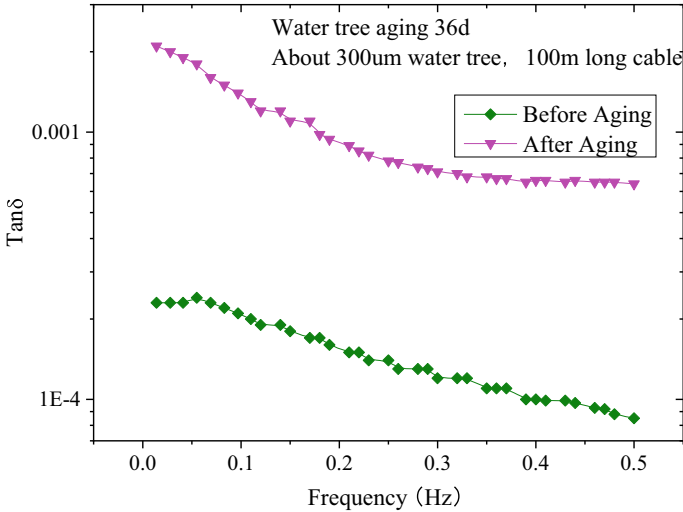


Fig. 14 Curve of the relationship between the low-frequency dielectric loss and the frequency of the cable sample

after accelerated aging, which is consistent with the results we observed on the water tree slice in the experiment.

4.2 Dielectric Loss Factor Measurement

The parameter reflecting the dielectric characteristics is the dielectric loss factor $\tan \delta$, it is the ratio of the active current component I_r to the total capacitor current I_c of the dielectric. The dielectric loss factor is used to identify the aging degree of XLPE insulation.

Under the action of a high voltage and strong electric field, the free ions inside the insulating material undergo polarization and conduction processes. Due to the hysteresis effect of this process, electrical conduction current and polarized current both generate energy loss inside the dielectric. The degree of loss generally uses unit time. The energy of internal loss is also called dielectric loss factor. Under DC voltage, the dielectric does not undergo periodic polarization and cannot reflect the loss caused by polarization current, which is not included in the concept of dielectric loss. In AC, the dielectric will have a polarization current at the same time I_c and electrical current I_r (Fig. 15)

A large amount of electrical energy is consumed inside the insulator due to the presence of dielectric loss, and the insulator will accumulate a large amount of thermal energy. If the heat cannot be dissipated in time, it will cause the performance of the insulating material to deteriorate. As the aging degree increases, it will eventually

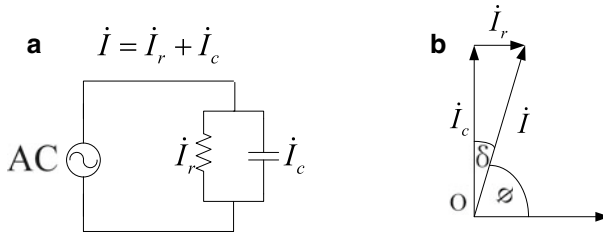


Fig. 15 Equivalent circuit and phasor diagram of dielectric under AC voltage. **a** Equivalent circuit. **b** Phasor diagram

lead to the total loss of insulation performance, the index for judging the energy loss is the power loss of the medium

$$P = UI \cos \varphi = UI_r = UI_c \tan \delta = U^2 \omega C_p \tan \delta \tag{32}$$

Where:

- ω AC voltage angular frequency $\omega = 2\pi f$,
- φ Power factor angle,
- δ Dielectric loss angle

There are three main methods for measuring dielectric loss factor angle: resonance method, voltammetry method and bridge method. Among them, the resonance method only works well under low-voltage and high-frequency conditions, but it is powerless for measurement of high-voltage equipment; voltammetry is widely used because of its poor anti-interference ability, large measurement error and high-harmonic. The suppression ability is poor, and its use has certain limitations; the bridge method has relatively high measurement accuracy and high sensitivity. It uses the bridge comparison principle, and the most representative is the Schering Bridge.

With the development of measurement technology, digital dielectric loss testers are widely used, which can effectively detect the overall moisture deterioration of electrical equipment insulation, as well as local defects. The measuring circuit of the instrument includes the standard circuit (C_n) and the test circuit (C_x). The standard circuit consists of a built-in high-stability standard capacitor and a measurement circuit. The test circuit consists of the test object and a measurement circuit. The measurement circuit consists of a sampling resistor, a preamplifier and an A/D converter. The current amplitude and phase of the standard circuit and the test circuit are measured by the measuring circuit. The capacitance value and the dielectric loss factor of the test object can be obtained by the single-chip computer using the digital real-time acquisition method and vector operation. However, because of the large capacitance of the cable, the conventional power frequency dielectric loss meter is often difficult to measure the data due to the output capacity limitation. Meanwhile, be affected by the field interference, its measurement repetition rate and accuracy are low. Table 4 lists some typical dielectric loss factor of the cable at power frequency.

Table 4 Typical values of normal and aged cables $\tan \delta$ [20]

Dielectric	Standard (%)	Determination
Dielectric loss tangent ($\tan \delta$)	$\tan \delta < 0.2$	Normal
	$0.2 < \tan \delta < 0.5$	Needed attention
	$\tan \delta > 0.5$	Severe aging

4.3 Breakdown Experiment

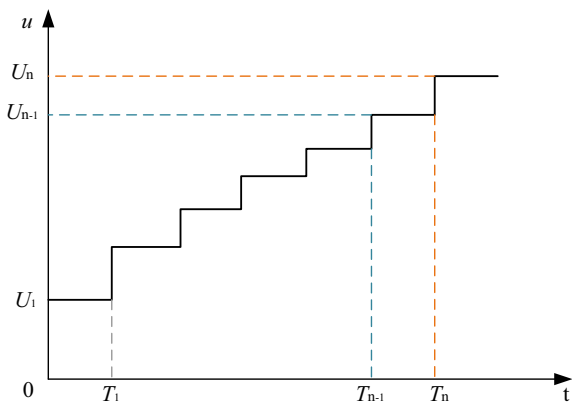
This part focuses on the electrical breakdown of XLPE insulation. The power frequency breakdown voltage test is an intuitive indicator for measuring the electrical strength of the insulating medium. The step-to-step power frequency breakdown voltage test is designed for the characteristic that the weak point of the insulation will first break down under the action of voltage. The power frequency breakdown voltage test is performed on the crosslinked polyethylene sheet as shown in Fig. 16.

The main steps are as follows:

- (a) The slice sample is placed in the center of the electrodes in the standard oil cup. The electrodes are ball-ball electrodes with a diameter of 11 mm. To avoid surface flashover, the oil cup contains transformer oil, and the sample is immersed in the transformer oil.
- (b) Apply 8 kV AC voltage to the slice sample through a protective resistor using a power frequency boost circuit for 1 min.
- (c) If the slice sample does not break down under 8 kV AC voltage, then take 1 kV as the increment, each stage voltage lasts for 1 min until the chip sample breaks down. Record the duration of the last stage voltage.
- (d) Use Ross Function and Weibull distribution to process the data.

According to a large number of studies, the probability distribution of the breakdown voltage of insulating materials obeys the two parameters Weibull distribution. Referring to the national standard GB/T 29310-2012 guide for *statistical analysis of*

Fig. 16 Step-by-step power frequency breakdown voltage test



electrical insulation breakdown data, according to Weibull probability statistics, the probability F of the breakdown of insulating materials under the voltage U is:

$$F(U, \alpha, \beta) = 1 - \exp\left(-\left(\frac{U}{\alpha}\right)^\beta\right) \quad (33)$$

In formula (33): U is the breakdown voltage of the tested object, α (kV) is the scale parameter of Weibull distribution, and β is the shape parameter of Weibull distribution.

Take logarithm on both sides of the formula (33):

$$\ln \ln \frac{1}{1-F} = \beta \ln U - \beta \ln \alpha \quad (34)$$

Set $Y = \ln \ln \frac{1}{1-F}$, $X = \ln U$, $C = -\beta \ln \alpha$, we have the following relationship:

$$Y = \beta X + C \quad (35)$$

According to the national standard GB/T 29310-2012 *guide for statistical analysis of electrical insulation breakdown data*, the Ross distribution function is used to calculate the Weibull distribution data point probability values:

$$F(i, n) \approx \frac{i - 0.44}{n + 0.25} \times 100\% \quad (36)$$

In formula (36): i is the sample number; n is the total number of samples.

When the breakdown voltage value of the sample is numbered from small to large, the formula (36) represents the failure probability of the sample at the breakdown voltage under the corresponding number.

5 Conclusions

Crosslinked polyethylene (XLPE) is a semicrystalline polymer, which is consisted of amorphous and crystalline regions. This chapter introduces the structure of XLPE and its chain movement. Secondly, detailed introduction of various physicochemical properties of XLPE is given.

1. The physical properties consist of electrical properties (such as polarization, dielectric constant, dielectric loss, breakdown voltage), and mechanical properties (such as high elasticity and viscoelasticity), and other performances.
2. The chemical properties mainly represent the abilities of anti-oxidation, thermal oxidation resistant and anti-corrosion.

3. The test methods are introduced for several important properties, which are divided into two units: physiochemical property tests and electrical property tests. In this chapter, each method is described from aspects of its basic principle, data processing, the results and the range for application.

References

1. Bower DI (2002) An introduction to polymer physics. Cambridge University Press, New York, pp 163, pp 290, pp 216
2. Guo H (2012) Electric wire and cable materials, the structures, properties, and applications. China Mechanic Press, Beijing, China, pp 70–166, pp 171–179
3. Han CD (2007) Rheology and processing of polymeric materials. V. I polymer rheology. Oxford University Press, New York, US, pp 400–736
4. Raharimalala V, Poggi Y, Filippini JC (1994) Influence of polymer morphology on water treeing. *IEEE Trans Dielectr Electr Insul* 1(6):1094–1103
5. Karakelle M, Phillips PJ (1989) The influence of structure on water treeing in crosslinked polyethylene: accelerated aging methods. *IEEE Trans Electr Insul* 24(6):1083–1092
6. Rdu I, Acedo M, Filippini JC, Notingher P, Frutos F (2000) The effect of water treeing on the electric field distribution of XLPE. *IEEE Trans Dielectr Electr Insul* 7(6):860–868
7. Ross R (1998) Water treeing theories current status, views and aims. In: Proceedings of 1998 international symposium on electrical insulating materials, Toyohashi, Japan, pp 535–540, 27–30 Sept 1998
8. Ross R, Smit JJ (1991) Water tree growth processes in XLPE. In: A proceedings of international conference of solid dielectrics 03rd, Tokyo, Japan, pp 214–217, 8–12 Jul 1991
9. Tanaka T, Fukuda T, Suzuki S (1976) Water tree formation and lifetime estimation in 3.3 kV and 6.6 kV XLPE and PE power cables. *IEEE Trans Power Appl Syst* 95(2):1892–1900
10. Faremo H, Selsjord M, Hvidsten S, Bengtsson KM, Ryen A (2006) Initiation of vented water trees from the conductor screen of MV XLPE insulated cables. *J Polym Sci, Part B: Polym Phys* 44(4):641–648
11. William AT et al (2014) Electrical power cable engineering. In: Sun J, Xu X et al (eds) translated. 3rd ed. China Machine Press, Beijing, China, pp 120–400
12. Seaner DA (1982) Electrical properties of polymer. Academic Press, New York, pp 1–26, pp 27–72, pp 186–210
13. Zhou K (2018) Aging diagnosis and rejuvenation of cable systems for medium and high voltage. Science Press, Beijing, China, p 73
14. Zhou K, Zhao W, Tao W (2013) Toward understanding the relationship between insulation recovery and micro structure in water tree degraded XLPE cables. *IEEE Trans Dielectr Electr Insul* 20(6):2135–2142
15. Sekii Y, Tanaka D, Saito M et al (2003) Effects of antioxidants on the initiation and growth of electrical trees in XLPE. In: Annual report conference on electrical insulation and dielectric phenomena, Albuquerque, America, Oct 19–22, pp 661–665
16. Bamji SS (2008) Luminescence and space charge phenomena in polymeric dielectrics. In: Annual report conference on electrical insulation dielectric phenomena, Québec City, Canada, Oct 26–29, pp 1–12
17. Oyegoke B, Birtwhistle D, Lyall J et al (2007) New techniques for determining condition of XLPE cable insulation from polarization and depolarization current measurements. In: 2007 IEEE international conference on solid dielectrics, Winchester, UK, Jul 8–13, pp 150–153
18. Kuschel M, Kryszak B, Kalkner W (1998) Investigation of the non-linear dielectric response of water tree-aged XLPE cables in the time and frequency domain. In: Proceedings of the 1998 IEEE 6th international conference on conduction and breakdown in solid dielectrics, Vasteras, Sweden, Jun 22–25, pp 85–88

19. Oonishi H, Urano F, Mochizuki T, Soma K, Kotani K, Kamio K (1987) Development of new diagnostic method for hot-line XLPE cables with water trees. *Power Eng Rev IEEE* 7(1):28–29
20. Jiang R (2009) Crosslinked polyethylene power cable line. China Electric Power Press, Beijing, China, p 114

Chapter 6

Morphology, Structure, Properties and Applications of XLPE



Khaled Aljoumaa and Abdul Wahab Allaf

1 Introduction

Polyethylene is widely produced under different grades by polymerization using different catalysts such as transition metal (Ziegler-Natta) catalysts [1]. The three major PE grades: high-density polyethylene (HDPE), linear low-density polyethylene (LLDPE) and low-density polyethylene (LDPE). Crosslinked polyethylene XLPE is created by introducing various crosslinking into the polyethylene different grades chains. Scheme 1 illustrates the different structures of PE grades.

It is well known that crosslinking of polyethylene polymers can be carried out under a controlled manner to yield materials that are extremely useful in many applications. The creation of a crosslink network between individual polymer chains leads to restriction in chain movement that makes the network structure hard to deform and some of the properties (e.g., dimensional stability, impact strength, creep and abrasion resistance) are retained at high temperatures. Moreover, the crosslinking of low-density polyethylene produces XLPE that is resistant to heat and mechanically durable as well as providing a high level of electrical insulation, which makes crosslinked polyethylene a material of choice for wire and cable coating, hot water tubing and heat shrinkable [2–4]. Table 1 shows the changes of physical properties for some different polyethylene grades.

XLPE can be produced either by chemical or physical methods [6]. The chemical processes of XLPE crosslinking can be done by silane crosslinking [7–12], peroxide

K. Aljoumaa (✉)

Industrial Irradiation Division, Department of Radiation Technology, Atomic Energy Commission of Syria, P.O. Box 6091, Damascus, Syria
e-mail: ascientific@aec.org.sy; kaljoumaa@aec.org.sy

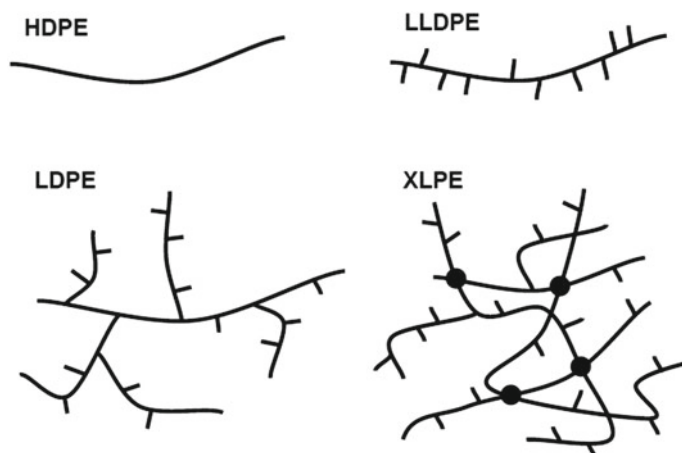
A. W. Allaf

Organic Synthesis Division, Department of Chemistry, Atomic Energy Commission of Syria, P.O. Box 6091, Damascus, Syria

© Springer Nature Singapore Pte Ltd. 2021

J. Thomas et al. (eds.), *Crosslinkable Polyethylene*, Materials Horizons: From Nature to Nanomaterials, https://doi.org/10.1007/978-981-16-0514-7_6

125



Scheme 1 Schematics of major polyethylene grades. Lines indicate hydrocarbon chains and intermolecular crosslinks are indicated with dots

Table 1 Some polyethylene grades parameters [5]

Property	Units	HDPE	LLDPE	LDPE	XLPE
Breakdown strength, E_B	kV/mm	100	75	75	50
Dielectric constant, ϵ_r		2.3	2.3	2.2	2.4
Volume resistivity, ρ	Ω cm	5×10^{17}	5×10^{17}	5×10^{17}	10^{16}
Dielectric loss, $\tan \delta$ (1 MHz)		10^{-3}	10^{-3}	2×10^{-4}	10^{-3}
Crystallinity	%	80–95	70–80	55–65	40–70 ^a
Density	g/cm ³	0.95	0.93	0.92	0.92
Melting point	°C	130	120	110	90–110 ^a
Tensile strength	Mpa	25	15	13	31

^aMelting point and crystallinity related to crosslinking density (discussed later in the chapter)

crosslinking [13–16], but Dicumyl Crosslinking Peroxide (DCP) is considered to be one of the most common substances to crosslink polyethylene by a peroxide process and generate primary radicals that attack the radicals in the polymeric chain. However, these crosslinking techniques involve high costs and risks of pre-curing during peroxide crosslinking [15]. Silane crosslinking is performed by grafting of vinyltriethoxysilane (VTES) or vinyltrimethoxysilane (VTMS) in polyethylene, followed by hydrolysis and condensation reaction to generate silanol groups [17]. While, the physical processes are produced using ionizing irradiation such as gamma rays and Electron Beam [18, 19].

During the process of fabrication, XLPE crystallization polymers display a strongly influenced behavior by cooling temperatures [20]. According to that, the morphology and the structure produced are dependent on crystallization [21, 22].

Moreover, crystalline structure formations are also inhibited by crosslinking and depend mainly on the crosslinking densities [23, 24].

Many additives were added to XLPE in order to improve its properties. Antioxidants are responsible of reducing the amount of aging, in particular chemical aging [25, 26]. Voltage stabilizers or water tree retardants that are added for wet designs as underground cables are chemical specimen's type materials which have the capability of absorbing the energy of high-energy electrons and reducing the electrical treeing process [27]. Pereira de Melo et al. [28] studied the effect of adding the coagent crosslinking at same time with silane and catalyst for increasing the distance between the linear chains, reducing crystallinity of grafted material which leads an improvement in the thermal degradation resistance and elastic modulus.

For different high-voltage cables applications, many limiting factors can affect the properties of XLPE insulation as the temperature in the cable core created as the result of joule heating that similarly occurs for hot pipes applications. The heating of polyethylene will cause polymer melting [29], while XLPE material will never melt and might become soft slightly, since the introduced crosslinks will retain stability.

In this chapter, the relation between the morphology, structure, properties and the application of XLPE will be discussed for essential applications.

2 XLPE Applications

Crosslinked polyethylene has a number of properties, which makes it suitable for several industrial applications at high and medium voltage insulation, tubing and piping, medical (hip replacement), auto components and other industrial applications. The crosslinking process converts thermoplastic polyethylene to a thermoset crosslinked polyethylene (XLPE) providing it with many enhanced properties, such as low-temperature impact strength, abrasion resistance, environmental stress-cracking resistance, tensile strength, flexibility, longevity as well as non-corrodibility. Moreover, XLPE is much less labor-intensive work and very low cost, which make it suitable for many interior and exterior applications such as insulation of high-voltage power cables plumbing due to easiness and cheap installation. The non-toxic and hypoallergenic nature of XLPE foams facilitates medical industrial applications; due to its light-weighting, this encourages the automotive sector to use XLPE in manufacturing vehicles.

In the upcoming paragraphs, the application will be discussed from a morphology point of view including XLPE structures and properties.

2.1 Cable Insulation

Electrical insulation in any high-voltage cable is the most considered important parts; these parts are used for expensive and important power cables. The type of insulation and its quality plays a major role to confirm the trustworthiness of cables.

Several layers of insulation with various functions and properties surround a typical high-voltage cable are the main concern. Figure 1 represents a simple schematic version of cable with more containing layers [30]. The conductor is made of copper or aluminum to obtain good conductivity in addition to good mechanical properties, the two layers of semiconductors action are to smooth surface around the layer afore and to prevent local field that results in the defect of conductor surface [31]. However, sometimes the second semiconductor layer usually is made of small copper wires or lead barrier especially for high-voltage submarine cables and having sealed layer to prevent water penetration [32]. The outer layers are often made of polymers such as PVC or polyethylene, providing good mechanical resistance at a low cost.

The uses of crosslinked polyethylene XLPE as the insulation material for high-voltage AC cables are growing in comparison with the commonly used oil or impregnated papers insulations [30], as shown in Fig. 2. Nevertheless, mass impregnated cables are recently still more suitable in particularly for high-voltage direct current (HVDC) cables due to its high direct current, DC reliability [33], the reason for that is due to space charge accumulates in the XLPE insulation and lowering the DC withstand characteristics. Recently, new DC-XLPE insulating material was developed with excellent DC characteristics that succeeded in its practical application and start to gain ground [34–37].

Nowadays, crosslinked polyethylene (XLPE) is used as the main insulation material for HVAC power cables due to its simplicity of manufacturing by extrusion, good electrical including stability of thermal and mechanical properties.

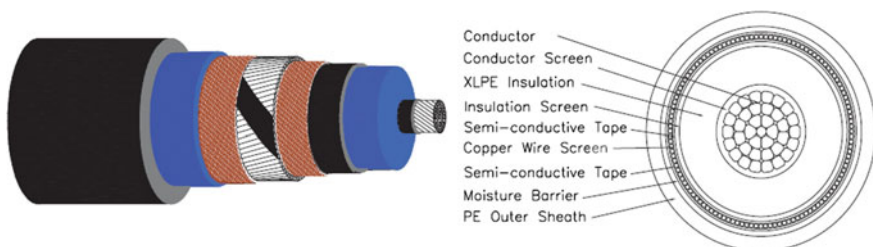
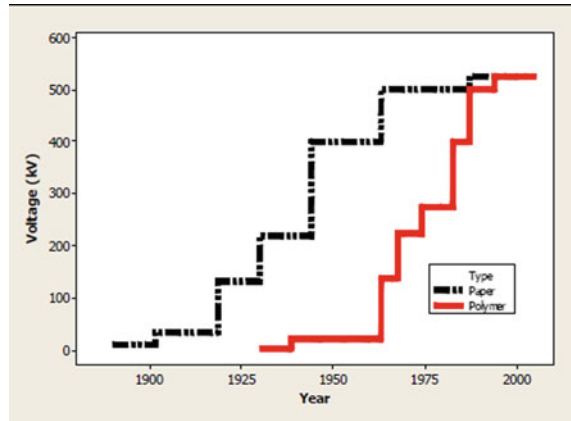


Fig. 1 Schematic of a typical single core XLPE insulated cable high voltage

Fig. 2 Evolution of the insulation of AC high voltage cable [38]



2.1.1 XPLE Cable Production

The manufacturing of high voltage cable is based on extruding the layer insulation around the conductor core. The process of crosslinking of polyethylene (PE) in order to produce XLPE material is performed by different chemical or physical techniques as described in the introduction. The crosslinking will change the thermoplastic polyethylene and transfer it to XLPE, which have a network, related the chain of polymer that improve the heat resistance. At, high voltage cable, the conductor temperature increases with the current transmitted through the cable, thus more power can be transmitted through XLPE cables compare with the non-crosslinked ones.

As aforementioned, the most widely method used for crosslinking polyethylene in the cable industry is by peroxide additives. The high temperature during the extrusion triggers the decomposition of peroxide into free radicals. These free radicals react with polyethylene molecules forming radicals on the polymer chains that will react with other radicals on the chains to create a crosslinking among chains.

Two typical manufacturing processes for crosslinked polyethylene (XLPE) of high voltage cables are usually used: a vertical continuous vulcanization (VCV) process line or a catenary continuous vulcanization (CCV) process line [39, 40]. The difference between these two processes is due to the physical location of cable. In a VCV production line, the cable is positioned vertically, whereas in a CCV production line the cable is positioned horizontally with a slight downward slope. Figure 3 presents the typical schematic of production stages, which starts by extruding the polymer onto a metal conductor, followed by crosslinking stage that can be achieved at different temperatures above the polymer melting point, the last stage is cooling the cable to room temperature by circulating water or gas around the cable. Gulmine and Akcelrud [41] studied the variation of the processing parameters (crosslinker concentration, cure time, and temperature) on the morphology of XLPE produced. They found also the suitable temperature, time of curing and high crosslinking density.

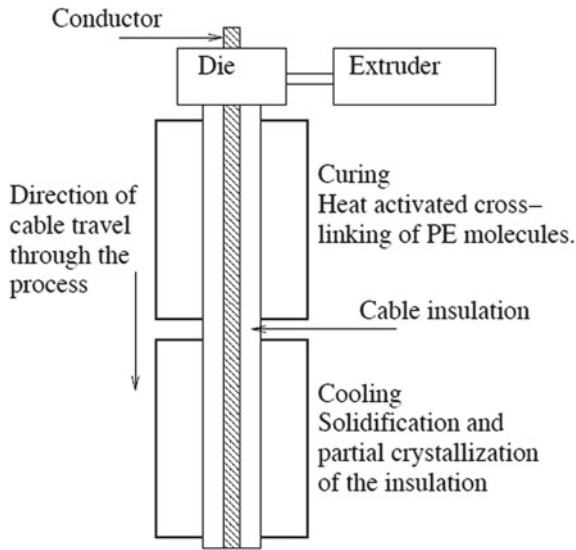


Fig. 3 Schematic of power cable manufacturing processes with its most important parts [42]

The cooling process is very important and is often considered a problematic manufacturing stage as it involves partial crystallization, besides that, the residual stresses influence both mechanical and electrical properties of the cable. It is known that mechanical stress affects the electrical breakdown strength which is also influenced by the presence of defects as voids (Fig. 4). Moreover, the residual stress may cause a problem at level of cable joints and also at termination joints due to the phenomenon called shrink-back which is regulated by an international standard IEC (2004) [43].

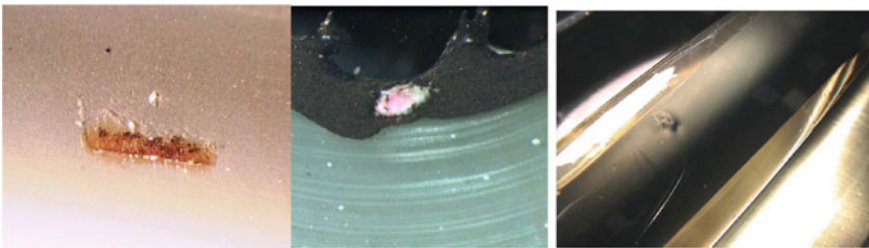
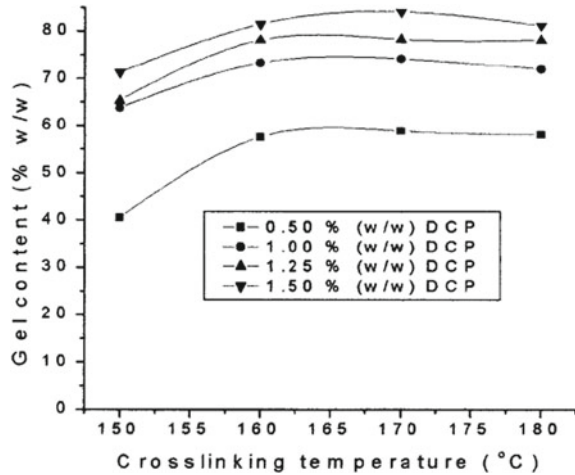


Fig. 4 Typical defects found in extruded cables [38]

Fig. 5 Crosslinking temperature dependence of gel content (cure time: 15 min) [41]



2.1.2 Morphology, Structure and Properties of XLPE for Cable Insulation

Crystallization Morphology of Crosslinked Polyethylene

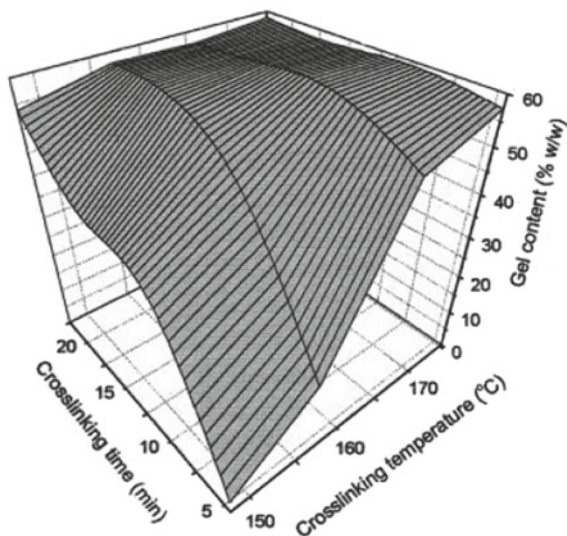
XLPE is usually made from LDPE and used for high voltage cable insulation. The crosslinking process results in creating a single large interwoven molecule (XLPE). As known, the polyethylene is crystalline, and the XLPE insulation properties will be influenced by the amount of crystalline and amorphous phases present. Moreover, chain branching, molecular weight and molecular weight distribution have also influences on the physical properties of cable.

LDPE is usually used for cable insulation because it contains short chain branches on the chain backbone that disrupt chain folding and thus reduce the degree of crystallinity to 40–60% in comparison with other type of polyethylene (70–90% for un-branched PE). This will lower the melting point, T_m and lays it between 105 and 115 °C (around 135 °C for un-branched PE) and occur over a wide temperature range that starts at 70–80 °C, and the density is lowered to 0.912–0.935 g/cm³ (0.960–0.970 g/cm³ for un-branched PE).

During the process of XLPE curing, a wide interval of crosslinking degree can be obtained that depends on the process and the material. In LDPE, the common base material for high voltage cables and gel content is between 70 and 80%. Gulmine and Akcelrud [41] studied the variation of gel content with crosslinking temperatures and time at different concentration of dicumyl peroxide (DCP). They found that the gel content reached a maximum over the temperature of 160 °C at different peroxide concentrations (Fig. 5). While a 5 min curing time was sufficient to obtain the maximum gel content (Fig. 6).

It is well known that crystalline structure in the semicrystalline PE is spherulites and consists of both crystalline lamellae and amorphous phase that are interconnected

Fig. 6 Correlation of the time, temperature and gel content with 0.50% DCP [41]



by amorphous regions as seen in Fig. 7, and spherulites which is developed from an initial central lamellae and subsequent branches leading to form the spherulite. By the way, the calculated density of a pure PE crystal is 1.00 g/cm^3 , whereas it is about 0.855 g/cm^3 for an amorphous phase. The cooling rate is essential for the formation of crystalline structure.

Several research reports studied the relation between the crystallinity of the XLPE [21–24, 45, 46] during the processing along with its relation with the morphology. Figure 8 shows the XRD pattern of LDPE and XLPE at different temperatures and the characteristic crystallization peaks (110) and (200) of polyethylene [47].

At slow cooling, rate lamella and spherulite structures are created while at fast cooling rate more amorphous structure with less ordered crystalline structures are obtained [46]. Moreover, it was reported that crystallization process was decreased with an increasing crosslink density and the fully developed spherulites is not preserved in XLPE, and the sheaf microstructure developed is smaller than spherulites. Figure 9 shows the change in the morphology of crystalline structure with the increase of peroxide concentration leading to increase the crosslinking density [48].

The development of crystal in XPLE stops before reaching fully developed spherulites, and that depends on the degree of crosslinking change. Whereas, high degree of crosslinking increases the nucleation of lamellar bundles while decreasing the crosslinking density forming the lamellae sheaf structures [22], as shown in Fig. 10.

Numerical simulation was used extensively to study the nucleation and growth of crystal using the simplest approach that homogeneous nucleation of crystals will be in the amorphous melt [49, 50]. Molecular simulation had some limitations, which are related to assumption, linearity and branched polymers structure. Recently, the

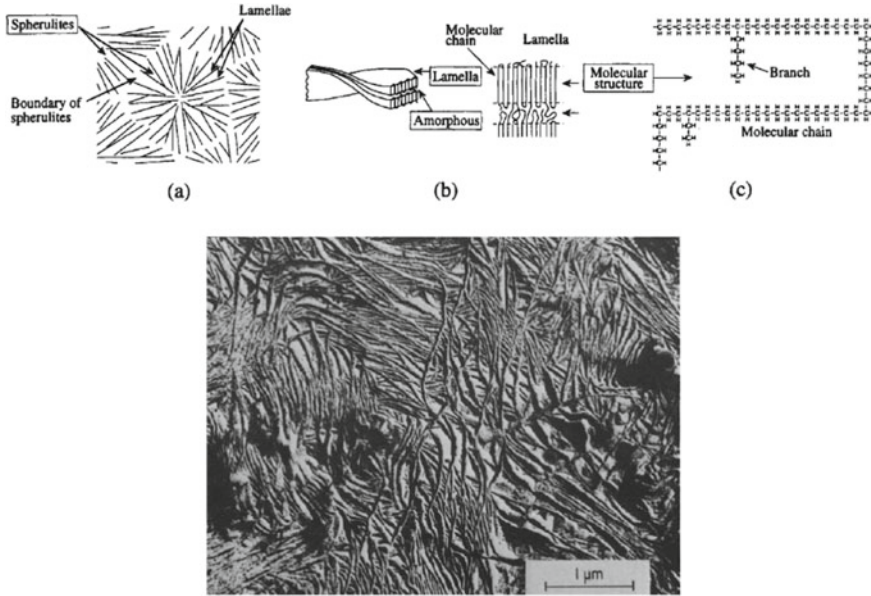


Fig. 7 a Schematic representation of spherulite structure [44], b electron micrograph showing infilling process by the growth of secondary lamellae in a banded spherulite of non-crosslinked polyethylene, $T \sim = 103.4 \text{ }^\circ\text{C}$ [22]

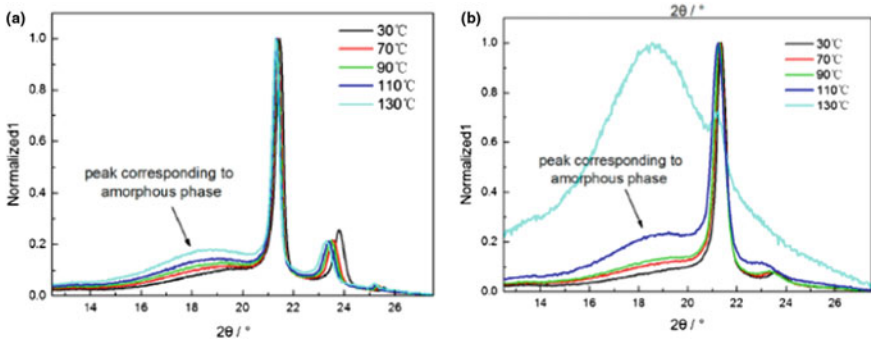


Fig. 8 XRD scanning spectrum for LLDPE (a), XLPE (b) with temperature [47]

groups of Paajanen et al. [24] have been using Molecular Dynamics (MD) simulations to study the crystallization of linear and crosslinked polyethylene with varying crosslink density. They performed the analysis in order to investigate the crystallization rates, final degrees of crystallization, behavior of crosslinks and last the properties of the un-crystallized material, they found that, the crosslinks are rejected from the crystals and accumulated in the amorphous inter-crystalline phase, Fig. 11.

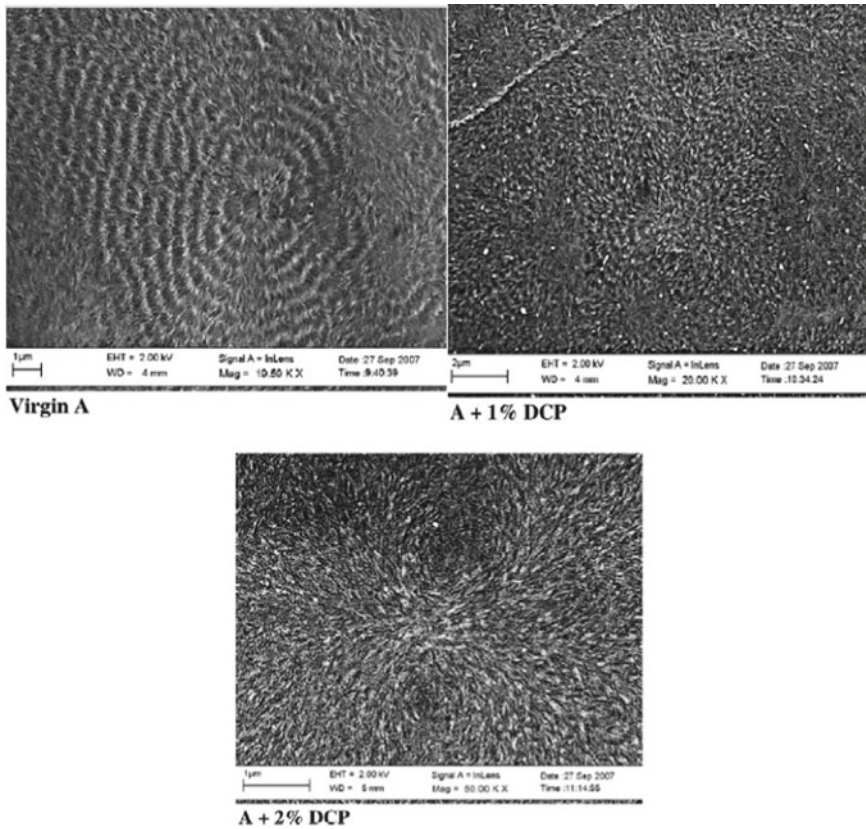


Fig. 9 Scanning electron micrographs of XLPE samples showing the change in spherulite size and structure and the appearance after crosslinking with DCP

XLPE Mechanical and Thermal Properties

During installation of the XLPE high voltage cables, it will be exposed to tensile and radial compressive forces. Moreover, there is also heat generation inside the metallic core of the cable. As known, the XLPE insulation is a critical component due to its relative low mechanical strength and thermal properties. Therefore, it is significantly important to investigate both thermal and mechanical time dependency behaviors.

During the last stage of cooling XLPE cable fabrication process into room temperature, secondary crystallization process takes place inside the insulation and residual stresses may develop into the final product. This may cause problems for loosening insulation around conductor; also a shrink-back of insulation in axial direction on the conductor at cable terminations will be appeared.

It is emphasized that, the XLPE cable has excellent anti-aging properties and a good heat-resistant deformation at working temperature lower than 90 °C [51]. Mo et al. [51] found that XLPE cable mainly experiences one stage of heat loss, due

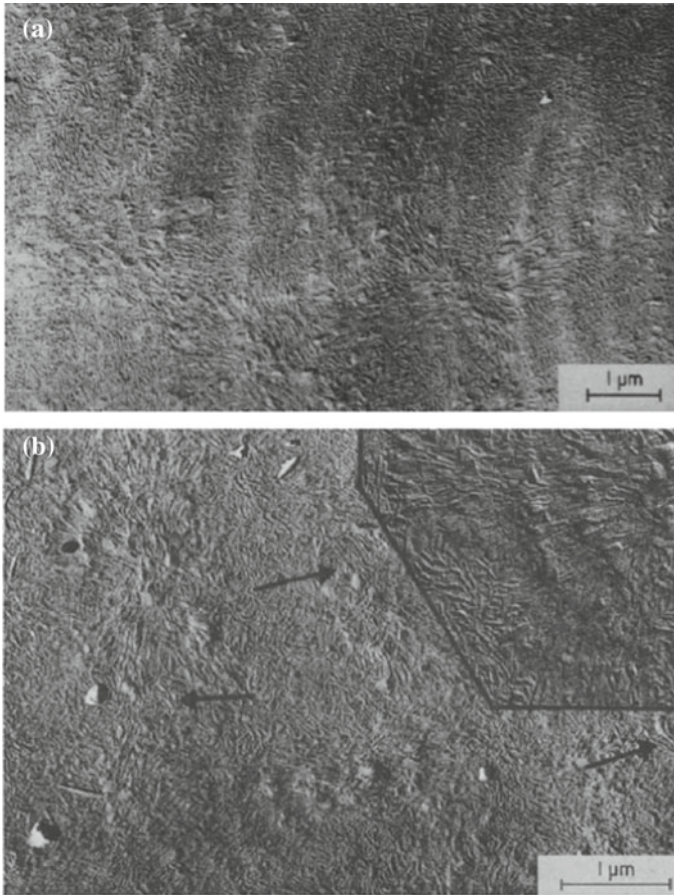


Fig. 10 An enlarged portion of a banded artifact developed in XLPE, $T \sim 103.8^\circ\text{C}$ (a). Electron micrograph of enlarged banded sheaves of XLPE-2, $T_c = 103.8^\circ\text{C}$; S-shaped lamellae are indicated by arrows (b) [22]

to additives, making the XLPE cable material starting from 400°C thermal weight loss stages. The cable absorbs heat, generating free radicals and a large amount of hydrogen chloride gas. During thermal decomposition observed on DSC curve at $550\text{--}690^\circ\text{C}$, the interaction between XPLE cable material and various additives will be accompanied by some reforms of structure, Fig. 12.

The manufacturing process influences clearly the thermal history and affects the radial profile of XLPE insulation due to the thermal gradient in the cooling process stage. Dissado et al. [52] found that the DSC thermal analysis of the crystallinity changes between the inner and outer surface and no variation of melting temperature as a function of the radial position was observed (Fig. 13).

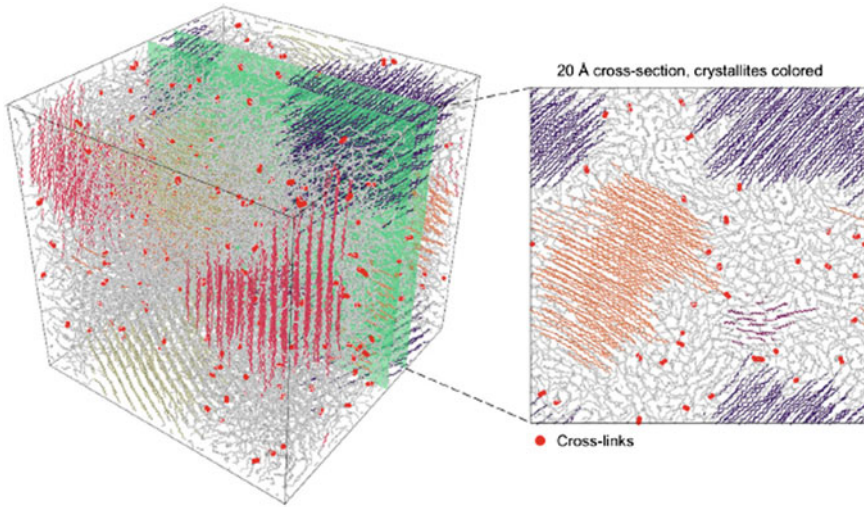


Fig. 11 Visualization of semicrystalline crosslinked system using stick representation of covalent bonds. Amorphous chain segments are shown in gray, crystalline segments are colored, and crosslinks are shown as red dots. The inset on the right shows a thick cross-section of the system, where crosslinks have accumulated to the amorphous inter-crystalline phase [24]

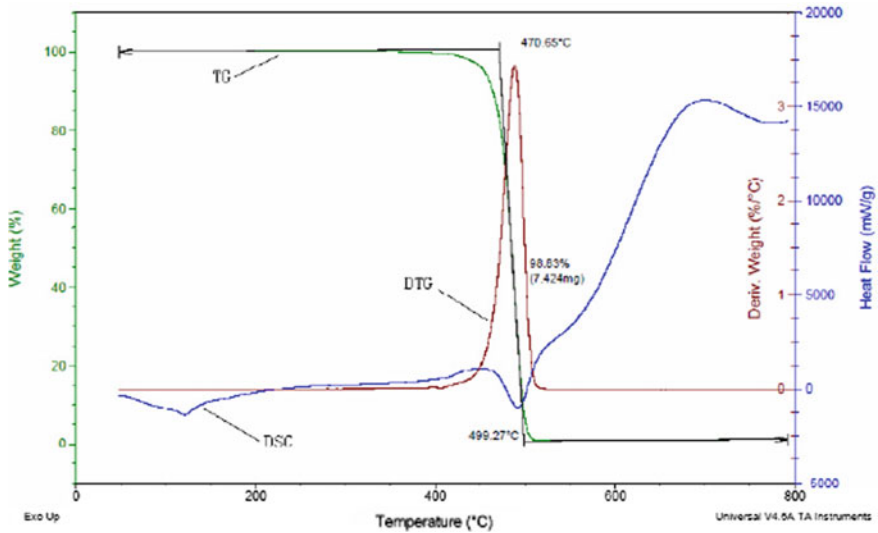


Fig. 12 TGA-DSC curve on XLPE cable material [51]

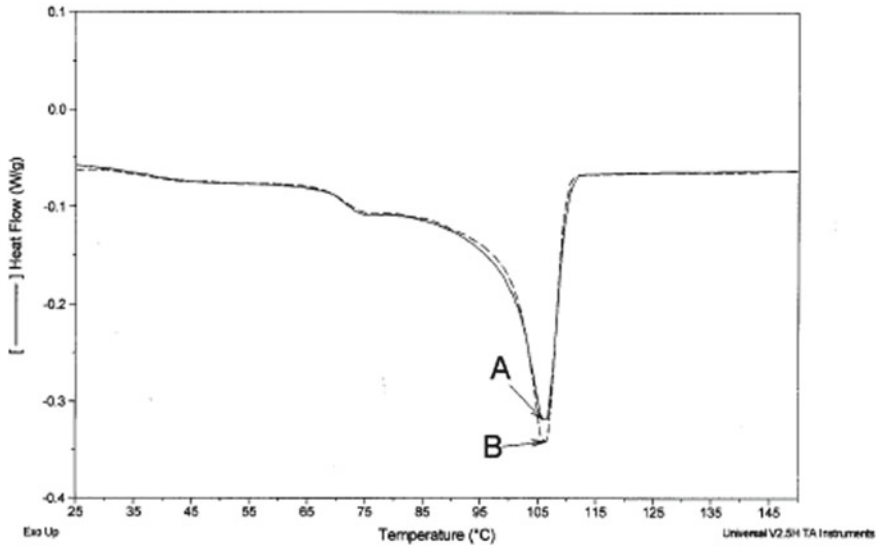


Fig. 13 DSC graphs for specimens taken from peels close (2 mm) to the inner semiconductor (A) and to the outer semiconductor screen (B) [52]

Nilsson et al. [48] show a decrease in elongation, melting point T_m , recrystallization point T_c , and crystallization degree X_c after crosslinking and the crosslinking density increased, due to the restraining effects of the incorporated crosslinks, as seen in Fig. 14.

Li et al. [47] studied the mechanical properties and the effect on temperature between LLPE and XLPE. They reported that the mechanical modulus was decreased with the temperature increasing, because the thermal motion of polyethylene molecules increases with the temperature rising, and the material became gradually soft, Fig. 15.

Many scientific researchers reported the predicting residual stresses in cable insulation to improve the production process [42, 53, 54]. Several models were used to calculate stress based on the change in density during cooling process. As crystalline regions grow during cooling, the elastic modulus changes influence the development of the residual stresses. Figure 16 shows the changes in the volumetric strain via the diameter of the XLPE insulation, which show the shrinking of cable during the cooling process.

The models used to calculate the residual stress are depending on thermo-elastic approach [53], or heat transfer approach [56]. While the effect of the relaxation of XLPE during cooling on the residual stress continues to be large, it is proof that the viscoelastic model gives an accurate prediction of residual stress. Figure 17 shows an example of the change in residual stress predicted by viscoelastic model.

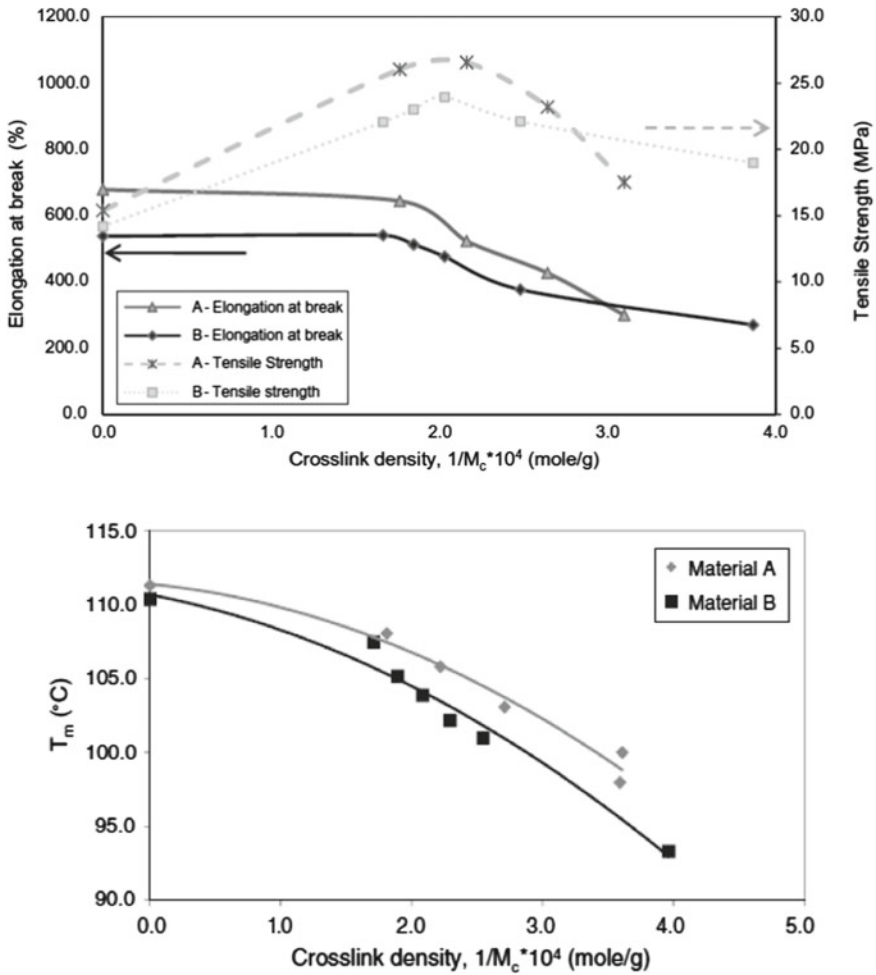


Fig. 14 Decrease in thermal and mechanical properties with the increase of crosslinking densities [48]

XLPE Electrical Properties

XLPE high voltage cables must have a good electrical stability during its lifetime service. Therefore, the electrical properties of XLPE are very important to cable insulation, and many research focused on studying the variation of XLPE electrical properties with manufacturing process and temperature. The relation between the morphology of XLPE and its electrical stability [44, 47] is crucial as it contributes to breakdown of the insulator through the phenomena called electrical treeing which will be discussed in details later on in this section.

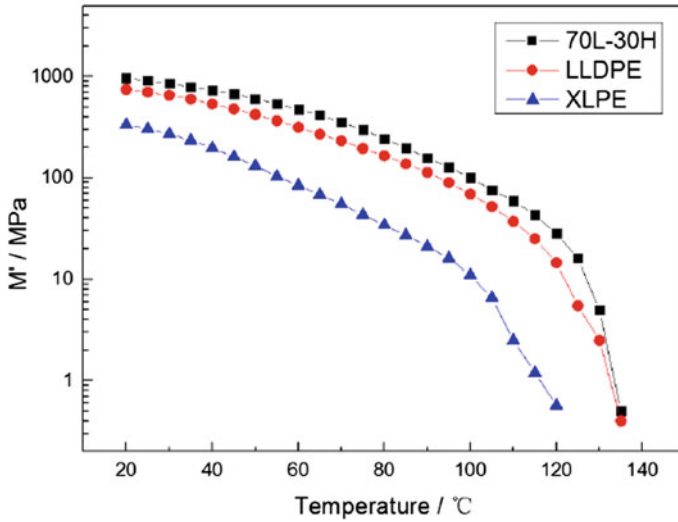


Fig. 15 Thermal spectrum for dynamic thermo mechanical of 70 L-30 H, LLDPE and XLPE [47]

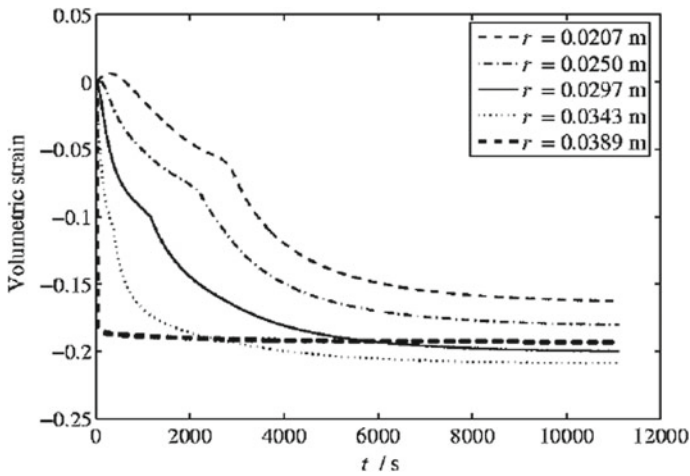


Fig. 16 Volumetric strain of the cable insulation at different radii during the cooling process [55]

Geng et al. [57] studied different electrical parameters as permittivity and current leak with temperature variation. They found that the real part of the complex permittivity begins to show a significant increase with a noticed decrease in electric field frequency for temperature above 140 °C, Fig. 18. This can be explained by the increase of the carriers in XLPE insulation at high temperature causing interface polarization. Moreover, the imaginary part of the complex dielectric constant increases with the increase of temperature.

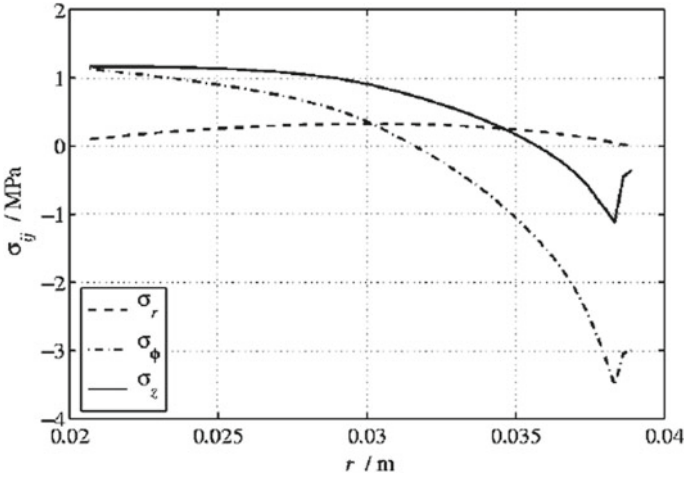


Fig. 17 Stress components in the insulation at the end of the cooling process calculated by the viscoelastic model [55]

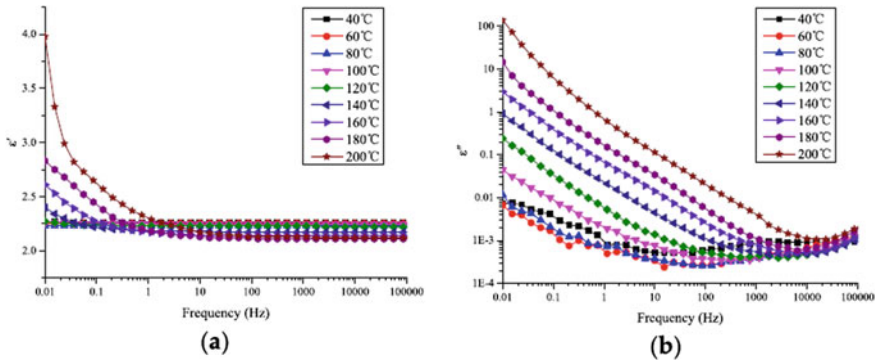


Fig. 18 **a** Frequency dependence of the real part of the complex permittivity, ϵ' , and **b** the imaginary part of the complex permittivity, ϵ'' under different test temperature

Geng et al. [57] also studied the variation in AC leakage current spectrum at different temperatures. They have shown that the AC leakage current is highly dependent on temperature and frequency due to its effect on the free charge and electric dipole movement. The active part of the leakage current increases with the increase of temperature at low-frequency range and tends to flatten. The reactive part of the leakage current increases significantly with the increase of frequency, but it is very little affected by the temperature (Fig. 19).

The measurement of breaking voltage on polyethylene crosslinked by silane showed that a 20% decrease and an increase of 30% on the leaking current were observed after three months of service (Figs. 20 and 21). This can be improved

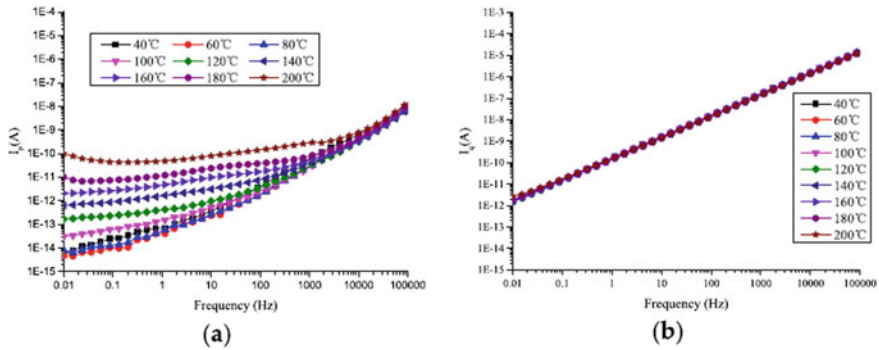


Fig. 19 **a** Frequency dependence of the active, I_p , and **b** reactive, I_q , parts of XLPE leakage current under different test temperature

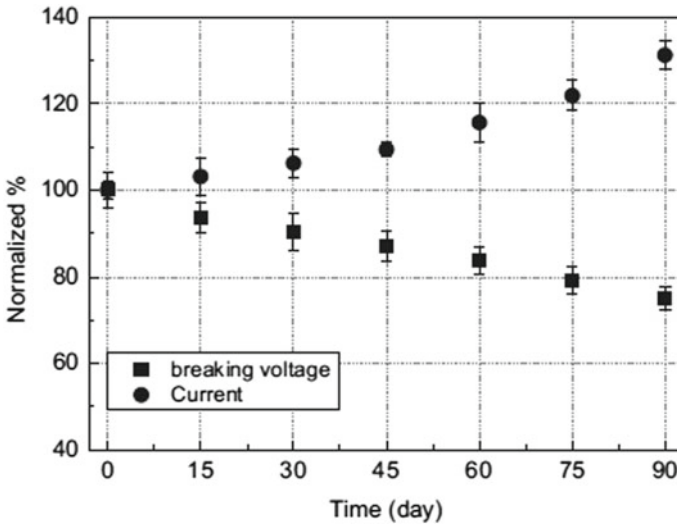


Fig. 20 Normalized breaking voltage, leakage current of PE/Silane samples versus annealing time at 80 °C

by using irradiation technique to enhance the crosslinking properties of XLPE as determined by Aljoumaa and Ajji [6].

Electrical treeing is a degradation phenomenon developing in dielectric insulation exposed to high electric fields [58]. Partial discharges initiate formation of a tree-like structure and cause the tree to propagate and eventually cross the entire insulation thickness, thereby short-circuiting it. Electrical trees can have shapes such as bush and branch depending on the electrical field intensity [59, 60] and applied voltage frequency [61]. The electrical tree can be initiated from contaminants, voids or cracks, and structure defects. It is a complicated electro-erosion phenomenon

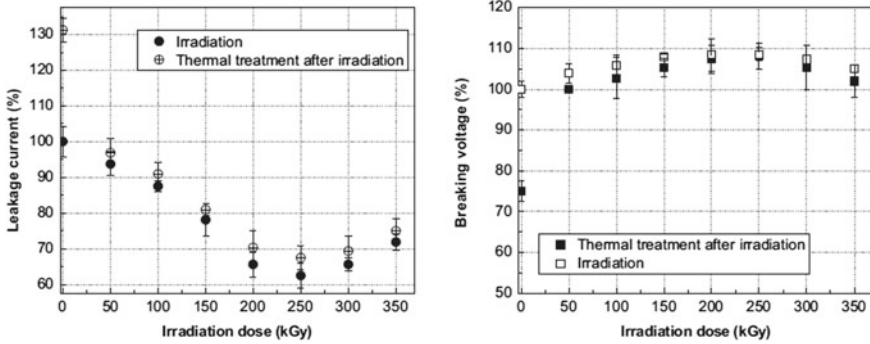


Fig. 21 Normalized leakage current (left), breaking voltage (right) of PE/Silane irradiated by gamma and annealed for 90 days at 80 °C

and a consequence of several processes including charge injection extraction, collision ionization, oxidation decomposition, partial discharge, partial high temperature, electro-mechanical stress, physics deformation, chemical decomposition, etc.

The process of electrical treeing can be described by three different stages: initiation, propagation and termination. The initiation process begins with the injection of space charge at high electrical field exceeding 100 kV/mm [31, 62, 63], where charge carriers can be injected or subtracted from the material near the stressed area and create local avalanches in the degraded area and the treeing begin to grow. The propagation of treeing continues via the ions produced in the avalanches which create positively charged bands and neutralize the injected electrons and forming a tube that extracts trapped electrons from the polymer at the tip of the tube, making the tree propagate into all directions by creating back avalanches [64]. Li et al. found that the polar groups, short branches, double bonds and impurities lying in crystalline and amorphous domains play an important role in acting as electron traps [65]. The created branches continue to grow in all directions by extracting electrons [66], Fig. 22.

As the tree propagates, the field at its tip will increase and the growth speed will begin to increase, to create a termination of treeing, the breakdown is prompted due to the polymer weakening. After this, a full short circuit of the insulation is created [67] (Fig. 23).

Many reports confirmed the relation between the crystalline morphology, cavities or voids, residual stress and the electrical failure of the insulation [68–71], where a network of cavities throughout the insulation layer represents a good pathway for the formation of electrical treeing that consists of consecutive discharges between the cavities.

According to Dissado and Fothergill [67], the other form of treeing is water treeing, which develops in the presence of an electrolyte at lower threshold electrical field at 1.9 kV/mm. Water trees are also initiated from deformations or contaminants in the material into two different forms: vented trees that are created by deformations at the edge of the insulation, and bow-tie trees which are created by contaminants inside the

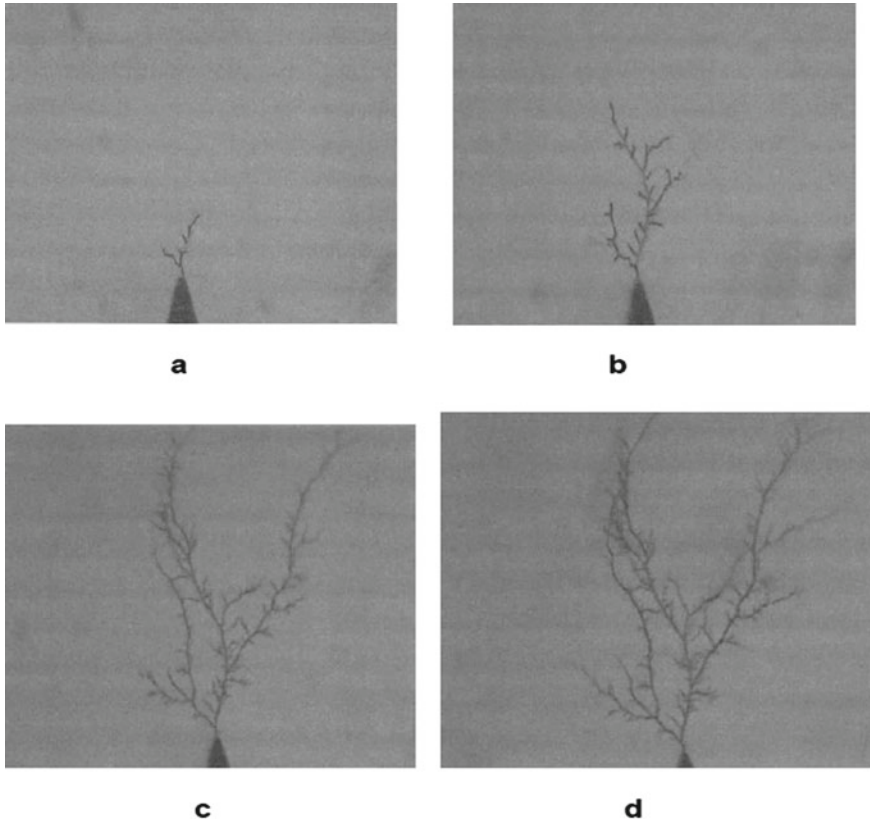


Fig. 22 Branch type electrical tree growth: **a** $L_m = 60 \mu\text{m}$, $t = 2 \text{ s}$; **b** $L_m = 500 \mu\text{m}$, $t = 7 \text{ s}$; **c** $L_m = 670 \mu\text{m}$, $t = 15 \text{ s}$; and **d** $L_m = 780 \mu\text{m}$, $t = 25 \text{ s}$. Applied voltage = 12 kV. L_m = Maximum axial tree length [60]

insulation, Fig. 24. There are a lot of factors which affect water treeing significantly: applied frequency (affects both initiation and propagation), degree of crosslinking [72, 73], morphology of the polymer matrix [74], magnitude of the applied electric field [75] and electrolyte's chemical content.

Furthermore, water trees take place on a micrometric through connecting the micro-voids in the structure of XLPE and reduce the breakdown strength during leading changes in the dielectric and viscoelastic responses. After a period of time, water trees give rise to electrical trees which in shorter time will lead to breakdown of insulator via arc discharge through electrical trees or via thermal breakdown if the tree is enough conductive, Table 2.

Sarathi et al. demonstrate that only XLPE thermal characteristics are altered due to electrical treeing and no new phases were observed in the electrical treed zone [70]. Zheng and Chen [69] studied the effects of the residual mechanical stress and the large crystal spherulite on the propagation of the electrical tree and they found that they

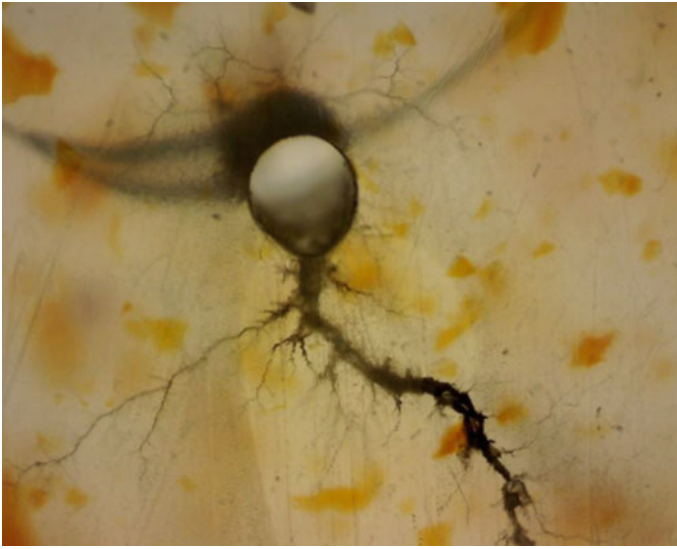


Fig. 23 Electrical treeing sample subjected to a full and irreversible breakdown [68]

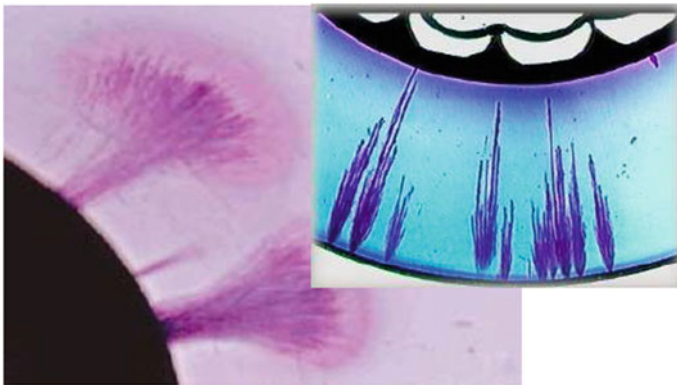







Fig. 24 Water trees growing from the inner (bottom) and outer (top) semiconductive screens [38]

have a significant influence. Figure 25a shows electrical tree propagation along the mechanical stress region and Fig. 25b shows the propagation around the boundary of the large crystalline spherulite. Ciuprina et al. [76] concluded that crosslinking plays a role in limiting water trees initiation due to the improvement of stress-cracking resistance of crosslinked polyethylene, while the crosslinking does not influence water tree propagation. Ciuprina et al. found that chemical crosslinking is not a retarding factor for water tree growth [77].

Undoubtedly, the micropores, inhomogeneous crystallization and the residual mechanical stress are the three important factors that cause the electrical tree to grow

Table 2 Propagation processes of the double structure electrical tree [69]

Phase	Item		Characterization
	The structure change of electrical tree		
	In the process	In the end	
1. Branch initiation process			(1) Charges injection and extraction to insulation from needle, then electrical tree is initiated (2) Single branch structure□ initiating
2. The electrical tree stagnant phase			(1) Charges injection and extraction to insulation from conducting tree (2) Dense and black tree□ or bush branch□ electrical tree □ appears
3. The double structure electrical tree appearing phase			Pine-branch tree initialization, Crown of vines-branch tree appears and grows rapidly The insulation would be broken down soon

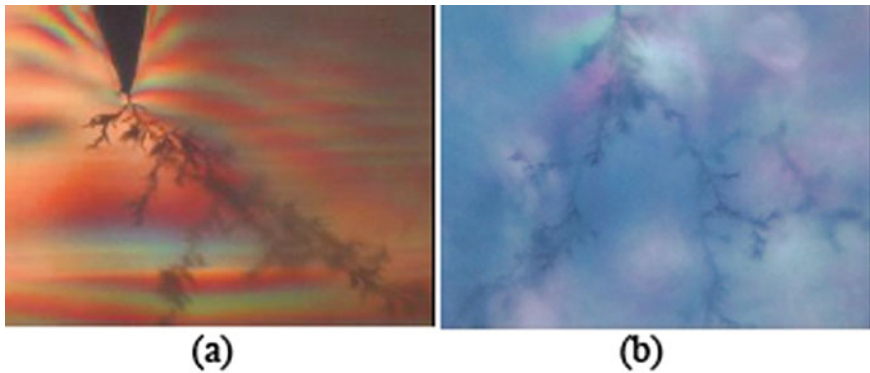


Fig. 25 The residual mechanical stress and uneven crystalline in sample taken by using the polarized microscope [69]

and raising a crucial problem that needs to be solved in manufacturing ultrahigh voltage XLPE cable with ultra-thick insulation [69].

Many reports mentioned that the electrical failure of XLPE cable insulation is caused by the growth of electrical treeing starting from weak points like contaminants, protrusions and voids (CPVs), therefore, the cable insulation has been recently

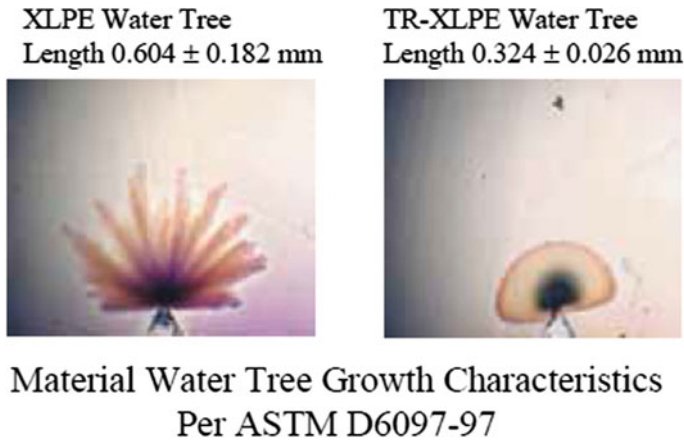


Fig. 26 Water tree growth patterns in XLPE and tree retardant-XLPE [82]

improved by manufacturing perfect and cleaner XLPE. Additives were used as voltage stabilizer [78], water tree retardant [79] to reduce the number and size of water trees in cable insulation, as seen in Fig. 26. Dong et al. [80] demonstrated that adding of 1-(4-vinyloxy) phenylethenone (VPE) can greatly improve the AC breakdown strength and the electrical tree initiation voltage, similar effect was found by adding Thioxanthone derivatives [81].

2.2 Hip Arthroplasty

Crosslinked polyethylene has many applications in the medical sector; the most important is the total Hip Arthroplasty that is the treatment for degenerative arthritis of the hip by replacement surgery of joint with an implant capable to recreate the articulation functionality. Several materials were used in order to combine biocompatibility and fatigue resistance, stiffness, toughness, withstanding static and dynamic loads, and finally high resistance to mechanical and chemical wear [83, 84]. Polyethylene (UHMWPE) was introduced for joint replacements since 1962 by Charnley for its potential properties [85], Fig. 27 shows some design of the designed acetabular cups. Nevertheless, the sterilization process by irradiation that created XLPE showed an oxidation-induced embrittlement.

Later, the modification in the treatment process has emerged to increase wear and oxidation resistance of the polymer. There are different treatments used to improve the mechanical and physical properties of the XLPE using irradiation and melting, irradiation and annealing, sequential irradiation with annealing, irradiation followed by mechanical deformation and irradiation and stabilization with vitamin E [86–89] or blending with tocopherol [90, 91]. Moreover, XLPE showed good mechanical properties (toughness, stiffness and hardness) material for hip bearing better than

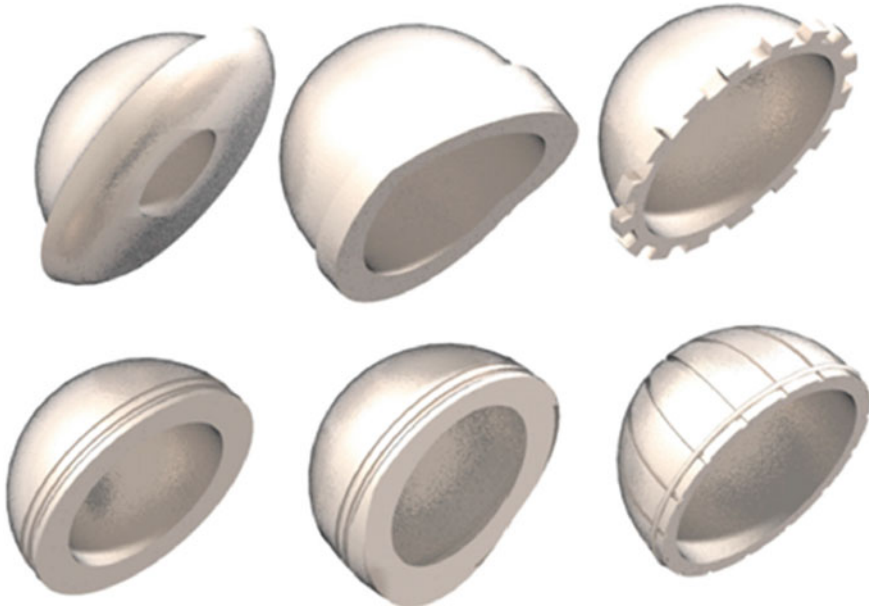


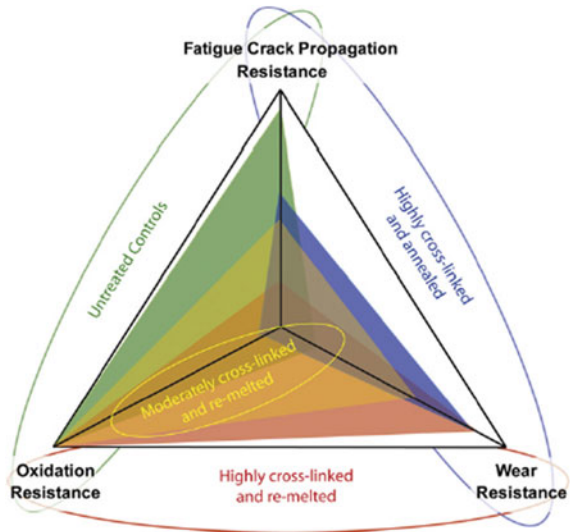
Fig. 27 Some of the designs that are achieved with XLPE for the acetabular cup [85]

conventional polyethylene (UHMWPE) [92–95]. However, the free radicals generated by irradiation through the process of crosslinking cause a problem of forming oxidized species that must be eliminated [96], where the correct level of irradiation to create XLPE should be regulated and thermal annealing must be used to remove the free radicals [89, 97]. Muratoglu et al. [98] and Puppulin et al. [99] studied the oxidation in the XLPE acetabular liners and assumed that lipids react with oxygen and provoke free radical generation via extracting hydrogen for polymer. Moreover, it is found that oxidation process in XLPE affects mechanical property through the oxidative chain scissions, which leads to variation in properties of acetabular liners [100, 101].

Atwood et al. [88] simultaneously evaluated the oxidative stability, fatigue crack propagation resistance, and wear resistance in ultrahigh polyethylene treated by different methods; they found that a trade-off among them as explained in Fig. 28. Where, the polymer behavior depends on both treatment (radiation, heating), radiation induce crosslinking causing an increase in wear resistance and decrease fatigue resistance while annealing reduce fatigue resistance.

Takahashi et al. [102] show that the percentage of the crystalline phases are rapidly changed within the first 35 μm from the surface articulating and a constant trend of crystallization in the depth while the lowest crystallinity at the surface due to surface finishing performance at the end process of manufacturing (lathe grinding, polishing) (Fig. 29). This confirms the existence of two structures in XLPE total hip replacement: anisotropic surface and isotropic bulk (Fig. 29), which is responsible

Fig. 28 Schematic showing the trade-offs in fatigue crack propagation resistance, wear resistance, and oxidation resistance. The vertices of the colored triangles on each axis represent the relative performance in that category [88]



for wear and creep resistance. Crystallinity of the crosslinked UHMWPE depends on the irradiation dose and the thermal treatment [103–105], whereas irradiation process causes smaller chain with augmented mobility leads to changes in crystallinity, while heat treatment increases the mobility of polymer chain yielding higher crystallinity that depending on the temperature reached. Nevertheless, during the cooling process with the presence of crosslinking, the crystallinity decreases and the wear resistance improves [104].

The morphology of UHMWPE changes due to mechanical movement, through a process called wear, which is an adhesive/abrasive that leads to the formation of micro-particles [106]. This process depends on the crystalline structure of XLPE causing plastic deformation of the articulating surface due to cyclic tension [104, 107]. The surface conditions of the femoral head component (roughness, hardness) affect the adhesion/abrasion wear mechanism, whereas the hardness should be higher than those of the acrylic bones and the head should be as smooth as possible.

After crosslinking, polyethylene showed a reduction in the abrasive and in the adhesive wear in several *in vitro* joint simulation studies [93, 108]. Muratoglu et al. [93] found that wear rates decrease with increasing the irradiation dose and reach the saturation at dose around 150 kGy (Fig. 30). However, crosslinking procedures affect also the polymer structure and its mechanical properties as strength, ductility, elastic modulus, fracture toughness, and crack propagation resistance [88, 94, 109–113].

Therefore, researches revise the first generation for XLPE total hip replacement and develop the XLPE material to produce almost ‘zero’ wear [114–116]. The first generation produced had improved wear resistance in comparison with basic UHMWPE and a reduction in volumetric wear was noticed [108, 117, 118]. Affatato et al. [94] show the internal surface of treated XLPE acetabular cups that crosslinked

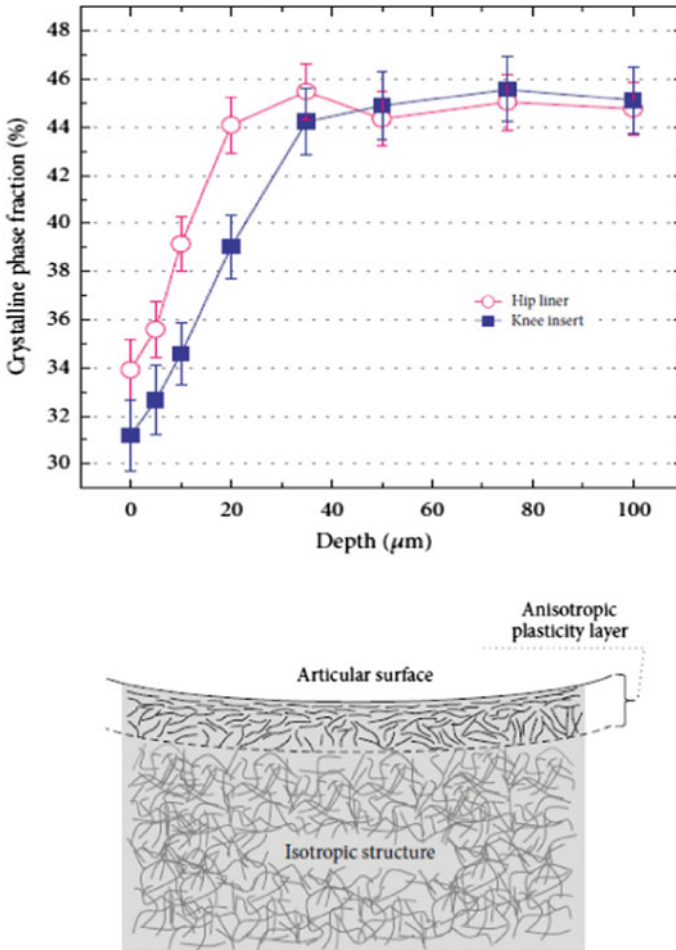


Fig. 29 Depth profiles of crystalline phase fraction collected in the as-received XLPE hip and knee components, schematic of XLPE microstructure consisting of anisotropic layer and isotropic random structure [102]

by different methods (Fig. 31), and the effect of wear on the surface. They found that, XLPE EtO-sterilized has less affected by wear.

Takada et al. [119] and D'antonio et al. [120] Compared the wear behavior in the two XLPE generations: the remelted (first-generation) and the annealed (second-generation). They found a better wear resistance in the second generation compared with the first one.

Nevertheless, a decrease in toughness, tensile strength and fatigue crack propagation resistance was noticed in acetabular liners [121–123]. Ansari et al. [124] studied the propagation of fatigue crack and its relation to stress intensity and showed that fibrillation and rippling on the fracture surfaces diminished due to crosslinking

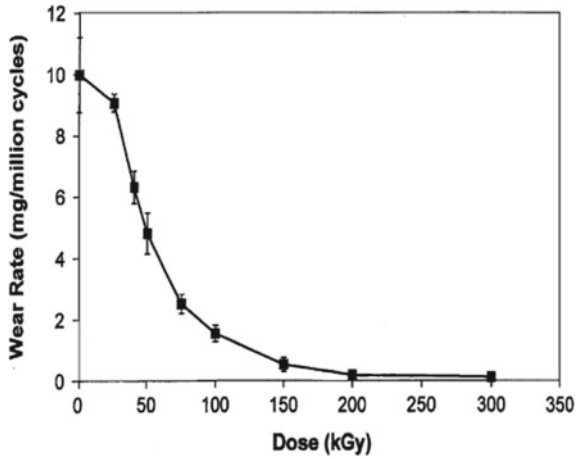


Fig. 30 Wear rate as a function of radiation dose

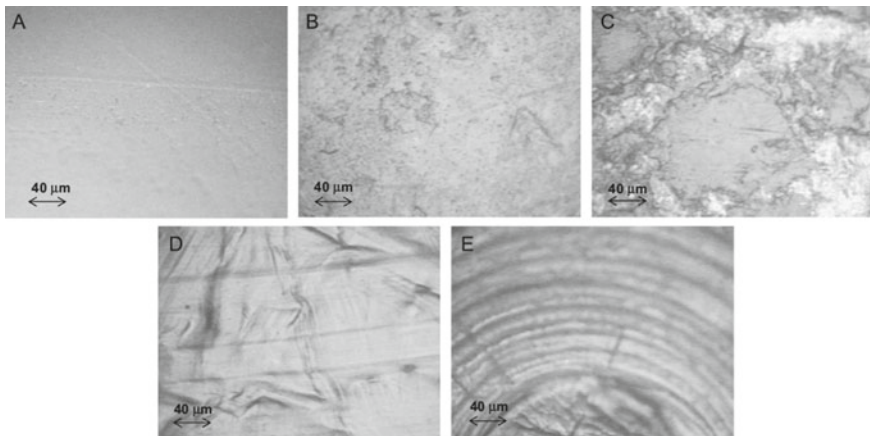


Fig. 31 Visual appearance of the center of the acetabular cups analyzed by Raman spectroscopy: **a** PE GUR1020 g-irradiated; **b** PE GUR1020 EtO sterilized; **c** PE GUR1050 g-irradiated; **d** XLPE-RT GUR1050 EtO-sterilized; **e** XLPE GUR1020 EtO-sterilized [94]

(Fig. 32). While Oral et al. [125] and others [109, 110] showed the relation between the irradiation doses, post-irradiation melting and the morphology of the fatigue crack propagation resistance that decrease with the increase of irradiation dose and with the decrease of the crystallinity. Cybo et al. [111] show that higher molecular weights are more advantageous and the irradiation results in improvement in wear resistance and young modulus.

Recently, different methods are developed to improve the properties of the second generation of highly crosslinked UHMWPEs. Diffusing vitamin E in irradiated UHMWPE to stabilize the free radicals was first clinically used in hip implant in

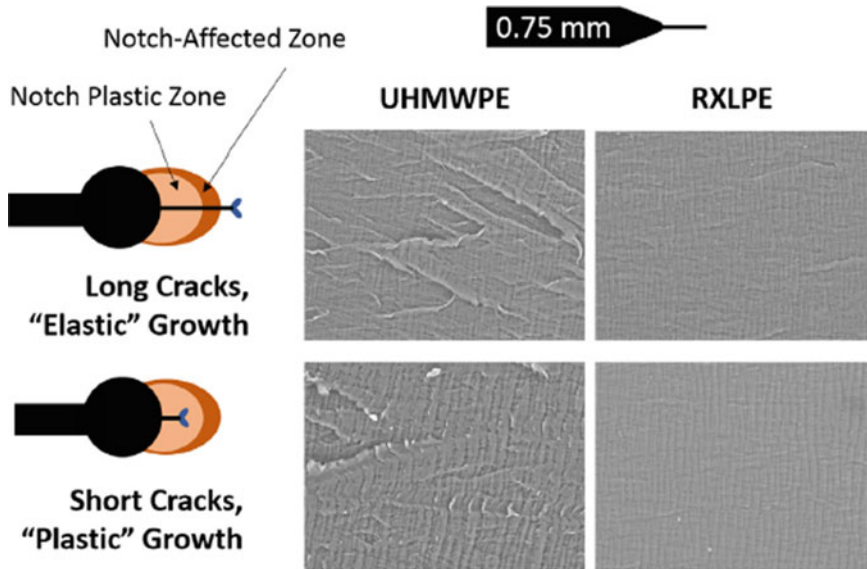


Fig. 32 SEM images of fracture surfaces for cracks growing outside the notch-affected zone and notch-plastic zone. UHMWPE samples demonstrate greater ductile features (rippling, criss-cross features) than both RXLPE

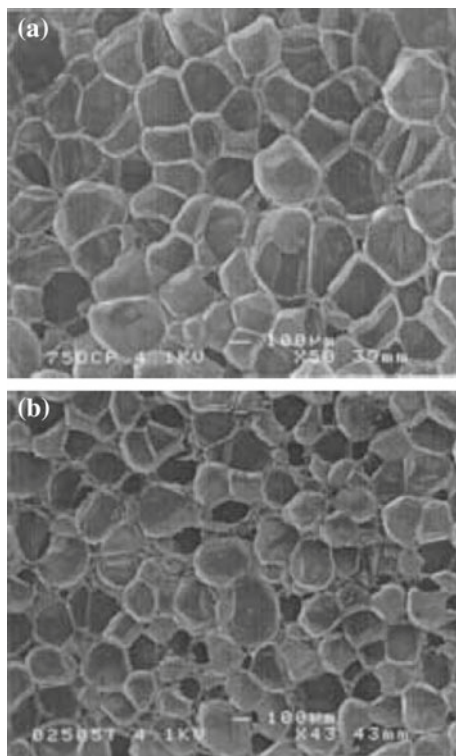
2007 [126]. However, these processes led to a decrease in the reactivity of the radicals and break the oxidation cycle and gave origin to the third generation hip implant XLPE [126–129].

2.3 XLPE Foam

The structure of foamed polymer consists of two phases: gas and polymer. Foaming can be produced by chemical or physical methods. In chemical methods, a chemical nucleation agent is added to the melting polymer and the gas is generated by the decomposition of the nucleator. While in physical foaming, external gas called the foaming agent is used. The growth of the foam cell is controlled by the gas pressure and the heating temperature [130].

Crosslinking technology is practical to polyolefin foaming, which can stabilize bubbles during foam expansion, enhance the thermal resistance, the mechanical properties (anti-creep, weather ability, impact, absorption, etc.) [131]. LLDPE, LDPE, HDPE foams are usually crosslinked during the manufacturing process [132]. Crosslinked polyethylene foams (XLPE foam) properties depend on the crosslinking process (chemical or physical) and on the blowing process (chemical or physical) [133, 134].

Fig. 33 Cell structure comparison of XLPE foam at similar gel content and density, **a** 0.75 phr DCP, 69.2% gel content, 62 kg m^{-3} and **b** 0.25 phr DCP with 0.5 phr TAC, 69.9% gel content, 64 kg m^{-3} [135]



Sims and Sipaut [135] studied the effect of dicumyl peroxide (DCP) as a chemical crosslinking agent with triallylcyanoate (TAC), a crosslinking promoter on the properties of obtained XLPE foam. They found that TAC increases the crosslinking density more than DCP alone, which resulted in a higher nucleation density in the foam, as presented in Fig. 33.

Moreover, Sims and Sipaut [135] demonstrated that it is not possible to predict foaming characteristics using gel content alone, particularly when crosslinking promoters are used.

Zhou et al. [136] prepared crosslinked HDPE foam using DCP as a chemical crosslinking and CO_2 as a physical blowing agents, respectively. They studied the effect of DCP content on the morphology of the foam cell and demonstrated that using SEM micrographs for the fracture surface of HDPE foam that DCP content affects the cell structure as shown in Fig. 34. Where good cell structure in x -HDPE foam was obtained for particular concentration of DCP, and the cell structure deformed to oval to pyritohedron with specific concentration, but the excessive DCP limit the foaming behavior of HDPE.

Physically crosslinked polyethylene foam can be prepared by two methods: treatment of pellets by irradiation followed by screw extrusion [137], or extruding followed by irradiation [138]. Xing et al. [138] studied the effect of the irradiation

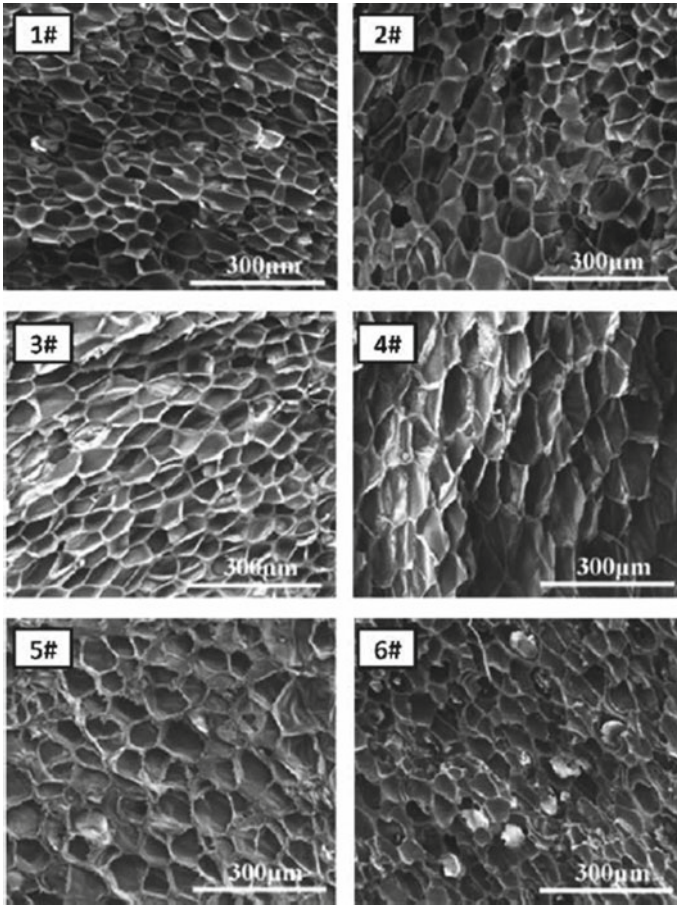


Fig. 34 SEM micrographs for foams of various HDPE samples (400 \times): 1: 0 phr, 2: 0.05 phr, 3: 0.10 phr, 4: 0.15 phr, 5: 0.20 phr, and 6: 0.25 phr

doses on the morphology of foaming using the two methods of preparation with CO₂ as a physical blowing agent. The crystallinity of prepared XLPE foam decreased with an increase in irradiation dose as seen for other type of XLPE. The fracture surface of the XPLE prepared foam using the two methods produced at 105 °C showed similar uniformly closed-cell structure (Figs. 35 and 36), with mean cell diameter less than 10 μm and cell density more than 10^9 cm^{-3} .

Moreover, Xing et al. [138] studied the effect of high temperature on the preparation of XLPE foam and observed the cells fusion and the breaking up of cell walls at foaming temperature of 130 °C for unirradiated LDPE which is due to weak elasticity modulus and stiffness of LDPE that cause cells collapsing during the depressurization. While the cells in crosslinked LDPE foam remained intact (displayed an impinging polygonal closed-cell structure as shown in Fig. 37), which demonstrated

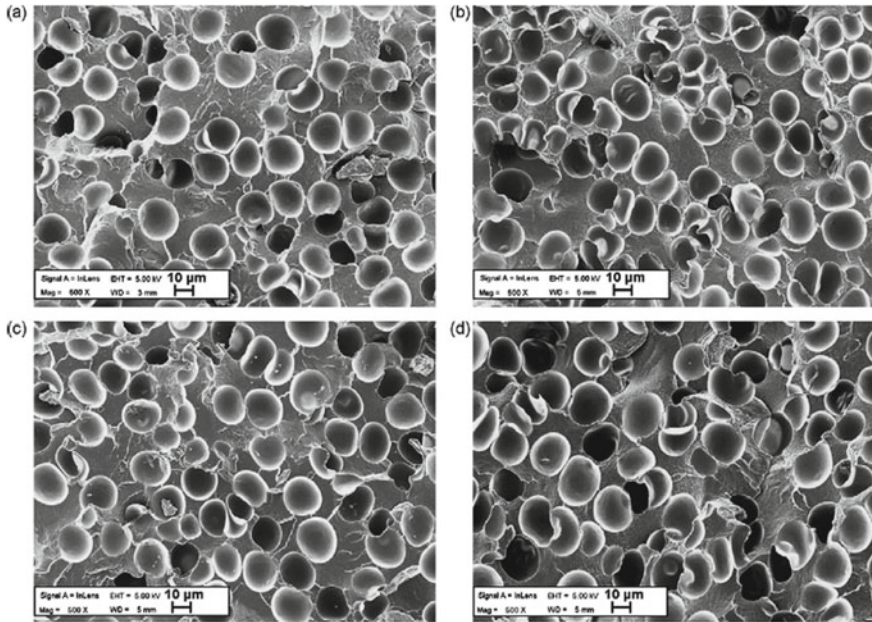


Fig. 35 SEM micrographs for the SB series (irradiated after foaming) of LDPE foams produced at 105 °C and at different doses (kGy): **a** 25; **b** 50; **c** 75; **d** 100 [138]

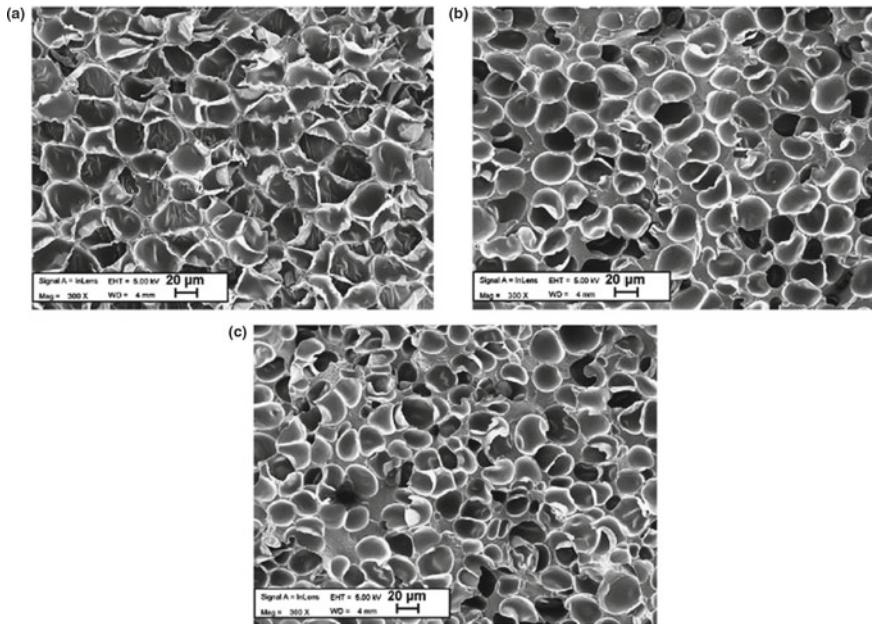


Fig. 36 SEM micrographs for the SA series (irradiated pellets) of LDPE foams produced at 105 °C and at different doses (kGy): **a** 50; **b** 75; **c** 100 [138]

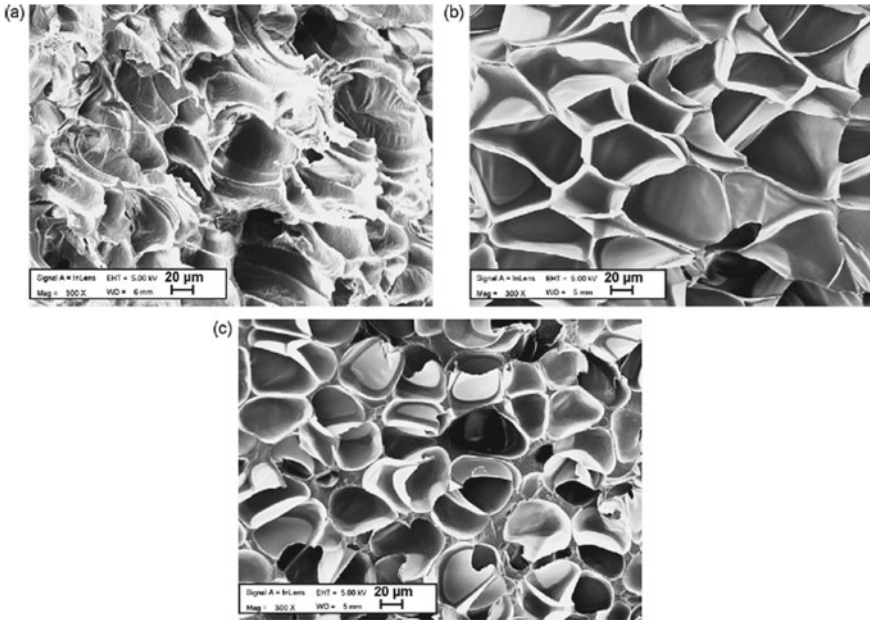


Fig. 37 SEM micrographs for three foaming specimens foamed at 130 °C **a** unirradiated (S0), **b** irradiated pellets at 50 kGy (SA50) and **c** irradiation at 50 kGy after foaming (SB50) [138]

that irradiation treatment increases foaming temperature range for LDPE due to the increase in melting strength and viscosity.

Furukawa [139] showed changes in morphology of the foaming cells that are due to the type of crosslinking (physical or chemical) as seen in Fig. 38. They obtained intact cells when a physically crosslinked foam was prepared (XLPE foam).

Closed-cells XLPE foam preserve good mechanical properties that make it suitable for various applications as Insulation/protection for pipes, air ducts, vessels and process equipment to prevent condensation, save energy and block sound propagation (Fig. 39). Moreover, the mechanical and the thermal properties can be ensured by using aluminum sheet to cover the foam that will be suitable for roofing insulation.

However, close-celled foam is not fit for applications that require a high permeability of gas or vapor, selective osmosis, and/or the absorption and dampening of sound, while the open-celled XLPE foam exhibits these properties and can be more suitable for applications as filters, separation membranes, diapers, etc.

There are many strategies to obtain open-celled foam, the basic one was to induce a hard/soft melt structure with crosslinking and to foam this non-homogeneous melt structure. The hard structure formed by the crosslinking maintains the shape of the cell while the soft section opens up the cell walls during the cell growth. The composition of the polymer and the additives must be optimized to obtain this structure [140].

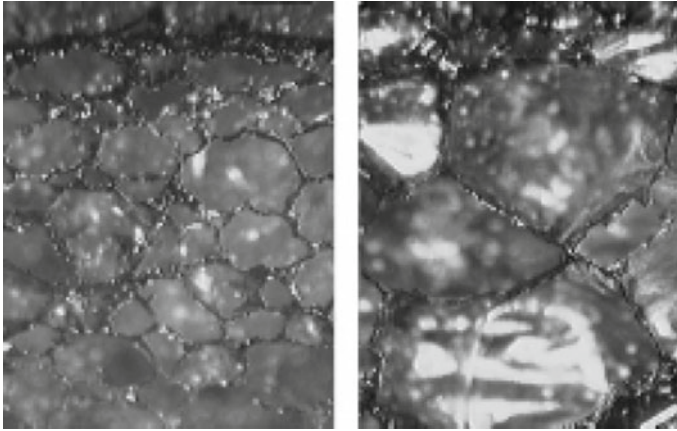


Fig. 38 Cell structure of two type of XLPE foam, physically crosslinked (left) and chemically crosslinked (right): (magnification 150 \times) [139]



Fig. 39 Some application of XLPE foam

2.4 Pipes

Crosslinked polyethylene used for many hot- and cold-water pipe systems is typically produced from HDPE (Fig. 40). In literature, the abbreviation PEX is well known in this application instead of XLPE. Crosslinking of polyethylene into PEX for pipes results in improved properties such as elevated temperature strength and performance,

Fig. 40 PEX pipes

chemical resistance, and resistance to slow crack growth, toughness, and abrasion resistance.

Irradiation technology was largely used for crosslinking of polyethylene pipes and used for the production of large diameter up to 450 mm with wall thickness up to 40 mm [141]. De Melo and Marques [142] studied the effect of crosslinking by peroxide (DCP) on the different properties of PEX, they found that adding a crosslinking coagent for the preparation of PEX improved the mechanical properties, increased modulus, and outstanding oil resistance properties, which make it suitable for oil pipes application. Samburski et al. [143] studied the oriented peroxide-crosslinked PE pipes by drawing process. The PEX pipe produced by this method had increase in melting temperature, degree of crystallinity and elastic modulus.

Crosslinking and stretching along the circumferential direction of the molten polyethylene during extrusion is one way of creating pipes with a predominantly circumferential molecular orientation. Higher degree of crystallinity and higher crystal thickness were found in oriented pipe material in comparison with conventionally crosslinked polyethylene, as shown in Fig. 41 [144].

Sun et al. [145] observed the variation in the crystalline morphology in XPE tubes, and they found, as seen in Fig. 42, that the anisotropic structures consisting of crystallites and lamellae stacked in parallel perpendicular to the crystallites, which is called shish-kebab morphology [146]. Moreover, the evolution of crystalline morphology caused by the different rotation extrusion rates was noticed, and mechanical properties were affected by the molecular orientation and degree of crystallinity.

Recently, Hiles et al. [147] proposed and developed a new methodology to classify different PEX pipe formulations and compare between them using the characteristic infrared (IR) spectroscopy absorbance peaks.

3 Summary

This chapter primarily demonstrates the up-to-date technology of polyethylene crosslinking manufacturing in general with emphasizing on the crosslinkable

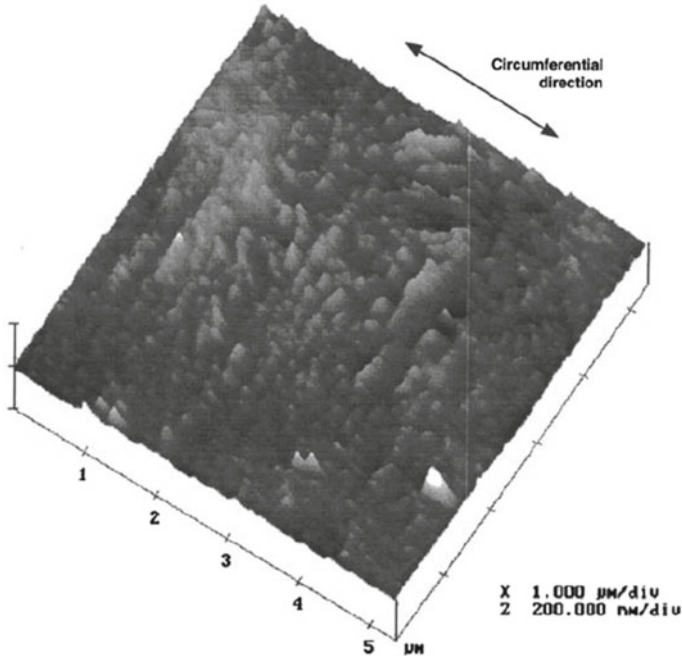


Fig. 41 Micrograph (AFM) showing the crystal lamellae texture from inner wall of oriented PEX [144]

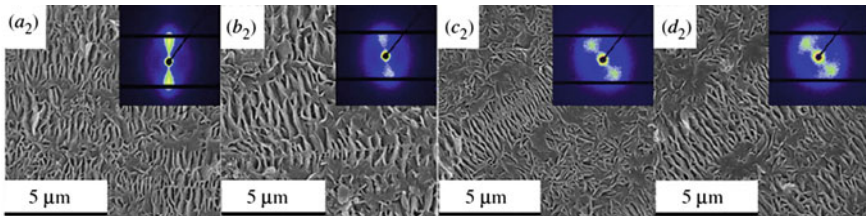


Fig. 42 XPE internal crystalline morphologies of (a_2) , (b_2) , (c_2) , (d_2) tubes with different mandrel rotation rates [145]

polyethylene compounds (XLPE) by investigation the morphology, structure, properties and applications of XLPE. The chapter explores also the XLPE applications starting from cable insulation. The different processes of production of XLPE cable insulation that alters the properties of final product were also discussed, in addition to that, an overview on the relation between crystallinity and crosslinking density and the morphology of crystallization after crosslinking have been considered. Mechanical and electrical properties of XLPE were argued widely showing the types of electrical failure inside the insulation.

Moreover, the XLPE for hip arthroplasty application has an essential part in this chapter, by going away through hip replacement fabrication using conventional or irradiation techniques and investigate the relationship between oxidation and wear resistances with fatigue crack propagation resistance.

In another paragraph, the application of XLPE foam was debated by explaining the fractures affecting the properties and the process of production that alters the formation of different types of foaming cells.

At the end, the productions of XLPE pipes and its thermal and mechanical properties are also covered in this fundamental chapter.

The chapter is supported by many interesting references covering all the raised points, which might help the readers for referring to them for more details.

References

1. Vaughan A, Davis DS, Hagadorn JR (2012) Industrial catalysts for alkene polymerization. In: Matyjaszewski K, Möller M (eds) *Polymer science: a comprehensive reference*. Elsevier, Amsterdam, pp 657–672
2. Whelton A, Dietrich A, Gallagher D (2010) Contaminant diffusion, solubility, and material property differences between HDPE and PEX potable water pipes. *J Environ Eng* 136(2):227–237
3. Shah GB, Fuzail M, Anwar J (2004) Aspects of the crosslinking of polyethylene with vinyl silane. *J Appl Polym Sci* 92(6):3796–3803
4. Sirisinha K, Boonkongkaew M, Kositchaiyong S (2010) The effect of silane carriers on silane grafting of high-density polyethylene and properties of crosslinked products. *Polym Test* 29(8):958–965
5. Wang X, Yoshimiura N (1998) In: *International symposium on electrical insulating materials*. Japan, 1998
6. Aljoomaa K, Aji Z (2016) Mechanical and electrical properties of gamma-irradiated silane crosslinked polyethylene (Si-XLPE). *J Radioanal Nucl Chem* 307:1391–1399
7. Morshedian J, Hosseinpour PM (2009) Polyethylene cross-linking by two-step silane method: a review. *Iran Polym J* 18(2):103–128
8. Kuan H-C, Kuan J-F, Ma C-C, Huang J-M (2005) Thermal and mechanical properties of silane-grafted water crosslinked polyethylene. *J Appl Polym Sci* 96:2383–2391
9. Barzin J, Azizi H, Morshedian J (2006) Preparation of silane-grafted and moisture cross-linked low density polyethylene: Part I: factors affecting performance of grafting and cross-linking. *Polym Plast Technol Eng* 45:979–983
10. Shah GB, Fuzail M, Anwar J (2004) Aspects of the crosslinking of polyethylene with vinyl silane. *J Appl Polym Sci* 92:3796–3803
11. Gl O, Mr C (2010) Optimization of process conditions, characterization and mechanical properties of silane crosslinked high-density polyethylene. *Mater Sci Eng* 527(18–19):4593–4599
12. Barzin J, Azizi H, Morshedian J (2007) Preparation of silane-grafted and moisture crosslinked low density polyethylene. Part II: electrical, thermal and mechanical Properties. *Polym-Plast Technol Eng* 46(3):305–310
13. Peschke E, Olshausen Rv (1999) *Cable systems for high and extra-high voltage: development, manufacture, testing, installation and operation of cables and their accessories*. Publicis MCD verlag
14. Hirabayashi H, Iguchi A, Yamada K, Nishimura H, Ikawa K, Honma H (2013) Study on the structure of peroxide cross-linked polyethylene pipes with several stabilizers. *Mater Sci Appl* 4(9):497–503

15. Vd R, Hm C, Ao P, McG R, As G (2004) Study of low concentrations of dicumyl peroxide on the molecular structure modification of LLDPE by reactive extrusion. *Polym Test* 23(8):949–955
16. Svoboda P, Poongavalappil S, Theravalappil R, Svobodova D, Mokrejs P (2013) Effect of octene content on peroxide crosslinking of ethylene-octene copolymers. *Polym Int* 62(2):184–189
17. Marcilla A, Ruiz-Femenia R, Hernández J, García-Quesada JC (2006) Thermal and catalytic pyrolysis of crosslinked polyethylene. *J Anal Appl Pyrolysis* 76(1–2):254–259
18. Lazar M, Rado R, Rychlý J (1990) Crosslinking of polyolefins. *Polym Phys* 149–197
19. Chmielewski AG, Haji-Saeid M, Ahmed S (2005) Progress in radiation processing of polymers. *Nucl Instrum Methods B* 236:44–54
20. Jiao C, Wang Z, Liang X, Hu Y (2005) Non-isothermal crystallization kinetics of silane crosslinked polyethylene. *Polym Test* 24(1):71–80
21. Phillips PJ, Kao YH (1986) Crystallinity in chemically crosslinked low density polyethylenes: 2. Crystallization kinetics. *Polymer* 27:1679–1686
22. Gohil RM, Phillips PJ (1986) Crystallinity in chemically crosslinked low density polyethylenes: 3. Morphology of the XLPE-2 system. *Polymer* 27:1687–1695
23. Gohil RM, Phillips PJ (1986) Crystallinity in chemically crosslinked low density polyethylenes: 4. Influence of crosslink density on morphology. *Polymer* 27:1696–1704
24. Paajanen A, Vaari J, Verho T (2019) Crystallization of cross-linked polyethylene by molecular dynamics Simulation. *Polymer* 171:80–86
25. Mason L, Doyle T, Reynolds A (1992) Effect of antioxidant concentration and radiation dose on oxidation induction time. In: *Electrical insulation, conference record of the 1992 IEEE international symposium on*, 7–10 Jun 1992, pp 169–172
26. Suh KS, Hwang SJ, Noh JS, Takada T (1994) Effects of constituents of XLPE on the formation of space charge. *IEEE Trans Dielectr Electr Insul* 1(6)
27. Englund V (2008) Voltage stabilisers for XLPE cable insulation. Thesis for the Degree of Doctorate of Engineering, Department of Chemical and Biological Engineering, Chalmers University of Technology
28. Melo RPD, Aguiar VdO, Marque MdFV (2015) Silane crosslinked polyethylene from different commercial PE's: influence of comonomer, catalyst type and evaluation of HLPB as crosslinking coagent. *Mater Res* 18(2):313–319
29. Cowie J, Arrighi V (2008) *Polymers: chemistry and physics of modern materials*, 3rd edn. CRC Press, Boca Raton
30. Ahmed N, Srinivas N (2001) Cable insulation. In: Webster J (ed) *Wiley encyclopedia of electrical and electronics engineering*. Wiley
31. Shimizu N, Laurent C (1998) Electrical tree initiation. *IEEE Trans Dielectr Electr Insul* 5(5):651–659
32. Zhang H, Zhang J, Duan L, Xie S, Xue J (2017) Application status of XLPE insulated submarine cable used in offshore wind farm in China. In: *The 6th international conference on renewable power generation (RPG)*, 19–20 Oct 2017
33. Worzyk T (2009) *Submarine power cables*. Springer, Berlin, Heidelberg
34. Nishikawa S, Sasaki K-i, Akita K, Sakamaki M, Kazama T, Suzuki K (2017) XLPE cable for DC link. *SEI Tech Rev* 84
35. Byggeth M, Johannesson K, Liljegren C, Palmqvist L, Axelsson U, Jonsson J, Törnkqvist C (1999) The development of an HVDC cable system and its first application in the Gotland HVDC light project. In: *JiCable*, Paris, 1999
36. Gustafsson A, Jeroense M, Ghorbani H, Quist T, Saltzer M, Farkas A, Axelsson F, Mondiet V (2015) Qualification of an extruded HVDC cable system at 525 kV. In: *JiCable 15*, Paris, 2015
37. Ghorbani H, Jeroense M, Olsson CO, Saltzer M (2014) HVDC cable systems—highlighting extruded technology. *IEEE Trans Power Delivery* 29(1):414–421
38. Hampton N, Rick H, Hakan L, Harry O (2007) Long-life XLPE insulated power cable. In: *Jicable*, 2007

39. Boysen RL (1970) An analysis of the continuous vulcanizing process for polyethylenes. In: IEEE Summer Power Meeting and EHV Conference, pp 926–933
40. Huotari P, Sistola M (1997) Production of XLPE insulated high and extra high voltage cable cores on catenary CV lines. *Wire Ind* 64(762):366–368
41. Gulmine JV, Akcelrud L (2004) Correlations between the processing variables and morphology of crosslinked polyethylene. *J Appl Polym Sci* 94:222–230
42. Olasz L (2006) Residual stresses and strains in cross-linked polyethylene power cable insulation. Doctoral thesis no. 63, KTH Engineering Sciences, Stockholm, Sweden
43. IEC (2004) Power cables with extruded insulation and their accessories for rated voltages above 30 kV ($U_m = 36$ kV) up to 150 kV ($U_m = 170$ kV)—test methods and requirements, 3rd edn. IEC
44. Fournier D, Robertson C (1996) Morphological study of aging phenomena in XLPE by TEM technique. *J Polym Sci: Part B Polym Phys* 34:1621–1628
45. Nilsson UH, Dammert RC, Campus A, Snec A, Jakosuo-Jansson H (1998) Morphology of polyethylene for power cable insulation: effects of antioxidant and crosslinking. In: IEEE international conference on conduction and breakdown in solid dielectrics. IEEE, pp 365–367
46. Woodward A (1989) Atlas of polymer morphology. Hanser Gardner Publications
47. Li L, Zhong L, Zhang K, Gao J, Xu M (2018) Temperature dependence of mechanical, electrical properties and crystal structure of polyethylene blends for cable insulation. *Materials* 11:1922
48. Nilsson S, Hjertberg T, Smedberg A (2010) Structural effects on thermal properties and morphology in XLPE. *Eur Polym J* 46:1759–1769
49. Lacevic N, Fried L, Gee R (2008) Heterogeneous directional mobility in the early stages of polymer crystallization. *J Chem Phys* 128:014903
50. Jabbari-Farouji S, Lame O, Perez M, Rottler J, Barrat J-L (2017) Role of the intercrystalline tie chains network in the mechanical response of semicrystalline polymers. *Phys Rev Lett* 118:217802
51. Mo Sj, Zhang J, Liang D, Chen Hy (2013) Study on pyrolysis characteristics of cross-linked polyethylene material cable. *Procedia Eng* 52:588–592
52. Dissado L, Fothergill J, See A, Stevens G, Markey L, Laurent C, Teyssedre G, Nilsson U, Platbrood G, Montanari G (2000) Characterizing HV XLPE cables by electrical, chemical and microstructural measurements on cable peeling: effects of surface roughness, thermal treatment and peeling location. *Electr Insul Dielectr Phenom* 1:136–140
53. Olasz L, Gudmundson P (2004) Viscoelastic model of cross-linked polyethylene including effects of temperature and crystallinity. Technical report 363, Royal Institute of Technology, Department of Solid Mechanics, Stockholm
54. Prat JÒ (2011) Study on conduction mechanisms of medium voltage cable XLPE insulation in the melting range of temperatures. Universitat Politècnica de Catalunya
55. Olasz L, Gudmundson P (2005) Prediction of residual stresses in high voltage cable insulation. In: SEM
56. Shugai G, Yakubenko PA (2003) Heat transfer processes in the curing tube during the production of XLPE insulated cables. In: Proceedings of HT2003 ASME summer heat transfer conference, pp 227–228
57. Geng P, Song J, Tian M, Lei Z, Du Y (2018) Influence of thermal aging on AC leakage current in XLPE insulation. *AIP Adv* 8:025115
58. Zhou YX, Luo XG, Yan P, Liang XD, Guan ZC, Yoshimura N (2001) Influence of morphology on tree growth in polyethylene. In: International symposium on electrical insulating materials (ISEIM), Himeji, Japan, 2001, pp 194–197
59. Sarathi R, Nandini A, Danikas MG (2011) Understanding electrical treeing phenomena in XLPE cable insulation adopting uhf technique. *J Electr Eng* 62(2):73–79
60. Qureshi MI, Malik NH, Al-Arainy AA (2012) Investigation of electrical treeing in cable grade crosslinked polyethylene (XLPE) insulations. *Int J Phys Sci* 7(1):132–138
61. Thiamsri R, Ruangakajonmathee N, Oonsivilai A, Marungsri B (2011) Effect of applied voltage frequency on electrical treeing in 22 kV cross-linked polyethylene insulated cable. *Int J Electr Comput Eng* 5(12)

62. Andrianjohanarivo J, Wertheimer M, Yelon A (1987) Nucleation of electrical stress in polyethylene. *IEEE Trans Electr Insul* EI-22(6):709–714
63. Krause G, Gottlich S, Moller K, Meurer D (1989) Space charge phenomena in partially crystalline polymers: on-line measurement of charge carrier motion under high AC-field stress. In: *Proceedings of the 3rd international conference on conduction and breakdown in solid dielectrics*, 3–6 Jul 1989, pp 560–564
64. Hozumi N, Okamoto T, Fukagawa H (1988) TEM observation of electrical tree paths and micro-structures in polyethylene. In: *Conference record of the 1988 IEEE international symposium on electrical insulation*, June 1988, pp 331–334
65. Jixiao L, Yewen H, Feihu Z, Changshun W, Zhongfu X (2003) The structure of XLPE and the distribution of space charge. *Sci China Ser G: Phys Mech Astron* 46(185)
66. Li Y, Zhang M, Liu H (2018) Research of grounded DC electrical tree growth properties in XLPE. *J Int Council Electr Eng* 8(1):93–98
67. Dissado L, Fothergill J (1992) Electrical degradation and breakdown in polymers. In: *IEE materials and devices series 9*. Peter Peregrinus, p 601
68. Doedens EH (2012) Organic contaminants in crosslinked polyethylene for demanding high voltage applications. Diploma Work in the Master programme of Electric Power Engineering, Chalmers University Of Technology, Gothenburg, Sweden
69. Zheng X, Chen G (2008) Propagation mechanism of electrical tree in XLPE cable insulation by investigating a double electrical tree structure. *IEEE Trans Dielectr Electr Insul* 15(3):800–807
70. Sarathi R, Venkataseshiah C, Kumar CRA (2002) Investigations of growth of electrical trees in XLPE cable insulation under different voltage profiles. In: *National power systems conference, NPSC, 2002*
71. Bellet JJ, Matey G, Rose J, Rose L, Filippini JC, Poggi Y, Raharimalala V (1987) Some aspects of the relationship between water treeing, morphology and microstructure of polymers. *IEEE Trans Electr Insul* 22:211
72. Nilsson S (2010) The effect of crosslinking on morphology and electrical properties in LDPE intended for power cables. Thesis for the Degree of Doctorate of Engineering, Department of Chemical and Biological Engineering, Chalmers University of Technology
73. Ciuprina F, Teissèdre G, Filippini J (2001) Polyethylene crosslinking and water treeing. *Polymer* 42:7841–7846
74. De Bellet JJ, Matey G, Rose L, Rose V, Filippini JC, Poggi Y, Raharimalala V (1987) Some aspects of the relationship between water treeing, morphology, and microstructure of polymers. *IEEE Trans Electr Insul* EI-22(2):211–217
75. Meyer C (1983) Water absorption during water treeing in polyethylene. *IEEE Trans Electr Insul* EI-18(1):28–31
76. Ciuprina F, Teissèdre G, Filippini JC, Smedberg A, Campus A, Hampton N (2010) Chemical crosslinking of polyethylene and its effect on water tree initiation and propagation. *IEEE Trans Dielectr Electr Insul* 17(3):709–715
77. Ciuprina F, Teissèdre G, Filippini JC, Notingher PV, Campus A, Zaharescu T (2004) Water treeing in chemically crosslinked polyethylene. *J Optoelectron Adv Mater* 6(3):1077–1080
78. Jarvid M, Johansson A, Bjuggren JM, Wutzel H, Englund V, Gubanski S, Müller C, Andersson MR (2014) Tailored side-chain architecture of benzil voltage stabilizers for enhanced dielectric strength of cross-linked polyethylene. *J Polym Sci, Part B: Polym Phys* 52:1047–1054
79. Boggs S, Xu J (2001) Water treeing-filled versus unfilled cable insulation. *IEEE Electr Insul Mag* 17(1):23
80. Dong W, Wang X, Tian B, Liu Y, Jiang Z, Li Z, Zhou W (2019) Use of grafted voltage stabilizer to enhance dielectric strength of cross-linked polyethylene. *Polymers* 11:176
81. Wutzel H, Jarvid M, Bjuggren J, Johansson A, Englund V, Gubanski S, Andersson MR (2015) Thioxanthone derivatives as stabilizers against electrical breakdown in cross-linked polyethylene for high voltage applications. *Polym Degrad Stab* 112:63–69
82. Caronia P, Mendelsohn A, Gross L, Kjellqvist J (2006) Global trends and motivation toward the adoption of TR-XLPE cable. In: *IEEE T&D conference, Dallas, 2006*

83. Aherwar A, Singh A, Patnaik A (2015) Current and future biocompatibility aspects of biomaterials for hip prosthesis. *AIMS Bioeng* 3:23–43
84. Affatato S (ed) (2014) *Perspectives in total hip arthroplasty: advances in biomaterials and their tribological interactions*. Elsevier Science, Amsterdam, The Netherlands
85. Merola M, Affatato S (2019) Materials for hip prostheses: a review of wear and loading considerations. *Materials* 12:495
86. Yamamoto K, Tateiwa T, Takahashi Y (2017) Vitamin E-stabilized highly crosslinked polyethylenes: the role and effectiveness in total hip arthroplasty. *J Orthop Sci* 22:384–390
87. Muratoglu O, Bragdon C (2015) Highly cross-linked and melted UHMWPE. In: Kurtz SM (ed) *UHMWPE biomaterials handbook: ultra high molecular weight polyethylene in total joint replacement and medical devices*. William Andrew, Norwich, NY, USA
88. Atwood SA, Citters DWV, Patten EW, Furmanski J, Ries MD, Pruitt LA (2011) Tradeoffs amongst fatigue, wear, and oxidation resistance of cross-linked ultra-high molecular weight polyethylene. *J Mech Behav Biomed Mater* 4(7):1033–1045
89. Oral E, Ghali B, Muratoglu O (2011) The elimination of free radicals in irradiated UHMWPEs with and without vitamin E stabilization by annealing under pressure. *J Biomed Mater Res Part B Appl Biomater* 97B:167–174
90. Oral E, Rowell S, Muratoglu O (2006) The effect of tocopherol on the oxidation and free radical decay in irradiated UHMWPE. *Biomaterials* 27:5580–5587
91. Oral E, Wannomae K, Hawkins N, Harris W, Muratoglu O (2004) Tocopherol-doped irradiated UHMWPE for high fatigue resistance and low wear. *Biomaterials* 25:5515–5522
92. Heisel C, Silva M, dela Rosa MA, Schmalzried TP (2004) Short-term in vivo wear of cross-linked polyethylene. *J Bone Joint Surg Am* 86-A(4):748
93. Muratoglu O, Bragdon C, O'Connor D, Jasty M, Harris W, Gul R, McGarry F (1999) Unified wear model for highly crosslinked ultra-high molecular weight polyethylenes (UHMWPE). *Biomaterials* 20:1463–1470
94. Affatato S, Zavalloni M, Taddei P, Foggia MD, Fagnano C, Viceconti M (2008) Comparative study on the wear behaviour of different conventional and cross-linked polyethylenes for total hip replacement. *Tribol Int* 41:813–822
95. Bracco P, Bellare A, Bistolfi A, Affatato S (2017) Ultra-high molecular weight polyethylene: influence of the chemical, physical and mechanical properties. *Materials* 10:791
96. Oral E, Ghali B, Muratoglu O (2011) The elimination of free radicals in irradiated UHMWPEs with and without vitamin e stabilization by annealing under pressure. *J Biomed Mater Res Part B Appl Biomater* 97 B:167–174
97. Burnett S, Abos D (2010) Total hip arthroplasty: Techniques and results. *BB Med. J.* 52:455–464
98. Muratoglu O, Wannomae K, Rowell S, Micheli B, Malchau H (2010) Ex vivo stability loss of irradiated and melted ultra-high molecular weight polyethylene. *JBJS* 92:2809–2816
99. Puppulin L, Miura Y, Casagrande E, Hasegawa M, Marunaka Y, Tone S, Sudo A, Pezzotti G (2016) Validation of a protocol based on Raman and infrared spectroscopies to nondestructively estimate the oxidative degradation of UHMWPE used in total joint arthroplasty. *Acta Biomater* 38:168–178
100. Reinitz S, Currier B, Levine R, Van Citters D (2014) Crosslink density, oxidation and chain scission in retrieved, highly cross-linked UHMWPE tibial bearings. *Biomaterials* 35:4436–4440
101. Currier B, Currier J, Mayor M, Lyford K, Van Citters D, Collier J (2007) In vivo oxidation of γ -barrier-sterilized ultra-high-molecular-weight polyethylene bearings. *J. Arthroplast* 22:721–731
102. Takahashi Y, Masaoka T, Pezzotti G, Shishido T, Tateiwa T, Kubo K, Yamamoto K (2014) Highly cross-linked polyethylene in total hip and knee replacement: spatial distribution of molecular orientation and shape recovery behavior. *BioMed Res Int*. <http://dx.doi.org/10.1155/2014/808369>
103. Bhateja S (1983) Radiation-induced crystallinity changes in linear polyethylene: influence of aging. *J Appl Polym Sci* 28:861–872

104. Muratoglu O, Bragdon C, O'Connor D, Skehan H, Delany J, Jasty M, Harris W (2000) The effect of temperature on radiation crosslinking of UHMWPE for use in total hip arthroplasty. In: 46th Annual Meeting, Orthopaedic Research Society, Orlando, USA
105. Oral E, Beckos C, Muratoglu O (2008) Free radical elimination in irradiated UHMWPE through crystal mobility in phase transition to the hexagonal phase. *Polymer* 49:4733–4739
106. Sinha R (2002) Hip replacement: current trends and controversies. Marcel Dekker, New York City, NY, USA
107. Sobieraj M, Rimnac C (2009) Ultra high molecular weight polyethylene: mechanics, morphology, and clinical behavior. *J Mech Behav Biomed Mater* 2:433–443
108. McKellop H, Shen FW, Lu B, Campbell P, Salovey R (1999) Development of an extremely wear-resistant ultra high molecular weight polyethylene for total hip replacements. *J Orthop Res* 17(2):157–167
109. Gencur SJ, Rimnac CM, Kurtz SM (2006) Fatigue crack propagation resistance of virgin and highly crosslinked, thermally treated ultra high molecular weight polyethylene. *Biomaterials* 27(8):1550–1557
110. Bradford L, Baker D, Ries M, Pruitt LA (2004) Fatigue crack propagation resistance of highly crosslinked polyethylene. *Clin Orthop Relat Res* 429:68–72
111. Cybo J, Maszybrocka J, Barylski A, Kansy J (2012) Resistance of UHMWPE to plastic deformation and wear and the possibility of its enhancement through modification by radiation. *J Appl Polym Sci* 25(6):4188–4196
112. Pruitt LA (2005) Deformation, yielding, fracture and fatigue behavior of conventional and highly cross-linked ultra high molecular weight polyethylene. *Biomaterials* 26:905–915
113. Hodrick JT, Severson EP, McAlister DS, Dahl B, Hofmann AA (2008) Highly crosslinked polyethylene is safe for use in total knee arthroplasty. *Clin Orthop Relat Res* 466:2806–2812
114. Muratoglu OK, Bragdon CR, O'Connor DO, Jasty M, Harris WH (2001) A novel method of cross-linking ultra-high-molecular-weight polyethylene to improve wear, reduce oxidation, and retain mechanical properties. *J Arthroplasty* 16(2):149
115. Muratoglu OK, O'Connor DO, Bragdon CR, Delaney J, Jasty M, Harris WH, Merrill E, Venugopalan P (2002) Gradient crosslinking of UHMWPE using irradiation in molten state for total joint arthroplasty. *Biomaterials* 23(3):717
116. Kurtz SM, Medel FJ, MacDonald D, Parvizi J, Kraay MJ, Rimnac CM (2010) Reasons for revision of first-generation highly cross-linked polyethylenes. *J Arthroplasty* 25(6):67–74
117. Muratoglu OK, Wannomae K, Christensen S, Rubash HE, Harris WH (2005) Ex vivo wear of conventional and crosslinked polyethylene acetabular liners. *Clin Orthop Relat Res* 438:158–164
118. Garcia-Rey E, Garcia-Cimbreno E, Cruz-Pardos A, Ortega-Chamarr J (2008) New polyethylenes in total hip replacement: prospective, comparative clinical study of two types of liner. *J Bone Joint Surg B* 90(2):149–153
119. Takada R, Jinno T, Koga D, Miyatake K, Muneta T, Okawa A (2017) Comparison of wear rate and osteolysis between second-generation annealed and first-generation remelted highly cross-linked polyethylene in total hip arthroplasty. A case control study at a minimum of five years. *Orthop Traumatol Surg Res* 103:537–541
120. D'Antonio J, Capello W, Ramakrishnan R (2012) Second-generation annealed highly cross-linked polyethylene exhibits low wear. *Clin Orthop Relat Res* 470:1696–1704
121. Atwood SA, Van Citters DW, Patten EW, Furmanski J, Ries MD, Pruitt LA (2011) Tradeoffs amongst fatigue, wear, and oxidation resistance of cross-linked ultra-high molecular weight polyethylene. *J Mech Behav Biomed Mater* 4(7):1033–1045
122. Oral E, Malhi AS, Muratoglu OK (2006) Mechanisms of decrease in fatigue crack propagation resistance in irradiated and melted UHMWPE. *Biomaterials* 27(6):917–925
123. Pruitt LA (2005) Deformation, yielding, fracture and fatigue behavior of conventional and highly cross-linked ultra high molecular weight polyethylene. *Biomaterials* 26(8):905–915
124. Ansari F, Gludovatz B, Kozak A, Ritchie RO, Pruitt LA (2016) Notch fatigue of ultra high molecular weight polyethylene (UHMWPE) used in total joint replacements. *J Mech Behav Biomed Mater* 60:267–279

125. Oral E, Malhi AS, Muratoglu OK (2006) Mechanisms of decrease in fatigue crack propagation resistance in irradiated and melted UHMWPE. *Biomaterials* 27(6):917–925
126. Bracco P, Oral E (2011) Vitamin E-stabilized UHMWPE for total joint implants: a review. *Clin Orthop Relat Res* 469:2286–2293
127. Affatato S, De Mattia J, Bracco P, Pavoni E, Taddei P (2016) Wear performance of neat and vitamin E blended highly cross-linked PE under severe conditions: the combined effect of accelerated ageing and third body particles during wear test. *J Mech Behav Biomed Mater* 64:240–252
128. Kurtz S, Bracco P, Costa L (2009) Vitamin-E-blended UHMWPE biomaterials. In: *UHMWPE biomaterials handbook*. Elsevier, Amsterdam, The Netherlands, pp 237–247
129. Kurtz S, Bracco P, Costa L, Oral E, Muratoglu O (2015) Vitamin E-blended UHMWPE biomaterials. In: Kurtz SM (ed) *UHMWPE biomaterials handbook: ultra high molecular weight polyethylene in total joint replacement and medical devices*. Elsevier, Norwich, NY, USA, 2015, p 840
130. Ramesh NS, Rasmussen DH, Campbell GA (1991) Theoretical and experimental study of the dynamic of foam growth in thermoplastic materials. *ANTEC*, pp 1292–1296
131. Lee S, Park CB, Ramesh NS (2007) *Polymeric foams*. CRC Press, New York
132. Rodriguez-Perez MA (2005) Crosslinked polyolefin foams: production, structure, properties, and applications. *Adv Polym Sci* 184:97–126
133. Klemmner D, Frisch KC (1991) *Handbook of polymeric foams and foam technology*. Hanser Publisher, New York
134. Danaei M, Sheikh N, Taromi FA (2005) Radiation cross-linked polyethylene foam: preparation and properties. *J Cell Plast* 41:551
135. Sims GLA, Sipaut CS (2001) Crosslinking of polyolefin foams: I. Effect of triallyl cyanurate on dicumyl peroxide crosslinking of low-density polyethylene. *Cell Polym* 20(4)
136. Zhou H, Wang Z, Xu G, Wang X, Wen B, Jin S (2017) Preparation of crosslinked high density polyethylene foam using supercritical CO₂ as blowing agent. *Cell Polym* 36(4)
137. Cheng S, Dehaye F, Bailly C, Biebuyck J, Legras R, Parks L (2005) Studies on polyethylene pellets modified by low dose radiation prior to part formation. *Nucl Instrum Methods Phys Res Sect B: Beam Interact Mater Atoms* 236:130–136
138. Xing Z, Wu G, Huang S, Chen S, Zeng H (2008) Preparation of microcellular cross-linked polyethylene foams by a radiation and supercritical carbon dioxide approach. *J Supercrit Fluids* 47(2):281–289
139. Furukawa (2002) Physically cross-linked polyethylene foam “SlimAce”. *Furukawa Rev* 22
140. Park CB, Padareva V, Lee PC, Nagui HE (2005) Extruded open-celled LDPE-based foams using non-homogeneous melt structure. *J Polym Eng* 25(3)
141. Below H, Quilitz G, Schumann W (2005) Electron beam crosslinking of large diameter thick-walled polyethylene pipes. *Plast Rubbers Compos* 34(1)
142. de Melo RP, Marques MF (2011) PEX synthesized via peroxide for oil pipes, starting from different commercial polyethylenes: influence of comonomer and catalyst type. *Macromol Symp* 299/300:246–253
143. Samburski G, Narkis M, Siegmann A (1996) The effect of drawing parameters on the orientation distribution in crosslinked high density polyethylene tubing. *J Mater Sci Lett* 15:1969
144. Jarvenkyla J, Johansson B, Ek C-G, Palmlof M, Ahjopalo L, Kuutti L, Pietila L-O, Neway B, Geddes UW (1999) Oriented crosslinked polyethylene pipes by a novel extrusion method. *Macromol Symp* 148:373–393
145. Sun F, Guo J, Li Y, Bai S, Wang Q (2019) Preparation of high-performance polyethylene tubes under the coexistence of silicone cross-linked polyethylene and rotation extrusion. *R Soc Open Sci* 6:182095
146. Kimata S, Sakurai T, Nozue Y, Kasahara T, Yamaguchi N, Karino T, Shibayama M, Kornfield JA (2007) Molecular basis of the shish-kebab morphology in polymer crystallization. *Science* 316:1014–1017

147. Hiles M, Grossutti M, Dutcher JR (2019) Classifying formulations of crosslinked polyethylene pipe by applying machine-learning concepts to infrared spectra. *J Polym Sci Part B: Polym Phys*

Chapter 7

XLPE: Crosslinking Techniques and Recycling Process



Nithin Chandran, Anjaly Sivadas, E. V. Anuja, Deepa K. Baby, and Ragin Ramdas

1 Introduction

Polyethylene is the most popular plastic in the world. It has a very simple structure, the simplest of all commercial polymers. The long chain of CH_2 group represented as $(-\text{CH}_2-\text{CH}_2-)$ is called linear or high-density polyethylene (HDPE). However, ethylene molecules attach as short branches on $(-\text{CH}_2-\text{CH}_2-)$ backbone leading to low-density polyethylene (LDPE). In fact, wide range of application of PE, such as shop bags, packaging, households, electronic devices protectors, medical field and so on [1]. The fundamental way to enhance material properties such as impact strength, chemical resistance and thermal characteristics is via crosslinking. Crosslinking of polyethylene (XLPE) in the early 1970s was a milestone in the field of plastic industry [2]. XLPE has a large market share due to its high properties related to other plastics. Several methods have been developed to crosslink polyethylene including: peroxide, silane, radiation, etc. [3]. These different crosslinking methods are generally classified to chemically and physically. In chemical process, a chemical initiator is required to induce links in polymer chains. Silane- and peroxide-based crosslinking belongs to this category. Radiation process is a physical method of crosslinking which involve

N. Chandran (✉)

Department of Chemistry, MES College, Marampally, Aluva, Kerala 683105, India
e-mail: nithinpc@gmail.com

A. Sivadas

School of Chemical Sciences, Mahatma Gandhi University, Kottayam, Kerala 686560, India

E. V. Anuja

Govt. Polytechnic College, Muttom, Thodupuzha, Idukki, Kerala 685587, India

D. K. Baby · R. Ramdas

Department of Basic Sciences and Humanities, Rajagiri School of Engineering and Technology, Kochi, Kerala 682039, India

© Springer Nature Singapore Pte Ltd. 2021

J. Thomas et al. (eds.), *Crosslinkable Polyethylene*, Materials

Horizons: From Nature to Nanomaterials,

https://doi.org/10.1007/978-981-16-0514-7_7

exposure to ionizing radiation from either radioactive sources or highly accelerated electrons, to liberate free radicals for crosslinking.

1.1 Chemical Process

Crosslinking is activated by chemical reactions.

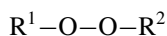
Peroxide method: this is a peroxide initiated crosslinking method. The crosslinked PE is known as PEX-A (European standards).

Silane method: Crosslinking of PE via silane- or moisture-based vinyl silane crosslinking. Crosslinked PE by this method is known as PEX-C (European standards).

1.1.1 Peroxide Method

The peroxide method involves the decomposition and creation of peroxide at higher temperature between the carbon bonds in the PE chains and the crosslinking occurs in the molten stage. The Engel process (German scientist Thomas Engel in the late 1960s), the granulated mixture of PE, peroxide and stabilizers are sintered together at high pressure; crosslinking occurs during extrusion through a long-heated die.

An organic peroxide is a carbon-based chemical which includes a minimum of two oxygen atoms bonded together ($-\text{O}-\text{O}-$) [4, 5]. The general representation is:



where R^1 and R^2 can be aryl, alkyl or acyl groups. There are also peroxides with a second $-\text{O}-\text{O}-$ bond and three R-groups. Based on the chemical structure, different families such as Alkyl, aryl, acyl peroxides and peroxyketals are considered as R groups. The alkyl peroxides such as dicumyl peroxide (DCP) (contains one $-\text{O}-\text{O}-$ group) and 1,3-1,4bis(tert-butylperoxyisopropyl) (contains two $-\text{O}-\text{O}-$ groups). The peroxide crosslinking reaction contains three steps:

First step: the addition of heat causes peroxide thermal decomposition. One unpaired electron remains in each oxygen atom and promotes the formation of peroxide radicals.

Second step: each peroxide radical reacts with the PE molecule, i.e., abstracts a hydrogen atom from the polymer chain, becoming a stable ROH species. The abstraction of hydrogen causes the formation of polymer radicals.

Third step: PEX is formed by the reaction between two polymer radicals.

DCP decomposes into two cumyloxy radicals $\text{Ph}-\text{C}(\text{CH}_3)_2\text{O}\cdot$ of equal reactivity. Alkoxy radicals are strong hydrogen abstracting agents and they quickly react with the polymer chains, releasing two macromolecular free-radical initiators $-\text{CH}_2-\text{CH}-\text{CH}_2-$ (Route A) [6], alternatively, a cumyloxy radical can undergo decomposition

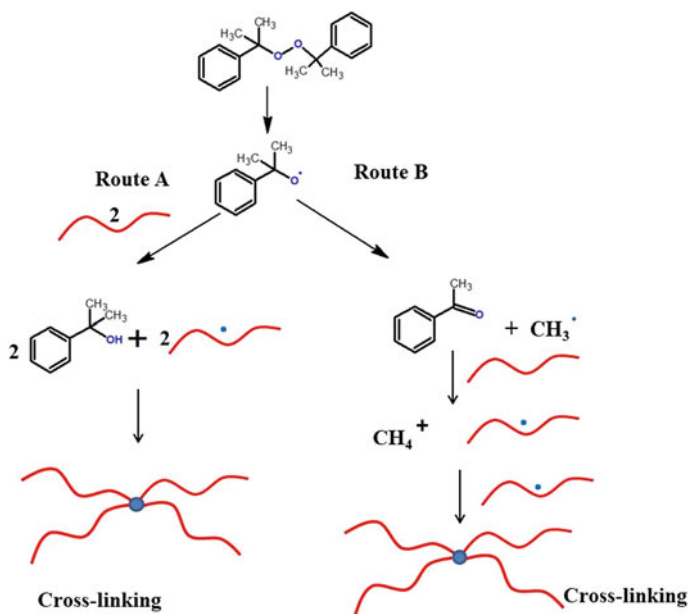


Fig. 1 Stages in dicumyl peroxide decomposition and radical crosslinking of polyethylene

through a β -scission reaction, leading to the formation of acetophenone and a methyl radical, CH_3^\bullet (Route B) (Fig. 1).

A free-radical macromolecule is produced by the reaction between the polymer and the methyl radical (a strong hydrogen abstracting agent). Considering the high reactivity of the alkoxy radicals, it is reasonable to expect that two macroradicals will be formed close to each other and upon recombination generate a crosslink [7]. The limitation of using peroxide, especially, DCP is formation of unwanted, low molecular weight and volatile by-products such as water, methane, acetophenone, cumyl alcohol and α -methyl styrene [6, 8–10].

A novel technique to surface crosslink consolidated UHMWPE/vitamin-E blends by diffusing two different organic peroxides into the polymer at moderate temperatures [11]. They characterized the surface crosslink density and wear rate of surface crosslinked UHMWPE/vitamin-E blends. The addition of the antioxidant vitamin-E led to higher oxidation resistance. Three synthesized reactive (graftable) antioxidants, r-AO, with hindered phenol and hindered amine antioxidant functions, were examined for their grafting efficiency in polyethylene and their retention and stabilizing performance in peroxide-crosslinked polyethylene pipe material [12]. The diffusion of emulsified DCP into vitamin E-blended ultrahigh-molecular-weight polyethylene (UHMWPE, 0.1 and 0.3 wt% vitamin-E) with subsequent thermal decomposition in situ to obtain surface crosslinking with the objective of achieving surface wear rate equivalent or lower than that of current clinically available materials [13]. Various vitamin E (0.1–1.0 wt% and peroxide concentration (0.5–1.5 wt%) combinations

changes in crosslink density, wear rate, mechanical properties, and oxidative stability in comparison with radiation crosslinked UHMWPE [14].

Low-density polyethylene (LDPE) was chemically crosslinked with of DCP. The crosslink density, determined by Flory–Rehner theory, showed an increase with various amounts DCP. The crystallinity, melting point, crystallization temperature, and elongation at break decreased with the increase in DCP. However, the maximum tensile stress increased with the increase in DCP, and the crosslinked samples showed a rubber-like behavior with no flow [15]. PEX-a pipes which were mixed with several stabilizers were tested to evaluate the effects on crosslink degree and the oxygen induction time and the effect of chlorine aqueous solution by the performance of the long-term hydrostatic pressure test and the long-term hydro-dynamic pressure test [16]. Influence of commercial phenol antioxidants Irganox 300, 1010, 1035 and 1076 on peroxide-cure reaction of low-density polyethylene (LDPE) was evaluated through isothermal dynamic rheological and nonisothermal differential scanning calorimetry (DSC) testing [17]. The phenol antioxidants could reduce storage modulus of LDPE completely crosslinked at 175 °C while they have a neglectable effect on gel fracture and activity energy of crosslinking reaction. The different by-products formed during the crosslinking reaction [acetophenone, a-cumyl alcohol, and a-methyl styrene (aMS)] were identified and quantified by Sahyoun et al. [8].

1.1.2 Silane Method

In silane method, crosslinking is activated by silane coupling agents. The organosilane moieties react with the polymeric chains, via typical organic chemistry reactions. The organic moieties of silanes have a central silicon atom (Si) bounded to two different categories of groups (vinyl and alkoxy), which exhibit different reactivity. Silane grafting on the PE main chain can be ensued by the vinyl group. The hydrolysable alkoxy groups in the presence of water or moisture react (via condensation and hydrolysis) and generate a three-dimensional network of siloxane linkages. There are two main processes for crosslinking PE with moisture-cured vinyl silanes.

In this process grafting of alkoxy silane onto the polyethylene chain takes place through radical formation [7, 18] (Fig. 2). The recombination of the radical molecules can be avoided by controlling the reaction conditions of the radical grafting. Moreover, the DCP produced free radicals readily react with vinyl group of silane reactants [7].

Afterward, the incorporated alkoxy groups $-(\text{CH}_2)_2-\text{Si}(\text{OR})_2\text{OR}$ are hydrolyzed in the presence of water and a catalyst to release silanol groups $-(\text{CH}_2)_2-\text{Si}(\text{OR})_2\text{OH}$ and ROH, which in a last step react with each other in a condensation reaction leading to the formation of a crosslinked polymer network (Fig. 3) [7, 18, 19].

The low mobility of water through PE makes the crosslinking of thick insulation and layers a slow process. Apart after crosslinking, it is necessary to remove water and ROH molecules from the polymer mass through a degassing step. So, the long processing times and the release of volatile by-products prevent the use of silane crosslinking.

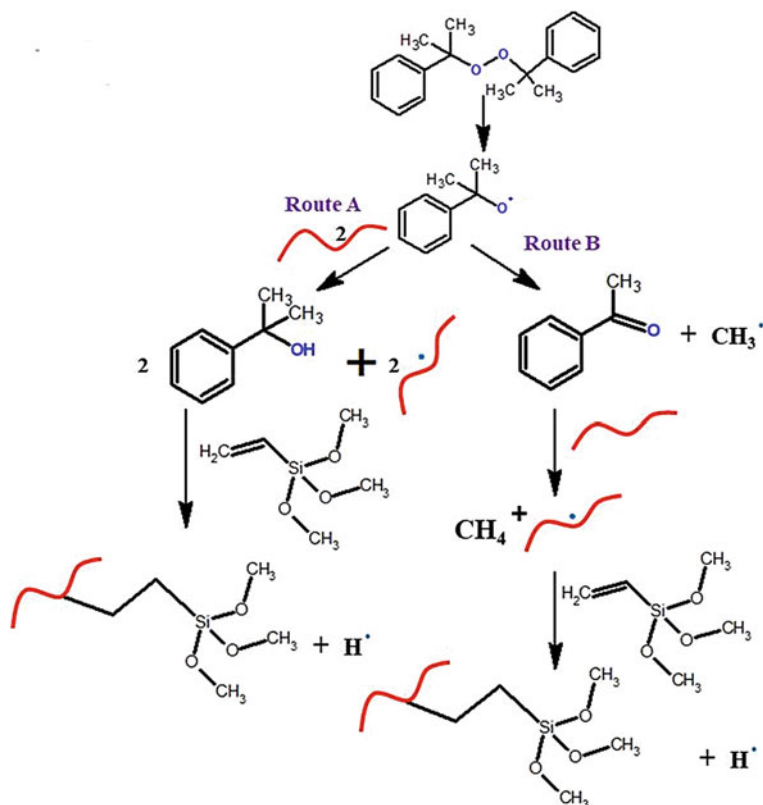


Fig. 2 Radical grafting of alkoxy silane crosslinkers onto polyethylene using DCP

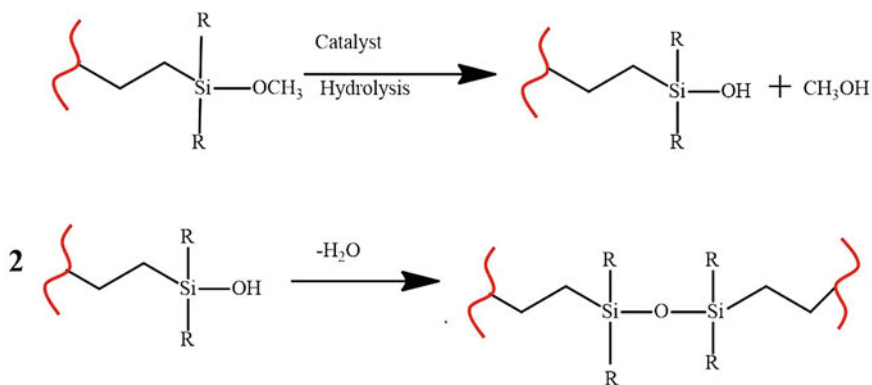


Fig. 3 Catalyzed hydrolysis of alkoxy silane, polyethylene-grafted curing agents and condensation reaction leading to PE crosslinking

Monosil (One-step) process, which involves a continuous feeding of liquid silanes during extrusion.

Sioplas (Two-step) process,

- (I) To prepare crosslinkable PE: a mixture of silane and peroxide are blended with PE by melt and formed into pellets.
- (II) To create the final product: the pellets are combined with a catalyst masterbatch, is extruded and cured in a high-temperature water bath, to reach the desired crosslinking level.

LDPE crosslinked with reduced graphene oxide (rGO) functionalized with vinyltrimethoxysilane (VTMOS) [20] produce a 3D network composed of LDPE and VTMOS-rGO resulting enhanced tensile properties.

To fulfill the requirements of automotive industry, crosslinks were introduced in a high molecular weight polyethylene (HMWPE) grade through grafting of vinyltrimethoxysilane (VTMOS) onto the polymer chain, promoted by DCP [21]. Crosslinked UHMWPE prepared by catalyst-free silane method by adding an additive ($\text{CaC}_2\text{O}_4 \cdot \text{H}_2\text{O}$) to generate water inside the materials [22]. To incorporate the functional group $-\text{O}-\text{C}_2\text{H}_5$, vinyltriethoxysilane functionalized with CNT and melt blended with PE resulting increase in melting temperature [23]. Composite prepared by the addition of aluminum (Al) particles and carbon fiber (CF) in Silane crosslinked polyethylene (XLDPE) for enhancing thermal conductivity for the thermal conductive pipes and semi-conductive products [24].

The crosslinked UHMWPE with excellent shape memory properties from the silane-grafted UHMWPE mixed with water-carrying agent by compression molding [25]. The samples incorporating more Si–O–Si crosslinking points have higher shape recovery ratio and faster shape recovery speed. Water treeing is one of the main deterioration phenomena observed in the polymeric insulation of extruded crosslinked polyethylene (XLPE) cables, which can affect the service life of power cables [26].

1.2 Radiation Method

Crosslinking of polyethylene wires and cables impart improved mechanical properties. They are having marked wear resistance. Several methods are currently utilized to bring about crosslinking in PE. These include chemical crosslinking with peroxide chemistry and ionizing methods such as an e-beam or gamma-radiation. The degree of crosslinking is affected by the amount of peroxide, level of ionizing energy, and whether the polymer is remelted or annealed to remove free radicals, and the environment. Peroxide crosslinking results in unwanted by-products and has to be removed by degassing for a long period of time at high temperature [10]. The volatile peroxide decomposition products impose considerable health hazard, which requires well-equipped work environment. Silane crosslinking chemistry requires water as an initiator and is not suitable for high-voltage insulation [27]. However, electron

beam irradiation offers good control of the radiation dose but is limited by a short penetration depth, which is insufficient for thick high-voltage cable insulation.

Gamma radiation of polyethylene readily penetrates thicker samples of polyethylene. It allows a crosslinking which produces products such as H_2 and low molecular-weight hydrocarbons, which would simplify the degassing process. Gamma radiation crosslinked LDPE is suitable for high voltage insulating material [28]. Radiation crosslinking is one of the effective methods that it requires low temperature. The flame retardant of polyolefins can be improved either by adding additives or by reactives. LDPE formulations were crosslinked by gamma-radiation in the presence of crosslinking agent. The formulations can be done by using various combinations of retardant fillers namely, zinc borate and aluminum trihydroxide $Al(OH)_3$ [29]. In addition, the formulations can be blended with ethylene-vinyl acetate (EVA) to improve the compatibility of the various fillers with LDPE. Gamma radiation in air and subsequent aging have detrimental impact on the structure and mechanical properties of the polyethylene and gamma radiation performed in an inert environment induces crosslinking and is beneficial to the wear behavior [30]. The Charles by–Pinner equation was used to determine the value of gel dose. It is given by

$$S + \sqrt{S} = P/Q + 2/quD \quad (1)$$

where S is the soluble fraction of polymer, D is the radiation dose in Mrad, q is the proportion of crosslinked units, p is the ratio of main chain breaks to chain units, and u is the weight average of the initial degree of polymerization [31]. When additives such as multifunctional monomers are used, gelation occurs at lower doses because these additives play the role as a center for crosslinking, and therefore gel dose is highly reduced [32].

2 Radiation Crosslinked Ultra-High-Molecular-Weight Polyethylene (UHMWPE)

Ultra-high-molecular-weight polyethylene (UHMWPE) is a semicrystalline polymer that has been used for over four decades as a bearing surface in total joint replacements [33]. UHMWPE is a member of the polyethylene family of polymers with the repeating unit $[C_2H_4]_n$. The International Standards Organization defines UHMWPE as having a molecular weight of at least 1 million g/mole, resulting in a minimum degree of polymerization of $n \approx 36,000$ [33]. The UHMWPEs used in orthopaedic applications typically have a molecular weight between 2 and 6 million with a degree of polymerization between 71,000 and 214,000.

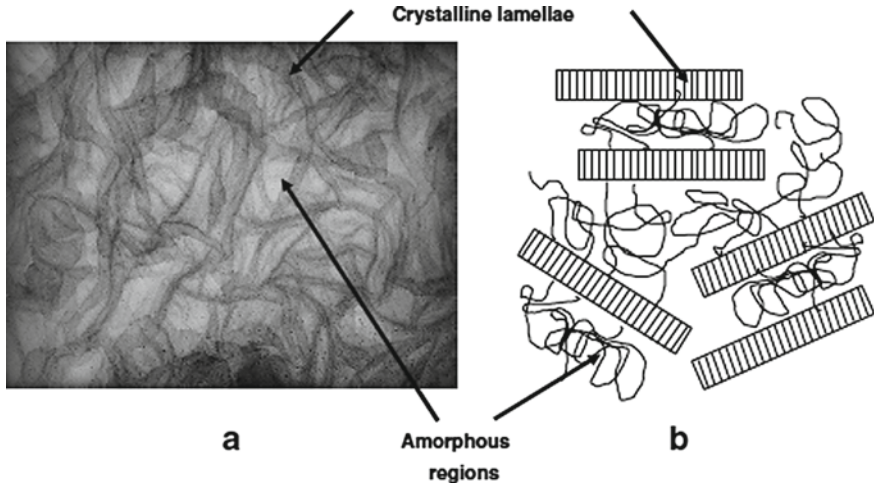


Fig. 4 A transmission electron micrograph (a) and schematic (b) depicting the semicrystalline morphology of UHMWPE (reproduced with permission from Elsevier)

3 Structure of UHMWPE

UHMWPE possess a composite structure with well-ordered crystalline lamellae embedded in a randomly oriented amorphous matrix (Fig. 4). Due to its high molecular weight, typically on the order of 2–6 million g/mol, it has high crystallinity (50–60%) and shape memory [34].

4 Purpose of Radiation Crosslinking in UHMWPEs

Its high mechanical strength under load and its favorable fatigue resistance are attributed to its composite structure, where, in addition to the crystalline content and associated strength, the mobility of the chains in the amorphous phase provides ductility and plasticity to the polymer. Increased plasticity allows the chains to be oriented in the direction of the applied stresses and weakens the material in the transverse direction, leading to the breakup of particles, especially under the multi-directional motion of the joints. Radiation crosslinking by high dose irradiation was proposed to increase the wear resistance of the polymer in general. Crosslinking of the polymer chains, which only occurs in the amorphous phase in polyethylene, introduces junctions between the polymer chains, reducing the mobility. Thus, it was hypothesized that wear would be reduced through a decrease in plasticity and thus orientation of the polymer.

Crosslinked UHMWPEs are of two generations. The first generation of highly crosslinked UHMWPEs has resulted in clinically reduced wear; however, the

mechanical properties of these materials, such as ductility and fracture toughness, are reduced when compared to the virgin material. Therefore, a second generation of highly crosslinked UHMWPEs is being introduced to preserve the wear resistance of the first generation while also seeking to provide oxidative stability and improved mechanical properties.

5 First-Generation Crosslinked UHMWPEs

First-generation crosslinked UHMWPEs were developed as a substitute to gamma sterilized UHMWPE, which had high wear and also displayed high oxidation *in vivo*. Induced radiolytic cleavage of the polyethylene produces C and H free radicals. As a result of the high molecular weight of UHMWPE, recombination responses along the spine are supported constraining chain scission. The decay of the staying free radicals is through recombination of the free radicals on various chains to form cross-joints. Some free radicals get trapped in the crystalline region of the lamellae for prolonged period of time [35, 36]. These free radicals migrate along the polymer chains to the crystalline/amorphous domain and undergo reaction with diffused oxygen over time. Highly reactive peroxy free radicals are produced by the combination of primary alkyl and allyl free radicals with oxygen. The stabilization of these peroxy radicals is occurred by the abstraction of hydrogen from nearby polymer chain and getting converted into hydroperoxides. The abstraction of hydrogen from polymer chain produces new primary alkyl free radicals which leads to further degradation and subsequent formation free radicals. This oxidative reaction of the free radicals is the reason for the embrittlement via oxidation through the local re-crystallization of the newly formed degraded short chains.

6 Second Generation of Crosslinked UHMWPEs

Second generation of highly crosslinked UHMWPE was developed by stabilizing the residual free radicals with the help of a chain-breaking antioxidant, i.e., vitamin E. The peroxidation of lipids is hindered by vitamin E similar to irradiated UHMWPE. Radiation cross-connecting of UHMWPE has been an incredible development in absolute joint arthroplasty bearing surfaces and shows guarantee in diminishing the event of osteolysis identified with the wear of UHMWPE.

There are two methods that can be used to incorporate vitamin E in UHMWPE; the first is by blending vitamin E, a viscous liquid with UHMWPE resin powder and consolidating them together before molding. The second is to diffuse vitamin E in molded and radiation crosslinked UHMWPE. The advantage of blending is the ease of obtaining a uniform concentration of vitamin E. The disadvantage is that the crosslinking efficiency of UHMWPE is reduced in the presence of vitamin E with increasing vitamin E concentration [37]. The advantage of this UHMWPE

over conventional, gamma sterilized UHMWPE is both its wear and oxidation resistance. By using vitamin E stabilization, the crystallinity of the radiation crosslinked UHMWPE is retained and the fatigue properties of this UHMWPE are improved over irradiated and melted UHMWPE [38, 39].

7 Applications of Radiation Crosslinked UHMWPE

The main domains which utilize these kinds of radiation crosslinked polyethylenes are follows.

7.1 Biomedical Field

Extensively crosslinked ultrahigh-molecular-weight polyethylene (HXPE) was prepared by compression molding of GUR 1050 UHMWPE bars [40]. Annealing of these bars conducted above melt temperature after exposing to electron beam irradiation of 90, 100 or 110 kGy. 100 ± 10 kGy is the processing limits of nominal processing dose for the clinically available Longevity material. The specimens after compression molding were sterilized by gas plasma. The wear properties of HXPE are better than that of conventional molded ultrahigh-molecular-weight polyethylene (UHMWPE) which is sterilized by 37 kGy of gamma radiation (Fig. 5). The

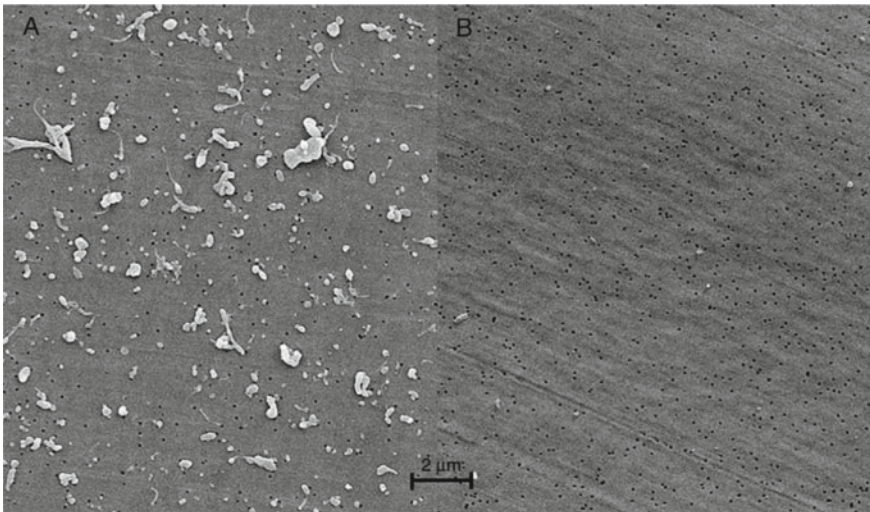


Fig. 5 Scanning electron micrographs of conventional UHMWPE (A) and HXPE (B) wear debris (white particles) generated in a hip simulator wear test (reproduced with permission from Elsevier)

HXPE is free from free radicals and they exhibit high resistance to oxidation. This lower sensitivity to oxidation of HXPE helps to preserve the wear advantage in clinical application. The strength and J-integral fracture toughness of UHMWPE were reduced by accelerated aging but the mechanical property of the HXPE was not that much affected by accelerated aging.

UHMWPE which is crosslinked with gamma radiation in different dosages in combination with aluminum head exhibits variation in properties like creep deformity, hardness, etc. After radiation process, UHMWPE displayed slight hydrophilicity with increase in hardness according to increase in radiation dose. There observed a slight reduction in creep deformity and a visible hike in the frictional torque of radiation crosslinked PE [41]. Radiation crossconnected UHMWPE brought about decreased rigidity and crack durability as a cost of sensational increment in the wear obstruction. First-generation crosslinked UHMWPE acetabular components exhibited clinical rim fracture due to neck-liner impingement. The second-generation, vitamin E blended highly crosslinked UHMWPE possesses the improved impingement resistance [42]. Radiation crosslinked UHMWPE (X-UHMWPE) powder was prepared by g-ray irradiation under inert nitrogen atmosphere with a dose of 50–200 kGy at a dose rate of 7 kGy/h and further annealing in vacuum at 120 °C for 4 h. A composite was prepared by mixing X-UHMWPE and pristine UHMWPE with 0–25 wt% filler. An improvement in wear resistance was observed with 25 wt%, 150 kGy dose X-UHMWPE. These kind of composites are potentially useful for artificial joint replacement and engineering devices [8].

7.2 Nuclear Reactor Field

Pristine, thermally-aged and gamma radiation-aged commercial crosslinked polyethylene (XLPE) was used for the quantitative analysis of antioxidant poly(1,2-dihydro-2,2,4-trimethylquinoline) (pTMQ) for nuclear power plant applications [43]. The polyethylene-based cable insulation materials are aged at temperatures 60, 90 and 115 °C, with gamma radiation exposure dose rates of 0, 120, 300 and 540 Gy/h for 15 days. The pristine XLPE is composed with 60% polymer matrix, decabromodiphenyl ether, octabromodiphenyl ether, etc. as the flame retardants, zinc sulfide as the white pigment, poly(1,2-dihydro-2,2,4-trimethylquinoline) and 1,3,5-Triazine-2,4,6(1H,3H,5H)-trione as the crosslinking booster. Isothermal aging was associated with decrease in quantity of antioxidant and oxidation induction time with increasing radiation dose.

7.3 Voltage Stabilizers

A theoretical study on the atomic and molecular level of benzophenone-initiated reaction mechanisms in the polyethylene UV radiation crosslinking process showed that

aromatic ketone voltage stabilizer and hindered phenol antioxidants molecules can be bonded to polyethylene chain during the polyethylene UV radiation crosslinking process [44]. Hot electrons bombarding C–C bond of XLPE matrix under the local high electric field can be prevented by the adulterant molecules benzophenone, voltage stabilizer, antioxidant, and by-product in XLPE insulation composite product with carbonyl or phenyl groups. This mechanism can be optimized to design voltage stabilizer real applications.

7.4 Disposal of Radiation Crosslinked PE

UV irradiation of high-density polyethylene (HDPE) and biodegradable polyethylene (PE-BIO) films of dimensions 40×50 mm with a thickness of 0.5 mm. were conducted using UV-B BYTEK lamp model Ultraviolet Multiprom Eraser in a 320–280 nm range wavelength at different exposure times, 0–60 days. Photo-oxidation of polyethylene which follows Norrish Type II mechanism is observed [45]. The photooxidation changes the molecular structure of polyethylene by forming the infrared bands.

Recently, researchers are focusing on the crosslinking of functionalized polyethylene resins by ring-opening reactions known as click chemistry, curing of polyethylene resins bearing various functional groups promises to be an appealing alternative [8, 46, 47].

7.5 Crosslinking with Epoxy Ring-Opening Reactions

The scope of PE-based materials is improved by the production of by-product-free curing process will considerably expand. Click-chemistry type's reactions, especially epoxy ring-opening methods are used to produce crosslinked polyethylene which involves a statistical ethylene-glycidyl methacrylate copolymer, p(E-stat-GMA), [48] which is commonly used as a compatibilizer for polymer blends [49, 50]. Maleimide/furan adduct as a crosslinking agent for the preparation of thermally reversible crosslinked polyethylene was prepared via Diels–Alder (DA) and retro Diels–Alder(rDA) reaction [48]. To improve network structure development of an ethylene-epoxy copolymer, thermally crosslinked with an amino acid (11-aminoundecanoic acid) [51].

7.5.1 Recycling

Recycling of crosslinked polymers is a serious and difficult problem in the recycling of plastic waste and it is a threat due to irreversible covalent crosslinking in the network [52]. Crosslinked polyethylene (XLPE) was widely used as an insulation

material for wires and cables. XLPE has low fluidity and poor moldability; it is rarely recycled, though its recycling is of crucial importance. Most of the industrial wastes were buried in landfills or removed by incineration. The current topic covers some of the efficient methods for the recycling of XLPE.

8 Chemical Recycling or Feedstock Recycling of Polymer Wastes

Chemical crosslinking endows a thermosetting polymer with admirable thermomechanical and solvent resistance properties. However, in comparison with those of thermoplastics, the re-processability and recyclability of these polymers are sacrificed because of the irreversible covalent bonds in the network [52, 53]. Feedstock recycling also known as chemical recycling or tertiary recycling aims to convert waste polymer into original monomers or other valuable chemicals.

9 By HDPE Vitrimers

Introducing exchangeable covalent bonds into the crosslinked network is an effective method for addressing the above challenges. Leibler and coworkers introduced the term vitrimers for crosslinked polymers which have the ability to rearrange their covalent bonds and they have made great efforts for recycling the thermosetting polymers. They introduced a novel method to prepare dioxaborolane-based vitrimers [54] which enabled polymers with backbones made of carbon-carbon single bonds to be reprocessed by extrusion or injection molding similar to thermoplastics. The stress relaxation property of vitrimer has been applied to the reprocessing of shape memory polymers (SMPs), liquid crystal elastomers and other functional materials [55, 56]. For SMPs, the exchangeable bonds enable topological rearrangement of the networks to occur in the solid state, which means that various permanent shapes can be achieved through secondary processing.

Polyolefins are composed of a large number of carbon-carbon single bonds as backbones, so it is difficult to alter the topology of crosslinked polyolefins. To achieve the high-value utilization and recycling of crosslinked polyolefins, introducing dynamic exchange bonds into the crosslinking system of polyolefins is an effective method. A simple way to prepare HDPE-vitrimers by triple shape memory effect. By melt-grafting of epoxy monomers, the functional monomers were incorporated into HDPE chains and served as active crosslinking sites. Therefore, the hydroxyl-ester transesterification reaction was enabled by the carbonyl group in the monomers during the post-processing step. Hydroxyl-terminated polytetrahydrofuran (HTPTF) and polycaprolactone (PCL) were chosen as crosslinkers. By this

reaction, polyethers and polyesters were introduced in the structure. The transesterification reaction in the HDPE vitrimers can be studied at different temperature by stress relaxation behavior at different temperature. This novel strategy of preparing HDPE vitrimers may be useful for the high-value utilization of crosslinked polyolefins [57].

10 By γ Radiation

Low-density polyethylene (LDPE) self-reinforced composites in which the fibers were irradiated with gamma rays prior to compression molding. The tensile tests of the single fibers revealed that the hot air-assisted melt-spun fibers had better mechanical performance than the same LDPE matrix material. The irradiation crosslinked fibers, which made it possible to widen the temperature window of the film-stacking method applied for composite production. The effect of irradiation on the mechanical properties of fibers themselves and the composites reinforced with these fibers were studied. Based on the mechanical and crystalline properties obtained, the fibers irradiated with an absorbed dose of 200 kGy were chosen as reinforcement for the composites [58].

11 By Ultrasonic Decross-Linking

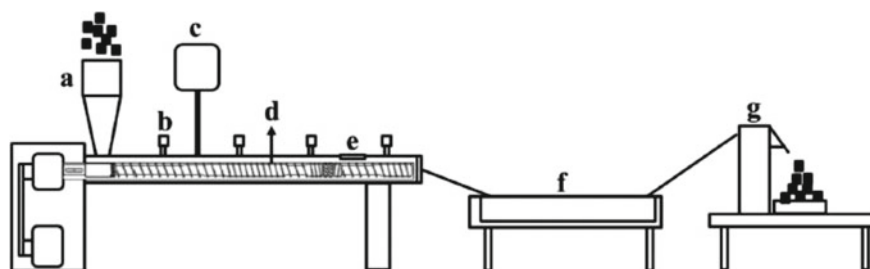
The ultrasonic batch reactor and ultrasonic extruder were used to decross-link various rubber vulcanizates and XHDPE. The analysis of the gel fraction-crosslink density relationship of various ultrasonically devulcanized rubbers showed that the ultrasound may induce a preferential breakage of crosslinks [59]. This mainly arises due to the difference in bond energy of main bonds and crosslinks. The type of bond breakage during the ultrasonic decross-linking of XHDPE revealed the structural factors governing this process and also leads to the possibility to obtain the decross-linked XHDPE with superior mechanical properties [60].

The increase of the barrel pressure with the degree of crosslinking is a result of the increase of viscosity. The decrease of the barrel pressure with the ultrasonic amplitude is due to both the thixotropic effect such as the shear thinning and permanent effect including the decrease in viscosity caused by the decrease of the gel fraction and crosslink density. The melting temperature, crystallinity and tensile properties of decross-linked XHDPE are significantly affected by the type of preferential bond breakage during decross-linking of XHDPE. The tensile properties of the decross-linked XHDPE are superior to those of the XHDPE.

12 By Supercritical Decross-Linking Extrusion Process

Supercritical fluids can act as a reaction medium for the depolymerization reaction of several condensation polymers and decross-linking reaction of XLPE [61, 62]. It is observed that the irradiation crosslinked, the silane crosslinked, and the peroxide crosslinked PE could successively be decross-linked into the thermoplastic PE using supercritical methanol [63]. The decross-linking reaction rate was observed as linearly proportional to the gel content [64]. The peroxide crosslinked PE was successfully decross-linked through reaction in supercritical methanol in a continuous multiscale single screw extrusion process [65]. XLPE was in contact with supercritical methanol for shorter than 2 min retention time in the continuous supercritical extruder and was successfully decross-linked at the methanol feeding rate. The decross-linking efficiency of the continuous supercritical extruder is expected to be improved through the optimization of extruder design to accept further methanol feeding rate and provide longer retention time. The depolymerization and decross-linking reactions using supercritical fluids were performed in the batch reactors. The batch process is time-consuming and cost-inefficient. To establish the recycling process at industrial scale, continuous supercritical reaction process needs to be developed. Goto et al. reported the recycling of silane crosslinked PE using the extruder at elevated temperature. However, it provided only limited information on the continuous extruder reactor and reaction conditions [61]. An extruder can be used as a reactor for the decross-linking reaction by supercritical fluids. The C–C crosslinking bond of peroxide crosslinked PE has much better thermal stability than the silane crosslinking bond in silane crosslinked XLPE [66, 67].

A schematic representation of the continuous supercritical process system, consisting of a multistage single screw extruder, is shown in Fig. 6. A multistage single screw composed of four divided zones of transfer, compression, reaction and discharge zones. The first transfer zone was in charge of feeding and transferring the XLPE waste material. The second compression zone was compressing the resin to attain supercritical pressure conditions of methanol. Methanol was injected to the



(a) Hopper, (b) temperature and pressure sensors, (c) A methanol injection pump, (d) A multistage single screw (e) Methanol gas ventilation (f) strand cooler (g) pelletizer

Fig. 6 Schematic representation of the continuous supercritical process system

end of compression zone of the extruder with a liquid injection pump. The third reaction zone was responsible for the decross-linking reaction of XLPE in supercritical methanol conditions. The discharge zone was for discharging the decross-linked XLPEs. The extrudate was a form of strand so as to be pelletized and collected as samples.

The dynamic storage modulus (G^1) and loss modulus (G^{11}) values of decross-linked XLPE samples were significantly affected not only by reaction temperature, but also by methanol content. The peroxide crosslinked PE was successfully decross-linked through reaction in supercritical methanol. Reaction temperature was set from 36 to 39 °C and the amount of methanol feeding was varied from 0 to 7 mL/min. The extruder with methanol injection pump was kept in the supercritical conditions of methanol during extrusion. The gel content value decreased with reaction temperature and methanol content. XLPE was in contact with supercritical methanol for shorter than 2 min retention time only in the continuous supercritical extruder; it was successfully decross-linked [68]. Another method for recycling silane crosslinked polyethylene is by closed recycling. In this thermosetting polyethylene having crosslinking element converts to thermoplastic polyethylene with no crosslinks and after shape forming, it changes to thermosetting polyethylene with crosslinks. The low fluidity and bad moldability of silane XLPE can be improved by the closed recycling without the deterioration of the properties [69].

13 As Toughness Enhancer

Silicon crosslinked polyethylene (Si-XLPE) can be blended with the high-density polyethylene (HDPE) for improved thermal endurance, stiffness and toughness. A series of Si-XLPE of different gel fraction and crosslink structure were used to study the recycling and properties of crosslinked waste. For this, the tensile and impact properties, crystallization and heat stability of the HDPE and Si-XLPE blends were investigated [70]. The results showed that crosslink gel in the blend could be as high as 70%. The tensile modulus and impact strength of the HDPE increased with increasing loading and content of gel in the crosslinked materials [71].

14 By Thermoplastic Vulcanizates (TPVs)

The process for obtaining a thermoplastic recycled material by breaking down the crosslinked structure of XLPE and reducing the molecular weight is referred to as thermoplasticizing. XLPE waste recovered from wires and cables; there are two types of XLPE.

1. XLPE-a (peroxide crosslinked polyethylene): a low-density polyethylene made by crosslinking using organic peroxide compounds, with a degree of crosslinking of approximately 80%.
2. XLPE-b (silane crosslinked polyethylene): a linear low-density polyethylene made by crosslinking using silane, with a degree of crosslinking (gel content) of approximately 60%.

The method involves sorting, feeding, thermoplasticization, cooling, pelletization and recycling [72]. The flow chart (Fig. 7) showing the thermoplasticizing of XLPE-a and XLPE-b is given below.

The properties and molecular weight distribution of recycled XLPE-a, XLPE-b and LDPE are provided in Table 1.

By mechanical decross-linking and dynamic vulcanization of ground tire rubber (GTR) and crosslinked polyethylene thermoplastic vulcanizates were prepared [73]. In this method, partial decross-linking of GTR and XLPE takes place. After mechanical milling, a new group carbonyl group was introduced into the structure. The blend

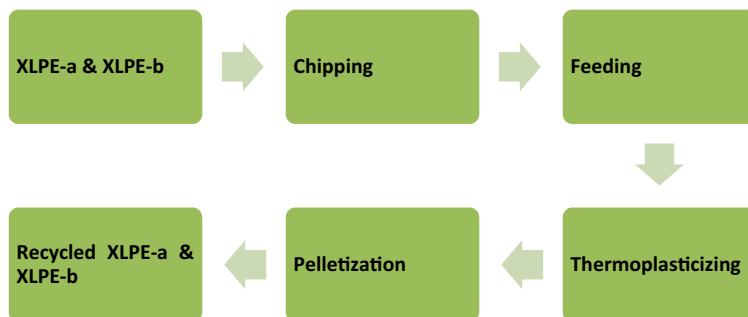


Fig. 7 Flowchart of thermoplasticizing of XLPE-a and XLPE-b

Table 1 Properties of recycled PCPE, SCPE and virgin LDPE

Property	Recycled XLPE-a	Recycled XLPE-b	LDPE
Surface	Good	Slightly rough	Good
Colour	Pale brown	Pale grey	Natural
Melt flow rate (g/10 min)	0.1–30	0.1–30	1.0
Gel content (%)	<1–10	20–40	0
Melting point (°C)	108	114	112
Heat of melting (mJ/mg)	121	103	126
Number-average molecular weight (Mn)	1.34×10^4	6.72×10^3	1.05×10^4
Weight-average molecular weight (Mw)	1.1×10^5	2.26×10^4	3.37×10^4
Polydispersity (Mn/Mw)	8.19	3.36	3.21
Peak top molecular weight	24,900	10,900	29,400

vulcanizates maintained the re-processability, and it has good thermoplastic processability. With the existing recycling methods, the TPV is cost-effective and easy for industrialization [74]. By mechanochemical milling, the breaking down of XLPE can be done and thereby a thermoplastic can be obtained. The advantage of this method is that it can be carried out at ambient temperature, no chemicals are needed, has low energy consumption and it is eco-friendly [75].

15 Particulate Infusion

Silane crosslinked polyethylene cable waste is recycled by infusion of the waste into virgin LDPE via mini compounder at different waste to virgin polyethylene weight fraction. The thermal analysis revealed that the heat absorbed during the melting of crosslinked PE is higher than that of the virgin LDPE. 15 wt% recycled SCPE to virgin PE displayed a hike in young modulus (17%), yield stress (37.2%), ultimate stress (22.4%) and a reduction in melting point (3.3%) [76]. By changing the thermal, static and dynamic properties, silane crosslinked polyethylene cable waste can be recycled as a filler or re-compounding it into cable product. The infusion of crosslinked PE waste into virgin LDPE provides another life for silane crosslinked polyethylene which saves million barrels of fossil fuel and converting cable industry into a greener and zero waste industry [77].

16 Conclusion

Commonly the manufacturing of XLPE is using peroxide method, which gives rise to hazardous by-products. Silane crosslinking is limited by the low mobility of water through PE, and the releases of polar by-products deteriorate the dielectric properties of the material. Radiation method is favorable because of the chain scission is low compared to chain recombination (the chemical bond strength of the C–H bond is greater compared to that of a C–C bond), and the by-products are H₂ with a small amount of low molecular weight hydrocarbons. The epoxy click chemistry reactions can be effectively used to crosslink polyethylene-based copolymers, meeting industrial requirements for cable production but without the release of volatile by-products.

Radiation-induced crosslinking of polyethylene is an efficient technique as it involves no chemicals and by-products obtained is very low. It effects the mechanical properties of crosslinked polyethylene and increases wear resistance. The recycling of cross linked polyethylene waste was conducted by various means to achieve an acceptable change in the mechanical and thermal properties, with the overall objective is to attain zero waste production.

References

1. Ronca S (2017) Polyethylene. In: Brydson's plastics materials. Elsevier, pp 247–278
2. Carlomagno GM, Meola C (2005) Cross-linked polyethylene. In: Lee S (ed) Encyclopedia of chemical processing. Taylor & Francis, pp 577–588
3. Morshedjian J, Hosseinpour PM (2009) Polyethylene cross-linking by two-step silane method: a review. *Iran Polym J* 18:103–128
4. Anbarasan R, Babot O, Maillard B (2004) Crosslinking of high-density polyethylene in the presence of organic peroxides. *J Appl Polym Sci* 93:75–81. <https://doi.org/10.1002/app.20390>
5. Smedberg A, Hjertberg T, Gustafsson B (2003) Effect of molecular structure and topology on network formation in peroxide crosslinked polyethylene. *Polymer* 44:3395–3405. [https://doi.org/10.1016/S0032-3861\(03\)00179-4](https://doi.org/10.1016/S0032-3861(03)00179-4)
6. Smedberg A, Hjertberg T, Gustafsson B (1997) Crosslinking reactions in an unsaturated low density polyethylene. *Polymer* 38:4127–4138. [https://doi.org/10.1016/S0032-3861\(96\)00994-9](https://doi.org/10.1016/S0032-3861(96)00994-9)
7. Patterson R, Kandelbauer A, Müller U, Lammer H (2014) Crosslinked thermoplastics. In: Handbook of thermoset plastics. Elsevier, pp 697–737
8. Sahyoun J, Crepet A, Gouanve F et al (2017) Diffusion mechanism of byproducts resulting from the peroxide crosslinking of polyethylene. *J Appl Polym Sci* 134:1–11. <https://doi.org/10.1002/app.44525>
9. Severengiz M, Sprenger T, Seliger G (2016) Challenges and approaches for a continuous cable production. *Procedia CIRP* 40:18–23. <https://doi.org/10.1016/j.procir.2016.01.040>
10. Andrews T, Hampton RN, Smedberg A et al (2006) The role of degassing in XLPE power cable manufacture. *IEEE Electr Insul Mag* 22:5–16. <https://doi.org/10.1109/MEI.2006.253416>
11. Gul RM, Fung K, Doshi BN et al (2017) Surface cross-linked UHMWPE using peroxides. *J Orthop Res* 35:2551–2556. <https://doi.org/10.1002/jor.23569>
12. Al-Malaika S, Riasat S, Lewucha C (2017) Reactive antioxidants for peroxide crosslinked polyethylene. *Polym Degrad Stab* 145:11–24. <https://doi.org/10.1016/j.polymdegradstab.2017.04.013>
13. Kayandan S, Doshi BN, Oral E, Muratoglu OK (2018) Surface cross-linked ultra high molecular weight polyethylene by emulsified diffusion of dicumyl peroxide. *J Biomed Mater Res B Appl Biomater* 106:1517–1523. <https://doi.org/10.1002/jbm.b.33957>
14. Oral E, Doshi BN, Gul RM et al (2017) Peroxide cross-linked UHMWPE blended with vitamin E. *J Biomed Mater Res B Appl Biomater* 105:1379–1389. <https://doi.org/10.1002/jbm.b.33662>
15. Liu S-Q, Gong W-G, Zheng B-C (2014) The effect of peroxide cross-linking on the properties of low-density polyethylene. *J Macromol Sci Part B* 53:67–77. <https://doi.org/10.1080/0022348.2013.789360>
16. Hirabayashi H, Iguchi A, Yamada K et al (2013) Study on the structure of peroxide cross-linked polyethylene pipes with several stabilizers. *Mater Sci Appl* 04:497–503. <https://doi.org/10.4236/msa.2013.49060>
17. Zhang X, Yang H, Song Y, Zheng Q (2012) Influence of binary combined systems of antioxidants on the stabilization of peroxide-cured low-density polyethylene. *J Appl Polym Sci* 126:1885–1894. <https://doi.org/10.1002/app.36754>
18. Shah GB, Fuzail M, Anwar J (2004) Aspects of the crosslinking of polyethylene with vinyl silane. *J Appl Polym Sci* 92:3796–3803. <https://doi.org/10.1002/app.20381>
19. Palmlof M, Hjertberg T, Sultan B (1991) Crosslinking reactions of ethylene vinyl silane copolymers at processing temperatures. *J Appl Polym Sci* 42:1193–1203. <https://doi.org/10.1002/app.1991.070420504>
20. Abbas SS, Rees GJ, Patias G et al (2020) In situ cross-linking of silane functionalized reduced graphene oxide and low-density polyethylene. *ACS Appl Polym Mater* 2:1897–1908. <https://doi.org/10.1021/acsapm.0c00115>
21. Rocha MCG, Moraes LR da C, Cella N (2017) Thermal and mechanical properties of vinyltrimethoxysilane (VTMOS) crosslinked high molecular weight polyethylene (HMWPE). *Mater Res* 20:1332–1339. <https://doi.org/10.1590/1980-5373-mr-2016-0552>

22. Li Q, Chen T, Sun L et al (2018) Cross-linked ultra-high-molecular-weight polyethylene prepared by silane-induced cross-linking under in situ development of water. *Adv Polym Technol* 37:2859–2865. <https://doi.org/10.1002/adv.21957>
23. Azizi H, Fallahi H, Ghasemi I et al (2020) Silane modification of carbon nanotubes and preparation of silane cross-linked LLDPE/MWCNT nanocomposites. *J Vinyl Addit Technol* 26:113–126. <https://doi.org/10.1002/vnl.21724>
24. Azizi H, Ghasemi I (2016) Thermal conductivity of silane cross-linked polyethylene composites. *Bul Chem Commun* 48:125–130
25. Chen T, Li Q, Fu Z et al (2018) The shape memory effect of crosslinked ultra-high-molecular-weight polyethylene prepared by silane-induced crosslinking method. *Polym Bull* 75:2181–2196. <https://doi.org/10.1007/s00289-017-2144-6>
26. Ma Z, Huang X, Jiang P, Wang G (2010) Effect of silane-grafting on water tree resistance of XLPE cable insulation. *J Appl Polym Sci* 115:3168–3176. <https://doi.org/10.1002/app.31421>
27. Knobel T, Minbiole PR, E-Beam Services Inc (1999) Method for irradiating organic polymers, p 75
28. Andersson MG, Jarvid M, Johansson A et al (2015) Dielectric strength of γ -radiation cross-linked, high vinyl-content polyethylene. *Eur Polym J* 64:101–107. <https://doi.org/10.1016/j.eurpolymj.2014.11.042>
29. Basfar A (2002) Flammability of radiation cross-linked low density polyethylene as an insulating material for wire and cable. *Radiat Phys Chem* 63:505–508. [https://doi.org/10.1016/S0969-806X\(01\)00545-X](https://doi.org/10.1016/S0969-806X(01)00545-X)
30. Baker DA, Hastings RS, Pruitt L (1999) Study of fatigue resistance of chemical and radiation crosslinked medical grade ultrahigh molecular weight polyethylene. *J Biomed Mater Res* 46:573–581. [https://doi.org/10.1002/\(SICI\)1097-4636\(19990915\)46:4%3c573:AID-JBM16%3e3.0.CO;2-A](https://doi.org/10.1002/(SICI)1097-4636(19990915)46:4%3c573:AID-JBM16%3e3.0.CO;2-A)
31. Shyichuk A, Tokaryk G (2005) A comparison of methods to determination of macromolecule crosslinking yield from gel fraction data. *Polimery* 50:219–221. <https://doi.org/10.14314/polimery.2005.219>
32. Danaei M, Sheikh N, Taromi FA (2005) Radiation cross-linked polyethylene foam: preparation and properties. *J Cell Plast* 41:551–562. <https://doi.org/10.1177/0021955X05059034>
33. Sobieraj MC, Rinnac CM (2009) Ultra high molecular weight polyethylene: mechanics, morphology, and clinical behavior. *J Mech Behav Biomed Mater* 2:433–443. <https://doi.org/10.1016/j.jmbbm.2008.12.006>
34. Li S, Burstein AH (1982) Current concepts review ultra-high molecular weight polyethylene. *J Bone Joint Surg* 64:147–152. <https://doi.org/10.2106/00004623-198264010-00023>
35. Jahan M, King M, Haggard W et al (2001) A study of long-lived free radicals in gamma-irradiated medical grade polyethylene. *Radiat Phys Chem* 62:141–144. [https://doi.org/10.1016/S0969-806X\(01\)00431-5](https://doi.org/10.1016/S0969-806X(01)00431-5)
36. Thomas DE, Jahan MS, Trieu HH et al (1996) A study of free radicals in irradiated/aged UHMWPE materials. In: Proceedings of the 1996 fifteenth southern biomedical engineering conference. IEEE, pp 207–209
37. Oral E, Muratoglu OK (2007) Radiation cross-linking in ultra-high molecular weight polyethylene for orthopaedic applications. *Nucl Instrum Methods Phys Res Sect B* 265:18–22. <https://doi.org/10.1016/j.nimb.2007.08.022>
38. Oral E (2004) α -Tocopherol-doped irradiated UHMWPE for high fatigue resistance and low wear. *Biomaterials* 25:5515–5522. <https://doi.org/10.1016/j.biomaterials.2003.12.048>
39. Oral E, Christensen SD, Malhi AS et al (2006) Wear resistance and mechanical properties of highly cross-linked, ultrahigh-molecular weight polyethylene doped with vitamin E. *J Arthroplasty* 21:580–591. <https://doi.org/10.1016/j.arth.2005.07.009>
40. Laurent MP, Johnson TS, Crowninshield RD et al (2008) Characterization of a highly cross-linked ultrahigh molecular-weight polyethylene in clinical use in total hip arthroplasty. *J Arthroplasty* 23:751–761. <https://doi.org/10.1016/j.arth.2007.06.006>
41. Oonishi H, Ishimaru H, Kato A (1996) Effect of cross-linkage by gamma radiation in heavy doses to low wear polyethylene in total hip prostheses. *J Mater Sci Mater Med* 7:753–763. <https://doi.org/10.1007/BF00121412>

42. Takahashi Y, Tateiwa T, Pezzotti G et al (2016) Improved resistance to neck-liner impingement in second-generation highly crosslinked polyethylene—the role of vitamin E and Crosslinks. *J Arthroplasty* 31:2926–2932. <https://doi.org/10.1016/j.arth.2016.05.049>
43. Liu S, Veysey SW, Fifield LS, Bowler N (2018) Quantitative analysis of changes in antioxidant in crosslinked polyethylene (XLPE) cable insulation material exposed to heat and gamma radiation. *Polym Degrad Stab* 156:252–258. <https://doi.org/10.1016/j.polymdegradstab.2018.09.011>
44. Zhang H, Shang Y, Li M et al (2016) Theoretical study on the reaction mechanism in the UV radiation cross-linking process of polyethylene. *RSC Adv* 6:110831–110839. <https://doi.org/10.1039/C6RA24433E>
45. Martínez-Romo A, Mota RG, Bernal JJS et al (2015) Effect of ultraviolet radiation in the photo-oxidation of High Density Polyethylene and Biodegradable Polyethylene films. *J Phys: Conf Ser* 582:012026. <https://doi.org/10.1088/1742-6596/582/1/012026>
46. Mauri M, Peterson A, Senol A et al (2018) Byproduct-free curing of a highly insulating polyethylene copolymer blend: an alternative to peroxide crosslinking. *J Mater Chem C* 6:11292–11302. <https://doi.org/10.1039/c8tc04494e>
47. Mauri M, Tran N, Prieto O et al (2017) Crosslinking of an ethylene-glycidyl methacrylate copolymer with amine click chemistry. *Polymer* 111:27–35. <https://doi.org/10.1016/j.polymer.2017.01.010>
48. Magana S, Zerroukhi A, Jegat C, Mignard N (2010) Thermally reversible crosslinked polyethylene using Diels-Alder reaction in molten state. *React Funct Polym* 70:442–448. <https://doi.org/10.1016/j.reactfunctpolym.2010.04.007>
49. Torres N, Robin JJ, Boutevin B (2001) Study of compatibilization of HDPE-PET blends by adding grafted or statistical copolymers. *J Appl Polym Sci* 81:2377–2386. <https://doi.org/10.1002/app.1678>
50. Chiono V, Filippi S, Yordanov H et al (2003) Reactive compatibilizer precursors for LDPE/PA6 blends. III: ethylene–glycidylmethacrylate copolymer. *Polymer* 44:2423–2432. [https://doi.org/10.1016/S0032-3861\(03\)00134-4](https://doi.org/10.1016/S0032-3861(03)00134-4)
51. Briceño Garcia RD, Keromnes L, Goutille Y et al (2014) Structural evolution of a constrained epoxy functional polyethylene network crosslinked by a bio-based reactant. *Eur Polym J* 61:186–196. <https://doi.org/10.1016/j.eurpolymj.2014.10.003>
52. Wojtecki RJ, Meador MA, Rowan SJ (2011) Using the dynamic bond to access macroscopically responsive structurally dynamic polymers. *Nat Mater* 10:14–27. <https://doi.org/10.1038/nmat2891>
53. Wu J, Cai L-H, Weitz DA (2017) Tough self-healing elastomers by molecular enforced integration of covalent and reversible networks. *Adv Mater* 29:1702616. <https://doi.org/10.1002/adma.201702616>
54. Röttger M, Domenech T, van der Weegen R et al (2017) High-performance vitrimers from commodity thermoplastics through dioxaborolane metathesis. *Science* 356:62–65. <https://doi.org/10.1126/science.aah5281>
55. Chen Q, Yu X, Pei Z et al (2017) Multi-stimuli responsive and multi-functional oligoaniline-modified vitrimers. *Chem Sci* 8:724–733. <https://doi.org/10.1039/C6SC02855A>
56. Cromwell OR, Chung J, Guan Z (2015) Malleable and self-healing covalent polymer networks through tunable dynamic boronic ester bonds. *J Am Chem Soc* 137:6492–6495. <https://doi.org/10.1021/jacs.5b03551>
57. Ji F, Liu X, Lin C et al (2019) Reprocessable and recyclable crosslinked polyethylene with triple shape memory effect. *Macromol Mater Eng* 304:1800528. <https://doi.org/10.1002/mame.201800528>
58. Mészáros L, Kara Y, Fekete T, Molnár K (2020) Development of self-reinforced low-density polyethylene using γ -irradiation cross-linked polyethylene fibres. *Radiat Phys Chem* 170:108655. <https://doi.org/10.1016/j.radphyschem.2019.108655>
59. Hong CK, Isayev AI (2002) Ultrasonic devulcanization of unfilled SBR under static and continuous conditions. *Rubber Chem Technol* 75:133–142. <https://doi.org/10.5254/1.3547665>

60. Huang K, Isayev AI (2014) Ultrasonic decrosslinking of crosslinked high-density polyethylene: effect of degree of crosslinking. *RSC Adv* 4:38877–38892. <https://doi.org/10.1039/C4RA04860A>
61. Goto T, Ashihara S, Kato M et al (2012) Use of single-screw extruder for continuous silane cross-linked polyethylene recycling process using supercritical alcohol. *Ind Eng Chem Res* 51:6967–6971. <https://doi.org/10.1021/ie202303y>
62. Goto T, Yamazaki T, Sugeta T et al (2005) Investigation of continuous process for recycling of silane cross-linked polyethylene by supercritical alcohol. *Kagaku Kogaku Ronbunshu* 31:411–416. <https://doi.org/10.1252/kakoronbunshu.31.411>
63. Lee HS, Jeong JH, Hong G et al (2013) Effect of solvents on de-cross-linking of cross-linked polyethylene under subcritical and supercritical conditions. *Ind Eng Chem Res* 52:6633–6638. <https://doi.org/10.1021/ie4006194>
64. Lee H-S, Jeong JH, Hong SM et al (2012) Recycling of crosslinked polypropylene and crosslinked polyethylene in supercritical methanol. *Korean Chem Eng Res* 50:88–92. <https://doi.org/10.9713/kcer.2012.50.1.088>
65. Goto T, Ashihara S, Yamazaki T, Watanabe K (2006) Evaluation of recycling technology of insulation of cross-linked polyethylene insulated cable using supercritical alcohol. *IEEJ Trans Power Energy* 126:400–406. <https://doi.org/10.1541/ieejpes.126.400>
66. Celina M, George GA (1995) Characterisation and degradation studies of peroxide and silane crosslinked polyethylene. *Polym Degrad Stab* 48:297–312. [https://doi.org/10.1016/0141-3910\(95\)00053-O](https://doi.org/10.1016/0141-3910(95)00053-O)
67. Yang Z, Peng H, Wang W, Liu T (2010) Crystallization behavior of poly(ϵ -caprolactone)/layered double hydroxide nanocomposites. *J Appl Polym Sci* 116:2658–2667. <https://doi.org/10.1002/app>
68. Baek BK, Shin JW, Jung JY et al (2015) Continuous supercritical decrosslinking extrusion process for recycling of crosslinked polyethylene waste. *J Appl Polym Sci* 132. <https://doi.org/10.1002/app.41442>
69. Okajima I, Katsuzaki A, Goto T et al (2010) Decomposition of silane-crosslinked polyethylene with supercritical alcohol. *J Chem Eng Jpn* 43:231–237. <https://doi.org/10.1252/jcej.09we303>
70. Ritums JE, Mattozzi A, Gedde UW et al (2006) Mechanical properties of high-density polyethylene and crosslinked high-density polyethylene in crude oil and its components. *J Polym Sci Part B: Polym Phys* 44:641–648. <https://doi.org/10.1002/polb.20729>
71. Sirisinha K, Chuaythong P (2014) Reprocessable silane-crosslinked polyethylene: property and utilization as toughness enhancer for high-density polyethylene. *J Mater Sci* 49:5182–5189. <https://doi.org/10.1007/s10853-014-8226-z>
72. Sirisinha K, Boonkongkaew M (2013) Improved silane grafting of high-density polyethylene in the melt by using a binary initiator and the properties of silane-crosslinked products. *J Polym Res* 20:120. <https://doi.org/10.1007/s10965-013-0120-x>
73. Grigoryeva OP, Fainleib AM, Tolstov AL et al (2005) Thermoplastic elastomers based on recycled high-density polyethylene, ethylene-propylene-diene monomer rubber, and ground tire rubber. *J Appl Polym Sci* 95:659–671. <https://doi.org/10.1002/app.21177>
74. Zhang X, Lu C, Liang M (2011) Preparation of thermoplastic vulcanizates based on waste crosslinked polyethylene and ground tire rubber through dynamic vulcanization. *J Appl Polym Sci* 122:2110–2120. <https://doi.org/10.1002/app.34293>
75. Wu H, Liang M, Lu C (2011) Morphological and structural development of recycled crosslinked polyethylene during solid-state mechanochemical milling. *J Appl Polym Sci* 122:257–264. <https://doi.org/10.1002/app.33863>
76. Qudaih R, Janajreh I, Vukusic SE (2011) Advances in sustainable manufacturing. In: Seliger G, Khraisheh MMK, Jawahir IS (eds) *Recycling of cross-linked polyethylene cable waste via particulate infusion*. Springer, Berlin, Heidelberg, pp 233–239
77. Janajreh I, Alshrah M (2013) Remolding of cross-linked polyethylene cable waste: thermal and mechanical property assessment. *Int J Therm Environ Eng* 5:191–198. <https://doi.org/10.5383/ijtee.05.02.012>

Chapter 8

Aging and Degradation Studies in Crosslinked Polyethylene (XLPE)



Meera Balachandran

1 Introduction

Crosslinked polyethylene (XLPE) has been in use since the 1930s in various applications. XLPE is extensively used in electrical cables, plumbing, chemical, mining, biomedical, watercraft and automotive industries. Crosslinked polyethylene is manufactured by crosslinking polyethylene with crosslinking agent or by irradiation [1]. Depending on the end application and properties required, XLPE is manufactured from different grades of polyethylene. For example, high-density polyethylene is used for tubing, low-density polyethylene for cable insulation and ultrahigh molecular weight polyethylene for artificial joints. The crosslinked bonds change the thermoplastic polyethylene to thermoset XLPE. The production process involving modification of polyethylene structure is generally optimized to maximize production, improve properties of interest and to reduce by-product generated during crosslinking. Crosslinking significantly enhances properties like impact and tensile strength, wear resistance, thermal resistance, chemical stability, insulating properties, resistance to brittle fracture, abrasion resistance, environmental stress cracking resistance and low-temperature properties [2]. The properties of XLPE can be tailored by appropriate degree of crosslinking [3]. For example, higher degree of crosslinking could induce stress cracking and brittleness whereas lower degree of crosslinking would give poor physical properties.

XLPE is used in artificial joints and composite material in dental restoration due to its wear and abrasion resistance. In automotive industry, XLPE is used in the manufacture of cold air intake systems and filter housings. XLPE is used in several countries in plumbing application as it is less expensive than alternatives like copper,

M. Balachandran (✉)

Department of Chemical Engineering and Materials Science, Amrita School of Engineering,
Centre of Excellence in Advanced Materials and Green Technologies, Amrita Vishwa
Vidyapeetham, Amrita Nagar, Coimbatore, TamilNadu 641112, India
e-mail: b_meera@cb.amrita.edu

© Springer Nature Singapore Pte Ltd. 2021

J. Thomas et al. (eds.), *Crosslinkable Polyethylene*, Materials

Horizons: From Nature to Nanomaterials,

https://doi.org/10.1007/978-981-16-0514-7_8

offers flexibility reducing the need for joints, easy to install and operate, is not affected by corrosion from minerals, moisture or freezing and is long lasting. XLPE is used to manufacture storage tanks used in chemical industries due to its strength, durability and ability to withstand heat and acidic corrosion.

One of the major and growing market for XLPE is power transmission cables industry. The high dielectric strength, very low dissipation factor at all frequencies, high insulation resistance and excellent dimensional stability of XLPE make it the ideal choice for insulation in medium and high-voltage electric cables. XLPE has higher strength, improved aging characteristics, water tree resistance and ability to retain electrical properties over a wider range of temperature than polyethylene. Additionally, they are also resistant to chemicals and oils even at elevated temperatures which make XLPE insulation halogen-free low-smoke material [4–6].

A typical high-voltage XLPE cable contains several layers with various functions viz. conductor, inner semiconducting layer, cable insulation, outer semiconducting layer, ground layer and the outer shell. A simplified representation of an XLPE insulated cable is shown in Fig. 1.

Electric lifetime of the cable is an important measure of its quality. Prolonged life time is also closely related to sustainable development, a key aspect of concern for engineers and researchers. The reliability and life time of cables depend on a number of different factors as shown in Fig. 2 [7]. The expected service life of the cables is around 20–30 years. However, service life of some of these is far shorter than expected and underground cables start to fail in about 5–10 years [8].

Fig. 1 XLPE insulated cable

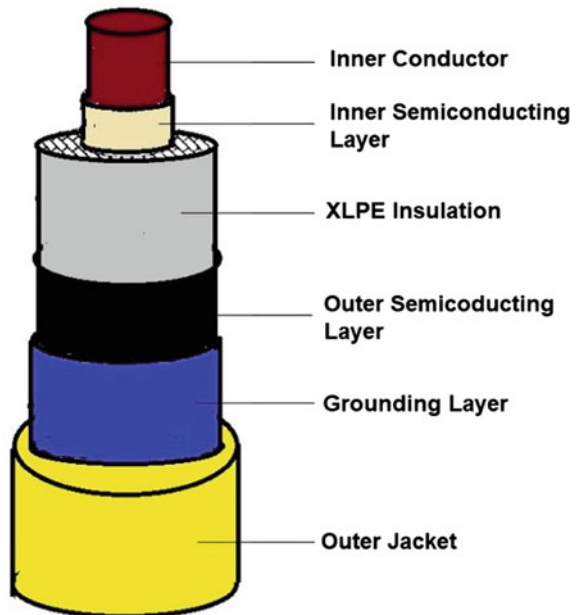
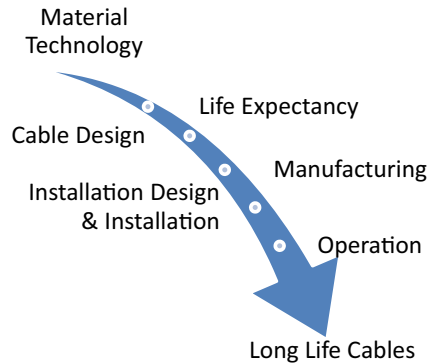


Fig. 2 Factors influencing reliability and life time of cables



A major concern in determining the life of an electric cable is the aging and breakdown of insulation. A local electrical field of more than 110 kV/mm is capable of injecting electrons into the insulation. The insulating layer of the cable should be able to withstand divergent field between the core conductor and the grounding layer. As all breakdown events occurring in the polymeric insulation are irreversible, they are to be avoided at all costs. The aging process is influenced by morphology as well as effect of additives, oxidation, ions and water. The major reasons for the failure of these cables are the combined effect of one or several of different factors like physical and chemical aging, electric breakdown, thermal breakdown, electromechanical breakdown and partial discharge breakdown [9]. Stresses (mechanical, electrical, thermal) exposure to ultraviolet or other radiations and diffusion of contaminants influence the aging process. This chapter examines the various degradation mechanisms in XLPE. The effect of additives and test procedures to evaluate the degradation is not considered in this chapter.

2 Aging and Degradation in XLPE

The major concern for all dielectric users is the aging and the breakdown of the insulation which depends on incipient changes in material properties. Fundamental origins of aging are still not clearly understood and there is still no consensus on what characterizes aging. However, it is generally accepted that morphology, additives, oxidation (or antioxidants), ions and water play major roles in the aging process of polymers. There are also many elements involved in creating conditions favorable to degradation and breakdown. Contributing processes include mechanical, electrical and thermal stress, exposure to ultraviolet radiation and, as mentioned before, the diffusion of contaminants into the insulator during its manufacturing and service time. The main mechanical, electrical, thermal and environmental factors that affect aging and degradation in XLPE are summarized in Table 1 [10].

Table 1 Factors that influence aging and degradation in XLPE insulation

Thermal factors	Mechanical factors	Electrical factors	Environmental factors
Maximum temp	Bending	Operating and transient voltage (AC, DC, impulse)	Gases
Ambient temp	Tension	Current	Water/humidity
Temperature gradient	Compression	Frequency	Corrosive chemicals
Temperature cycling	Torsion	Partial discharge	Lubricants
	Vibration	Charge injection	Radiation
	Compression cycle		

The degradation in XLPE insulation can be caused due to intrinsic or extrinsic factors. Extrinsic factors are due to micro-voids, physical imperfections, poorly dispersed components and contaminants in the insulation. On the other hand, intrinsic factors are chemical and physical changes in the polymer or trapped charges [10]. Intrinsic breakdown is caused due to the electronic behavior of the dielectric, with no effect of ambient or temperature rise and is also called electronic breakdown. The intrinsic breakdown when electrons in the insulator gain sufficient energy from the applied field to cross the energy gap from the valence to the conduction band [9]. Intrinsic type of degradation affects the properties of the material. When the property falls below a critical value, the insulation fails. These changes may or may not lead to electrical failure. Intrinsic effects are generally not confined to local area and affect large part of the insulation. Extrinsic factors affect local areas of the insulation which eventually can result in failure of the insulation.

3 Electrical Degradation and Treeing

The most hazardous and damage inducing degradation in XLPE insulation is the electrical degradation. Electrical degradation can reduce the service life of XLPE cables. In high-voltage XLPE cables, voltage difference between the conductors creates an electric field that causes ionization in the XLPE. This generates current that creates short circuit path through the insulation. This phenomenon results in electrical breakdown of the material [9]. The electric field in high-voltage cables accelerate the charge carriers (electrons, ions, etc.) in the insulation in the direction of the electric field. The acceleration increases the kinetic energy of the charge carriers. When they collide with insulation and transfers the energy which is manifested as increase in temperature. This phenomenon is called Joule heating. When the heat generated by Joule heating is not dissipated and the temperature of the material increases, the amount and mobility of charge carriers increases resulting in exponential increase in the electrical conductivity. The increased conductivity causes more current to flow through the insulation which further increases the heat input. The heating also softens the insulation. The heat generated is transferred to the surrounding medium by conduction through the solid dielectric and by radiation from its outer surfaces. This process eventually initiates thermal breakdown in XLPE and breakdown occurs

when the heat generated exceeds the heat dissipated [11]. The combined effect is the electromechanical breakdown of the insulation. Another cause of breakdown in insulation is the partial discharge (pd) breakdown that is initiated by small voids in the material. In current carrying cables, the presence of voids and contaminations in XLPE induced during the manufacturing process, coupled with ionic contaminants give rise to voltage stresses in the insulation. The high electrical stresses induce partial discharge that causes dendritic growth of microscopic cavities called trees. Electrical treeing and water treeing are the two types of trees, which are discussed in the following sections. The formation of trees is accelerated by several factors, moisture being the major accelerating factor. Formation of trees ultimately leads to complete failure of the insulation. The sequence of activities leading to electrical breakdown is summarized in Fig. 3.

A major factor influencing the dielectric properties like tree growth and breakdown in polymer dielectric materials is the non-uniformity of electric field distribution [12]. Electrical degradation due to treeing is initiated by partial discharge. Treeing is a random process that affects localized areas of the insulator. As mentioned earlier, trees are initialised at imperfections where the electrical field is highly divergent.

Electrical trees contain hollow tubules that are connected to form a treelike structure. The stem of a tree has typical dimensions in the range of tens of micrometers

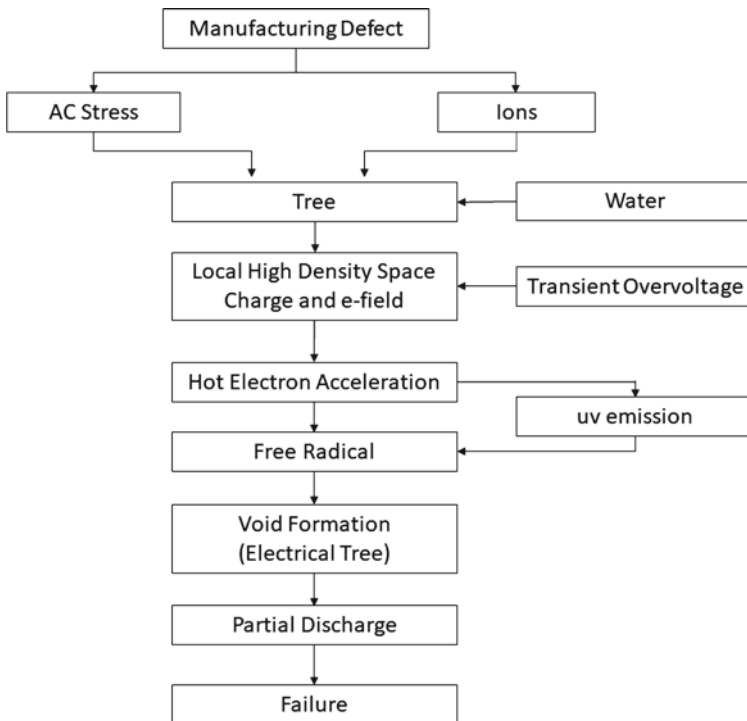


Fig. 3 Electrical breakdown in XLPE cable insulation

in diameter while the branches have sizes in micrometer range. The shape of the electrical tree can be bush type or branch type. Generally, higher fields create more bushy trees, while trees generated at lower fields have a more branch-like shape. In the general working environments of the cable, the growth of the tree is slow spanning several months or years. The tip of the water tree can initiate an electrical tree. As the electrical tree initiated by a water tree grow rapidly, the insulation will not be capable of withstanding the high voltage and the insulation fails [13–15].

3.1 Electrical Treeing

Electrical tree is the prime reason for insulation failure in XLPE cable insulation [16]. Electrical trees are interconnected channels that are generally initiated in void and are strongly influenced by defects (voids, impurities, etc.) in the and the partial discharge activity. The phenomenon of tree growth is illustrated in a sample model containing an air-filled void. Voltage is applied with a needle tip. As illustrated in Fig. 4a, the maximum electric field is observed near to the needle tip. The electric field stress at void is greater than the dielectric strength of air filled in the void. When the voltage across the void exceeds the breakdown voltage, partial discharge is initiated in the void. Partial discharge further leads to formation of electrical discharge path and a tree like structure as illustrated in Fig. 4b. The tree growth is initiated inside the void and penetrates toward the point at which electrical stress is maximum [17].

The phenomenon of electrical treeing occurs in three phases namely initiation, propagation or growth and bridging as illustrated in Fig. 5. The tree is initiated due to high and divergent stress at the interface of an imperfection or void and XLPE. The stresses may be of electrical, chemical or mechanical nature and can be caused by several factors including temperature, chemical reaction, partial discharge, etc. Among the above-mentioned factors, a major factor that initiates insulation degradation is partial discharge [18]. According to International Electrotechnical Commission Standard 60,270, partial discharge is a localized electrical discharge

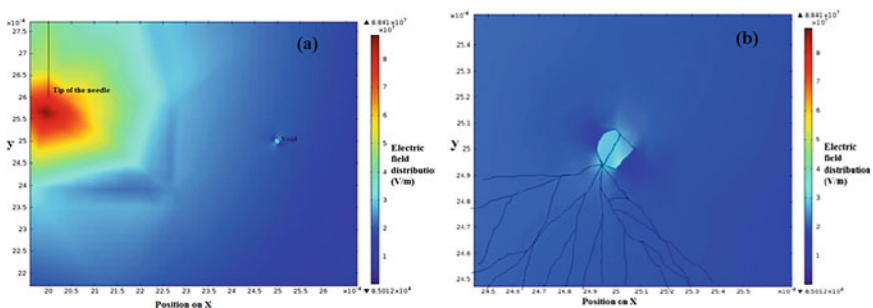


Fig. 4 **a** Electric field distribution in insulation with void **b** electrical tree growth [17]

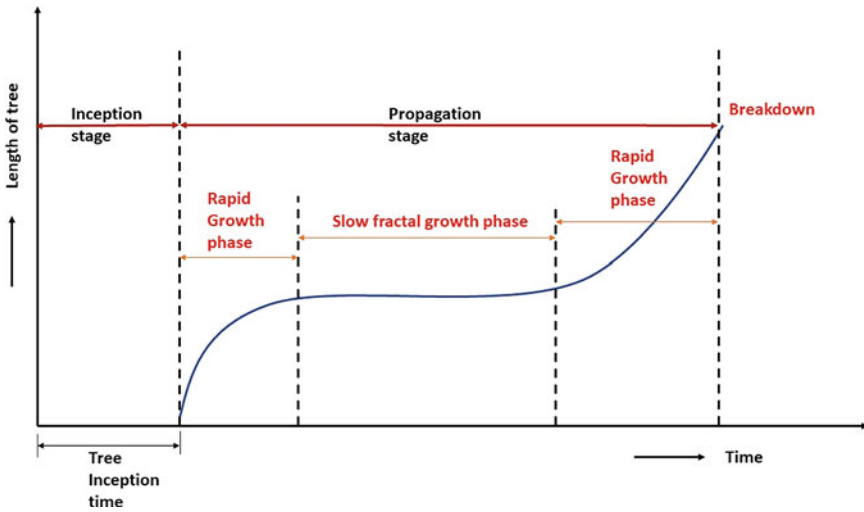


Fig. 5 Growth Stages in Treering

that only partially bridges the insulation between conductors and which may or may not occur adjacent to a conductor.

Several mechanisms have been proposed to explain initiation of electrical trees. Electrical trees can be initiated by charge carriers, mechanical fatigue, electrophotoluminescence or high field electron avalanche [19, 20]. When the insulation is subjected to AC voltage, injection of charge carriers takes place in one half cycle while extraction of charge carriers takes place in the other half cycle. The charge carriers also known as space charges can be electrons, holes or ions. When the space charges gain sufficient energy, they initiate chemical reactions that cause polymer degradation. The degradation eventually leads to formation of hollow channels in which partial discharge take place that initiates a tree [21]. It has also been reported that insulation subjected to mechanical stresses and fatigue develop cracks. Electrical trees are initiated at the cracks due to partial discharge [20]. Another phenomenon that initiates electrical tree is electro- photoluminescence. When subjected to AC voltages above a certain threshold, due to the changing polarities, XLPE emits UV and visible light. Electroluminescence spans a broad spectrum in the visible range and partial discharge light exhibits peak in the UV range. The UV light induces photochemical reaction that generates free radicals, which are capable of breaking the chemical bonds in the polymer chain. They are accelerated by electric field, collide with polymer chains and produce more free radicals. These reactions initiate the channels in electrical tree as explained earlier. Localized electron avalanche is another mechanism that initiates electrical tree. When a voltage surge (impulse voltage) happens, it can cause the local field to exceed the breakdown threshold of the

insulation. This leads to localized electron avalanche and local breakdown that initiates electrical tree [19]. The growth/propagation of the tree occurs in the direction toward the region where electric field stress is maximum.

The partial discharge depends on the geometry of the void, impurities present in the insulation and permittivity of the insulation material [22]. Several factors like magnitude and frequency of applied electric field, temperature, environmental stresses and mechanical stresses influence the propagation of electrical tree. Finally, when the tree is long enough, bridging occurs resulting in total breakdown of insulation [9]. Treeing can be controlled by adopting several strategies like ensuring smoothness of the semiconductive shield, minimizing contamination and defects during manufacture of semiconductive shield, insulation and cable and minimizing ingress of moisture into the insulation [23].

A partial discharge occurs when there is sufficiently high field and presence of an electron. The enhancement in electric field at the defect site induces partial discharge. This enhanced field consists of an enhancement in background field and the field produced by local space charges formed from previous PD events. The avalanche of electrons is formed at a minimum local inception field that corresponds to the partial discharge inception voltage (PDIV). PDIV is the lowest voltage at which partial discharges is termed partial discharge inception voltage. The magnitude of PDIV depends on the size of the defect, composition of the constituents of the defect, operating temperature and pressure. The electrons are initially produced by gas ionization by energetic photons and field detachment of electrons from negative ions. The rate of production of electron depends on the magnitude of electric field. Another mechanism by which electrons are produced is from surface emissions due to ion impact, detrapping of electrons due to field emission or by the photon effect. The PDIV in newly formed virgin defects is higher than that in aged defects (defects that have been there in the insulation for longer duration or exposed to aging conditions). On occurrence of partial discharge, charges are deposited on the surface and in traps in the insulator surface. When sufficient energy is acquired, the surface liberates free electrons. The charges decay when they diffuse through gases in the voids or by conduction along the surface or by ion drift [19]. When an XLPE high-voltage cable is in operation, due to high voltage and aging, there is accumulation of space charge in the insulation that distorts the local electrical field.

Several mechanisms have been proposed to explain initiation of electrical trees. Electrical trees can be initiated by charge carriers, mechanical fatigue, electrophotoluminescence or high field electron avalanche [20, 21]. When the insulation is subjected to AC voltage, injection of charge carriers takes place in one half cycle while extraction of charge carriers takes place in the other half cycle. The charge carriers also known as space charges can be electrons, holes or ions. When the space charges gain sufficient energy, they initiate chemical reactions that cause polymer degradation. The degradation eventually leads to formation of hollow channels in which partial discharge take place that initiates a tree [24]. It has also been reported that insulation subjected to mechanical stresses and fatigue develop cracks. Electrical trees are initiated at the cracks due to partial discharge [21]. Another phenomenon that initiates electrical tree is electro-photoluminescence. When subjected to AC

voltages above a certain threshold, due to the changing polarities, XLPE emits UV and visible light. Electroluminescence spans a broad spectrum in the visible range and partial discharge light exhibits peak in the UV range. The UV light induces photochemical reaction that generates free radicals, which are capable of breaking the chemical bonds in the polymer chain. They are accelerated by electric field, collide with polymer chains and produce more free radicals. These reactions initiate the channels in electrical tree as explained earlier. Localized electron avalanche is another mechanism that initiates electrical tree. When a voltage surge (impulse voltage) happens, it can cause the local field to exceed the breakdown threshold of the insulation. This leads to localized electron avalanche and local breakdown that initiates electrical tree [20]. The growth/propagation of the tree occurs in the direction toward the region where electric field stress is maximum.

During cycling of voltage of sufficient amplitude, charges are released and extracted in the alternate half cycles. These charge carriers can move around in the dielectric material under the influence of electric field or become trapped in the bulk of material. The trapped electrons can build up the heterocharge that cause increase in local electric field. When the local electric field exceeds the breakdown threshold, local deterioration is initiated. Recombination of charges releases energy. When the magnitude of energy released is higher than the bond energy, breakage of polymer chains occurs. The trapping, detrapping and recombination of charges release energy that ultimately leads to breakdown of the material. Attempts have been made to study the AC space charge characteristics of XLPE cable insulation at various stages of accelerated aging. The trap energy level gradually increased with aging time due to breakage of XLPE chains, decomposition of additives and generation of space charge traps at deeper levels. The non-uniformity of the applied field also affects the trapped charge in XLPE insulation [25].

Several factors like the magnitude and nature (AC, DC or impulse) of applied voltage, electric field enhancement, frequency, partial discharge and temperature influence the growth of electric trees. The strength of the electric field near the defect depends on the magnitude of applied voltage and if this induced field exceeds the dielectric strength of the material, tree growth and initiation commence [26]. The type of tree formed also depends on the type and magnitude of applied voltage. At lower voltage branched type tree growth was observed in XLPE whereas bush type was observed at higher voltages [27, 28]. The three phases of electrical tree viz. initiation, growth and breakdown of XLPE insulation are greatly influenced by temperature. In a recent study, the effect of temperature gradient on electrical tree was studied [29]. The tree was initiated with AC voltage with RMS of 12 kV and frequency of 50 Hz in needle plate electrodes. The needle temperature varied from -122 to 18 °C while the ground temperature varied from -196 to 0 °C. The notation (needle temperature, ground temperature) will be used to discuss the effect of temperature gradient. The tree structure formed depended on the temperature gradient. In samples with lower temperature gradient, the electrical trees formed consisted of an upper region with large amount of channels that interlaces with each other and a vine region with vine-structure channels. With increase in temperature gradient, trees with pine structure with 3–5 main branches with several tiny channels were formed. Further increase

in temperature gradient resulted in branch-structure where the main branch was not very obvious. Electrical tree formation was suppressed in lower temperature regions. The effect of temperature gradient on the tree size was also analyzed. It was found that both the length and width of the tree (at 60 min) decreased with decrease in ground temperature, i.e., increase in temperature gradient. The reason for the lower length and width of the tree at lower temperature is that the partial discharge, the major reason for electrical treeing, is limited at low temperature. At lower temperature, the pressure induced by gaseous products of partial discharge that accelerates tree growth will also be lesser. The rigidity of XLPE at lower temperature also limits tree growth. The tree initiation voltage increased while the tree growth speed decreased with increase in temperature gradient [29]. Effect of temperature and electric field on charge accumulation properties in XLPE were studied by Li et al. by correlating the polarization and depolarization processes. It was shown that there was an increase of 2 or 3 orders in steady current with a temperature increasing from 25 to 90 °C. Above 70 °C, electric field dependence of charge conduction is weaker as effect of thermal vibration becomes significant [30]. Another factor that influences tree growth is the moisture content. The fractal dimensions of the tree increase whereas the growth time reduces with increase in moisture content [31]. Fractal dimensions are used to describe the nature of the electrical tree and it represents the density of branches in the electrical tree.

As discussed above, the initiation and propagation of electrical tree are influenced by both electrical and mechanical stresses. Jones et al. studied whether the electrical stress can produce the same effect as mechanical stress in XLPE, viz. creation of sub-microvoid, cavity and crack initiation [32]. According to classical electromagnetic theory, a force density is generated when a dielectric is subjected to an electric field. This force density gives rise to mechanical stress. When the developed mechanical stress exceeds, the yield stress of the material, plastic deformation and craze formation occurs [32, 33]. The degradation by electrical treeing can be triggered through enlargement of microvoids and progresses through propagation of cracks. Mechanical stress has been correlated with reduction in tree initiation voltage and dielectric strength. Electrical breakdown is initiated at the weakest point in the insulation [33]. It has been proven that XLPE samples subjected to deformation by applied tensile stress forms more ionizable chemical species that result in more space charge than undeformed samples. When the sample is deformed, the by-products of crosslinking locked between polymer chains are released and they form ionizable species. Higher the mechanical stresses, shorter the tree inception time and longer the tree growth. The microcracks developed during deformation also contribute to the treeing mechanism. Internal mechanical stress developed during manufacture of the cable can also result in enhancing electrical trees [34].

3.2 Water Treeing

The moisture content in soil makes underground cables prone to degradation by water treeing. Moisture ingress into the cable insulation can occur through joints, termination points or physical damage in the cable. Water tree itself cannot cause failure, however, water trees facilitate the initiation of electrical tree which grow fast and leads to breakdown [35, 36]. The risk of failure due to water tree depends on the impurity content in the insulation. The trees that originate from an impurity or imperfection within the insulation or residual moisture present after crosslinking process is generally bow-tie type. These trees have length in the range of micrometers and do not very dangerous to degrade the cable. The trees that originate at the interface between semiconductor shield and insulation are vented type water tree that propagate in the direction of the electric field. The propagation continues till it reaches ground. Vented trees physically divide the insulation and hence are more detrimental to the cable than bow-tie tree.

It has been shown in several studies that the initiation of water tree in polymer dielectric is mainly influenced by the magnitude of electric field and availability of water content [37–39]. Water trees are formed at lower electric field strengths than electrical trees. Water tree formation also depends on temperature, mechanical stresses developed in the insulation material and the quality of insulation. Water tree initiation and growth are also influenced by voltage, frequency, amount of water, water quality, type of solvent, additives in insulation, irradiation, ions and oxidation, presence of impurities [40–42].

To understand the process of water tree formation, the author and co-workers performed experiments with water-needle arrangements [43]. The XLPE samples were pressed with abrasive paper (P240 grit 50 micron defect size) on one face for 2 min at 50 MPa at room temperature to create initiation sites on the surface of the samples. Samples were exposed to AC voltage of 5 kHz frequency and 5 kV amplitude for 24 h. 0.1 molal sodium chloride solution was used in the needle plane cell. The samples were dyed in rhodamine solution at 60 °C for 3 days. Slices of 200 μm thickness were microtomed from the XLPE samples and the average length of the tree formed was measured to be 50 μm . The water-needle arrangement and water tree length measurement are represented in Fig. 6.

Water treeing is affected by temperature, type of electrolyte and pH. In sodium chloride solution, water tree propagates faster at room temperature than at 50 °C.

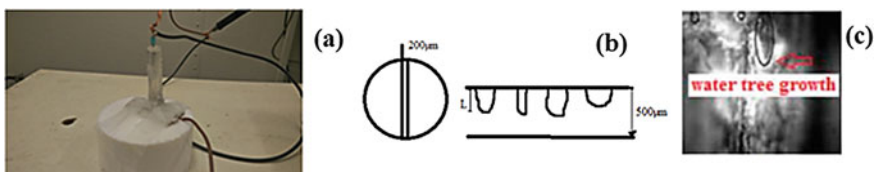


Fig. 6 **a** Experiment setup for water tree growth, **b** representation of water tree measurement on microtomed specimen **c** water tree in XLPE

In copper sulfate solution, however, the tree propagation was faster at 50 °C than at room temperature. The treeing in NaCl solution was vented type whereas in CuSO₄ solution, both vented and bow-tied treeing occurred. The propagation of water treeing depends strongly on the pH level. Lower pH gives higher propagation of water tree and vice versa [44].

Studies have shown that water treed regions of XLPE are prone to oxidative degradation, which has been linked to lowering of breakdown strength and voltage [14, 15, 45–48]. The breakdown voltage of XLPE cables aged at 90 °C for 50 h were found to be 144 ± 8 kV/mm as compared to 174 ± 6 kV/mm in unaged cables [49]. Li et al. studied the effect of accelerated aging on XLPE insulation. Aged XLPE showed higher conductivity, increased dielectric loss, decrease in crystallinity and density and the change in properties were dependent on the aging time [50].

4 Chemical Degradation Mechanisms

Crosslinked polyethylene is produced by cross linking polyethylene with crosslinking agents. During crosslinking, several by-products like acetophenone, cumyl alcohol, α -methyl styrene, methane, and moisture are generated that remain in the XLPE matrix [51]. These by-products lead to generation of negative hetero-charges, increases conductivity and eventually leads to degradation and aging in XLPE [52, 53].

Chemical degradation in XLPE occurs due scission of polymer chains, depolymerization, crosslinking reactions, oxidation and/or hydrolysis. Scission can occur in the main chain or on the side chains as shown in Fig. 7. In elimination reaction, a

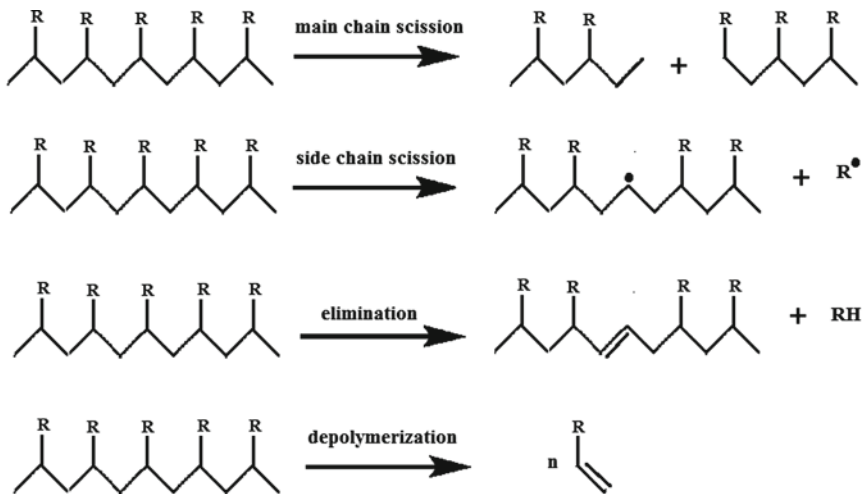


Fig. 7 Schematic representation of degradation by scission in XLPE

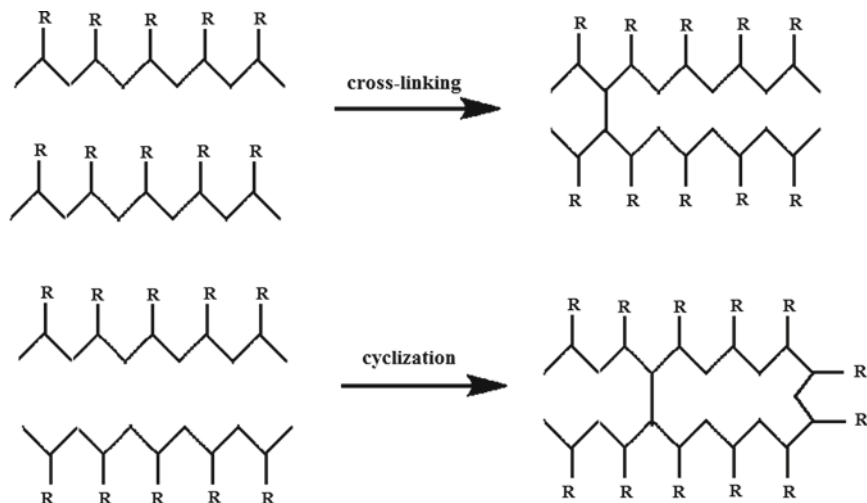
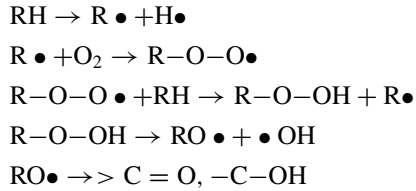


Fig. 8 Schematic representation of degradation by crosslinking and cyclization

side chain or molecule along with a proton (H) is detached from the main chain [54]. Scission of polymer chains results in shorter chains with lower molecular weight and consequent loss in mechanical properties. In extreme cases, depolymerization occurs with polymer chains getting converted back to monomer units. The schematic representation of the scission in XLPE is represented in Fig. 7.

Chemical degradation can also occur due to crosslinking and cyclization. Crosslinking results in three-dimensional network formed by covalent bonds between adjacent chains. Side cyclization refers to the grouping of side chains to form ring structures in the chain. Crosslinking and cyclization are schematically represented in Fig. 8. Excessive crosslinking results in increase in stiffness, loss of ductility and embrittlement of material. Both scission and crosslinking can occur simultaneously and the net effect depends on which process dominates.

In XLPE insulation exposed to atmosphere and ambient conditions, oxidation is the major cause of degradation. Both chain scission and crosslinking are largely influenced on the presence of oxygen. Oxidation, chain scission and crosslinking are strongly dependent on the temperature. Oxidation in XLPE progresses through a series of reactions. In the first step (initiation), a radical ($R\bullet$) is formed on the polymer chain (represented by RH). The initiation step can be induced by temperature or energy (UV, radiation, etc.). The radical thus formed reacts with oxygen in the atmosphere to form peroxy radical ($R-O-O\bullet$). In the propagation step, the peroxy radical reacts with hydrogen from another chain to form hydroperoxide ($R-O-OH$) and a new radical on the second chain. The hydroperoxide thermally decomposes to form poly-oxy radical ($RO\bullet$) and hydro-oxy radical ($\bullet OH$). The poly-oxy radical decomposes to form oxidation products (carbonyl groups, alcohols). This process continues till the radicals are combined [55]. The reaction scheme for oxidation reaction is as shown below.



In XLPE, oxidation reduces the molecular weight and introduces functional groups that contain oxygen. Oxidation increases brittleness in XLPE and causes cracking. Degradation by oxidation is an auto-acceleration phenomenon that proceeds initially at a slow pace. When XLPE is subjected to hydrolysis, the chain undergoes scission with one part containing a hydroxyl group and the other containing a hydrogen from water. The chemical degradation process is complex, with multi-stage chemical reactions that end either in crosslinking or in chain scission. Each of these reactions has its own reaction rate and activation energy.

There are several studies done on the effect of various factors on the degradation of XLPE. Chemical degradation in XLPE is influenced by the temperature. Oxidative stability tests can be conducted in isothermal conditions or in a ramp temperature test. The occurrence of oxidation in XLPE is characterized by the formation of carbonyl compounds which can be measured by FTIR. It has been observed that oxidation in regions of XLPE with treeing was more than in non-tree region of the insulation. The presence of contaminants like metal ions catalyzes oxidation through hydroperoxide mechanism and reduce the oxidative stability in the treed regions of insulation. Progressive oxidation at the trees eventually results in breakdown of the insulation [56].

Extensive studies have been carried out by Garcia et al. on the degradation reaction and products in XLPE subjected to partial discharge. Upon occurrence of partial discharge in XLPE, several reactions take place that result in the formation of aromatic and non-aromatic compounds. The chemicals that are produced during crosslinking reaction like acetophenone play vital role in the formation of non-aromatic reaction products like oxalic acid, formic acid, carbon monoxide, carbon dioxide and water. In XLPE subjected to corona discharge, aromatic compounds like benzoic acid, benzamide and toluene are formed as degradation products. Generally, the amount of water and oxalic acid formed is low. If the insulation operates in moist environment, the discharges may be extinguished by the water or acid present in cavities. But, if the intensity of pd is high, the degradation and erosion will also be faster [57].

5 Thermal Degradation

The normal operating temperature of XLPE insulation is up to 90 °C and it may go up to 150 °C. In short circuit conditions, the temperature may go up to 250 °C

[58]. The exposure to higher temperature during service life and very high temperature even for short durations during short circuiting results in degradation of the material that eventually alters chemical and physical structure along with deterioration in dielectric properties [59]. Similar to chemical degradation, thermo-oxidative degradation produces low molecular weight oxygenated products, chain scission and causes structural changes. These changes result in variation of crystallinity, heat of fusion, melting points, mechanical and electrical properties [60, 61].

6 Aging in XLPE

Aging is the irreversible change in properties of a material under the influence of its environment during its operational life. Aging of XLPE arises from changes in its physicochemical structure. Degradation of polymer chains is the major aging mechanism in XLPE. Aging significantly reduces the properties of cable insulation. In XLPE cables subjected to electrical stress and aged underwater, the breakdown voltage/strength decrease with time of aging and the magnitude of change can be more than 50%. Temperature cycling increased the number of breakdowns occurring in XLPE significantly [62].

Accelerated aging test has been conducted on XLPE insulation to evaluate the thermal aging effects. In a study conducted on medium voltage XLPE insulation by Mecheri et al., volume resistivity by two orders of magnitude decreased from $7 \times 10^{14} \Omega \text{ cm}$ to $2.57 \times 10^{12} \Omega \text{ cm}$ value after aging at 90°C for 1350 h. At higher temperatures of 135°C and 150°C , the resistivity further dropped further to $4.6 \times 10^{11} \Omega \text{ cm}$ and $2 \times 10^{11} \Omega \text{ cm}$, respectively, for the same aging. This phenomenon is an indication of deterioration of the XLPE material [62]. The dissipation factor was relatively unaltered with only slight increase at 90°C and had a value of 3.7×10^{-3} . The dissipation factor but increased rapidly beyond 680 h to 20.5×10^{-3} and 57.1×10^{-3} at 135°C and 150°C , respectively. This change is caused due to thermal degradation involving decomposition, chains scission and oxidation. The formation of $-\text{C} = \text{O}$ is responsible for increase in the dielectric loss factor. The breakdown voltage decreases rapidly with the thermal aging time. The breakdown strength decreased by 32.5%, 50% and 52.5%, respectively, in XLPE sampled aged for 1350 h at 90°C , at 135°C and 150°C , respectively. The thermal aging also results in loss of mass and decrease in mechanical properties. The deterioration in tensile strength increased with increase in aging temperature and can be as high as 75% reduction at 150°C . The decline in mechanical properties can also be attributed to deterioration in chemical and physical structure of the insulation arising from thermal degradation [63].

A recent study by Boukezzi et al. also concluded that thermal aging cause losses factor to increase and volume resistivity to decrease. At temperature above melting point, the loss factor increase is faster due to the higher concentration of carbonyl groups produced during oxidation. They also postulated that the activation energy for thermal degradation and resistivity is affected by aging time [61]. Low-temperature

aging increases XLPE crystallinity while high-temperature aging decrease the crystallinity [64]. At higher temperatures, the crystalline regions of XLPE become amorphous making diffusion of oxygen. As temperature increases the volatile by-products of crosslinking move out of the amorphous region of XLPE and are replaced with oxygen or water (if aging is in wet condition). Both these factors increase degradation during thermal aging. Both chain scission and/or crosslinking can occur.

In high-temperature environment and in the presence of air, several physical and chemical changes occur in XLPE. Zhang et al. compared the effect of thermo-oxidative aging at constant temperature (473.5 K) to aging under thermal cycling (5 cycles from 293.5 to 473.5) for 30 h. Samples subjected to temperature-frequency aging were more damaged than the sample of constant temperature heat aging due to deterioration of the crystallization zone in XLPE due to repeated melting and crystallization. In the initial stages of aging, there was release of gaseous isobutene while in the later stages of aging, oxygen containing compound increased whereas amount of isobutylene gas decreased [65].

Thermal aging in XLPE not only influences the electrical, physicochemical and mechanical properties, but also affects the initiation and propagation of water tree. In a study by Kim et al., it was reported the most influential factor in the initiation and growth of water trees in thermally aged XLPE insulation. Aged samples displayed higher tree density and length [66]. A study on the influence of thermal aging on AC leakage current demonstrated that the dielectric constant and AC leakage current of XLPE increased with both aging temperature and aging time [67].

7 Radiation Aging

Electrical cables are used in nuclear plants in power transmission, control and instrumentation. The insulation and jacket materials for these cables are polymer-based. Unlike other polymer components like seals that can be replaced during maintenance, replacement or removal of cables are difficult and expensive.

Aging of XLPE in nuclear environments is very complex. The degradation behavior of XLPE exposed to radiation polymeric displays non-linear behavior and is a function radiation dose and temperature [68]. In XLPE, the predominant aging mechanism in radiation environment is oxidative degradation that includes both crosslinking and chain scission and radiation induced crosslinking as depicted in Fig. 9.

When exposed to radiation, XLPE generates free radicals. The free radicals directly involve in crosslinking between the polymer chains and/or chain scission that causes deterioration in mechanical and electrical properties. The primary factors that affect degradation in radiation exposed XLPE are temperature, radiation dose rate, cumulative dose of radiation exposure and presence of oxygen [69]. As seen in the previous discussions, degradation increases with increasing temperature. The dependence of degradation on radiation dose rate is quite significant when irradiated in the presence of air or oxygen. At low radiation dose rate, chain scission due to

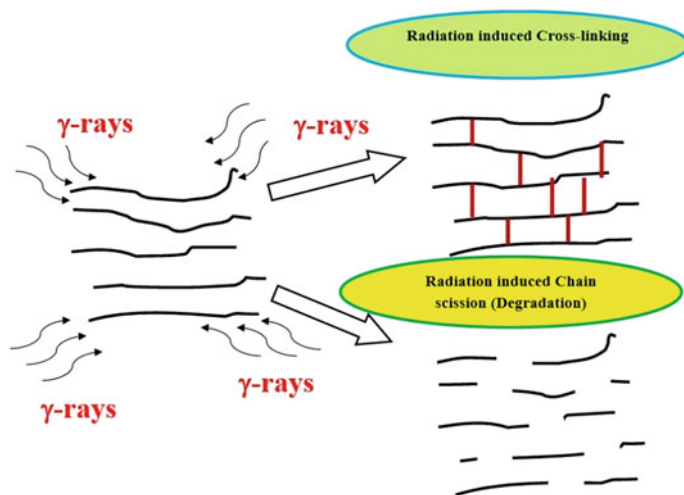


Fig. 9 Effect of gamma radiation on XLPE

oxidative degradation is predominant whereas at higher doses the crosslinking effect cancels the effect of chain scission due to oxidative degradation [69]. These effects along with oxidative products change the mechanical as well as electrical properties of XLPE. The dose of radiation required to result in a specific level of degradation (e.g., 50% loss of weight or tensile strength) decreases as the dose rate decreases. In addition, secondary factors like moisture, mechanical stress, presence of ozone and chemical contamination also affect the radiation aging in XLPE [70].

The main factors that are considered in radiation aging effects are diffusion-limited oxidation, effect of dose rate, synergy between radiation and temperature and reverse temperature effects. The magnitude of degradation in both thermal and radiation aging depends on the diffusion of oxygen into the component aged. Under normal operating conditions (low temperature, lower dosage rate and long exposure time), the rate of diffusion of oxygen is slow. The degradation is uniform throughout the sample. At higher radiation dosage rate, higher temperature or shorter times, the oxygen diffused into the component is rapidly consumed in the degradation reaction and the concentration difference drives more oxygen molecules to diffuse into the matrix [69, 71]. This results in heterogeneous degradation effects with surface and edges being degraded/oxidized more than the interior of the component.

The dose rate of radiation is an important factor that governs the extent of degradation in XLPE. In a study on the dose required to reduce the elongation at break of XLPE cable insulation material to 100% absolute, it was observed that the dose required decreases from 600 kGy at 400 Gy/h to 150 kGy at 9 Gy/h [72]. For most polymers, the effect of radiation aging is generally dependent on temperature. At rate of radiation dose, the degradation is dominated by radiation aging and the effect of temperature is not dominant. At lower dosage rates, the degradation is largely affected by the temperature at which the component is exposed to radiation. However, in the

case of XLPE exposed to radiation, degradation is greater at lower temperatures than at higher temperatures. This phenomenon is called reverse temperature effect. For XLPE reverse temperature effect is significant in the temperature range 20–120 °C, the service temperature range in nuclear plants [73].

In a recent study on XLPE cable insulation material exposed to heat and gamma radiation, it was found that for isothermal aging, the oxidation induction time decreased with increasing gamma radiation dose. At fixed gamma radiation dose, the induction time for oxidation decreased with increasing temperature of aging. In thermally aged XLPE that is not exposed to gamma radiation, the breakage C–C bond caused by temperature generates free radicals. When exposed to high energy gamma radiation, the degradation is faster because the rate at which free radicals are formed is higher and the high energy radiation generates secondary electrons that break additional polymer C–C bonds, producing more free radicals. Additionally, the chain scission in XLPE and changes in crystalline and semicrystalline content in the matrix reduces the oxidation induction time [74].

The effect of UV radiation on XLPE has also been studied. Aging due to UV radiation deteriorates XLPE and affects the dielectric properties. Dielectric constant, dissipation factor, dielectric loss index increased while AC volume resistivity decreased after UV aging. Aging introduces more dissociative ions and additional polar groups which act as charge carriers which leads to increase of polarization, electrical conductivity and dissipation factor. The formation of electrically unsymmetric carbonyl compounds is responsible for the increase in $\tan\delta$ [75].

8 Conclusion

The durability of cable insulation is governed by the aging and degradation of the insulation. In XLPE insulation, aging and degradation are affected by mechanical, electrical, thermal and environmental factors. Electrical breakdown is the most hazardous and damage inducing degradation in XLPE insulation. Various phenomena that lead to electrical degradation like electric treeing, partial discharge, water treeing and electromechanical stresses are investigated. The stages and the mechanism electrical tree growth affected by the charge carriers, mechanical fatigue, electro-photoluminescence or high field electron avalanche are discussed. Chemical degradation in XLPE occurs due scission of polymer chains, depolymerization, crosslinking reactions, oxidation and/or hydrolysis. The mechanism of chemical degradation and its effects has been elaborated. Thermal and radiation aging effects in XLPE insulation cables have also been discussed.

References

1. Dyson RW (ed) (1990) Engineering polymers. Chapman and Hall, New York

2. Barzin J, Azizi H, Morshedian J (2007) Preparation of silane-grafted and moisture crosslinked low density polyethylene. Part II: electrical, thermal and mechanical properties. *Polym Plast Technol Eng* 46:305–310
3. Nilsson S, Hjertberg T, Smedberg A (2010) Structural effects on thermal properties and morphology in XLPE. *Eur Polym J* 46:1759–1769
4. Orton H (2013) History of underground power cables. *IEEE Electr Insul Mag* 29:52–57
5. Precopio F (1999) The invention of chemically cross linked polyethylene. *IEEE Electr Insul Mag* 15:23–25
6. Hampton N, Hartlein R, Lennartsson H et al (2006) Long-life XLPE-insulated power cables *SMAR Tech* 1853/27815
7. Zhou C, Yi H, Dong X (2017) Review of recent research towards power cable life cycle management. *High Volt* 2:179–187
8. Ezrin M, Lavigne G (2007) Unexpected and unusual failures of polymeric materials. *Eng Fail Anal* 14:1153–1165
9. Kuffel E, Zeangle WS, Kuffel J (eds) (2000) High voltage engineering fundamentals. Butterworth-Heinemann, Oxford
10. Densley J, Bartnikas R, Bernstein BS (1993) Multi-stress ageing of extruded insulation systems for transmission cables. *IEEE Electr Insul Mag* 9:15–17
11. Naidu MS, Kamaraju V (1995) High voltage engineering. McGraw-Hill, New York
12. Mahajan A, Seralathan KE, Nandini G (2007) Modelling of electric tree propagation in the presence of voids in epoxy resin. Paper presented at the international conference on solid dielectric, winchester, 8–13 July 2007
13. Uematsu T (1992) Bow-tie-tree in EPR cables are accelerated water treeing test. *IEEE Trans Power Deliv* 7:1667–1676
14. Yoshimitsu T, Mitsui H, Hishida K et al (1983) Water treeing phenomena in humid air. *IEEE T Dielect El In* 4:396–401
15. Yoshimitsu T, Mitsui H, Hishida K et al (1983) Water treeing phenomena in humid air *IEEE T Dielect El In* 4:396–401
16. Bin LJ, Quan Z, Di Y et al (2008) Study on propagation characteristics of electrical trees in different electrode system. Paper presented at the international conference on high voltage engineering and application, Chongqing, China, 9–12 Nov 2008
17. Kavitha D (2016) Theoretical and experimental investigation on dielectric properties of epoxy and XLPE Nanocomposites. Ph.D. Thesis, Amrita Vishwa Vidyapeetham
18. Ramu TS, Nagamani HN (2010) Partial discharge based condition monitoring of high voltage equipment. New Age International (P) Ltd, New Delhi
19. Wu J, Mor AR, Smit JJ (2019) The effects of superimposed impulse transients on partial discharge in XLPE cable joint. *Int J Electr Power Energy Syst* 110:497–509
20. Shimizu N, Laurent C (1998) Electrical tree initiation. *IEEE T Dielect El In* 5:651–659
21. Ahmad MH, Bashir N, Ahmad H et al (2014) An overview of electrical tree growth in solid insulating material with emphasis of influencing factors, mathematical models and tree suppression indones. *J Electrical Eng Comput Sci* 12:5827–5846
22. Illias H, Tunio MA, Abu Bakar AH et al (2016) Partial discharge phenomena within an artificial void in cable insulation geometry: experimental validation and simulation. *IEEE T Dielect El In* 23:451–459
23. Poggi Y, Raharimalala V, Filippini JC et al (1990) Water treeing as mechanical damage. *IEEE Trans Electr Insul* 25:1056–1065
24. Tanaka T, Greenwood A (1978) Effects of charge injection and extraction on tree initiation in polyethylene. *IEEE Trans Power Appar Syst PAS-97(5):1749–1759*
25. Gao C (2019) A study on the space charge characteristics of AC sliced XLPE cables. *IEEE Access* 7:20531–20537
26. Sarathi R, Das S, Anil Kumar CR et al (2004) Analysis of failure of crosslinked polyethylene cables because of electrical treeing: a physicochemical approach. *J Appl Polym Sci* 92:2169–2178

27. Densley R (1979) An investigation into the growth of electrical trees in XLPE cable insulation. *IEEE T Dielect El In EI-14*: 148–158
28. Yoshimura N, Noto F (1982) Voltage and frequency dependence of bow-tie trees in crosslinked polyethylene. *IEEE T Dielect El In, EI-17*:363–367
29. Fang S, Du B, Member S et al (2019) Effect of temperature gradient on electrical tree in XLPE from 0 to $-196\text{ }^{\circ}\text{C}$. *IEEE T Appl Supercon* 29:1–4
30. Li G, Zhou X, Hao C et al (2019) Temperature and electric field dependence of charge conduction and accumulation in XLPE based on polarization and depolarization current. *AIP Adv* 9:015109
31. Fan Y, Zhang D, Li (2018) Study on the fractal dimension and growth time of the electrical treeing degradation at different temperature and moisture. *Adv Mater Sci Eng* 2018:6019269
32. Jones JP, Llewellyn JP, Lewis TJ (2005) The contribution of field-induced morphological change to the electrical aging and breakdown of polyethylene. *IEEE T Dielect El In* 12:951–966
33. Montanari GC, Mazzanti G, Simoni L (2002) Progress in electrothermal life modeling of electrical insulation during the last decades. *IEEE T Dielect El In* 9:730–745
34. Danikas M, Papadopoulos D, Morsalin S (2019) Propagation of electrical trees under the influence of mechanical stresses: a short review. *Eng Appl Sci Res* 9:3750–3756
35. Gulski E, Cicecki P, Wester F et al (2008) On-site testing and PD diagnosis of high voltage power cables. *IEEE T Dielect El In* 15:1691–1700
36. Hui L, Schadler LS, Nelson JK (2013) The influence of moisture on the electrical properties of cross linked polyethylene/silica nanocomposites. *IEEE T Dielect El In* 20:641–653
37. Zazoum B, David E, Ngo AD (2014) Simulation and modelling of polyethylene/clay nanocomposite for dielectric application. *Trans electr electron mater* 15:175–181
38. Chan JC (1978) Electrical performance of oven-dried XLPE cable. *IEEE T Dielect El In* 13:444–447
39. Eccles L, Dissado A, Fothergill JC (1992) Water tree inception-experimental support for a mechanical/chemical/electrical theory. Paper presented at the sixth international conference on dielectric materials, measurements and applications, Manchester, UK, 7–10 Sept 1992
40. Yuan Y, Lu G, Wang W (2003) Dielectric loss and partial discharge test analysis of 10 kV XLPE cable. Paper presented at the 2013 annual report conference on electrical insulation and dielectric phenomena, Shenzhen, China, 20–23 Oct. 2013
41. Ogiwara J (2010) Temperature characteristics of water tree propagation in a wide temperature range using XLPE sheets. Presented at the 2010 annual report conference on electrical insulation and dielectric phenomena, West Lafayette, IN, USA
42. Kim C, Jin Z, Huang X et al (2007) Investigation on water treeing behaviours of thermally aged XLPE cable insulation. *Polym Degrad Stabil* 92:537–544
43. Kavitha D, Balachandran M (2019) XLPE—layered silicate nanocomposites for high voltage insulation applications: dielectric characteristics, treeing behaviour and mechanical properties. *IET Sci Meas Technol* 13:1019–1025
44. Promvichai N, Boonraksa T, Marungsri B (2018) The effect of pH and temperature on the propagation of water treeing in XLPE insulated underground cable. *ECTI Trans Electric Eng Electron Comm* 16:83–89
45. Radu I, Notinger PV, Filippini JC (2000) Influence of water trees on the electric field distribution and breakdown in the point–point geometry. *J Electrostat* 48(3):165–178
46. Radu I, Notinger PV, Filippini JC (2000) The effect of water treeing on the electric field distribution of XLPE. Consequences for the dielectric strength. *IEEE T Dielect El In*. 7:860–868
47. Elayyan HSBA, Abderrazzaq MH (2005) Electric field computation in wet cable insulation using finite element approach. *IEEE T Dielect El In* 12:1125–1133
48. Meyer CT, Filippini JC (1979) Water-treeing seen as an environmental stress cracking phenomenon of electric origin. *Polymer* 20:1186–1187
49. Faedah HN, Azreen MAM, Lau KY et al (2019) Breakdown properties of aged low voltage cross-linked polyethylene insulated cable. *I IOP Conf Ser Mater Sci Eng* 513:012014
50. Li J, Zhao X, Yin G et al (2011) The effect of accelerated water tree ageing on the properties of XLPE cable insulation. *IEEE T Dielect El In* 18:1562–1569

51. Maeno Y, Hirai N, Ohki Y et al (2005) Effects of crosslinking byproducts on space charge formation in crosslinked polyethylene. *IEEE T Dielect El In* 12:90–97
52. Hirai N, Minami R, Tanaka T et al (2003) Chemical group in crosslinking byproducts responsible for charge trapping in polyethylene. *IEEE Trans Dielect Elect Insul* 10:320–330
53. Sekii Y (2019) Charge generation and electrical degradation of cross-linked polyethylene. *IEEE T Electr Electr* 14:4–15
54. Ebewele RO (2000) *Polymer science and technology*. CRC Press, New York
55. Gugumus F (2002) Re-examination of the thermal oxidation reactions of polymers 2. Thermal oxidation of polyethylene. *Polym Degrad Stabil* 76:329–340
56. Garton A, Bamji SS, Bulinski A et al (1986) Oxidation and water treeing in XLPE cable insulation. In: *Proceedings of the 3rd international conference on conduction and breakdown in solid dielectrics, rondheim, Norway, 3–6 July 1989*
57. Gamez-Garcia M, Bartnikas R, Wertheimer MR (1987) Synthesis reactions involving XLPE subjected to partial discharges. *IEEE T Dielect El In* EI-22:199–205
58. Bernstein BS (1989) Service life of cross-linked polyethylene as high voltage cable insulation. *Polymer Eng Sci* 29:13–18
59. Struik LCE (1978) *Physical ageing in amorphous polymers and other materials*. Elsevier Press, Amsterdam
60. Boukezzi L, Boubakeur A, Lallouani M (2007) Presented at IEEE international conference on electrical insulation and dielectric phenomena (CEIDP) (Canada, 2007), p 65
61. Boukezzi L, Boubakeur A (2018) Effect of thermal aging on the electrical characteristics of XLPE for HV cables. *Trans electr electron mater* 19:344–351
62. Bulinski A, Bamji S, Densley J (1982) The effects of moisture content, frequency and temperature on the life of miniature XLPE cables. Presented at the 1982 IEEE international conference on electrical insulation, Philadelphia, PA, USA, 7–9 June 1982
63. Mecheri Y, Bouazabia S, Boubakeur A et al (2013) Effect of thermal ageing on the properties of XLPE as insulating material for HV cables. In: *International conference on electrical Insulation, IET Centre, Birmingham, UK*
64. Li W, Shi Q, Xiao W (2015) Investigation on thermal aging of HVDC XLPE. In: *Proceedings of 5th international conference on advanced design and manufacturing engineering, advances in engineering research, Atlantis Press, pp 428–432*
65. Zhang F, Xie C, Wang T et al (2019) Study on XLPE temperature-frequency aging based on combined analysis of laser induced breakdown spectroscopy and gas chromatography study on XLPE temperature-frequency aging based on combined analysis of laser induced breakdown spectroscopy and gas chromatography. *IOP Conf Ser Mater Sci Eng* 493:012003
66. Ciuprina F, Teissède R, Filippini JC (2001) Polyethylene crosslinking and water treeing. *Polymer* 42:7841–7846
67. Geng P, Song J, Tian M et al (2018) Influence of thermal aging on AC leakage current in XLPE insulation. *AIP Adv* 8:025115
68. Sugimoto M, Shimada A, Kudoh H et al (2013) Product analysis for polyethylene degradation by radiation and thermal ageing. *Radiat Phys Chem* 82:69–73
69. Kuriyama I, Hayakawa N, Nakase Y et al (1979) Effect of dose rate on degradation behavior of insulating polymer materials. *IEEE T Dielect El In* EI-14:272–277
70. Matsui T, Takano T, Takayama S et al (2002) Degradation of crosslinked polyethylene in water by gamma-irradiation. *Radiat Phys Chem* 63:193–200
71. Seguchi T, Tamura K, Shimada A et al (2012) Mechanism of antioxidant interaction on polymer oxidation by thermal and radiation ageing. *Radiat Phys Chem* 81:1747–1751
72. Burnay SG (2018) Degradation of polymeric components in nuclear power applications. educational material for engineers. In: *Energiforsk*. Available via DIALOG. <https://energiforsk.se/en/programme/polymeric-materials-in-nuclear-applications/reports/degradation-of-polymeric-components-in-nuclear-power-applications/>. Accessed 20 Mar 2020
73. Burnay SG, Dawson J (2001) Reverse temperature effect during radiation ageing of XLPE cable insulation. In: *Mallinson LG (ed) Ageing studies and lifetime extension of materials*. Springer, Boston, MA

74. Liu S, Veysey SW, Fifield LS et al (2018) Quantitative analysis of changes in antioxidant in crosslinked polyethylene (XLPE) cable insulation material exposed to heat and gamma radiation. *Polym Degrad Stabil* 156:252–258
75. Hedir A, Moudoud M (2016) Effect of ultraviolet radiations on medium and high voltage cables insulation. *Int J Eng Technol* 8:2308–2317

Chapter 9

Flame-Retardant Aspects of XLPE



Jeffrey M. Cogen, Bharat I. Chaudhary, Abhijit Ghosh-Dastidar, Yabin Sun,
and Scott H. Wasserman

1 Introduction

Crosslinked polyethylene (XLPE) represents a small subset of polyethylene (PE) for applications requiring enhancement of characteristics such as mechanical properties, thermo-mechanical performance and chemical resistance. Flame-retardant (FR) XLPE represents a subset of XLPE and is required in some applications where XLPE is to be used in and around enclosed spaces, where there could be a significant safety risk posed by the flammability of non-flame-retardant polyethylene.

Polyethylene, which includes a variety of polymers having ethylene as the majority of its repeat units, has a relatively high fuel load on account of the large number of $-CH_2-$ groups. Polyethylene thermally decomposes primarily via random scission leading to hydrocarbon monomers and oligomers, which exothermically yield carbon dioxide and water during combustion. Some polyethylene copolymers can also have participation of more complex decomposition mechanisms in parallel with random scission. To put this in perspective, enthalpy of combustion of wood fuel can give a value of up to about 20 kJ/g (under the most favorable laboratory conditions), whereas

J. M. Cogen (✉) · B. I. Chaudhary · A. Ghosh-Dastidar · S. H. Wasserman
The Dow Chemical Company, Collegeville, PA, USA
e-mail: jmcogen@dow.com

B. I. Chaudhary
e-mail: bichaudhary@dow.com

A. Ghosh-Dastidar
e-mail: ghoshda@dow.com

S. H. Wasserman
e-mail: wassersh@dow.com

Y. Sun
The Dow Chemical Company, Shanghai, China
e-mail: sysun@dow.com

the heat of combustion of polyethylene is about 40–50 kJ/g. In order to reduce the fuel load (enthalpy of combustion) and/or ease of ignition and flame spread, polyethylene is often formulated with FR additives, which interfere with one or more elements of the fire triangle needed to sustain a fire: fuel, oxygen and heat. These include various brominated or chlorinated molecules, which decompose to form HBr or HCl to break the combustion cycle; metal hydroxides, which endothermically decompose to produce water; intumescent systems typically based on phosphorus and nitrogen compounds, which decompose to form an insulating foam layer; and various FR synergists. It is not uncommon for flame-retardant grades of polyethylene to achieve enthalpy of combustion of 10 kJ/g or lower. Therefore, FR XLPE is frequently found in applications including wire and cable; building and construction; appliances; and shipboard, automotive, railroad and other transportation applications.

FR applications are driven heavily by various standards, such as the National Electrical Code (NEC) and Underwriters Laboratories (UL) in the USA. Applicable standards include fire, smoke and other property tests on either materials and/or finished articles.

There are some important industry trends pertaining to FR plastics applications, including FR XLPE. One such trend is the drive toward halogen-free flame retardants (HFFR) to reduce the amount of smoke released during combustion, since smoke is one of the leading causes of death in fires. Even in cases where halogenated flame retardants are still used, there is a drive toward use of halogenated flame retardants that are not environmentally persistent, bioaccumulative and toxic (PBT). As in many industries, there is also an increasing focus on sustainability in general.

2 Flammability of Polyethylene

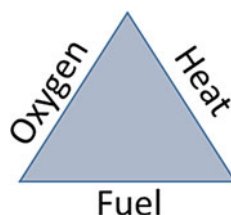
Fires are complex phenomena involving a variety of chemical and physical aspects. The progression and outcome of a fire involving a given material will vary widely depending on many variables such as ignition source, airflow, proximity of other combustible materials, dimensions of the article containing the material, dimensions of the room or enclosure and many others.

Pure polyethylene is a relatively rich fuel source. Ethylene homopolymer consists almost entirely of saturated hydrocarbon groups, primarily $-\text{CH}_2-$ units. More broadly, the term polyethylene is often taken to include polymers that have a majority of their units coming from ethylene, but may also contain one or more other units derived from polymerizable monomers such as alkenes (e.g., octene, hexene, butene, propylene), acrylates (e.g., ethyl acrylate, methyl acrylate, etc.), vinyl acetate, vinyltrimethoxysilane. The energy released upon combustion of such polymers results mainly from oxidation to form carbon dioxide and water. Although the presence of other comonomers in polyethylene can result in slight reduction of the enthalpy of combustion (Table 1), the presence of large number of C–H bonds

Table 1 Gross enthalpy of combustion calculated by the authors using the group contribution method of walters [1]

Polymer	Estimated enthalpy of combustion (kJ/g)
Polyethylene homo polymer	48
Ethylene-vinyl acetate (25 wt% vinyl acetate)	42
Ethylene-vinyl acetate (40 wt% vinyl acetate)	38
Ethylene-ethyl acrylate (25 wt% ethyl acrylate)	43

Fig. 1 The fire triangle. All three elements—oxygen, heat and fuel—must be present for combustion



in all type of polyethylene results in relatively high enthalpy of combustion. Nevertheless, the differences among various polyethylene, such as those in Table 1, can be significant in a fully formulated composition.

In general, the burning of polymers involves several discrete steps, [2] which can involve feedback loops. These steps include heating, decomposition, ignition (and smoldering), flame spread and heat release. It is generally accepted that the surface of a burning polymer is a relatively oxygen deficient environment, whereas the gas phase above the burning polymer is where oxygen is available and where exothermic oxidation of fuel vapor occurs during combustion. In order for a fire to occur, all three elements of the fire triangle must be present in sufficient quantity: fuel, oxygen and heat (Fig. 1).

Enthalpy of combustion is an important thermodynamic property and is just one parameter to consider when assessing flammability. Kinetic parameters are also important. Variations in polyethylene molecular structure can also impact the rate of combustion. For example, ethylene homopolymer primarily undergoes random scission leading to hydrocarbon monomers and oligomers, including propylene, butane, pentene, hexane and various alkanes [3]. Ethylene-vinyl acetate copolymers can release acetic acid upon pyrolysis with concomitant formation of carbon-carbon double bonds in the polymer backbone. These double bonds include conjugated polyene sequences that can undergo intermolecular reactions that lead to a protective layer that can delay the breakdown of the polymer into gaseous fuel fragments [4]. Figure 2 shows thermal gravimetric analysis results for five different types of polyethylenes, highlighting significant differences in the rate of volatile fuel release resulting from pyrolysis.

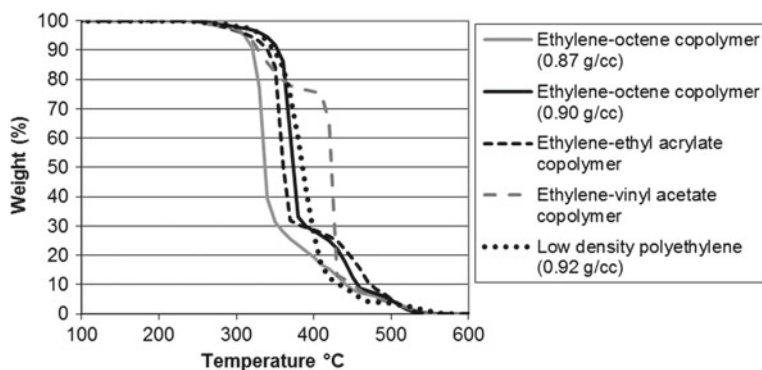


Fig. 2 Thermogravimetric analysis (TGA), conducted at 10 °C/min heating rate in air, of five different polyethylenes measured in a laboratory of The Dow Chemical Company. The ethylene-ethyl acrylate contains 18 wt% ethyl acrylate. The ethylene-vinyl acetate contains 15 wt% vinyl acetate. This test measures the rate of weight lost to the gas phase from a sample as it is heated

An interesting question arises as to whether or not crosslinking polyethylene to make XLPE results in an improvement of flame retardancy due to slower mass loss upon pyrolysis and an accompanying slower rate of burning compared to PE. However, the reality is complicated by many factors. Since XLPE for flame-retardant applications is typically highly formulated with additives, which operate via a variety of complex chemical and physical mechanisms, any potential impact of crosslinking on flame retardancy can become obscured by other variables, and flame-retardant XLPE is not universally found to have significantly different fire performance than PE.

For example, Liu et al. [5] studied HDPE/EVA/magnesium hydroxide composites and determined that irradiation crosslinking increased thermal stability as determined by TGA. Yet the flame retardancy as measured using cone calorimetry suggested that crosslinking had a detrimental effect as indicated by reduced time to peak heat release rate (PHRR) and increased PHRR, which was attributed to improved char structure in the un-crosslinked sample. Shafiq and Yasin [6] studied linear low-density polyethylene/magnesium hydroxide/sepiolite composites that were crosslinked with gamma irradiation. They found that at high doses, thermal stability of the composites was lower than an un-crosslinked composite, which they attributed to detrimental structural change in the magnesium hydroxide flame retardant caused by irradiation. Wang et al. [7] studied silane-crosslinked polyethylene with and without magnesium hydroxide as flame retardant. While the silane crosslinking increased the temperature to 10% weight loss in TGA from 445 to 475 °C, the effect on limiting oxygen index, which is a measure of flame retardancy, was minimal, increasing by only about 0.6 LOI units from about 17.5% LOI to about 18.1% LOI. This very small difference in LOI could potentially be due to presence of the silane in the crosslinked sample rather than the crosslinking itself.

Table 2 Crosslinked (XL) or thermoplastic (TP) insulated wires in two industry wire flame tests (test 1 = MS8288, test 2 = SAEJ1128) based on data from Ref. [8]

	All formulations		High LOI (group A)		Low LOI (group B)	
	Flame test 1	Flame test 2	Flame test 1	Flame test 2	Flame test 1	Flame test 2
XL better than TP	4	5	0	2	4	3
TP better than XL	2	1	2	0	0	1
XL ~equal to TP	1	1	1	1	0	0

Cogen et al. [8] measured LOI on seven different un-crosslinked HFFR formulations, which were subsequently extruded as insulation onto wire. Insulated wire that was irradiation crosslinked was compared to un-crosslinked wires in two wire and cable industry flame tests (Table 2). The compositions can be arbitrarily divided into two groups, with group A (three formulations) having LOI from 33 and 40, and group B (four formulations) having LOI from 20 to 28. Careful examination of the data shows that with the first type of wire burn test, in two out of three of the group A formulations non-crosslinked formulations outperformed crosslinked insulation, while the third group A formulation showed burn performance that was about equal in crosslinked and un-crosslinked samples. In the group B tests, all four of the crosslinked specimens outperformed the un-crosslinked specimens. With the second type of wire burn test, in one out of three of the group A formulations non-crosslinked formulations outperformed crosslinked insulation. In the group B flame test 2, three out of four of the crosslinked specimens outperformed the un-crosslinked specimens, with one un-crosslinked formulation outperforming its crosslinked counterpart. These results indicate that in this limited set of materials and tests, overall the crosslinked wires tended to slightly outperform the un-crosslinked wires, but the differences became less significant (or even disappeared) in materials with high FR performance ($LOI \geq 33$).

Overall then, what emerges from the literature is a picture that crosslinking polyethylene does not universally have a significant impact on flame-retardant performance, but may help or hinder it, depending on the specific type of formulation, finished article and test (fire conditions).

As mentioned above, for most XLPE applications requiring flame retardancy, flame-retardant additives (“flame retardants”) must be included in the polymer composition. Therefore, it is relevant to review the most commonly used flame-retardant additives for XLPE, along with their mechanisms.

3 Flame Retardants for Polyethylene

Flame retardancy of materials can be achieved by attacking one or more elements of the fire triangle (Fig. 1) by physical and chemical interactions.

3.1 Physical Interaction

Endothermic decomposition, dehydration or phase transformations of flame-retardant additives reduce the amount of heat released during combustion. For example, at elevated temperatures metal hydroxides will endothermically dehydrate to release water vapor. It is calculated that the heat absorbed in such a process is comparable to the heat required to increase the temperature of low-density polyethylene from room temperature to decomposition temperature [9]. The water vapor generated from metal hydroxides also plays a role of fuel diluent in the gas phase and decreases the possibility of ignition. In addition to water vapor, ammonia and carbon dioxide are generated from decomposition of certain flame retardants to dilute fuel. Incorporation non-combustible mineral fillers decrease the flammability of polymer by reducing the amount of combustible material. In addition, mineral fillers have high heat capacity to absorb energy generated during combustion. A protective char layer formed either from flame-retardant decomposition or carbonized polymer/charring agents at the interface between the condensed and gas phases can inhibit the exchange of heat, oxygen and fuel between the condensed and gas phases. The quality of such protective layers can significantly impact the flame-retardant performance. For example, high strength (to slow release of fuel through cracks) and foaming (low thermal conductivity) of such char layers can provide enhanced performance.

3.2 Chemical Interaction

One of the major chemical interactions is the radical scavenging in the gas phase to inhibit the free-radical combustion process. Effective radicals such as $\text{Cl}\cdot$, $\text{Br}\cdot$ and $\text{PO}\cdot$ can react with highly reactive species (such as $\text{H}\cdot$ and $\text{OH}\cdot$) to inhibit the radical chain reactions involved in combustion, in turn reducing the corresponding heat generated from these reactions, decreasing the temperature and reducing the amount fuel produced from pyrolysis.

In the condensed phase, the main chemical interactions are the decomposition of flame retardants to release inert gas and aid in formation of a char layer on the polymer. Additional charring agents (e.g., polyhydroxyl organic compounds) can enhance char layer formation when used with certain flame retardants. For example, ammonium polyphosphate (APP) will decompose to release NH_3 to foam the polymer and polyphosphoric acid to dehydrate polymer and/or polyhydroxyl compound to

form a protective char layer to slow exchange of heat, oxygen and fuel between the condensed and gas phases. In addition, some additives such as polyphosphoric acid can also form a glassy layer on the surface as a protective layer.

A combined chemical and physical interaction is the accelerated depolymerization in the presence of heat and flame retardants. This can increase the melting and flow rate of the polymer, enabling it to drip away from the flame before decomposing to fuel. A large amount of the fuel can be taken away by dripping. However, in some flame-retardant industry tests, the presence of flaming drops can result in failure. In addition, the compatibility of the dripping mechanism with other mechanism should be carefully considered when designing a flame-retardant material. For example, generally a dripping mechanism is not compatible with a protective layer mechanism.

3.3 Halogenated Flame Retardants

Various brominated and chlorinated compounds are widely used as flame retardants. For example, decabromodiphenyl oxide (DBDO) is one of the most effective brominated flame retardants due to the very high bromine content, 83.3% by weight, and the excellent match between the temperatures at which bromine is released from the flame retardants and decomposition profile of polyethylene [10]. However, due to certain environmental health and safety (EH&S) concerns, DBDO and some other brominated flame retardants are facing increasing scrutiny and de-selection. Decabromodiphenyl ethane (DBDE) has been a viable alternative to DBDO for some time but is now itself coming under increasing scrutiny. Flame-retardant suppliers continue to develop alternative brominated flame retardants.

Halogenated compounds are known to primarily operate via gas phase mechanisms involving HX (HCl or HBr) as major pyrolysis byproducts, which play critical roles as radical scavenger to terminate the reactive radicals, HO· and H· to inhibit flame propagation [11].



In addition, it is reported that the halogens in the gas phase change the density and heat capacity of the gaseous mixture of fuel and oxidants, while the presence of these additives in the formulation itself lowers the overall fuel content (by displacing some polymer in the composition).

In addition to the halogenated flame retardant itself, various synergists are important to enhance the FR performance. For example, antimony oxide is frequently used with halogenated flame retardants. Antimony oxyhalides and antimony trihalides are formed in the condensed phase by reactions at elevated temperatures and can

enhance the FR performance by multiple mechanisms. Laboratory flammability [11] tests indicate that the optimum halogen/antimony atom ratio in many polymers is about 2:1–3:1. At the ratio of 3:1, antimony trihalide is most likely to form and is generally regarded as more effective than antimony oxyhalide in the gas phase. The series of chemical reactions of antimony trihalide and active radicals were summarized by Boryniec [11]. Recently, Valeri built up a kinetic gas phase model for the antimony-halogen flame-retardant system in hydrocarbons, summarizing the possible antimony-halogen volatiles in the gas phase and the corresponding reactions with active radicals [12].

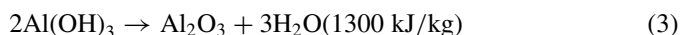
Factors that bind the halogens into the condensed phase can reduce the flame-retardant effect of such additives. For example, metal cations from color pigments and basic fillers such as calcium carbonate may compete with antimony oxide to form metal halides.

3.4 Mineral Flame Retardants

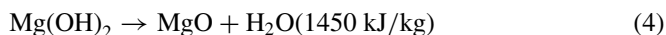
Non-combustible fillers will reduce the flammability of a polymer composition by reducing the total amount of fuel available from the polymer (condensed phase diluent). In addition, in some cases an inert metal oxide or related inorganic layer can form during combustion to limit the exchange of oxygen and fuel between the condensed and gas phases. And endothermic decomposition with release of inert gases or water vapor may occur with some mineral flame retardants.

3.5 Metal Hydroxides

Aluminum trihydroxide (ATH) decomposes around 180 to 200 °C to form alumina (Al_2O_3) with the release of water vapor [13]. The decomposition is endothermic by around 1300 kJ/kg. In addition to absorbing heat, the released water vapor dilutes the fuel and radicals in the flame, and the resulting alumina builds up a protective layer to suppress the exchange of oxygen, fuel and heat between the condensed and gas phases.



Magnesium dihydroxide (MDH) acts in a similar way to ATH but decomposes endothermically at a slightly higher temperature of about 300 to 340 °C, absorbing slightly more heat, around 1450 kJ/kg, enabling MDH to often be somewhat more efficient as a flame retardant and being suitable for higher processing temperature compared to ATH [13].



Metal hydroxides help to minimize formation of smoke during combustion because water vapor is the only volatile decomposition product. It was also reported that both ATH and MDH will suppress the smoke formation compared to calcium carbonate [14]. In practice, resistance to the formation of smoke and toxic gases is critical because almost 80% of fatalities in fires involving polymeric materials have been caused by the inhalation of smoke [15].

Usually high loadings of metal hydroxide are required to pass some of the more challenging FR test. For example, in order to pass UL 94 V0, the loading of ATH in crosslinked polyethylene is around 60% by weight, which increases the density and viscosity of the polymer melt and reduces the mechanical properties and flexibility [16].

3.6 *Hydroxyl Carbonates*

Besides the widely used ATH and MDH flame retardants, hydroxyl carbonates such as hydromagnesite/ $Mg_5(CO_3)_4(OH)_2 \cdot 4H_2O$, Dawsonite/ $NaAl(OH)_2CO_3$, UltraCarb (hydromagnesite/huntite = 60/40), synthetic magnesium carbonate hydroxide pentahydrate/ $(MgCO_3)_4 \cdot Mg(OH)_2 \cdot 5H_2O$ can be used as flame retardants in polyethylene due to suitable endothermic decomposition temperatures in the range of 220 to 400 °C [9]. In addition, some of these undergo additional decomposition steps at even higher temperatures that do not further contribute to flame retardancy beyond playing a role as inert fuel diluent (e.g. huntite). These operate through a series of decomposition steps releasing water and carbon dioxide [17, 18]. Although these are less widely used in high value applications than the more effective MDH and ATH, they offer flexibility to the formulator in balancing various properties as well as cost.

3.7 *Borates*

Zinc borates such as $2ZnO \cdot 3B_2O_3 \cdot 3.5H_2O$ are used in plastics and rubber products as effective FR synergists. These additives will endothermically decompose (503 kJ/kg) between about 290 and 450 °C to release water [19]. Furthermore B_2O_3 can form a glassy protective layer around 350 to 500 °C. This insulation layer protects the polymer by limiting the exchange of heat, oxygen and fuel between condensed and gas phases [20].

3.8 Phosphorus Containing Flame Retardants

Phosphorus and its organic and inorganic compounds are widely used as flame retardant in polymers, including red phosphorus, phosphates, phosphonates, phosphinates, phosphine oxides and phosphate esters. These involve both chemical and physical interactions in their flame-retardant mechanisms.

Phosphorus flame retardants work in both condensed and gas phases. In the condensed phase, protective layers can be formed by polyphosphoric acid. In the gas phase, phosphorus-based flame retardants can also form active radicals ($\text{PO}_2\cdot$, $\text{PO}\cdot$ and $\text{HPO}\cdot$) to scavenge $\text{H}\cdot$ and $\text{OH}\cdot$ radicals [11].

Red phosphorus is a highly combustible hazardous material, which is used in the striking surface for matches. However, when a small amount of red phosphorus is mixed with a flammable resin, the resin becomes less likely to burn. The most attractive feature of red phosphorus is the relatively low concentrations required to achieve excellent flammability results in most polymers because of its high phosphorus content compared to other phosphorus-containing flame retardants. Therefore, red phosphorus is sometimes used to meet the high requirements on flammability.

In a fire, red phosphorus will be oxidized to phosphoric acid which will dehydrate certain polymer intermediates to form a char layer to protect polymer in the condensed phase. It becomes significantly more effective in oxygen- or nitrogen-containing polymers. For example, to achieve UL-94 V0 rating, 3% red phosphorus is necessary for polyethylene terephthalate (PET) while at least 10% is required for polyethylene. However, additional charring agents, like pentaerythritol (PER), can be incorporated to enhance the char formation. It was also reported that red phosphorus can also generate volatile phosphorus radicals (P_2 , $\text{PO}\cdot$, $\text{PO}_2\cdot$, $\text{HPO}\cdot$) to scavenge $\text{H}\cdot$ and $\text{OH}\cdot$ radicals in gas phase.

Red phosphorus powder can be stabilized and encapsulated in melamine-formaldehyde (MF) resin to make it less ignitable and to suppress formation of hazardous phosphine gas. However, the red-brown color is the major disadvantage limiting its application.

Another well-developed inorganic phosphorus flame retardant is ammonium polyphosphate (APP). Various forms are available with differing molecular weight, water solubility and thermal stability. The type of APP most commonly used as a flame retardant in polymers decompose at about 240 °C to form ammonia and polyphosphoric acid. In the gas phase, the release of non-flammable ammonia helps to dilute fuel and oxygen of the air. In the condensed phase, the resultant carbonaceous char helps to shield the underlying polymer from attack by oxygen and radiant heat, thereby inhibiting the pyrolysis of the substrate. One disadvantage of APP is that it often contributes to carry over of water during polymer processing.

The main groups of organophosphorus compounds are phosphate esters, phosphonates and phosphinates shown in Fig. 3. They mainly operate in the gas phase by quenching the species such as $\text{H}\cdot$ and $\text{OH}\cdot$ radicals. The phosphorus-based radicals are reported to be five times more effective than bromine and 10 times more effective than chlorine radicals [21]. Because of the need for gas-phase activity, a number

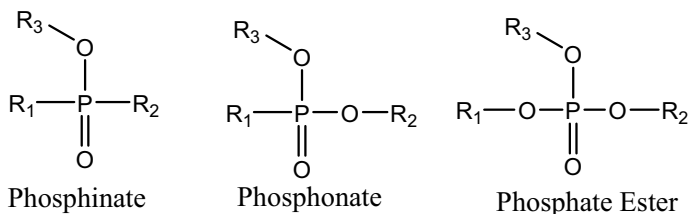


Fig. 3 Structures of some phosphorus flame retardants

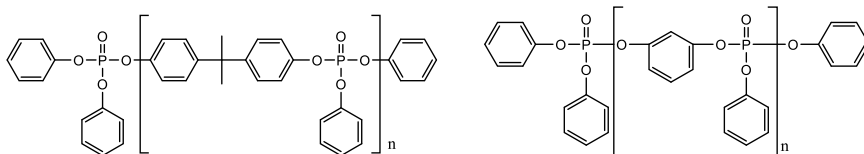


Fig. 4 Structures of BDP and RDP

of volatile phosphorus flame retardants, tributyl phosphate (TBP), triphenylphosphate (TPP) and triphenylphosphine oxide (TPPO), have been identified as possible substitutes for Br flame retardants in some formulations.

Many organic phosphorus compounds have flame-retardant properties but limited used in polymers due to high volatility. For example, TPP volatilizes before decomposition of the polymers. Therefore, oligomeric phosphates such as resorcinol bis(diphenyl phosphate) (RDP) and bisphenol A bis(diphenyl phosphate) (BDP), shown in Fig. 4, with lower volatility than TPP have been developed for the plastic industry.

3.9 Nitrogen-Based Flame Retardants

Melamine is one of the more widely used nitrogen-based flame retardants, which will vaporize or sublime at around 350 °C, which absorbs a significant amount of heat. Furthermore, decomposition of the melamine vapors will absorb additional heat. Ammonia will be released to the gas phase which is also a diluent to oxygen and combustible gases. In the condensed phase, the char layer stability is enhanced by multi-ring structures formed during self-condensation of melamine.

Melamine salts are well-developed nitrogen-based flame retardant, like melamine cyanurate (MC), melamine phosphate (MP) and melamine pyrophosphate (MPP), etc. During combustion, some melamine will be released from these melamine salts and volatilizes to gas phase, while some melamine may stay in the condensed phase. Besides melamine, acid can be released from melamine salts. For example, heating

melamine phosphate will lead to melamine polyphosphate, melamine and phosphoric acid [22]. As discussed above, such phosphorus acids can aid in char formation.

3.10 Intumescent Flame Retardants (IFRs)

Intumescent flame retardants (IFR) are most commonly composed of three major components: an acid source, a charring agent and a foaming agent [23–25]. When burning, the IFR forms a foamed char layer that serves as an effective physical barrier to limit the exchange of heat, fuel and oxygen between condensed and gas phases.

In principle, the working temperatures for each component must be carefully matched with each other. The gas must be released during the thermal decomposition of the carbonizing agent in order to trigger the expansion of the char layer. The acid has to be liberated at a temperature below the decomposition temperature of the charring agent and its dehydration should occur around the decomposition temperature of the polymer. Flame-retardant manufacturers offer such systems for use in polymers.

A representative IFR for polyolefins is composed of APP as acid source, PER as charring agent and melamine as blowing agent. However, from the application point of view, such IFR systems have seldom been used in the plastic industry due in part to the low water resistance of APP. Several alternative acid sources were developed for IFR, like melamine modified APP, piperazine pyrophosphate [26] with improved water resistance.

Some synergists have been studied in IFR for polyolefin, like zeolite, [27] zinc borates, [28] expandable graphite, [29] beta-cyclodextrin, [30] colemanite [31] and triazine polymers [32, 33]. However, one must be careful with other additives in the system, such as various inorganic particles, which can destroy the integrity of foamed char layer.

Despite the large number of flame-retardant additives reported in the literature for polyethylene and XLPE—several of which were discussed above—ATH, MDH and brominated flame retardants remain by far the most widely used flame retardants for high value applications requiring high levels of flame retardancy.

4 Key Crosslinking Methods Used in FR XPLE Applications

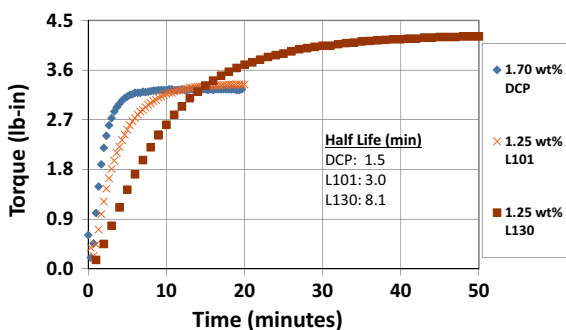
Crosslinking of polyethylene in flame retarded applications is done to impart improvements in resistance to heat, abrasion, chemicals, etc. [34–37]. The major approaches to accomplish crosslinking are through the use of peroxides, irradiation, silanes, and/or sulfur agents. The first two revolve around free-radical

chemistries, with peroxide or irradiation serving as radical initiators, and conceptually yield carbon-carbon crosslinks in the polymer; graftable polyfunctional components (sometimes referred to as coagents, cure boosters, etc.) are often used in the formulations, resulting in connections of polymer chains through other bridges as well [38–40]. Silane crosslinking is brought about by moisture in the presence of a suitable catalyst and involves hydrolysis and dehydrocondensation of alkoxy-silane groups that are attached to the polyethylene. Sulfur cure is less frequently used and occurs by a complex mechanism potentially involving both radical and ionic intermediates.

In the case of peroxide crosslinking, it is required that the initiator be stable at the temperatures used to imbibe or compound the peroxide into a polymer composition and also that it not decompose prematurely during the melt processing step(s) used in fabricating articles. For instance, when making wire and cable constructions by coating conductors with molten polymer layers comprised of such additives, little or none of the peroxide should ideally decompose during the melt extrusion process conducted at temperatures less than 140 °C. However, it needs to decompose sufficiently or fully in the subsequent step used to effect crosslinking in the continuous vulcanization tube, where the temperatures can be as high as 300 °C. Thus, a key attribute of an organic peroxide is its decomposition half-life (time required to decompose 50% of the initiator at a specified temperature), [41] or alternatively, the temperature at which a peroxide has a half-life of fixed number of hours [42]. Representative peroxide free-radical generators are dicumyl peroxide (DCP), 2,5-bis(tert-butylperoxy)-2,5-dimethylhexane (L101) and 2,5-bis(tert-butylperoxy)-2,5-dimethyl-3-hexyne (L130). The latter two decompose at comparatively higher temperatures than DCP. Also necessary to consider are the byproducts of peroxide decomposition, such as methane (from methyl radicals [39]), making it essential for the crosslinked articles to be adequately degassed in order to prevent flammability hazards.

Figure 5 shows the crosslinking at 180 °C of low-density polyethylene (of 2 dg/min melt index measured at 190 °C with 2.16 kg load) using the three different peroxides mentioned above. The measured time to 50% of maximum torque at these conditions, which is related to peroxide half-lives but may also be influenced by other

Fig. 5 Peroxide crosslinking of low density polyethylene at 180 °C in a moving die rheometer, which measures the material stiffness. Data were generated in laboratories of The Dow Chemical Company



factors, were 1.5 min, 3.0 min and 8.1 min with DCP, L101 and L130, respectively. These values are considerably greater than the half-lives measured of these peroxides in solutions. For example, the half-life of L101 in a hydrocarbon at 180 °C has been reported to be 0.9 min, [41] which is approximately one-third that observed in polyethylene (Fig. 5). This is due to cage effects in the much more viscous polymer media.

Peroxide crosslinking of polyethylene is accomplished in its molten (amorphous) state and leads to decreased crystallinity upon cooling the crosslinked material to room temperature [43, 44]. DCP is a widely used peroxide for polymer modification. The mechanism by which this peroxide functions as a crosslinking initiator has been studied in polyethylene (and hydrocarbons that serve as models for this class of polymers) [45]. Homolytic cleavage of the O-O bond in DCP occurs at elevated temperatures to yield cumyloxy radicals that abstract hydrogen from polyethylene chains, and β -scission of the cumyloxy radicals further yields methyl radicals and acetophenone. The methyl radicals are also able to abstract hydrogen from polyethylene. Hydrogen abstraction (by cumyloxy and/or methyl radicals) leads to the formation of polymer carbon-centered radicals, as well as cumyl alcohol and methane. Carbon-carbon crosslinks are formed when two polymer carbon-centered radicals react.

When selecting fire retardants for peroxide-crosslinked systems, it is necessary to avoid those that can have deleterious effects on crosslinking efficacy (or the stability of formulated compounds containing peroxides and such flame-retardants). Most of the commonly available flame retardants (and fire-retardant synergists) are generally suitable for use with peroxide crosslinking, such as ammonium polyphosphate [46], metal hydrates [47] and calcium carbonate [47]. However, differences in crosslinkability have been observed across different types, with organoclays having particularly adverse effects on peroxide crosslinking of polyethylene [47]. Carbon black is another filler that is well known to impart not just black color and ultraviolet light resistance to polymer systems, but also enhanced limiting oxygen index [48], a measure of burn performance. However, carbon blacks that are acidic in nature can lead to acid-catalyzed decomposition of peroxides [49], leading to products that are consistent with ionic decomposition [50, 51] and thus decreased free-radical initiated crosslinkability of such flame-retarded polyethylene formulations. The mechanism of acid-catalyzed decomposition of dicumyl peroxide has been well studied [45]. Furthermore, even if the fire retardants used are compatible with peroxides, it needs to be ensured that other additives in the formulation are as well. For example, it has been shown that the antioxidant bis(octadecyloxy-carbonyl) ethyl sulfide can be transformed to sulfur acids under certain conditions, that in turn lead to depletion of active peroxide [52].

One important consideration for peroxide crosslinking of PE compositions that contain flame retardants is processing temperature window. Most flame retardants operate via intended thermal decomposition mechanisms. Care must be taken to ensure that the flame retardant is stable at the temperatures required for peroxide crosslinking. Furthermore, some PE compositions with very high flame-retardant levels have very low melt flow rates, requiring high processing temperatures to

reduce viscosity, and/or slow processing speeds, which can cause premature peroxide decomposition.

Irradiation is another well-established mode of free-radical crosslinking of polyethylene [53–55] and has been shown to be effective in making flame retarded crosslinked compositions [34, 46]. Unlike peroxide crosslinking, which occurs in the molten state of the polymer, radiation crosslinking is done on finished articles in solid state, below the peak melting points of the semicrystalline polyethylene. Electron beams are applied at doses as high as 20 MRad to relatively thin polymeric layers, resulting in hydrogen abstraction from the polymer and subsequent crosslinking of largely the amorphous fraction of the polymer.

Silane crosslinking requires that the polymer have alkoxy silane functionality incorporated in it and use of suitable catalysts to induce hydrolysis of the alkoxy silane groups followed by condensation of the resulting silanols to form crosslinks (achieved through water diffusion into the polymer during cure in humid environments). Alkoxy silane groups can be introduced by copolymerizing vinylalkoxy silanes with ethylene in a high-pressure reactor, [56] to make so-called reactor ethylene silane copolymers, or grafting vinylalkoxy silanes to ethylenic polymers using peroxides as free-radical initiators. The latter ‘post-reactor’ approach leads to the alkoxy silane groups being two extra carbons removed from the polymer backbone, [57, 58] making them considerably more reactive to hydrolysis and condensation reactions. Thus, significant differences are observed between reactor ethylene-silane copolymers and silane-grafted polyethylenes in terms of shelf stabilities at ambient conditions of room temperature and humidity (in the absence of catalyst), propensities for premature crosslinking during extrusion, and rates of crosslinking after article fabrication [58]. Furthermore, silane-grafted polyethylenes are of the following two types: SIOPLAS (which involve an additional step of grafting vinylalkoxy silane to the polymer, prior to use in article fabrication) or MONOSIL type (grafting done in situ during the article manufacturing process, by single-step melt blending, reaction and extrusion of ethylenic polymer compositions containing peroxide, vinylalkoxy silane and catalyst). Additionally, the type of alkoxy silane used to make silane-functionalized ethylenic polymers influences moisture cure characteristics, with vinyltrimethoxy silane (VTMS) resulting in faster crosslinking than vinyltriethoxy silane [56].

In making moisture-curable (silane crosslinkable) compositions, any flame-retardants that are employed need to be not only compatible with the alkoxy silane functionalized ethylenic polymers, but also with the silanol condensation catalysts that are used to effect crosslinking. Any water that is present in a flame retardant can cause premature polymer crosslinking during melt processing. Typical catalysts for moisture cure are Lewis acids (such as dibutyltin dilaurate) or Brønsted acids (such as dodecylbenzene sulfonic acid). Although the latter are generally more efficient catalysts than the former (at fixed loadings), flame retardants (and flame-retardant synergists) that are of basic characteristics can neutralize the acids, making them ineffective. Examples of such flame-retardant additives are metal hydrates and zinc oxide. These issues are much more prevalent with halogen-free flame-retardant formulations, and less so with systems based on halogenated flame retardants.

Ethylenic polymers such as ethylene-propylene-diene monomer rubber (EPDM) that have adequate unsaturation can also be vulcanized through the use of sulfur [40, 59, 60]. The mechanism of crosslinking polymers with sulfur, leading to formation of sulfur bridges, has been illustrated elsewhere, [40] including in the presence of accelerators. A variety of flame retardants are suitable for use with sulfur crosslinking, including ammonium polyphosphate and aluminum trihydroxide.

5 Main Applications for FR XLPE

Technical innovation and new product and technology development are generally motivated by a specific need in the marketplace, or even by the discovery of new science that might be looking for a commercial use. However, in a competitive commercial environment, the most innovative new technologies and certainly those that have the potential to have the greatest impact in the marketplace are generally accompanied by one or more patent applications. In many cases, such patent applications are filed locally at the individual country level and then eventually filed in other countries or groups of countries around the world in which the inventors see potential value. Patents that result from such applications enable the patent owners to prevent their competitors from practicing the same technology—a distinct commercial advantage. For the above reasons, detailed patent analysis is an effective method for identifying key applications within a given field. In this section, results of such a search are summarized. State-of-the-art methods were used to search for patents related to FR XLPE and to analyze the search results to enable conclusions about the key applications of FR XLPE, to delineate details related to any geographical concentrations, temporal trends, and to identify the key leaders in this marketplace.

5.1 *Mapping the Intellectual Property (IP) Landscape for FR XLPE*

In order to adequately delineate the application spaces in which FR XLPE is found as a technical solution, the IP landscape that would certainly under-pin new technology development was assessed. As with any other strategic IP search, a broad, high-level set of search terms was initially utilized to get an initial sense of the breadth of the respective IP landscape. As an example, the following search string within the titles, abstracts and claims of the international patent art was initially utilized:

```
(flame OR fire OR ignition)AND(resist * OR retard*)AND
((XLPE OR XL – PE)OR((cross – link * OR crosslink*)AND
((poly – ethylene OR polyethylene)OR(ethylene AND(polymer OR copolymer))))))
```

The resulting set of patent documents contained nearly 10,000 patent families; in general, a patent family refers to a set of patents or patent applications that are linked up to a common priority patent application (or set of priority applications). As very broad patent searches are completed, in particular, having result sets collapsed to the level of patent families is very useful to facilitate evaluation and analysis.

Using some of the available patent search analysis tools, it became clear that the search results fell into a number of high-level categories, including crosslinked polyethylene, outer sheaths, cable materials, refractory layers, halogen-free flame retardants, halogenated flame retardants and flame retardancy.

In fact, further analysis allowed another level deeper assessment to examine the sub-topics within each of those high-level categories. The latter three categories were, as expected, focused primarily on the underlying science related to flame-retardant technologies, both halogenated and halogen-free, including melamines, red phosphorus, common inorganic minerals, and low-smoke or other coagents in flame-retardant systems such as antimony trioxide and zinc borate. As a result, those groups were not considered further as the focuses of those innovations were on the underlying FR science, and not the applications used therein.

So, focusing on the first four categories, their respective sub-topics were examined. The ‘Cable Materials’ sub-topics were repetitive with respect to those for the ‘Cable Materials’ so only the latter was considered further, along with those for ‘Crosslinked Polyethylene’ and ‘Refractory Layers’ as being inclusive of the application spaces represented by the results set. In fact, Table 3 lists a representative list of the sub-topics in the three remaining categories.

In order to gain more specific information on the application spaces for which FR XLPE would be represented in the patent literature, the three selected search

Table 3 The three key high level, application-based search result categories included these sub-topics

Crosslinked polyethylene (XLPE)	Outer sheath	Refractory layer
<ul style="list-style-type: none"> • Armor layer • Flame-Retardant sheath • Irradiation XLPE • Flame-Retardant XLPE • XLPE • Flame-Retardant polyvinylchloride • Flame retardant XLPE • Tin plated copper wire • Radiation XLPE • Tin plated copper conductor • XLPE insulation 	<ul style="list-style-type: none"> • Core insulation • Cable core • Oxygen barrier layer • XLPE insulating layer • Halogen inflaming • Flame retardant layer • Shield layer insulation • Insulating layer • Outer shield layer • Shield layer • Outer sheath 	<ul style="list-style-type: none"> • Mica tape • Fire resistant electrical cable • Fire resistant cable • Refractory layer • XLPE insulating

result categories shown in Table 3 were isolated as a new result set. Search analysis tools were then used to find trends and other application-related information from that resulting set of 4,338 patent families. The results from the analyses of both the original results set and the second, narrower results set will be discussed in the subsequent section.

5.2 Key Applications and Trends Delineated by IP Landscaping

Within the initial broad search and analysis that resulted in nearly 10,000 patent families, we sought to observe some key indicators, including filing activity over time, geographical trends, and leading companies within the field of FR XLPE. One key qualifier to consider as one discusses patenting activity over time is the fact that it generally takes 18 months after a priority patent application is filed before that application is published; as a result, searches are blind to those cases that may have been filed within the prior 18 months. In the graphics reporting results related to patent families over time, reliable data ceases at the end of 2017, given that the results are based on searches conducted in mid-2019. As an example, Fig. 6 shows the numbers of patent families filed over the prior 20 years. As shown, starting somewhat in 2008, but especially starting in 2010, there was a significant increase in the rate of patents filed in FR XLPE, continuing well into 2016. Of course, it will not be until 2020 that it can be confirmed whether the decrease from 2016 to 2017 is an anomaly or is indicative of decreased patenting activity.

Figure 7 provides an analysis of the top assignees in this technology area. It is evident that the results set is dominated by companies that manufacture wire and cable. Companies such as Sumitomo Electric Industries (headquartered in Japan), Furukawa Electric (Japan), Hitachi Cable (Japan), Fujikura (Japan), LS Cable (South Korea), and Lubao Cables (China) represent a highly Asia-centric concentration of

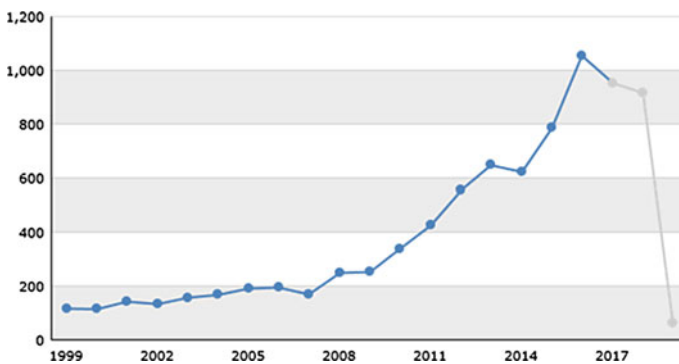


Fig. 6 Number of worldwide patent families supporting FR XLPE technology filed in last 20 years

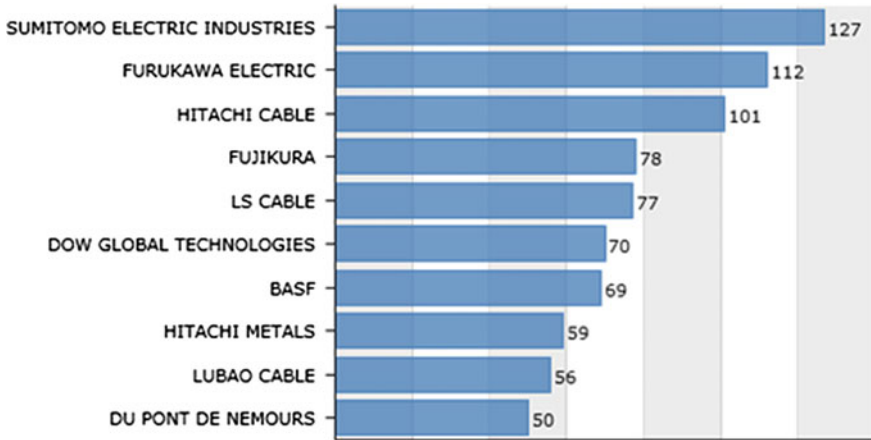


Fig. 7 Specific assignees within the broader FR XLPE search since 1999 with the most patent families

wire and cable companies, plus materials suppliers such as Dow Global Technologies (USA), BASF (Germany), Hitachi Metals (Japan) and Du Pont de Nemours (USA), all of whom have businesses supplying the wire and cable industry, as well as others.

After completing the analysis of the original result set of approximately 10,000 patent families, an analogous analysis was done on the subset of patent families that appeared to represent well the more specific areas related to applications of FR XLPE, as summarized above in Table 3. That focused result set of approximately 4300 patent families delineated some similar qualitative trends as did the larger results set, but a number of the key conclusions were even more accentuated.

Figure 8 again shows the 20-year trend in the number of distinct patent families filed within the narrower application space of this result set. As observed earlier,

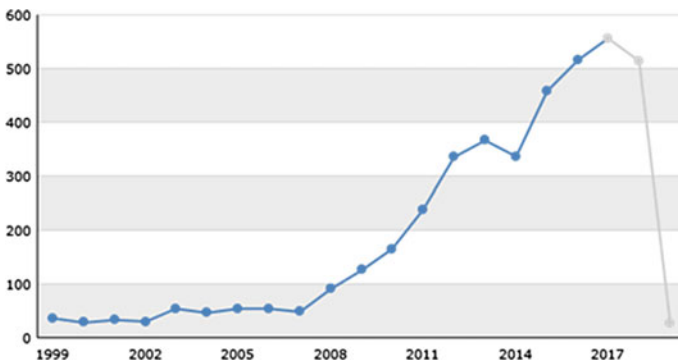


Fig. 8 Number of patent families supporting FR XLPE technology filed in last 20 years for the narrower application-specific results set

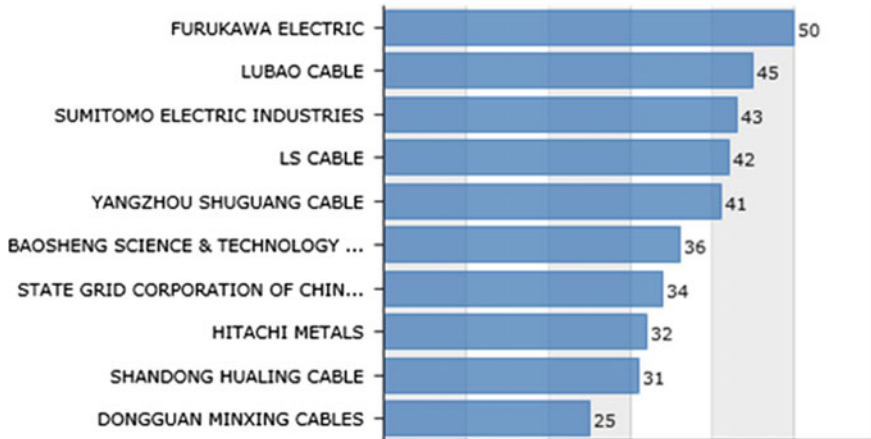


Fig. 9 Specific assignees within the application-specific FR XLPE search since 1999 with the most patent families. Specific use of FR XLPE in wire & cable applications

a significant acceleration in filing activity began in 2008, but in this case the more specific application-based categories maintained the growth in filings moving into 2017, as well (as mentioned earlier, the data after 2017 is unknown since in most cases, patent applications take 18 months to be published after filing, and therefore 2017 is the last complete year of data available for this study).

Finally, a further analysis was completed on the application-specific data set to identify those key players that represent the greatest number of patent families. Those results are summarized in Fig. 9. Once again, the results are dominated by players in the wire and cable industry, particularly those headquartered in Asia. While key players identified in the broader results set remain from Japan and South Korea—Furukawa Electric (headquartered in Japan), Sumitomo Electric Industries (Japan), LS Cable (South Korea) and Hitachi Metals (Japan)—Lubao Cable is now joined in the results set by a number of other China-based players, including Yangzhou Shuguang Cable, Baosheng Science & Technology, State Grid Corporation of China, Shandong Hualing Cable and Dongguan Minxing Cables. As might be expected, global materials suppliers, such as Dow Global Technologies (USA), BASF (Germany) and Du Pont de Nemours (USA), have fallen further down the list of assignees of more application-specific patent families as their focus would tend to be more on materials solutions as opposed to innovations related specifically to applications. In the next section, connections will be made between specific assignees and respective FR XLPE applications covered in their patent families, leading to some illustration of FR XLPE technology for wire and cable applications.

Having examined the more application-specific results set to elucidate a steady increase in patenting activity in FR XLPE since 2008, specific applications were then examined to determine that the specific application areas represented most often in the result set are:

- **Cable Core:** components and layers within the cable structure that surround and/or protect the distribution of power or data signals via metal conductors or glass fibers
- **Low Smoke:** cable constructions in sensitive installments in which human exposure to smoke during a fire scenario needs to be minimized to allow for escape; these applications are often coupled with halogen-free requirements for regulatory (human exposure) and critical equipment preservation concerns (e.g., in data centers)
- **Halogenated Flame Retardants:** cable constructions and applications for which regulatory limitations still allow halogen use, often due to a lack of suitable non-halogen solutions
- **Shield Layer:** these include those layers that are exposed to external stresses, requiring the crosslinking of the PE for toughness, and environmental concerns to protect the inner layers and components of the cable; in fire scenarios, these are the layers that are first exposed to the burn, hence the cable construction-specific FR requirement.

Collectively, FR XLPE application in wire and cable markets addresses a combination of those physical property needs dictated by the end use, as well as the FR performance dictated by their use in spaces with significant human exposure potential in a fire scenario. While crosslinked PE in general finds use in cables that need to maintain key properties in their designs (medium and high voltage power cable insulation, for example), FR XLPE finds its utility in those markets that simultaneously require FR and a need to maintain resistance to one or more chemical or environmental stresses. Good examples of those market spaces requiring FR XLPE include military, shipboard, aviation, railway and automotive use in which human exposure is an obvious concern.

For illustrative purposes, some examples of intellectual property are provided for some of those key application areas. In one example, CN102,637,473A, [61] assigned to Baosheng Science & Technology Innovation, describes a ‘Low-smoke halogen-free flame-resistant type-a stainless steel armored cable and preparation method thereof’ that comprises a core and an outer protective layer that encompasses a multi-layer core within the cable. Here, the FR XLPE-incorporated outer layer, or sheath material, is present to enable the cable to satisfy low-smoke, zero-halogen requirements while at the same time, provide ‘superior mechanical shock resistance.’ As a point of interest, the multi-layer cable sheath design includes an additional flame-retardant inner layer to further facilitate flame-retardant behavior for the cable design. JP2,005,350,578A [62] describes electrical wire with excellent properties such as colorability, resistance to external damage, water and acid, but which is also free of heavy metals and phosphorus compounds due to concerns with post-use landfilling and incineration. More specifically, the proposed invention is concerned with reduction of potentially ‘large volume of smoke or corrosive gas’ during combustion. Its solution encompasses, in addition to a crosslinked PE base, the use of silane-coated metal hydrate (often used for both flammability and smoke reduction). An example of an application in which halogenated solutions remain acceptable is given in US6,204,318B1 [63] which describes wires and insulated

tubes used in 'high-frequency current transmission, for example, in the field of high-density wiring of internal circuits in electronic appliances.' Claimed is a multi-layer cable construction including a conductor and a coating 'wherein said coating is a cross-linked flame-retardant resin composition' that includes among other ingredients, a 'halogen-containing flame retardant.' The FR XLPE composition is said to have sufficiently high tensile and elongation properties, but also able to satisfy the requirements for VW-1 [64] burn rating.

5.3 *Additional Applications*

Beyond the prevalent use of FR XLPE in wire and cable applications, the other widespread use of that materials technology appears to be in a number of foamed FR XLPE constructions. In particular, applications are seen in the following markets:

- **Aviation and Aerospace:** aircraft seating, wall insulation, seals, ducts, buoyancy aids, soft touch trim, etc.
- **Building and Construction:** flooring underlayment, sealing, thermal insulation, etc.
- **Air Conditioning and Ducting:** thermal insulation
- **Automotive:** car floor mat, seating, soft trim areas, etc.
- **Railroad:** floor and roof insulation of passenger railway carriages and buses
- **Marine:** buoyancy fillers in amphibious cars

As expected, those market spaces in which foamed FR XLPE technology is found combine the physical requirements for which foamed material and crosslinking is ideal and the FR requirements specific to human safety. Analogous to those applications discussed in the wire and cable area, these applications require physical properties that both crosslinking and foaming deliver, such as thermal insulation, comfort and light-weighting. In fact, in many cases, the crosslinking itself provides the right rheological properties in which the desired foam structure can be generated. In addition, these applications are often found in enclosed spaces and, therefore, have high potential for human exposure to the flame, and especially generated smoke during a fire scenario. For that reason, these applications tend to be governed by regulatory agencies and specific flame or smoke limits that are designed for each space.

5.4 *Key Conclusions on Applications*

Based on the analysis described in this section, it is possible to make some key observations:

- A broad search of prior intellectual property provides a set of results dominated by the application of FR XLPE to wire and cable (sheaths, barrier layers, insulations, etc.).
- Activity around FR XLPE started taking off in 2008, rising quickly year after year thru 2017 (the last year of relevant data currently available due to timing of new patent application publications).
- Beyond use in wire and cable applications, FR XLPE is most often found in foamed applications that need to deliver comfort, energy absorption or other related properties in those end uses related to human safety or enclosed spaces.

6 Types of Polyethylene Used in FR XLPE

Polyethylenes used in FR XLPE applications are generally semicrystalline polymers, ranging in crystallinity from approximately 5 wt% to about 80 wt% (Fig. 10). They are either homopolymers or copolymers, and are made by different processes. Depending on the type of reactor, polymerization catalyst (if any) and type of comonomers employed, very different polymer architectures are obtained. In the case of ethylene homopolymers, non-polar ethylene copolymers and blends of these two types, the polymer density at room temperature decreases with decreasing crystallinity (Fig. 10). For these systems, with decreasing density (i.e., crystallinity), there is a corresponding decrease in flexural modulus (Fig. 11). However, when a polar comonomer such as ethyl acrylate (EA) is copolymerized with ethylene to make ethylene-ethyl acrylate copolymer (EEA), the density increases with decreasing

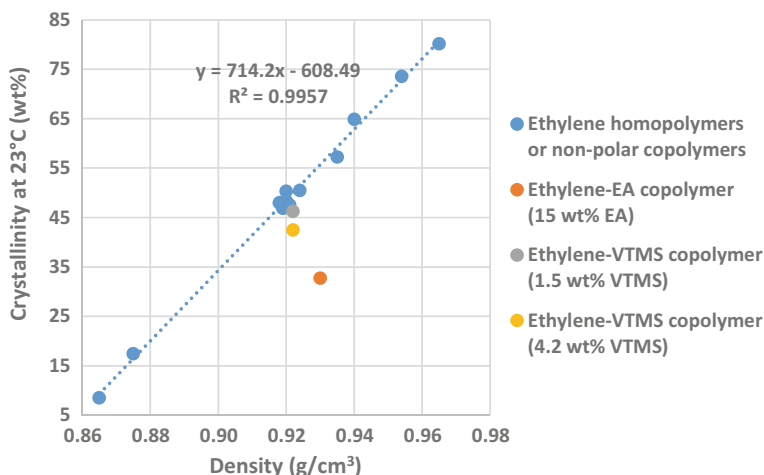


Fig. 10 Crystallinities and densities of some polyethylenes. Data were generated in laboratories of The Dow Chemical Company

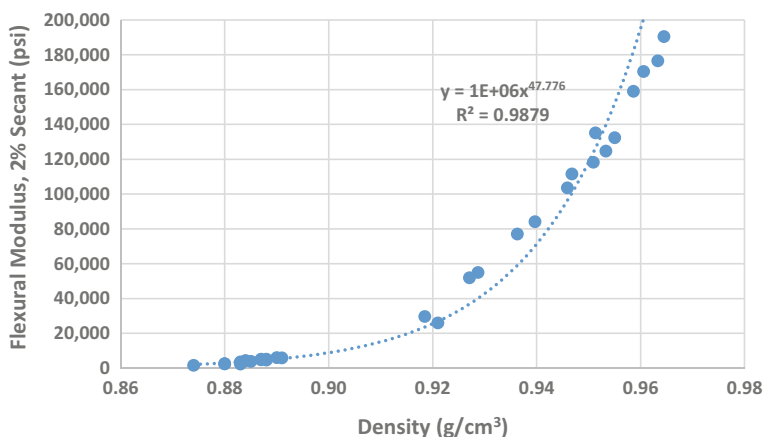


Fig. 11 Flexural modulus of ethylene homopolymers or non-polar ethylene copolymers (and blends thereof). Data were generated in laboratories of The Dow Chemical Company

crystallinity (Fig. 10). Reactor ethylene-VTMS copolymers also exhibit lower crystallinities with increasing amounts of VTMS (Fig. 10) and correspondingly faster moisture-induced crosslinking due largely to higher VTMS content [56]. Unsaturation types, distributions and extents in ethylenic polymer (as well as molecular weight characteristics and branch architectures) particularly affect crosslinkability through free-radical mechanisms, [39, 65–67] as do functional groups in reactor copolymers or grafted polymers, such as the acetate groups in ethylene-vinyl acetate copolymer (EVA) [44].

Low polymer crystallinity is generally preferable in terms of flame retardant acceptance (ability to maintain, for example, decent mechanical properties when containing high levels of flame retardants). Additionally, broad molecular weight distributions and long chain branching are often desirable attributes of polyethylene for extrusion processability, especially when flame retardants having low decomposition temperatures are present in the formulations, such as aluminum trihydroxide (which has been observed to release water at temperatures as low as 180 °C) [68]. The presence of polar moieties in copolymers such as EVA and EEA also facilitates incorporation and dispersion of flame-retardant additives, through decreased crystallinity as well as improved compatibility with fillers [69]. The polymer also serves as fuel during combustion and, as is discussed above, EVA resins exhibit considerably lower heats of combustion than polyethylene, which is a beneficial attribute for flame retardancy as it results in less thermal energy being produced [70]. Thus, the peak heat release rate measured by cone calorimetry of EVA (having 18 wt% VA content) has been shown to be about 19% lower than that of LDPE [46]. Furthermore, in compositions containing ammonium polyphosphate as flame-retardant, blends of LDPE with increasing amounts of this EVA have been observed to exhibit desirably increased limiting oxygen index [46]. The use of maleic anhydride functionalized PE as compatibilizers in halogen-free flame-retardant systems is also well recognized.

Alkoxysilane functionality (as in, for example, reactor ethylene-VTMS copolymers) is, of course, required for moisture crosslinking. Introducing additional polar functionality into such copolymers (to make, for instance, ethylene-VTMS-acrylate terpolymers) further enhances moisture permeability and compatibility with flame retardants. For example, a reactor ethylene-VTMS-butyl acrylate terpolymer (containing 17 wt% butyl acrylate) has been shown to substantially reduce moisture crosslinking times at fixed temperature and humidity, in comparison with the use of a reactor ethylene-VTMS copolymer [71]. A similar reactor ethylene-VTMS-butyl acrylate terpolymer (containing 8 wt% butyl acrylate and 2 wt% vinyltrimethoxysilane) has been used to make moisture-curable halogen-free compositions with calcium carbonate and silicone gum as the flame-retardant components for wire and cable applications [72].

Increased loadings of flame retardants in crosslinked polyethylene compositions can have deleterious effects on mechanical and other properties [73]. These issues can be mitigated through judicious choices of types of polyethylenes selected as components of the formulations, to obtain blends that provide the desired balance of properties. In the case of moisture cure systems, flame-retardant additives are generally delivered in the form of concentrates in polymer carriers (masterbatches). In this context, it has been demonstrated that increased crystallinity (i.e., modulus) of the polyethylene used as carrier resin of the flame-retardant masterbatch results in a cable construction made with moisture-cured (silane crosslinked) ethylenic polymer sheathing that exhibits significantly improved retention of dielectric strength after glancing impact [74]. In a MONOSIL silane grafting operation of flame retarded polyethylene compositions, both cable crush resistance and cable glancing impact performance are improved through the use of polyethylenes of narrower molecular weight distributions, likely because polymer toughness improves with decreasing polydispersity [58, 75].

7 Overview of Test Methods and Standards

Testing of materials or fabricated articles for their performance in a fire situation is rooted in the concept of fire safety, which is based on defining the fire safety objectives and deciding what will be the minimum level of safety that must be achieved. The objectives of fire safety vary by the structures and establishments that they intend to protect. Depending on the type and occupancy levels, sometimes they are designed toward protecting the property and in other situations, especially for high-occupancy establishments, they emphasize more on product features that will allow greater flexibility for evacuation of the occupants in a fire.

Testing methods are designed to verify whether the fire safety objectives will be met with the product used under a specified fire condition. The tests are typically carried out in the laboratory or pilot scale. Size and shape of the specimens are important, and so are the orientation of the specimens in a fire test. For most samples, usually horizontal or vertical orientations are specified. The type and intensity of the

ignition sources are also important. For example, matches and various kind of gas burners, such as small flame burners (Bunsen burners) are used. Methane, propane or other flammable gases can be specified as the fuel for these burners.

In most geographies, the prevalent fire safety standards that are followed have been developed and issued by the IEC (International Electrochemical Commission) or the ISO (International Organization of Standardization) technical committees. In the USA, International Code Council (ICC) and National Fire Protection Association (NFPA) are two organizations that have been responsible for developing many of the key fire safety standards. Fire test standards on the other hand have been primarily developed by the American Society of Testing and Materials (ASTM), NFPA and Underwriters Laboratories (UL) [76]. The discussion that ensues in this section is by no means a comprehensive account of all the tests and standards, but is an attempt to introduce readers to some key representative examples in both fire performance testing and the standards associated with them, where applicable.

An easy and basic test for flame-retardant properties of polymers is the test for limiting oxygen index, or LOI. This test is designed to determine the critical oxygen index of a sample by measuring the minimum volume concentration of oxygen in a flowing stream of oxygen and nitrogen required to sustain continuous burning of that sample. The test follows the standard ASTM D2863 in the United States, or the international standard, ISO 4589. A typical laboratory set up for LOI is shown in Fig. 12.

While limiting oxygen index does not always correlate with a flame-retardant compound's performance in the field, it is a useful tool for laboratory screening of multiple formulation options. Typical LOI value for a pure Polyethylene sample is between 17 and 18, whereas polyethylene compounded with halogenated flame-retardants exhibits an LOI value of 24–30. PE or ethylene copolymers such as EVA or EEA, when formulated with flame-retardant mineral fillers, such as aluminum

Fig. 12 Laboratory set up of the test for limiting oxygen index (LOI); photo from a laboratory of the dow chemical company



trihydroxide or magnesium hydroxide, show a wide range of LOI values, between 29 and 48. Higher loading of flame retardant in the compound leads to a higher LOI value. It is often difficult to measure a flame-retardant additive's sole contribution to increasing the LOI number for a compound since higher loading of the additive also reduces the amount of the polymer in the formulation, and hence reduces the total fuel load. Therefore, a careful consideration of the dilution effect must be made before drawing any conclusion on the flame-retardancy efficacy of the additive only from the LOI data.

One of the more important fundamental flame-retardancy tests is cone calorimetry. Although a detailed discussion is beyond the scope of this text, it is important to mention. In cone calorimetry, [77] a specimen is subjected to a radiant heater that delivers a specified heat flux to the sample surface, with a spark (ignition) source located above the sample. Gases liberated from the specimen are swept through the calorimeter, enabling determination of the energy release as a function of time via oxygen consumption calorimetry. In a typical test, after some time under the radiant heater, decomposition of the specimen releases sufficient fuel into the vapor phase to cause ignition of the sample by the spark source. The heating continues and the test is monitored until the sample extinguishes as a result of insufficient fuel generation to maintain combustion. A large amount of useful data are generated, typically including time to ignition, peak heat release rate, time to peak heat release rate, flameout time, total heat released. In addition, various parameters related to smoke and carbon monoxide levels during combustion are obtained. Because the test specimen sits on a load cell, mass loss data are also available.

With the global market shifting to more and more halogen-free flame-retardant formulations, the tests such as smoke density, acid gas generation and toxicity have gained acceptance into the specifications for the commercial flame-retardant polymeric compounds. ASTM E662 is the standard for smoke density test that covers determination of the specific optical density of smoke generated by solid materials and assemblies mounted in the vertical position. Measurement is made of the attenuation of a light beam by smoke produced and confined in a closed chamber due to non-flaming pyrolytic decomposition and/or in the flaming or combustion mode. Results are expressed in terms of specific optical density, which correlates with the concentration of smoke produced by the sample under testing.

Acid gas test is covered by the international standard IEC- 60754 and measures the acidity of gases evolved during the combustion of electric cable materials by measuring the pH & conductivity of a solution of the evolved gases.

As discussed in other sections, flame-retardant crosslinked polyethylene foams also find significant use in construction, trains and in automotive applications. As discussed in detail above, patent searching revealed that wire and cable appears to be the largest application for FR XLPE. The following section discuss some of the commonly used standards for crosslinked foams in non-wire and cable applications as well as for solid (non-foam) insulations for wires and cables.

Pipe insulation is one end use for foamed FR XLPE, which if installed in Germany, is required to meet the country specific Din 4102 B1/B2 fire standard [78]. In the B2 test, the specimen is suspended vertically and a 20 mm high flame is applied for

15 s to both the foam surface and edge. The test for flaming droplets is conducted by placing a piece of filter paper under each specimen. A B2 classification is attained if the tip of the flame fails to reach a reference line marked on the sample within 20 s after the application of the flame. For a B1 classification, the test configuration is different as well as the passing criteria. The smoke gas temperature is measured for this test, and it is required that the mean smoke gas temperature is below 200 °C.

As FR XLPE foam is used in large quantities in the automotive industry, the standard fire test they need to pass for this application in USA is FMVSS302 (Federal Motor Vehicle Safety Standard 302). FMSVSS302 is one of the least stringent fire tests and is relatively easy to comply with. The rationale behind such low fire retardancy requirement is that the reason for using flame-retardant materials in a car is primarily to allow the occupants sufficient time to exit the car in the event of a fire. The '100 mm/min' burn rate is considered adequate for most automotive applications that are not placed near the engine or high output electrical equipment.

UL-44 [79] standard issued by Underwriters laboratories based in USA specifies the requirements for single-conductor and multiple-conductor thermoset insulated wires and cables rated 600–5000 V for use in accordance with the guidelines set by the Canadian, Mexican, and National Electric Code (NEC), NFPA-70 in the USA. The standard covers many types of thermoset compounds, such as crosslinked polyethylene, crosslinked polyvinyl chloride or crosslinked ethylene-vinyl acetate or blends thereof. It also includes thermoset insulations made with chlorosulfonated polyethylene, chlorinated polyethylene and ethylene-propylene rubber. The specifications not only require that the insulated wires pass the flame resistance tests, but also stipulate that they pass a host of mechanical and electrical tests. For example, passing the hot creep test indicates that the insulation is sufficiently crosslinked to have the necessary thermo-mechanical strength during use. Long-term wet insulation resistance test conducted in high temperature (75 °C or 90 °C) water bath ensures integrity of insulation is maintained over its long life in a moist environment. Minimum values of tensile strength and tensile elongation of the insulation are needed and their retention to an acceptable level after heat-aging is also important. Furthermore, the wires need to exhibit abuse resistant properties such as glancing impact and crush resistance. The scientists who develop such FR XLPE compounds therefore have a challenging task of balancing all these properties, especially the mechanical ones which are adversely affected by increasing loading of flame-retardant additives.

All the test methods including the flame-retardant tests that are specified in UL-44 standard are described in detail in UL-2556 [80]. For crosslinked polyethylene single-layer insulation (XHHW, or crosslinked high heat), a minimum of horizontal burn rating (FT2/FH) is required. For uses in specific locations and applications, vertical burn rating may also be required, which is more difficult to pass and is typically met by enhanced level of flame-retardant additives. As the name suggests, horizontal burn test (FT2) is a method designed to determine the resistance of a wire or cable to the horizontal propagation of flame, and it also requires resistance to formation of flaming droplets or particles. Passing FT2 is required for all XHHW-2 type wires including wires with optional VW-1 (vertical burn) markings. Both the horizontal and vertical burn tests are conducted in an enclosed chamber where typically three-wire

samples, with specified length (250 mm) are secured horizontally to the specimen supports. The test flame from a Bunsen burner is adjusted to 125 ± 10 mm (5.0 ± 0.4 in), with an inner blue cone 40 ± 2 mm (1.5 ± 0.1 in). Cotton batting is placed below the specimen at the bottom of the draft-free chamber. The burner is positioned to impinge upon the specimens at an angle of 20° from vertical and withdrawn after 30 s. The specimens are allowed to burn until they self-extinguish. The length of damage to the specimen is measured and recorded. Damage is defined as charring, burning or melting. Failure of a horizontal burn test can occur if the damage to the wire exceeds 4 in (100 mm) or if the cotton is ignited. For the vertical burn test (FV-2), the wires are suspended vertically and unlike the horizontal test, each specimen is subjected to five, 15 s application of flame. The interval between flame applications is 15 s and the interval is maintained for all applications where the specimen self-extinguishes prior to the elapse of the 15 s. For samples burning longer than 15 s but shorter than 60 s, the next application of flame is done when the sample self-extinguishes. In order for a sample to pass the VW-1 burn test, all of the following criteria must be met:

- Less than 25% of the Kraft paper indicator is burned.
- The specimen does not burn longer than 60 s after any of the 5 applications of flame.
- The cotton batting is not ignited by either flaming or glowing particles or flaming drops.

8 Trends

The predominant trend in the flame-retardant polymeric systems has been a move away from using halogenated flame retardants to the use of more sustainable and environmentally friendly halogen-free additives. Not all regions of the globe have adopted halogen-free alternatives with the same speed, and the US market has lagged behind Europe and China in this respect. The trend toward HFFR has resulted in replacement of polyvinyl chloride in many applications, including some in wire and cable, with halogen-free flame-retardant systems where base resin is polyethylene or ethylene copolymers. For applications where halogenated FR additive has been traditionally used with XLPE, there is also increasing demand to switch to a halogen-free solutions. However, the movement away from halogenated systems has been hampered by lack of available HFFR solutions that can deliver on the hard-to-meet flexibility, cold temperature, processability and electrical property targets (in the case of cable insulation) for the intended applications. For wire and cable, using inorganic mineral additives with moisture cure crosslinking technology has proven to be challenging since the hygroscopic nature of these additives results in premature crosslinking during the fabrication step. The mineral fillers also adversely affect the mechanical and long-term wet insulation resistance properties (UL-44) of the cable. One way to overcome the problem of using inorganic fillers with moisture

crosslinking systems is through irradiation or peroxide aided crosslinking of the article that is carried out in the post-fabrication step.

In Europe, the absence of the long-term wet insulation resistance (wet IR) requirement for wire and cable has made the move away from halogenated insulation easier. In USA, the formulators have been able to develop and introduce a moisture-crosslinkable halogen-free solution that meets the UL-44 horizontal burn requirement, taking advantage of the relatively lower amount of mineral fillers needed to achieve that flame-retardancy requirement, while passing the wet IR and making wire insulation that is free of defects from premature moisture crosslinking (scorch) [81, 82]. More recently, halogen-free products have also been introduced for photovoltaic wires in the Americas with moisture cure as the crosslinking technology.

The halogenated flame-retardant market is also experiencing ongoing changes due to evolving regulations. A decade ago, the most commonly used brominated flame-retardant additive, decabromodiphenyl ether, was deemed to be not ROHS (Restriction of Hazardous Substance, EU) compliant, and was replaced by a different chemical decabromodiphenyl ethane. However, the new chemical has also come under increasing attention from regulators for its long-term impact in the environment, or PBT (persistence, bioaccumulative, toxic) properties, and it is anticipated that in few years, import or use of this chemical will be banned in Canada. Work is underway by the compound suppliers to find a suitable alternative.

Another important recent trend is harmonization in the EU, with introduction of the Construction Product Regulation (CPR) by the European Union Directive 305/2011. The regulations are intended to harmonize the mechanical resistance and stability of products in buildings across Europe and include fire safety standards. The scope of the regulations cover all products used in the permanent structure of a building such as doors, windows, building insulation, and wires and cables. The cables are classified from Aca to Fca, where Aca classification requires the most stringent fire safety performance. There are additional criteria around smoke production, flaming droplets and smoke acidity for the cables classified in the B to D classes. All the cable used in the buildings are expected to have CPR ratings. The move to CPR has ushered in a flurry of activities in fire testing of cables as well as new innovations from the polymer formulation compounders and cable makers with the aim of achieving higher classes with their products to gain a competitive edge.

9 Summary

Polyethylene is crosslinked for use in a variety of applications to improved various properties including thermo-mechanical resistance and chemical resistance. When crosslinked polyethylene is to be utilized within enclosed spaces, such as buildings and cars, fire safety performance is often required.

Polyethylene, which includes a variety of copolymers that are based on ethylene as a majority monomer, has a relatively high fuel load (enthalpy of combustion) and must be formulated with flame retardants to pass the fire safety requirements for many applications. The flame-retardant additives operate by interfering with one or more elements of the fire triangle—oxygen, heat, and fuel—all three of which must be present to sustain a fire. Crosslinking sometimes slightly improves the fire performance of PE compositions, though there are also situations where it can decrease the performance, and overall, crosslinking is not a significant means for impacting flame retardancy. The most prevalent flame retardants for PE include brominated or chlorinated molecules, metal hydrates and a variety of phosphorus and/or nitrogen-containing organic molecules.

Methods for crosslinking PE for FR applications are generally the same as those used for un-crosslinked PE, including peroxide crosslinking, silane-based moisture crosslinking, irradiation crosslinking and sulfur crosslinking. However, careful consideration must be made with respect to chemical compatibility between flame retardants and crosslinking additives as well as process compatibility, such as stability of flame retardants and crosslinking additives at the required processing and crosslinking temperatures.

Based on detailed patent analysis, wire and cable is the largest application area for FR XLPE, with significant usage also in building and construction, appliances, shipboard, automotive, railroad and other transportation applications.

Many type of polyethylene are available. The type of polyethylene selected for a composition can have a large impact on the resulting properties, due to factors including enthalpy of combustion, decomposition mechanism, crystallinity, polarity, mechanical and electrical properties.

FR applications are driven heavily by various standards, such as the National Electrical Code (NEC) and Underwriters Laboratories (UL) in the USA. Applicable standards include fire, smoke and other property tests on either materials and/or finished articles.

There are some important industry trends pertaining to FR plastics applications, including FR XLPE. One such trend is the drive toward halogen-free flame retardants (HFFR) to reduce the amount of smoke released during combustion, since smoke is one of the leading causes of death in fires. Even in cases where halogenated flame retardants are still used, there is a drive toward use of halogenated flame retardants that are not environmentally persistent, bioaccumulative and toxic (PBT). As in many industries, there is also an increasing focus on sustainability in general.

References

1. Walters R (2002) Molar group contributions to the heat of combustion. *Fire Mater* 26:131–139
2. Troitzsch J (2004) *Plastics flammability handbook: principles, regulations, testing, and approval*. Carl Hanser Verlag GmbH & Co, KG
3. Madorsky S, Strauss S (1954) Thermal degradation of polymers as a function of molecular structure. *J Res Natl Bur Stand (US)* 53:361–370

4. Hull T, Price D, Liu Y, Wills C, Brady J (2003) An investigation into the decomposition and burning behaviour of ethylene-vinyl acetate copolymer nanocomposite materials. *Polym Degrad Stab* 82(2):365–371 and references cited therein
5. Liu H, Fang Z, Peng M, Shen L, Wang Y (2009) The effects of irradiation cross-linking on the thermal degradation and flame-retardant properties of the HDPE/EVA/magnesium hydroxide composites. *Radiat Phys Chem* 78:922–926
6. Shafiq M, Yasin T (2012) Effect of gamma irradiation on linear low density polyethylene/magnesium hydroxide/sepiolite composite. *Radiat Phys Chem* 81:52–56
7. Wang Z, Hu Y, Gui Z, Zong R (2003) Halogen-free flame retardation and silane crosslinking of polyethylenes. *Polym Testing* 22:533–538
8. Cogen J, Lin T, Lyon R (2009) Correlations between pyrolysis combustion flow calorimetry and conventional flammability tests with halogen free flame retardant polyolefin compounds. *Fire Mater* 33:33–50
9. Hull T, Witkowski A, Hollingbery L (2011) Fire retardant action of mineral fillers. *Polym Degrad Stab* 96(8):1462–1469
10. Bocchini S, Camino G (2010) Halogen-containing flame retardants, in Grand A, Wilkie C. *Fire Retardancy of Polymeric Materials*, United States, CRC Press p 76
11. Boryniec S (2001) Polymer combustion processes. 3. flame retardants for polymeric materials. *Prog Rubber Plast Technol* 17(2):127–148
12. Babushok V, Deglmann P, Krämer R, Linteris G (2017) Influence of antimony-halogen additives on flame propagation. *Combust Sci Technol* 189(2):290–311
13. Troitzsch J *Plastics (2004) Flammability Handbook*, Hanser Gardener Publications, Cincinnati pp 145–146
14. Hornsby P, Watson C (1989) Mechanism of smoke suppression and fire retardancy in polymers containing magnesium hydroxide filler. *Plast Rub Proc Appl* 11:45–51
15. Green J (1996) Mechanisms for flame retardancy and smoke suppression—a review. *Flame Retardants-101: Basic Dynamics*, 1996 –Spring Conference, FRCA, Baltimore, 13–30
16. Weil E, Levchik S (2008) Flame retardants in commercial use or development for polyolefins. *J Fire Sci* 26:5–43
17. Hollingbery L, Hull T (2010) The fire retardant behaviour of huntite and hydromagnesite—a review. *Polym Degrad Stab* 95:2213–2225
18. Hollingbery L, Hull T (2012) The thermal decomposition of natural mixtures of huntite and hydromagnesite. *Thermochim Acta* 528:52–54
19. Adewale K (2016) *Thermoplastic Additives: Flame Retardants* in Olabisi O, Adewale K. *Handbook of Thermoplastic*, Taylor & Francis Group, Boca Raton, FL p 889
20. Laoutid F, Bonnaud L, Alexandre M, Lopez-Cuesta J-M, Dubois P (2009) New prospects in flame retardant polymer materials: from fundamentals to nanocomposites. *Mater Sci Eng R: Reports* 63(3):100–125
21. Babushok V, Tsang W (2000) *Combust Flame* 124:488
22. Levchik SV, Costa L, Camino G (1996) *Polym Degrad Stab* 43:43
23. Bourbigot S, le Bras M, Duquesne S, Rochery M (2004) Recent advances for intumescent polymers. *Macromol Mater Eng* 289(6):499–511
24. Bourbigot S, Bras ML, Delobel R (1993) Carbonization mechanisms resulting from intumescence association with the ammonium polyphosphate-pentaerythritol fire retardant system. *Carbon* 31(8):1219–1230
25. Camino G, Costa L, di Cortemiglia MPL (1991) Overview of fire retardant mechanisms. *Polym Degrad Stab* 33(2):131–154
26. United States patent 9,056,973
27. Bowbigot S, Le Bras M, Delobel R, Breant P, Tremillon J-M (1996) 4A zeolite synergistic agent in new flame retardant intumescent formulations of polyethylenic polymers—study of the effect of the constituent monomers. *Polym Degrad Stab* 54:275–287
28. Feng C, Zhang Y, Liang D, Liu S, Chi Z, Jiarui X (2015) Influence of zinc borate on the flame retardancy and thermal stability of intumescent flame retardant polypropylene composites. *J Anal Appl Pyrol* 115:224–232

29. Xie R, Qu B (2001) Expandable graphite systems for halogen-free flame-retarding of polyolefins. I. Flammability characterization and synergistic effect, *J Appl Polym Sci* 80:1181–1189
30. Michel Le Bras, etc (1997) *Polymer Degradation and stability* 56:11–21
31. Atikler U, Demir H, Tokath F, Tihminliog F, Balko'se D, Ulku S (2006) Optimization of the effect of colemanite as a new synergistic agent in an intumescent system, *Polym Degrad Stab* 91:1563–1570
32. WO2009016129
33. US20090281215
34. Jia S, Zhang Z, Wang Z, Zhang X, Du Z (2005) A study of γ -radiation-crosslinked HDPE/EPDM composites as flame retardants. *Polym Int* 54(2):320–326
35. Sener AA, Demirhan E (2008) The investigation of using magnesium hydroxide as a flame retardant in the cable insulation material by crosslinked polyethylene. *Mater Des* 29(7):1376–1379
36. Biggs JW, Maringer MF (1984) Flame retardant crosslinked polyolefin insulation material. US Patent 4,477,523
37. Tamboli SM, Mhaske ST, Kale DD (2004) Crosslinked polyethylene. *Indian J Chem Technol* 11(6):853–864
38. Chaudhary BI, Chopin LJ, Klier J (2007) Nitroxyls for scorch suppression, cure control, and functionalization in free-radical crosslinking of polyethylene. *Polym Eng Sci* 47(1):50–61
39. Chaudhary BI, Peterson TH, Wasserman E, Costeux S, Klier J, Pasztor AJ Jr (2010) Thermoreversible crosslinking of polyethylene enabled by free radical initiated functionalization with urethane nitroxyls. *Polymer* 51(1):153–163
40. Manaila E, Stelescu MD, Craciun G (2012) Aspects Regarding Radiation Crosslinking of Elastomers, *Advanced Elastomers - Technology, Properties and Applications*, Anna Boczkowska, IntechOpen, DOI:10.5772/47747
41. Pesetskii SS, Jurkowski B, Krivoguz YM, Kelar K (2001) Free-radical grafting of itaconic acid onto LDPE by reactive extrusion: I effect of initiator solubility. *Polymer* 42(2):469–475
42. Akiba M, Hashim AS (1997) Vulcanization and Crosslinking in elastomers. *Prog Polym Sci* 22(3):475–521
43. Liu SQ, Gong WG, Zheng BC (2014) The effect of peroxide cross-linking on the properties of low-density polyethylene. *J Macromol Sci Part B* 53(1):67–77
44. Reyes-Labarta JA, Olaya MM, Marcilla A (2006) DSC and TGA study of the transitions involved in the thermal treatment of binary mixtures of PE and EVA copolymer with a crosslinking agent. *Polymer* 47(24):8194–8202
45. Conley ML et al (2016) Mechanism of acid-catalyzed decomposition of dicumyl peroxide in dodecane: intermediacy of cumene hydroperoxide. *Ind Eng Chem Res* 55(20):5865–5873
46. Shukri TM, Mosnáček J, Basfar AA, Bahattab MA, Noireaux P, Courdeuse A (2008) Flammability of blends of low-density polyethylene and ethylene vinyl acetate crosslinked by both dicumyl peroxide and ionizing radiation for wire and cable applications. *J Appl Polym Sci* 109(1):167–173
47. Kudla S (2009) Assessment of the influence of mineral fillers on polyethylene crosslinking process in the presence of peroxide by rheometric method. *Polimery* 54(7–8):577–580
48. Ramesan MT (2004) The effects of filler content on cure and mechanical properties of dichlorocarbene modified styrene butadiene rubber/carbon black composites. *J Polym Res* 11(4):333–340
49. Dannenberg EM, Jordan ME, Cole HM (1958) Peroxide crosslinked carbon black polyethylene compositions. *J Polym Sci* 31(122):127–153
50. Kharasch MS, Fono A, Nudenberg W (1950) The chemistry of hydroperoxides I. The Acid-Catalyzed Decomposition of α,α -Dimethylbenzyl (α -Cumyl) hydroperoxide. *J Org Chem* 15(4):748–752
51. Robinson AE, Marra JV, Amberg LO (1962) Ethylene-propylene rubber vulcanization with aralkyl peroxide and coagents. *Ind Eng Chem Product Res Dev* 1(2):78–82
52. Sarnghadhan SC et al (2019) Interactions of Bis(1-methyl-1-phenylethyl) peroxide with the secondary antioxidant Bis(octadecyloxycarbonylethyl) sulfide: mechanistic studies conducted in dodecane as a model system for polyethylene. *Ind Eng Chem Res* 58(31):14569–14578

53. Pearson RW (1957) Mechanism of the radiation crosslinking of polyethylene. *J Polym Sci* 25(109):189–200
54. Manas D et al (2018) The effect of irradiation on mechanical and thermal properties of selected types of polymers. *Polymers* 10(2):158–179
55. Przybytniak G (2017) Crosslinking of polymers in radiation processing. In: *Applications of Ionizing radiation in materials processing*, 2nd Ed., Chapter 11, pp 249–267
56. Ishino I, Hikita M, Mizutani T, Ieda M (1991) Molecular structure and electric breakdown of ethylene/silane copolymers. *Jpn J Appl Phys* 30(4):720–726
57. Dias DT et al (2003) Study of cross-linking process in grafted polyethylene and ethylene based copolymer using a phase resolved photoacoustic method. *Rev Sci Instrum* 74(1):325–327
58. Chaudhary BI et al (2019) Effect of silane functionalized polyethylene structure on properties of moisture-crosslinked compositions and cable constructions. In: *Society of plastics engineers (SPE) ANTEC conference proceedings*, Mar 18–21, Detroit, Michigan
59. Zirnstein B, Schulze D, Schartel B (2019) Mechanical and fire properties of multicomponent flame retardant EPDM rubbers using aluminum trihydroxide, ammonium polyphosphate, and polyaniline. *Materials* 12(12). <https://doi.org/10.3390/ma12121932>
60. Wu W, Tian L (2012) Preparation of EPDM flame-resistant cable materials. *Appl Mech Mater* 151:240–244
61. Yang Z et al (2012) Baosheng Sci & Tech Innovation, assignee. Low-smoke halogen-free flame-resistant type-a stainless steel armored cable and preparation method thereof. CN publication 102,637,473A. 15 Aug 2012
62. Masami N (2005) Furukawa electric, assignee. In: *Flame-retardant resin composition and insulated electric wire*. JP publication 2,005,350,578A. 22 Dec 22 2005
63. Hiroshi H et al (2001) Sumitomo electric industries, assignee. In: *Insulated wire comprising a flame-retardant polyolefinic resin composition*. US patent 6,204,318 B1. 20 Mar 2001
64. Babrauskas V et al (1991) Fire performance of wire and cable: reaction-to-fire tests—a critical review of the existing methods and of new concepts. In: *NIST technical note 1291*, United States department of commerce, Washington, DC, p 17
65. Smedberg A, Hjertberg T, Gustafsson B (1997) Crosslinking reactions in an unsaturated low density polyethylene. *Polymer* 38(16):4127–4138
66. Smedberg A, Hjertberg T, Gustafsson B (2003) Characterization of an unsaturated low-density polyethylene. *J Polym Sci Part A* 41(19):2974–2984
67. Bremner T, Rudin A, Haridoss S (1992) Effects of polyethylene molecular structure on peroxide crosslinking of low density polyethylene. *Polym Eng Sci* 32(14):939–943
68. Sabet M, Hassan A, Wahit MU, Ratnam CT (2009) thermal characterization of alumina trihydrate (ATH) and flammability studies of ATH filled low density polyethylene. *Journal of Industrial Technology* 18(1):83–93
69. Basfar AA, Mosnáček J, Shukri TM, Bahattab MA, Noireaux P, Courdreuse A (2008) Mechanical and thermal properties of blends of low-density polyethylene and ethylene vinyl acetate crosslinked by both dicumyl peroxide and ionizing radiation for wire and cable applications. *J Appl Polym Sci* 107(1):642–649
70. Lyon RE, Janssens ML (2005) Polymer flammability. Report DOT/FAA/AR-05/14, office of aviation research, Washington, D.C. 20591, national technical information service (NTIS), Springfield, Virginia 22161
71. Sultan BA, Hampton N, Arora A, Mattila A (2002) A review of fifteen years development in moisture curable copolymers and a future outlook. Presented at *Cablewire in Mumbai*
72. Andreasson U, Uematsu T, Sultan BA, Anker M, Prieto O (2016) Flame retardant polymer composition. US Patent 9,249,288 B2
73. Azizi H, Barzin J, Morshedian J (2007) Silane crosslinking of polyethylene: the effects of EVA, ATH and Sb₂O₃ on properties of the production in continuous grafting of LDPE. *eXPRESS Polym Lett* 1(6):378–384
74. Dreux P, Tomer V, Mundra MK, Chaudhary BI, Ghosh-Dastidar A, Patel RM, Sehanobish K (2018) Flame-Retardant, moisture-cured wire and cable constructions with improved glancing impact performance. Patent Application WO2018160846A1

75. Chaudhary BI, Talreja M, Zhang Y, Bawiskar S, Dreux PC, Mundra MK, Ghosh-Dastidar A, Patel RM, Sehanobish K, Heah CY, Leong KOH (2019) Moisture-cured wire and cable constructions. Patent application WO2019005439A1
76. Hirschler MM (2010) Regulations, codes, and standards relevant to fire issues in the United States. In Wilkie CA, Morgan AB (eds) Fire retardancy of polymeric materials, 2nd edn. CRC Press
77. Babrauskas V (2016) The cone calorimeter. In: Hurley M et al (eds) SFPE handbook of fire protection engineering. Springer, New York, NY
78. DIN EN ISO 1402: rubber and plastics hoses and hose assemblies—hydrostatic testing (ISO 1402:2009)
79. UL-44: Thermoset-insulated wires and cables, underwriters laboratories
80. UL-2556: Wire and cable test methods, underwriters laboratories
81. Lindsay, D (2018) Technology for high productivity moisture cure crosslinked low voltage cables. In: Conference proceedings, polymers in cables, PA
82. Marconi AP (2018) Innovative low smoke zero halogen compound technology for control and instrumentation cable. In: Conference proceedings, polymers in cables, PA

Chapter 10

Structural Design and Performance of XLPE for Cable Insulation



Timothy J. Person, Saurav S. Sengupta, and Paul J. Caronia

1 Introduction

Not long after the invention of the telegraph in 1839, the race to long-distance and even trans-Atlantic communication began. In many applications including submarine and buried wires, a suitable electrical insulation system was required. Early insulation systems were based upon strips of India rubber. By the late 1840s, gutta-percha (a natural gum) was utilized as wire insulation due to the ability to easily melt and coat wires in combination with good electrical insulating properties. As electrical demand increased in the late 1870s with a drive to electric lighting, excessive deformation of natural rubber insulations was experienced due to the low-temperature softening of such materials. Rigid cables designed by Edison with a wrapped conductor isolated by bitumen inside an iron conduit provided a solution for urban lighting. In the 1890s, an electrical cable system was introduced which employed a paper insulation which was saturated with oil. Paper-insulated cables enabled power cable voltages of 10 kV and higher and remained the primary power cable insulation technology for decades with various design improvements. Paper-insulated cable proved reliable, but had several drawbacks associated with the use of oil impregnant and the complexity of forming joints. While these issues were later addressed with the use of polyethylene as an electrical insulation, paper-insulated cables are still utilized in many power cable applications today [1–4].

The discovery of ethylene polymerization is credited to Fawcett and Gibson in 1933, although German scientists claimed to have documented production of $(-\text{CH}_2-)_x$ from diazomethane chemistry as early as 1897. Fawcett and Gibson, however, produced polyethylene directly from ethylene in a high-pressure process in which

T. J. Person · S. S. Sengupta (✉) · P. J. Caronia
The Dow Chemical Company, Collegeville, PA, USA
e-mail: SSSengupta@dow.com

© Springer Nature Singapore Pte Ltd. 2021
J. Thomas et al. (eds.), *Crosslinkable Polyethylene*, Materials
Horizons: From Nature to Nanomaterials,
https://doi.org/10.1007/978-981-16-0514-7_10

247

oxygen had (accidentally) been introduced into the methane. Difficulties in reproducing the initial experience were later explained by the work of Perrin and colleagues in 1935, where the presence of trace amounts of oxygen as an initiator for the polymerization reaction was recognized, and ultimately resulted in a granted patent in 1937 [5–10].

Polyethylene was rapidly industrialized and utilized as an electrical cable insulation as early as 1942. By 1947, it was utilized in 15 kV cable for residential power distribution. Polyethylene provided excellent insulating properties, reduced electrical losses and reduced installation and maintenance costs compared to paper-insulated cables [2]. The application use temperature (ampacity) could be increased with polyethylene-insulated power cables relative to paper-insulated cables, but temperatures were still limited by the softening and deformation of the polymer as temperatures exceeded 70 °C [1]. This temperature limitation was later addressed with the advent of crosslinked polyethylene (addressed in the following section).

The fundamental design elements of polyethylene-insulated cable have not changed significantly between its early use and the present day, yet there has been continual drive to increase voltage (as a means to reduce current and associated resistive losses) for more efficient power delivery.

Electricity is generated typically in the range of 2–30 kV depending on the source of energy and then stepped up to higher voltages using a step-up transformer. Electricity is then transmitted at high voltages (69–700 kV) using underground insulated cables or over-head metal wires. In nearby neighborhoods, a step-down transformer reduces the voltage and distributes the power to houses at 5–46 kV. Underground cables further distribute the power/electricity to residences or commercial end users at lower voltages (500 V–5 kV) for consumption and use. The cables employed in such a grid can be physically located underground (UG), overhead (OH) or in submarine environments (entrenched in the sea bed or laying of the ocean floor). The common classification of these power delivery systems is depicted in Fig. 10.1.

UG, OH and sea cables require protection from the elements and reliable operations over a long period of time. The designs of such cables have evolved over time and can vary based on the specific needs of utilities and end users. The common design elements are presented in Fig. 10.2. The conductor is chosen by the utilities based on the grid (power demand, voltage and ampacity, and thermal designs) and connectivity requirements, and it is not in scope for this discussion. The jacket materials (which were not always employed in early cable designs) are typically thermoplastic-formulated polyethylenes sufficient to provide mechanical protection and to protect the metallic neutral or ground materials from corrosion.

The insulation shield is typically formulated with carbon black in a polymer matrix and serves the following purposes:

- (a) Prevents partial electrical discharge between the metallic neutral or ground materials and the cable insulation,
- (b) Provides uniform ground potential around the insulation,
- (c) Minimizes charge buildup on outside of cable for operator safety,

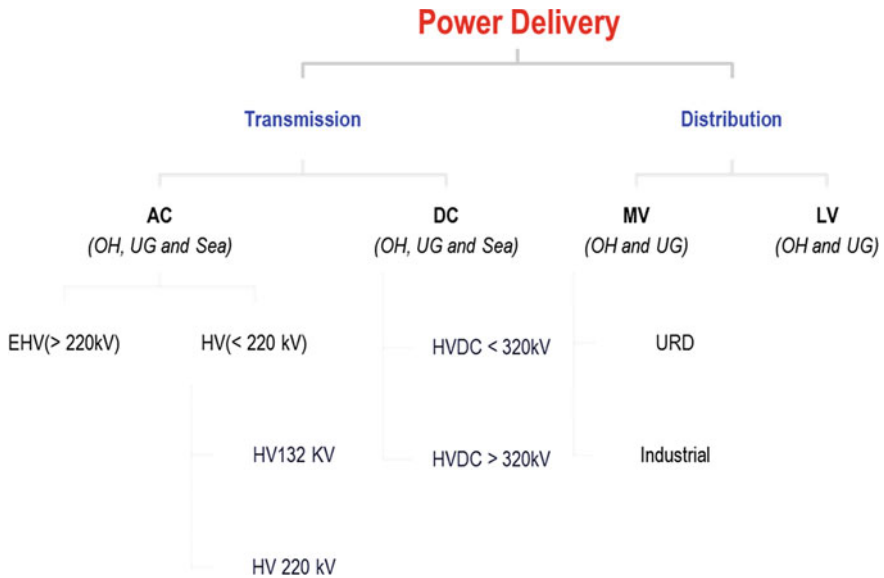


Fig. 10.1 Common classification of the power delivery systems

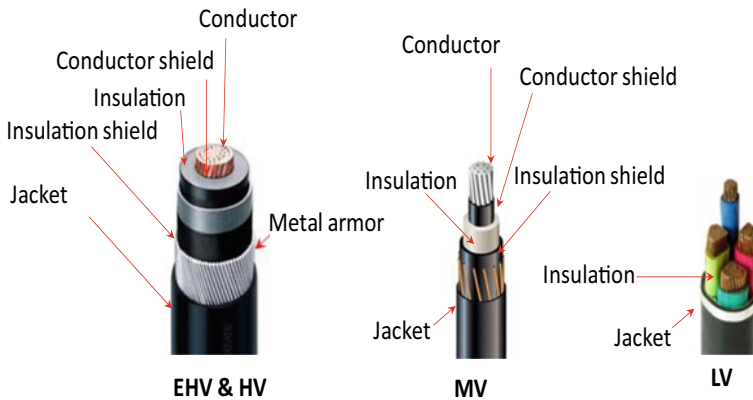


Fig. 10.2 Typical construction of XLPE cables

(d) Provides a material layer of intermediate conductivity/permittivity between the insulation and metallic neutral or ground materials which must be removed without damage to the underlying insulation for effective installation of splices, terminations and joints.

The insulation requirements and technical aspects will be further discussed in this chapter, but generally three key considerations come into play:

(a) Thermo-mechanical properties,

- (b) Ease of fabrication,
- (c) Dielectric properties:
 - Dielectric losses,
 - Dielectric strength.

2 History of XLPE Insulation

In 1945, Pinkney and Wiley filed a patent describing a means to crosslink polyethylenes using an organic peroxide. Their work demonstrated gel formation in an ethylene-vinyl acetate copolymer, and potential use as a wire coating was contemplated [11]. However, Precopio and Gilbert have been recognized with the invention of crosslinked polyethylene and filed patents for radiation-induced crosslinking of polyethylene in February of 1955 and peroxide-initiated crosslinking of polyethylene in May of 1955 [12]. These patents included the demonstration of crosslinking of ethylene homopolymers. In an interview published in 1999, Gilbert described how dated and witnessed notes were essential in resolving the issues at the US Patent Office [13, 14].

The work of Precopio and Gilbert spread quickly to colleagues in the General Electric Company. By 1957, Vostovich and Bailey had filed a patent describing the process of crosslinking polyethylene and producing coated wires [15]. In this process, peroxide is mixed into a polyethylene composition and extruded onto a wire, and then immediately contacted with pressurized steam as a means to initiate the crosslinking of the polyethylene. Ward filed a separate patent in 1958, in which a carbon-black-filled semiconductive layer was introduced over the conductor and crosslinked, followed by the polyethylene insulation which could also be crosslinked [16]. Even at this time the presence of the intermediate semiconductive layer was known to reduce the electric field gradient and reduce the presence of corona discharges in high-voltage cables. The insulation and semiconductive layers could be extruded as thermoplastic followed by crosslinking, pre-crosslinked and milled followed by extrusion, or could be applied as thin crosslinked and stretched (oriented) tapes around the conductor and subsequently heated to shrink into void-free layers. Irradiation crosslinking was noted as particularly useful for the thin extruded tapes.

Another means of crosslinking polyethylene utilizes silane functionality incorporated into the polymer. In 1961, Union Carbide Corporation demonstrated that trialkoxysilane functionality could be introduced into an ethylene polymer, and the resulting polymer could be crosslinked upon heating to cause a reaction between the silane groups [17]. It was later determined that these ethylene-vinylsilane copolymers could be effectively crosslinked with moisture and a silanol condensation catalyst. The silane-functionalized polyethylene can be formed as a copolymer of ethylene and vinyl silane in a high-pressure polymerization process or can result from grafting of vinyl silane to polyethylene using a radical-initiated process (typically initiated using organic peroxide). The silane-functionalized polyethylene can then be melt

processed along with a separate masterbatch compound to form an insulation layer; the masterbatch will introduce a suitable catalyst, typically of organotin or sulfonic acid type. Grafting and melt extrusion may also take place simultaneously in a single process to form an insulation coating. The insulated wire can then be crosslinked as moisture diffuses into the insulation layers, either under ambient conditions or under accelerated conditions through the use of a water bath or sauna. The diffusion-limited crosslinking rate often limits the application of moisture-cure polyethylene to lower voltage applications and thinner insulation thicknesses [18].

Crosslinking of polyethylene provided enhanced thermo-mechanical deformation resistance and enabled an increase of the use temperature, and thereby the ampacity, of insulated power cables. Today, crosslinked polyethylene-insulated cables are rated for maximum of 90 °C (and in some cases 105 °C) conductor temperature. Where overload conditions are allowed, these temperature ratings can reach 130 °C (and in some cases 140 °C) for a limited time throughout the cable lifetime.

The incorporation of mineral fillers into crosslinkable polyethylene provided a means to impact the thermal and mechanical properties of the resulting compounds. Crosslinkable filled ethylene-propylene elastomers were first commercially available in the early 1960s. The presence of the filler will generally reduce electrical properties (increase electrical losses and reduce breakdown strength), but filled elastomeric insulating compounds based on ethylene propylene rubber (EPR) have become common in many power distribution applications where a high degree of flexibility, heat resistance and chemical resistance is desired [19].

3 Insulation Requirements

Two key reasons for using XLPE insulation are its high dielectric strength and very low dissipation factor characteristic. The high dielectric strength of XLPE is a key feature for its use in power cables rated from 5 kV to 500 kV with an intrinsic breakdown strength reported at above 200 kV/mm [28] and well made XLPE insulated distribution cable having a breakdown strength in excess of 26 kV/mm (based on minimum within ICEA S-94-649 standard). The low dissipation factor characteristic is reflected by a global experience that XLPE insulated cables should have a dissipation factor of less than 0.10% between room temperature to 130 °C and electrical stresses up to 20 kV/mm. For water tree retardant crosslinked polyethylene (TR-XLPE), which will be discussed shortly, its specialized formulation technology includes the incorporation of polar components and it is generally not able to meet this dissipation factor requirement. For TRXLPE, the industry has accepted a dissipation factor of less than 0.50% between room temperature to 130 °C and electrical stresses up to 10 kV/mm.

In the 1970s, with the growing use of crosslinked polyethylene in power cables, the industry became aware of the electrical degradation phenomenon of treeing; both electrical treeing and water treeing. Though there are a number of variables that impact XLPE treeing, one factor common to both electrical and water treeing

is the impact of electrical stress enhancements due to contaminants. Based on the recognition that contaminants can have a role in a XLPE insulated cable's live performance, some industrial specifications include specific cable insulation inspection requirements. Other industrial specifications address insulation cleanliness indirectly with requirements on a cable's minimum AC withstand voltages, minimum impulse strength and maximum partial discharge requirements. Defects, as due to contaminants, would make achieving the required properties difficult. Based on the differences in operating stresses and conditions between transmission and distribution class cables, there are differences in the cleanliness requirements for the XLPE materials used in these cables [20, 21].

Additionally, compound manufacturers monitor the cleanliness of XLPE compounds, wherein a selected quantity of material is extruded into a molten tape and then examined by associated contamination detection and sizing equipment. As this is a destructive test, a small quantity of material is tested such that tape inspection is generally one component of an overall assessment of insulation cleanliness.

For cables that will be exposed to moisture as well as be under electrical and mechanical stress, XLPE insulation can undergo a phenomenon known as 'water treeing.' Water trees in the XLPE insulation are generally considered to be degraded, chemically oxidized structures that are observed as a dendritic pattern of water-filled micron and sub-micron-sized cavities. As water trees grow, the electrical stress on the insulation can increase to the point where an electrical tree initiates at the tip. Once initiated, electrical trees grow rapidly and lead to catastrophic failure of the cable [22–25].

In order to avoid or minimize this phenomenon, two different approaches are taken. One option is to modify the design of the cable to eliminate the possibility of water or moisture ingress. This is done by the use of a metal sheath resulting in a so-called dry-design cable [1]. Although successful, this is a relatively expensive solution, especially for a medium voltage cable installation. It can also impact cable flexibility and the complexity and difficulty of the cable installation process. The alternative is to use a more cost-effective 'wet design,' whereby the moisture-impervious metal sheath is eliminated and replaced by diffusion-resistant polyethylene jackets, water-absorbing tapes and conductor strand filling compound. However, in this case, the cable insulation needs to be more robust toward the growth of water trees in a wet electrical aging environment. As a result, the wet design cable preferably employs a water tree retardant insulation. The vast majority of wet cable designs are used in the manufacture of medium voltage (6–46 kV) cables [2].

The key industry specifications for MV through EHV cables are outlined below, and a summary of the requirements as related to insulation contamination is discussed.

HV/EHV Specifications

- IEC 60840: Power cables with extruded insulation and their accessories for rated voltages above 30 kV up to 150 kV—Test methods and requirements,
- IEC 62067: Power cables with extruded insulation and their accessories for rated voltages above 150 kV up to 500 kV,

- AEIC CS9: Specification for Extruded Insulation Power Cables and their Accessories rated above 46 kV through 345 kVac,
- ICEA S-108-720: Standard for Extruded Insulation Power Cables Rated Above 46 Through 500 kV,
- Chinese National Standard/Specification GB/T 11017 for 110 kV Cable,
- Chinese National Standard/Specification GB/TZ 18890 for 220 kV Cable,
- Chinese National Standard/Specification GB/T 22078 for 500 kV Cable.

MV Specifications

- IEC 60502 Part 1 and 2: Power cables with extruded insulation and their accessories for rated voltages from 1 kV up to 30 kV,
- CENELEC Harmonization Document (HD 620),
- AEIC CS8: Specification for Extruded Dielectric Shielded Power Cables rated 5 through 46 kV,
- ICEA S-94-649: Standard for Concentric Neutral Cables Rated 5 through 46 kV,
- ICEA S-97-682: Standard for Utility Shielded Power Cables Rated 5 through 46 kV,
- Chinese National Standard/Specification GB/T 12706 for 1 kV up to 35 kV Cables.

The IEC specifications do not have a cleanliness specification or requirement. However, the factory cable electrical requirements (AC Breakdown and Impulse) would limit contaminant sizes in order to pass the tests. The AEIC/ICEA specifications have insulation contamination requirements for MV, HV and EHV cables. The method for examining the insulation as well as the requirements is outlined in the specifications. The insulation contamination requirements vary based on cable voltage class. In China, the Chinese National Standard/Specifications also have contamination requirements on the incoming insulation compound. These requirements also vary based on the cable voltage class.

4 Choice of Insulation Materials for Cables

Insulation in cables is a vital layer to prevent the leakage or loss of power from being transmitted. This layer demands the following balance of properties [1]:

- a. Excellent Electrical Properties:
 - Low Dielectric Constant,
 - Low Power Factor,
 - High Dielectric Strength.
- b. Excellent Moisture Resistance:
 - Low Moisture Vapor Transmission.
- c. High Resistance to Chemicals and Solvents.

Table 10.1 Available materials for wire and cables

Material	Common name
<i>Thermoplastic</i>	
• Polyvinyl Chloride	PVC
• Polyethylene	PE
• Polypropylene	PP
• EA/VA copolymers	EEA/EVA
• Chlorinated polyethylene	CPE (also crosslinked)
• Thermoplastic elastomer	TPE
• Nylon	Nylon
• Fluorocarbon polymers	PTFE, FEP, CTFE
• Polyurethanes	
<i>Crosslinked</i>	
• Polythylene	XLPE
• Rubber	NR, SBR, Butyl, Silicone
• Neoprene	
• Nitrile-Butadiene/Polyvinyl Chloride	NBR/PVC
• Chlorosulphnated polyethylene	CSPE
• Ethylene propylene rubber	EPR/EPDM

The materials commonly used in wire and cable are listed in Table 10.1. PVC has been widely used as a non-metallic jacketing material since its introduction in 1935. Low cost, ease of processing and excellent combination of overall properties including fire and chemical resistance are some of the value propositions for this material. It has a fairly linear molecular structure with 5 to 10% crystallinity [26]. Usually, it is formulated with plasticizers and stabilizers to maintain good flexibility, heat resistance and low temperature properties. However, under high current fault conditions, the insulation may be permanently damaged by melting or loss of plasticizers. Polypropylene also offers unique properties as a jacket or insulation material and has electrical and chemical resistance properties similar to those of polyethylene. From the perspective of mechanical properties, it is harder and stiffer than polyethylene [27]. It is also characterized by a higher melting point and poor low temperature properties as compared to polyethylene. Nylon presents an interesting blend of properties and is a tough material but stiff in cold weather conditions. It has excellent resistance to hydrocarbon fluids, lubricants and organic solvents but not toward strong acids. It is almost exclusively used as jacket material because of its sensitivity to moisture [28]. Sometimes fluorocarbon polymers are used in special cable applications. They offer low flame ability, excellent abrasion and abuse resistance properties. They are characterized by a high dielectric constant but offer good resistance to moisture, weathering ozone and UV radiation. It is not a material of choice in high-voltage insulation because of propensity to degrade under corona

discharge conditions [29]. Rubbers are often used as insulation materials where excellent resistance to oil, harsh chemicals and flexibility is needed. Polyethylene as an insulation offers excellent electrical properties and good chemical resistance and is characterized by a very low moisture vapor transmission rate. These polymers offer excellent UV stability when formulated with proper grade of carbon black or UV stabilizers. These materials are unaffected by ozone as compared to the rubbers and offer excellent retention of functional additives as compared to PVC products. They offer a good balance of toughness versus flexibility and are easy to fabricate via extrusion. In some cases, these may be foamed by chemical or physical foaming agents. The polyethylene materials are inexpensive and readily available on small and large scales. Upon proper formulation, they offer very long-life performance and reliable cable operation. The upper use temperatures are limited for polyethylene materials since they start to soften from 90 °C.

Consider the dielectric constant of polyethylene (ϵ) which is related to the polarizability of the material (α) through the Clausius–Mossotti–Debye equation [30]:

$$\frac{(\epsilon - 1)M}{(\epsilon + 2)\rho} = \frac{4\pi N\alpha}{3} \quad (1)$$

where N is the Avogadro number,

ρ is density,

M is the molecular weight of a material.

The polarizability is usually understood as contributions from electronics and due to the orientation of permanent electrical dipole moments. According to Debye, this orientation is proportional to the dipole moment of the molecule. In polyethylene, these dipoles may arise from CH bond moments, C=C bond moments and impurities. The dielectric constant is affected by the temperature, frequency and pressure since these parameters affect the variables used to describe this property. From a molecular structure standpoint, density and hence crystallinity have a direct impact on the dielectric constant.

Even when segmental level polarization is taken into account, the fact that polyethylenes have hydrocarbon structures and are essentially non-polar may lead one to believe that no dielectric loss occurs over the useful range. Although the losses are low compared to existing materials, they are still measurable and are an important consideration for the design of the insulation materials. The dielectric losses are always more sensitive to small concentration of polar groups present in the material. This property is the result of relaxation of the polar impurity groups which seem to be always present. These polar molecules are often free to rotate even though they may be confined to a rigid lattice. Such behavior is to be expected in polyethylene where the intermolecular forces are weak and appreciable portion of the structure is amorphous.

Design considerations on current-carrying capacity (ampacity) as well as voltage ratings for any given cable system allow the use of very limited materials as insulation in power cables. The dielectric heating and energy loss in power cables are given by:

Table 10.2 Electrical properties of insulating materials

Material	Dielectric constant	Dielectric loss
Air	~1	~0.0000
Teflon	2.1	0.0002
PE	2.4	0.0005
Nylon	3.5	0.0065
PVC	6	0.1000

$$\text{Power loss per phase} = 2\pi fCU_0^2 \tan \delta \quad (2)$$

where f = supply frequency (Hz),

C = capacitance per core (F/m),

U_0 = voltage to earth (V),

$\tan \delta$ = dielectric loss angle of insulation.

Table 10.2 lists the $\tan \delta$ values for various common insulating materials and for the same type of constructions and under similar operating conditions also gives a relative idea of expected loss characteristics. The paper and oil materials have inherently low susceptibility toward discharges and treeing. As paper-insulated cable ages under load cycling and voltage stress, impregnated fluids migrate with temperature changes and lead to the formation of waxes and detrimental microvoids. This along with the complexity associated with splicing and terminating these cables places those at a disadvantage compared to solid extruded cables. While extruded cable has become the dominant technology, it is expected that paper/oil cables will continue to be utilized in some applications due to proven longevity. Polyethylene-based insulations have low loss characteristics and high dielectric strength which are advantages in this application. However, the cable environment impacts the susceptibility of polyethylene insulation to electrical discharges and treeing. This has led to the use of formulated compounds in this area to achieve the required performance.

The manufacture of power cables with extruded polyethylene insulation began with the use of thermoplastic polyethylene. In order to improve upon high temperature performance and achieve thermal stability, thermoset compounds such as XLPE came into use. There are mainly two classes of polyethylenes, linear and branched. The branched family of resins is made by a high-pressure reactor and is usually referred to as LDPE (low-density polyethylene). This was the original PE discovered in 1935 and has been prevalent in the power cable industry since its introduction in 1950s. Since then, other polyethylenes have been synthesized with different molecular architectures. Table 10.3 lists the various kinds of polyethylene available for use, their properties and year of development. LDPE resins are typically characterized by broad molecular weight distributions and long-chain branched (LCB) molecules. The other linear resins are noted for their narrow molecular weight distribution and short-chain branched (SCB) molecules.

Table 10.3 Different grades of polyethylenes

	Density (gm/cc)	Melting point (°C)	Crystallinity (%)	Developed year
LDPE	0.915–0.93	106–120	40–60	1935
HDPE	0.94–0.965	125–135	65–80	1955
LLDPE	0.91–0.94	120–125	40–60	1975
VLDPE	0.89–0.91	118–122	25–40	1983

Extruded cable manufacturing assets are usually designed to accept ready-to-extrude pellets which are fed in an extruder. A proper process control (and extrusion screw design) leads the compound to be melted and forced through a die-head arrangement that deposits the melt on the conductor core being passed through the crosshead. State-of-the-art cable extrusion processes consist of co-extrusion of three material layers over a metallic conductor (semiconductive inner shield, insulation and semiconductive outer shield) to form a cable core, which is subsequently crosslinked to increase the use temperature. After allowing the crosslinking by-products to diffuse out of the cable core, a metallic neutral ground is applied (typically wires wrapped helically around the core), and a thermoplastic protective jacket is extruded over the neutral to complete the cable construction. Curing or crosslinking is enabled through technologies such as peroxide crosslinking, silane crosslinking and radiation crosslinking. Peroxide curable insulation compounds are typically formulated with dicumyl peroxide as the radical initiator to allow for extrusion above the melt temperature of polyethylene with limited initiator activity, followed by crosslinking at elevated temperatures sufficient to dramatically increase initiator activity. This process of elevated temperature crosslinking is referred to as vulcanization. Following extrusion onto the conductor, the compound is exposed in a continuous vulcanization chamber to a pressurized high temperature environment. The environment can be high-pressure steam (about 250 psi) which yields a temperature of about 400 °F. Alternatively, dry nitrogen may be used to process the crosslinkable insulation at a pressure of about 150 psi when used in conjunction with a vulcanization tube wall temperature of approximately 650 °F. These high temperatures cause the peroxide to decompose into reactive free radicals. The pressure is required to reduce void formation from volatile peroxide decomposition by-products. A number of design and process configurations exist for the overall process and selected based on the type of cable being manufactured and volume requirements. The cable manufacturing process as discussed very briefly above imposes serious material properties consideration for the selection of insulation compounds. Most of the current cable manufacturing process is an optimized design around LDPE resins.

The final properties of solid crosslinked insulation at the molecular level can be roughly correlated with the molecular weight of the polymer (M_w). From the physical property data listed in Table 10.3, high-density polyethylene (HDPE) can be ruled out based on its higher melting point and density characteristics. Based on a first pass assessment, linear low-density polyethylene (LLDPE) on the other hand

Table 10.4 Comparison of LDPE and LLDPE flow properties

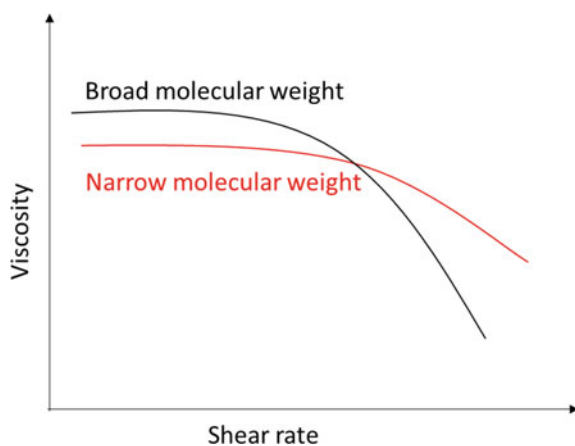
Mw (g/mol)	LDPE MI	LLDPE MI
815,600	0.45	0.001
251,320	0.21	0.064
153,400	2.3	0.36
125,000	6.9	0.75

presents itself as a viable option for use as insulation material. Listed in Table 10.4 are melt indices of LDPE and LLDPE at various molecular weights. For any given molecular weight, the melt index (MI) of an LDPE resin is at least an order of magnitude higher than LLDPE resin that translates into an easier flowing material at the same melt temperature, or a similar flow at a lower temperature which can be an advantage when trying to limit premature crosslinking reactions.

Figure 10.3 shows the viscosity (Pa s.) dependence of typical LDPE as compared to that of linear PE resins as a function of shear rate (1/s). Narrow molecular weight distribution PE shows a prolonged Newtonian behavior. Broad molecular weight distribution allows higher low-shear viscosities (or zero shear viscosities) and lower high-shear viscosities (shear thinning). These are principal attributes that facilitate sag-resistance in the vulcanization process and ease of extrusion during fabrication, respectively. VLDPE resin made via Ziegler Natta process is very similar to LLDPE. This discussion suggests that in terms of processing ease, LDPE presents the best option in existing equipment.

Detailed study of crosslinking efficiency and scorch retardance had been carried out in the past with LLDPE and LDPE resins. It was found that increase in compound viscosity was enhanced with LLDPE due to the degree of polymer chain entanglement as compared to probability of intra-chain crosslinks in highly branched and more

Fig. 10.3 Comparison of rheology of PE resins



tightly coiled LDPE. However, these resins performed poorly in terms of scorch retardance. LDPE resins presented a balance of cure and scorch retardance. This suggests that LLDPE being more efficient in the curing step would pose serious challenges in extrusion. Considering typical rheology and shear-thinning behavior of LLDPE, it is expected that it would require slightly higher melt processing temperatures in order to achieve the same output compared to LDPE and this will further aggravate any pre-mature crosslinking concerns. However, all studies were conducted using DCP as the peroxide initiator. Use of LLDPE may be conceived with different peroxides or mixtures having higher activation temperatures and tailored decomposition kinetics. The other option is to use conventional peroxides with coagents like AMSD.

Electrical performance limits the selection of base resins even further. Generally, LDPE has a dissipation factor of around 0.0005 as compared to LLDPE which can have an order of magnitude higher owing to catalyst residues from its synthetic process. Earlier experimentation had revealed that dissipation factor and break-down strength of LLDPE were inferior compared to LDPE but acceptable. However, particular grades of LLDPE resins are available that meet the electrical requirements.

Choice of base resin for insulation compounds in power cables is governed by the balance of electrical properties (low DC/DF, high VR, high dielectric strength), mechanical properties (good elongation, LTB, crosslinked modulus at high temperature), functionality (high unsaturation) and flow properties (high shear thinning, high zero shear viscosity). These impact the cable manufacturing process as well as final cable properties like lifetime, flexibility, etc. Figure 10.4 presents a high-level comparison of available resins, based on the discussion above, from the standpoint of use in insulation materials. This analysis represents why LDPE resin is the material of choice in cable designs using current extruder cable fabrication equipment.

		Extrudability	Crosslinking efficiency	Electrical Property	Mechanical Property	
PE	Linear	HDPE	--	+	+	
		VLDPE	-	+	-	+
		LLDPE	-	+	_*	+
	Branched	LDPE	+	-	+	+/-

Fig. 10.4 Material selection for peroxide curable power cable insulation. * = selected resin grades with preferred catalysts can meet electrical performance requirements

5 Factors Affecting Dielectric Performance

An effective power cable insulation is one that enables efficient delivery of electrical power. Clearly, this delivery must first avoid an electrical breakdown or fault between the high potential conductor and the ground, throughout the expected lifetime of the cable. As a second aspect, the efficiency of the power delivery is focused on minimizing energy loss during the operation of the cable. If one is to discuss these aspects, it becomes important to first establish a general basis of electrical behavior of materials. Bartnikas and Eichhorn provide a detailed foundation, while only a few essential concepts are provided in the following section [31].

5.1 Material Permittivity, Dissipation Factor and Conductivity

Consider an ideal parallel plate capacitor separated by vacuum with charge, Q , at the plates under a steady voltage, V_0 . The capacitance, C_0 , is the ratio of the charge to the voltage, Q/V_0 . When a dielectric material is placed between the plates, the voltage is reduced to V and the capacitance to Q/V . A material parameter, known as the relative permittivity (or dielectric constant), can be described as

$$\epsilon_r = V_0/V = C/C_0 \quad (3)$$

The reduction in voltage results from electric polarization of the material. Polarization occurs with the orientation of permanent dipoles within the molecular structure of the dielectric. Polarization may also be induced within non-polar materials, as an applied field will result in a displacement of the electron clouds within an atomic or molecular structure.

The above representation of the relative permittivity can also be termed the static permittivity and represents an equilibrium value. The rate of polarization is dependent upon the structure of the dielectric material (e.g., the strength of dipoles, atomic and molecular interactions, and crystallinity), and polarization contributes to dielectric loss. The permittivity is a complex quantity and can be expressed as $\epsilon = \epsilon' - j\epsilon''$ where ϵ'' is related to the energy stored within the material and ϵ'' is related to energy dissipation or loss. When an alternating voltage is applied across a dielectric material, the resulting current can be separated into two components, one in-phase with the voltage and one leading the voltage by 90° . The leading current is the charging current of an ideal capacitor, while the in-phase current represents the loss current. The ratio of loss current to charging current, which is often equated to the ratio of dielectric loss to dielectric storage, ϵ''/ϵ' , is referred to as $\tan \delta$ (tangent delta) or dissipation factor. However, materials are not ideal capacitors, and loss current measurements also include a conductivity component due to displacement of charge carriers. The conductivity, σ , defined as the ratio of current density to applied field, will have both

an ac and a dc component. Thus, an apparent dissipation factor will then take the form of

$$\tan\delta = \sigma/\omega\varepsilon' = \varepsilon''/\varepsilon' + \sigma_{dc}/\omega\varepsilon' \quad (4)$$

where total conductivity $\sigma = \sigma_{ac} + \sigma_{dc}$. At high frequencies, the component associated with dc conductivity becomes negligible, while at very low frequencies the losses can become dominated by dc conduction. For further information on dielectric polarization and losses, the reader is directed to references by Bartnikas and Raju. Typical electrical properties of several polymeric materials are provided in Table 10.5, as reported by Raju. The table refers to volume resistivity, which is the inverse of conductivity [32, 33].

Table 10.5 Typical electrical properties of several polymeric materials as reported by Raju [28]

Material	Dielectric strength (kV/mm)	Volume resistivity (Ω cm)	Dielectric constant (–)	Dissipation factor ($\times 10^{-4}$)
Polyethylene (LDPE)	200	10^{16}	2.3 (50–60 Hz) 2.2 (1 kHz) 2.2 (1 MHz)	2–10 (50–60 Hz) 3 (1 kHz) 3 (1 MHz)
Polyethylene (HDPE)	200	10^{16}	2.35 (50–60 Hz) 2.4 (1 MHz)	2.4 (50–60 Hz) 2–7 (1 MHz)
Polyethylene (XLPE)	220	10^{16}	2.3 (1 MHz)	3 (1 MHz)
Polypropylene (biaxially oriented)	200	3×10^{14}	2.27 (50–60 Hz) 2.2 (1 kHz) 2.2 (1 MHz)	3 (1 kHz) 3 (1 MHz)
Polytetrafluoroethylene (PTFE)	88–176	10^{18}	2.1 (50–60 Hz) 2.0 (1 kHz) 2.0 (1 MHz)	2 (50–60 Hz) 1 (1 kHz) 1 (1 MHz)
Polyester (PET)	275–300	10^{18}	3.2 (1 kHz) 3.0 (1 MHz)	50 (1 kHz) 160 (1 MHz)
Ethylene-propylene diene rubber (EPDM)	20–	10^{16}	2.5–3.5 (50–60 Hz)	70 (1 kHz)
Silicone rubber	20–30	–	2.5–3.2 (50–60 Hz) 2.5–3.2 (1 kHz) 3.0–3.6 (1 MHz)	4–25 (50–60 Hz) 3–10 (1 kHz) 20–50 (1 MHz)

5.2 *Electrical Breakdown*

A large air gap represents an effective insulation, and bare overhead conductors suspended from poles or large towers serve this purpose very well. In this case, the cables are suspended far enough away from trees, structures, and ground so that the air is able to sustain the resulting electrical field without a breakdown. However, aspects such as aesthetics, vegetation management, right-of-ways, power delivery across large bodies of water, power theft and reliability in adverse weather conditions all represent drivers for underground or submarine power cables. Such applications require an insulating layer over the conductor which must also be able to sustain the electric field without a breakdown throughout the expected lifetime of the cable. Electrical breakdown of polymeric insulation is discussed in depth within [Dissado and Fothergill], with various breakdown mechanisms identified as electrical, thermal, electromechanical and partial discharge breakdowns. In the electronic breakdown, a high-energy charge carrier within free volume of the dielectric is accelerated by the applied field. The energy gained can become sufficient to damage the polymer matrix upon charge carrier collision or to result in ejection of a number of additional charge carriers (e.g., electrons), which themselves are accelerated due to the applied field. The result is an electron avalanche and numerous high-energy collisions resulting in failure of the polymer dielectric [34].

Polyethylene is recognized as having a high breakdown strength. The intrinsic breakdown strength of polyethylene has been estimated to be above 700 kV/mm, yet breakdown strength is reduced dramatically when practical volumes are electrically stressed [Fischer, 1976]. Such behavior has been attributed to the presence of critical defects and an increased probability of having a critical defect as the tested volume is increased. The similarity in the intrinsic breakdown strength was also observed in comparison with the peak ac to dc breakdown characteristics for a given low-density polyethylene. In that same work, various LDPEs with different average molecular weights were shown to exhibit an increase in breakdown strength with an increase in average molecular weight [35].

The breakdown strength of polyethylene has been observed to increase with increased density. This effect is consistent with free-volume breakdown mechanisms described in Dissado and Fothergill, as an increase in density effectively reduces the available free volume for such charge carrier acceleration. Additional aspects of crystalline morphology as related to breakdown strength have been studied through the use of polyethylene blends. Breakdown strength is also known to drop as the temperature is increased, where temperature not only assists in overcoming the energetic barrier to break bonds, but also contributes to the formation of more amorphous volume as the edges of crystallites begin to melt [36, 37].

A common method of characterization of polyethylene breakdown strength or initiation of a pre-breakdown phenomenon known as electrical treeing incorporates the use of needle-shaped electrodes into polyethylene blocks or samples of cable insulation. Breakdown stress has been approximated at 300 kV/mm in this manner. Using needle tips of different radii, researchers have also found a limitation in the

expected breakdown due to geometric stress enhancement. It was found that a needle tip radius of less than 10 microns did not provide a further reduction in breakdown voltage. This was considered that local field decay becomes very rapid with smaller tip radii such that it may become more difficult to realize a critical electric field over a critical length to sustain a breakdown event. There is also evidence of injected charge near the needle tip which will provide effective field-screening to manage the local field and thus limit the localized damage. The combination of a critical tip radius ($\sim 10 \mu$) and a critical breakdown strength ($\sim 300 \text{ kV/mm}$) has become important elements utilized in the estimation of a critical-sized contaminant (addressed shortly) [38, 39].

Numerous studies have considered so-called voltage stabilizers of various functionalities which can be added to a polymer composition with the intent of capturing the energy of the high electrons and transforming it into a less damaging form of energy release. Various electron donor-acceptor structures have been studied based upon this hot-electron mechanism with varied degrees of success. Fused aromatic structures were found to be highly effective voltage stabilizers, yet their poor solubility in polyethylene brings concern of long-term effectiveness if the additive is fugitive. Functionalized aromatics such as alkylated pyrene and anthracene were also explored. Acetophenone is a known voltage stabilizing additive and is also a major by-product of the crosslinking of XLPE with dicumyl peroxide as an initiator. However, acetophenone is volatile and will slowly evacuate from the insulation layers of the XLPE cable, such that cable breakdown strength can be significantly reduced after the concentration of volatile by-products are reduced via a 'degassing' process. [This has raised some concern in the use of partial discharge testing as a cable manufacturing quality test before the cable is sufficiently 'degassed,' as a cable defect could be masked in the presence of acetophenone shortly after manufacturing. But later, that same cable could be delivered for installation with much lower levels of residual acetophenone, which enable the detection of that defect through positive partial discharge testing.] The effective voltage stabilizing nature of acetophenone led to further investigations of larger molecules with similar structures, such as benzophenone and various derivatives thereof with the intent of improving the solubility and finding a voltage stabilizing additive which was less fugitive. Voltage stabilizers continue to be a critical area of research, but have not yet made significant commercial impact. The benefits seen in the laboratory using highly divergent fields from wires or needle tips do not appear to have a significant effect on a manufactured cable [40–45].

5.3 Impact of Contaminants

While structural properties of polyethylene can impact electrical breakdown, the practical breakdown strength of polyethylene is still found to be much lower than the intrinsic values measured by Fischer. In order to better appreciate this, we must consider the presence of a contaminant within the polyethylene and the impact that it may have on the resulting breakdown strength. The properties of the insulation

volume are no longer spatially uniform as the electrical properties of the contaminant can be much different than that of the insulation. In this case, the relevant material property is the permittivity, which relates the displacement field to the electrical field, $\mathbf{D} = \varepsilon\mathbf{E}$. The divergence of the displacement field is equal to the free charge density, such that $\text{div } \mathbf{D} = \text{div } (\varepsilon\mathbf{E}) = \rho$, which is a form of Gauss's law where the permittivity can still vary with position. Thus, for an example domain in which there is no free charge ($\rho = 0$), the spatial variation of the material permittivity will define the local electrical field. If the permittivity is spatially constant, then the field takes the form of the Laplacian, where $\text{div } \mathbf{E} = 0$. But, if a contaminant of differing permittivity exists within the domain, then large field enhancements can exist [33].

The field enhancements for contaminants of different shapes and permittivities have been calculated in this manner. The most common models are based upon ellipsoidal contaminant geometries. An expression for the stress enhancement as a function of assumed ellipsoidal geometry and contaminant permittivity is provided in Böstrom and appears to be an extension of the 1912 work of Larmor and Larmor.

$$\text{SEF} = 1 - \frac{1}{\alpha} \left\{ \frac{1}{2} \ln \left(\frac{\lambda + 1}{\lambda - 1} \right) - \frac{\lambda}{\lambda^2 - 1} \right\} \quad (5)$$

$$\alpha = \frac{1}{2} \ln \left(\frac{\lambda + 1}{\lambda - 1} \right) - \frac{1}{\lambda} + \frac{1}{(k - 1)\lambda(\lambda^2 - 1)} \quad (6)$$

$$\lambda = \frac{1}{\left\{ 1 - \left(\frac{R}{a} \right) \right\}^{\frac{1}{2}}} \quad (7)$$

where R is the tip radius, a is the half-length of the major ellipsoidal axis, and k is the ratio of the permittivities of the contaminant particle to the matrix (originally focused on the impact of contaminants within the insulation). For a conductive ellipsoid, the value of k will be very high, such that the third term in the expression for α will become very small. [This equation has been reproduced here in corrected form, as a typographical error in the placement of the parentheses was noted within Böstrom. The corrected form above is now easily validated to yield the expected stress enhancement of 3 for a high permittivity spherical contaminant, which has been published by Bowers and Cath.] Bahder provides an alternate form for ellipsoidal contaminants with reference to the work of Larmor and Larmor, and Malik refers to yet a third representation with credit given to Bateman. Each of these models has been found equivalent to the representation provided above. The calculated stress enhancement factor for ellipsoidal contaminants of different permittivity ratios is shown in Fig. 10.5 [46–49].

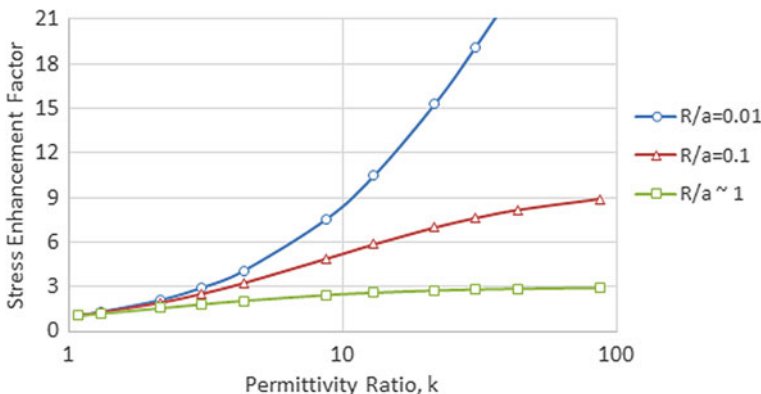


Fig. 10.5 Stress Enhancement Factor of an ellipsoidal contaminant as a function of shape and permittivity ratio

5.4 Electrical Aging

A high initial breakdown strength does not ensure that an insulation will sustain a high electrical stress over the lifetime of the cable insulation. Constant stress evaluations of time-to-failure (t) under different applied electrical fields (E) give rise to an aging correlation which has become known as the inverse power law. A plot of $\log E$ versus $\log t$ is found to yield a straight line (with a slope $-1/n$), such that the product $E^n t$ is constant. Values for the lifetime exponent, n , can range from 5 to 8 for distribution cable systems, but are typically 10–15 for XLPE insulation utilized in high-voltage applications [50].

One can also consider the constant in the inverse power law to represent a measure of lifetime, such that any increment of time at a given field will represent a fraction of that lifetime (or a degree of aging). Such concepts have been applied to step-wise or ramped stress evaluations as a means to characterize the parameters of the aging model in a shorter duration. The use of such concepts involves the assumption that the inverse power law is a reasonable approximation of material aging over the entire range of stress conditions and can lead to considerable uncertainty in the resulting estimates.

5.5 Critically Sized Contaminants

If one starts with the needle tests discussed by Ishibashi, which suggested 300 kV/mm as a critical failure stress during 15 min time steps, the inverse power law provides a means to define a critical stress for another duration such as that of a qualification test or the expected cable lifetime. Additional correction factors can be applied to account for the temperature difference between the needle tests and the cable

operating temperature. The result is a critical stress for cable survival. One can then assume a worst-case scenario that a contaminant could be present at the position of highest design stress of the cable and that contaminant is of sufficient size to cause a failure. A very high permittivity ratio, representative of a metallic contaminant, would be consistent with the worst-case scenario. Based upon the needle tests and demonstration of effective shielding, a tip radius of 10 microns can be assumed to determine the dimension of this ‘critical contaminant’ according to the stress enhancement factor described earlier.

Following the approach described by Ishibashi,

$$E_c > E_{\max} k_T k_m k_f \quad (8)$$

where E_c is the critical failure stress of 300 kV/mm, E_{\max} is the maximum design stress of the cable construction, k_T is a temperature correction factor, k_m is a correction according to the aging model (Ishibashi utilized $n = 15$ from the inverse power law with a cable life expectation of 30 years), and k_f is a geometric stress enhancement factor. With $k_T = 1.2$, $k_m = 2.52$ and an ellipsoidal stress enhancement, Ishibashi estimated that a 500 kV AC cable with inner insulation radius of 19 mm and outer radius of 46 mm would have a largest permissible contaminant of 67 μ (major ellipsoidal axis).

Through the use of the ellipsoidal stress enhancement model previously discussed, this approach can be taken for any proposed cable design where a critical stress enhancement factor can be tolerated, and thereby defines a critical contaminant size (e.g., the major axis length $2a$ where the tip radius R is assumed to be 10 microns using the notations described in Eq. 7). Such an approach has led to industry specifications (as discussed in Sect. 3) to limit protrusions and contaminants, with particular attention to sizes down to 70 μ and even 50 μ , with some specific references to metallic contaminants.

5.6 Dielectric Losses

Dielectric energy dissipation (losses) can result in localized heating of the dielectric if the rate of thermal conductivity out of the dielectric is insufficient. An increased temperature can not only reduce breakdown strength, but will also reduce energetic barriers to enhance dipole and charge carrier mobility and promote further heat generation. Such a condition can lead to ‘thermal runaway’ and result in a thermal failure of the dielectric.

Dielectric power loss in an ac cable (watts per unit length) is proportional to the product of the dielectric constant (real part of the permittivity), the dissipation factor and the square of the applied voltage. Thus, low dielectric constant and dissipation factor are desired and become more important as the application voltage is increased. In the case of a dc cable, the losses associated with the dielectric are due to leakage current, and thus, low conductivity is desired. Leakage current and dc losses will

also increase with the application voltage. However, for both ac and dc applications, the efficiency of power transmission is improved at higher voltages, as losses are dominated by Joule heating from the conductor current. The magnitude of power transmitted is the product of the conductor current and the conductor voltage; thus, the conductor current can be reduced in proportion to the increase in application voltage as a means to reduce transmission losses [51].

5.7 Electrical Aging in Wet Environments

Up to this point, the discussion of electrical aging and breakdown has focused on mechanisms which are typically associated with ‘dry-design’ power cables, where the structure of the cable has been designed to resist water penetration into the insulating layer. However, as mentioned in an earlier section, the presence of water has been shown to introduce a different mode of electrical aging which leads to considerable acceleration of the deterioration of the insulation even at relatively low alternating electrical fields (a few kV/mm). This mode of degradation has become known as ‘water treeing’ due to the tree-shaped and bush-shaped structures which form within the insulation and grow predominantly along field lines. An ASTM method for characterization of water treeing resistance was developed, and most distribution cable standards now incorporate wet electrical aging and retention of electrical breakdown strength into material qualifications [52–54].

While some debate may be found regarding the role of electrochemical oxidation of polyethylene in the water treeing mechanism, the demonstration of acceleration of water treeing with increased frequency seems to have generated more consensus in an electromechanical driving force. The permittivity difference between small water clusters and the surrounding polyethylene matrix can create a frequency-dependent electromechanical stress on the polymer matrix. Over time, much like mechanical crack propagation, small water-filled channels can form and continue to provide a conductive path and stress enhancement at the crack tip. Materials designed to resist water treeing have now become well established, either through the use of polymer blends or through the use of water tree retardant additives. Water tree retardant additives (such as polyethylene glycol) are water soluble and can reduce the permittivity difference between additive water solution domains and that of the polyethylene matrix, thereby resulting in a reduced driving force for electromechanical stress. Introduction of a polar polymer (such as an ethylene-alkyl acrylate copolymer) into a blended composition with polyethylene serves to provide a thermodynamically preferred location for any water present within the higher-permittivity polar phase [43, 55, 56].

The introduction of polar species into water tree retardant XLPE compositions results in an increase in the dissipation factor of the compound. Thus, the use of water tree retardant materials in wet designs has been primarily limited to power distribution applications, with some limited extensions into wind farm array cables and wet design high-voltage applications. Recent material developments have been

reported which identify water tree retardant compound approaches with substantially reduced dissipation factor at power frequencies, which may result in a greater utility of water tree retardant technology at higher voltages [57–59].

6 Concluding Remarks

Power cables are critical infrastructure component in delivering power or electricity to consumers. The design and specifications vary by region and application. Utilities design the cables and expect the grid to work reliably for a long time. XLPE as an insulation material offers advantages over other polymers. The XLPE materials should be carefully selected based on several criteria, including cleanliness, dielectric properties (high dielectric strength, low dielectric loss), processability and scorch retardance. The molecular structure of polyethylene has an impact on the insulating properties. Rheology and polymer architecture are fine-tuned for this application during the polymerization process by tailoring molecular weight distribution, branching and unsaturation. This provides shear thinning for good processability, high melt strength to avoid flowing due to gravitational forces as the insulation exits the extrusion die and hasn't yet crosslinked (ensures round cross-section), and good peroxide response during cure. There is ongoing research on molecules that interfere with the electrical breakdown processes to improve the performance of these materials.

References

1. Bernstein B, Thue W (2003) Historical perspectives of electrical cables. In Thue W (ed) *Electrical power cable engineering*, 2nd ed, Marcel Dekker, New York
2. Black R (1983) *The history of electric wires and cables*. Peter Peregrinus Ltd.
3. Edison, US Pat 251552, "Street Pipes" Dec 1881
4. Orton H (2013) History of underground power cables. *IEEE Electr Insulation Mag* 29(4)
5. Bamberger E, Tschimer F (1900) Ueber die Einwirkung von Diazomethan auf b-Arylhydroxylamine. *Berichte der Dueschten chemischen Gesellschaft zu Berlin* 33:955–959
6. [claims student Hindermann mentioned white substance, later determined to be $(-CH_2)_x$, in his dissertation in Zurich in 1897]
7. Von Pechmann H (1989) Ueber Diazomethan und Nitrosoacylamine. *Berichte der Dueschten chemischen Gesellschaft zu Berlin* 31:2640–2646
8. Fawcett EW, Gibson RO, Perrin MW, Paton JG, Williams EG (1937) Improvements in or relating to the polymerization of ethylene. British Patent 471590
9. Perrin MW (1953) The story of polythene. *Research* 6
10. Dobbin C (2017) An industrial chronology of polyethylene. In Spalding M, Chatterjee A (eds) *Handbook of industrial polyethylene and technology*. Wiley and Sons
11. Pinkney P, Wiley RH (1953) Curing of polyethylenes. US Patent 2628214
12. Gilbert A, Precopio F (1963) Irradiated filler-containing polyethylene. US Patent 3084114
13. Precopio F, Gilbert A (1959) Curable polyethylene comprising a peroxide containing tertiary carbon atoms, and a filler, and process of curing same. US Patent 2888424

14. Precopio F, Gilbert A (1999) The invention of chemically crosslinked polyethylene. *IEEE Electr Insulation Mag* 15(1)
15. Vostovich J, Bailey C (1960) Extrusion of crosslinked polyethylene and process of coating wire thereby. US Patent 2930083
16. Ward R (1967) Method of making polyethylene insulated electrical conductors. US Patent 3325325
17. US Patent US3225018A to Union Carbide Nathan Zutty, filed in Dec 1961, published in Dec 1965
18. GB1286460A to Dow Corning, Henry George Scott, filed 12-20-1968, published in 8-23-1972
19. A Brief History of EPR Dielectric, EPR Cable Technology Consortium—University of Connecticut; <https://eprcable.ims.uconn.edu/epr-cables/>; contact Dr. Y. Cao
20. Vahlstrom W (1971) Paper presented at IEEE Conference on Underground Distribution, Detroit, Mich.
21. Lawson RH, Vahlstrom W (197) *IEEE Trans PAS* 824
22. Lawson J, Vahlstrom Jr W (1973) Investigation of insulation deterioration in 15 kV polyethylene cables removed from service, Part II. *IEEE Trans PAS* 92:824–831
23. Miyashita T (1971) Deterioration of water-immersed polyethylene coated wire by treeing. *IEEE Trans Electr Insul* 6:129–135
24. Lawson JH, Vahlstrom W Jr (1973) Investigation of insulation deterioration in 15 kV and 22 kV polyethylene cables removed from service—part II. *IEEE Trans PAS* 92:824–835
25. Bahder G, Katz C, Lawson JH, Vahlstrom Jr W (1974) Electrical and electrochemical treeing effects in polyethylene and crosslinked polyethylene cables. *IEEE Trans PAS* 93:977–990
26. Ballard DGH, Burgess AN, Dekoninch JM, Roberts EA (1987) The ‘crystallinity’ of PVC. *Polymer* 28:3–9
27. Noel OF, Carley JF (1975) Properties of polypropylene-polyethylene blends. *Polym Eng Sci* 15(2):117–126
28. Kohan Melvin (1995) *Nylon plastics handbook*. Carl Hanser Verlag, Munich
29. Hougham GG, Cassidy PE, Johns K, Davidson T (1999) *Fluoropolymers 2*. Springer
30. Ryszelberghe PV (1932) Remarks concerning the Clausius-Mossotti Law. *J Phys Chem* 36(4):1152–1155
31. Bartnikas R (1983) Dielectric loss in solids. In: Bartnikas R, Eichhorn R (eds) *Engineering dielectrics—Volume IIA—Electrical properties of solid insulating materials: molecular structure and electrical behavior*. ASTM Publications
32. Bartnikas R (ed) *Engineering dielectrics: volume IIB—electrical properties of solid insulating materials: measurement techniques*. American Society for Testing and Materials—Special Technical Publication 926
33. Raju G (2003) *Dielectrics in electric fields*. Marcel Dekker, Inc
34. Dissado LA, Fothergill JC (1992) *Electrical degradation and breakdown in polymers*. Peter Peregrinus Ltd.
35. Fischer and Nissen (1976) Breakdown behavior of polyethylene. *IEEE Trans Electr Insul* EI-11(2)
36. Li D et al (2019) Effect of crystallinity of polyethylene with different densities on breakdown strength and conductance property. *Materials* 12(11):1746
37. Hosier I, Vaughan A, Swingler S (1997) Structure-property relationships in polyethylene blends: the effect of morphology on electrical breakdown strength. *J Mater Sci* 32:4523
38. Shimizu N et al (1998) Electrical tree initiation. *IEEE Trans Dielectrics Electr Insul* 5(5):651
39. Ishibashi A et al (1998) A study of treeing phenomena in the development of insulation for 500 kV XLPE cables. *IEEE Trans Dielectrics Electr Insul* 5(5):695
40. Gross R, Hunt G (1967) Dielectric compositions containing halogenated voltage stabilizing additives. US Patent 3,350,312; Simplex Wire and Cable
41. Heidt L (1970) Solid dielectric polyolefin compositions containing various voltage stabilizers. US Patent 3,522,183; Simplex Wire and Cable
42. Hunt G (1970) Voltage stabilized polyolefin dielectric compositions using liquid-aromatic compounds and voltage stabilizing additives. US Patent 3,542,684; Simplex Wire and Cable

43. Eichhorn R (1983) Treeing in solid organic dielectric materials. In: Bartnikas R, Eichhorn R (eds) *Engineering dielectrics—Volume IIA—electrical properties of solid insulating materials: molecular structure and electrical behavior*. ASTM Publications
44. Kisin S et al (2009) *Polym Degrad Stab* 94:171
45. Englund V et al (2009) *Polym Degrad Stab* 94:823
46. Bostrom J-O et al (2003) Stress enhancement of contaminants in XLPE insulation used for power cables. *IEEE Electr Insul Mag* 19(4)
47. Bahder G, Eager, GS, Silver DA, Lukac R (1912) Criteria for determining performance in service of crosslinked polyethylene insulated power cables. *IEEE Trans Power Apparatus Syst* 95(5):1552, with reference to a 1912 paper by Larmor and Larmor (Royal Society of London, 1912)
48. N.H. Malik, et al, *Electrical Insulation in Power Systems*, Marcel Dekker, New York 1998, with reference to H. Bateman, *Partial Differential Equations of Mathematical Physics*, Cambridge University Press, New York, 1944
49. Bowers AB, Cath PG (1941) The maximum electric field strength for several simple electrode configurations. *Phillips Tech Rev* 6, #270
50. Orton H, Hartlein R (eds) *Long-life XLPE-insulated power cables*. Orton Consulting Engineers International, Ltd.
51. Thue W (2003) *Electrical power cable engineering*, 2nd edn. Marcel Dekker, New York
52. Steennis EF, Kreuger FH (1990) Water treeing in polyethylene cables. *IEEE Trans Electr Insul* 25:989
53. Pelissou S, Harp R, Bristol R, Densley J, Fletcher C, Katz C, Kuchta F, Kung D, Person T, Smalley M, Smith J (2008) A review of possible methods for defining tree retardant crosslinked polyethylene (TRXLPE). *IEEE Electr Insul Mag* 24(5):22
54. ASTM D6097 (2016) Standard test method for relative resistance to vented water tree growth in solid dielectric insulating materials. ASTM International
55. US Patent 4305849A (1980) Polyolefin composition containing high molecular weight polyethylene glycol useful for electrical insulation. Nippon Unicar Company
56. Farkas A (1985) Insulation composition for cables. WO 1985005216A1
57. CIGRE TB722 (2018) Recommendations for additional testing for submarine cables from 6 kV ($U_m = 7.2$ kV) up to 60 kV ($U_m = 72.5$ kV). CIGRE Study Committee—WG B1.55
58. Cree S et al (2015) Potential use of new water tree retardant insulation in offshore wind farm array cables. In: *Jicable '15*, B1.3
59. Caronia P et al (2019) Advancements in TR-XLPE insulation technology to enable use in high-voltage cable applications. In: *Jicable'19*, B5.1

Chapter 11

Failure Mechanisms in XLPE Cables



Petru V. Noțingher, Cristina Stancu, and Ilona Pleșa

1 Introduction

Crosslinked polyethylene (XLPE) is widely used as electrical insulation in conductors and cables of all voltage and frequency ranges and is especially well suited to medium and high-voltage power applications (Fig. 11.1) [1]. The first XLPE insulated cables were performed in Canada and USA (in the 1960s) and are used predominantly in Northern America, Japan and Northern Europe. The use of XLPE as insulation of medium, high and very high-voltage power cables (Fig. 11.1c) is due to its remarkable properties, as follow: very good electrical properties, mechanical properties and operating temperature (90 °C) superior to low-density polyethylene (70 °C), good resistance to environmental stresses (acids, bases, radiation, etc.), easy processability, low maintenance costs, long lifetime, etc. [1, 2]. Table 11.1 shows the values of XLPE and other thermoplastic polymers properties used as insulation for power cables [1].

The transition from fluid-impregnated paper systems to polymeric-insulated system was favored by reduced installation and maintenance costs for polymer-insulated cables, no fluid leaks to locate and repair, weight reduction (allowing for the installation of longer cable lengths), reduced risk of fire during earthquakes, and reduced dielectric losses [3].

P. V. Noțingher (✉) · C. Stancu
University Politehnica of Bucharest, Splaiul Independentei 313, 060042 Bucharest, Romania
e-mail: petrunot@elmat.pub.ro

C. Stancu
e-mail: cstancu@elmat.pub.ro

I. Pleșa
Polymer Competence Center Leoben GmbH (PCCL), Roseggerstrasse 12, Leoben 8700, Austria
e-mail: ilona.plesa@pccl.at

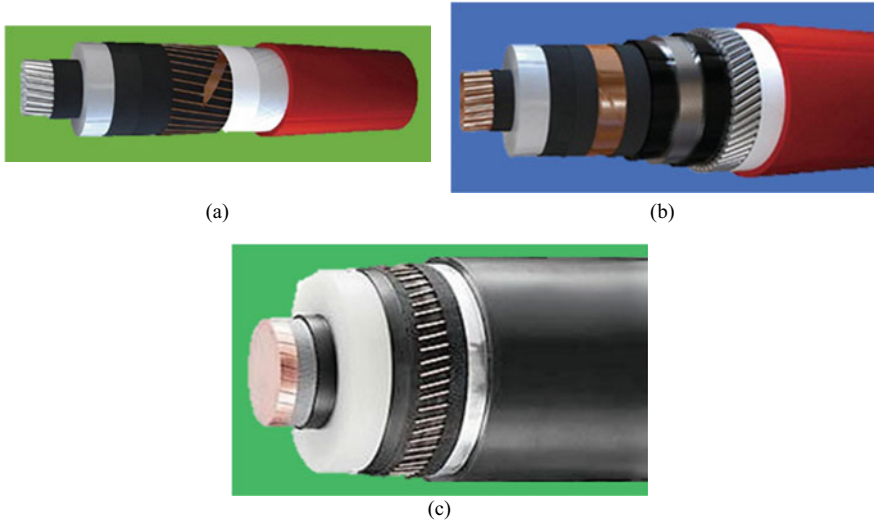


Fig. 11.1 Medium (a), high (b) and very high-voltage cables (c) insulated with XLPE. Redrawn and adapted figure from reference [1]

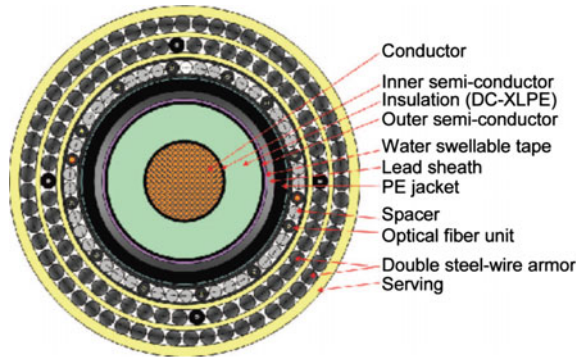
Table 11.1 Properties of polymers used for insulation of power cables [1]

Properties	LDPE ^a	MDPE ^a	HDPE ^a	XLPE ^a	EPR ^a
Volume resistivity (Ωm)	$>10^{14}$	$>10^{14}$	$>10^{13}$	$>10^{13}$	$10^{13}\text{--}10^{15}$
Dielectric strength (MV/m)	18.5–28	20–28	18–20	22	36
Dielectric constant at 60 Hz	2.3	2.3	2.35	2.3	3.17–3.34
Loss factor at 60 Hz	0.0002	0.0002	0.0002	0.0003	0.0073
Density (g/cm^3)	0.910–0.925	0.926–0.940	0.941–0.965	0.920	0.86
Modulus of elasticity (MPa)	117–242	173–380	552–1035	790	210–470
Elongation (%)	20–650	100–600	15–700	550	200

^aLDPE—Low-density polyethylene, MDPE—Medium density polyethylene, HDPE—High-density polyethylene, EPR—Ethylene propylene rubber

However, the use of XLPE for high and very high-voltage cables requires a drastic reduction in the contaminants content of the insulation. The presence of contaminants (primarily high-permittivity or conductive particles) increases locally the electrical stresses to the point that electrical trees initiate. Unlike water trees, these trees rapidly grow and lead to the cable failure. For this reason, compound manufacturers have developed extra-clean insulation compounds for HV cable applications. Beside the proper part of insulation, XLPE is also used for the manufacture of semiconductor screens and cable sheaths, especially in the case of submarine cables for the energy transport, both alternating (AC) and direct current (DC) [4] (Fig. 11.2).

Fig. 11.2 Cross-sectional configuration of the bipolar 250-kV DC-XLPE



The estimated lifetime of an XLPE insulated power cable is at least 30 years [4]. During the operation of the cables, their insulation is subjected to simultaneous or consecutive electrical, thermal, mechanical and environmental stresses. These stresses contribute to the initiation and development of some processes of XLPE degradation; processes that lead, in time, to the insulation breakdown and, therefore, to the removal and failure of the cables.

This chapter presents the mechanisms of XLPE insulations degradation generated by the electric field, namely the electric discharges, the electric and water trees. Initially, the distribution of the electric field inside the insulations (i.e., in the absence and in the presence of the space charge) is analyzed and shown to be non-uniform. The existence of macroscopic defects (e.g., protuberances, non-uniformities of the semiconductor layers, cavities, clusters of impurities, etc.).

Submarine cable within the Hokkaido-Honshu HVDC link [4] determines large local values of the electric field, which can exceed the maximum permissible limits imposed on each type of cable (starting from which the mechanisms of insulations degradation are initiated). It is outlined then the phenomena of aging, degradation and failure of the XLPE insulation due to the electric field and its values are presented for each characteristic phenomenon and degradation mechanism. Further, the physical processes of initiation and development of partial discharges and electric and water trees, their characteristic parameters, the factors that contribute to the intensification of these processes, as well as the methods of increasing the initiation times and reducing the development speed of the mechanisms are analyzed in detail. The resistance of the XLPE insulations to each of the three degradation mechanisms is studied in detail, and some results from literature regarding methods of increasing their values are presented, respectively, the improvement of the XLPE characteristics and of the insulations manufacturing technologies. In addition, the mechanisms of space charge accumulation and its influence on the degradation mechanisms of XLPE insulations are investigated.

2 Cables Insulation Stresses

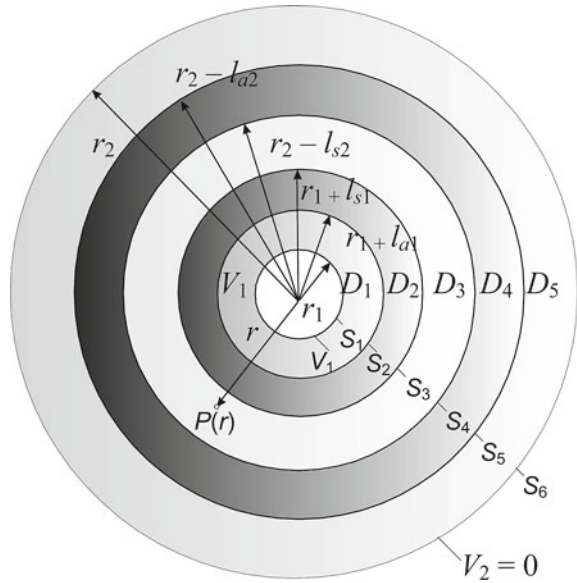
During cable operation, XLPE insulations are subjected to the combined action of electrical, mechanical, thermal and environmental stresses. As a result, physico-chemical processes of aging and degradation are initiated and carried out, leading to the reduction of the electrical and mechanical properties of the insulation below the accepted values for a safe operation of the cables or even their removal from the operation (failure). The rate of these processes are directly related to the shape, intensity and frequency of the requested stresses. It should also be noted that all types of stresses vary within the insulation, both in space (i.e., due to the shape of electrodes, material defects, etc.) and in time (i.e., as a result of aging, degradation and space charge accumulation within insulation, etc.). Thus, both the temperature and the electric field show higher values in the areas adjacent to the inner semiconductor layer and lower in the areas adjacent to the outer semiconductor layer (e.g., oxygen and radiation penetrate the insulation from the outer semiconductor layer, etc.). As a result, aging and/or degradation does not occur uniformly within the volumes of insulation. Some models and methods of estimation the electric field distribution in the XLPE insulation of a power cable, in the absence and presence of trees and space charge, are presented below [5, 6]. Regarding the estimation of the electric field, a medium voltage cable insulated with XLPE with the nominal voltage $U = 8.7$ kV, the length l , the outer radius of the inner semiconductor $r_1 = 8$ mm and the inner radius of the outer semiconductor $r_2 = 13$ mm, was considered. It has been also assumed that within the insulation of the cable, continuous water trees have been developed (i.e., especially observed within the insulation of the highly degraded cables [5]) or individual ones (i.e., especially occurred within the insulation of the recently manufactured cables, in which, the number of volume defects is lower). They show lengths between 0.5 and 1.5 mm (i.e., developed from one or both semiconductor layers) and a space charge content, whose density varies parabolically with the coordinate r [6].

Considering that $l \gg r_1$ and $l \gg r_2$ and continuous water trees (with the lengths $l_{a1} = l_{a2} = l_a$) and space charge layers (with the thickness $l_{s1} = l_{s2} = l_s$ and $l_s \geq l_a$), the electric field is plane-parallel and shows axial symmetry. The numerical calculation was performed in the plan domain D , formed by five subdomains, as follow: D_1 (with a variable permittivity $\varepsilon_1(r) = c_1 e^{-dr}$), containing trees and space charge, D_2 (with a constant permittivity $\varepsilon_2(r) = 2.2 \varepsilon_0$), containing space charge, D_3 (with a constant permittivity $\varepsilon_3(r) = 2.2 \varepsilon_0$), with no content of trees and space charge, D_4 (with a constant permittivity $\varepsilon_4(r) = 2.2 \varepsilon_0$) containing space charge, and D_5 (with a variable permittivity $\varepsilon_5(r) = c_2 e^{dr}$), containing trees and space charge (Fig. 11.3).

The space charge layers were considered to have average densities and equal thicknesses ($\rho_{vmed1} = \rho_{vmed2} = \rho_{vmed}$), but parabolic variable densities of coordinate r , potential conductor V_1 and external potential semiconductor $V_2 = 0$ (obviously, $U = V_1 - V_2 = V_1$) [5].

Considering the electrostatic field and using the polar coordinate system (r, φ) , the potential will be estimated by the Poisson's equation:

Fig. 11.3 Computation domain of the electric field in the presence of trees and layers of space charge, developed from both semiconductor layers. Reprinted, with permission, from author [6]



$$\frac{1}{r} \cdot \frac{d}{dr} \left[r \varepsilon_i(r) \frac{dV_i}{dr} \right] = -\rho_{vi}(r), i = 1, 2, \dots, 5 \tag{11.1}$$

where $V_i(r)$ is the analytical value of the potential in the point P of radius r of the domain D_i , $\varepsilon_i(r) = \varepsilon_0 \varepsilon_{ri}(r)$, $\varepsilon_0 = 8.85 \cdot 10^{-12}$ F/m—the absolute permittivity of vacuum, $\varepsilon_{ri}(r)$ —relative permittivity and $\rho_{vi}(r)$ —volume density of space charge in the point $P(r)$ from D_i [7].

Equations (11.1) are added to the conditions on the boundaries $S_{1,6}$ (Fig. 11.3):

$$\begin{aligned} V(P) &= V_1, & P \in S_1 \\ V(P) &= V_2 = 0, & P \in S_6 \end{aligned} \tag{11.2}$$

and the boundary conditions on the surfaces $S_{2,3,4,5}$:

$$V_i(P) = V_{i+1}(P), \quad P \in S_{i+1}, i = 1, 2, 3, 4 \tag{11.3}$$

$$\frac{dV_i(P)}{dr} = \frac{dV_{i+1}(P)}{dr}, \quad P \in S_{i+1}, i = 1, 2, 3, 4 \tag{11.4}$$

where $V_i(P)$ are the values of the potential in points $P \in S_{2,3,4,5}$ estimated by the equations corresponding to the subdomains D_1, D_2, D_3, D_4 and D_5 , respectively.

By deriving the potential $V_i(r)$, the expression of the electric field $E_i(r)$ in each subdomain D_i is obtained (see [7] in Appendix, for details):

$$E_i(r) = -\frac{dV_i(r)}{dr}, i = 1, 2, 3, 4, 5. \tag{11.5}$$

In the absence of trees and space charge (homogeneous D), results:

$$E(r) = -\frac{V_1}{r \ln \frac{r_1}{r_2}}, \tag{11.6}$$

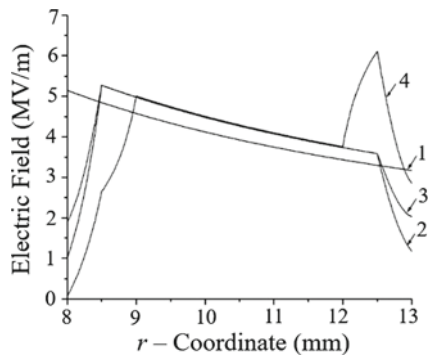
equation used for a first estimation of the electrical field near the inner semiconductor layer.

Using the analytical expressions of the electric field, Stancu et al. [7] present the results of the numerical estimation of the electric field in D , both in the presence and in the absence of water trees and/or the space charge in the form of continuous layers (Fig. 11.3). In the case of individual trees and variations of the space charge with r , the estimation of the electric field was performed by using Flux 2D [8] or COMSOL Multiphysics® software [9].

Figure 11.4 shows the variation of the electric field with the coordinate r within the XLPE insulation of a 20 kV voltage cable, in the absence of trees and space charge (1), in the presence of two continuous trees of lengths $l_{a1} = l_{a2} = 0.5$ mm (2), for two continuous trees and two positive charge layers of lengths $l_{a1} = l_{a2} = l_{s1} = l_{s2} = 0.5$ mm (3), and lengths $l_{a1} = l_{a2} = 0.5$ mm and $l_{s1} = l_{s2} = 1$ mm (4), considering that the average space charge density takes the same value within both layers, $\rho_{vmed1} = \rho_{vmed2} = + 0.106$ C/m³, respectively. The existence of two layers of space charge causes a decrease of the electric field in the subdomains $D_{1,2}$ and an increase in the subdomains $D_{3,4,5}$ (Fig. 11.4). It was observed that the existence of trees and space charge (Fig. 11.4, curves 2–4 and Fig. 11.5, curves 2–3) leads to a considerable increase of E values in certain areas, in the absence of trees and/or space charge (Figs. 11.4 and 11.5, curve 1).

The presence of space charge produces, as expected, a reduction of the field in the areas with space charge ($D_{1,2} \cup D_{4,5}$) and an increase in the area without space charge (D_3). These variations are more important as l_s and ρ_{vmed} take higher values (Fig. 11.6). It should be noted that maximal and minimal values of the electric field

Fig. 11.4 Variation of the electric field with coordinate r in the absence of trees and space charge (1) and in the presence of two trees of lengths $l_{a1} = l_{a2} = 0.5$ mm (2), two trees and two layers of positive charge of lengths $l_{a1} = l_{a2} = l_{s1} = l_{s2} = 0.5$ mm (3) and $l_{a1} = l_{a2} = 0.5$ mm and $l_{s1} = l_{s2} = 1$ mm (4). Reprinted, with permission, from author [6]



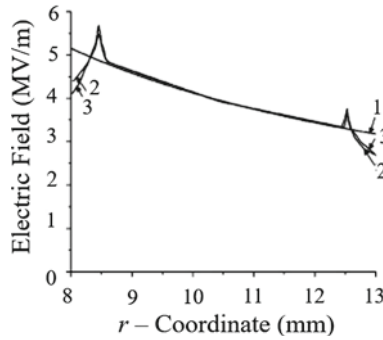


Fig. 11.5 Variation of the electric field with coordinate r in the absence of water trees and space charge (1), in the presence of two individual water trees of length $l_{a1} = l_{a2} = 0.5$ mm (2), and in the presence of two individual water trees of length $l_{a1} = l_{a2} = 0.5$ mm and of two space charge layers with $l_{s1} = l_{s2} = 0.5$ mm and $\rho_{vm1} = \rho_{vm2} = 0.106$ C/m³ (3). Reprinted, with permission, from author [7]

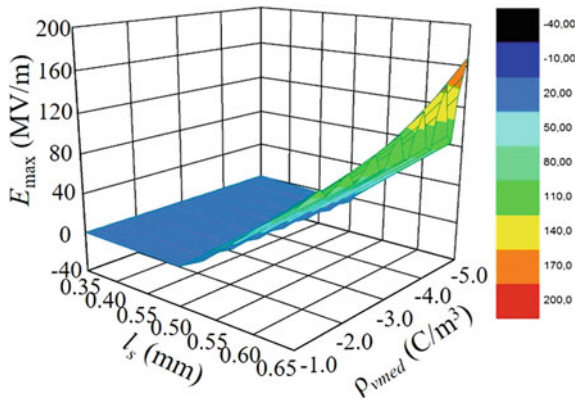


Fig. 11.6 Variation of the maximal electric field E_{max} with the layer thickness l_s and average density of the space charge ρ_{vmed} in the presence of a continuous trees of length $l_a = 0.35$ mm ($V_1 = 39$ kV, $r_1 = 0.55$ mm, $r_2 = 1.35$ mm). Reprinted, with permission, from author [5]

are reached after certain times (Fig. 11.7), depending on the electrical conductivity values of the XLPE insulation [6]. However, by increasing the thickness of the space charge layer, the electric field in the area of the outer semiconductor increases.

By disconnecting high-voltage cables operating in DC from the voltage source, the space charge being accumulated within the XLPE insulation, a residual electric field appears (Figs. 11.8 and 11.9). This must be as small as possible due to, on the one hand, its injuriousness to the operators' lives and, on the other hand, its contribution to further processes of the insulation degradation (i.e., by maintaining partial discharges and trees).

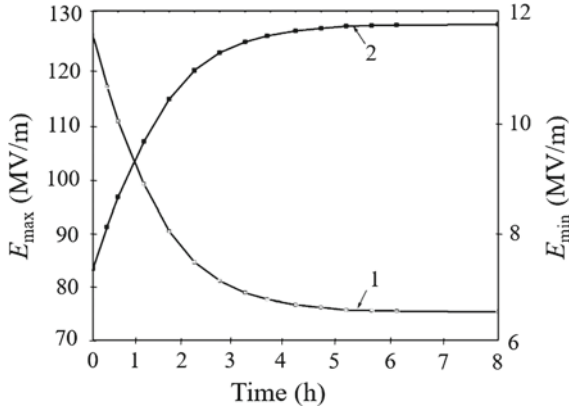


Fig. 11.7 Variation in time of the maximal electric field E_{\max} (1) and minimal E_{\min} (2) estimated in quasi-stationary regime ($V_1 = 39$ kV, $r_1 = 0.55$ mm, $r_2 = 1.35$ mm, $l_a = 0.35$ mm, $l_s = 0.65$ mm, $\rho_{\text{vmed}} = -2$ C/m³). Reprinted, with permission, from author [5]

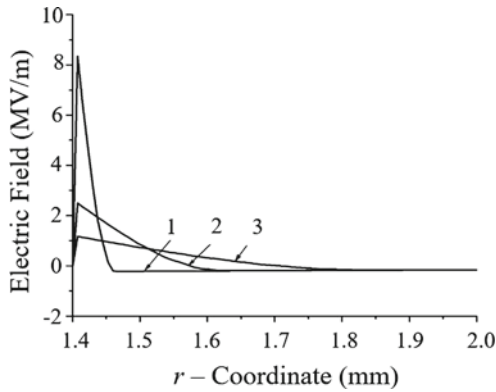


Fig. 11.8 Variation with coordinate r of the residual electric field E for trees with $L_m = 370 \mu\text{m}$, $D_m = 110 \mu\text{m}$ (1), $D_m = 400 \mu\text{m}$ (2) and $D_m = 790 \mu\text{m}$ (3). Reprinted, with permission, from author [5]

The variation curves of the residual electric field intensity versus coordinate r represent the maximal points identified in the areas with water trees (Fig. 11.8.). With the increase of the water trees average diameter D_m , the maximal values of E decrease, and the maximal points are approaching the inner semiconductor layer (Fig. 11.8, curve 3).

The values of the residual electric field depend on the dimensions (average length L_m and diameter D_m) of the water trees (Fig. 11.8.) and on the concentration of the water within trees c_{aw} (Fig. 11.9). The maximal electric field is obtained near the inner semiconductor layer and an increase by almost 70% was obtained when c_{aw} reached 2%.

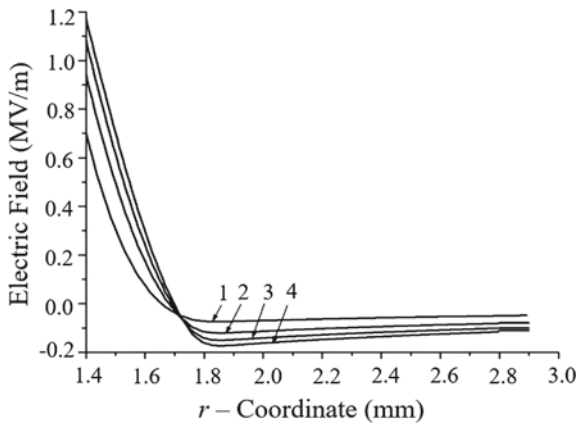


Fig. 11.9 Variation with coordinate r of the residual electric field in the absence (1) and in the presence of water trees with $c_{aw} = 1\%$ (2), 1.5% (3) and 2% (4). Reprinted, with permission, from author [5]

3 Aging, Degradation and Failure

Under the action of the electric field, three important physical phenomena, namely aging, degradation and breakdown, may occur over time in the cable insulation during operation. These phenomena were analyzed and presented in numerous papers, including those of Fothergill [10], Dissado and Fothergill [11], O'Dwyer [12], Notinger [13–16], etc. Figure 11.10 shows that aging, degradation and breakdown of the insulation occur at certain values of the electric field E with different

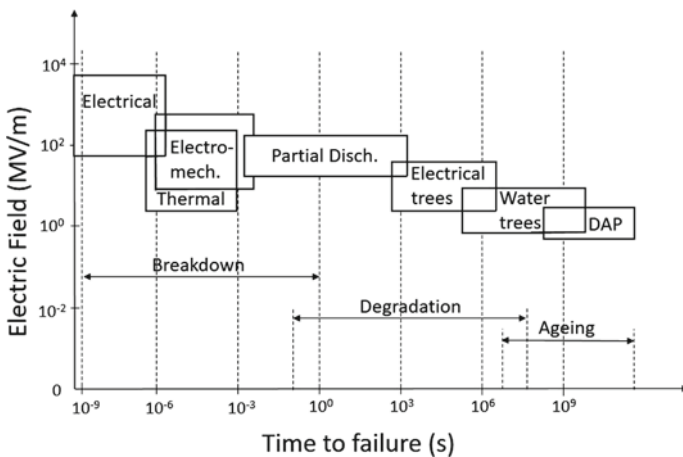


Fig. 11.10 Times and electric fields over which various electrical breakdown, degradation and aging mechanisms are operative (DAP—Different Aging Processes) [10]

running time intervals between them, whereas in the case of some other values of E , these phenomena can occur simultaneous. For example, for low electric fields (2–3 MV/m), both aging and degradation of the insulation can occur and for medium electric fields (10 MV/m), degradation and breakdown can appear, etc.

Aging is a complex physicochemical process that takes place over a relatively long time interval under the influence of aging factors on the operational cables insulation, which cause a change of one or more properties of the insulation. Densely [17] groups the aging factors as follow: thermal (maximum temperature, low temperature, temperature gradient, temperature cycling), electrical (voltage, frequency, current), environmental (gases, lubricants, water/humidity, corrosive chemicals, radiation) and mechanical (bending, tension, compression, torsion, vibration) and stated that, the cable insulation will fail after a period of exposure to these aging factors. Dissado and Fothergill [11] consider that, depending on the nature and magnitude of these factors, within insulation occurs physical, chemical, electrical and mechanical aging.

Physical aging occurs due to the time changes in the polymer as a result of the structural relaxation of the polymer's chain through segmental motion in the amorphous region because of the variation in glass transition temperature [11]. The glass transition temperature T_g is a critical parameter that determines the polymer states (i.e., a slight change in T_g can show if aging will take place or not). In the case of amorphous regions of polymers, physical aging can be associated with inefficiency of molecular packing (i.e., free volume), which can prevent all the potential lattice sites from being occupied due to chain structure and steric hindrances [11].

Chemical aging changes the behavior of the polymer as a result of the electrons and ions release (i.e., by breaking molecular chains and bond breakage) under the action of light. Chemical degradation is the breaking of the polymer's chain, namely the phenomenon of depolymerization. As a result, new crosslinking bridges may occur, and the insulation will be more brittle. Chemically reactive free radicals are part of the reaction. The formation rate of the free radicals depends on temperature, the amount of oxygen and the presence of radiation [18]. Polymer aging caused by the polymer radicals can be grouped in three categories as follow: addition to the polymer chain by branching or net formation, chain scission and oxidation by absorbed oxygen. Branching will make the material harder, while scission and oxidation will cause loss in molecular weight and brittleness increase. Oxidation also increases polarity and the loss factor of the insulated material. It also increases electrical conductivity, which leads to the increase of Joule losses and local heating that cause, at high fields, current flow and thermal runaway. While physical aging may be reversible [19], chemical aging is irreversible due to the morphological changes in the composition of the material produced after chemical reactions [20].

Electrical aging is due to the action of the electric field, which, through the energy transmitted directly to the polymer, can be accelerated by physical, chemical and mechanical processes. Thus, Crine [21] shows that the intense local fields can lead to the appearance of cavities with characteristic dimensions of 5–10 nm. However, several papers emphasize the great difficulties encountered during the experiments and measurements of the electrical aging in nominal conditions of operational cables [22].

Mechanical aging is due to the torsional vibrations, tensions and bending, which lead to physical and chemical changes within the insulation structure, mechanical rupture, respectively, loss of adhesion, separation, delamination at the interfaces, loss of liquids, gases, etc.

Densely [17] characterized aging as intrinsic and extrinsic. Intrinsic aging was defined as a result of the aging factors interaction that can induce changes in the material properties by acting singly or in combination on the insulation system. Extrinsic aging was defined as a degradation caused by the interaction between aging factors and defects (i.e., such as protrusions, cavities and voids) within the material bulk or at the interfaces. The author does not make a clear distinction between aging and degradation of the cable insulation, 'degradation' being included in the generic term of 'aging.'

Fothergill [10] shows that aging process is less clear and that there are questions as whether aging due to an electrical field actually exists at all [22]. However, it is generally accepted that the time to breakdown decreases as the electric field increases, even in the apparent absence of any degradation mechanisms such as water or electrical treeing. In this regard, Crine and Vijn [23] proposed 'an approach to physicochemical factors in the electrical breakdown of polymers,' considering the processes at a molecular and morphological level.

The research carried out so far has not led to the elaboration of a 'single theory' on the electrical aging, in order to explain the effect of long-term action of the existing electric field in cable insulation operating under nominal conditions. However, in a series of papers published recently, the space charge accumulated in cable insulation was taken into account, the characteristics of the aging process (Table 11.2. [10]) and the formation of reduced density regions or free volume throughout the insulation are assumed and models of electrical, electro-thermal or electromechanical aging are developed [20, 24–38].

The aging rate is assumed to increase in regions of high space charge concentration (model A), high electromechanical stress (model B) or in regions of free volume that allow high local currents (model C). In all cases, such aging may result in sub-micro-cavities (nano-cavities) and a greater prevalence of charge traps. Fothergill presents an analysis of these models in [10]. Thus, model A assumes that space charge is the cause, whereas model C assumes that it is the effect of aging [38]. In model A, space charge accumulates at centers giving rise to enhanced electric fields and to the formation of aging centers (local chain scission). In model C, electrically induced mechanical deformation of intermolecular bonds is the first step, whereas at high fields, electrons injected into nano-voids can acquire enough energy to generate further damage. Model B considers that the morphology is changed at points throughout the material, principally through electromechanical forces that unravel crystallites.

In the case of intense electric fields (especially in areas with insulation defects, Fig. 11.11), non-existent phenomena in low fields can be initiated and intensified (i.e., partial discharges, electrical and water trees), which contribute to the degradation of insulation (Table 11.2 [10]). The defects may be formed during extrusion processes or/and in service, contributing to the local increase of the electric field values at

Table 11.2 Characteristics of breakdown, degradation and aging processes [10]

	Breakdown	Degradation	Aging
Effect	Catastrophic: insulation cannot be used afterward	Leads to breakdown: reduces breakdown voltage	May lead to degradation: may not reduce breakdown voltage
Rate	Fast: occurs in $\ll 1$ s	Less than required service life: hours—years	Continuous process: whole service life
Evidence	Direct observation: normally by eye—hole (channel) through insulation	Observable directly: may require microscopic or chemical techniques	Difficult to observe: may even be difficult to prove existence
Place	Continuous filament: bridges electrodes	Occurs in weak zones: may form fractal structures	Assumed to occur throughout insulation
Size	>mm: dependent on energy of event	> μ m: may form larger structures	>nm: molecular scale
Examples	Thermal electromechanical Mixed mod Avalanche Intrinsic	Electrical trees Water trees Partial discharges	Bond scissions Nano-voids Traps formation Non-electrical changes (oxidation, etc.)

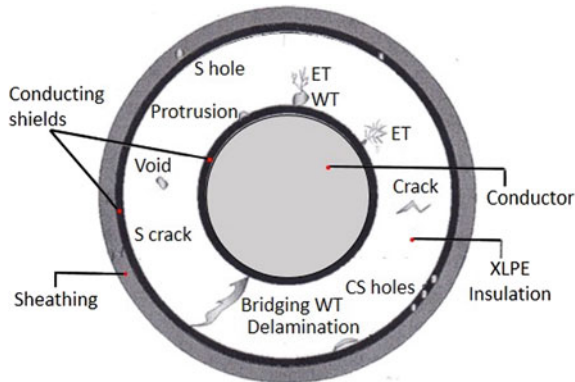


Fig. 11.11 Defects in insulation and shields of power cables (ET—electrical tree, WT—water tree, CS—conducting shield, S—sheathing) [19]

higher ones compared to those of partial discharges and trees initiation, which cause the degradation of the insulation [11].

The degradation of insulation under the action of the electric field is a process that runs faster compared to aging, causing a reduction in the breakdown strength and an important increase in the probability of insulation breakdown [10]. Breakdown is evidenced by the local transition of the insulation into a conductor, respectively, by

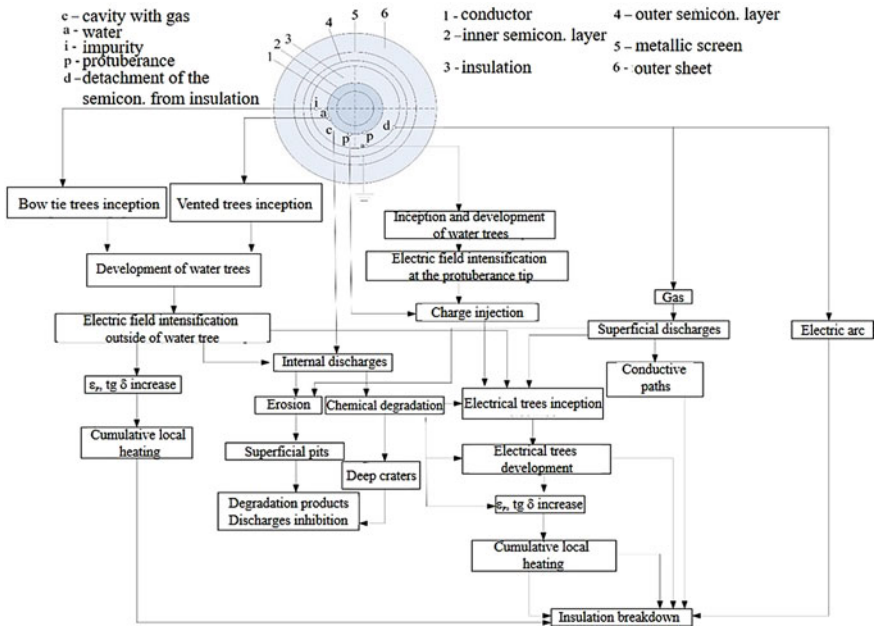


Fig. 11.12 General diagram of the physical processes leading to the breakdown of polymeric insulation of a power cable. Reprinted, with permission, from author [5]

the appearance of a macroscopic channel with conducting (semiconducting) walls that cross the insulation from the inner semiconductor shield to the outer one.

Unlike breakdown that is a sudden and catastrophic event (i.e., the insulation cannot withstand the service voltage following breakdown), degradation is a process that runs slower. After a period of hours to weeks, the degradation process leads to a breakdown (i.e., a discharge arc through the electrical tree or/and thermal breakdown if the tree is sufficiently conductive) [10]. A general diagram of the physical processes that take place within polymeric insulation, leading to the insulation breakdown, is shown in Fig. 11.12. It must be noted that, the aging is harder to be detected by direct methods, while degradation and breakdown are directly observable.

4 Failure Mechanisms

The failure of XLPE insulation is due to their slower or faster degradation under the action of intense electric fields occurring in certain areas of the insulation.

The degradation mechanisms of XLPE are related to the types of stresses (electrical, thermal, mechanical, environmental) to which the insulation is subjected during the operation of the cable, leading, in the end, to the insulation’s failure.

It should be emphasized that for the process of properties modification of the insulation under the action of (simple or synergistic) stresses, either the term aging [17] or degradation [18] is used in literature. Also, it should be noted that aging causes slow changes (deterioration) of the insulation's properties, while degradation involves macroscopic localized changes that lead to its breakdown in a shorter time than expected lifetime. In the following it will be analyzed the processes of XLPE insulations' degradation of medium and high-voltage cables under the action of the electric field (i.e., electrical degradation).

XLPE is formed by mixing low-density polyethylene (LDPE) with the activation chemical agent (i.e., dicumyl peroxide). During XLPE manufacturing process, several crosslinking by-products are formed. These include water bubbles formed inside the crosslinked polyethylene. Other harmful and reactive chemical agents such as acetophenone and cumyl alcohol are also formed during polyethylene crosslinking. In addition, while cooling down the cable, residual mechanical stresses are formed inside the insulation due to difference in the temperature gradients. These stresses may not be uniformly distributed across the cable insulation resulting in a large number of stress points. These stress points are the weakest points in insulation where electrical trees can be initiated, leading eventually to the cable breakdown [18].

On the other hand, during the curing process, crosslinking by-products are formed, too. Water is formed while crosslinking polyethylene and resulting XLPE. At the same time acetophenone and cumyl alcohol are formed in the quantity of 1 wt% of the fresh vulcanized insulation. Up to 99.5% of the peroxide will be consumed during the curing process. After degassing the insulation, the peroxide residual will be less than 4000 ppm and the water by-product should be less than 150 ppm [39]. The long-term performance of XLPE insulation can be improved by using additives that can improve the electrical and water tree retardant capabilities. Furthermore, antioxidants are added to the cable insulation to capture highly reactive and harmful free radicals.

Electrical degradation is a local phenomenon that does not affect the entire cable length [40] and is the result of three important mechanisms, such as: partial discharges, electrical and water treeing. The presence of contaminants, defects, protrusions and voids (CPDV) inside the insulation is the major stress point for these degradation phenomena. Practically, it is impossible to remove the presence of CPDVs completely from the polymeric insulated cables.

Cable terminations and joints are most likely sites for the formation of CPDVs and considered as the most vulnerable for the insulation degradation. However, CPDVs' influence on the insulation degradation is relatively small if their concentrations, shapes and sizes are controlled to very low levels during XLPE manufacturing process [41].

4.1 Partial Discharges

4.1.1 General Characteristics

Due to the presence of impurities and formation of gas bubbles during the manufacturing, installation and/or local insulation stresses during cable operation, micro-cavity and stress enhancement sites are formed within solid insulation or at the insulation/semiconductor layers interfaces. Formally, a cavity is defined as gas filled void and is a weak point of insulation as it has relatively lower electrical permittivity ϵ_r and breakdown strength as compared to the rest of solid insulation. This leads to local electric field enhancement, which may exceed the intrinsic field strength resulting in the initiation of self-sustaining electron avalanches [2].

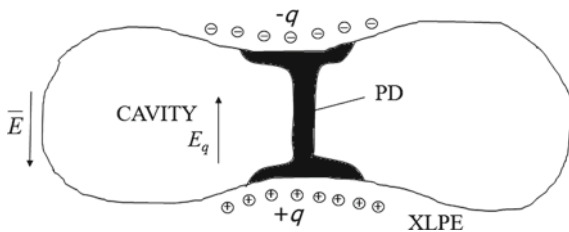
Partial discharge (PD) is defined as localized electrical discharge that only partially bridges the insulation between conductors and which can or cannot occur adjacent to a conductor [18, 42]. Partial discharges (PDs) appear as pulses with the duration of much less than 1 μ s [18]. PDs can occur at operating voltages in electrical trees, voids, cuts, cracks, fillers and contaminants with poor adhesion to the insulation and delamination at the interfaces [17].

PDs deteriorate the insulation (through combination of chemical, mechanical, thermal and radiative processes), but it does not cause immediate failure or breakdown. If PDs continue to occur for long time, it might take up to several years for complete failure of the insulation. There are two necessary conditions for initiation of PDs within a cavity, respectively, the electrical field must be larger than certain critical value E_c and free electrons must be available to start the electron avalanche [2]. If the electric field is below the E_c , the amount of electron generation is not sufficient to keep the discharge self-sustained.

The phenomenon of PDs is associated with the ionization of gas molecules. PDs ionize the gas in the cavity and the resulting charges move toward cavity surfaces in the direction of the electric field E (Fig. 11.13). These charges are trapped at the cavity surface resulting in a net accumulation of the cavity charge ($+q$ and $-q$) that generates an electric field opposite to the one existing in the cavity ($E_q < E$). As a result, the total electric field E_{tot} ($E_{tot} = E + E_q$) weakens, leading to the extinction of the discharge within the cavity.

During the PDs activity, it is quite possible that the electrical field in the cavity exceeds the critical value for PD ignition without starting any discharge. This might

Fig. 11.13 Schematic representation of partial discharges inside a cavity [18]



happen due to lack of free electrons. The average waiting time needed by free electron to appear when the electrical field condition for PDs is fulfilled is known as statistical time lag (τ_{stat}) [11, 18].

The Townsend theory is used to analyze the discharges (electrons avalanches) produced in gas cavities [2]. The dimensions of avalanche begin to grow very quickly, due to the change in the electric field distribution produced by the accumulation of positive space charge in the entire cavity volume. Due to physical degradation and injection of warm electrons, the anode surface becomes more (electrically) conductive. This, associated with the development of positive space charge, tends to enhance further the field in certain areas. The decreasing of the electrical resistance of the cavity and cavity tension causes a quick extinction of the discharge.

In general, the development of streamers in the XLPE cable insulation is conditioned by two essential conditions, such as: the existence of macroscopic cavities (tens of microns [11]) and the appearance in the cavities of some electric fields superior to the ones that initiate Townsend discharges. Their existence is due to water vapor, which cannot be evacuated outside during the quick cooling of the insulation. Concentration (c) and maximum cavity diameters (d_{max}) depend on the used crosslinking process. Thus, in the case of XLPE with peroxides $c = 10^5 - 10^6$ cav./mm³ and $d_{\text{max}} = 30 \mu\text{m}$ (if water vapors are used) and $c = 10^{3-6} \cdot 10^4$ cav./mm³ and $d_{\text{max}} = 15 \mu\text{m}$ (if hot nitrogen is used), and in the case of crosslinking with silanes $c = 10^4$ cav./mm³ and $d_{\text{max}} = 15 \mu\text{m}$. The ratio of the cavities' total volume and polyethylene in which they are located ranges from 0.7 to 7%, when the water vapor is used for crosslinking, of approx. 0.07% when silanes are used and from 0.007 to 0.4% when using hot nitrogen [5].

The mechanisms by which XLPE degrades in the presence of PDs have been the objective of numerous studies [43]. It has been found that PDs result in gaseous by-products (CO₂, CO, CH₄, H₂ and H₂O) [43, 44] and liquid droplets (mixtures of simple organic compounds, such as formic, acetic and carboxylic acids) [43, 45], in association with solids, such as oxalic acid crystals [43, 46] (Fig. 11.14).

Fig. 11.14 Cluster of crystals after 100 h of PD activity in a cavity in polyethylene © 2005 IEEE. Reprinted, with permission, from [45]

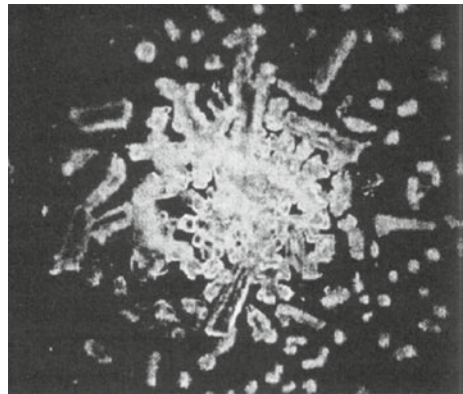
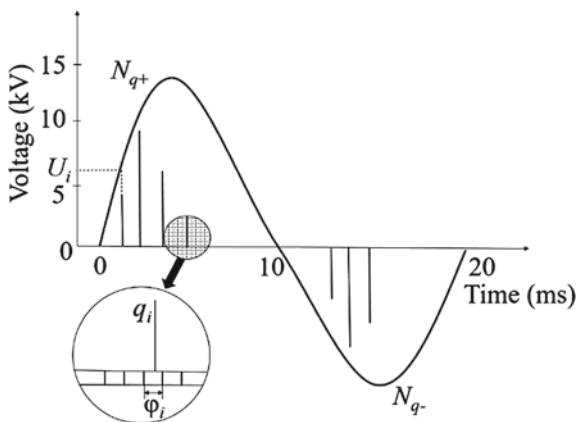


Fig. 11.15 Schematic diagram of partial discharges quantities



It should be emphasized that the droplets deposited in an earlier stage are crystallized at the point of PD impact [47, 48]. Oxalic acid causes a reduction in the level of PDs and, as a result, of the amounts of CO₂ and CO. If the cable is in a moist environment, then it is possible that discharges within its cavities may be extinguished due to both formation of acids within the cavities' walls, and to direct water ingress into the cavities [43].

In order to describe the characteristics of PDs, many quantities have been introduced:

- basic quantities (i.e., quantities observed during one voltage cycle) as the discharge of magnitude q_i , the apparent charge q associated to the PDs, the inception voltage U_i , the position of the discharge related to the phase angle φ_i of the test voltage and the number of discharges for each halve period of the voltage cycle N_q (Fig. 11.15);
- derived quantities (i.e., integrated values of basic quantities observed throughout several voltage cycles) and statistical operators (i.e., operators for the statistical analysis of the deduced parameters) [42, 49].

In terms of basic quantities are used, the maximum discharge magnitude $q_{i,max}$, the PD inception U_i and extinction voltage U_e , the position of the PD related to the phase angle φ_i of the test voltage and the number of discharges for each halve period of the voltage cycle N_q (Fig. 11.15) [42]. These quantities can provide information about the nature of a defect, its size, location and the extent of damage it may cause within the insulation [19]. Thus, the maximum discharge magnitude indicates the location and size of the defect in the insulation, the discharge pulse repetition rate indicates the severity of defect, the discharge phase angle indicates the defect's ignition condition, etc.

Derived quantities (e.g., the apparent energy W , the average discharge power P , the average discharge current I , the quadratic rate D , etc.) are obtained from the basic quantities measured for a large number of cycles (>100 cycles) and are analyzed as functions of time and phase angle [42, 50]. The quantities as function of the phase angle represent the recurrence of PDs related to their phase angle. Therefore, the

voltage cycle is divided into phase windows representing the phase angle axis (0 to 360°) (Fig. 11.15). Four quantities can be determined in phase window: the sum of the discharge magnitudes, the number of discharges, the average value of discharges and the maximum value of discharges.

By measuring pulse distributions as a function of the phase angle, it is possible to obtain information on the phenomena that cause these distributions [49]. For this following phase-position quantities can be processed: the pulse count distribution $H_n(\varphi)$, which represents the number of observed discharges in each phase window as a function of the phase angle and the mean pulse height distribution $H_{qn}(\varphi)$ that represents the average amplitude in each phase window as a function of the phase angle. $H_n(\varphi)$ contains information of the intensity of discharges as a function of their inception phase angle and allows the recognition of discharge sources and their behavior in time. $H_{qn}(\varphi)$ allows noise reduction due to the difference between the statistical characteristics of the discharge pulses and that of noise pulses as a function of phase angle [5, 6, 14]. Therefore, the $H_{qn}(\varphi)$ and $H_n(\varphi)$ quantities are characterized by two distributions, as follow: for the positive ($H_{qn}^+(\phi)$ and $H_n^+(\phi)$) and for the negative half of the voltage cycle ($H_{qn}^-(\phi)$ and $H_n^-(\phi)$).

As statistical quantities can be used, as follow: discharge asymmetry (the quotient of the mean discharge level of the $H_{qn}(\varphi)$ distribution in the positive and negative half of voltage cycle), phase asymmetry (the ratio of the inception phase of the $H_{qn}(\varphi)$ distribution in the positive and negative half of the voltage cycle), the cross-correlation factor (to evaluate the difference in shape of distributions $H_{qn}^+(\phi)$ and $H_{qn}^-(\phi)$), the skewness factor (to evaluate the asymmetry of a distribution with respect to a normal distribution), the kurtosis factor (to evaluate the deviation from the normal distribution), etc. [49].

4.1.2 Methods of Detection and Measurement

Non-electrical Methods

Non-electrical methods of PDs detection include acoustical, optical and chemical methods and where practicable, the subsequent observation of the effects of any discharges on the test object [42]. The *acoustic detection* is based on aural observations, the use of selective microphones with high sensitivity above the audible frequency range, acoustic transducers, etc. *Optical detection* is based on visual observations (in a darkened room) or the use of binoculars or photographic records. *Chemical detection* is based on gas analysis resulting from the insulation degradation under PDs.

Electrical Methods

The electrical meaning of PDs detection can be classified into detection for internal, surface and corona discharges. Surface and corona discharges are accompanied by

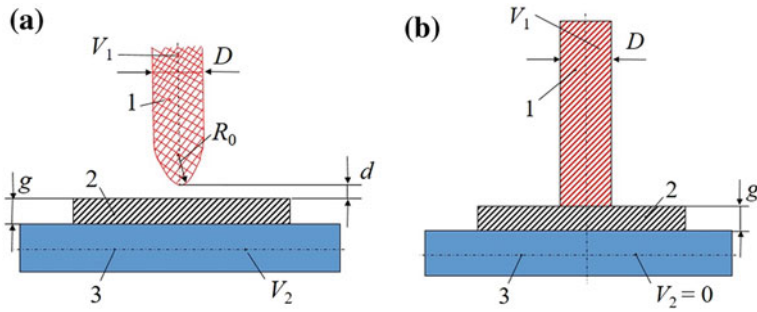
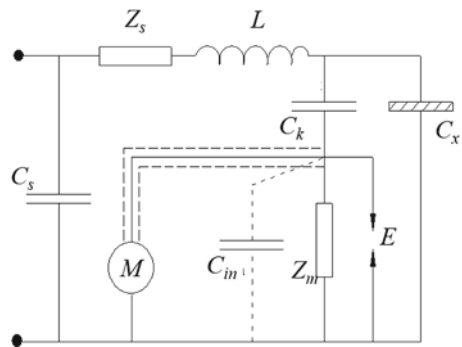


Fig. 11.16 **a** Rod-plane electrode configuration for partial degradation tests: 1: Rod electrode; 2: Specimen; 3: Plane electrode; **b** Rod-plane electrodes system (similar to IEC electrode) for surface erosion by PDs. Reprinted, with permission, from author [53]

Fig. 11.17 Parallel scheme for PDs measurement. Reprinted, with permission, from author [54]



large discharge magnitudes and usually occur at the insulations' surface or at sharp points around conductors [51]. Surface and corona discharges are generally less harmful as compared to internal discharges, which are triggered in cavities internal to the insulation with low discharge amplitudes and are often hidden or mistaken for disturbances [52].

To study the PDs action on insulations, different types of setups are used, including comparably simple ones (Fig. 11.16) that consist of a rod electrode from a tungsten wire with rounded tip, connected to the high-voltage terminal of an AC supply and a plane electrode connected to the ground. The sample to be analyzed is placed between the two electrodes (Fig. 11.16a) [53]. In the case of an electrical equipment insulation (cables, joints, electrical machines, etc.), installations with a more complex structure are used (see [54]).

Due to the PDs in the cavities, the voltage applied to the insulation drops rapidly for short periods, resulting in successive voltage pulses, which are reflected in the cable supply circuit by the occurrence of current pulses. As a result, PDs detection is based on the detection of voltage or current pulses. In Fig. 11.17, direct detection and measurement scheme of PDs are shown, where C_x represents the object to be tested,

C_k —coupling capacitor, Z_m —measuring impedance, M —measuring device of PDs parameter, E —protective gap, Z_s —internal impedance of the source, C_s —capacity of source output and L —filtering inductance (at high frequencies).

In some XLPE insulation, the detectable PD inception voltage may be much higher than the PD inception voltage appearing in small voids adjacent to projections with a high stress enhancement factor [55]. The smallest value of the inception voltage, regardless of the apparent charge generated, is called ‘threshold voltage.’ This name has been adopted in order to distinguish it from the ‘inception voltage’ which is determined by the PD detection system.

4.1.3 Influence of Partial Discharges

Although DPs have a reduced duration (10^{-8} s), they develop in smaller volumes compared to cavity volumes and the transported charge and energy have very low values that contribute to the worsening of the XLPE insulation characteristics due to:

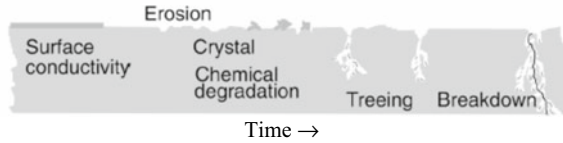
- (a) the rise of local bodies temperature (due to the collisions of charge carriers with gas molecules and cavity walls);
- (b) the erosion of cavity walls produced by the charge carriers;
- (c) the radiation generated by atoms excitation and charge carriers recombination;
- (d) the intensification of chemical degradation reactions of the insulation and the initiation of new chemical reactions (due to the temperature increase).

Degradation due to PDs is localized and minute in magnitude, nonetheless it can cause progressive damage that in time leads to the equipment failure [51]. In [2], it is shown that PDs degradation is due to the chemical reactions between the excited molecules (especially, oxygen) and the polymer, the chemical reactions between molecules in metastable states (e.g., ozone), between them and the molecules from dielectric in which they diffused, the bombardment of the cavities surface with electrons and ions, the production of high energy gases (which causes local heating, softening and degradation of the dielectric), etc. As the mechanical shock waves produced have relatively low energies (below 0.1 J), the general fracturing of molecules is unlikely. However, on the surfaces of the cavities appear small craters, which, due to the intensification of the electric field, can lead to the occurrence of electric trees and, therefore, the insulation failure.

Ions Action

The experiments on samples containing nitrogen cavities showed that PDs cause the appearance of pits and craters on the cavity walls as a result of ions bombardment. Although the ions’ own energies are generally not large enough to cause intermolecular breakage (i.e., the fracture of macromolecules), the concentrated action of ions in a streamer on small areas [11] associated with the rise of local temperature (with a

Fig. 11.18 Stages of PD-induced damage at the XLPE surface [56]



few hundred Kelvin) is enough to produce these defects on the surfaces of the cavities. Mason [62] has estimated that the erosion of material produced by a discharge can reach 10^{-21} m^3 (a cube with the side of $0.1 \mu\text{m}$).

In the case of XLPE, this degradation progresses at a reasonable rate, if the charge density corresponding to the ions exceeds 150 C/m^2 . However, the effect of electrons' bombardment is insignificant, since their required energy to produce superficial damage must exceed 500 eV . Ions' bombardment does not generally lead to the initiation of a significant degradation process, but can play an important role in enhancing the existing degradation process. For example, in the case of micro-cracks due to the mechanical or chemical stresses, ions' bombardment will contribute to their deepening, followed by chain cracking and/or electric tree, and, finally, by a breakdown.

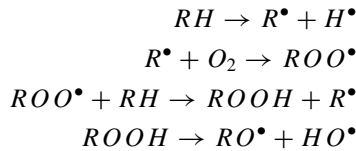
The degradation process of a XLPE under the PD action follows the steps [45]:

1. The conductivity of the cavity surface increases due to the reaction processes of humidity and the dissociation products of air caused by PDs;
2. The surface roughness increases due to charge carriers' bombardment and deposition of PDs by-products;
3. PDs activity leads to the formation of localized solid by-products (hydrated oxalic acid);
4. The field enhancement at crystal tips leads to a further intensification and localization of the PDs process and pit formation. Consequently, the electrical tree is initiated;
5. The tree growth may lead to breakdown (Fig. 11.18).

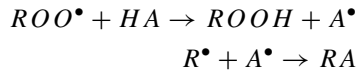
Action of Chemical Agents

Relatively high-energy values involved in an electrons' avalanche allow the production of highly active oxygen species (e.g., O , O_3 , O_2^-) and the development of endothermic reactions. A uniform degradation (due to the oxidation of molecules) of the cavity walls (as a result of the diffusion of these particles in the insulator) occurs in contrast to the formation process of cracks activated by ions' bombardment. The effect of several air constituents on polyethylene has been analyzed in many cases (due to the multitude of conditions in which XLPE insulated cables can be found) [11]. The most important and most active factor is oxygen. In the absence of oxygen, the only possible reactions that involve breaking C–H and C–C bonds and the formation of free radicals, C–C bonds and the appearance of crosslinking. In the presence

of oxygen, if sufficient energy is provided to form an R^\bullet radical, OH groups can be build-up according to the reactions:



This chain reaction stops if the supplied energy is consumed or if there is an antioxidant (HA) that reacts with the radical R^\bullet :



In the case of the existing XLPE cavities, the occurred PDs lead to the formation of oxalic acid (i.e., due to humidity, oxide and carbon dioxide, oxygen and acetophenone in the cavities). As a result, the cavity surfaces become semiconductor, voltage drops in cavity are reduced and discharges are extinguished. Obviously, the volume resistivity of the insulation is reduced if it is maintained for a certain time at a voltage above the inception one of PDs (U_i).

PDs also produce nitrogen oxides and carbonates, which can also lead to the degradation of cavity walls over a longer period. However, under the action of PDs, cavity walls are oxidized and eroded. Initially, the walls oxidation alongside to an increase in the cavity volume occurs. Then, the streamers inject locally the electric charges, facilitating the local oxidation and the appearance of semiconductor zones ('spots'). This causes a more significant localization of streamers, avoiding damaged areas with increased electrical conductivity.

Initiation and Development of Electric Trees

To explain the initiation and the propagation of breakdown channels in polyethylene insulation as a result of cavity discharges produced within cavities, a simple model, proposed by Badher [55], which is based on charges injection from cavities to polymer, can be used. Starting from the idea of a non-zero permeability of polymers for fluids, Badher believes that there is a very fine network of channels in the polymer that makes connections between cavities and/or microcavities [57, 58]. The occurrence of PDs into these cavities is originated by an existing electron in the gas or by a created electron by cold emission from the cathode. Considering the studies [59–63], Badher believes that the inception voltage stress of voids encapsulated in the polymeric insulation is close to that appearing between metal electrodes and can be defined by the Paschen curve [2]. Since cavities with diameters substantially larger than 0.01 mm are commonly observed in XLPE insulations, the PDs appearing in such insulations originates from the existing electrons in the gas rather than from

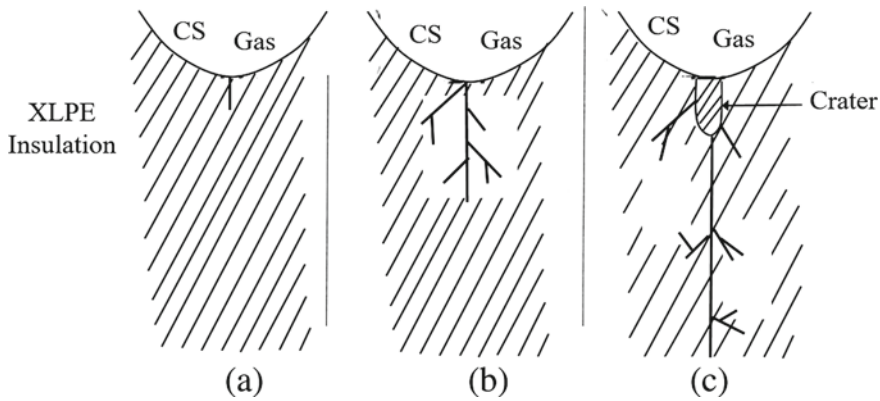


Fig. 11.19 Tree-like pattern of space charge flow into channels of XLPE insulation [55]

the cold electron emission [63]. If the voltage stress increases further above the PD threshold level, then the space charge previously deposited on the cavity surface enters the gas channels existing in the structure of the polymeric insulation adjacent to the cavity. The entry of the space charge into gas channels occurs in discrete places where the diameter and the shape of the gas channels create favorable conditions for the flow of charges at the applied voltage stresses (Fig. 11.19a). In the gas channels, the space charge moves along the paths resembling tree-like patterns (Fig. 11.19b). The degree of branching of the space charges' paths depends on the structure of the polymeric insulation, especially on the diameter and the distribution of the gas channels within the polymeric insulation.

The small diameter of the channels generates very high-voltage stresses at their tips that accelerate the charged particles (space charge), which collide with the neutral gas particles and with the channel walls. As a result, ionization takes place in the gas, and decomposition occurs in the polymeric insulation adjacent to the channels. These collisions also lead to high-energy losses and to a decreased density of the space charge along the channels. The branching of the charge flow pattern causes additional decrease in the space charge density. Consequently, the voltage stress and the intensity of ionization 'at the tips' of the space charge decrease with the progression of the space charge into the channels.

For values of the electric field higher to the threshold level, the charge carriers progress along the channels to a depth at which the electric field 'at the tips' of the space charge is less than the minimum electric field necessary for the charge carriers propagation in the channels. In the case of a field equal to the dielectric strength of the insulation, the electric field at the branch tips of the moving space charge does not drop below the minimum value required for flow along the channels. At a certain depth of charge flow in the channels, a self-sustaining ionization of gas develops in one of the channel branches. This self-sustaining ionization leads to the formation of an electric tree and, ultimately, to the complete breakdown of the insulation (Fig. 11.19c).

Fig. 11.20 Breakdown channel in a XLPE sample. Reprinted, with permission, from author [64]



A degradation process of the XLPE insulation may take place when the energy of the charge carriers in the cavities (i.e., electrons, ions) exceeds 10 eV (for producing scissions of hydrocarbon chains). The highest degree of degradation will occur in the localized areas where the electric stress is the highest, respectively, where the narrow channels become filled with space charge and act as conducting projections in the insulation. Due to the high field strengths, the charges penetrate the unaged insulation in a tree-like pattern for a few molecular distances only. The flow of charges forward and backward along the channels causes the scission of molecular chains of insulation adjacent to the channels and in this way increases the diameter of the channels. The greatest amount of charge flows in the stem of the tree-like pattern, its diameter increasing faster than the diameters of the branches, forming a crater (Fig. 11.19c).

The voltage drop along a crater is significantly reduced as compared to the voltage drop existing at the charge flow in the original channel. As a result, there is an increase of voltage stress at the end of the tree-like charge flow pattern, and consequently, the charge will penetrate deeper into the insulation. As the depth of the crater increases, the voltage stress at its end increases and the charge penetrates deeper into the gaseous channels adjacent to the crater. Once the crater achieves a critical depth, the electrical field at its end becomes sufficiently high for development of local PDs, which are independent of the PDs in the cavity. These local PDs lead to an electric tree that causes the complete breakdown of the insulation (Fig. 11.20) [64].

Badher's model was developed by Notingher [14–16], which takes into account the energy transported by PDs into the cavities and transferred to their walls. A parabolic cavity with a gas of permittivity and initial pressure known is considered. By using Poisson's equation (for the electric field E), Fourier equation (for the temperature T) and gas state equation developed inside a cavity (for the gas pressure p), the values E , T and p are initially calculated, followed by the minimum values of the electric field intensity E_{\min} in the cavity and the superficial power density $p_{s\min}$ transmitted to the cavity walls (crater, Fig. 11.19.c) by the PDs for a breakdown channel initiation. In addition, the initiation and development periods of a breakdown channel are calculated. It is demonstrated that if the conditions for initiating a channel

from an existing crater (produced, e.g., by mechanical stress), $E > E_{\min}$ and $p > p_{s\min}$ are fulfilled and sufficient for further development of a thermal breakdown channel with a relatively large diameter (tens of μm).

In general, charge carriers erode the surface of the samples and the walls of the channels [65]. Considering the harmful effect of PDs, in the case of high and very high-voltage cables insulation, restrictions are imposed on cavities dimensions and concentrations, such that their apparent charge does not exceed certain limits. For example, for $U_o = 110$ kV voltage cable and a XLPE insulation, the apparent charge measured at voltage $U = 1.5 U_o$ should not exceed 10 pC. However, PDs may occur at high-voltage cable joints interfaces manufactured from two distinct insulating layers due to the defects introduced during the technological process or during operation (i.e., metallic particles, fibers, cavities and layer depletions) [66].

4.1.4 Experimental Results

Numerous experimental results highlight the influence of PDs on aging and degradation of power cables XLPE insulation and underline the fact that PDs are responsible for the initiation of electrical breakdown [55]. Thus, the studies [67–70] showed that a very small PD plays an important role in aging and degradation processes of XLPE insulation. However, by using more accurate detection equipment for PDs and a cable samples of 20 m, in [71] appears that after an accelerated thermal aging (90 °C) and 15 kV/mm (for 6 months) no correlation between aging and PDs activity could be established in these samples. It could be possible that the aging time is too low for important physical transformations (increase in the cavities volume) in insulation.

The XLPE insulation behavior of a medium voltage cable (24 kV) with a thickness of 4.3 mm is analyzed in [18]. Within insulation are produced cavities of 10 μm , and the samples were subjected to a voltage of 15 kV for 500 h. It has been found that the PDs charge has increased with the duration of stress and the PDs intensity increased sharply once the electrical treeing starts, resulting in severe degradation of the insulation. The highlighting of a direct relationship between PDs level and aging (degradation) of the XLPE insulation of medium voltage cables is analyzed by Wolzak et al. [71]. The authors developed a PDs detection equipment with charges below 1 pC. Then, measurements of PDs parameters on 30 m length samples of 30 kV cables unaged and electrically and thermally aged (at 15 kV/mm and 90 °C) were performed for two months. In the meantime, the results showed no significant aging and therefore no correlation between aging and PDs activity could be established (due to the reduced test duration).

An analysis of the products nature that arise as a result of the PDs action on the cavity walls of XLPE cable insulation was presented by Gamez-Garcia et al. in [72] and [43]. The authors subjected XLPE foils (of 160 μm in thickness) to PDs action and analyzed the resulting chemical compounds. It was shown that, under PDs action, both gaseous (CO , CO_2 , H_2O) and liquids and solids products resulted. The liquid and solid products have been found to result from synthesis reactions taking place in the vapor phase across the interelectrode gap-space. Acetophenone, which

evaporates from the XLPE surface after the crosslinking, plays an important role in the formation of other observed degradation products. Benzoic acid, benzamide, toluene and other aromatic compounds result from corona-chemical reactions of this volatile compound during the degradation process. The influence of temperature on XLPE degradation under PDs is analyzed by Gamez-Garcia et al. in [73]. The authors studied the modification of XLPE exposed to PDs at temperatures up to 160 °C using an air gap of 50 μm . A change in nature of the reaction products at the gap surface was found, but more important, enhanced bulk and surface oxidation was observed with rising temperature.

The introduction of power electronics systems (inverter stations) has led to a XLPE cable insulation stressed with repetitive transients of relatively high frequency [74]. As a result, PDs have a strong detrimental effect on the insulation due to short rise time of voltage surges [75]. The effect on the PDs behavior of the resulting voltage distortion is not satisfactorily explained yet. An intricate interaction between injected space charge and PDs activity complicates the understanding of these processes [45].

Several authors [76, 77] have used simultaneous optical and electrical recording of the PDs process to obtain information on their physics. For flat cavities in polyethylene, Morshuis [76] found a characteristic pulse shape for every aging stage. Initially, narrow pulses of large magnitude (streamer-like) appear in the virgin cavity. These PDs discharge only part of the cavity surface and often parallel PD events are seen, both in the electrical and optical recordings (Fig. 11.21a). When a conductive layer appears at the cavity surface, the PD pulse shape becomes wide and of low amplitude (Fig. 11.21b). In the aging stage when crystals appear, the PD pulse shape changes to small amplitude and intermediate pulse width (Fig. 11.21c) [76].

The PD acts as a source of charge injection into the dielectric resulting in a modification of the space charge density inside or on the insulation surface [45, 78].

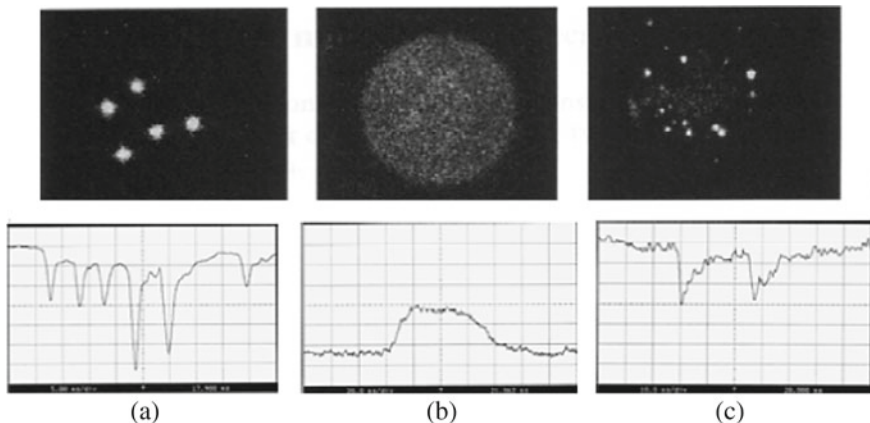


Fig. 11.21 Optical (top) and electrical (bottom) recordings of PD activity: **a** Parallel, streamer-like PD events in a virgin, polyethylene cavity; **b** Single, diffuse Townsend-like PD in a slightly aged cavity; **c** Minute discharge pulses (pitting) in a significantly aged cavity [76]

Thus, a part of the charge involved in the discharge process is trapped at the cavity surface and part of the charge migrates deeper into the dielectric. This contributes to the modification of the electric field distribution and to the facilitation of the insulation failure.

Mechanically pre-stressing insulation can definitely have a beneficial effect on insulation resistance against PDs [79]. While many constructions could benefit from well-designed pre-stressing insulations, the effect of mechanical stress on PDs is often disregarded and deserves more attention. It should be noted that, based on the experimental results obtained, various mechanisms have been proposed through which PDs affect the XLPE insulation [55]. Thus, Mason [80] believes that mainly localized heating causes the detrimental effect of PDs. Artbauer [81], Frohlich [82], Yoda and Sakaba [83] take into consideration the detrimental action of hot electrons. Golinski [84] suggests that the discharges between ionization centers existing in the polymer insulation are responsible for the breakdown. Bahder, Dakin and Lawson [85] conclude that scissions of molecular chains, caused by the electric charges moving forward and backward in the insulation, are the most detrimental effect of PDs, etc.

4.1.5 Partial Discharges Effects Attenuation

The reduction of PDs level may provide high reliability for a XLPE insulation, so that many methods have been attempted to eliminate PDs. The most effective method is the suppression of the voids in the insulation [86]. However, the voids removal is very difficult in the case of insulation systems made of two layers of different polymers (XLPE + EPR, XLPE + EPDM, etc.). Although the compositions are prepared carefully in order to keep it free of air at the interfaces, however, during the system operation, the two layers may be separated by heat, vibration, etc., appearing certain voids to interfaces. In these voids, the electric field is more intense than in the polymer [2] and PDs may appear. Therefore, it is necessary to establish methods for achieving PDs free insulation, even if the voids occur during operation.

A widely used method in manufacturing XLPE insulations for HV power cables consists of introducing additives that inhibit PDs initiation and development processes. Thus, it is known that the depth and number of charge traps in a polymer can be controlled by the radicals type in the molecule and by additives, electron donors or acceptors [86, 87]. In the case of an electron acceptor radical, if the surface of the material with the additive is in contact with the surface without additive, the surface with additive tends to be negatively charged after accepting the electron to the radical. In this case, it is considered that the electron trap sites are brought about in the material as a result of the additive. In the case of an electron donor radical, the surface tends to be positively charged. Therefore, if an additive is added to the insulating material that forms the walls of a void, PDs in the voids might be diminished (as a result of prevention of the secondary electron emission due to electron trapping on the wall).

This phenomenon is highlighted by Yamano et al. [86], in experiments carried out on PE samples with azobenzo additives. The samples used were sandwiches made of 5 layers (films) of PE. The middle layers of the samples contained three cavities with a diameter of 1 mm and for some of the samples the adjacent layers were coated with additives. The authors used four types of azobenzo compounds, namely Azobenzene (Az), Y-Aminoazobenzene (Az_a)—containing a NH_2 radical, P-Nitroazobenzene (Az_n)—containing a NO_2 radical and P-Nitrobenzeneazo-resorcinol (Az_{hn})—which contains a NO_2 radical and two OH radicals. For the characterization of PDs, the values of charge impulses related to discharges were measured. The performed tests showed a reduction in the level of PDs in the samples in function of the type and concentration of the additive [86]. This decrease is due to the excitation of additives, charge traps introduced by the additives' molecules and the increase of the electrical conductivity of the cavity walls.

The stimulation of the additives is due to electrons generated by PDs in the void that will attach to the XLPE wall of the anode side. When the electric field (AC) is reversed, the wall on which an electron is attached will become the cathode, and the positive ion will collide with the cathode wall. Some of the electrons on the wall will be emitted if the positive ions have the adequate range of the kinetic energy and the energy is delivered to the electrons. This may correspond to the secondary electron emission in the case of insulating surfaces charged with electrons. The secondary emission enhances the PDs generation and supports the sustenance of the PDs. However, the azobenzo compounds absorb UV energy in the range of 2.8 and 3.8 eV. Thus, if the azobenzo compound added to the insulating wall can absorb this range of kinetic energy of the positive ions at the collision, the secondary electron emission might be reduced, which will lead to diminished PDs in the void.

The second factor is the influence of charge traps introduced by molecules of the additives. Electrons generated by PDs in the void will attach to the insulating wall of the anode side. When the AC electric field is reversed, some of the attached electrons on the wall will be removed. This may correspond to the first electron emission in the case that the surface is charged with electrons. The emitted electrons drift to the opposite side of the wall. The number of electrons removed from the wall depends on the number and depth of the electron traps on the wall surface of the void.

Nevertheless, the type of radicals on the additive molecules significantly influences the condition of charge traps on the void surface with additive. Thus, in the case of an electron-accepting radical, the additive near the surface of the anode wall is negatively electrified after that the additive has accepted the attached electron. This electron acceptance corresponds to an electron trap. The trapped electron cannot remove from the wall surface by the electric field if the trap level is sufficiently deep. Furthermore, the trap from the additive will decrease the secondary electron emission and PDs in the void will be diminished.

The third factor is the increase of the electrical conductivity of the cavity walls by introducing the additives (about 2.5 times), which leads to a reduction of the electric field in the cavities and thus to an increase of the initiation voltage (U_i) of the PDs.

Experiments showed that the number of pulse events in the voids for PE with additive is 80% less than in PE without additive. The concentration used was in the range of 0.05 to 0.5%wt., and the best concentration appears between 0.05 and 0.1%wt. [86].

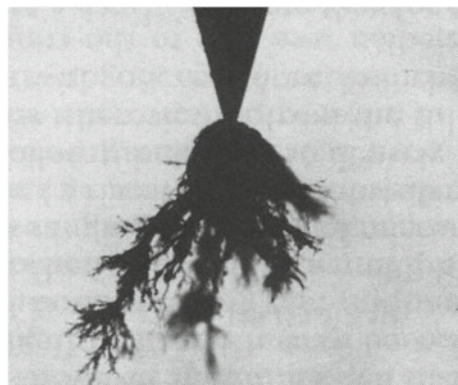
4.2 Electrical Treeing

4.2.1 General Characteristics

Electrical treeing is one of the main causes of damage and failure in electrical power cable with XLPE insulation [11]. Electrical trees are very fine channel networks (including gases at high pressures) initiated near insulation and/or electrodes defects, which develop in the insulation during the electrical equipment operation [2, 54]. Propagation of the electrical trees into XLPE solid insulation can bridge the electrode gap, leading to the breakdown of the insulation. Nevertheless, the breakdown does not occur when the channels of the trees reach the opposite electrode. In general, a certain time is required for thin channels to turn into thick ones, which are able to cause a breakdown [53].

The electric tree channels (Fig. 11.22) are formed by the local destruction of the material under the synergetic action of the electric field, the PDs (from the voids and channels), the heat and the mechanical stresses produced by the electric field and the gases from the channels (resulting from the material decomposition). The electric trees initiated near the electrodes are called vented trees, and they are developed from the electrode to the 'inside' of the material (Fig. 11.23). In contrast, the ones generated inside the insulation (near voids, metal inclusions, etc.) have a channels structure developed along the electric field lines on both sides of the defect (electric field concentrator) and they are called bow-tie trees [2]. The branch trees (Fig. 11.23.a) are networks of thin and thick channels. In bush trees (Fig. 11.23.b), the empty and

Fig. 11.22 Vented electrical tree in XLPE. Reprinted, with permission, from author [2]



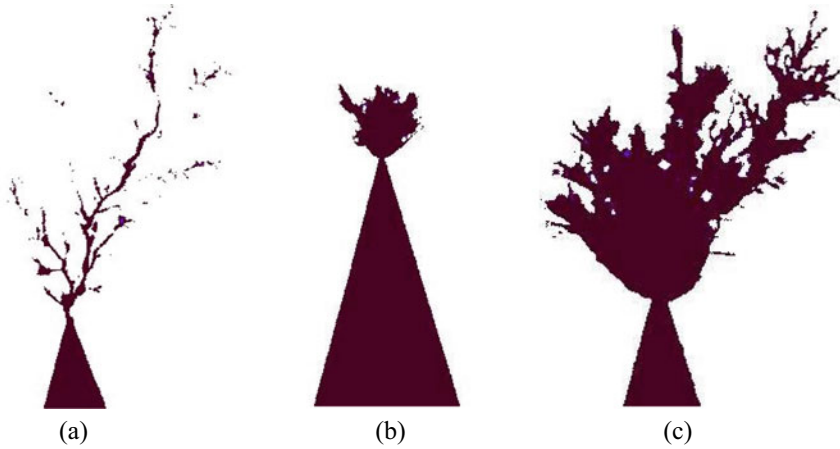


Fig. 11.23 Shapes of electrical trees: **a** branch-type tree; **b** bush-type tree; **c** bush-branch tree. Reprinted, with permission, from author [2]

very fine channels are so ‘tightly packed’ that they appear as a solid mass of a bush shape. The bush-branch trees (Fig. 11.23.c) are, in fact, bush trees with one or more branches exiting from inside the bush.

The electrical treeing has been studied in the laboratory, using electrodes with special shapes, in order to intensify, locally, the electric field. The most used system of electrodes is the system needle-plan (with metallic needles or needles from thin strips of semiconductor polymeric materials). With this system of electrodes, electrical treeing has been achieved by applying alternative or step (continuous) voltages, performing some electrodes shortcuts or reversing their polarity, applying some voltage impulses, etc. The electric trees made in PE with needle-plan electrode in harmonic fields of 50 Hz has form of trees (or branches) for $E < 5.4$ GV/m, shape of bush for values of E ranging between 5.4 GV/m and 6 GV/m and shape of bush-branch for $E > 6$ GV/m (these values decreasing with the increase in the frequency).

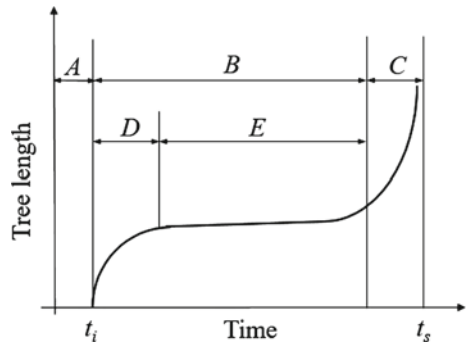
The inception of the electric trees is characterized by a long duration of inception t_i , defined as ‘the required timeframe for generating a noticeable tree (with the length of 10 μm usually) or detectable by non-optical methods.’ The t_i duration is strongly influenced by the electric field intensity, according to the relation:

$$t_i = A E^{-a} \quad (11.7)$$

where A is a constant of material and $a \in (5, 20)$ [2].

For each polymer, a critical inception field E_i is defined. Its values are much higher in AC compared to DC (0.5 GV/m), which is assigned to the reduction effect of the field by the formed space charge. For higher rate ($\gg 5$ GV/ms), the space charge does not have enough time to form itself completely and the critical field reduces to a higher value of the dielectric strength. If the tree is initiated by PDs in a void

Fig. 11.24 Schematic representation of the development of an electrical tree: *A*—inception stage; *B*—development stage; *C*—runaway stage (preceding the breakdown); *D*—area of slow growth; *E*—area of slow propagation. Reprinted, with permission, from author [2]



located on the top of the needle electrode, the critical inception field depends on the sizes of the void, taking values between 1 GV/m—for sub-micron voids - and 3.5 MV/m—for large voids (over 1 mm).

The propagation of the electrical trees is made, in general, with a lower rate in the first development stages, area *E* (Fig. 11.24) being called slow propagation area. If, after a certain time, the rate increases (Fig. 11.24, area *C*), it will (certainly) lead, for $t = t_s$, to the development of a very long tree, respectively, to the breakdown of the sample.

The process of electrical trees propagation is discontinuous, with sudden growth in the trees sizes (for instance, length L), followed by local failures. During τ_c of the first sudden growth (corresponding to the area *D*, Fig. 11.24), where the tree reaches the length L_m , its length at the time t (respectively, $L(t)$) can be calculated with the equation:

$$L(t) = L_m \left[1 - \exp\left(-\frac{t - t_i}{\tau_c}\right) \right] \tag{11.8}$$

After the formation of the first branch, the tree develops by forming other branches after a certain time. The stagnation stage of the tree growth is regarded as an inception stage (incubation) for the occurrence of a ‘cleavage’ of the (initial) branch (channel). During this time, PDs extend on the newly formed channels, contributing (by the energy sent to their walls) to the increase of their diameters (and of the lengths of the last formed branches). It is considered that for XLPE, in order to continue the tree propagation, a higher intensity DC electric field of a threshold value $E_p = 0.85$ GV/m for the positive polarity of the needle electrode and 1 GV/m for its negative polarity is necessary. After the formation of a certain number of branches, some of those keep on growing, while others stagnate. This evolution is to be noticed until the stage of ‘accelerated’ development (Runaway Stage *C*, Fig. 11.24). It is noticed that the full description of the tree development stages is not possible with the relation (11.8) (Fig. 11.25).

The temporary cease of the electric tree development is due to the impossibility of eliminating the gas resulting from the polymer decomposition. This phenomenon

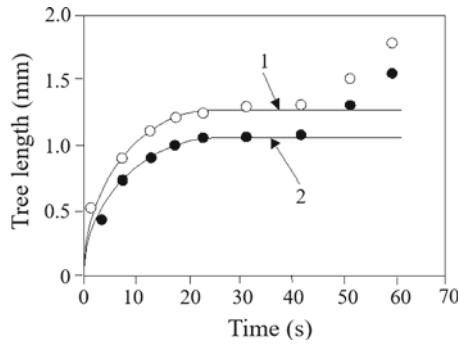


Fig. 11.25 Variations in time of the electrical trees lengths in two types of XLPE (1 and 2), established experimentally (empty and full circles) and by calculation with the relation (11.9) (continuous line). Reprinted, with permission, from author [2]

was highlighted on voids allowing for gas exhausting and, with the aid of which, it was possible to demonstrate that the trees length depends directly on the size of the applied voltage ($L \approx U^4$) and of its frequency ($L \approx f^{-1/3}$) (Fig. 11.26) [87].

In the final stage of tree development, its accelerated increase occurs, corresponding to a fast development on branches, in the shape of some filaments (with diameters of $\approx 1 \mu\text{m}$), which lead to breakdown of the insulation. However, the breakdown does not occur as soon as the tree channels completely crossed the testing sample [2].

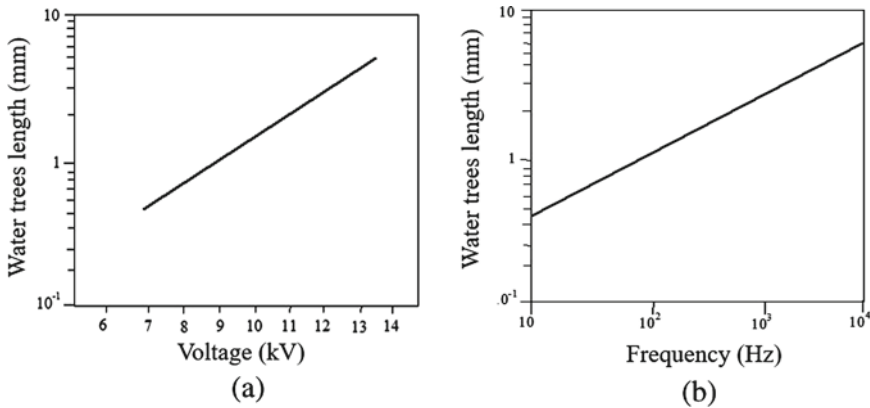


Fig. 11.26 Variation of the tree length with voltage (a) and frequency (b) [11]

4.2.2 Inception of the Electrical Trees

The most recent theories consider the inception of the electrical trees as a process of local breakdown occurred as result of the local intensification of the electric field over the material dielectric strength E_b . This occurs in relatively reduced areas in the neighborhood of the insulations defects (protuberances, voids, impurities, etc.), which will delimit nevertheless the lengths of the initial trees channels lengths. The higher values of the inception field than E_b are explained for the DC voltages by the presence of the space charge that (locally) reduces the electric field intensity. For the AC electric fields, the trees inception field takes lower values than E_b , as the injected charges do not move very far. In addition, it is considered that resulted heat due to the dielectric losses may cause a void or that the Maxwell stresses may cause a fissure where PDs occur, leading to electrical treeing.

A needle electrode introduced, at room's temperature, into a XLPE sample is presented in Fig. 11.27a. It can be noticed an area of deformed PE around the needle top, produced by the pressure exerted by the needle. After applying the needle-plan electrodes voltage, due to the electrical and thermic stresses, this area reduces continuously its mechanical properties, generating a void (Fig. 11.27b). PDs occur in the void due to which an electrical tree will be initiated (Fig. 11.27c). Same phenomenon occurs also if, at the needle top, a micro-crack or a crack occurred (Fig. 11.28). If several cracks were created at the top of the needle, two or more

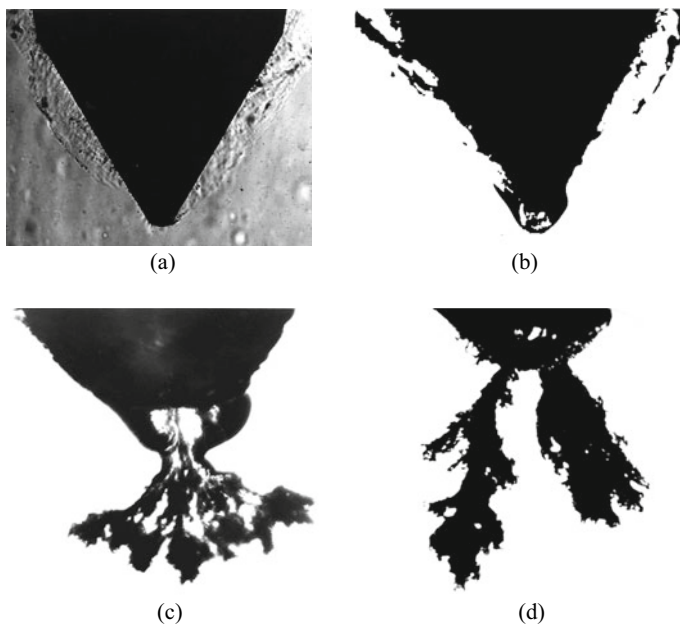


Fig. 11.27 Trees initiated in a void produced at the needle top in a sample of XLPE. Reprinted, with permission, from author [2]

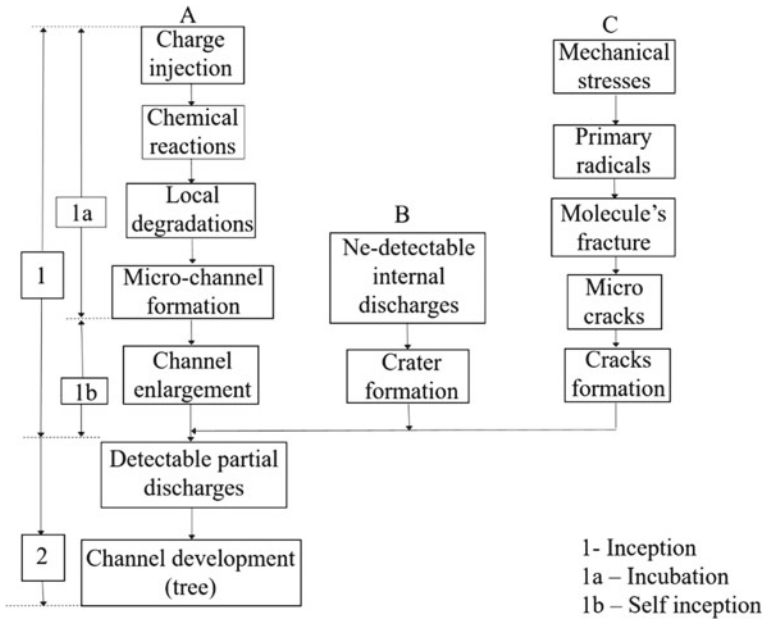


Fig. 11.28 Models of inception of the electrical trees. Reprinted, with permission, from author [2]

channels can be initiated (Fig. 11.27d), and the tree development will correspond to the channel situated in the area of maximum intensity of the electric field. In the absence of mechanical stresses or cracks, the space charge plays an important part in initiating the electrical trees, especially as the charge injection is made in fields ranging between one-fifth and one-third of the E_b for the homogenous samples and reaches $E_b/10$ —for the non-homogenous samples. For XLPE, the critical field of injection of the space charge is $E_{ss} = 0.1$ GV/m.

The models of electrical trees' inception under the action of the injected charge of PDs and of mechanical stresses are presented (schematically) in Fig. 11.28.

The electrical charge issued by an electrode may move inside the polymer if the electric field goes above a critical value E_{dc} . The depth of penetration of the space charge 'cloud' depends obviously on the voltage applied to the electrodes. In the typical tests, the values of the electric field are approx. 1 GV/m and the depth of penetration of the space charge is up to 10 μm [2].

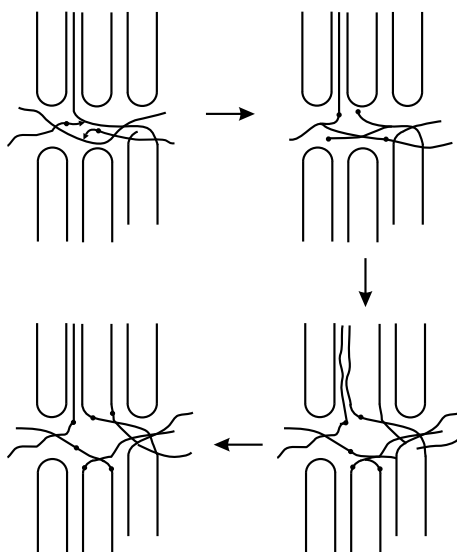
In general, it is considered that the time of the trees inception is highlighted more by the occurrence of some current impulses. Certain charge impulses can be noticed in PE before the first channel is visible, but they have relatively low amplitudes (0.04...0.3 pC). These impulses correspond to the extractions of some electrons held in deep traps. The charge density corresponding to these impulses may be of the order of 10^{-3} ... 10^{-2} pC/ μm^3 and the volume that this charge takes may have values of about 10^3 μm^3 .

The extraction of the charge carriers to give current impulses occurs only when the local value of the electric field caused by hetero-charges reaches a value sufficiently higher to generate an electrons avalanche, which starts to ‘erode’ the polymer. Thus, the electrons accelerated by the electric field accumulate enough (kinetic) energy to ionize the polymer (>10 eV), to form cationic radicals (<10 eV) and to break the polymer bonds (≈ 3.5 eV). The electrons captured by the cationic radicals lead to the formation of free radicals that can cause breaks (scissions) of molecular chains.

An important factor intervening in the inception of the trees is the spatial distribution of the injected charge. If the electrons extraction follows the electric field lines, the electrons injection is spatially homogenous. In this last case, the field has to be sufficiently intense so that the front of the space charge to be unstable and to generate ‘filaments’ to support the electron avalanche. If the electron injections is carried out only in small areas, a filamentary distribution of the spatial charge occurs which, if the field is not very intense to produce a channel, it extends uniformly.

The type of degradation associated to these processes depends on the nature of the polymer: micro-cracks appear in poly (α -methyl-styrene), PMMA may decompose itself, micro-voids appear in PE (by chain crosslinking, Fig. 11.29), etc. Due to the lack of uniformity of the electrons’ extraction field, the degradation converges to the top of the needle, generating (probably due to the Maxwellian stresses) chains of micro-voids along the field lines. However, generally, these micro-cavities have very small sizes (<10 nm) [11]. On the other hand, there has to be emphasized that the morphology of extruded XLPE insulation present high importance on the values of the inception voltage of the electrical trees [88].

Fig. 11.29 Schematic representation of the forming of a micro-void by generating free radicals as result of the scission of the chains, followed by a crosslinking reaction. Reprinted, with permission, from author [2]



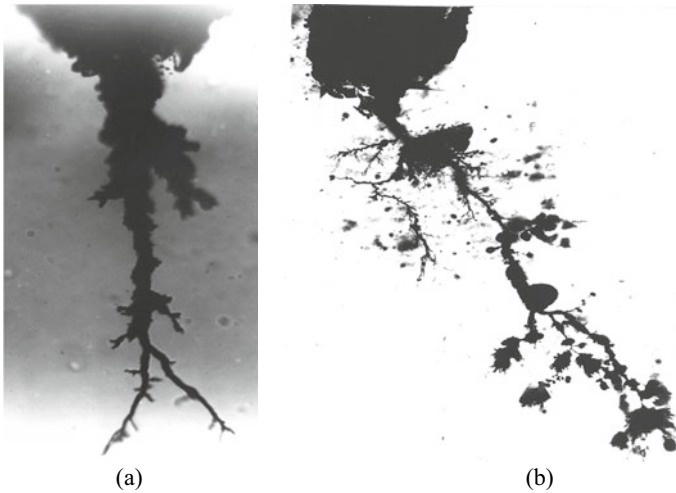


Fig. 11.30 Enlargement of the main channels (a) and the development of side branches (b). Reprinted, with permission, from author [2]

4.2.3 Propagation of the Electrical Trees

Main Channel

For AC voltages, the first generated channel (also called tree ‘foot,’ Fig. 11.28) has a limited growth. This is due to the dependency of the polymer electro-fracturing process of the size of the energy transferred to the dielectric by the electric field. Gas formed by the chemical decomposition of the channel wall leads to a constant increase of the gas pressure inside the channel and its deepening (Fig. 11.30a). Nevertheless, this does not modify the value of the PD’s inception voltage in the voids of more reduced size. In the moment of reaching the maximum length L_{\max} , the first channel contains on its walls enough positive charge to extinguish the previous discharges, thus, avalanches can be further generated only by extracting electrons in positive alternation. The electrons extraction from the surface of the channel will initiate local deterioration in a similar way to that of the first channel inception and it will produce impulses of similar sizes. Therefore, if the electrons extraction takes place with higher probability on the channel lateral walls than on its extremity, then ‘local’ deteriorations will occur and tree branches will show up (Fig. 11.30b). In the same time, several discharges on channel lateral walls occur, neutralizing the cations and causing erosion and channel enlargement.

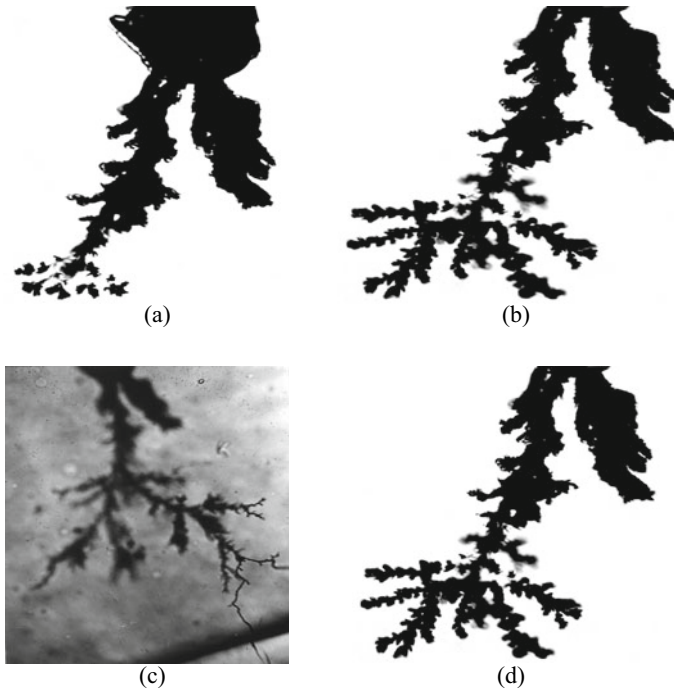


Fig. 11.31 Runaway development of trees (a, b and c) until the sample breakdown (d). Reprinted, with permission, from author [2]

Branches Development

After the formation of the main channel, the tree development process continues by forming side branches, departing from the main channel (Figs. 11.30 and 11.31). At this stage, the neutralization and diffusion of cations in the polymer allow the development of discharges, both ‘forward’ (from the needle electrode) and ‘backward’ (toward the needle electrode) inside the tree. When there are enough cations on the main channel walls or the existing side branches, there are ‘backward’ avalanches formed by electrons that are fixed in deep traps in the polymer and which cause the tree progress through the formation of new branches, even if discharges are extinguished in certain channels. This tree propagation stage is characterized by the occurrence of sound and light waves (pulses) associated with gas discharge, which can be evidenced by the occurrence of charge (current) acoustic and light impulses of more than 1 pC [11].

The mechanical shockwaves, which appear during the tree development stage, have very low energy (only 0.002% of the energy corresponding to the discharge) and cannot produce local deformations in the polymer. Unlike the mechanical waves, the electrons flow corresponding to each discharge may reach a kinetic energy of up to 10 eV in a discharge to the top of the channel, sufficient for breaking the connections,

and, thus the channel expansion. However, the most important degradation is caused by the cations flow, which may cause a local growth of the temperature of hundreds of Kelvin in the impact point. The discharges in the channels cause erosions and voids on the channels' walls, leading to their elongation and the sudden appearance of some gas decomposition products, such as acetylene, CO_2 , H_2 and CO .

Runaway Propagation

The stage of runaway (uncontrolled) propagation of the branch-like trees (Fig. 11.31) is characterized by the stop of the light emission and the reduction in PDs (the afferent charge being reduced below 5 pC). Though, in general, the PDs extinguishing is assigned to the increase in the gas pressure. It seems that this is rather due to the reduction in the electric field as a result of the cations deposition and of the occurrence of semiconducting products on the channels walls. Thus, the tree behavior after the interruptions of the electric stresses takes a closer path to that of walls charge dissipation than that of gas pressure reduction by its diffusion in the polymer. The small discharges are forming new channels, where new discharges occur. In the first case, a delay in the uncontrolled tree propagation occurs, while, in the second, there is an acceleration of the propagation process leading to the polymer breakdown (Fig. 11.31c, d).

In the stage of runaway propagation, filamentary channels are produced, having 2–3 μm in diameters and very low network of branches. The values of the charges and discharges observed during the development stage show that the same processes are carried out as during the previous stage, but now being limited at the uncontrolled branches channels. It seems that this type of growth is initiated by the time where enough charge is accumulated on the channels walls so that it blocks the discharges development in the main channel.

The filamentary formation continues in a reduced area of the tree surface and is characterized by a (favorable) intensification of the stress. Once the formed channel becomes large enough, the repulsion forces between the cations constrain the cations from the main channels' walls to enter inside them. The return of the cations formed in the small discharges will reinforce the previous extension of the branches, while the layer of space charge will stop quickly the development of the branches network.

Propagation of the Bush-Type Trees

Initially, the bush trees propagate like the branch trees, the bush shape appearing as a result of the faster development of new branches (from the channels situated in the vicinity of the needle electrode) than the existing channels. During this process, the discharges are carried out continuously, inside the trees (their charge reaching up to 500 pC). Once the tree started to grow, the local field is more strongly influenced by the produced space charge than by the form of the electrodes (needles). Consequently,

it is possible that the space charge deposited on the channels' walls cause local values of the electric field higher than its initial value at the top of the needle.

It may be considered that the transition to the bush shape is due to the accumulation of charge on channels' walls during the previous development, sufficient to generate branches on their lateral walls. The branches inception will take place, probably in the 'pits' on the channels' areas. The removal or neutralizing of the electric charges on the channels' walls favor the continuity of the discharges development and the increase of the electrical tree channels density.

Development Under Continuous Voltage

By applying continuous voltage, the local degradation may be achieved only through the action of the avalanches and discharges that are produced. A voltage impulse or a step voltage will generate charge impulses (injected by electrodes or extracted from traps), which initiate several avalanches to produce the first channel. The length of this channel depends on the length of the ionization area by impact and the polymer characteristics. Currently, the charges deposited on the channel walls are removed or neutralized by the needle electrode and the maximal electric field is moving to an area located on the top ('front') of the channel. The tree advances by the repeated action of erosion of the avalanche, each (new) channel top acting as a high potential point. The penetration of the avalanche inside the polymer stops only when the field corresponding to the space charge in any point in the tops area is too low to initiate a new avalanche.

Badher-Fothergill Model

It is considered that the space charge, constituted from the ionized gas molecules, may be injected by the streamers formed in the created micro-channels. These charge carriers will move through the micro-channels network, creating a (fractal) tree structure. At the peaks of these 'charge branches' the electric field is very intense, which makes the charge to continue to move. As the charge penetrates deeper and deeper in the channels, its density reduces and the intensity of the electric fields at the branches peaks is decreasing. If the electric field set in the dielectric causes superior local fields to those developing branches networks at the extremities of the branches, the dielectric is broken (criterion of breakdown). For the dense branches' networks, the charge reduces more rapidly as the length of the tree is increasing, and the branches which are practically closed (close channels) do not allow an intensification of the electric field. This structure represents a tree or a fractal type, comprising electrons and mobile ions. The most important electrical charge movement takes place through the 'trunk' of this tree structure and, thus, it is natural to be considered that the most significant degradation will occur in the same area.

For the Badher-Fothergill model, it is considered that the diameter of this area increases continuously until the extinguishing of all discharges. The Badher-Fothergill model is a simplified model (filamentary model), but there is a development of it in the more general case of a tree shape structure [10].

Based on these models, a critical value of the voltage is established (called threshold voltage U_p) under which the polymer degradation does not occur. For values of the voltage higher than this critical value, there is a direct relation between the breakdown duration and the value of the applied voltage (law of the inverse power).

A more evolved filamentary breakdown model, which take into consideration the density of transmitted energy by PDs to the dielectric and the pressure of the developed gas from the molecules fracturing within the channel walls (under the action of PDs), was proposed by Nottingher in 1986 [15, 16].

Observations. 1. The electrical tree constitutes the stage preceding the breakdown of the solid dielectric and, in general, of the insulation systems.

2. The development of the electrical trees (from the area where the electric field is more intense to the area where the electric field is weaker) leads to the reduction of the resistivity and of the dielectric strength of the insulation. Nevertheless, the contact moment of a tree and the second electrode (Fig. 11.31c) does not coincide with the breakdown occurrence moment (Fig. 11.31d). This is achieved a bit later, namely only after transferring to the electric field, the required energy for ‘digging’ the breakdown channel.

A general schema of the XLPE insulation breakdown in the presence of the electrical trees is present in Fig. 11.32.

4.2.4 Experiments

Such as shown above, the electrical treeing constitutes the stage preceding the cables insulations breakdown. Therefore, several surveys were taken, on various types of XLPE, in order to understand the mechanisms of inception and development of the electrical treeing and, mostly, of estimating its resistance to electrical treeing. In order to produce and measure the sizes of the electrical trees, needle-plan electrodes (Fig. 11.33a) and installations with recording the trees time evolution (Fig. 11.33b) are mostly used [89]. The inter-relationship between tree discharges, tree propagation and tree shape is discussed in [90] and theoretical models for these processes are proposed and evaluated in terms of their ability to reproduce experimental data, especially tree shapes and discharge sequences in time and space [91].

In [92] Zhu et al. present the results of an experimental survey on the electrical treeing processes in XLPE and polypropylene (PP) under different temperatures. The authors show that the inception probability and growth rate of PP at the same temperature is lower than that of XLPE. With the temperature decreasing, the inception probabilities and growth rate decrease. On the other hand, the values of the branch density for the trees developed in XLPE are reduced if the temperature is decreasing (Fig. 11.34).

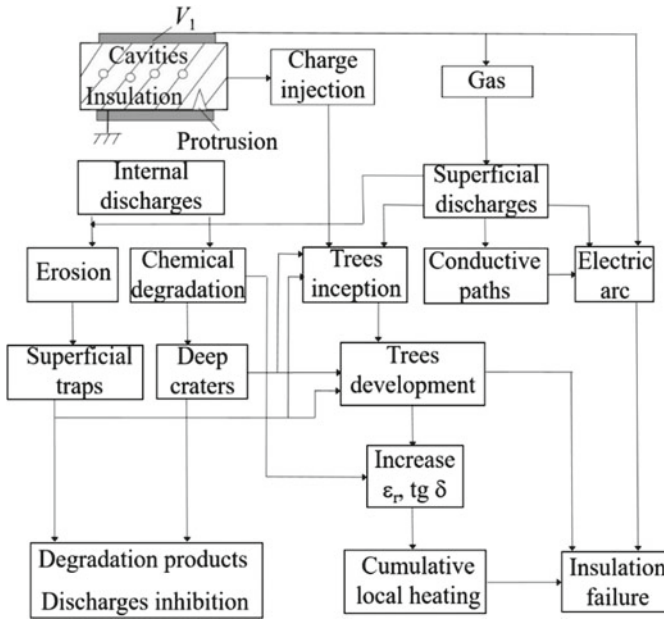


Fig. 11.32 Insulations breakdown in the presence of the electrical trees. Reprinted, with permission, from author [2]

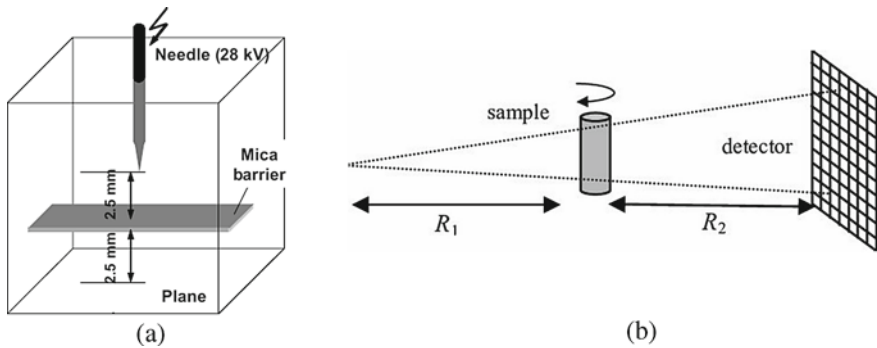


Fig. 11.33 System of needle-plan electrodes (a) and schematic diagram of a typical laboratory micro-system (b) for measuring the electrical trees [89]

In [93] Liu et al. present the results of a study for the development of electrical trees under DC voltages on which they overlapped AC voltages, performed on XLPE extruded rectangular bars, with needle-plan electrodes. The authors explain the trees shapes based on the electrons avalanches and charge accumulations and show that the AC component will greatly promote the growth rate of the electrical trees. Also,

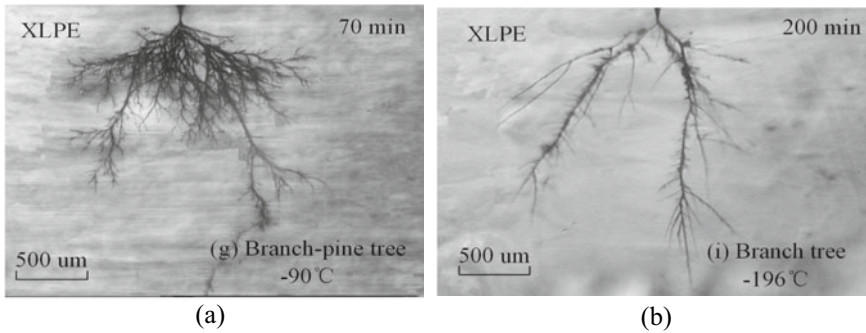


Fig. 11.34 Electrical trees in XLPE at 183 K (a) and 77 K (b) ($U = 12$ kV) [92]

the influences of the positive and negative DC bias voltages on the electrical tree growth properties were quite different.

The influence of the electric field frequency on the characteristics (fractal dimensions) of the electrical trees produced in XLPE samples for power cables was analyzed by Chen et al. in [94]. The authors showed that, contrary to our expectation, the fractal dimension prior to the breakdown showed no significant changes when frequency of the applied voltage increases. On the other hand, it was found an accelerated breakdown process with higher frequency leading to a faster breakdown. This could be due to the higher number of PDs at higher frequency. A more precise characterization of the fractal dimensions developed in XLPE samples, using 3D models and 2D projections, for two types of tree topology, respectively, bush- and branch types was proposed by Schurch et al. in [95].

The formation of electrical trees inside the XLPE cable insulation samples and the increase of their lengths with the increase of the voltage and of its duration of application are presented in [96] and these are in accordance with those presented in [2] and [14].

The influence of the mechanical stresses on the electrical trees' inception was analyzed by Varlow et al. in [97]. The authors showed that the mechanical properties (specifically, tensile strength, elastic modulus and fracture toughness) of the dielectric material strongly affect the inception and growth of electrical trees in single-cast homogeneous specimens. It is also shown, that the insertion of barrier materials in the path of the tree presents an obvious impediment to the tree growth.

Liu et al. study the effect of continuous voltage on the development of electrical trees in the XLPE insulations of the DC cables [98]. The authors show that the electrical tree cannot be easily caused by constant DC voltages, even under the combined action of a high voltage and an elevated temperature. For example, the continuous application of 60 kV and 90 °C on specimens for 20 days did not trigger an electrical tree in the DC XLPE insulation. In their opinion, the detectable damage in XLPE insulation is a joint result of space charges' injection and extraction. The deterioration caused by charge extraction will be more serious than injection.

The effects of frequency, voltage, temperature and mechanical stress on the times to breakdown of the XLPE cable insulation subjected to highly divergent fields were presented by Densley in [99]. The author showed that the temperature and mechanical stress reduce the times to breakdown, but tests with increased voltage and high frequency produced unexpected results that could not be explained by the existing theory of electrical tree growth. Results of PDs measurements indicate that space charge is dominant in determining the shape of the tree and the time to breakdown of the insulation. The influence of the electric field frequency on the shapes of the electrical trees is also analyzed by Gao in [100]. The author showed that bush-type trees are formed at a high frequency range and the density of the tree appears to increase with the frequency.

The influence of PE structure on the electrical trees' inception was experimentally studied also by Shimizu et al. [101]. The authors showed that in PE subjected to high electric fields, a deteriorated region is formed before tree inception. The chemical analysis of the deteriorated region performed with FT-IR and Raman spectroscopy showed that it contains excess carbonyl groups (C=O) and double bonds (C=C) compared to normal PE. Scanning electron microscope observation found in the deteriorated region a number of voids with diameter $<0.5 \mu\text{m}$. The observation by transmission electron microscope revealed that the lamellar structure was destroyed in the deteriorated region. It was found that tree inception voltages for AC ramp and positive impulse are increased after the formation of the deteriorated region. The change of PE structure is considered to be responsible for the increase of treeing resistance.

The relationship between electrical tree propagation and the material morphology in XLPE has been studied by Zheng and Chen in [102]. It has been found that, due to the influence of uneven congregating state, difference in crystalline structure, and the existence of residual stress in semicrystalline polymer, five types of electrical tree structures (branch, bush, bine-branch, pine-branch and mixed configurations) would propagate in XLPE cable insulation. Three basic tree propagation phases (inception, stagnation and rapid propagating phases) are presented in electrical tree propagating process. If inception phase is very active, the single branch tree will propagate, while if this phase is weak then the bush tree will occur more easily.

An analysis of the experimental results obtained by various researchers for the electrical trees inception was presented by Shimizu and Laurent in [103]. There are given information on the inception mechanisms of the electrical trees and phenomena occurring during the induction period in the discharge free condition. The importance of charge injection in electrical tree inception is well established, not only under DC or impulse stresses, but also under AC stress. Electroluminescence can be used as a monitor for charge injection. Tree inception from field enhancing locations under moderate stress proceeds through cumulative degradation reactions and void formation caused by injected charge. The dependence of tree inception on temperature and the nature of dissolved gases underlines the importance of free volume processes, and therefore of polymer morphology. Electron avalanche type tree inception is strongly influenced by the field modification due to the space charge and also by the size of the high field region.

4.2.5 Electrical Trees Effects Attenuation

Performing cables of increasingly higher voltages imposed to manufacturers the need to find solutions for inhibiting the phenomenon of electrical treeing. During the last years, two practical and technological approaches have been developed for XLPE cables, as follow: the development of new types of manufacturing process and the incorporation of a certain additives into solid insulation [104]. The improvement of the technological processes led to insulations with much lower sizes and concentrations of voids, reduced impurities concentration, eliminated protuberances of the semiconducting layers, etc., respectively, reduced areas with intense electric fields and increased treeing inception voltages. The second method consists in introducing some substances to reduce the inception and development of electrical trees. The concept of adding voltage stabilizers has been tested since the late 1960s [105–110], but without substantial impact in commercial cable manufacturing [105]. The reason is the lack of compatibility between the voltage stabilizer and the polymeric matrix. Solubility of the voltage stabilizer in the polymer matrix is crucial for achieving a homogeneous material. This is important to ensure constant dielectric properties along the whole service length of the cable [105]. A voltage stabilizing effect has however always been present in peroxide XLPE cables, as the peroxide decomposition product acts as a voltage stabilizer [111, 112]. The composition products contain aromatic species with low molecular weight, prone to migrate to the surface from the bulk where they evaporate, resulting in a reduction of breakdown strength. These compounds and their effect on the insulation material have been widely studied, but the focus has primarily been on pre-treeing phenomena, such as space charge formation [113, 114]. The efficiency of antioxidants in electrical tree suppression has also been investigated [112, 115–117], where some work have led to patents. However, there were problems regarding the efficiency or solubility, as the utilization of these molecules as voltage stabilizers has been very limited commercially.

Martinotto et al. [118] studied the influence of a series of alkylated derivatives of benzophenone [23] on the inhibition of the electrical treeing phenomenon. They achieved a high content of voltage stabilizer, even after aging it at elevated temperature, when attaching long alkoxy side chains to the benzophenone. The attached alkyl side chains were of an alkoxy structure to avoid benzylic hydrogens that would otherwise contribute to a non-stable structure, where the alkyl side chains are susceptible to detaching. In [105] Englund et al. present the findings of an experimental survey on the use of new voltage stabilizers. The authors used a commercial grade of XLPE, pre-impregnated with dicumylperoxide. The voltage stabilizers were N-octylcarbazole, 4-methoxy-9-octyloxyacridine, 1,5-dioctyloxynaphthalene and 4-dioctyloxy-benzophenone, which were all alkylation of a phenolic hydroxyl to an octyloxy. It has been shown that a significant increase in the electrical treeing resistance can be achieved with only a 0.76 wt% addition of a voltage stabilizer and that hetero-aromatics are potent stabilizers.

In [104] Kato et al. present a new type of voltage stabilizer, constituted from a mix of ferrocene and 8-hydroxyquinoline. Ferrocene ($\text{Fe}(\text{C}_5\text{H}_5)_2$) is an organometallic compound with the molecule consisting of two cyclopentadienyl rings bound on

opposite sides of a central iron atom. This may capture and deactivate injected electrons, siloxane oligomer may migrate in voids and/or defects and then 8-hydroxyquinoline may stabilize metal ions through trap. The authors showed that the incorporation of ferrocene contributes prominently to the elevation of the tree inception voltage of XLPE and that this growth gets more important with the increase of the additive concentration. On the other hand, the corresponding effect of siloxane oligomers clearly depends on the degree of oligomerization and their structures, especially on types of functional groups attached to the silicone atom. As it is shown in [119], electrochemical processes on ferrocene may cause rapid formation of a ferrocenium cation that would produce a redox complex reaction with a neutral ferrocene molecule. Subsequent capture of electrons by this redox complex reaction would reversibly reproduce two molecules of neutral ferrocene. Such behavior and reactivity of ferrocene with electrons suggests that ferrocene would play an important role as a scavenger and a deactivator of electrons under electric stress, increasing the electrical tree inception time.

4.3 Water Treeing

4.3.1 General Characteristics

Water trees represent diffuse regions, which appear inside the insulation under the action of the electric field and consist of microcavities filled with water. In [121] Ross proposes a more complex definition, namely that water trees represent structures of polymer's degradation, which: (i) are permanent; (ii) increase due to moisture and electric field; (iii) have a lower dielectric strength than the original polymer, but are not a local breakdown channel and (iv) are more hydrophilic than the original polymer. In the following, it is believed that a water tree is a diffuse area (structure) in a polymer of bush or fan shape, build-up of a plurality of water-filled microcavities, connected by very narrow channels [120].

Water trees are developing along the electric field lines similar to electric trees, from regions with a higher field to those in which the field is weaker. If the water trees start on the surface of electrodes, they are called vented trees. This is the case of trees' growth in the XLPE insulation of medium and high-voltage electrical cables, which starts from the semiconductor layers in samples appointed with needle electrodes (Fig. 11.35a) and in plate samples with surface defects (Fig. 11.35b) [53]. If the cables are subjected to moderate stresses (below 4 kV/mm), open trees have, generally, a wedge shape. They grow toward the inside of the insulation, from the inner (Fig. 11.36a) or outer (Fig. 11.36b) semiconductor layer and exhibits distinct branches, which extend in such a way that each branch of an open tree takes the form of a feather [2].

Bow-tie trees (Fig. 11.37) start at defects within the bulk material (impurities, cavities, etc.) and grow inside the insulation, along the electric field lines \vec{E} , in the sense or contrary to \vec{E} . The lengths of the bow-tie trees are limited and, therefore,

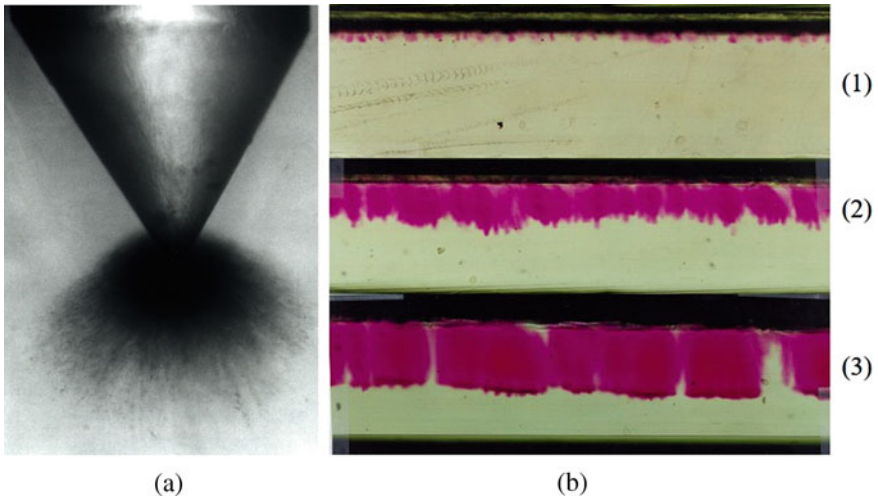


Fig. 11.35 Water trees: **a** Vented tree developed at the tip of water needle electrode; **b** Water trees developed in laboratory from the defects located at the surface of XLPE samples as a function of time t_1 (1), $t_2 > t_1$ (2) and $t_3 > t_2$ (3). Reprinted, with permission, from author [2]

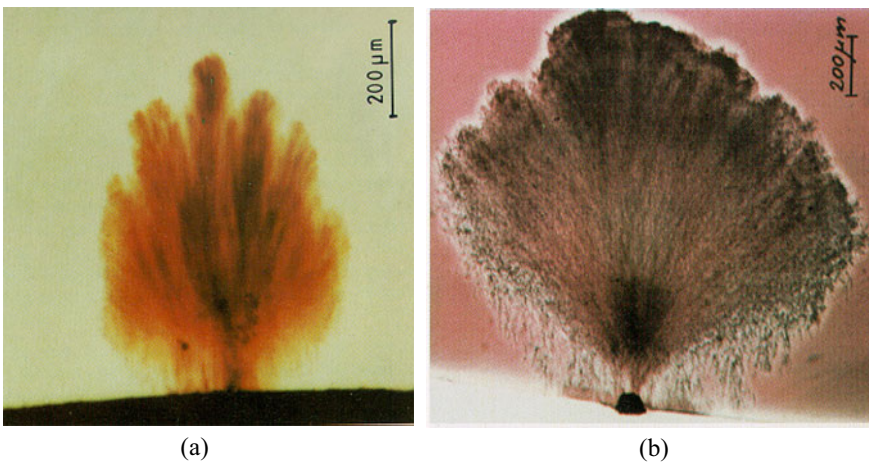
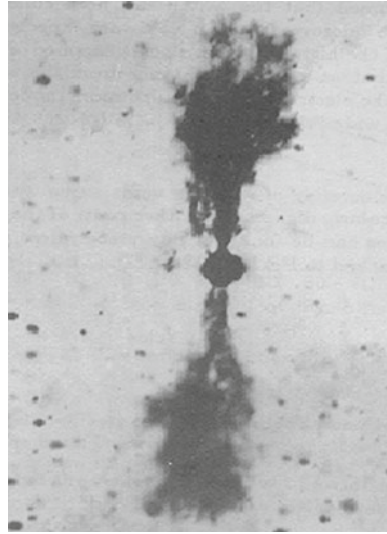


Fig. 11.36 Open trees in a XLPE insulated cable from the inner **(a)** and outer **(b)** semiconductor screen. Reprinted, with permission, from author [2]

only occasionally cause electrical breakdown of the insulation in which they develop. However, they obviously lead to a worsening of the insulation characteristics and, therefore, a reduction in their lifetimes.

Meyer [122] determined the water content of the open trees obtained in needle-plane samples (where the needle is a ‘water needle’). Near the top of water needles, the trees contain 10% water (of the total trees volume) and the water content drops

Fig. 11.37 Bow-tie tree developed in XLPE cable insulation from an impurity. Reprinted, with permission, from author [53]



to 1–2% over the trees ends [122, 123]. Besides the water clusters from the cavities, there are water molecules dispersed in other areas of the trees, attached to the PE molecules [2, 124].

The typical characteristic of water tree branches is given by the presence of spherically shaped micro-cavities with a radius of 1–5 μm (10^6 – 10^9 mm^{-3}) [125]. By drying, the cavities close and cannot be seen, but if the sample is introduced into the water, the tree reappears. ‘Boiling’ in water leads to the stabilization of existing cavities and, moreover, to the appearance of other very small cavities (<0.5 μm). The concentration of cavities has higher values at the base of the tree and lowers in its front, the maximum values being between 10^7 and 10^9 mm^{-3} [125]. Several parameters are used to characterize water treeing, such as: electric field and voltage inception, length at a given time, maximum length, average growth rate, area and volume occupied by trees, density of trees, etc. [6, 11]. Regarding the water trees growth in the operating cables’ insulation, different metal ions were detected, as follow: Fe, Al, S, Na, K and C in the bow-tie trees and Cu, Si, S, K, Ca and Fe in vented trees [122, 123]. During the development of water trees, ions from the electrolyte drift with the water molecules and the concentration of water in the ‘tree regions’ (regions containing water trees) increase with the applied voltage (up to 10%) [123].

Chemical transformations produced in polymers during trees development cannot always be easily identified. The permanent coloring of zones with trees (called *tree zones*) indicates that in these regions has been an oxidation phenomenon. Infrared spectroscopy highlights the oxidized area of a tree region, bordered by loose chain ends and folded surface of the lamellae. For the study of water treeing resistance of polymers, trees are accelerated by the uniform or strongly irregular electric fields in plane samples, minicables, needle-plane and needle-needle samples, etc.

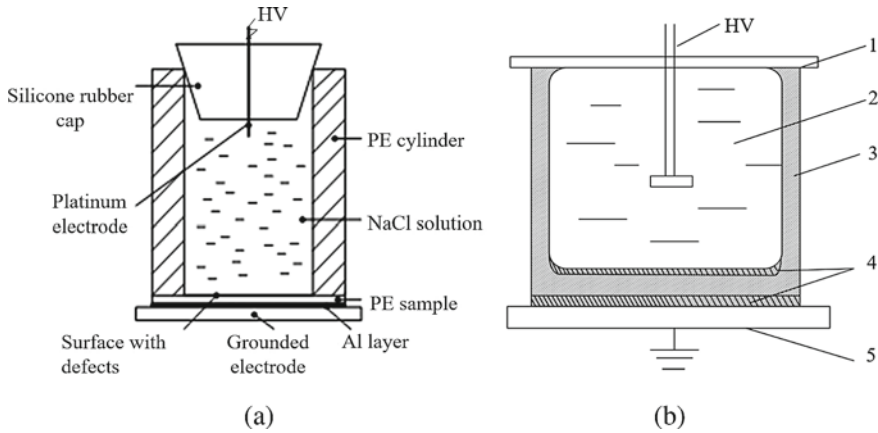


Fig. 11.38 Cells for the production of water trees in plane-plate (a) and plate-shaped (b) samples: 1—Cover; 2—Water tank; 3—XLPE sample; 4—XLPE semiconductor layers; 5—Earth electrode. Reprinted, with permission, from authors [6, 131]

Minicables (cables model) have the advantage of performing tests in conditions as close as possible to those in which real cables operate and are used, in particular, for testing new insulations [126]. The resistance to water treeing is determined by measuring the breakdown voltage after producing water trees [2].

Plane samples have the shape of films, plates or plate-shaped pieces and are components of test cells (Fig. 11.38) [127, 128]. High-voltage plane electrodes are generally build-up of water, but can also be made of semiconductive PE layers (blended with black carbon) (Fig. 11.38b). Plane samples are used both for the characterization of insulation materials and for the insulation. However, they are not allowing the trees visualization during their development, but only at the end of the test (by sampling with thicknesses of 50–200 μm).

Water-needle electrodes are used to produce very intense electric fields in selected areas of samples in order to control initiation sites, reduce initiation times and speed up the development of water trees. The model proposed by Ashcraft [129] consists in producing surface defects on the inner surfaces of plate-shaped samples with needles of reduced curvature (about 5 μm). The second model consists of producing superficial defects on the surfaces of the samples by sandblasting [130] or by pressing some layers of abrasive paper [131, 132]. The produced superficial defects are filled with electrolyte and forms ‘water-needle electrodes.’

A perfect localization of trees initiations, reduction of initiation times, increase of speed up the development and the possibility of tracking the evolution over time of trees (shapes, dimensions, etc.) are in the samples with water needle-plane electrodes proposed by Filippini et al. [133].

The study of water trees development requires analysis of three distinct phases: initiation, propagation and long-term development.

4.3.2 Water Trees Initiation

The existence of the initiation phase is characteristic for vented trees in all sample and electrode configurations. In the case of ‘miniature’ cables, the initiation time t_i is related to the electric field intensity (E) and the frequency (f) applied by the empirical relation:

$$t_i = A \cdot f^{-1} \cdot E^{-3.5}, \quad (11.9)$$

where A represents a constant of material [2].

The value of the electric field E_i at which the water trees initiation take place is called ‘minimum field of initiation.’ This quantity is used to show that, at a given frequency, there is a lower limit value of the electric field strength under which trees cannot be initiated. The initiation process can also be followed by setting up the density of trees produced after different times of applying stress t ($N(t)$).

During the water trees initiation it can be observed, first, their initiation points [Fig. 11.35b (1)] in the form of micro-trees (i.e., at the interfaces between the electrolytes and the samples in which they develop), then the ‘continuous’ trees that are developing in time [Fig. 11.35b (2 and 3)]. Initiation of water trees occurs, particularly in the lower density regions of insulation (amorphous regions) [123] and they are influenced by several factors, such as: the intensity and frequency of the electric field [2, 11], the characteristics and concentration of the salts in the liquid, which is in contact with the insulation [135], the concentration of additives [136], the temperature [137, 138], the degradation degree of the material [137, 139], the quality of the electrode surfaces and semiconductor layers, etc. [121].

Notingher et al. [140] showed that a critical field (depending on the nature and state of the material) exists for each material over which water trees are induced. Over the years, various types of mechanisms have been proposed regarding the initiation and water trees growth. An overview of them is given by Notingher [2], Dissado and Fothergill [11], Steennis and Kreuger [123], Crine [137], Ross [121], Nunes and Shaw [141], Shaw and Shaw [142], etc. It is considered that there are two groups of mechanisms seemed to play a decisive role in water trees growth: mechanisms based on the electrochemical degradation of the insulation and mechanisms based on the mechanical action of the electric forces on the material [120]. A detailed analysis of these mechanisms can be found in Refs. [2, 11].

4.3.3 Water Trees Propagation

After initiation, water trees follow a rapid growth phase. The variation of the tree length (L) in time (t) can be estimated by the empirical relation (power law):

$$\frac{dL}{dt} = L_\infty \cdot k^{-1} \cdot (t - t_i)^{-n}, \quad t \geq t_i \quad (11.10)$$

where L_∞ represents the length of the tree after a very long time ($t \rightarrow \infty$), k —the constant of the initiation rate, t_i —the duration of the tree initiation and n —a constant of the material [2].

The experimental dependence of the trees development rates on their length is obtained by plotting its variation curves over time. It was found that the increase rate of trees varies inversely proportional with the square of their lengths. It should be noted, however, that in the case of samples taken from the power cables insulation, on the surfaces where feather channels were produced, the results differ from those obtained on the samples [i.e., most of them resulting in a variation of the trees growth rate with the inverse of their lengths (L^{-1} , respectively)] [2].

For the estimation of the insulation resistance to water treeing, the average maximum length $L_{\max,a}$ of trees developed in one or more samples was determined experimentally. However, as the most damaging trees are vented trees with the longest length, $L_{\max,a}$ is a value that can be used to characterize the degradation of the material, but cannot be used for comparisons with the lengths resulting from models of individual trees growth.

4.3.4 Long-Term Development

Acceleration after a certain time of the trees development process may be due to the local increase in the intensity of the resulting electric field, especially in the case of the trees development from the outside toward the inside of a cable (i.e., the field being obviously more intense in the areas closer to the conductor). Therefore, a reliable prediction of the water treeing influence on the cable failure requires knowledge of the propagation mode, density and trees length distribution for long periods, because the negative effects of the treeing phenomenon on dielectric strength are determined by the vented trees with the longest lengths.

The systematic study of water treeing has led to the development of some models and the proposal of some mechanisms for their development. The most important mechanisms are based on the capillary action, osmosis, coulombic forces, dielectrophoresis, partial discharges, thermal and chemical degradation [133, 143–146].

As water trees consist of microcavities generated and/or augmented by treeing process, it is natural to assume that mechanical forces play a relatively important role in this process. This information is experimentally proven by accelerated propagation of trees in the case of stretching stresses application and by reducing propagation rate in the case of isotropic compression. A model of initiation and development of water trees based on the assumption of nanocavity formation in insulation, which increase if the pressure imposed by the electric field on the liquid contained in nanocavities, exceeds the permissible limit of the polymer is presented by Crine in [146].

The essential role of chemical reactions in the propagation process is not very clear, but it is known that antioxidants reduce the rate of propagation, while oxidizing agents increase it. Furthermore, it was found that the treeing process is inhibited by inert gases (e.g., nitrogen). From the analysis of areas containing water trees results that

they are oxidized and, therefore, oxidation is an essential factor in the mechanisms of water treeing development.

4.4 Experiments

4.4.1 Factors Affecting Water Treeing

Numerous experiments conducted over the years have shown that the development of water trees is influenced by a number of factors, such as: electrical, chemical, mechanical, thermal, structural, and environmental (Fig. 11.39) [137, 147].

Electric Field

Experimentally, it was found that the increase of the intensity of the electric field E leads to an important increase, both of the lengths (Fig. 11.40) [147] and concentrations of vented water trees [2, 148, 149]. With the increase of the electric field frequency, there was a significant reduction of the initiation time and an increase in the propagation rate of water trees [151–156]. Furthermore, the rate of water trees development decreases as their length increases [156]. The increase of E also leads to an increase in the developing rate of the bow-tie trees [151, 152, 157, 158].

Furthermore, some researchers found that the average rate of water trees development is much stronger influenced by the number of applied voltage zero-crossings of the samples than its frequency [159–162]. An explanation of this phenomenon could be based on the model of the trees' growth by ion diffusion and attraction of water molecules by these molecules (i.e., ionic displacement being influenced by the changes in the electric field direction, respectively, of the electrostatic forces which are acting on the ions and their relaxation times).

In the case of bow-tie trees, the experiments on cables have also shown an increase in the rate of trees development with the increase in the electric field frequency, but much lower than in the case of vented trees [149, 164, 165].

Temperature

In some papers are presented aspects of the vented trees development at constant temperatures, without taking into account the existence of a temperature variation inside the insulation. Most of the tests were performed on LDPE and XLPE insulation in water baths using samples with water needle [2, 166–168]. From these studies resulted that the vented trees concentration increases and their length decreases if the insulation temperature is higher than 50 °C [167]. It seems that, excepting the results obtained in water needle tests, the most favorable temperature values—for the development of water trees—are between 30 and 50 °C [2, 168].

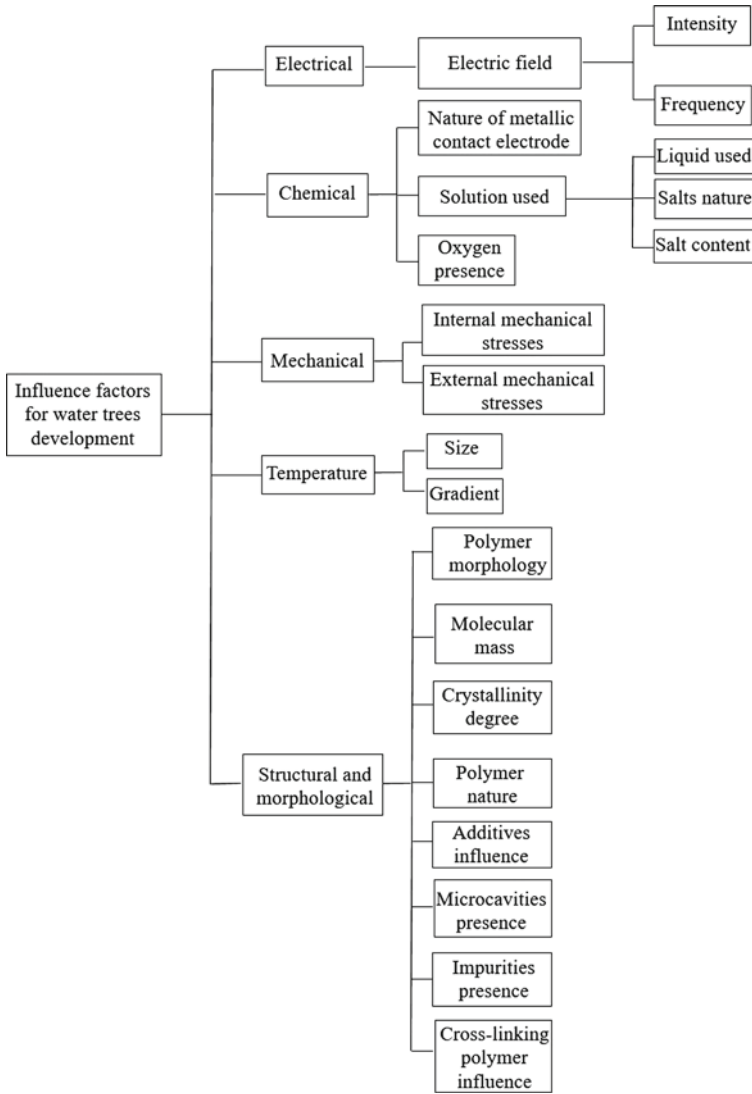
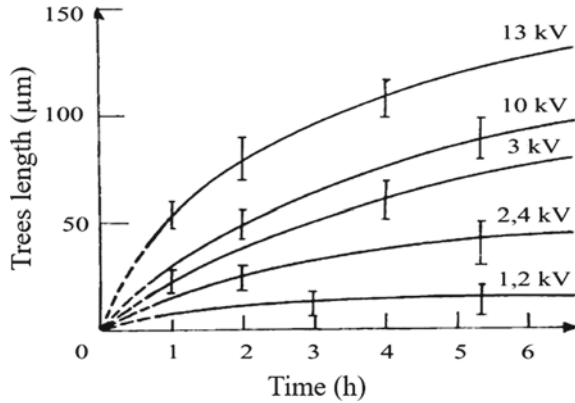


Fig. 11.39 Factors affecting water trees development. Reprinted, with permission, from author [2]

Some experiments were conducted on real cables and miniature cables to analyze the influence of cyclical thermal stresses of conductors and external screens on the development of water trees [155, 169]. It has been found that the development of trees is strongly affected by the cyclical stresses of the external screen (e.g., trees density is drastically reduced with respect to the case of continuous thermal stresses) [155].

Fig. 11.40 Variations of trees lengths in time for PE samples at different voltage values (at $f = 2$ kHz). Reprinted, with permission, from author [2]



Mechanical Stresses

Tanaka et al. [170] studied the influence of internal mechanical stresses on the development of water trees. They used foils (thin plates) of the cable insulation, aged in different ways. It was found that vented trees were concentrated, especially in regions with significant, but non-destructive mechanical stresses between 1 and 8 MPa, respectively. Such internal stresses may occur both in the cable manufacturing process and during operation.

Other results were published by Tu and Kao [171], by subjecting the samples under water needles at pressures ranging from 0.1 to 3 MPa, for relatively short times of stress (15 h). The authors found that, in case of high pressures, trees initiation was faster, but their development was slower than in lower pressures.

Fluid and Salts

The first study conducted by Badher et al. [164] on the trees development in insulated cables based on LDPE and XLPE in contact with fluids of different chemical species (e.g., pure water, salt water, ethylene-glycol, paraffinic solution, etc.) showed that in all cases, with the exception of paraffin solution, trees appeared. From the analysis of water trees from cables, it was found that they contain a wide variety of ions (especially of transition metals), such as: K^+ , Na^+ , Ca^{2+} , Al^{3+} , Mg^{2+} , Fe^{3+} , Fe^{2+} , Cu^+ , Cu^{2+} , Zn^{2+} , Si^{4+} , S^{4+} , etc. [164, 172, 173]. The role of ions in the water trees development is not yet fully elucidated. If they move under the electric field action and attract water molecules or vice versa, the water molecules facilitate the displacement of ions. Furthermore, Meyer [174] showed that the permeability of sodium ions in PE is approx. five orders of magnitude smaller than that of water molecules (i.e., which is strongly influenced by the crosslinking degree of PE), leading to the conclusion that there are layers of ionic space charge in front of the water trees. Subsequent

studies have analyzed the influence of salt nature and concentration, the nature of the electrode, the acidity of the solution, etc. [2, 175, 176].

An information regarding the effect of salt dissolved in water on the water trees development is given by Bamji et al. in [127], whom were using XLPE samples and water needle electrodes for this type of testing. The highest rates of trees development were obtained by using CuSO_4 , followed by NaCl and CaCl_2 .

Ross et al. [177] carried out tests on similar samples and under the same conditions, but the aging time was 1200 h. Electrodes made of stainless steel and salts of different types such as NaCl , Na_2SO_4 , CuCl_2 and CuSO_4 were used. The longest vented trees were obtained with CuSO_4 , and the shortest with NaCl . The other salts resulted in intermediate lengths.

The nature of ions from trees strongly influences their electrical conductivity. Thus, the study conducted by Li et al. [178] on PE samples and electrolytes based on LiCl , $\text{LiCl} + \text{HCl}$, MnCl_2 and FeCl_3 , showed that the values of the currents measured on samples with trees are the highest in the case of ferric chloride. The experiments performed with electrolytes based on NaCl and CuSO_4 and water needle-plane electrodes have shown that higher salt concentrations result in higher values of trees propagation rate [2, 158, 179, 180]. It is noted that in the case of NaCl concentrations less than 2 M/l, the growth rate increases with the electrolyte concentration, but decreases if its concentration exceeds this value [2].

Polymer Nature

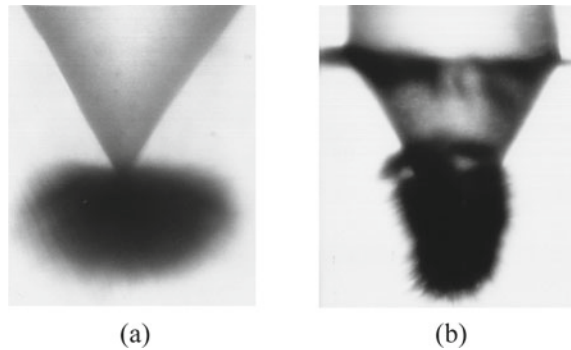
Ashcraft [181] studied the rate of water trees development (at 8.5 kHz) in samples of polystyrene, polyethylene, ethylene-propylene-diene-terpolymer (EPDM), low-density polyethylene (LDPE) and crosslinked polyethylene (XLPE). The trees development rate has maximum values in polybutene and minimum in freshly XLPE, probably due to crosslinking residual products, especially acetophenone. Moreover, it is known that acetophenone added to PE inhibits or even blocks the development of water trees [150].

Some studies were conducted on samples of miniature cables or taken from real LDPE or XLPE cables insulation [2, 164, 182, 183]. Generally, it was found that trees development rates were higher in LDPE samples than in XLPE. The reduction in the rate of trees growth in XLPE insulation was attributed to the inhibitory effect of crosslinking residual products.

Polymer Morphology

Some papers showed that there is no direct relationship between the morphological parameters of the materials (e.g., melting point, density, crystallinity index) and the way of water trees development. Thus, Morita et al. [184] carried out tests on PE and other materials with the melting point between 0.3 and 2 g/10 min, density between 0.92 and 0.927 g/cm³ and crystallinity index between 72 and 76%. They

Fig. 11.41 Water trees in non-aged (a) and thermo-oxidative aged (b) samples (reprinted, with permission, from author [2])



failed to establish a relationship between the rate of trees development and these morphological parameters.

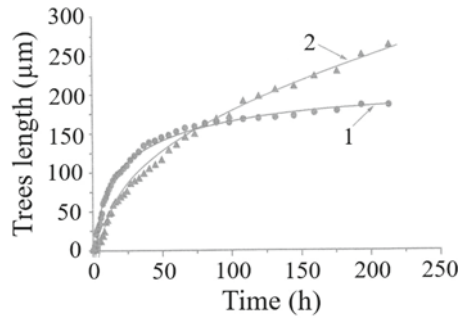
Saure and Gözl [185] studied the development of vented trees (at 50 Hz) in tests with water needle. The melting point values of the LDPE and XLPE samples varied within a fairly wide range (from 0.2 to 10 g/10 min.). They could not establish a relationship between morphological parameters and the development of water trees. Namiki et al. [186] have come to the conclusion that the thermal treatment of XLPE samples leads to an additional development of water trees. Namiki attributes this effect to the increase in samples fragility as a result of the material crystallization. An explanation of the increase in the rate of water trees development due to thermal treatments could also be the elimination of residual crosslinking products [187].

Poggi et al. [188] analyzed the influence of the parameters of the technological process of preparing samples with water trees, using needle-plane electrodes. The authors established a link between the mechanical properties of the polymers and the shapes and dimensions of the trees. Thus, the existence of internal mechanical stresses leads to defects of polymer spherulites and dislocation lines which become preferential directions for the water trees development. An annealing treatment greatly changed the rate of trees development as a result of the crystallinity index modification [189]. Also, a degassed sample leads to a reduction in trees propagation rate (more, as the degassing time is higher) [189].

Oxygen and Radiation

Both oxygen and radiation result in a reduction in initiation times and an increase in mean rates of trees growth, by chemical degassing of samples and by generation of polar products (e.g., ketones, aldehydes, carboxylic acids, etc.) that facilitate the penetration of water into samples [134, 189, 190]. As a result of the material degradation, the minimum value of the trees initiation electric field decreases and the shape of the trees is also changed. If, in the case of non-aged samples, water trees occur only at the tip of the needles (i.e., where the electric field intensity is maximum (Fig. 11.41a), in the case of oxidized samples, trees are initiated in any of the areas

Fig. 11.42 Variation of trees lengths with the aging time of polyethylene:
 1—non-aged samples;
 2—irradiated samples with 70.4 Mrad (reprinted, with permission, from author [2])



where the electric field intensity exceeds the new critical value (Fig. 11.41b). As a result, the trees became ‘elongated’ and completely cover the surfaces of the water needles.

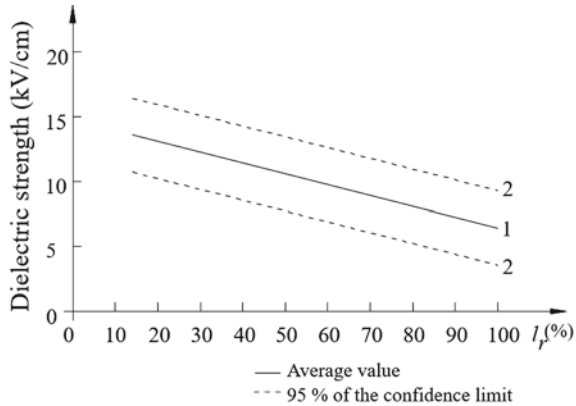
The studies conducted by Garton et al. [191] and Bulinski et al. [134] on samples of PE subjected to oxidation showed that oxidation and resulting oxidation products (carbonyl and carboxylate groups) do not have a major influence on the water trees initiation, but can play an important role in their development and especially in the initiation of electrical trees [191]. After the irradiation, it first noticed a reduction of the trees development rates with the increase of the total radiation dose (i.e., due to the facilitated crosslinking process) [191, 192], followed by their increase (i.e., due to polymer degradation—Fig. 11.42).

Furthermore, it is noted that for high radiation doses (over 2000 kGy) the water trees concentration increases [12, 18]. This is probably due both, the increase in samples defects (i.e., generated by the radiation-sample interaction) and the reduction of the critical voltage values of the trees’ initiation (i.e., by the occurrence, in some areas, of intense electric fields).

4.4.2 Water Trees Characteristics

Koo et al. [120] and Cross et al. [193] studied the dielectric properties of vented trees obtained experimentally with water needles at 1.5 kHz. They measured the capacity between the water needle and the opposite plane electrode during the development of vented trees, and concluded that a vented tree behaves more like a dielectric than a conductor. If vented trees were conductive, then, increasing from one side to the other of the insulation, it would initiate a thermal breakdown or an electric tree, which would be followed by a total breakdown of the insulation. In most cases, it was found that, although very long vented trees appeared, they did not cause the insulation breakdown at 2 kV/mm (or even more). Furthermore, it was noted that the breakdown voltage (thus, the dielectric strength E_b) decreases with increasing the lengths of vented trees [2]. Generally, water trees cause a reduction in breakdown voltage (measured at both 50 and 0.1 Hz, c.c. or pulse) [123, 194, 195]. It was found that E_b decreases with the increase in trees lengths (Fig. 11.43). Furthermore, the

Fig. 11.43 Variation of the dielectric strength on the relative length of trees $l_r = l/g$ (l —tree length, g —insulation thickness) (reprinted, with permission, from author [2])



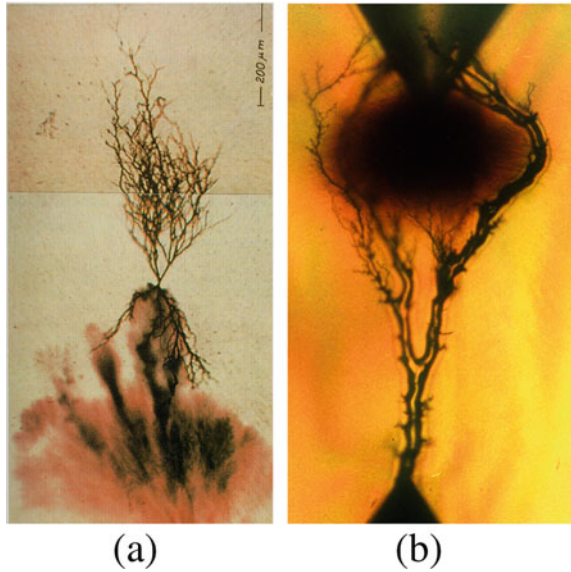
development of vented trees does not necessarily cause an immediate breakdown of the insulation. Such insulation often maintains a withstand voltage and therefore a dielectric strength (in fact a maximum permissible stress) of more than 2 kV/mm. By drying the insulation, the maximum stress level increases, reaching at least 50% of the permissible level (initial) [196]. However, the effect of water trees does not disappear if the insulation comes into contact with water or water steam. The water molecules will be absorbed by the insulation and the values of the breakdown voltage will be reduced again [197].

As a result of the water trees development, the loss factor increases [198–201] and the resistivity (thus, the insulation resistance) decreases [168, 198, 202–206]. For example, Tharning et al. [205] found that, after two weeks of accelerated aging (electric field + water) of some PE samples, the loss factor increased more than 10 times.

The electrical conductivity increases (more than 10^6 times) in XLPE insulation tree areas due to the increased concentration and mobility of the ions from trees [207–209]. Also, the relative permittivity values ϵ_r increase. Thus, if for XLPE without trees it is assumed that $\epsilon_r = 2.3$, in the presence of trees the values of ϵ_r can reach up to 4–5. This is due, in particular, to the increase in concentration of the electrical dipoles (e.g., water molecules) [2].

The water trees development is not normally accompanied by the occurrence of detectable PDs [198, 204, 210]. However, in certain situations (e.g., when using high voltages), water trees can initiate electrical trees, which, as is known, facilitate the initiation of electric breakdown [2] (Fig. 11.44a). It is considered that the initiation of electrical trees is predominantly produced in the area where the vented trees path encounters an electric field concentrator (e.g., an impurity or a cavity), as seen in Fig. 11.44b.

Fig. 11.44 Electric trees developed in the presence of water trees: **a** the electric tree starts from the water tree; **b** the electric tree avoids the water tree (Reprinted, with permission, from author [2])



4.4.3 Mechanisms and Models of Water Trees Development

Over the last few decades, numerous mechanisms have been proposed to explain the propagation of trees, a description of which is presented by Dissasdo and Fothergill in [11]. These mechanisms have been grouped, depending on their applicability, to explain the initiation or propagation of trees. Most of the mechanisms can be considered as versions of an electrochemical process, some of which are essentially electrical, electrochemical or electromechanical-chemical ones, and a small part is based on thermodynamic forces. It is clear from this group that most authors identify either a mechanical or a chemical component as essential in the process of treeing, and although an author considers some or others of the processes as alternatives, only in one case a combination of them was used. Therefore, although so many mechanisms have been proposed, none of them can fully describe all the aspects observed in the initiation and propagation of water trees. However, it should be noted that in all the mechanisms, the electric field plays an essential role in the initiation and development of water trees. The most important mechanisms are based on capillary action, osmosis, coulombic forces, dielectrophoresis, PDs, thermal degradation and chemical degradation [2, 11, 143, 145, 163, 211].

As water trees consist of microcavities generated by the treeing process, it is natural to assume that mechanical forces play a relatively important role in this process. This information is experimentally proven by accelerating propagation of trees in the event of application stretching stresses and by reducing propagation rate in the case of isotropic compression. A model of initiation and development

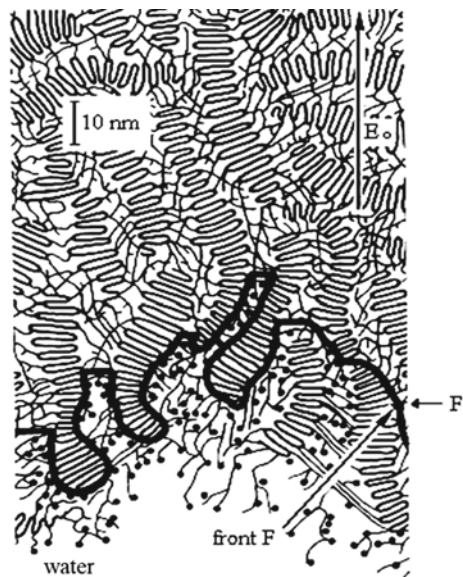
of water trees, based on the assumption of formation nanocavities in the insulation, which increase if the pressure applied by the electric field on the liquid contained in nanocavities, exceeds the permissible limit of the polymer is presented by Crine in [146].

The essential role of chemical reactions in the propagation process is not very clear, but it is known that antioxidants reduce the rate of propagation, while oxidizing agents increase it. Furthermore, it is observed that the process of treeing is inhibited by inert gases (e.g., nitrogen). From the analysis of areas containing water trees resulted that they are oxidized and that, therefore, oxidation is an essential factor in the mechanisms of trees development.

Steennis [210] showed that water penetrates the amorphous regions of the polymers if they contain polar particles. The occurrence of a polar zone (i.e., a process that can be considered as the initiation of vented trees) may be due to the oxidation of the cable insulation during the manufacturing process, the diffusion of impurities from the inner semiconductor of the cable in the insulation volume [212] and the insulation surface scratching during or after the cable production, process which generates polymeric chain ends (easily oxidizable) [2].

Figure 11.45 illustrates the development of a water trees by electrochemical action. The water penetrates the amorphous regions to the points where the polar groups are located. The front of this area where the water penetrated is marked by the continuous line F . In the polar region (up to the line F), an ions displacement from the electrolyte in contact with PE can occur. Behind the front-line F , the polymer is pure and behaves like a dielectric with permittivity ϵ_p , which corresponds to a capacitive electric current (when establishing an electric field). Ions displacement is stopped at the interface

Fig. 11.45 Water penetration through the polar surface of the insulation (© 1990 IEEE. Reprinted, with permission, from [123])



F , where a charge transfer by electrolysis occurs, as described by Kao et al. [213]. As a result, free radicals or oxidizing agents such as H_2O_2 are formed. The polymer is attacked, the front F penetrates deeper inside the polymer, creating a polar zone (path) containing water and actually forming a water tree. The formed vented tree can be considered as an electrolyte with very high resistivity (the potential difference that ‘falls’ on the tree is very high). Since the remaining potential difference is important, the vented tree path may contain several fronts F in series. As the ionic current in the water tree is maintained (in this theory) by the capacitive current through the dielectric area unaffected by tree, the tree development occurs only in a.c.

In 1990, Ross et al. [177] proposed a more advanced model of water trees structure in which the hydrophilic nature of water trees is explained by the presence of ionic bonding groups (chemical or physical). It is assumed that oxidation occurs during the development of water trees, and carboxyl and/or sulfur-oxygen ionic groups are regarded as possible oxidation products. It is suggested that sulfur-oxygen acid groups may be the result of antioxidants oxidation and that, in contact with water, these groups can be converted into salts.

Considering the action of the harmonic electric field on the ions displacement in solid dielectrics, Fouracre et al. and Given et al. [214–216] proposed a mechanism for the penetration of ions in front and within the trees regions. The authors showed that when establishing a harmonic electric field in a sample, the potential barrier that ions need to escalate [2] reduces in a semi-period and increases in the other, leading to the generation of an ions flux in the direction of the electric field lines. It is assumed that initially an ions penetration occurs in the polymer, leading to a local damage of the polymer, especially in its amorphous zones (a separation of polymer chains), facilitating the penetration of water molecules. In the ion-penetrating process, their rays play a significant role.

Sletback [217] highlighted the role of ions in the water trees development, but does not explain the values of their concentrations in trees’ area.

All mechanisms that were explaining the propagation of water trees based on forces proportional to the square of the electric field intensity showed an increase in the rate of development with frequency. By eliminating those models that are inevitably linked to cracks production, the most promising mechanisms are based on the formation of microcavities.

Electromechanical models consider that the force, which cause the degradation (causing the advancement of the tree, respectively) is proportional to E^2 . The same dependence is also proposed in the case of chemical degradation, as a result of a sustained reaction by the electric field. The chemical reaction leads to a local increase of the permittivity. In any model, the energy required to produce trees comes either directly from the electric field, or from the dissipated heat. In the proposed models, these energies are converted into a ‘mechanical stress’ dependent on the electric field E , which is responsible for producing trees. A general scheme of water trees development in XLPE insulation of cables is shown in Fig. 11.12.

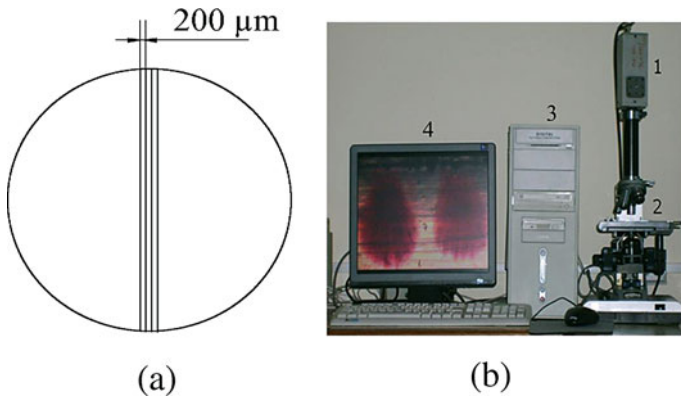


Fig. 11.46 Measuring equipment for the water trees dimensions of water: **a** Sampling from a plan sample; **b** Measuring equipment: 1—Video camera; 2—Optical microscope; 3—Computer; 4—Monitor (Reprinted, with permission, from author [6])

4.4.4 Water Tree Resistance

The evaluation of XLPE insulation resistance to water trees and, in particular, the evaluation of XLPE with inhibitors against water treeing phenomenon can be done by accelerated aging tests. The purpose of such tests is to obtain, in a short period, as complete as possible information on the behavior of insulation to water trees during the operation of the electrical equipment. In this respect, it can be developed, accelerated (at electrical stresses higher than those used in operation) water trees at different time intervals. Their dimensions and samples (with and without trees) parameters are measured.

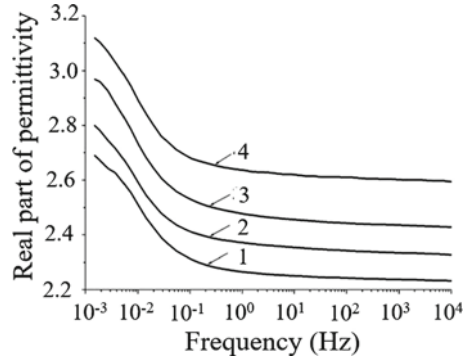
Measurement of Trees Dimensions

To measure trees dimensions, electrically aged samples are placed in a solution of rhodamine or blue methylene and kept in an oven for 72 h at temperature $T = 60\text{ }^{\circ}\text{C}$. Using a microtome, 3–5 samples (flat circular plates or crowns) of 200–300 μm (Fig. 11.46a) are taken from each sample, and the dimensions of the trees are measured with a simple equipment consisting of an optical microscope, a video camera and a color monitor (Fig. 11.46b) [6].

Determination of Trees Concentration

Determination of trees concentration is carried out by counting trees on taken samples or directly on samples (Fig. 11.46, [6]). The smaller the trees size and concentration, the greater is the material resistance to water treeing.

Fig. 11.47 Variation of the permittivity with the frequency for electrically aged XLPE samples at different aging periods τ : 1— $\tau = 0$, 2— $\tau = 48$ h, 3— $\tau = 72$ h, 4— $\tau = 96$ h (Reprinted, with permission, from author [220])



Space Charge Measurement

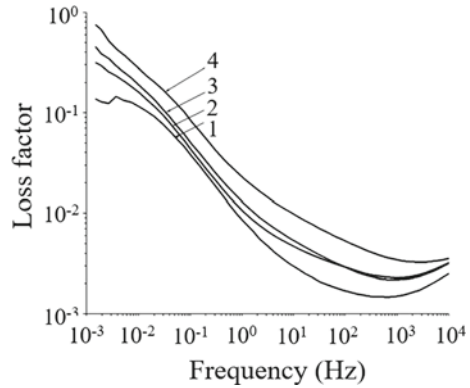
Different methods can be used to measure the space charge associated with water trees: Thermal Pulse Method (TPM), Laser Intensity Modulation Method (LIMM), Pulsed Electro-Acoustic Method (PEAM), Thermal Pulse Method (TPM), Thermal Wave Method (TWM), etc. [6, 218, 219]. An increase in density of ionic space charge means an increase in the concentration and/or the dimensions of the trees, thus a lower resistance of the sample to the water treeing [6].

Dielectric Spectroscopy

Dielectric spectroscopy in the time domain involves the measurement of the absorption and desorption currents on the samples or the cables insulation subjected to DC voltages and the calculation of the conductivity of the samples in the presence of water trees [6]. Increasing the absorption currents (and the electrical conductivity) means an increase in the concentration and/or the dimensions of the water trees. Dielectric spectroscopy in the frequency domain involves the measurement of the real and imaginary components of the complex permittivity and the loss factor at frequencies between 1 μ Hz and 1 GHz. Increasing the values of these parameters with the duration of the electrical stress (Figs. 11.47 and 11.48) [220] means the increase in the dimensions and/or the concentrations of water trees [6].

The modification of XLPE insulation properties due to accelerated aging tests for determining the water treeing resistance of some medium voltage cables is presented by Li et al. in [221]. The authors found that with increasing aging time, an increase in the electrical conductivity, a change in the lamellar structure (a reduction in the thickness of the lamellae) and a reduction in density, crystallinity index and melting temperature of the tested samples are produced.

Fig. 11.48 Variation of loss factor with the frequency for electrically aged XLPE samples at different aging periods τ : 1— $\tau = 0$, 2— $\tau = 48$ h, 3— $\tau = 72$ h, 4— $\tau = 96$ h (Reprinted, with permission, from author [220])



4.4.5 Water Trees Effects Attenuation

To improve the performance of cables insulation operating in high humidity environments, two different methods can be applied. On the one hand, it is possible to produce cables in a sealed construction, which do not allow direct contact of the insulation with water, and, on the other hand, the contact of the insulation with water can be accepted, but the insulation should contain water-inhibiting materials against water trees.

Sealed Construction

In many countries, sealed power cables construction with longitudinal water barriers (located along the conductor, inside or outside insulation) or radial (located outside the insulation) is used [123, 222, 223]. Longitudinal barriers along the conductors are achieved by partially or totally reducing the gaps volume between the constituent wires of the cables’ conductors. In this regard, fillings with compounds or materials that absorb water (hygroscopic) are used to fill the gaps or conductors are produced without gaps (full), preventing the longitudinal water penetration into the cable.

The filler compounds may be semiconductor or insulating materials and must be with stable to variable temperature, high chemical resistance, deformable and elastic for long periods and do not attack the cable components. Water absorbing materials are organic or inorganic powders and are introduced into the conductor gaps during cable manufacturing. After absorbing water, they turn into gels, which prevent the penetration of other water molecules into the conductor gaps. The water absorbing longitudinal jackets are disposed over the outer semiconductor screens under or over the metal screens (Fig. 11.49). Radial barriers are achieved by using copper or aluminum strips coated with two layers of acrylic copolymer [224].

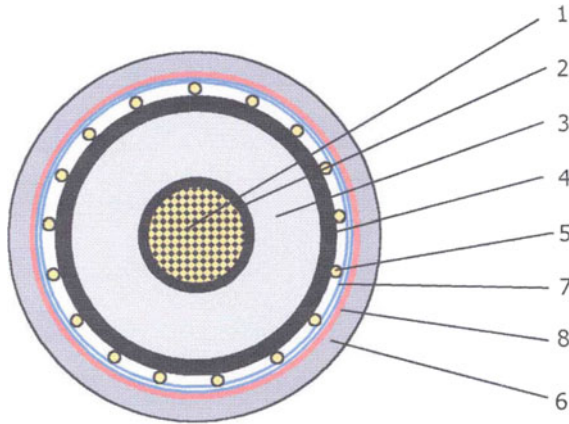


Fig. 11.49 Power cable with longitudinal and transversal protection to water trees: 1—Conductor (copper wire); 2—Inner semiconductor layer (polyethylene with black carbon); 3—Insulation (XLPE); 4—Outer semiconductor layer (polyethylene with black carbon); 5—Metal screen (conductors + copper tape); 6—Outer coating (polyethylene or polyvinyl chloride); 7—Longitudinal protection layer against water penetration (very low water permeability band); 8—Radial protection layer against water penetration (aluminum laminated tape) [224]

Water Trees Inhibitors

Manufacturers of polymeric materials and cables are making great efforts to obtain water trees inhibitors ('water tree retardants' or WTR) [225]. These inhibitors are modified polymers, polymers with chemical additives and their mixtures. Considering that electrochemical reactions underlie the initiation and development of water trees, Henkel et al. [226] carried out a detailed study on the mechanism of hydrogen peroxide formation and its important role in generating organic radicals that facilitate the process of PE oxidation and thus the development of water trees. By using barbituric acid and a series of their derivatives (1-methylbarbituric acid, isobarbituric acid, 2,4,6-trimethoxypyrimidine, 4-aminouracil, etc.), the authors obtained a reduction in the sizes and rate of trees development depending on the concentration of the additives. They showed that if a concentration value above a limit value is used, these additives lose their inhibitory effect.

The inhibitor effect (retardant) of residual crosslinking products on the development of water trees has been confirmed by Saure et al. [227] (by tests at 50 Hz). Moreover, Saure discovered that an antioxidant used as a stabilizer of PE has a contrary effect in this test. Furthermore, he found that PE crosslinked with silanes was less susceptible to water trees than the one crosslinked with peroxides.

Kato et al. [104] have succeeded in blocking the initiation of water trees in XLPE by introducing mixtures of various additives (ferrocene, siloxane oligomer and 8-hydroxyquinoline) into samples. The resistance to trees initiation was attributed to the combined action of migration of these additives into microcavities and the deactivation of electrons and ions by trapping.

Another water tree inhibitor additive has been disclosed by McMahon et al. [228]. This is a dodecanol that has been tested on water needle-plane electrode samples at different frequencies for 28 days on PE samples and on cables insulation (220 days at 90 °C). In the latter case, it has been found that the concentration of dodecanol has not changed, which means that this additive retains its inhibitory effect for a long time.

In 1986, Fisher et al. [229] prepared the inhibitor called HF-DA 4202. This is a non-filler polymer and a ‘non-stepper’ additive (which fits into the polymer), an organometallic compound, respectively. Short-term tests with water needles have highlighted the very good inhibitory properties of this material.

Excluding inhibiting insulating materials, it is assumed that smooth and low impurities concentration of semiconductor layers would help to delay the development of water trees, especially the vented ones [230]. Therefore, one way of reducing the number and size of water trees is to produce semiconductor screens with very smooth surfaces and low-hygroscopic XLPE insulation doped with trees inhibitors, respectively (TR-XLPE) [230]. TR-XLPE type insulation contain hydrophilic molecular clusters (TR) dispersed in a hydrophobic XLPE matrix. It can be considered that the water trees consist of a single channel and that this channel develops until meets such a cluster which, being hydrophilic can stop its propagation (by preventing water condensation in the electro-oxidized regions) [231]. Considering that the average cluster spacing is 0.2–0.3 mm, Boggs [231] showed that a typical water tree can reach 0.3–1 mm (for a 5% probability). This model gives a qualitative explanation and a quantitative basis for estimating trees lengths in TR-XLPE insulation, consistent with experimental results.

A study of the methods regarding the insulation testing based on XLPE and TRXLPE (XLPE with water tree inhibitors) of medium voltage cables is presented by Pelissou et al. in [225], according to the existing norms and standards [232, 233]. The authors conclude that there is still insufficient data to define a material as *water tree resistant material* based on the ASTM D6097-97 [233].

4.5 Space Charge Influence

Space charge is considered an excess of electric charge, continuously distributed in a space region (volume or surface) and consists of electrons, holes and ions. In terms of power cables, space charge is generally understood as a separation of free charge in the volume or interface of their insulation components due to: (i) carriers generated in the technological processes, (ii) space charge injection on the electrodes, (iii) the field-assisted thermal ionization of impurities from the insulation and (iv) the insulation degradation under the action of (electrical, thermal, mechanical, etc.) stresses during operation. In addition, space charge can accumulate in the case of the electric tree development [2] and/or in electrochemical approach (e.g., by water trees) [1, 2, 6, 234].

With respect to DC power cable joints with multi-layered insulation, electric charges accumulate at the interfaces of the layers during operation due to the different values of the charge carriers' relaxation time in the adjacent layers τ :

$$\tau = \varepsilon/\sigma, \quad (11.12)$$

in which ε represents the permittivity and σ —the electrical conductivity of the layer.

Space charge density is measured by different methods such as the piezoelectric-induced pressure wave propagation PIPWP method, the laser-induced pressure propagation LIPP method, the thermal step method TSM method, the pulsed electro-acoustic PEA method, etc. [1, 2, 6].

The accumulation in time of the space charge contributes to the local intensification of the electric field, which accelerates the degradation process of the material, respectively, an increase in PDs and a reduction in initiation times and an increase in the rate of the electric and electrochemical (water) trees. Although the analysis of the global action of space charge on the insulation is difficult to achieve, it is still necessary to control and to reduce space charge accumulation in high-voltage DC systems.

5 Conclusions

The degradation of XLPE insulation of medium and high-voltage cables under the action of the electric field is mainly due to the development of partial discharges and electric and electrochemical (water) trees. These phenomena can occur individually, eventually consecutively (unifactor degradation) or together at the same time (multifactor degradation). The three degradation factors influence each other, their effect on the insulation degradation being synergistic. Thus, partial discharges can lead to the initiation of electric trees, which cause an enhancement of partial discharges, the water trees facilitate the intensification of partial discharges and the appearance of electric trees, etc.

The action of partial discharges, electric and water trees over time leads to a worsening of the electrical characteristics of XLPE insulation and in the end to the insulation breakdown (followed by the failure of electrical equipment). Therefore, it is necessary to develop methods for slowing down or eliminating these phenomena, respectively, increasing the insulation resistance to electrical degradation.

Among the methods to reduce the XLPE insulation degradation, can be distinguish:

1. Producing XLPE granules of highest purity (no impurities);
2. Obtaining compounds and nanocomposites based on XLPE with high resistance to electrical degradation;
3. Improvement of conductor and semiconductor shields manufacturing technologies (high insulation adherence, low protrusions, etc.);

4. Producing equipment with metallic protection against the water and impurities penetration from the environment, etc.

Acknowledgements Ilona Plesa's contributions were accomplished within the K-Project Poly-Therm at the Polymer Competence Center Leoben GmbH (PCCL, Austria) within the framework of the COMET-program of the Federal Ministry for Transport, Innovation and Technology and the Federal Ministry for Digital and Economic Affairs. Funding is provided by the Austrian Government and the State Government of Styria.

References

1. Bartnikas R (2000) Characteristics of cable materials. In: Bartnikas R (ed) Power and communication cables. Theory and applications. IEEE Press, New York, pp 134–137
2. Notingher PV (2004) Materials for electrotechnics. In: Structure. Properties, vol 1. Politehnica Press, Bucharest, Romania, pp 350–403
3. Orton H (2013) History of underground power cables. IEEE Electr Insul Mag 29(4):52–57
4. Ohki Y (2013) Development of XLPE-insulated cable for high-voltage DC submarine transmission line (2). IEEE Electr Insul Mag 29(5):85–87
5. Stancu C, Notingher PV (2012) Electrical stresses of medium voltage cable insulations. Ed. Printech, Bucharest, Romania
6. Stancu C (2018) Méthodes d'estimation de l'état de vieillissement des câbles d'énergie. Editions universitaires européennes, Schaltungsdienst Lange o.H.G, Berlin
7. Stancu C, Notingher PV, Notingher P (2013) Computation of the electric field in aged underground medium voltage cable insulation. IEEE Trans Dielectrics Electr Insul 20(5):1530–1539
8. Stancu C, Notingher PV, Ciuprina F, Notingher Jr P, Castellon J, Agnel S, Toureille A (2009) Computation of the electric field in cable insulation in the presence of water trees and space charge. IEEE Trans Ind Appl 45(1):30–49
9. Taranu LV, Notingher PV, Stancu CR (2019) Accumulation and effects of space charge in direct current cable joints, Part I: model and methods for space charge density determination. Rev Roum Sci Tech Electr et Energy 64(2):1–6
10. Fothergill JC (2007) Aging, space charge and nanodielectrics: ten things we don't know about dielectrics. In: Proceedings of the IEEE International Conference on Solid Dielectrics, Winchester, UK, pp 1–10
11. Dissado LA, Fothergill JC (1992) Electrical degradation and breakdown in polymers. Peter Peregrinus Ltd.
12. O'Dwyer JJ (1973) Theory of electrical conduction and breakdown in solid dielectrics. Oxford University Press, Oxford, UK
13. Notingher PV, Ioan D (1978) A numerical method for computing the electrical stress in dielectrics. Revue Roum Sci Tehn Electr Et Energy 23(3):363–372
14. Notingher PV (1979) On the breakdown mechanism of inhomogenous solid dielectrics. Revue Roum Sci Tehn Electr Et Energy 24(4):651–663
15. Notingher PV (1979) Méthodes de calcul de la durée de rupture dans le système pointe-plan. Revue Roum Sci Tehn Electr Et Energy 31(1):59–68
16. Notingher PV (1979) Le calcul des durées de rupture des diélectriques solides. L'influence des gas de l'intérieur des cavités. Revue Roum Sci Tehn Electr Et Energy 31(2):133–144
17. Densley J (2001) Aging mechanisms and diagnostics for power cables - an overview. IEEE Electr Insul Mag 17(1):14–22
18. Ahmed Z, Hussain GA, Lehtonen M, Varacka L, Kudelcik J (2016) Analysis of partial discharge signals in medium voltage XLPE cables. In: 17th International scientific conference on electric power engineering (EPE), Prague, pp 1–6

19. Idrissu I (2016) Study of electrical strength and lifetimes of polymeric insulation for DC applications. Ph.D. Thesis, University of Manchester, Manchester, UK
20. Dissado LA, Mazzanti G, Montanari GC (1997) The role of trapped space charges in the electrical aging of insulating materials. *IEEE Trans Dielectr Electr Insul* 4(5):496–506
21. Crine JP, Parpal JL, Lessard G (1989) A model of aging of dielectric extruded cables. In: *Proceedings of 3rd ICSD*, pp 347–351
22. Rowe SW (2007) Electrical aging of composites: an industrial perspective. In: *2007 International conference on solid dielectrics*, Winchester, UK, pp 401–406
23. Crine J-P, Vijnh AK (1985) A molecular approach to the physicochemical factors in the electric breakdown of polymers. *Appl Phys Comm* 5(3):139–163
24. Dissado LA, Mazzanti G, Montanari GC (1995) The incorporation of space charge degradation in the life model for electrical insulating materials. *IEEE Trans DEI* 2(6):1147–1158
25. Dissado LA, Mazzanti G, Montanari GC (1997) Discussion of space-charge life model features in dc and ac electrical aging of polymeric materials. In: *Annual Report CEIDP*, pp 36–40
26. Mazzanti G, Montanari GC, Dissado LA (1999) A space-charge life model for ac electrical aging of polymers. *IEEE Trans Dielectrics Electr Insul* 6(6):864–875
27. Dissado LA, Mazzanti G, Montanari GC (2001) Elemental strain and trapped space charge in thermoelectrical aging of insulating materials. Part 1: elemental strain under thermo-electrical-mechanical stress. *IEEE Trans DEI* 8(6):959–965
28. Mazzanti G, Montanari GC, Dissado LA (2001) Elemental strain and trapped space charge in thermoelectrical aging of insulating materials. Life modelling. *IEEE Trans DEI* 8(6):966–971
29. Lewis TJ, Llewellyn JP, van der Sluijs MJ, Freestone J, Hampton RN (1996) A new model for electrical aging and breakdown in dielectrics. In: *IEE DMMA, Conference Publication No. 430*, pp 220–224
30. Lewis TJ (2001) Aging—a perspective. *IEEE Electr Insul Mag* 17:6–16
31. Lewis TJ, Llewellyn JP, van der Sluijs MJ, Freestone J, Hampton RN (1995) Electromechanical effects in XLPE cable models. In: *Proceedings of 5th ICSD (IEEE Pub. 95CH3476–9)*, pp 269–273
32. Griffiths CL, Freestone J, Hampton RN (1998) Thermoelectric aging of cable grade XLPE. In: *Proceedings of IEEE ISEI*, pp 578–582
33. C. L. Griffiths, S. Betteridge, J. P. Llewellyn, T. J. Lewis. The Importance of Mechanical Properties for Increasing the Electrical Endurance of Polymeric Insulation. *IEE DMMA, Conf. Pub. No 473*, 2000, p. 408–411
34. Jones JP, Llewellyn JP, Lewis TJ (2005) The contribution of field-induced morphological change to the electrical aging and breakdown of polyethylene. *IEEE Trans DEI* 12(5):951–966
35. Dang C, Parpal J-L, Crine J-P (1996) Electrical aging of extruded dielectric cables review of existing theories and data. *IEEE Trans DEI* 3(2):237–247
36. Parpal JL, Crine JP, Dang C (1997) Electrical aging of extruded dielectric cables—a physical model. *IEEE Trans DEI* 4(2):197–209
37. Crine JP (1997) A molecular model to evaluate the impact of aging on space charges in polymer dielectrics. *IEEE Trans DEI* 4(5):487–495
38. Mazzanti G, Montanari GC (2005) Electrical aging and life models: the role of space charge. *IEEE Trans DEI* 12(5):876–890
39. Harlin A, Danikas MG, Hyvönen P (2005) Polyolefin insulation degradation in electrical field below critical inception voltages. *J Electr Eng* 56(5–6):135–140
40. Hyvönen P (2008) Prediction of insulation degradation of distribution power cables based on chemical analysis and electrical measurements. Ph.D. Thesis, Helsinki University of Technology (TKK), Espoo, Finland
41. Oyegoke B, Hyvönen P, Aro M, Gao N (2003) Application of dielectric response measurement on power cable systems. *IEEE Trans DEI* 10(5):862–873
42. ***IEC 60270, High-voltage test techniques—Partial discharge measurements, Geneva, 1 November 2015
43. Gamez-Garcia M, Bartnikas R, Wertheimer MR (1987) Synthesis reactions involving XLPE subjected to partial discharges. *IEEE DEI EI-22(2)*:199–205

44. Wolter KD, Tanaka J, Johnson JF (1982) A study of the gaseous degradation products of corona-exposed polyethylene. *IEEE Trans Electr Insul* EI-17(3):248–252
45. Morshuis PHF (2005) Degradation of solid dielectrics due to internal partial discharge: some thoughts on progress made and where to go now. *IEEE Trans DEI* 12(6):1275–1275
46. McMahon EJ (1968) The chemistry of corona degradation of organic insulating materials in high voltage fields under mechanical strain. *IEEE Trans Electr Insul* EI-3(1):3–10
47. Foulon Belkacemi N, Goldman M, Goldman A, Amouroux J (1995) Transformation of nodules into crystals on polymers submitted to corona discharges with streamers. *IEE Proc Sci Measur Techn* 142(6):477–481
48. Morshuis P (1995) Assessment of dielectric degradation by ultrawide-band PD detection. *IEEE Trans DEI* 2(5):744–760
49. Gulski E, Kreuger FH (1992) Computer-aided recognition of discharge sources. *IEEE Trans Electr Insul* 27(1):82–92
50. James J, Kulkarni SV, Parekh BR (2009) Partial discharge in high voltage equipment-HV cable. In: Proceedings of IEEE 9th international conference on the properties and applications of dielectric materials (ICPADM), Harbin, China, pp 445–448
51. Kreuger FH (1989) Partial discharge detection in high-voltage equipment. Butterworths, London
52. Montanari GC, Cavallini A, Puletti F (2006) A new approach to partial discharge testing of HV cable systems. *IEEE Electr Insul Mag* 22(1):14–23
53. Pleşa I, Nojinger PV, Stancu C, Wiesbrock F, Schlögl S (2019) Polyethylene nanocomposites for power cable insulations. *Polymers* 11(1):24
54. Notinger PV (2002) Insulation systems. PRINTECH Publishing House, Bucharest
55. Bahder G, Garrity T, Sosnowski M, Eaton R, Katz C (1982) Physical model of electric aging and breakdown of extruded polymeric insulated power cables. *IEEE Trans PAS* PAS-101(6):1379–1390
56. Temmen K (2000) Evaluation of surface changes in flat cavities due to aging by means of phase-angle resolved partial discharge measurement. *J Phys D Appl Phys* 33:603–608
57. Yoda B, Muraki K (1973) Development of EHV cross-linked polyethylene insulated power cables. *IEEE Trans PAS* PAS-92(2):506–513
58. Muccigrosso J, Phillips PJ (1978) The morphology of cross-linked polyethylene insulation. *IEEE Trans Electr Insul* EI-13(3):172–178
59. Nitzer H (1966) Teilentladungsvorgänge in dielektrischen Hohlräumen. Technische Hochschule Illmenau, XI, Internationale Wissenschaftliche Kolloquium, pp 25–31
60. Pedersen A (1968) Partielle Udladninger i kunstige Hulrum. Vasteras, Nord-PD 68
61. Kreuger FH (1964) Discharge detection in high voltage equipment. Heywood, London
62. Mason JH (1951) The deterioration and breakdown of dielectrics resulting from internal discharges. *Proc Inst Electr Eng Part I General* 98(109): 44–59
63. Dakin TW, Berg D (1959) Luminous spots on electrodes in insulating oil gaps. *Nature* 184(120):120
64. Notinger PV, Plopeanu M (2009) Fast development of electrical trees. Part I—a: trees inception. *EEA Electr Eng Electron Autom* 57(4):11–19
65. Tanaka T, Ohki Y, Ochi M, Harada M, Imai T (2008) Enhanced partial discharge resistance of epoxy/claynanocomposite prepared by newly developed organic modification and solubilization methods. *IEEE Trans DEI* 15(1):81–89
66. Arief YZ, Ahmad H, Hikita M (2008) Partial discharge characteristics of XLPE cable joint and interfacial phenomena with artificial defects. In: Proceedings of IEEE 2nd international power and energy conference (PECON), Johor Bahru, Malaysia, pp 977–982
67. Lyle R, Kirkland JW (1981) An accelerated life test for evaluating power cable insulation. *IEEE Trans Power Appar Syst* PAS-100(8):3764–3774
68. Okamoto H, Kanazashi M, Tanaka T (1977) Deterioration of insulating materials by internal discharge. *IEEE Trans PAS* PAS-96(1):166–177
69. Rageb MHSA, Pearmain AJ (1984) An approach to the prediction of the lifetime of electrical insulations. *IEEE Trans Electr Insul* EI-19(2):107–113

70. Eriksson AJ, Kroninger H (1984) Accelerated life performance studies on a sample 132 kV XLPE industrial cable installation. In: Proceedings of 30th Session CIGRE, Paris, Paper 15–05
71. Wolzak GG, van de Laar AMFJ, Steennis EF (1986) Partial discharges and the electrical aging of XLPE cable insulation. EUT Report 86-E-160, Eindhoven University of Technology
72. Gamez-Garcia M, Bartnikas R, Wertheimer MR (1984) Circular degradation patterns on XLPE surfaced electrodes. In: IEEE international symposium on electrical insulation, pp 356–359
73. Gamez-Garcia M, Bartnikas R, Wertheimer MR (1990) Modification of XLPE exposed to partial discharges at elevated temperature. IEEE Trans Electr Insul 25(4):688–692
74. Fabiani D, Montanari GC (2001) The effect of voltage distortion on aging acceleration of insulation systems under partial discharge activity. IEEE Electr Insul Mag 17(3):24–33
75. Stone G, Campbell S, Tetreault S (2000) Inverter-fed drives: Which motor stators are at risk? IEEE Ind Appl Mag 6(5):17–22
76. Morshuis PHF (1993) Partial discharge mechanisms. Ph.D. Thesis, Delft University of Technology
77. Devins JC (1984) The physics of partial discharges in solid dielectrics. IEEE Trans Electr Insul 19:475–495
78. Jeon SI, Nam SH, Shin DS, Park IH, Han MK (2000) The correlation between partial discharge characteristics and space charge accumulation under AC voltage. In: IEEE conference on electrical insulation and dielectric phenomena (CEIDP), pp 653–656
79. Al-Ghamdi SA, Varlow BR (2004) Treeing in mechanically prestressed electrical insulation. IEEE Trans Dielectr Electr Insul 11(6):130–135
80. Mason JH (1959) Dielectric breakdown in solid insulation. In: Progress in dielectrics, New York, Wiley, pp 1–58
81. Artbauer J (1965) Elektrische Festigkeit von Polymeren. Kolloid-Zeitschrift und Zeitschrift für Polymere 202:15–25
82. Fröhlich H (1947) On the theory of dielectric breakdown in solids. R Soc London Proc A 188(1015):521–532
83. Yoda B, Sakaba M (1969) Treeing degradation of high voltage polyethylene insulated cable. Hitachi Rev 18:406–412
84. Golinski J (1968) Mehrphasiger Mechanismus des Ionisations-Durchschlages von festen Kunststoffen. Wissenschaftliche Zeitschrift der Elektrotechnik 10:193–205
85. Bahder G, Dakin TW, Lawson JH (1974) Analysis of treeing type breakdown. In: International conference on large high voltage electric systems (CIGRE). Paris, Conference report 15-05
86. Yamano Y, Okada M (2001) Reduction of PD in a void by additives of azobenzoic compound in HDPE insulating material. IEEE Trans DEI 8(6):889–896
87. Notingher PV, Plopeanu M (2010) Fast development of electrical trees. Part II: trees development. EEA-Electrotehnica Electronica Automatica 58(1):24–31
88. Harlin A, Shuvalov M, Ovsienko V, Juhanoja J (2002) Insulation morphology effects on the electrical treeing resistance. IEEE Trans DEI 9(3):401–405
89. https://www.researchgate.net/publication/251880167_Imaging_and_Analysis_Techniques_for_Electrical_Trees_using_X-ray_Computed_Tomography
90. Dissado LA (2002) Understanding electrical trees in solid: from experiment to theory. IEEE Trans DEI 9:483–497
91. Dissado LA, Dodd SJ, Champion JV, Williams PI, Alison JM (1997) Propagation of electrical tree structures in solid polymeric insulation. IEEE Trans Dielectrics Electr Insul 4(3):259–279
92. <https://www.google.ro/search?q=electrical+trees+in+polypropylene>
93. Liu M, Liu Y, Li Y, Zheng P, Rui H (2017) Growth and partial discharge characteristics of electrical tree in XLPE under AC-DC composite voltage. IEEE Trans Dielectrics Electr Insul 24(4):2282–2290
94. Chen G, Tham CH (2009) Electrical treeing characteristics in XLPE power cable insulation in frequency range between 20 and 500 Hz. IEEE Trans DEI 16:179–188
95. Schurch R, Ardila-Rey J, Montana J, Angulo A, Bradley RS (2019) 3D characterization of electrical tree structures. IEEE Trans DEI 26(1):220–228

96. Karmakar S (2018) Study of degradation phenomena of solid insulation used in extra high voltage cable under alternating voltage stress. In: 2nd IEEE international conference on dielectrics (ICD-2018), Budapest, Hungary
97. Varlow BR, Auckland DW (1998) The influence of mechanical factors on electrical treeing. *IEEE Trans Dielectr Electr Insul* 5:761–765
98. Liu Y, Xiao Y, Su Y, Chen X, Zhang C, Li W (2016) Electrical treeing test of DC cable XLPE insulation under DC voltage and high temperature. In: IEEE international conference on dielectrics (ICD). <https://doi.org/10.1109/icd.2016.7547725>
99. Densley RJ (1979) An investigation into the growth of electrical trees in XLPE cable insulation. *IEEE Trans Electr Insul* 14:148–158
100. Gao Y, Deng YD, Du BX, Li SW, Wang N (2016). Electrical treeing behavior in XLPE under kHz-AC voltage. In: IEEE international conference on dielectrics (ICD). <https://doi.org/10.1109/icd.2016.7547718>
101. Shimizu N, Uchida K, Rasikawan S (1992) Electrical tree and deteriorated region in polyethylene. *IEEE Trans Electr Insul* 27(3):513–518
102. Zheng X, Chen G (2008) Propagation mechanism of electrical tree in XLPE cable insulation by investigating a double electrical tree structure. *IEEE Trans DEI* 15:800–807
103. Shimizu N, Laurent C (1998) Electrical tree initiation. *IEEE Trans DEI* 5:651–659
104. Kato H, Maekawa N, Inoue S, Fujita H (1974) Effect and mechanism of some new voltage stabilizers for cross-linked polyethylene insulation. In: Proceedings of conference electrical insulation & dielectric phenomena. <https://doi.org/10.1109/ceidp.1974.7735913>
105. Englund V, Huuva R, Gubanski SM, Hjertber T (2009) Synthesis and efficiency of voltage stabilizers for XLPE cable insulation. *IEEE Trans DEI* 16(5):1455–1461
106. Gross RE, Hunt GH (1967) Dielectric compositions containing halogenated voltage stabilizing additives. Patent US3350312, Simplex Wire and Cable Co
107. Hunt GH (1967) Stabilized dielectric composition containing 2-bromonaphthalene. Patent US3346500, Simplex Wire and Cable Company
108. Hunt GH (1969) Voltage stabilized solid polyolefin dielectric. Patent US3445394, Simplex Wire and Cable Company
109. Hunt GH (1970) Voltage stabilized polyolefin dielectric compositions using liquid-aromatic compounds and voltage stabilizing agents. Patent US3542684, Simplex Wire and Cable Company
110. Kenney ND, Petterson VS (1969) High voltage polyolefin insulated cable. Patent US3482033, Simplex Wire and Cable Co.
111. Sekii Y, Maruta K, Okada T (1998) Effect of inclusions in XLPE insulations on electrical trees generated by AC and grounded DC voltage. In: IEEE 6th international conference on conduction and breakdown in solid dielectrics, Vaesteras, Sweden, pp 317–320
112. Sekii Y, Ohbayashi T, Uchimura T, Mochizuki K, Maeno T (2002) The effects of material properties and inclusions on the space charge profiles of LDPE and XLPE. In: IEEE conference on electrical insulation and dielectric phenomena (CEIDP), pp 635–639
113. Hirai N, Maeno Y, Tanaka T, Ohki Y, Okashita M, Maeno T (2003) Effect of crosslinking on space charge formation in crosslinked polyethylene. In: IEEE 7th international conference on properties and applications of dielectric material, Nagoya, Japan, pp 917–920
114. Hirai N, Minami R, Tanaka T, Ohki Y, Okashita M, Maeno T (2003) Chemical group in crosslinking byproducts responsible for charge trapping in polyethylene. *IEEE Trans DEI* 10:320–330
115. Sekii Y, Hirota K, Chizuwa N (2001) Effects of antioxidants on electrical tree generation in XLPE. In: IEEE 7th International conference on solid dielectrics, Eindhoven, Netherlands, pp 460–464
116. Sekii Y, Tanaka D, Saito M, Chizuwa N, Kanasawa K (2003) Effects of antioxidants on the initiation and growth of electrical trees in XLPE. In: IEEE conference on electrical insulation and dielectric phenomena (CEIDP), pp 661–665
117. Bamji SS, Bulinski AT, Densley J (1989) Electrical tree suppression in high-voltage polymeric insulation. Patent US4870121, Canadian Patents and Development Ltd., Canada

118. Martinotto L, Peruzzotti F, Del Brenna M (2001) Cable, in particular for transport or distribution of electrical energy and insulating composition. Patent WO0108166, Pirelli Cavi e Sistemi S.p.A., Italy
119. Gubin SP, Smirnova SA, Denisovich LI, Lubovich AA (1971) Redox properties of cyclopentadienylmetal compounds I. Ferrocene, ruthenocene, osmocene. *J Organometallic Chem* 30(2):243–255
120. Koo JY, Cross JD, El-Kahel M, Meyer CT, Filippini JC (1983) Electrical behaviour and structure of water trees in relation to their propagation. In: Conference on electrical insulation & dielectric phenomena, pp 301–306
121. Ross R (1998) Inception and propagation mechanisms of water treeing. *IEEE Trans DEI* 5:660–680
122. Meyer CT (1983) Water absorption during water treeing in polyethylene. *IEEE Trans Electr Insul* 18:28–31
123. Steennis EF, Kreuger FH (1990) Water treeing in polyethylene cables. *IEEE Trans Electr Insul* 25:989–1028
124. Ross R, Geurts WSM, Smit JJ (1988) FTIR microspectroscopy and analysis of water trees in XLPE. In: IEE conference on publication no. 289, DMMA, pp 313–137
125. Chen JL, Filippini JC (1993) The morphology and behavior of the water tree. *IEEE Trans Electr Insul* 28:271–286
126. Steennis EF, van den Heuvel CC, Boone W (1987) Accelerated aging to predict water tree behavior in extruded cables. In: international conference on polymer insulated power cables, Paris, pp 161–167
127. Bamji S, Bulinski A, Densley J, Garton A, Shimizu N (1984) Water treeing in polymeric insulation. In: Proceeding of CIGRE, Paper 15-07
128. Visata O (2001) Influence des arborescences d'eau sur les propriétés diélectriques des polymères. Thèse, Université POLITEHNICA de Bucarest—Université Joseph Fourier Grenoble
129. Ashcraft AC (1977) Treeing update part III: water trees, Kabelitems 152, Union Carbide Corporation. Based on water treeing in polymer dielectrics. In: World electrotechnical congress
130. Radu I (1997) Behavior of some insulating materials in high electric fields. Ph.D. Thesis, UPB, Bucharest
131. Stancu C, Notingher PV (2010) Influence of the surface defects on the absorption/resorption currents in polyethylene insulations. *Sci Bull Univ Politehnica Bucharest Ser C* 72(2):161–170
132. Stancu C (2008) Caractérisation de l'état de vieillissement des isolations polymères par la mesure d'arborescences et de charges d'espace. Ph.D. Thesis, University POLITEHNICA of Bucharest
133. Filippini JC, Meyer CT, El-Kahel M (1982) Some mechanical aspects of the propagation of water trees in polyethylene. In: Proceedings of CEIDP, pp 629–637
134. Bulinski AT, Crine J-P, Noirhomm B, Densley RJ, Bamji S (1998) Polymer oxidation and water treeing. *IEEE Trans DEI* 5(4):558–570
135. Visata OI, Teissedre G, Filipinni JC, Notingher PV (2001) An investigation on the distribution of ions and water in water trees by FTIR microspectroscopy. In: Proceedings of IEEE 7th international conference on solid dielectrics, (ICSD), Eindhoven, Netherlands, pp 373–376 (2001)
136. Chiru O, Notingher PV, Jipa S, Setnescu T, Setnescu R (1996) Influence of antioxidant concentration on the water trees propagation. In: *Electrotehnica '96*, Bucharest, Romania, pp 157–164, 6–7 Dec 1996
137. Crine J-P (1998) Electrical, chemical and mechanical processes in water treeing. *IEEE Trans DEI* 5:681–694
138. Nagao M, Watanabe S, Murakami Y, Murata Y, Sekiguchi Y, Goshowaki M (2008) Water tree retardation of MgO/LDPE and MgO/XLPE nanocomposites. In: International symposium on electrical insulating materials (ISEIM), Mie, Japan, pp 483–486

139. Notingher PV, Ciuprina F, Radu I, Filippini JC, Gosse B, Jipa S, Setnescu T, Setnescu R, Mihalcea T (1996): Studies on water treeing and chemiluminescence on irradiated polyethylene. In: Proceedings of international symposium on electrical insulation, Montreal, Canada, pp 163–167
140. Notingher PV, Ciuprina F, Radu I (1998): The influence of ageing process on the shape and the propagation kinetics of the water trees in needle-plane polyethylene samples. In: Proceedings of the 1998 IEEE 6th international conference on conduction and breakdown in solid dielectrics (ICSD), Västerås, Sweden, pp 341–344
141. Nunes SL, Shaw MT (1980) Water treeing in polyethylene—a review of mechanisms. *IEEE Trans Electr Insul* 15:437–450
142. Shaw MT, Shaw SH (1984) Water treeing in solid dielectrics. *IEEE Trans Electr Insul* 5:419–452
143. Swapan K, Battacharya K, Brown N (1984) Micromechanisms of crack initiation in thin films and thick sections of polyethylene. *J Mater Sci* 19:2519–2532
144. Zeller H (1991) Noninsulating properties of insulating materials. In: Proceedings of IEEE conference on electrical insulation and dielectric phenomena, pp 19–30
145. Wang Z, Evans JW, Wright PK (2011) Thermodynamics of water treeing. *IEEE Trans DEI* 18(3):840–846
146. Crine J-P, Jow J (2005) A water treeing model. *IEEE Trans DEI* 12(4):801–808
147. Filippini JC, Meyer CT (1988) Water treeing using the water needle method: the influence of the magnitude of the electric field at the needle tip. *IEEE Trans DEI* 23(2):275–278
148. Bernstein BS, Srinivas N, Lee PN (1975) Electrochemical treeing studies: voltage stress, temperature, and solution penetration effects under accelerated test conditions. In: Annual report conference on electrical insulation & dielectric phenomena, pp 296–302
149. Srinivas NN, Doepken HC (1978) Electrochemical treeing in PE and XLPE insulated cables—frequency effects and impulse degradation. In: IEEE conference on electrical insulation dielectrics phenomena, pp 106–109
150. Srinivas NN, Allam SM, Doepken Jr HC (1976) The effect of crosslinking and crosslinking agent by products on tree growth in polyethylene. In: Proceedings of conference on electrical insulation & dielectric phenomena, pp 380–385
151. Bulinski A, Densley RJ (1981) The voltage breakdown characteristics of miniature XLPE cables containing water trees. *IEEE Trans DEI* 16(4):319–326
152. Favrie E, Auclair H (1980) Effect of water on electrical properties of extruded synthetical insulations application on cables. *IEEE Trans PAS* 99(3):1225–1234
153. Filippini JC, Meyer CT (1982) Effect of frequency on the growth of water trees in polyethylene. *IEEE Trans DEI* 17(6):554–559
154. Densley J, Bulinski A, Sudarshan T (1979) The effects of water immersion, voltage and frequency on the electric strength of miniature XLPE cables. In: Annual report CEIDP, pp 469–479
155. Bulinski AT, Bamji SS, Densley RJ (1986) The effect of frequency and temperature on water tree degradation of miniature XLPE cables. *IEEE Trans DEI* 21(4):645–650
156. Dissado LA, Wolfe SV, Fothergill JC (1983) A study of the factors influencing water tree growth. *IEEE Trans DEI* 18:565–585
157. Dissado LA, Wolfe SV, Filippini JC, Meyer CT, Forthergill JC (1988) An analysis of field – dependent water tree growth models. *IEEE Trans DEI* 23(3):345–356
158. Yoshimura N, Noto F (1982) Voltage and frequency dependence of bow-tie trees in crosslinked polyethylene. *IEEE Trans DEI* 17(4):363–367
159. Suzuki H, Mukai S, Ohki Y, Nakamichi Y, Ajiki K (1988) Water-tree characteristics in low-density PE under simulated inverter voltages. *IEEE Trans DEI* 5(2):256–260
160. Kaneko D, Maeda T, Ito T, Ohki Y, Konishi T, Nakamichi Y, Okashita M (2004) Role of number of consecutive voltage zero-crossings in propagation of water trees in polyethylene. *IEEE Trans DEI* 11(4):708–714
161. Maeda T, Kaneko D, Ohki Y, Konishi T, Nakamichi Y, Okashita M (2005) Voltage zero-crossing as a factor inducing water trees. *IEE J Trans Fundam Mater* 125(1):51–56

162. Ohki Y, Ishikawa H, Morita G, Konishi T, Nakamichi Y, Tanimoto M (2008) Role of the voltage zero-crossing in the growth of water trees—effect of superposition method of a high-frequency voltage and a low-frequency voltage. In: International conference on condition monitoring and diagnosis, pp 328–331
163. Ohki Y (2008) Aiming at a more rigorous understanding in electrical insulating materials research. *IEEE Trans DEI* 15(5):1201–1214
164. Bahder G, Katz C, Lawson J, Vahlstrom W (1974) Electrical and electrochemical treeing effect in polyethylene and crosslinked polyethylene cables. *IEEE Trans PAS* 93:977–990
165. Bahder G, Katz C (1972) Treeing effects in PE and XLPE insulation. In: Conference on electrical insulation & dielectric phenomena, pp 190–199
166. Yoshimitsu T, Mitsui H, Hishida K, Yoshida H (1983) Water treeing phenomena in humid air. *IEEE Trans DEI* 18(4):396–401
167. Ross, R., Megens, M.: Dielectric properties of water trees. In: *IEEE International Conference on Properties and Applications of Dielectric Materials*, pp 455–458 (2000)
168. Tabata T, Nagai H, Fukuda T, Iwata Z (1972) Sulfide attack and treeing of polyethylene insulated cables—cause and prevention. *IEEE Trans PPAS* 91(4):1354–1360
169. Sletbak J, Ildstad E (1983) The effect of service and test conditions on water tree growth in XLPE cables. *IEEE Trans Power App* 102(7):2069–2076
170. Tanaka T, Fukuda T (1974) Residual strain and water trees in XLPE and PE cables. In: Conference on electrical insulation & dielectric phenomena, pp 239–249
171. Tu DM, Kao KC (1983) Effects of hydrostatic pressure on water treeing properties of polyethylene. In: Conference on electrical insulation & dielectric phenomena, pp 307–311
172. Mashikian M, Groeger JH (1987) Ionic impurities in extruded cable insulation. In: *Proceedings of JICABLE, Versailles*, pp 199–205
173. Garton A, Groeger JH, Henry JL (1990) Ionic impurities in crosslinked polyethylene cable insulation. *IEEE Trans DDEI* 25(2):427–434
174. Meyer CT, Chamel A (1980) Water and ion absorption by polyethylene in relation to water treeing. *IEEE Trans DEI* 15(5):389–393
175. Duna M, Senchiu M, Notingham PV, Radu I, Ciuprina F (1996) Influence of nature and impurities concentration on water trees propagation. In: “*Electrotehnică ’96*”, Bucharest, pp 165–171
176. Fournie R, Perret J, Recoup P, Le Gall Y (1978) Water treeing in polyethylene for HV cables. In: Conference of IEEE international symposium on electrical insulation, pp 110–115
177. Ross R, Geurts WSM, Smit J, Van der Maas JH, Lutz ETG (1990) The hydrophilic nature of water trees. In: Conference Record of International Symposium on Electrical Insulation
178. Li HM, Fouracre RA, Crichton BH, Banks VAA (1994) The influence of ions on the thermally stimulated discharge current spectra of water-treed additive-free low-density polyethylene. *IEEE Trans DEI* 1(6):1084–1093
179. Filippini JC, Koo JY, Chen JL (1989) Electrode Influence on the Properties of Water Trees in Polyethylene. *IEEE Trans. DEI* 12(1):75–82
180. Henkel HJ, Kalkner W, Muller N (1981) Electrochemical Treeing—Strukturen in Modelkabelisolierungen aus Thermoplastischem oder Vernetztem Polyethylen. *Siemens Forschungs und Entwicklungs Bericht*, vol 10, no 4, pp 205–214, Springer Verlag
181. Ashcraft AC (1977) Factors influencing treeing identified. *Electrical World*, p 3840
182. Kalkner W, Muller U, Peschke E, Henkel HJ, von Olshausen R (1982) Water treeing in PE and XLPE Insulated HV Cables. *CIGRE. Paper No. 21-07*
183. T. G. Marsh, A. P. Smith, J. Drysale. Long Term Aging of Water Immersed XLPE Insulations. *Int. Conf. on Polym. Insul. Power Cables*, 1987, p. 181–186
184. Morita M, Hanai M, Shimanuki H (1973) Some preventive methods for water treeing in PE and XLPE insulation. In: *Annual Report CEIDP*, pp 303–312
185. Saure M, Golz W (1985) Über den Einfluss von Mischungskomponenten auf das Water-Tree Wachstum in Polyolefin-Materialien und Prüfverfahren zur Bewertung des Water-Tree Wachstums. *Electrotechnische Gesellschaft Fachberichte* 16, VDE-Verlag GmbH, pp 127–131

186. Namiki Y, Shimanuki H, Aida F, Morita M (1980) A study on microvoids and their filling in crosslinked polyethylene insulated cables. *IEEE Trans Electr Insul* 15(6):473–480
187. Golz W (1985) Water-tree growth in low-density polyethylene. *Coll Polym Sci* 263:286–292
188. Poggi Y, Raharimalala V, Filippini JC, De Bellet JJ, Matey G (1990) Water treeing as mechanical damage. *IEEE Trans Electr Insul* 25(6):1056–1065
189. Ross R (1993) Effect of aging conditions on the type of water treeing. *IEEE Trans Electr Insul Mag* 9(5):7–13
190. Notingher PV, Ciuprina F, Radu I, Filippini JC, Gosse B, Jipa S, Setnescu T, Setnescu R, Mihalcea T (1996) Studies on water-treeing and chemiluminescence on irradiated polyethylene. In: Conference of IEEE international symposium on Electrical Insulation, pp 163–167
191. Garton A, Densley RJ, Bulinski A (1987) Oxidation and water tree formation in service-aged XLPE cables. *IEEE Trans DEI* 22:405–412
192. Spadaro G, Calderaro E, Rizzo G (1989) Radiation induced degradation and crosslinking of low density polyethylene. Effect of dose rate and integrated dose. *Acta Polym* 40:702–705
193. Cross JD, Koo JY (1984) Some observations on the structure of water trees. *IEEE Trans DEI* 19(4):303–306
194. Franke H, Heumann H, Kaubisch D (1984) Testing possibilities and results regarding water aging of PE/XLPE insulated medium voltage cables. In: International conference on polymer insulated power cables, pp 113–118
195. Matsuura K, Ohno H, Ishibashi A, Yatsuka K, Hirotsu K, Kajiki I, Shinagawa J (1987) Investigation on deterioration of 22 to 66 kV XLPE cables removed from actual service lines. In: International conference on polymer insulated power cables, pp 471–476
196. Katz C, Eager Jr GS, Leber ER, Fischer FE (1984) Influence of water on dielectric strength and rejuvenation of in-service aged URD cables. In: International conference on polymer insulated power cables, Paris, pp 127–134
197. Oyegoke BS, Birtwhistle B, Lyall J, Saha TK (2006) Water migration in degraded XLPE cables. In: Annual report CEIDP, pp 704–707
198. Bahder G, Eager GS, Lukac RG (1974) Influence of electrochemical trees on the electrical properties of extruded polymeric insulation. In: Annual report CEIDP, pp 289–301
199. Tanaka T, Fukuda T, Suzuki S, Nitta Y, Goto H, Kubota K (1974). Water trees in crosslinked polyethylene power cable. Paper T73497-5. IEEE PES summer meeting & EHV/UHV conference, pp 693–702
200. Fukagawa H, Okamoto T, Hozumi N, Shibata T (1987) Developments of methods to estimate the residual life of XLPE cables deteriorated by water trees. In: International conference on polymer insulated power cables, pp 457–462
201. Karner H, Stietzel U, Saure M, Golz W (1984) Determination of small water contents in solid organic insulating and the influence of moisture on the dielectric properties. In: Conférence Internationale des Grandes Réseaux Electriques à Haute Tension, CIGRE, Paper 15-02
202. Wojtas S (1987) Investigations of polyethylene insulation resistivity of power cables. In: International conference on polymer insulated power cables, pp 436–440
203. Notingher PV, Stancu C, Notingher Jr P (2009) Water trees—electrical aging factor for power cable insulation. *Science Bulletin of the “POLITEHNICA” University of Timisoara*, Tom 54, No. 68, Special Issue (Proceedings of the 8th International Power System Conference), pp 369–376
204. Srinivas NN, Doepken HC, McKean AL, Biskeborn MC (1978) Electrochemical treeing in cable. EPRI Final Report EL-647
205. Tharning P, Gafvert U (1995) High voltage dielectric frequency response measurements on polyethylene samples during water tree aging. In: IEEE 5th international conference on conduction and breakdown in solid dielectrics, pp 671–675
206. Densley J (1995) Aging and diagnostics in extruded insulations for power cables. In: IEEE 5th international conference on conduction and breakdown in solid dielectrics, pp 1–15
207. Toyoda T, Mukai S, Ohki Y (1999) Conductivity and permittivity of water tree in polyethylene. In: Annual Report CEIDP, pp 577–580

208. Thomas AJ, Saha TK (2008) A new dielectric response model for water tree degraded XLPE insulation—Part A: model development with small sample verification. *IEEE Trans DEI* 15(4):1131–1134
209. Katsuta G, Toya A, Ying L, Okashita M, Aida F, Ebinuma Y, Ohki Y (1999) Experimental investigation on the cause of harmfulness of the blue water tree to XLPE cable insulation. *IEEE Trans Electr Ins* 6:887–891
210. Steennis EF (1989) Water treeing, the behavior of water trees in extruded cable insulation. Ph.D. Thesis University Delft. ISBN 90-353-1022-5; KEMA, Arnhem
211. Radu I, Acedo M, Nottingher PV, Frutos F, Filippini JC (1997) The danger of water-trees in polymer insulated power cables evaluated from calculations of electric field in the presence of water trees of different shapes and permittivity distributions. *J Electrostat* 40–41:343–347
212. Crine J-P, Pelissou S, St-Onge H, St-Piere J, Kennedy G, Houdayer A, Hinrichsen P (1987) Elemental and ionic impurities in cable insulation and shields. In: International conference on polymer insulated power cables, pp 206–213
213. Kao KC, Hwang W (1981) Electrical transport in solids. In: International series in the science of the Solid State, vol 14. Pergamon Press
214. Fouracre RA, Given MJ, Crichton BH (1986) The effects of alternating electric fields on migration in solid dielectrics. *J Phys Chem* 19:1949–1958
215. Given MJ, Fouracre RA, Crichton BH (1987) The role of ions in the mechanism of water tree growth. *IEEE Trans DEI EI-22(2)*:151–156
216. Fouracre RA, Banford HM, Given MJ (1993) Charge migration processes in insulators. *High Temp Chem Proc* 2:257–264
217. Slebak J (1979) A theory of water tree initiation and growth. *IEEE Trans PAS* 98(4):1358–1365
218. Toyoda T, Mukai S, Ohki Y, Li Y, Maeno T (2001) Estimation of conductivity and permittivity of water tree in PE from space charge distribution measurements. *IEEE Trans. DEI* 8:111–116
219. Holé S, Ditchi T, Lewiner J (2003) Non-destructive methods for space charge distribution measurements: what are the differences? *IEEE Trans DEI* 10(4):670–677
220. Plopeanu M (2012) Estimation of power cables lifetime. Ph.D. Thesis, University POLITEHNICA of Bucharest
221. Li J, Zhao X, Yin G, Li S, Zhao J, Ouyang B (2011) The effect of accelerated water tree ageing on the properties of XLPE cable insulation. *IEEE Trans Dielectrics Electr Insul* 18(5):1562–1569
222. Bow KE (1989) The development of underjacket moisture barrier cable as a counter measure against treeing. *IEEE Trans Power Energy Soc* 5(1):47–53
223. Powers WF Jr (1993) An overview of water-resistant cable designs. *IEEE Trans Ind Appl* 29(5):831–833
224. Malik NH, Qureshi MI, Al-Arainy AA, Saati MN, Al-Natheer OA, Anam S (2012) Performance of water tight cables produced in Saudi Arabia under accelerated aging. *IEEE Trans DEI* 19(2):490–497
225. Péliou S, Harp R, Bristol R, Densley J, Fletcher C, Katz C, Kuchta F, Kung D, Person T, Smalley M, Smith JT III (2008) Review of possible methods for defining tree retardant crosslinked polyethylene (TRXLPE). *IEEE Electr Ins Mag* 24(5):22–30
226. Henkel H-J, Muller N, Nordmann J, Rogler W, Rose W (1987) Relationship between the chemical structure and the effectiveness of additives in inhibiting water-trees. *IEEE Trans DEI EI-22(2)*:157–161
227. Saure M, Kalkner W (1987) On water tree testing of materials. Rep. of CIGRE TF 15 – 06 – 05, CIGRE Symp. 05 – 87, Section 6.2, No. 620–10
228. McMahon EJ (1981) A tree growth inhibiting insulation for power cable. *IEEE Trans DEI* 16(4):304–318
229. Fisher EJ, McClung LB (1986) Long-life insulation for industrial and utility cables. *IEEE Trans Ind Appl* 5:946–951
230. Boggs SA, Mashikian MS (1994) Role of semiconducting compounds in water treeing of XLPE cable insulation. *IEEE Electr Insul Mag* 10(1):23–27

231. Boggs SA, Xu JJ (2001) Water treeing-filled versus unfilled cable insulation. *IEEE Electr Insul Mag* 17(1):23–29
232. *** Standard Test Method for Relative Resistance to Vented Water-Tree Growth in Solid Dielectric Insulating Materials, ASTM D6097–97 (1997)
233. *** Specifications for Thermoplastic and Cross-Linked Polyethylene Insulated Shielded Power Cables Rated 5 Through 46 kV, AEIC CS5–82, 8th ed (1982)
234. Ohki Y, Ebinuma Y, Katakai S (1998) Space charge formation in water-treed insulation. *IEEE Trans DEI* 5(5):707–712

Chapter 12

Short Overview of Practical Application and Further Prospects of Materials Based on Crosslinked Polyethylene



Ter-Zakaryan Karapet Armenovich and Zhukov Aleksey Dmitrievich

1 Introduction

The usage of products made of crosslinked polyethylene (XLPE) is of great importance in the world practice. More than 40% of the entire market of commercial plastics is accounted for the total share of polyethylene [1]. Polyethylene is the most widespread due to its relatively low cost and easy processing of the products made of it. However, simple polyethylene will lose its physical properties at high temperatures, which leads to the limitations in application. The process of crosslinking of the polyethylene is performed in order to preserve the desired properties of the material and acquire new qualities [1]. XLPE is the most dense among other polyethylene materials and has higher technical characteristics and operating properties, which arise from the structure of its polymer base and particularities of molecular structure.

XLPE is characterized by a range of unique qualities, such as thermal resistance, durability, chemical resistance, resistance to stress fracture, low dielectric losses, high resistance to microorganisms and many other particularities, which allowed the products made of it to be introduced into the majority of areas of modern human activity [1, 2].

Modern XLPE production is based on several fundamental principles of crosslinking using chemical and physical methods. Depending on these methods,

T.-Z. K. Armenovich (✉)
Tepofol, Moscow, Russia
e-mail: karo73@mail.ru

Z. A. Dmitrievich
National Research Moscow State University of Civil Engineering (NRU MSUCE), Moscow,
Russia

Russian Academy of Engineering, Moscow, Russia

a material with predetermined properties is obtained within the process of manufacture of products intended for solving various technological problems. Let us take a closer look at the prospects and practical methods of application of this polymer.

1.1 Base Methods of XLPE Production

XLPE is manufactured by means of different technologies and can be divided into two subtypes: chemically crosslinked polyethylene (using chemical reagents) and physically crosslinked polyethylene (using hard radiation). Final physical and chemical properties of the end product will depend on the method and type of additives by means of which the granulated raw material was processed.

The industrial production of XLPE uses three basic crosslinking technologies—peroxide, silane (XLPE is produced by means of chemical method) and radiant (XLPE is produced by means of physical method using hard radiation) methods [3, 4].

Peroxide crosslinking technology (Engel's method) represents a free radical process that leads to the formation of carbon bonds between polymer chains. Polyethylene is melted together with antioxidants and peroxides before extrusion in order to obtain a crosslinked polymer. Along with the temperature increase, peroxides decompose and build radicals (molecules with a free bond). Peroxide radicals detach one hydrogen atom from the polyethylene joints, which leads to the appearance of a free bond at the carbon atom. The carbon atoms are uniting in the adjacent macromolecules. A three-dimensional network is formed, which excludes the possibility of crystalline grain formation during polymer cooling. This method requires strict monitoring of the temperature conditions during the extrusion and the preliminary crosslinking as well as during further heating to complete bonds formation. The decomposition of peroxides takes place after extrusion with the help of extended lines of continuous vulcanization, a salt bath or a nitrogen system. Peroxide crosslinking technology is mainly used in the manufacture of cables of low and medium voltage, as well as for pipes production.

Radiation crosslinking technology is based on physical principles. Free radicals are formed during the irradiation of polymers with electrons, beta or gamma rays, which leads to the appearance of structures similar to those obtained as a result of peroxide crosslinking. Products are irradiated after the extrusion process, which often requires the usage of separate producing operations. This process is quite expensive and longstanding. The inevitable unevenness of crosslinking over the thickness of XLPE-layer can be considered as another disadvantage of this method. Radiation crosslinking of polyethylene is used in the manufacture of films, heat-shrink tubings and cable insulation [4].

Silane technology is based on the wet vulcanization process and has been used in production for many years. Usage of silanes provides more flexible and efficient crosslinking process. Silane-crosslinked polyolefins are bonded by Si–O–Si bridges, in contrast to the C–C bonds resulting from the peroxide or radiation method.

The technology of production of XLPE consists of two stages. Initially, silane is introduced into the polymer either by grafting vinylsilane on the polymer chain or by copolymerization of vinylsilane with ethylene in a polymerization reactor. Further, the crosslinking is performed in the presence of water accelerated by tin-based catalysts or others. Silane crosslinking (SC) expands the framework of the manufacturing process. The polymerization speed is determined by moisture diffusion speed, therefore, a hot water bath, steam sauna or low-pressure autoclave is frequently used in order to accelerate the reaction. This technology is used in the manufacture of cables of low/medium voltage, polymer pipes for floor heating and drinking water, in the production of sheet, film and foam materials [5].

Extrusion is the simplest and most widespread industrial method of production of XLPE foam [5]. The material increases in volume and acquires a closed cellular structure. The size of the bubbles does not exceed 1 mm, what increases the density and technical characteristics of the product.

1.2 Utilization and Recycling

The durability of XLPE is its advantage in the quality of a consumer good and represents its disadvantage as one of the main factors of environmental pollution. XLPE-based products will decompose in the rubbish dumps for hundreds of years whereas the accumulated plastic wastes poison vital natural resources.

Utilization of products made of XLPE is effected with the help of 50% nitric acid at a room temperature, as well as under gaseous or liquid chlorine or fluorine affecting the material during the chemical production. Also, the utilization of XLPE is effectively performed in water heated up to 1800°, or with the help of other processes, provoking thermal aging and fragility. In any case, the process of recycling of XLPE occurs together with the release of harmful substances and can only be performed within the framework of specialized production operations [6].

The basic methods of XLPE recycling are as follows:

Thermochemical (pyrolysis). Production of valuable gases and liquids that can be used in the quality of fuel, as well as in the process of manufacture of other organic compounds.

Mechanical. Milling of XLPE wastes with further usage as a filler in the production of granules from high-density and low-density polyethylene.

Hot cutting with partial oxidation. Fracturing of XLPE wastes at elevated temperatures leads to the breaking of carbon bonds between the molecule chains and to the increase of material's fluidity.

Hydrolysis. Water and alcohol used in the process are capable to break carbon crosslinking of XLPE. The resulting product does not differ from synthesized polyethylene, but this method is not always applicable.

Ultrasonic processing. The destruction of three-dimensional structure of PEX by means of high-frequency pulses. This method allows leaving the main polymer chains unchanged [7].

The fact that should be taken into consideration is that not all types of XLPE are recyclable for further production of granules and fillers. Thus, for instance, wastes of XLPE pipes used in gas and petrochemical industries cannot be reprocessed into granulate. So, the utilization of such products is performed by means of the technologies that enable wastes recycling into energetic raw:

Pyrolysis. The process of bond-breaking in XLPE in light of air absence.

Hydrogenation. The process of bond-breaking in XLPE in the presence of hydrogen.

Gasification. The process of breaking the molecular bonds in XLPE in the presence of a limited amount of oxygen.

Recycling of XLPE wastes into energy raw materials does not require special energy expenditures, it is environmentally safe and allows obtaining of up to 70% of liquid fuel and up to 25% of pyrolysis oils from the total amount of wastes [7, 8].

2 XLPE and Modern Technologies

2.1 Industrial Application of XLPE

XLPE produced by means of chemical technologies is used within the process of industrial manufacturing of pipes of a plain (cylindrical) or corrugated profile (Fig. 1), including metal-plastic pipes of 16–1600 mm in diameter (corrugated up to 1600 mm) [9, 10]. Endurance and thermal resistance which are rather high for a polymer material allow pipes made of this material (or rather, of its varieties) to be used in a



Fig. 1 Polyethylene foam pipes: **a** plain profile (open sources, <https://www.shutterstock.com/g/4level>); **b** corrugated profile (open sources, <https://www.shutterstock.com/g/Anatoliy%20Berislavskiy>)

wide range of pipeline systems: from electrical pipes to cold-/hot-water supply and heating systems, as well as from pipelines within the frame of food, chemical and pharmaceutical industries to pipes meant to be used in underfloor heating and gas supply. The pipes are manufactured by means of continuous extrusion [11].

Polymer pipes compare favorably with analogous steel pipes for a number of parameters: durability, weight, high anti-corrosion effect, inertness, ease of transportation and assembling, lightness of construction, cost-effectiveness. XLPE is resistant to aggressive chemical substances and does not require additional electrochemical protection. However, the installing of communications made of XLPE on manufacturing sites should be executed only in correspondence with subsurface (closed) method. Such products cost less than metal ones, what is considered to be the fundamental choice factor for many construction companies [12].

The production of industrial high-voltage cables with a nominal voltage of 110 kW with XLPE insulation began in the 1970s of the last century. At that time, the durability of such cables represented a disadvantage, being inferior to electric cables with paper-oil insulation (25–30 years). This weak point was caused by the aging of the insulation shell, what led to the appearance of electric breakdowns. The studies on improvement of production technology and application of various additives to polyethylene with XLPE insulation were conducted and have still being conducted in many countries (FRG, France, the USA, Italy, Japan, etc.). As a result, some companies started production of the electric cables with a nominal voltage of up to 400 kW and a service life of up to 25 years.

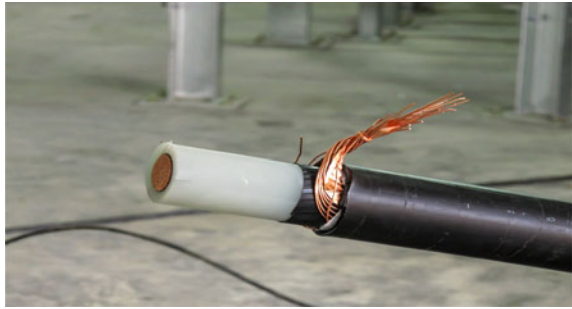
The leading foreign manufacturers of high-voltage XLPE-cables are the following companies: ABB, NEXANS, Pirelli, NKT Cable, Sumitomo Electric and others. In Russia, there have been produced electrical cables with XLPE insulation with a nominal voltage of up to 110 kW [13].

Two crosslinking technologies—peroxide and silane, as well as highly pure raw materials—are used in the manufacture of electric cables with XLPE insulation. When using peroxide technology, the chemical crosslinking process is performed using dicumyl peroxide as a reagent. Crosslinking is evenly executed over the entire thickness of the insulation, without forming of voidness and foreign impurities. This technology is used in vertical extrusion lines [14].

More advanced MDCV method, ‘dry’ crosslinking or vulcanization is used in order to improve electrical insulating properties and eliminate possible defects of the insulation. An insulating compound free of moisture and foreign impurities is immediately applied to the core that is supplied from the barrel. Then the core enters the ‘vulcanization pipe’ which is heated under the influence of direct current and the crosslinking of insulation is consequently produced. The extrusion of electrically conducting shield over the insulation as well as the extrusion of an insulation layer and of electrically conducting shield along the core is proceeded simultaneously—it means that a three-layer extrusion takes place. This technology ensures the absence of gaseous impurities at the border of the shields and in the insulation as well as provides good adhesion between the insulation and the shields [13, 14].

Aluminum or copper conductive leads of cables with XLPE insulation are made sealed and thickened, and if the cross-section of the lead is more than

Fig. 2 Polyethylene insulation (open sources, <https://www.shutterstock.com/g/SB7>)



1000–1200 mm²—the leads are produced in a segmented way, which allows reducing the surface effect. The electrically conducting external layer, the insulation, and the electrically conducting inner layer are simultaneously extruded from crosslinked polyethylene compositions of high-frequency. The metal shield of the cable consists of spirally applied copper tape and of copper wires. The shield's cross-section is selected according to the condition of short-circuit currents flow. A layer of water swelling material is used to provide longitudinal sealing, and a sheath of aluminum-polymer tape is used to protect the cable insulation from moisture in a more reliable way. The aluminum-polymer sheath is welded with PVC or polyethylene sheath to ensure radial sealing.

XLPE is actively applied in the quality of electrical insulation in commercial power cables of all voltage ranges, but is particularly suitable for cables of medium (up to 6–35 kW) and high (36–110 kW) voltage [15].

Polyethylene insulation is used in the production of both single-wire and multi-wire cables (Fig. 2) applied in single-line and group laying in open areas, in cable constructions, under the ground. As compared with the other insulation materials, cables with XLPE insulation have a low failure and damage rate, high throughput capacity, high frost resistance. Cables with XLPE insulation require smaller cross-section to transfer high load currents in comparison with cables with other types of insulation. The permissible heating level of a current-carrying conductor for cables with XLPE insulation reaches 250 °C at a short circuit [15].

Depending on the quality of the supplementary sheath, copper and aluminum-core cable within the scope of polyethylene insulation can be used:

- In a polyethylene (PE) sheath—for laying indoors and in the air,
- In an armored polyethylene sheath (PA)—for laying on complicated ground areas,
- In a PVC sheath (Y)—for a single-line laying in areas where its mechanical damage is excluded (indoors and dry soil),
- With protection from PVC of lower flammability (Ylf)—for group laying,
- With supplementary sealing (s, 2 s)—for laying in humid areas, in the ground with subsoil waters,
- Armored with a metal wire or tape (A)—in the areas with a probability of mechanical damage.

Cables with XLPE insulation are laid out in correspondence with closed (underground) and opened method. Laying of underground cables is performed in trenches to a depth of not less than 0.7 m from finished grade for cables with voltage of up to 20 kW and not less than 1 m for cables with voltage over 35 kW.

Opened laying across the territory of the enterprise is performed within the cable structure. The laying is executed according to the opened method along the supporting structures represented by poles, wall-mounted shelves and others [15].

In the automotive industry, physically crosslinked XLPE is used in manufacturing of air intakes and filters, in fabrication of buffer gaskets for automobile components and parts, of various weather strips, within the process of lining the better half of the car salon in the quality of vibration insulation and soundproofing. The main properties that contributed to this material being selected for these systems in the automotive industry are rather good thermal resistance and resistance to temperature fluctuations, good impact resistance, soundproofing and vibration insulation, resistance to chemicals damage, low flexural modulus and good resistance to stress cracking.

Low coefficient of friction of physically crosslinked XLPE is comparable with polytetrafluoroethylene (Teflon) and wear-resistant coatings of ultrahigh-molecular-weight polyethylene (UHMWPE), the fact that allows applying it in unstrained dry friction assemblies. Looking ahead, the new types of bearings made of wear-resistant XLPE are expected to be massively introduced in the future (Fig. 3).

Strict demands are applied to the XLPE materials in the area of food service regarding cleanliness, environmental and infectious safety for humans. Besides, products made of XLPE easily withstand processing in hot (boiling) water. Such materials should be disinfected easily, and the XLPE together with its resistance to microorganisms is perfectly suitable for cabinets, refrigerators and other equipment of the production base of modern kitchens, cafes and restaurants. XLPE material creates a corrosion-resistant smooth surface that remains durable for years.

Fig. 3 Slider bearing made of wear-resistant polyethylene (open sources, <https://www.shutterstock.com/g/marekusz>)



2.2 *Application of XLPE Within the Scope of Modern Production*

The key properties of crosslinked polyethylene foam designated within the scope of modern manufacturing technologies are the following:

- Resistance to high and low temperatures and to the dynamics of their changes,
- High resistance to hydrolysis,
- High electrical and heat-insulating properties,
- High durability under conditions of mechanical wear and abrasion,
- Preservation of dimensional stability at predetermined temperatures,
- The ability to dampen noise and vibration,
- Environmental safety while storing liquids and products intended for human consumption.

These physical properties of the material became the key reason for widespread usage of XLPE in modern industry.

For instance, heat-insulating, waterproofing properties of XLPE as well as the ability of the material to dampen vibrations are used in light of erection of manufacturing objects. At the same time, the combustibility of XLPE should be taken into consideration. It cannot be used within the premises of hot shops, metalworking enterprises and foundries. On the other hand, XLPE has perfectly proven itself as a universal, easy-to-install and reliable heat-insulating and waterproofing material within the process of insulation of warehouses, industrial refrigerators, transportation departments and other objects of industrial infrastructure [16]. So, during the installation and thermal insulation of manufacturing facilities of hangar-type (warehouses, shops, parking lots), an insulating envelope is created with the help of XLPE foam rolls using the technology of seamless heat-insulating coating over the entire area of the room (Fig. 4). Herewith, heat-insulating material made of XLPE can have a metallized reflective surface that creates additional benefit due to the fact that such a surface reflects heat flows in the infrared range [17, 18].

The operating temperature of XLPE insulation varies from -60 to $+150$ °C what creates all the necessary conditions for performance of all-season installation. The works on thermal insulation of the objects do not depend on the outside air temperature and can be performed 365 days a year. Furthermore, the rolled polyethylene foam itself is not prone to destruction under the influence of seasonal temperature fluctuations what makes it weatherproof and suitable for regions with extreme temperature conditions, including severe climatic conditions.

Suchlike thermal insulation system has a high degree of reliability, and the XLPE elasticity enables its deformation in accordance with the temperature deformations of the metal coating of the hangar simultaneously maintaining the overall integrity of heat-insulating structure [19].

Within the process of implementation of inline (assembly line) production cycle, following properties of XLPE products are used: vibration damping, soundproofing and waterproofing. The material is used in the quality of components of the concrete

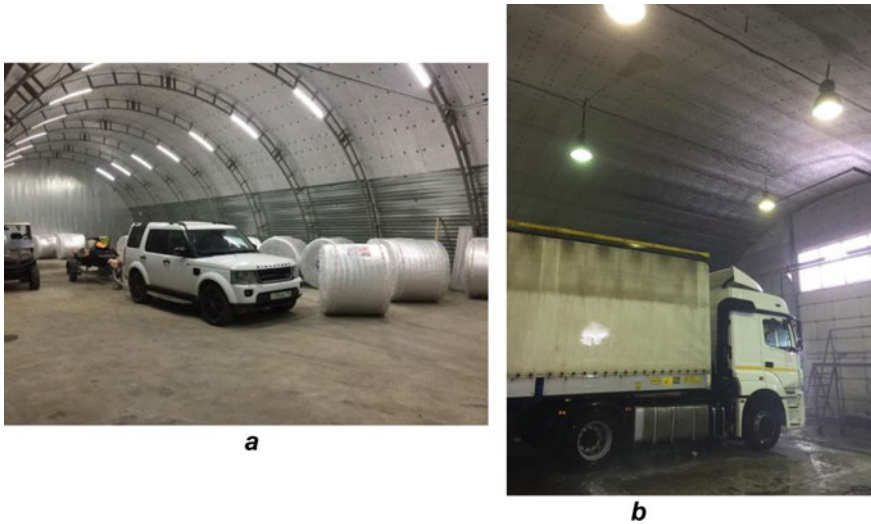


Fig. 4 Interior of heat-insulated parking areas (owned by our company)

foundation during the equipment mounting, in compensation couplings and shock absorbers of moving elements of assembly-line equipment, as the elements of personal protective equipment (helmets, noise-canceling headphones) for enterprise workers and in other areas.

When equipping the commercial refrigerators, including those designed for the food industry, the XLPE property of maintaining a predetermined indoor temperature is used. It has to be considered that commercial refrigerators have large areas of premises what leads to significant energy expenditure in order to maintain the necessary storage temperature. The following can be used in the quality of the storage:

- Already built constructions of any purpose,
- Framed or frameless hangars,
- Purposely constructed projects.

Additional requirements are imposed toward the insulating material of such facilities. Except high thermal characteristics, the material should be hermetic, light, easy-to-install and simple-to-use, durable, resistant to bacterial contamination and fungi, non-odorous and easily bear the temperature fluctuations. The problem is solved with the help of impermeable insulation based on foamed XLPE materials, installation of special hermetic doors and cold generators (Fig. 5) [20, 21].



Fig. 5 Commercial refrigerator built on the base of single-floor storage (open sources, <https://www.shutterstock.com/g/Aleksandar%20Milutinovic>)

2.3 XLPE in Insulation Systems of Industrial Pipelines and Heating Plants

XLPE products in the form of hollow cylindrical pipes as well as rolled up sheets, mats and other forms, in a simple or self-adhesive implementation, with or without reflective coatings are used within the scope of insulation of equipment and heat network pipelines of industrial heating systems, main lines of hot and cold water supply systems, technological systems; within the frame of insulation of air-ducts of the ventilation and air conditioning systems. The types of coatings used can be different: polished aluminum foil, reflective metallized coating and polymer film [22].

When referring to heat-insulating structures on the pipelines, XLPE-based thermal insulating products in the form of tubes should be used as thermal insulation. If the required nominal size in the manufactured nomenclature of tubes is unavailable, insulating products in the form of rolls should be applied.

The assembly option of heat-insulating structure on the pipeline consisting of a heat-insulating tube, glue and a reinforced self-adhesive tape is demonstrated in Fig. 6.

When installing the heat-insulating products made of XLPE in the form of rolls or mats on the pipelines, bands (Fig. 7) located at intervals from 500 to 600 mm have to be arranged. Metal tapes with anti-corrosion coating of stainless steel, aluminum alloys or polyamide are allowed to be used as a band. Material of the band used for fixation of the covering layer should correspond to the material the coating is made of [23].

In case of multilayer insulating structures intended for pipelines, the installation of the second and subsequent layers of XLPE thermal insulation is implemented

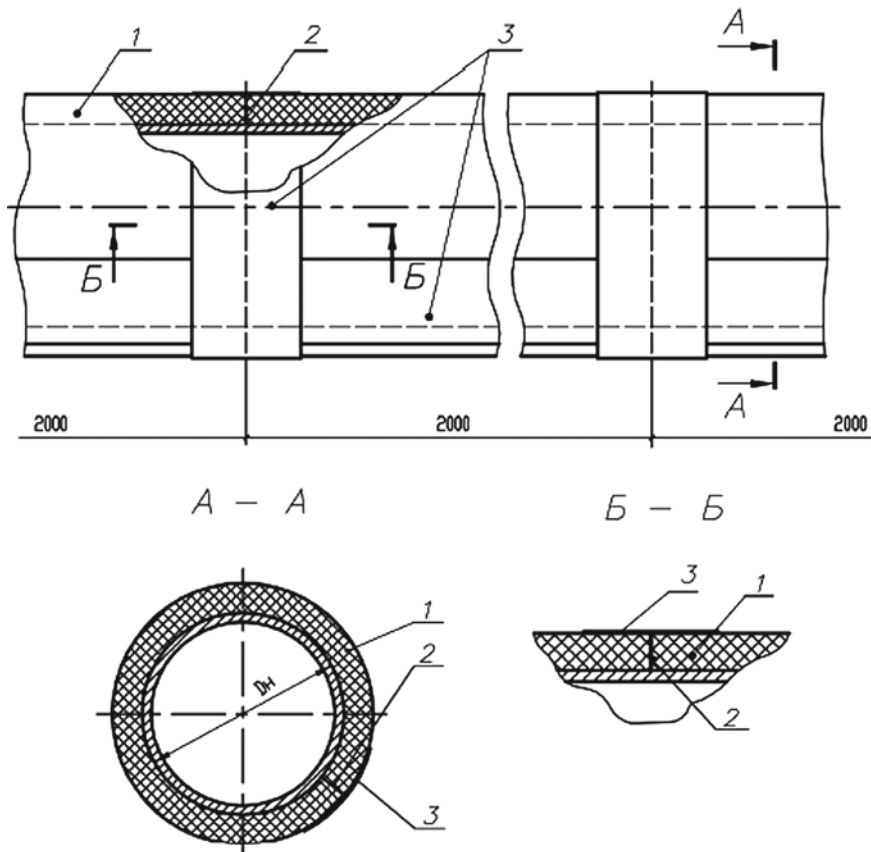


Fig. 6 Heat-insulating structure of the pipeline of diameter D_H : 1—tube made of heat-insulating material; 2—glue; 3—reinforced self-adhesive tape (provided by co-author Zhukov A.D.)

together with seams overlapping of each previous layer. The seams of all layers of thermal insulation are stuck together with contact glue.

It is additionally recommended to glue the seams of the outer layer with a reinforced self-adhesive tape. Fixed thermal insulation of screwed valves installed on pipelines is implemented by means of products in the form of tubes or rolls, together with thermal insulation of the pipeline.

Within the scope of insulating structures of the tanks, heat-insulating products in the form of rolls and mats should be applied in the quality of thermal insulation. The variant of implementation of thermal insulation is demonstrated in Fig. 8. In case the temperature of the insulated surface is below $+90\text{ }^\circ\text{C}$; it is recommended to use XLPE products in the form of rolls with a self-adhesive base layer.

In order to ensure the quality of work performance during the installation of thermal insulation (Fig. 9) within the scope of ventilation and air conditioning systems, the above-mentioned requirements have to be taken into consideration.

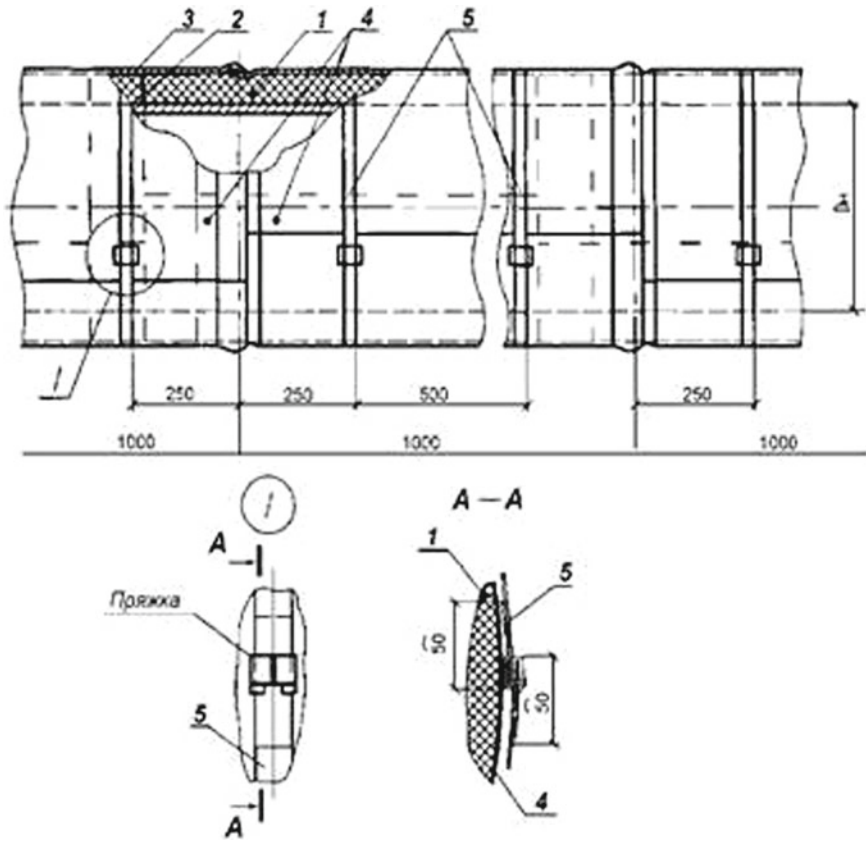


Fig. 7 Heat-insulating structure with a band fixation: 1—tube made of heat-insulating material of $D_H \leq 160$ mm (heat-insulating material sheet of $D_H > 160$ mm); 2—glue; 3—reinforced self-adhesive tape; 4—metal covering; 5—band with buckle (provided by co-author Zhukov A.D.)

Within the process of assembling of heat-insulating structures intended to prevent moisture condensation arisen from the outdoor air on the surface, XLPE materials are chosen in the quality of thermal insulation materials as they are characterized by a closed cellular structure and high hygroscopicity [23, 24].

2.4 Application of XLPE in the Medical Field and Dentistry

It is worth mentioning that the polymers, and particularly the XLPE, are widely used in the medical field. They are used within the process of manufacturing blood substitutes, for prosthetics of separate bones in light of fractures of the skeleton, ribs, braincase, for the manufacture of prosthetic dentures, blood vessels, heart valves and much more.

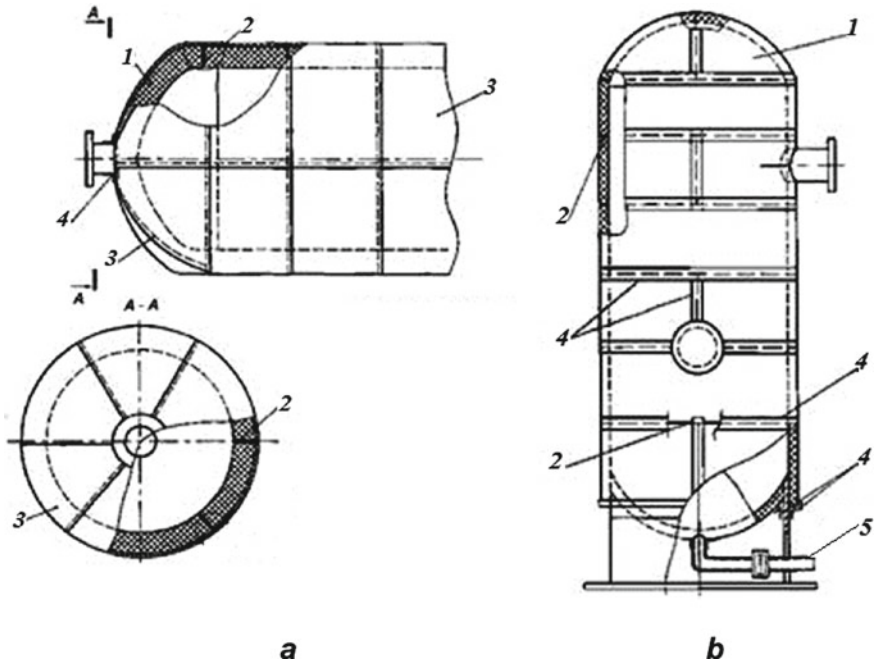


Fig. 8 Heat-insulating structure of a tank: **a** horizontal; **b** vertical; 1—sheet of heat-insulating material; 2—glue; 3—metal covering; 4—self-adhesive aluminum tape; 5—insulation of the socket (provided by co-author Zhukov A.D.)

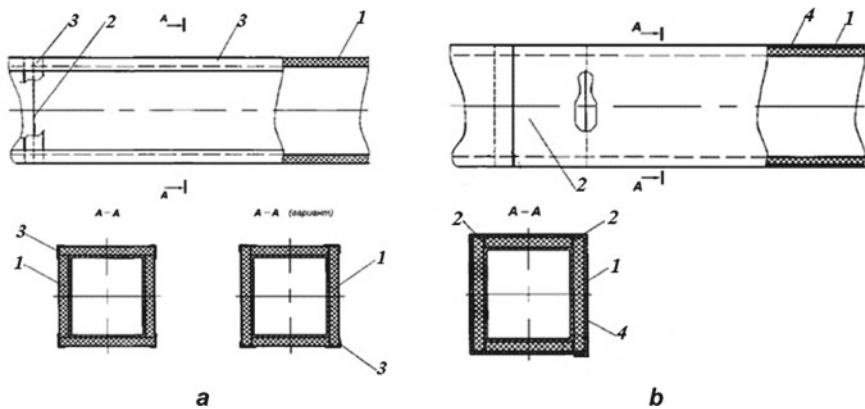


Fig. 9 Heat-insulating structure of an air-duct: **a** performed with the help of a self-adhesive heat-insulating material; **b** performed with the help of a self-adhesive heat-insulating material and self-adhesive coating; 1—sheet of self-adhesive heat-insulating material; 2—glue; 3—reinforced self-adhesive tape; 4—self-adhesive metal covering (provided by co-author Zhukov A.D.)

In particular, within the scope of prosthetics in dentistry and in the artificial joints in the quality of wear-resistant material, the crosslinked polyethylene is considered to be a preferable material by the hip joint replacement due to its abrasion resistance qualities in the friction joints of the juncture (Fig. 10) [25, 26].

At the same time, knee replacement requires several types of materials to be used including XLPE, as the strain in the knee joints is rather various (Fig. 11).

For instance, the cancellous bones implants based on the composite material, where XLPE serves as internal (porous) base, have already passed the successful tests. It is about the most accurate imitation of the porous structure of the bone tissue. This ensures complete elimination of bone defect, the initiation of the recovery process and allows maintaining functional abilities of the limbs. The prosthesis is suitable for patients who require replacement of bones destroyed by cancer, trauma or surgery [27].

Prostheses and their elements made on the base of XLPE are remarkable not only for its high strength and impact resistance, but also for wear resistance, frost

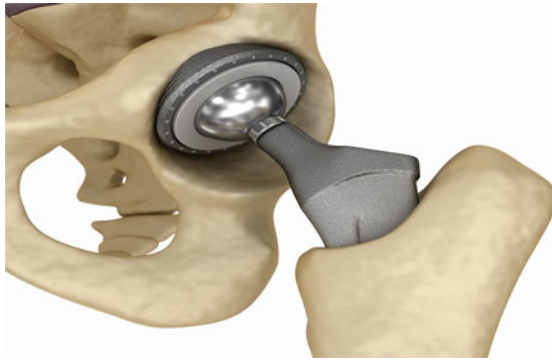


Fig. 10 Hip joint construction (open sources, <https://www.shutterstock.com/g/Alex%20Mit>)



Fig. 11 Joint implant made of polyethylene (open sources, <https://www.shutterstock.com/g/Denis%20Simonov>)

Fig. 12 Dental prosthesis
(open sources, <https://www.shutterstock.com/g/fresco>
movie)



resistance, chemical resistance, inertness toward the impact of salts, alkalis and acids. These properties of the material are widely used in modern dentistry, and when manufacturing various types of maxillofacial prostheses.

It is worth pointing out that a dynamic transition from implantation of dental prostheses to the manufacture of removable prosthetic systems is outlined in modern dental technologies. Such prostheses are characterized by usability, aesthetic qualities and high durability. When using them, the periosteum of the patient remains absolutely undamaged and the prosthetics process itself is reversible (Fig. 12). Creation of suchlike constructions became possible only through the application of the materials resistant to alkaline conditions, corrosion, cracking, high temperatures and being characterized by the strength on a par with bone strength. In this respect, polymer-based materials are preferable to metals and ceramics, as they allow making a prosthesis practically of any shape and installing it without implantation, avoiding the irrevocable periosteum trauma [28].

The application of polymers in modern cardiovascular surgery is related to the prosthetics of heart valves and blood vessels. Following materials are used for this purpose:

- Fibers made of fluoropolymers, polypropylene, polyethylene, lavsan are used for prosthetics of blood vessels.
- Silicone rubbers, XLPE, fibers of fluoropolymers are used for prosthetics of heart valves.

Alongside the general surgical requirements for such materials, specific demands are placed as well: they should not cause blood destruction and thrombus formation. Lavsan, polytetrafluoroethylene and XLPE have no impact on the thrombosis process. And some of them suspend it. So, for instance, the surface made of XLPE and treated with heparin is able to extensively delay the blood coagulation what is considered to be the good sign within the process of prosthesis manufacture.

Generous amount of abdominal surgeries on the diaphragm, in light of herniae removal, thoracic tissues replacement and others, is performed within the application of mesh materials made of nylon fiber, polyester fibers, XLPE and fluoropolymer.

Nowadays, prosthetics surgeries on intracavitary canals have already been successfully performed by means of special tubes made of crosslinked polyethylene and organosilicone rubbers. These technologies have already been approved and will be implemented in the near future.

Manufacturing of the products intended for medical technique and serial production of medical instruments, items of patient care, special utensils, various types of packaging for drugs, which prevail over similar metal and glass products, became possible due to the physical properties of XLPE, its chemical inertness and safety for the human body.

2.5 *XLPE in Sports Industry*

The properties of XLPE, such as the ability to dampen vibration and load impact, elasticity, environmental friendliness, closed-cell structure of the material, have found their application in sports, tourism and leisure industry. All these qualities of the material are used in the production of inventory, facilities, floorings and equipment items. It includes the production of travel mats, sports and gymnastic mats and roll mats, shock absorbers for helmets and rucksacks, fillers for floating life-saving equipment and much more [29].

For example, roll mat—today's popular type of sports flooring and wall coating—consists of segments seamlessly connected to one another what enables to mount the coatings of practically any area size. Such coatings are used not only in the gym halls but also in kindergartens, schools and big sport arenas. Roll mats tatami with imitation of rice straw and many others are produced as well (Fig. 13) [30].

Among other properties of XLPE implemented in the sports industry is the ability of the foamed material to maintain a predetermined temperature inside insulated rooms. For instance, the erection of sports venue with artificial ice rinks (Fig. 14) represents a rather difficult task. In order to keep the ice covering applicable for all-year exploitation, the preset climate has to be constantly maintained inside the building. An easy and inexpensive way of solving this problem is a seamless thermal insulation of the construction roof and walls with the help of XLPE insulant. Supply and exhaust ventilation providing fresh air supply is also obligatory. Such a method prevents from heat penetration inside the room, ice melting, allows decreasing the power of cooling plant and reduces the costs for electricity.

Large thermal insulating envelope made of XLPE with a reflective metallized coating is used for snow conservation in the off-season (from spring to fall) for the purpose of its early use at ski resorts. The hot welding technology of separate XLPE sheets is used within the scope of manufacturing of suchlike structure [19, 31, 32].

XLPE rolls are prepared and laid out on an insulated surface, then joined together in order to form an integral seamless coating. In order to increase the durability of the insulation system and to enable its reuse, it is recommended to install a tent covering



Fig. 13 Products for sports, tourism and leisure (open sources, **a** <https://www.shutterstock.com/g/wavebreakmedia>; **b** <https://www.shutterstock.com/g/Stanisic%20Vladimir>; **c** <https://www.shutterstock.com/g/Evgeny%20Bakharev>)



Fig. 14 Insulating coating of ice skating rink (owned by our company)

Fig. 15 Installation of a protective coating with the help of crosslinked polyethylene foam rolls (snow conservation) for ski resorts (owned by our company)



a



b

fastened along the perimeter of the snow storage and surface area with the help of tensile structures: ropes, fixed around the perimeter and forming a net (Fig. 15) [33, 34].

2.6 Application of XLPE in Construction of Residential Buildings

Mineral wool and polystyrene foam are traditionally used in the quality of insulation materials within the scope of construction of private residential buildings and structures. Over the last years, brand new heat insulants based on foamed crosslinked polyethylenes (XLPE) entered the construction market. In addition, XLPE foam is widely used in thermal insulation within the construction process of different private, commercial and industrial facilities. XLPE materials fulfill their functions so much

successfully that the engineers lean toward the application of foamed polyethylene over other types of insulation. Such a modern and promising method of insulation allows solving the problem of heat conservation to the maximum benefit and a minimum input [35, 36].

Crosslinked polyethylene foam combines thermal insulation, vapor barrier properties, water- and soundproofing at the same time. Although the cost XLPE is higher than that of mineral wool or polystyrene foam, it is not so much expensive in total when taking the universality, simplicity of technical solutions, high durability and easy mounting of insulating coatings made of materials based on XLPE into account. And their reliability, durability, heat-insulating and soundproofing properties count in favor of crosslinked polyethylene foam in comparison with other types of insulating materials [37, 38].

XLPE produced by means of chemical method and presented in the form of rolls and mats is generally used in the construction field. One of the particularities of the insulation technology performed with the materials based on XLPE is the creation of an integral hermetic insulating coating over the entire contour of the insulated objects (Fig. 16). Various technical solutions are used for this: application of various adhesive joints, tapes and others for joint hermetization of heat-insulating coatings. However, the best result was shown by the patented elaboration of the Russian company TEPOFOL concerning the creation of a homogeneous thermal insulating coating by means of heat (thermal) welding [39, 40].

Due to the fact that the best result of thermal insulation of a construction object is achieved when using the technology of a hermetic heat-insulating coating, the accepted standards of normative air exchange and conditioning of the indoor space should be respected.

Apart from the thermal insulation of building structures of various systems, XLPE is used for soundproofing of indoor premises, such as floors, walls, ceilings, inter-floor overlappings and others. High elasticity, ease of insulation with XLPE, absence of protective garment, respiratory protection equipment and special tools significantly simplify the mounting of XLPE insulation coverings in comparison with the application of traditional types of thermal insulation. Crosslinked polyethylene foam is not harmful to health as it does not contain phenolic resin binders, glass fragments

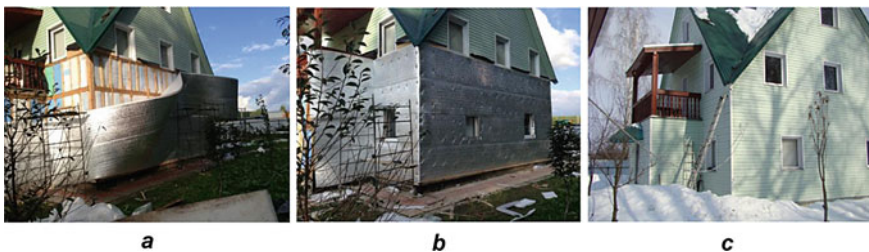


Fig. 16 Thermal insulation of the cottage with the material based on XLPE: **a** unreeling of the XLPE heat-insulating roll; **b** formation of heat-insulating coating; **c** final siding and exterior of the insulated house (owned by our company)

and does not cause skin irritation. It is not prone to decay, does not emit harmful substances, is environmentally friendly and durable.

3 XLPE Within the Scope of Individual Household

The usage of XLPE within the scope of individual household can be divided into several categories, as follows:

- Heating, water supply, sewerage of a private house,
- Power supply of private houses and apartments,
- Thermal insulation and soundproofing of houses and apartments,
- Objects of everyday use.

3.1 XLPE in Heating, Water Supply and Sewerage Systems

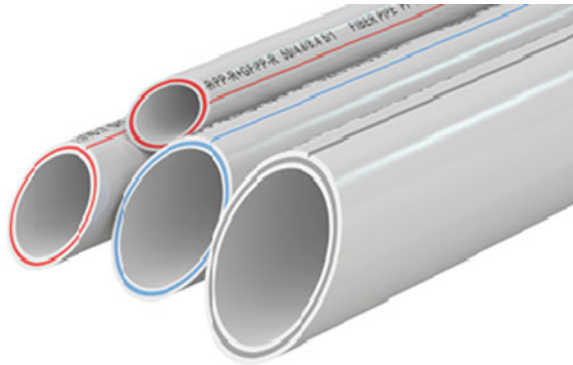
An important factor when selecting the pipeline products based on XLPE is the corrosion of metal pipes and structures as well as their high cost. Unlike common polyethylene, which melts at a temperature of $+80\text{ }^{\circ}\text{C}$, XLPE can withstand greater heating temperatures, which is rather enough to provide private residences with heating and hot water, in networks of which the temperature usually does not exceed $+95\text{ }^{\circ}\text{C}$ [41].

Household pipes made of XLPE are marked with PEX and are widely applied in urban distribution networks and in the private sector. They are produced in several basic ways:

PEX-C are produced by means of physical crosslinking technology with the help of irradiation with hard X-rays. As a result, the crosslinking of the material over the pipe thickness is uneven: the largest percentage of crosslinking molecules falls at the external surface, and only small percentage (average crosslinking percentage amount to 78%) falls at the inner surface. Corrugations on such a pipe can only be fixed using transition joints. No chemical additives that would improve the characteristics of the pipes are used in the process of manufacture.

PEX-B are made by means of chemical crosslinking technology. The displacement of hydrogen atoms takes place under the influence of chemicals in the molecules of polyethylene. Silane (silane crosslinking) is applied in this case as one of these chemicals. Leaving the extruder, polyethylene pipe is placed in a silane bath, while crosslinking moves from the external and inner surfaces deep into the pipe wall. As a result, the crosslinking percentage on both surfaces is high, and it is low in the middle of the pipe thickness (average crosslinking percentage amounts to 75%). As for flexibility characteristics: such a pipe is less flexible than PEX-A. Corrugations can only be fixed with the help of transition joints. The pipe withstands high-pressure indices.

Fig. 17 Samples of marking of PEX—pipes for heating and water supply (open sources, <https://www.shutterstock.com/g/AlexLMX>)



PEX-A are produced using peroxide crosslinking technology. The process takes place in the extruder in a molten state, under high pressure and under the influence of laser light. The average percentage of crosslinking of such a pipe amounts to 85%, the properties of the material are the same along the entire pipe, independently on its thickness. The corrugations of such a pipe can be easily restored by means of a hot air gun, but the withstand pressure is slightly lower than by PEX-B. As for the properties: this type of pipe is the most flexible [42].

PEX-A, PEX-B and PEX-C pipes (Fig. 17) are applied in heating and water-supply systems of private houses and apartments. Herewith, the limitations linked to the material's plasticity and durability are taken into account since the material of PEX-B and PEX-C pipes has a heterogeneous structure. For instance, the pipe loses its elasticity in course of time, pipe's walls gradually shrink, the impermeability of the mechanical joints decreases, which necessitates the occasional tightening of the pipe fittings. In addition, PEX-C pipes cause the greatest difficulties during the recycling process.

As concerned PEX-A pipes—at a short-term peak temperature from -100 to $+100$ degrees Celsius—they are capable to maintain their thermophysical and strength properties, and are also characterized by shape memory effect, which significantly expands the scope of their application in heating networks as well as hot and cold water-supply networks [43].

It should be taken into account that XLPE does not tolerate the impact of solar ultraviolet radiation. In order to solve this problem, PEX pipes are varnished.

The modern design of the pipe intended for heating, hot and cold water supply has a multilayer structure. For instance, an EVON pipe with an anti-diffusion (oxygen) barrier has a five-layer construction (Fig. 18). The inner part of the pipe consists of PEX-A or PEX-B polyethylene, followed by an adhesive layer, an anti-diffusion barrier and an external protective polymer layer. This construction provides high-temperature resistance of the product, while maintaining its flexibility.

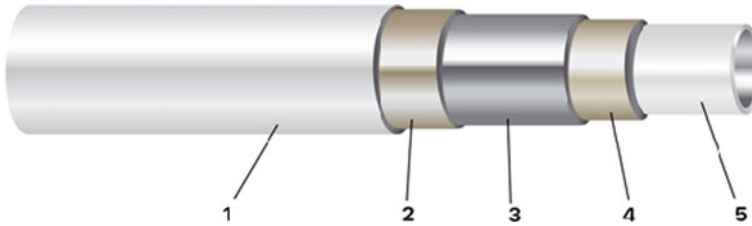


Fig. 18 Heating pipe construction. 1—external protective polymer layer, 2—adhesive layer, 3—anti-diffusion (oxygen) barrier, 4—adhesive layer, 5—internal PEX pipe (owned by our company)

Apart from polyethylene pipes, metal-plastic pipes are used as well within the process of installation of individual heating systems. But unlike PEX pipes, metal-plastic products are not flexible enough. The advantages of XLPE pipes over other products can be defined as follows:

- High elasticity of PEX-A pipes. In case of deformation of the pipe wall surface, it can retain its shape until the problem is fixed. Suchlike pipes do not lose plasticity in course of time.
- Pipes made of crosslinked polyethylene do not lose their consumer performance characteristics even if system temperature increases above 95 °C; the same in case of the emergency situations, when the temperature can reach 200 °C.
- XLPE pipes are resistant to aggressive environments, pressure drops, effects of oils and solvents.
- In case of ignition, they do not emit substances harmful to humans.

Pipes made of XLPE are not only applicable for hot water supply and room heating, but also in the underfloor heating system, heating of pools and outdoor areas, stairs assemblies, greenhouses.

It should be considered that despite the important advantages, pipes based on XLPE can cause consumers some inconvenience: they cannot be welded and they do not allow recycling (except pyrolysis) [44, 45].

Plastic pipes based on XLPE are widely used in sewerage systems. The operational life of XLPE pipes is not limited by corrosive wastes, mixed household wastes or the environment in comparison with the traditional metal pipes [46, 47].

XLPE pipes are easy-to-install, do not require gas welding, electric welding and are characterized by ease of maintenance as well. The operating pressure of suchlike pipes amounts to 2.5–16 atm. Pipes are produced with a diameter of up to 1000 mm, have high thermal resistance and are most practical if used in storm drains and flow sewerage systems (Fig. 19). Their advantages are the following:

- Long lifespan (up to 50 years),
- Low coefficient of thermal conductivity allows decreasing the condensation on the external surface of the pipes,
- Do not require insulation,
- Resistance to thermal loads.

Fig. 19 XLPE pipe intended for laying of force main sewage (open sources, <https://www.shutterstock.com/g/P%20A>)



XLPE water pipes (PEX-B and PEX-A) are used in inexpensive and effective private cold water supply systems. In addition to the advantages mentioned in other sections of the chapter, a distinguishing feature of XLPE pipes is increased throughput capability. This particularity can be explained by several reasons.

For instance, corrosion spreading over the internal part of a metal pipe reduces its inner diameter. XLPE, like all polymers, is prone to creeping, and the inner diameter of such a pipe increases without compromising their performance characteristics during the exploitation. Such an increase in the inner dimension of the pipe can reach up to 3% of the initial value of the pipe section throughout the entire lifespan of the product.

An important advantage over metal pipes is a wide range of operating temperatures and the elasticity of the pipe material. For instance, XLPE pipe can withstand a negative temperature of up to -70°C , and if the liquid in it freezes, the pipe will not collapse, and will be applicable when the liquid defrosts. The ability to re-install the system throughout its entire service life remains as well [48].

Another important factor is resistance of XLPE to fungal infections and those triggered by microorganisms. The construction and reconstruction of water supply networks based on pipes made of crosslinked polyethylene foam are 40% cheaper in comparison with traditional methods.

3.2 XLPE in Power Supply Systems of Private Houses and Apartments

Until recently, electrical cables with insulation based on impregnated paper or PVC were used within power supply systems of private residences and apartment blocks. In comparison with these methods, electrical cables with XLPE insulation have a number of advantages (Fig. 20). For instance, the electrical performance characteristics of XLPE insulation are much better in comparison with the insulation made of impregnated paper or PVC. Its thickness is less; the dielectric permeability is 1.7 times lower. During the equal current transfer, a cable with insulation made of PVC

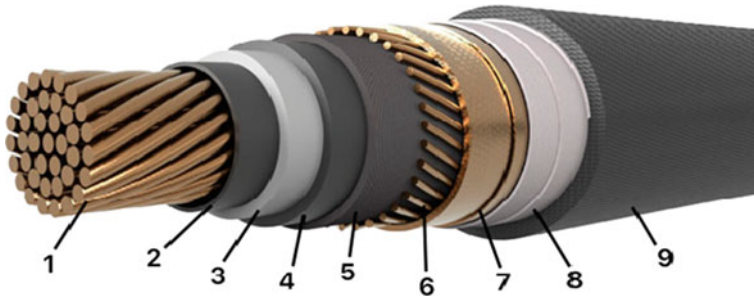


Fig. 20 Configuration of a single-wire cable with XLPE insulation: 1—round stranded conductor, 2—sheet of semiconducting crosslinked polyethylene, 3—insulation of crosslinked polyethylene, 4—sheet of semiconducting crosslinked polyethylene, 5—separating layer of semiconducting tape or semiconducting water-blocking tape, 6—a screen made of copper wires fastened with a copper tape; 7—separating layer of two polymer tapes; 8—separating layer of aluminum-polyethylene tape; 9—polyethylene or PVC coating (owned by our company)

plastic and cross-section of 120 sq mm can be advantageously substituted by cables with XLPE insulation and cross-section of 95 sq mm. Herewith, within the process of manufacture of suchlike cable, copper consumption is decreased in 1.6 times. Under the conditions of equal cross-section, the current-conducting loads of the cable with XLPE insulation are 20–30% higher than of the cables with PVC insulation [49].

XLPE-cables in the power supply systems of private houses are presented in a single-core design in the most cases, and the usage of various types of sheaths together with the possibility of sealing allows using the cable for both subsurface laying and cable structures, including group installation (Fig. 20).

Usage of XLPE insulation improves the thermal performance characteristics of the product as well. The operating heating temperature of copper wire of a cable with XLPE insulation is 20–30 °C higher than of cables with traditional insulation. The permissible heating temperature of the wires during short circuits amounts up to 230 °C, as compared to 160 °C with PVC insulation, and 200 °C with paper impregnation. Higher factory length of 450 m (with a cross-section of up to 16 sq mm), minimum bend radius in dependence on the outer diameter, the possibility of laying under conditions of any altitude difference, up to the vertical line, and ease of mounting can be indicated as additional advantages as well.

On the basis of the above comparison, it is possible to identify the areas where the application of XLPE cable in power supply systems of private and high-rise buildings is mostly reasonable—based on the cost, these are the voltage levels of 15, 20, 35 kW, where even the initial capital expenditures for the cable will be lower, if higher power transfer is required [50].

3.3 XLPE in Soundproofing and Thermal Insulation Systems of Private Apartments

Thermal insulation on the basis of XLPE foam produced by means of chemical method represents a product with a closed-cell structure produced in the form of rolls, plates or mats. These materials have a range of universal properties that allow using them in the quality of thermal insulation, waterproofing and soundproofing of the rooms. For instance, the coefficient of thermal insulation material based on XLPE amounts only 0.038 W/(m·K). As a comparison, the thermal conductivity of drywall amounts to 0.15 W/(m·K), wood—0.09 W/(m·K), mineral wool—0.07 W/(m·K). Considering the increased strength, excellent humidity resistance, low vapor permeability, high values of sound absorption, environmental safety of XLPE materials, we can safely say that this thermal insulation material suits the best for usage in the rooms designed for a comfortable human living [51, 52].

Following criteria of crosslinked polyethylene foam are considered within the process of soundproofing of inter-floor overlappings, floor, walls and other elements: density 33 kg/m³; thickness up to 10 mm; sound reduction index 23 dB; thermal conductivity coefficient 0,038 W/(m·K); water absorption by full immersion (by volume) 96 h to 1%; dynamic modulus of elasticity up to 0.77 MPa; tensile strength up to 0.34 MPa; elongation at break up to 127%. The material is used in the form of rolls and mats (Fig. 21).

Traditional methods of insulation of balconies, loggias, mansards and other elements lying outside the living area imply a combination of three groups of materials: heat-insulating, ensuring vapor barrier and waterproofing filling the gaps between the elements of the substructure. Suchlike system is unreliable as it requires very accurate mounting. The application of XLPE-based insulant allows creating the insulating coating of any objects and therewith completely eliminating splits, gaps and other cold bridges with the help of seamless technology what considers to the full extent all the advantages of polyethylene foam (Fig. 22) [53–55].



Fig. 21 Polyethylene foam used in insulation of inter-floor overlappings: **a** dry screed; **b** reinforced screed (owned by our company)

Fig. 22 Insulated loggia before the facing (owned by our company)



a



b

During the indoor repair work, substrate layers, damping tapes, shock-absorbing coatings and other products made of XLPE foam are actively used. So, for example, the XLPE substrate layer is made of high-quality material of 5 mm in thickness, with double-sided paper coating. Fastening to the wall is performed using strong wallpaper adhesive. Suchlike solution allows thermal insulation and sound insulation to be performed without imposing any constraints on the room finish.

4 Conclusion

Short overview of the practical application of XLPE showed that products based on this polymer became a significant part of everyday life of modern society and are actively used in various fields of human activity.

Products made on the basis of XLPE compare favorably with analogue products made of other materials in a number of parameters: durability, weight, high anti-corrosion effect, inertness, ease of transportation and installation, ease of construction, cost-effectiveness, good heat-insulating and waterproofing parameters and other properties. XLPE is resistant to aggressive chemicals and does not require additional electrochemical protection. As a result, basic areas where XLPE is used are: hydraulic heating and cooling systems, industrial and urban power grids, heat-insulating materials, products for food and chemical industries, as well as medicine.

A serious disadvantage of XLPE products usage is the complicated recycling process. Utilization of large amount of wastes into energy raw materials requires the construction of specialized enterprises.

References

1. Tamboni SM, Mhaske ST, Kale DD (2004) Cross-linked polyethylene. *Indian J Chem Technol* 20(11):853–864. <https://doi.org/10.1021/cen-v032n014.p1392>
2. Osipchik BC, Sravnitel'nyj (2006) Comparative analysis of the structure and properties of polyethylenes crosslinked by various methods. D. Mendeleev University of Chemical Technology of Russia, Moscow, p 4. Research report
3. Watanabe S, Komura K, Nagaya S, Morita H, Nakamoto T, Hirai S, Aida F (2003) Development of cross-linked polymer material recycling technology by supercritical water. In: Proceedings of the 7th international conference on "Properties and Applications of Dielectric Materials", vol 2. IEEE, pp 595–598. <https://doi.org/10.1109/ICPADM.2003.1218487>
4. Pikaev AK (1987) Modern radiation chemistry. Rigid body and polymers. Application aspects. Science, Moscow, pp 320–354
5. Evseeva KA (2008) To the question of the effectiveness of various peroxides in the crosslinking reaction of PEX-A polyethylene. In: Abstracts at the XX international symposium "Modern Chemical Physics", 15–26 Sept, Russia, Tuapse, p 32
6. Goto T et al (2008) Selective decomposition of the siloxane bond constituting the crosslinking element of silane-crosslinked polyethylene by supercritical alcohol. *J Appl Polym Sci* 109(1):144–151. <https://doi.org/10.1002/app.27928>
7. Chalov K, Lugovoy Y, Suman E (2019) Study of the kinetics of thermal destruction of crossed polyethylene. *Bull Sci Pract* 5(12). <https://doi.org/10.33619/2414-2948/49>. AGRIS T01
8. Nikolaev OO, Brittov VP (2019) Analysis and technological solutions for the recycling of cross-linked polyethylene. Saint-Petersburg State Institute of Technology, pp 102–106. DOI:10.6.160/2587-75.77-2019-2-102-106
9. Tsunaga M, Matsunami S, Sato M, Nakata K (1998) Cross-linked PE pipes for hot water and geothermal applications reliability and fusion technology. *Plastics Pipeline Systems for the Millennium X*. Svenska Massan Centre Goteborg, Sweden, pp 595–603
10. Scheelen A (2005) Facilitating the pipe system choice of European water engineers. *European Plastics News*, Belgium, pp 105–121
11. Shepherd M (2005) Benefits of plastics pipes from the water utility's point of view. *European Plastics News*, Belgium, pp 129–144
12. Frost SR, Gibson AG (2001) Reinforced thermoplastic pipes (RTP) in the oil and gas industries. *Plastics Pipes XI*. Munich Germany, pp 731–740
13. Konstantinov GG, Arsent'ev OV (2010) Cables with XLPE insulation. *Nat Res Irkutsk State Tech Univ.* 46(6):218–224. UDK 621.315.21.3002. (075.3)
14. Golynina NG, Nekrasov ML (2008) Insulated power cables made of XLPE. *Specifications Appl Tests Cable-News*. 3:17–24

15. Hakimulin BR, Bagautdinov IZ (2016) Advantages of power cables insulated with XLPE. *Innov Sci.* ISSN 2410-6070, UDK 621.315
16. Zhukov AD, Bobrova EY, Zelenshchikov DB, Mustafaev RM, Khimich AO (2014) Insulation systems and green sustainable construction. *Adv Mater Struct Mech Eng* 1025–1026:1031–1034
17. Rumiantcev BM, Zhukov AD, Zelenshchikov DB, Chkunin AS, Ivanov KK, Sazonova YV (2016) Insulation systems of the building construction. In: MATEC web of conferences, vol 86. <https://doi.org/10.1051/mateconf/20168604027>
18. Rumiantcev BM, Zhukov AD, Bobrova EY, Romanova IP, Zelenshchikov DB, Smirnova TV (2016) The systems of insulation and a methodology for assessing the durability. MATEC web of conferences, vol 86. DOI: <http://dx.doi.org/10.1051/mateconf/20168604036>
19. Zhukov AD, Ter-Zakaryan KA, Semenov VS (2018) Insulation systems with the expanded polyethylene application. *ScienceDirect IFAC PaperOnLine* 51(30):803–807. <https://doi.org/10.1016/j.ifacol.2018.11.191>
20. Zhukov A, Dovydenko T, Kozlov S, Ter-Zakaryan K, Bobrova E (2019) Insulation systems of the building constructions. Published online: <https://doi.org/10.1051/e3sconf/20199102032>
21. Zhukov A, Ter-Zakaryan A, Bobrova E, Bessonov I, Medvedev A, Mukhametzyanov V, Poserenin A (2018) Evaluation of thermal properties of insulation systems in pitched roofs. Published online: 02 April 2019 TPACEE 2018 DOI:<https://doi.org/10.1051/e3sconf/20199102047>
22. Zhukov AD, Ter-Zakaryan KA, Tuchaev DU, Petrovsky ES (2019) Energy-efficient insulation of food warehouses and vegetable stores. *Int Agric J* 361(1):65–67
23. Shitikova MV, Bobrova EY, Popov II, Zhukov AD (2019) Energy efficiency technical thermal insulation. In: International multi-conference on industrial engineering and modern technologies, FarEastCon, No 8934917 Cat. No. CFP19M35-ART, code 156113. DOI:101109/FarEastCon.2019.8934917
24. Krashchenko V, Tretyakov N, Chernov A, Shaykhalov I, Zhukov A (2019) Modeling and thermal calculation of a pipeline insulation system. In: TPACEE E3S web of conferences, vol 164, 14021
25. Muratoglu OK et al (2000) The comparison of the wear behavior of four different types of crosslinked acetabular components. In: 46th annual meeting of the orthopaedic research society, p 0566
26. Li MG, Zhou ZK, Wood DJ et al (2006) Low wear with high-cross linked polyethylene especially in combination with OXINIUM heads. A RSA evaluation. In: Poster no. 643 presented at: orthopaedic research society annual meeting; 19–22 Mar 2006; Chicago, IL
27. Bragdon CR et al (2009) Seven-to-ten year follow-up of highly crosslinked polyethylene liners in total hip arthroplasty. Annual Meeting of the Orthopaedic Research Society, 55th Las Vegas. Poster No. 2444
28. Oonishi H, Saito M, Kadoya Y (1998) Wear of high-dose gamma irradiated polyethylene in total joint replacement—long-term radiological evaluation. In: 44th annual meeting, Orthopaedic Research Society, March 16–19
29. Cross-linked polyethylene. Applications fields. Web: ProPolyethylene.ru, 2019
30. Cross-linked polyethylene. Web: ru.knowledgr.cor., 2017
31. Zhuk PM, Zhukov AD (2018) Normative legal base of environmental assessment of building materials: prospects for improvement. *Ecol Ind Russia* 4:52–57
32. Zhukov AD, Konoval'tseva TV, Bobrova EY, Zinovieva EA, Ivanov KK (2019) Thermal insulation: operational properties and methods of research. MGSU, IPICSE. Published online. DOI:<https://doi.org/10.1051/mateconf/201825101016>
33. Zhukov AD, Ter-Zakaryan KA, Semenov VS, Kozlov SD, Zinovieva EA, Fomina ED (2019) Insulation systems for buildings and structures based on polyethylene foam. MGSU, IPICSE. Published online: DOI:<https://doi.org/10.1051/mateconf/201825101014>
34. Pilipenko A, Bobrova E, Zhukov A (2018) Optimization of plastic foam composition for insulation systems. Published online: 02 Apr 2019. TPACEE 2018 DOI:<https://doi.org/10.1051/e3sconf/20199102017>

35. Bobrova E, Pilipenko A, Zhukov A (2018) Insulating sheath system and energy efficiency of buildings. Published online: 02 Apr 2019. TPACEE 2018 DOI:<https://doi.org/10.1051/e3sconf/20199102019>
36. Ter-Zakaryan KA, Zhukov AD, Bessonov IV, Semenov VS, Starostin AV (2018) Systems of building insulation with the use of polyethylene foam. *Constr Mater* 2018(9):58–61
37. Semenov VS, Zhukov AD, Ter-Zakaryan KA, Sazonova YV (2018) Features of the implementation of insulation systems in the Far North. *Constr Mater* 2018(4):65–69
38. Ter-Zakaryan KA, Zhukov AD, Bobrova EY (2018) Innovative technologies for rural construction. *Moscow Econ J (QJE.SU)*. 2018(5)
39. Pilipenko A, Bobrova E, Zhukov A (2019) Optimization of plastic foam composition for insulation systems. 02017. Published online: 02 Apr 2019. DOI: <https://doi.org/10.1051/e3sconf/2019910201>
40. Bobrova E, Pilipenko A, Zhukov A (2019) Insulating sheath system and energy efficiency of buildings. Published online: 02 Apr 2019. TPACEE 2018. DOI:<https://doi.org/10.1051/e3sconf/20199102019>
41. Storb M (2005) Examining market trends for PEX pipes 11. *European Plastics News*, Belgium
42. Schiess A, Maillefer K (2008) PEX technology for pipes of various applications. In: *Materials of the International Conference "Polymer pipes"*
43. Bar Y (1998) Large diameter cross-linked P.E. Pipes. *Plastics pipeline systems for the Millennium X*. Svenska Massan Centre Goteborg, Sweden
44. Scheelen A (2005) Facilitating the pipe system choice of European water engineers. *European Plastics News*, Belgium
45. Honda H (1998) The evolution and present state of polyethylene (PE) water pipes in Japan. *Plastics pipeline systems for the Millennium X*, Svenska Massan Centre Goteborg, Sweden
46. Beech SH, Duncan JN, Millar JB (2001) Polyethylene pipeline systems the big success story. *Plastics pipes XI*, Munich Germany
47. Tsunaga M, Matsunami S, Sato M, Nakata K (1998) Cross-linked PE pipes for hot water and geothermal applications reliability and fusion technology. *Plastics pipeline systems for the Millennium X*, Svenska Massan Centre Goteborg, Sweden
48. Gorilovskij MI, Kalugina EV, Ivanov AN, Satdinova FK (2005) Examination of crystallinity and thermal stability in pipes produced from various types of polyethylene. *Scientific and technical magazine "Plasticheskie massy"*, no 4
49. Bulatova VM (2012) Comparative analysis of the operational characteristics of modern high-voltage cables. *All-Russian Academy of Sciences, Kazan National Research Technological University*. UDK 621.315.1.015.38
50. Korotkevich MA, Podgaiskiy SI (2017) The efficacy of the cables of 6–110 Kw with XLPE insulation, Part 2. *Energetika. Proc. CIS Higher Educ. Inst. and Power Eng. Assoc.* 60(6):505–522 505. <https://doi.org/10.21122/1029-7448-2017-60-6-505-522>
51. Zhukov A, Dovydenko T, Kozlov S, Ter-Zakaryan K, Bobrova E (2018) Innovative technologies for low-rise construction. Published online: 02 Apr 2019. TPACEE 2018. DOI:<https://doi.org/10.1051/e3sconf/20199102032>
52. Zhukov A, Ter-Zakaryan A, Bobrova E, Bessonov I, Medvedev A, Mukhametzyanov V, Poserenin A (2019) Evaluation of thermal properties of insulation systems in pitched roofs. Published online: 02 Apr 2019. DOI:<https://doi.org/10.1051/e3sconf/20199102047>
53. Zhukov A, Medvedev A, Poserenin A, Efimov B (2019) Ecological and energy efficiency of insulating systems. 03070. In: *E3S web of conferences*, vol 135, (ITESE-2019) Published online: 04 Dec 2019. DOI:<https://doi.org/10.1051/e3sconf/201913503070>
54. Zhukov AD, Ter-Zakaryan KA, Bobrova EY, Pilipenko AS (2019) Insulation sheath materials for cold preservation. In: *Materials and technologies in construction and architecture II*, pp 452–457
55. Pilipenko A, Ter-Zakaryan K, Bobrova E, Zhukov A (2019) Insulation systems for extreme conditions International. In: *Conference on modern trends in manufacturing technologies and equipment*. 19:1819–2586

Chapter 13

Industrial and Commercial Importance of XLPE



Shah Mohammed Reduwan Billah and Waseem Ibrahim

1 Introduction

Polyethylene (PE) is a low cost, widely available and easily processable polymer. It is used as a raw material to manufacture different types of crosslinked polyethylenes (XLPEs) which have very interesting features that include cost-effectiveness and versatility in technical properties compared to their competitors. XLPEs are prepared from PE by using different types of crosslinking techniques [1–15]. Polyethylenes are of different types, which include—(a) LLDPE (linear low-density polyethylene); (b) HDPE (high-density polyethylene); (c) UHMWPE (ultrahigh molecular weight polyethylene) [16–19]. These varieties of polyethylenes have different levels of physical and chemical properties suitable for a wide range of applications. Due to crosslinking, XLPEs usually attain a higher level of physicochemical properties compared to the polyethylene varieties from where they have been produced. For example, typically when XLPEs are produced from LDPE and HDPE (high-density polyethylene), they usually have higher tensile strength compared to that of original LDPE or HDPE [16–21]. It is a current trend where LLDPE is being popularly used for the covering of electrical cables. However, there are a few limiting factors that affect certain qualities of XLPEs when LLDPEs are used as raw materials to produce them. For example, there are complexities during the synthesis of XLPE from LLDPE and a reduction of gloss [1–5, 22–24]. Among different classes of polyethylenes, the UHMWPE (ultrahigh molecular weight polyethylene) is very

S. M. R. Billah (✉)

School of Engineering and Materials Science, Queen Mary University of London, Mile End, London, UK

e-mail: reduwan.shah@gmail.com

Department of Chemistry, The University of Durham, Durham, UK

S. M. R. Billah · W. Ibrahim

School of Textiles and Design, Heriot-Watt University, Galashiels, UK

© Springer Nature Singapore Pte Ltd. 2021

J. Thomas et al. (eds.), *Crosslinkable Polyethylene*, Materials

Horizons: From Nature to Nanomaterials,

https://doi.org/10.1007/978-981-16-0514-7_13

tough and highly robust in terms of physical and chemical properties [3–6, 25–32]. It is because the UHMWPE has very long chains with molecular weight generally ranging from 2 to 6 million. The UHMWPE has a wide range of applications some of which include—(a) bullet-proof vests (such as police and military ballistic-resistant vests), (b) helmets and (c) armored vehicles [1–8, 33–46]. Additionally, polyethylene is one of the widely used commodity polymers which have vast usages in different areas that include a variety of industrial products (e.g., carrier bags, bulletproof jackets, fuel tank), household items (e.g., water tank, container for food items), product for packaging and certain medical applications (such as implants) [1–8, 46–63].

1.1 Basic Features of the Crosslinking Operation and Its Importance in Enhancing Technical Performances

In very simple and typical consideration, one of the most general purposes of the crosslinking of polyethylene is mainly to enhance certain desired properties of polyethylene that transform polyethylene into a crosslinked polyethylene (XLPE) to have highly technically robust expected properties that include—(a) resistance to extreme environmental conditions such as at high temperature and pressure resistance, (b) retention of technical performances for a considerable period of time and (c) compliance with other sets of industrial criteria (such as yielding a non-melting robust polymer matrix at relatively cost-effective price) [12, 64–72].

1.2 Crosslinked Polyethylenes

The crosslinked polyethylene is expressed as XLPE or PEX. In general, three major technologies may be used to make crosslinked polyethylene products [1–5, 12, 13, 33–36]. All three methods link single strands of PE through radical reactions between the molecules to form a dense network. In typical consideration, all three processes are suitable to produce XLPE-based insulating materials such as pipes meet the set of ASTM standard requirement of the degree of crosslinking which is 65–80% [66, 71, 73–75]. Additionally, the crosslink density depends on the number of links between the molecules and this crosslink density also controls the physical properties of the resultant XLPE. Different tests can be carried out to analyze the degree and the nature of crosslinks formed by any of these three methods. For example, the xylene extraction process (as stated in ASTM D2765) is a typical method to quantify the degree and nature of crosslinking formed by any of these three techniques [1–4, 12, 76–78].

1.3 Crosslinking Improves the Technical Properties of Crosslinked-Polyethylenes

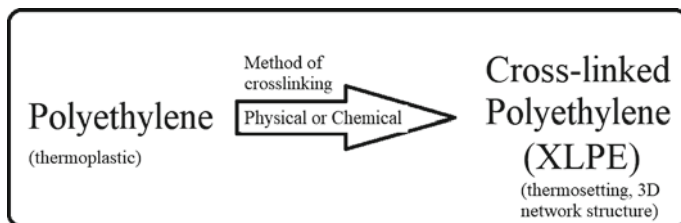
Crosslinking contributes to improve the desired technical properties (such as thermal and mechanical stabilities of the XLPEs) of polyethylene. After crosslinking and subsequent chain entanglement, the resultant XLPE becomes technically robust and it also retains certain characters of the polyethylene from where it has been produced. Some of these examples include—(a) lightweight, (b) flexibility, (c) good chemical resistance and (d) non-toxicity [1–4, 12, 79–84]. Selectively, some of these physical properties are included in the following table (Table 13.1).

2 Methods of Crosslinking

Different methods are usually used to produce crosslinked polyethylene where two principal groups of methods include—(a) physical crosslinking methods and (b) chemical crosslinking methods [1–4, 12]. Scheme 13.1 shows the production of crosslinked polyethylene from polyethylene.

Table 13.1 A precise presentation of various fundamental impacts of crosslinking on the properties of crosslinked polyethylene (XLPE) produced after crosslinking from different types of polyethylene HDPE (High-Density Polyethylene) or LDPE (Low-Density Polyethylene) [1–4, 12, 73, 81–86]

Different parameters	Nature of changes usually observed in XLPE when produced after crosslinking of HDPE or LDPE
Molecular weight	Increases significantly
Density	Usually no change or decrease
Melt Flow Index	Decreases
Tensile strength	Little change or increase very slightly
Elongation at break	Decreases
Impact resistance	Improves significantly
Resistance to abrasion	Improves significantly
Resistance to stress-crack	Improves considerably
Resistance to higher temperature	Improves significantly (e.g., a boost in the increase in long-term working temperature to 95 °C)
Resistance to environmental stress cracking	Improves considerably
Elastic properties	Enhances significantly
Resistance to slow crack growth	Improves greatly
Resistance to chemical attack	Improves significantly



Scheme 13.1 Production of crosslinked polyethylene from polyethylene

2.1 Selected Usually Used Methods of Crosslinking for the Preparation of XLPE from Different Types of Polyethylene

Various techniques are usually used for crosslinking in order to prepare XLPE from different types of polyethylenes (such as HDPE and LDPE) to improve desired technical properties suitable for different types of expected commercial and industrial applications. In this context, the first commercially widely used crosslinking method looks almost identical to the method typically used in rubber vulcanization process where the peroxide-based chemical(s) are employed to generate direct carbon-to-carbon links within the structure of polyethylene molecules that in turn contributes to produce the general structure of the XLPE. For more than two decades, many commercially available crosslinked polyethylene compounds or XLPEs have been produced based on this technique [1–4, 12]. A summary of generally used methods for the crosslinking reaction for the preparation of XLPE from different types of polyethylenes is presented here.

2.2 Different Methods of Producing Crosslinked Polyethylenes (XLPEs) and Their Specific Applications

In typical consideration, different techniques can be used to produce crosslinked polyethylenes or XLPEs which fall into two major groups; they are (i) physical methods and (ii) chemical methods. Each method has merits and demerits where a suitable method is usually selected based on the nature of final application of the XLPE product under consideration. Some of these points to consider a crosslinking method include—(a) the technical requirements of the XLPE product under consideration, (b) the total cost of the crosslinking operation, (c) the gel content, (d) the nature of hazards produced during the reaction and (e) the health and safety or the risks associated with the materials used in the whole production cycle [1–4, 7, 12, 87–96].

Methods of crosslinking differ considerably. In different methods, the physical state of polyethylenes is different (such as solid or melt). Additionally, it also differs in the type of initiator used to generate free radicals. During physical methods of

crosslinking, polymers (such as LDPE and HDPE) are exposed to high-energy radiations such as gamma rays or ultra-violet (UV) radiation to initiate the crosslinking reaction. For chemical methods of crosslinking, different techniques are used. For example, using free radical polymerization technique, crosslinking reaction can be controlled significantly [1–4, 12, 97–99]. However, for industrial applications, one of the most frequently used techniques is the use of accelerated electrons, because in this system the energy reached per unit time is relatively high [12, 100, 101]. The selection of crosslinking technique depends on the final use of the crosslinked polymer-based products. For instance, as the radiation provides an opportunity for sterilization, radiation crosslinked polymers such as crosslinked polyethylenes produced by radiation are suitable candidate for biomedical applications [2–6, 12, 46–63, 102–105]. However, the degree of crosslinking achieved from different radiation crosslinking techniques differs widely, and sometimes photo-initiators are also used to speed up radiation-based crosslinking of different polymers. For example, photo-initiators (e.g., benzophenone, benzyl dimethyl ketal, etc.) are usually used during crosslinking of polymers by using UV radiation technique [1–4, 12, 103–113]. Electron beam radiation-based crosslinking technique is generally used to produce thin-wall products (e.g., films, foams) since electron beams typically penetrate on the surface of the product for up to a few centimeters [3–5, 12, 114–118]. Usually, the radiation crosslinked polyethylenes have been used for different purposes some of which include—(a) electrical insulation, (b) packaging films and (c) medical implants [4–7, 12, 119–126]. Besides this, in certain methods of chemical crosslinking, free radicals are also generated by using appropriate techniques. In this context, two principal chemical crosslinking techniques are – (a) organic peroxide-based technique and (b) silane-based (moisture cured) technique [3–6, 12, 127–132]. Moreover, sometimes azo compounds are also employed for crosslinking of different polymers. One of the main reasons for the frequent application of the peroxide-based technique is, it helps to produce the highest and uniform degree of crosslinking in comparison with other radiation techniques [2–4, 12, 133–136].

In a precise diagram, Fig. 13.1a illustrates the generally used technologies to produce XLPEs, Fig. 13.1b shows the typically used silane-based crosslinking technologies, while Fig. 13.1c generally used peroxide-based crosslinking technologies. Table 13.2 describes a brief analysis of the nature of crosslinks. A detailed discussion on all these techniques is beyond the scope of this current chapter, hence for more information please consult the respective textbooks, reviews and related journal articles [1–7, 12–15, 137–316].

For XLPE production, peroxide crosslinking is one of the most usually employed techniques which are used to crosslink PE and it is the first commercially used technique to produce crosslinked polyethylenes [2–4, 12, 87–93]. During the application of organic peroxide to generate the free radicals for the crosslinking of polyethylene, as a by-product methane gas is released due to the reaction between DCP and PE that sometimes causes to generate pinholes or pores; thus, the process is usually carried out at higher pressure environment [2–5, 12, 94].

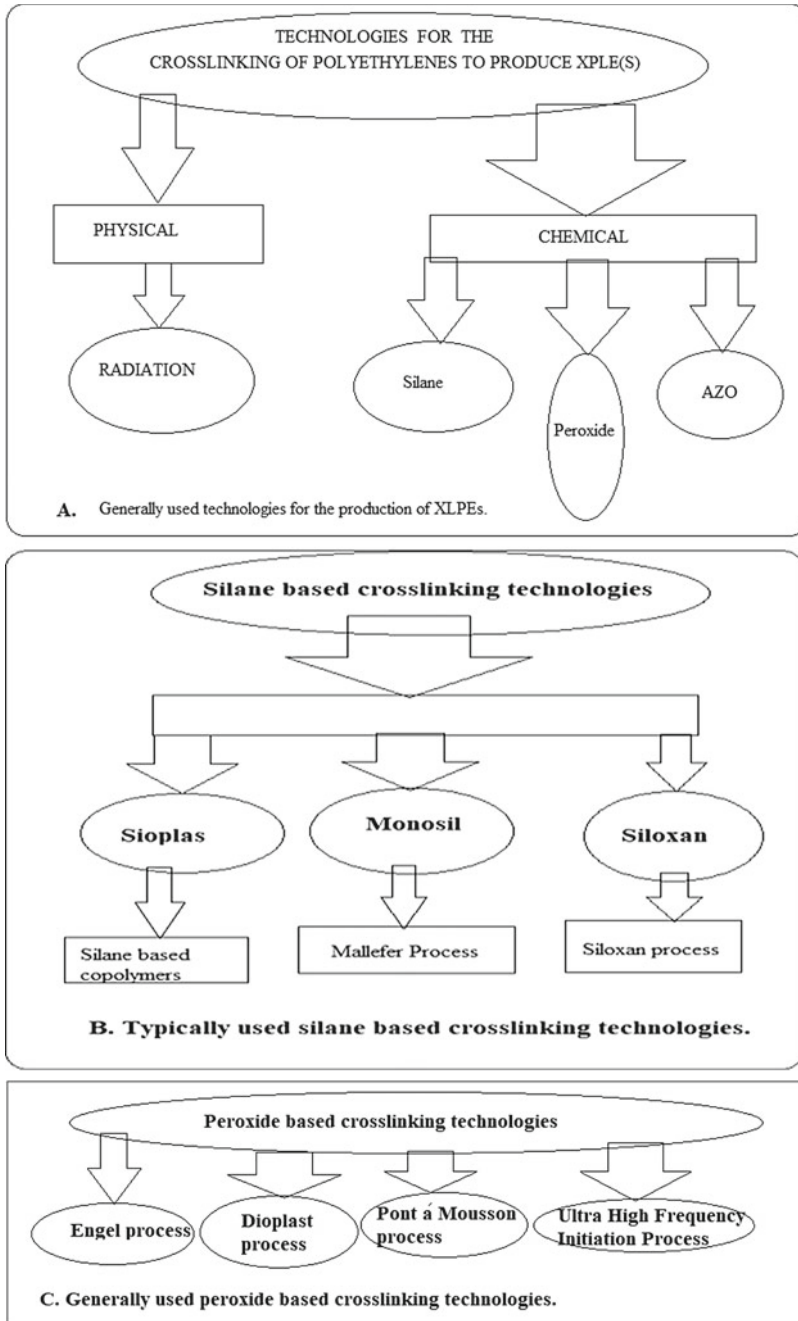


Fig. 13.1 a Generally used technologies to produce XLPEs. b Typically used silane-based crosslinking technologies. c Generally used peroxide-based crosslinking technologies

Table 13.2 A brief analysis of the nature of crosslinks [2–5, 12, 13, 87–89]

Features	Organic peroxide-based crosslinking technique	Silane-based crosslinking technique
Degree of crosslinking	Up to 90%	45–70%
Nature of crosslinks	C–C crosslinks are formed	Si–O–Si crosslinks are formed
Strength	C–C crosslinks are stronger	Si–O–Si crosslinks are relatively weaker

3 Principal Applications of XLPEs

Polyethylene (PE) is a relatively low cost, widely available, easily processable polymer. Commercially available in different forms of polyethylene includes—(a) low-density polyethylene (LDPE), (b) linear low-density polyethylene (LLDPE), (c) high-density polyethylene (HDPE) and (d) ultrahigh molecular weight polyethylene (UHMWPE) [3–5, 12, 60–64]. Usually, polyethylene is produced by a polymerization of ethylene. Polyethylene is one of the most commonly used commodity polymers in a wide range of areas that include—(a) packaging; (b) plumbing and building pipes for domestic and industrial applications; (c) automobiles, marine vehicles and certain component of space-crafts; (d) products for everyday life (such as household items); (e) insulation of low, medium and heavy-duty cables; (f) product used in the areas of material science and biomedical applications; (g) products for defense applications (such as police and military ballistic-resistant vests, helmets and armored vehicles) [2–12, 47–62, 137–139].

Table 13.3 demonstrates a comparative study on different properties of polyvinyl alcohol (PVC), polyethylene (PE) and crosslinked polyethylene (XLPE). This study clearly illustrates the advantages of using XLPE-based products for both industrial and commercial applications [1–5, 66–84, 92–94, 140–156].

4 Applications of XLPEs in Electrical Insulations

One of the main uses of XLPEs is in electrical insulation. They have attractive required technical features that make them suitable to be used in effective insulation of high-voltage cables for electricity transmission without causing any hindrance or limitations on the performances of the electric cables. In addition, XLPE insulated cables have superior qualities compared to the cables insulated with many other alternating insulating materials (e.g., silicon rubbers, ethylene-propylene rubber or EPR) [1–12, 66–94, 140–145]. Figure 13.2 illustrates the basic construction of a high voltage cable (HVC), and in this type of cable, sometimes the XLPE can be used in primary insulation [66–68, 146–152].

Figure 13.2 also illustrates the basic construction of a high-voltage cable that contains different parts such as – (a) a jacket, (b) a metallic sheath, (c) a primary

Table 13.3 Comparative studies on different properties of polyvinyl alcohol (PVC), polyethylene (PE) and crosslinked polyethylene (XLPE)

Properties	Polyvinyl alcohol (PVC)	Polyethylene (PE)	Crosslinked polyethylene (XLPE)
Typical thickness (insulation), mm	1.0	0.70	0.70
Density, g/cm ³	1.4	0.92	0.92
Dielectric strength (Kvcm ⁻¹)	20–35	20–35	35–50
Dielectric constant (60 Hz)	6–8	2.3	2.3
Dielectric loss tangent (60 Hz)	0.1	10.4	10.4
Volume resistivity (Ω cm)	1012–1015	1017	1017
Insulation resistance (m Ω K m ⁻¹)	20	1000	1000
Instantaneous short-circuit temperature (°C)	135	150	250
Typically, maximum operating temperature (°C)	60–70	75	95
Typically, softening temperature (°C)	120	105–115	127
Chances of embrittlement at low temperature	Fair	Good	Excellent to outstanding
Resistance to oil	Fair	Good	Excellent to outstanding
Resistance to aging	Fair	Good	Excellent to outstanding
Resistance to weathering	Fair	Good	Excellent to outstanding

insulation and (d) a primary conductor. In this type of cable when XLPE is used mainly for insulation, it also serves some other purposes which include (a) protection of the conductor from being damage and (b) providing fire and chemical resistance or other adverse environmental impacts [1–4, 12, 13, 153–165]. In order to prolong the product life of the cable by keeping it in a safe environment, sometimes the XLPE is complemented with other materials used in the insulated cable manufacture. For example, the cross-section of two different types of XLPE insulated cable is shown in Fig. 13.3a, b.

Figure 13.3a demonstrates the cross-section of a XLPE insulated cable, Fig. 13.3b shows the cross-section of a XLPE insulated cable with a different construction pattern, while Fig. 13.3c exhibits a basic construction of a XLPE insulated cable.

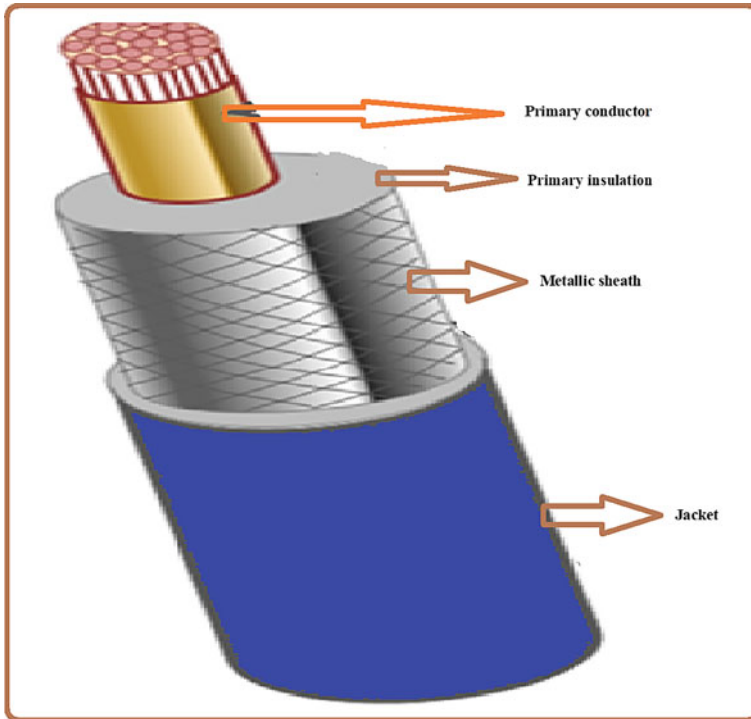


Fig. 13.2 Illustration of the basic construction of a high-voltage cable

The nature of the current rating of cables is affected by the installation conditions and the cable design and materials used in the manufacture of these cables. Some of the factors that have impact on current rating that include—(a) conductor size, (b) sheath bonding arrangement, (c) enclosing in conduit, (d) exposure to direct solar radiation, (e) groups of cables and those installed in randomly filled cable trays and (f) overall nature of insulation used in the cable manufacture. For different types of cable, different parameters are important. For example, for buried underground cables, the effect on the current rating is influenced by different parameters that include—(a) conductor size, (b) soil dry-out, (c) conductor material, (d) sheath bonding arrangement, (e) enclosing in conduit, (f) phase separation, (g) soil thermal resistivity, (h) conduit size, (i) soil ambient temperature and (j) overall nature of the insulating materials used [2–5, 33–36, 166–192]. Thus, in both cases, it is important to note that the insulating material used in the cable manufacture is one of the most important factors that play vital role to keep the cable safe and contribute in its work life-time. The uses of XLPE are increasing in different sectors, for example, both in electrical cable insulation and in the plumbing and construction industry for making different components that include pipes, storage tanks and other similar components [1–5, 32–36, 193–212].

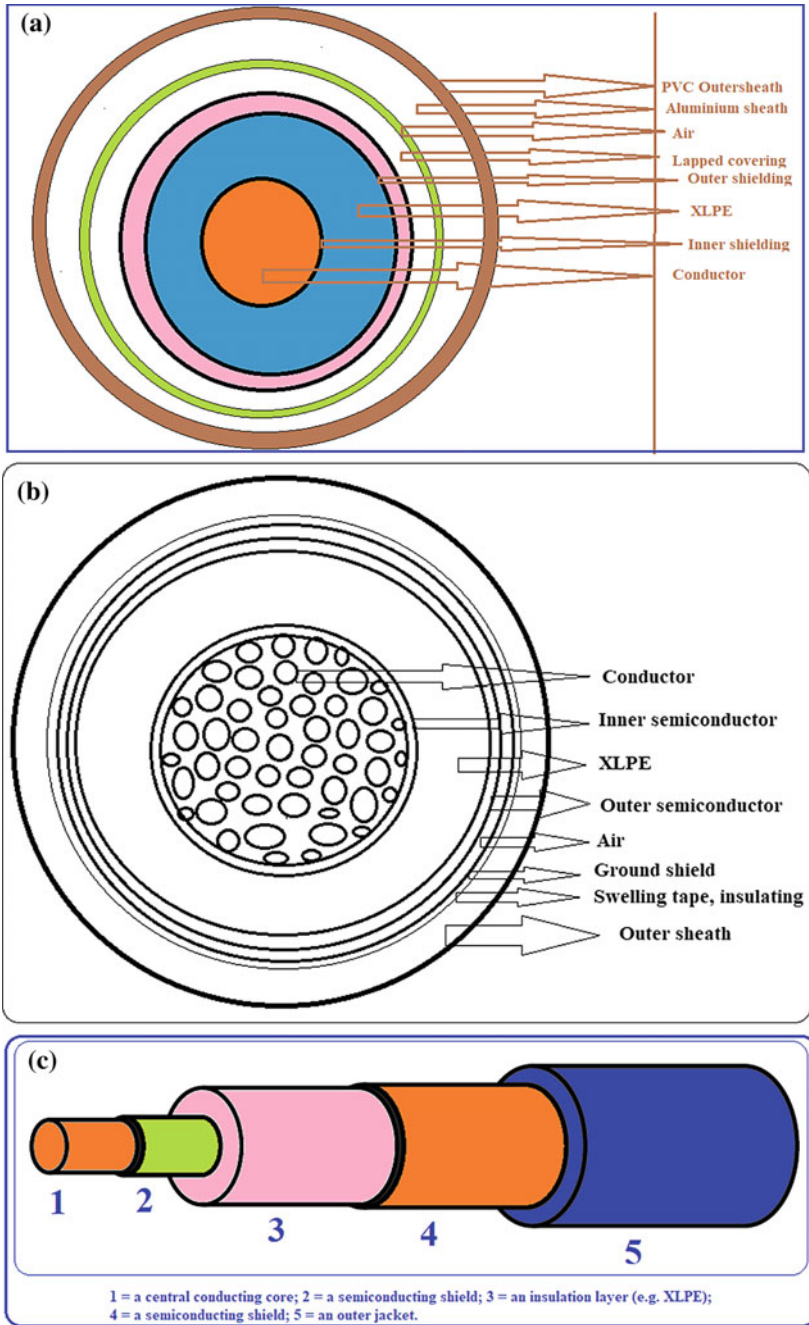


Fig. 13.3 a Cross-section of a XLPE insulated cable. b A cross-section of a XLPE insulated cable with a different construction pattern. c A basic construction of a XLPE insulated cable

5 XLPEs in High-Voltage Cable Insulation

In general, the wind farms use high-voltage alternating current (HVAC) and high-voltage direct current (HVDC) cables for the transmission of power from the sea as well as across offshore for the use of this power by the end users [3–5, 12, 189–193]. HVDC cables are usually employed to transmit power at a long distance. In addition, HVDC underground cables provide several of the merits (compared to overhead lines) that include—(a) protecting aesthetic views, (b) reducing the level of disruption living environment and (c) providing a relatively safer way to transmit the power using this type of insulated cables at a desired long distance. Besides this, the transmission of power through the HVDC cables provides other advantages that include—(i) a full control of transmission process, (ii) a rapid and accurate level of power transmission and (iii) cost-effective (e.g., HVDC channels have relatively lower capital costs) [7, 12, 194–196]. The different parts as a HVDC cable are (a) a conductor core, (b) semiconductor screen, (c) main insulation and (d) sheath, armoring and related accessories [2–5, 12, 189, 193–231]. This is similar to AC cables (Fig. 13.3c).

6 Different Types of HVDC Cables

Different types of HVDC cables are used for a variety of purposes where the some of the main categories are briefly summarized here.

(a) Oil-filled DC cables

In oil-filled DC cables as the main insulation component, multilayer-impregnated kraft papers are used where the pressured oil is used in the oil channels. However, HVDC cables of this type show different unexpected features that include—(a) limited cable length, (b) requirements of oil feed equipment and (c) the risk of oil leakage [2–5, 189–198]. Currently, these types of HVDC cables are being replaced with extruded HVDC and mass-impregnated cables [228].

(b) Mass-impregnated cables

For mass-impregnated cables, for the insulation of the mass-impregnated cable mainly kraft paper is used where the operation temperature of this type of cable can rise to 55 °C. To enhance the insulation and operation temperature of the mass-impregnated, laminated polymer film can be used [228–231].

(c) Extruded HVDC cables:

For this type of extruded HVDC, XLPE is mainly used for insulation by using extrusion technique and it is a new trend in developing extruded HVDC for a variety of purposes. Extruded HVDC produced from XLPE offers a wide range of attractive

features, some of which include—(i) the capability to withstand a higher operational temperature (up to 90 °C) which in turn allows higher level of electricity transmission through a given conductor cross-section compared to that of a mass-impregnated cable; (ii) typically, the XLPE-based HVDC cables are technically robust and have relatively less weight; (iii) it provides the scope for an easy and quicker installation process; (iv) it helps to avoid the environmental issues like oil leakage; and (v) it offers the ability to recycle and reuse. Because of these highly attractive significant features, extruded XLPE-based HVDC is being successful to draw more active current research both in academia and in industry. For example, recently, in different HVDC projects, XLPE-based extruded HVDC cables have been successfully used [186–194, 230–294].

For example, some typical methods of producing different types of XLPE insulated HVDC cables are demonstrated in Fig. 13.4a which illustrates a method of producing XLPE insulated single wire, while Fig. 13.4b demonstrates the method of producing XLPE insulated power cables.

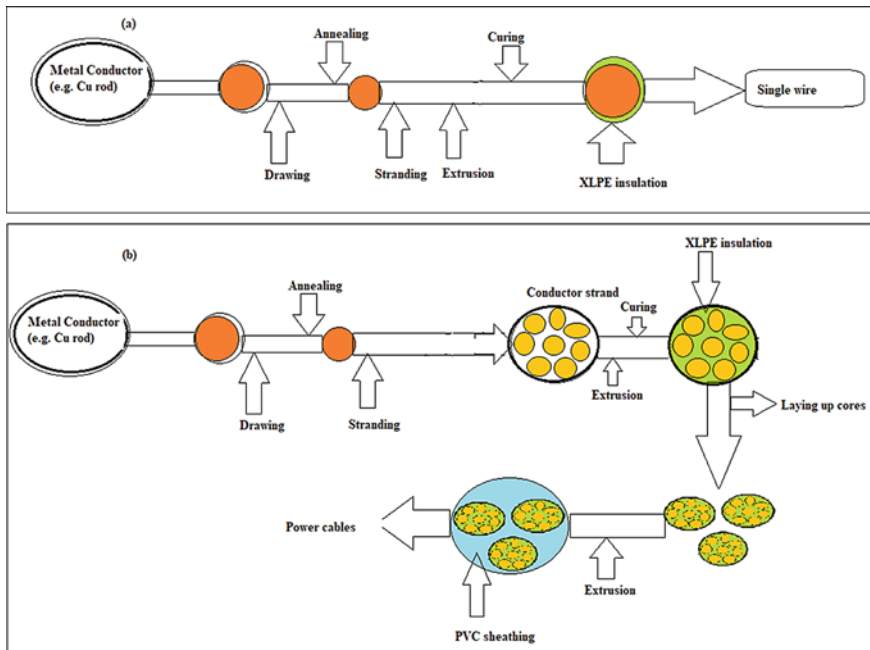


Fig. 13.4 a Examples of the method of producing XLPE insulated single wire. b Examples of the method of producing XLPE insulated power cables

7 XLPE for Domestic and Plumbing Applications

Recently, one of the biggest markets where the application of XLPE growing steadily is the domestic use of XLPE in plumbing (such as in domestic pipes) and other related areas that include water tanks, tanks for chemical storage and pipes for radiators used in heating purposes. This growing trend in domestic is mainly due to the fact that the XLPE provides high level of technical properties that include—(a) chemical resistance, (b) heat resistance, (c) dimensional thermal and mechanical stabilities, (d) environmental stress crack resistance/notch sensitivity, (e) long-term hydrostatic strength, (f) toughness and (d) long product life at a relative cost-effective price [2–5, 7, 14–21, 193–256].

8 Commercial and Industrial Importance of XLPE

Different projects show that the estimated year market size in 2019 is USD 6.2 billion, while forecasted market size in year 2024 is 8.1 billion USD with a compound annual growth rate or CAGR of 5.4% (Fig. 13.5) (according to Forencis Research) [231]. However, different research groups have varying level of projects on the market size and growth; hence, for more information, relevant sources of information can be consulted for more up-to-date information [232–235]. Projections on the global XLPE market show nearly sustained growth year by year [231]. For example, the global XLPE market is highly influenced by the investments made by APAC countries. Additionally, the market growth is significantly contributed by the increasing uses of wires and cables due to the boost in global building and construction industry.

Fig. 13.5 A graphical illustration of the volume (estimated market size in 2019 and forecasted market size in 2024) of crosslinked polyethylene (XLPE) in two different years. [231]



9 Market Based on Crosslinked Polyethylene Foam (XLPE Foam)

Crosslinked polyethylene foam (XLPE foam) insulation is highly attractive and flourishing day by day. During XLPE foam insulation, the molecular structure of polyethylene changes from a linear molecular structure to a three-dimensional network structure (similar to the change as shown in Scheme 13.1) by converting it from a thermoplastic material to a thermosetting material; it contributes to increase the operating temperature from 70 to 90 °C and also enhances the mechanical properties. Relatively, there are very limited manufacturers who produce the XLPE foams, and some of the principal producers of XLPE foam are (a) Armacell, (b) Sekisui Chemical, (c) BASF, (d) Furukawa and (e) Zhejiang Jiaolian. XLPE-based foams are being increasingly used in different sectors some of which include—(a) building and construction industry, (b) automotive parts industry, (c) anti-static and electronics hardware industry and (d) sports and leisure [1–7, 12, 13, 234, 236–250]. The global XLPE-based foam market size is projected to reach USD 1968.4 million by 2026, from USD 1356.6 million in 2020 at a CAGR of 6.4% during the financial years from 2021 to 2026 [233]. In addition, in the year 2018, the size of global XLPE market was valued at USD 5.73 billion which has been projected to expand at a CAGR of 6.0% from 2019 to 2025 [234]. Over the next few years, some of the principal factors that are positively driving the XLPE market are – (a) increasing demand from the plumbing and construction-related industries and (b) insulations for electrical wires and cables manufacturing sectors [234, 235, 248, 265–273].

9.1 Basic Features on the Commercial and Industrial Importance of XLPE

Crosslinked polyethylene (XLPE) is one of the very useful polymers that have a wide range of applications in a variety of commercial and industrial uses. However, it possesses some attractive characteristics of polyethylene (that include high chemical and moisture resistance) and it also has its own attractive features such as a higher thermal insulation capability that makes it suitable for its uses in high voltage and temperature conditions. For example, commercial applications of XLPE include—(a) plumbing systems used in building (or pipework) and (b) applications for insulating high-voltage cables (that has been successfully used to replace PVC (polyvinyl chloride) for wire insulation and also to replace copper tubing usually used in water pipes in the buildings or other commercial or industrial applications [1–8, 11–31, 51–62, 81–93, 201–231, 248, 263–282, 294–330].

When the polyethylene is crosslinked by using physical or chemical crosslinking methods, it helps to boost certain properties of the resultant crosslinked polyethylene (XLPE) by increasing its particular technical performances (such as higher thermal

and chemical resistances) that make it suitable for a wide range of applications [1–7, 23–46]. For example, the XLPE which is used in the insulation of ground wire does not melt easily and can withstand higher temperature (such as 120 °C) for a significantly long period with maintaining its original mechanical and chemical characteristics efficiently [15, 35–39]. In addition, this crosslinking also enhances other technical performances; for example, young modulus, resistance to abrasion and environmental stress of the XLPE are also increased [32–45, 121–126]. It is indeed the crosslinking operation that causes a structural change which turns the thermoplastic structure of polyethylene (before crosslinking) into a 3D-structured thermoset structure (after crosslinking) and eventually improves the technical performances of XLPE [1, 63–76, 127–132]. For instance, high-voltage ground cable insulated with XLPE can work fine for a considerably long time even in the very harsh environmental conditions [1, 133–136]. Additionally, XLPE shows higher level of technical performance in terms of insulation compared to that of PVC-insulated wires since PVC-based insulation is more suitable in low tension applications. In brief, XLPE insulated cable shows the following technical robust characteristics—(a) highly technically performing electrical, thermal and physical characters; (b) robust moisture and flame resistance; and (c) very high resistance to crush and heat deformation [137–141]. Some of the technical performances of XLPEs are shown in Table 13.3.

The crosslinking of polyethylene to prepare XLPE is similar to vulcanizing the rubber with the addition of little amount of chemical additives to cause a rearrangement of the molecular structure into a lattice which effectively hinders the movement of molecules in the presence of heat that effectively protects the physical and chemical structure of the insulated wire from being damaged from the harsh environmental conditions ensuring higher level of product life for a significant amount of time, the crosslinking contributes to enhance the insulation performances of XLPE cable at high temperatures that also helps to boost the XLPE wire current rating for short circuits and normal loading conditions when used in different environmental conditions (e.g., XLPE high-voltage cable insulation for underground electricity transmission). Besides this, when XLPE is used for cable insulation, it helps to mitigate or remove (to some extent) the issue of accelerated aging due to the impacts of electrical, environmental and mechanical stress which ensures the product life of XLPE insulated cable for a considerably longer period [1–5, 23–27, 142–153].

Crosslinked polyethylenes (XLPEs) have got their applications in a wide range of areas due to their attractive properties. As for example, in the manufacture of chemical storage vessels, they have been popularly used due to their very high technical performances (such as physical strength and chemical resistance), while their applications in mines are highly pronounced for their outstanding capability to withstand and resist any deformation that may cause by the high pressure and temperature from the surrounding environment [154–163].

10 Current Trends and Future Perspective of XLPEs

Table 13.4 illustrates the continuous level of scientific research and breakthrough on the fundamental progress in the development of insulated cable (such as XLPE cables). This research and development activity is a continuous process and constantly deals with issues generating from the practical uses of XLPE-based cable or other insulated cables as well as the tireless effort to enhance new desired level of technical performances to overcome many existing issues and widening the scope of future potential application areas.

Generally, polyethylenes are widely used low-cost commodity polymers which provide the opportunities for recycle and reuse. When these polyethylenes are crosslinked to prepare crosslinked polyethylenes (XLPEs), the resultant XLPEs show enhanced desired technical properties suitable for many commercial and industrial

Table 13.4 Fundamental progress in the development of XLPE cables [1–12, 231–236]

Milestones	Major events
1812	To detonate a mine, a company called Schilling (Russia) at first used a rubber varnish-insulated wires
1850	Subsea telegraph cable between Dover (England) and Calais (France) was used to enhance communication using trans-Atlantic submarine telegraph cable for the first time
1880	Thomas Edison used DC cables insulated with jute in ‘Street Pipes’
1890	Sebastian Ferranti of Great Britain pioneer the use of 10 kV tubular cable having paper insulation
1900	Introduction of natural rubber for cable insulation
1925	Start of the use pressurized paper cables
1930	In this year, polyvinylchloride was commercially manufactured in Germany
1937	Development of polyethylene in Great Britain
1942	Introduction of polyethylene for cable insulation
1954	Sweden introduced the DC power transmission cable
1963	General Electric Company reported the intention of crosslinked polyethylene (XLPE) and its application in cable insulation
1968	The introduction of XLPE for medium voltage cable insulation
1972	Extruded semi-conducting screens were introduced in this year
1978	The widespread use of jackets in the cable was observed in North America from this year
1988	From this year in Japan, for the first time 500 kV XLPE cables were applied without joints within a pump storage scheme
2000	Again, in Japan, 500 kV XLPE cables were applied with joints installed under long distance
2006	For the first time, the world’s longest submarine cable has been employed in Basslink (Australia)

applications. After crosslinking operation, the thermoplastic polyethylene changes into a thermosetting crosslinked polyethylene. Different studies on the market analysis show that high-density polyethylene (HDPE) is one of the many polyethylene derivatives that dominated the current market for its commercial and industrial applications. Both high-density polyethylene and low-density polyethylene are typically used in the manufacture of crosslinked polyethylenes (XLPEs). The commercial and industrial applications of XLPEs are growing for a number of reasons that include—(a) relatively cheaper raw materials (such as HDPE and LDPE), (b) higher technical properties (such as higher thermal resistance and mechanical strength, and higher stress crack resistance), (c) processing flexibility and compatibility, (d) providing the opportunity to recycle and reuse, and (e) economic compatibility over its competitors. XLPEs are widely used in medium to high-voltage cable insulations as well as in domestic and industrial plumbing applications. They are also used in a few other areas that include—(a) automobiles, (b) fuel and water tanks, (c) packaging, (d) preparation of marine vehicles and (e) biomedical applications (such as hip and knee joints, and bone repair) [1–12, 24–43, 46–66, 123–168, 189–214, 220–229, 232–245, 294–330].

In different industrial applications, the uses of XLPEs are growing steadily. As for example, in 2016, plumbing was the highest application area in the global consumption of crosslinked polyethylene. Typically, copper and PVC are usually used in plumbing applications, but their performances in terms of resistance to high temperature and highly chlorinated water (i.e., generally transported through the water pipes for a long time) are relatively poor compared to the performances of XLPEs; as a result, there is a current trend in the applications of XLPEs for these types of products manufacture. As a result, there are intensive comprehensive research and development activities on the production of XLPEs in most effective and economically viable ways to increase their resistance to higher or extreme environmental conditions as well as resistance to certain chemicals (such as resistance to chlorinated water, acidic corrosions and gaseous environments) to occupy this domestic plumbing markets [228–236]. This research also contributes to excel the technical properties of XLPEs that can make them more robust competitors in their general uses in medium and high-voltage applications [1–7, 237–247]. In the chemical industry, XLPEs are used to manufacture storage tanks because of their resistance to certain chemicals (such as acidic corrosion) and heat [12–22, 193–226, 230–238, 249, 250]. As a result, there is steady growth in the applications of XLPEs in commercial and industrial applications. For example, in 2016, the value of the global crosslinked polyethylene market was at US\$ 5323.1 million (for 2941.2 kilotons of XLPE-based products). So, the current projection of growth of global XLPE-based products during 2017–2025 stands at a CAGR of 6.6% in terms of revenue, and in terms of volume, it is 6.1% [231–235].

10.1 Recycle, Reuse and Eco-Compatibility of XLPEs

XLPEs are widely used in a variety of commercial and industrial applications which have been mentioned in previous sections of this chapter. However, for a steady and sustainable growth, environmental concerns must be addressed properly. But it is practically very expensive and difficult to decrosslink XLPEs to ensure recyclability and reuse for various purposes [12–21, 193–203]. It is a matter of great hope that there is continuous research in this area which shows some rays of hope that in the future there would more viable environmentally sustainable products based on XLPE [1–7, 12–16, 121–124]. In order to mitigate future challenges and to draw active and continuous commercial and industrial scale research and developments on XLPE-based products must have to comply with environmental regulations and they must be eco-compatible.

In a very precise statement on the facts that there are several major influencing factors which drive current trends and future perspectives for the research and development activities on XLPEs. Thus, one of the major objectives is reiterated here once again (as they have already been stated elsewhere in the above sections).

10.2 Finding the Most Effective Methods for the Manufacturing of XLPEs to Enhance Desired Technical Performances at Cost-Effective Ways Meeting All the Environmental Issues

In very simple and typical consideration, one of the most general purposes of the crosslinking of polyethylene is mainly to enhance certain desired properties of polyethylene that transform polyethylene into a crosslinked polyethylene (XLPE) to have highly technically robust expected properties that include—(a) resistance to extreme environmental conditions such as at high temperature and pressure resistance, (b) retention of technical performances for a considerable period of time and (c) compliance with other sets of industrial criteria (such as yielding a non-melting robust polymer matrix at relatively cost-effective price) [1–7, 295–330]. In other words, the crosslinking reaction plays an active role to change the thermoplastic polyethylene into a thermoset XLPE with a robust three-dimensional network structure that provides the many significant properties that include—(a) improved thermal resistance, (b) resistance to environmental stress, (c) creep resistance and (d) higher impact strength. XLPEs are attractive and practically used in many industrial applications due to properties obtained from the crosslinked polyethylenes or XLPEs. Some of these properties are (a) high operational temperature, (b) higher dielectric strength, (c) reliability, (d) low dielectric loss, (e) good dimensional stability, (f) solvent resistance and (g) long life [1–13, 294–333].

Thus, to find the most effective methods for the manufacturing of XLPEs to enhance desired technical performances in cost-effective ways was one of the main

impetus in the past for the research and development activities on XLPEs. It is still one of the main targets for the research and development activities on XLPEs and it will remain as one of the main aims for the research and development activities on XLPEs for foreseeable future [1–13, 228–234].

11 Conclusion and Perspective

The commercial and industrial importance of XLPEs is growing steadily and significant efforts have been employed to overcome different issues and to realize the wider rigorous exploitation of other potential applications in existing and new areas of potential uses. It is almost impossible to give a comprehensive picture of the wide range of applications of XLPEs and the detailed explanations of the technological breakthrough of different recent achievements within the very limited scope of this current chapter. For more up-to-date information, readers can have an eye on the new research articles in the relevant journals and electronic information on the news on the latest developments in terms of trade and business relating to XLPEs and their application. A concerted effort has been made to provide most up-to-date information on types of applications of XLPEs along with relevant references for more detailed information. Additionally, for detailed mechanisms and the methods of applications of XLPEs in a wide range of potential and practical applications, readers are advised to consult the relevant reference(s).

References

1. Malpass DB (2010) Introduction to industrial polyethylene: properties, catalysts, and processes. First published 14 June 2010, Print ISBN 9780470625989, Online ISBN 9780470900468, Wiley Online Books, <https://doi.org/10.1002/9780470900468>
2. Peacock A (20 Jan 2000) Handbook of polyethylene: structures: properties, and applications. CRC Press
3. Spalding MA, Chatterjee A (eds) (2017) Handbook of industrial polyethylene and technology: definitive guide to manufacturing, properties, processing, applications and markets set. ISBN 978-1-119-15976-6, Wiley Online Library
4. Kurtz S (ed) (2004) The UHMWPE biomaterials handbook: ultra high molecular weight polyethylene in total joint replacement and medical devices. Elsevier Academic Press, London, UK. eBook ISBN 9780323354356, Hardcover-ISBN 9780323354011
5. Tamboli SM, Mhaske ST, Kale DD (2004) Crosslinked polyethylene. *Indian J Chem Technol* 11:853–864
6. Visakh PM, Morlanes MJM (2015) Polyethylene-based blends, composites and nanocomposites. Scrivener Publishing LLC. First published 24 July 2015, Print ISBN 9781118831281, Online ISBN 9781118831328, <https://doi.org/10.1002/9781118831328>
7. Li Lunzhi, Zhong Lisheng, Zhang Kai, Gao Jinghui, Man Xu (2018) Temperature dependence of mechanical, electrical properties and crystal structure of polyethylene blends for cable insulation. *Materials (Basel)* 11(10):1922

8. Zhang K, Li L, Zhong L, Chen N, Xu M, Xie D, Chen G (2015) The mechanical properties of recyclable cable insulation materials based on thermo-plastic polyolefin blends. In: Proceedings of the 11th international conference on the properties and applications of dielectric materials (ICPADM), Sydney, Australia. 19–22 July 2015, pp 532–535
9. Barzin J, Azizi H, Morshedian J (2006) Preparation of silane-grafted and moisture cross-linked low density polyethylene: Part I: factors affecting performance of grafting and cross-linking. *Polym Plastic Technol Eng* 45(8):979–983
10. Barzin J, Azizi H, Morshedian J (2007) Preparation of silane-grafted and moisture crosslinked low density polyethylene. Part II: electrical, thermal and mechanical properties. *Polym Plastic Technol Eng* 46(3):305–310
11. Morshedian J, Hoseinpour PM (2009) Polyethylene cross-linking by two-step silane method: a review. *Iran Polym J* 18(2):103–128
12. Thomas J, Joseph B, Jose JP, Maria HJ, Main P, Rahman AA, Francis B, Ahmad Z, Thomas S (2019) Recent advances in cross-linked polyethylene-based nanocomposites for high voltage engineering applications: a critical review. *Ind Eng Chem Res* 58(46):20863–20879
13. Gao Y, Huang X, Min D, Li S, Jiang P (2019) Recyclable dielectric polymer nanocomposites with voltage stabilizer interface: toward new generation of high voltage direct current cable insulation. *ACS Sustain Chem Eng* 7(1):513–525
14. Zhao Y, Choi BH, Chudnovsky A (2013) Characterization of the fatigue crack behavior of pipe grade polyethylene using circular notched specimens. *Int J Fatigue* 51:26–35
15. Miao W, Zhu H, Duan T, Chen H, Wu F, Jiang L, Wang Z (2018) High-density polyethylene crystals with double melting peaks induced by ultra-high-molecular-weight polyethylene fibre. *R Soc Open Sci* 5:180394. <https://doi.org/10.1098/rsos.180394>
16. Frank A, Pinter G, Lang RW (2009) Prediction of the remaining lifetime of polyethylene pipes after up to 30 years in use. *Polym Test* 28:737–745
17. Pérez-González J, Denn MM (2001) Flow enhancement in the continuous extrusion of linear low-density polyethylene. *Ind Eng Chem Res* 40:4309–4316
18. Williams JG, Hodgkinson JM, Gray A (1981) The determination of residual stresses in plastic pipe and their role in fracture. *Polym Eng Sci* 21:822–828
19. Nie M, Wang Q, Bai SB, Li Z, Huang A (2014) The formation and evolution of the hierarchical structure of polyethylene pipe during extrusion processing. *J Macromol Sci B* 53:205–216
20. Li Y, Nie M, Wang Q (2017) Facile fabrication of electrically conductive low-density polyethylene/carbon fiber tubes for novel smart materials via multi-axial orientation. *ACS Appl Mater Interfaces* 10:1005–1016
21. Nie M, Wang Q, Bai SB (2010) Morphology and property of polyethylene pipe extruded at the low mandrel rotation. *Polym Eng Sci* 50:1743–1750
22. Nie M, Bai SB, Wang Q (2010) High-density polyethylene pipe with high resistance to slow crack growth prepared via rotation extrusion. *Polym Bull* 65:609–621
23. Miao W, Wang B, Li Y, Zheng W, Chen H, Zhang L, Wang Z (2017) Epitaxial crystallization of precisely bromine-substituted polyethylene induced by carbon nanotubes and graphene. *RSC Adv* 7:17640–17649
24. Pi L, Hu X, Nie M, Wang Q (2014) Role of ultrahigh molecular weight polyethylene during rotation extrusion of polyethylene pipe. *Ind Eng Chem Res* 53:13828–13832
25. An M, Xu H, Lv Y, Gu Q, Tian F, Wang Z (2016) An in situ small-angle X-ray scattering study of the structural effects of temperature and draw ratio of the hot-drawing process on ultra-high molecular weight polyethylene fibers. *RSC Adv* 6:51125–51134
26. Sun FS, Bai SB, Wang Q (2018) Structures and properties of waste silicone cross-linked polyethylene de-cross-linked selectively by solid-state shear mechanochemical technology. *J Vinyl Addit Technol* 25:149–158
27. Li YJ, Nie M, Wang Q (2016) Synergistic effect of self-assembling nucleating agent and crystallization promoter on polypropylene random copolymer pipes via rotation extrusion. *Polym Eng Sci* 56:866–873
28. Cho S, Jeong S, Kim JM, Baig C (2017) Molecular dynamics for linear polymer melts in bulk and confined systems under shear flow. *Sci Rep* 7:9004

29. Ramos J, Vega JF, Martínez-Salazar J (2018) Predicting experimental results for polyethylene by computer simulation. *Eur Polym J* 99:298–331
30. Bornarel AC, White JR (1998) Birefringence and shrinkage during thermal reversion of oriented polymers. *Polym Polym Compos* 6:287–294
31. Lamberti G (2014) Flow induced crystallisation of polymers. *Chem Soc Rev* 43:2240–2252
32. Orton H (2013) History of underground power cables. *IEEE Electr Insul Mag* 29(4):52–57
33. Zhu WW, Zhao YF, Han ZZ, Wang XB, Wang YF, Liu G, Xie Y, Zhu NX (2019) Thermal effect of different laying modes on cross-linked polyethylene (XLPE) insulation and a new estimation on cable ampacity. *Energies* 12(15):2994
34. Orton H (2015) Power cable technology review. *High Volt Eng* 41:1057–1067
35. Shwehdi MH, Morsy MA, Abugurain A (2003) Thermal aging tests on XLPE and PVC cable insulation materials of Saudi Arabia. In: *Proceedings of the IEEE conference on electrical insulation and dielectric phenomena, Albuquerque, NM, USA, 19 November 2003*, pp 176–180
36. Liu X, Yu Q, Liu M, Li Y, Zhong L, Fu M (2017) DC electrical breakdown dependence on the radial position of specimens within HVDC XLPE cable insulation. *IEEE Trans Dielectr Electr Insul* 24:1476–1486
37. Ouyang B, Li H, Li J (2017) The role of micro-structure changes on space charge distribution of XLPE during thermo-oxidative ageing. *IEEE Trans Dielectr Electr Insul* 24:3849–3859
38. Diego JA, Belana J, Orrit J, Cañadas JC, Mudarra M, Frutos F, Acedo M (2011) Annealing effect on the conductivity of xlpe insulation in power cable. *IEEE Trans Dielectr Electr Insul* 18:1554–1561
39. Xie Y, Zhao Y, Liu G, Huang J, Li L (2019) Annealing effects on XLPE insulation of retired high-voltage cable. *IEEE Access*
40. Xie Y, Liu G, Zhao Y (2019) Rejuvenation of retired power cables by heat treatment. *IEEE Trans Dielectr Electr Insul* 26:668–670
41. Celina M, Gillen KT, Clough RL (1998) Inverse temperature and annealing phenomena during degradation of crosslinked polyolefins. *Polym Degrad Stab* 61:231–244
42. Kalkar AK, Deshpande AA (2010) Kinetics of isothermal and non-isothermal crystallization of poly (butylene terephthalate) liquid crystalline polymer blends. *Polym Eng Sci* 41:1597–1615
43. Wang Y, Shen C, Li H, Qian L, Chen J (2010) Nonisothermal melt crystallization kinetics of poly (ethylene terephthalate)/clay nanocomposites. *J Appl Polym Sci* 91:308–314
44. Xie AS, Zheng XQ, Li ST, Chen G (2010) The conduction characteristics of electrical trees in XLPE cable insulation. *J Appl Polym Sci* 114:3325–3330
45. Xie A, Li S, Zheng X, Chen G (2009) The characteristics of electrical trees in the inner and outer layers of different voltage rating XLPE cable insulation. *J Phys D Appl Phys* 42:125106–125115
46. Insulated Conductors Committee of the IEEE Power Engineering Society (1981) *IEEE GUIDE for soil thermal resistivity measurements. IEEE Std 442, Reaffirmed 2003. IEEE, Piscataway, NJ, USA*
47. Malatray M, Roux J-P, Gunst S, Pibarot V, Wegrzyn J (2017) Highly crosslinked polyethylene: a safe alternative to conventional polyethylene for dual mobility cup mobile component. A biomechanical validation. *Int Orthop* 41(3):507–512
48. Lambert B, Neut D, van der Veen HC, Bulstra SK (2019) Effects of vitamin E incorporation in polyethylene on oxidative degradation, wear rates, immune response, and infections in total joint arthroplasty: a review of the current literature. *Int Orthop* 43(7):1549–1557
49. Massin P, Achour S (2017) Wear products of total hip arthroplasty: the case of polyethylene. *Morphologie* 101(332):1–8
50. Leclercq S, Benoit JY, de Rosa JP, Tallier E, Leteurtre C, Girardin P (2013) Evora® chromium-cobalt dual mobility socket: results at a minimum 10 years' follow up. *Orthop Traumatol Surg Res* 99:923–928

51. Paxton EW, Inacio MCS, Namba RS, Love R, Kurtz SM (2015) Metal-on-conventional polyethylene total hip arthroplasty bearing surfaces have a higher risk of revision than metal-on-highly crosslinked polyethylene: results from a US registry. *Clin Orthop Relat Res* 473:1011–1021
52. Glyn-Jones S, Thomas GE, Garfjeld-Roberts P, Gundle R, Taylor A, McLardy-Smith P, Murray DW (2015) The John Charnley Award: highly crosslinked polyethylene in total hip arthroplasty decreases long-term wear: a double-blind randomized trial. *Clin Orthop Relat Res* 473:432–438
53. Sobieraj MC, Rimnac CM (2009) Ultra high molecular weight polyethylene: mechanics, morphology, and clinical behavior. *J Mech Behav Biomed Mater* 2:433–443
54. Gencur SJ, Rimnac CM, Kurtz SM (2006) Fatigue crack propagation resistance of virgin and highly crosslinked, thermally treated ultra-high molecular weight polyethylene. *Biomaterials* 27:1550–1557
55. Pruitt LA (2005) Deformation, yielding, fracture and fatigue behavior of conventional and highly cross-linked ultra high molecular weight polyethylene. *Biomaterials* 26:905–915
56. Sirimamilla A, Furmanski J, Rimnac C (2013) Peak stress intensity factor governs crack propagation velocity in crosslinked ultra-high-molecular-weight polyethylene. *J Biomed Mater Res B Appl Biomater* 101:430–435
57. Baker DA, Bellare A, Pruitt L (2003) The effects of degree of crosslinking on the fatigue crack initiation and propagation resistance of orthopedic-grade polyethylene. *J Biomed Mater Res A* 66:146–154
58. Medel FJ, Peña P, Cegoñino J, Gómez-Barrena E, Puértolas JA (2007) Comparative fatigue behavior and toughness of remelted and annealed highly crosslinked polyethylenes. *J Biomed Mater Res B Appl Biomater* 83:380–390
59. Ast MP, John TK, Labbisiere A, Robador N, Valle AG (2014) Fractures of a single design of highly cross-linked polyethylene acetabular liners: an analysis of voluntary reports to the United States food and drug administration. *J Arthroplasty* 29:1231–1235
60. Furmanski J, Kraay MJ, Rimnac C (2011) Crack initiation in retrieved cross-linked highly cross-linked ultrahigh-molecular-weight polyethylene acetabular liners. an investigation of 9 cases. *J Arthroplasty* 26:796–801
61. Birman MV, Noble PC, Conditt MA, Li S, Mathis KB (2005) Cracking and impingement in ultra-high-molecular-weight polyethylene acetabular liners. *J Arthroplasty* 20:87–92
62. Kurtz SM, Austin MS, Azzam K, Sharkey PF, MacDonald DW, Medel FJ, Hozack WJ (2010) Mechanical properties, oxidation, and clinical performance of retrieved highly cross-linked crossfire liners after intermediate-term implantation. *J Arthroplasty* 25:614–623
63. Kurtz SM, Manley M, Wang A, Taylor S, Dumbleton J (2002–2003) Comparison of the properties of annealed crosslinked (Crossfire) and conventional polyethylene as hip bearing materials. *Bull Hosp Jt Dis* 61:17–26
64. MacDonald D, Sakona A, Ianuzzi A, Rimnac CM, Kurtz SM (2011) Do first-generation highly crosslinked polyethylenes oxidize in vivo? *Clin Orthop Relat Res* 469:2278–2285
65. Muratoglu OK, Oral E (2011) Vitamin E diffused, highly crosslinked UHMWPE: a review. *Int Orthop* 35:215–223
66. Cornelia V, Seymour RB (1993) *Handbook of polyolefin's*. Marcel Dekker, New York
67. Gowariker VR, Viswanathan NV, Sreedhar J (1993) *Polymer science*, 7th ed. New Delhi Publisher, Bangalore
68. Ulrich H (1993) *Introduction to industrial polymer*, 2nd ed. Hanser, Munich
69. Brydson J (1999) *Plastics material*. 7th ed. ButterworthHeinemann, Oxford
70. Mori T (1998) Process For producing silane crosslinked polyolefin. U.S. Patent 5,756,582
71. Mori T (2000) Process for producing flame-retardant, silane crosslinked polyolefin. U.S. Patent 6,107,413
72. Shieh Y-T, Tsai T-H (1998) Silane grafting reactions of low density polyethylene. *J Appl Polym Sci* 69:255–261
73. Shieh Y-T, Liu C-M (1999) Silane grafting reactions of LDPE, HDPE and LLDPE. *J Appl Polym Sci* 4:3404–3411

74. Shieh Y-T, Hsiao K-I (1998) Thermal properties of silane grafted water-crosslinked polyethylene. *J Appl Polym Sci* 70:1075–1082
75. Han SO, Lee DW, Han OH (1999) Thermal degradation of crosslinked high density polyethylene. *Polym Degrad Stab* 63:237–243
76. Shieh Y-T, Chuang H-C, Liu C-M (2001) Water crosslinking reactions of silane grafted polyolefin blends. *J Appl Polym Sci* 81:1799–1807
77. Shieh Y-T, Chuang H-C (2001) DSC and DMA studies on silane grafted and water crosslinked LDPE/LLDPE blends. *Journal of Applied Polymer Science* 81:1808–1816
78. Kumar S, Pandya MV (1997) Thermally recoverable crosslinked polyethylene. *J Appl Polym Sci* 64:823–829
79. Muñoz PMAP, Vargas MD, Werlang MM (2001) High density polyethylene modified by polydimethylsiloxane. *J Appl Polym Sci* 82:3460–3467
80. Kang T-K, Ha C-S (1999) Effect of processing variables on the crosslinking of HDPE by peroxide. *Polym Test* 19:773–783
81. McCormick JA, Royer JR, Hwang CR, Khan SA (2000) Tailored rheology of a metallocene polyolefin through silane grafting and subsequent silane crosslinking. *J Appl Polym Sci Part B Polym Phys* 38:2468–2479
82. Huang H, Lu H, Liu NC (2000) Influence of grating formulations and extrusion conditions on properties of silane-grafted polypropylenes. *J Appl Polym Sci* 78:1233–1238
83. Yamazaki T, Seguchi T (1997) ESR study on chemical crosslinking reaction mechanisms of polyethylene using a chemical agent. *J Appl Polym Sci Part Polym Chem* 35:279–284
84. Abraham D, George KE, Francis DJ (1998) Structure-property-processing relationships in chemically modified LDPE and LDPE/LLDPE blend. *J Appl Polym Sci* 67:789–797
85. Smedberg A, Hjertberg T, Gustafsson B (1997) Crosslinking reaction in an unsaturated low density polyethylene. *Polymer* 38(16):127–138
86. Miyashita Y, Kato H (1988) Crosslinking reaction of LDPE and the behavior of decomposition products from crosslinking agents. *IEEE Trans Dielectr Electr Insul* 259–262
87. Wang Z, Chan CM, Zhu SH, Shen J (1998) Compatibilization of polystyrene and low density polyethylene blends by two-step crosslinking process. 39:6801–6806
88. Krupa I, Luyt AS (2001) Mechanical properties of uncrosslinked and crosslinked linear low-density polyethylene/wax blends. *J Appl Polym Sci* 81:973–980
89. Bremner T, Rudin A (1993) Peroxide modification of linear low density polyethylene: a comparison of dialkyl peroxide. *J Appl Polym Sci* 49:785–798
90. Penfold et al (1998) Silane crosslinkable, substantially linear ethylene polymers and their uses. U.S. Patent 5,824,718
91. Sajkiewicz P, Phillips PJ (1995) Peroxide crosslinking of linear low-density polyethylene's with homogeneous distribution of short chain branching. *J Appl Polym Sci Part A Polym Chem* 33:853–862
92. Sajkiewicz P, Phillips PJ (1995) Changes in sol fraction during peroxide crosslinking of linear low-density polyethylenes with homogeneous distribution of short chain branching. *J Appl Polym Sci Part A Polym Chem* 33:949–955
93. Bremner T, Rudin A (1995) Effect of antioxidant on peroxide modification of LLDPE. *J Appl Polym Sci* 57:271–286
94. Lachtermacher MG, Rudin A (1998) Reactive processing of LLDPE in co rotating no intermeshing twin-screw extruder. III. Methods of peroxide addition. *J Appl Polym Sci* 59:1775–1785
95. Isac SK, George KE (2001) Reactive processing of polyethylene on a single screw extruder. *J Appl Polym Sci* 81:2545–2549
96. Yamaguchi M, Suzuki K-I (2001) Rheological properties of linear and crosslinked polymer blends: relation between crosslink density and enhancement of elongational viscosity. *J Appl Polym Sci Part B Polym Phys* 39:228–235
97. Nield SA, Tzoganakis C, Budman HM (2000) Chemical modification of low density polyethylene through reactive extrusion: Part I: process development and product characterization. *Adv Polym Technol* 19:237–248

98. Jeong H-G, Lee K-J (1999) Effect of discontinuous phase size on physical properties of LLDPE/PP blends obtained in the presence of peroxide. *J Adv Polym Technol* 18:43–51
99. Lachtermacher MG, Bremner, Rudin A (1995) Reactive processing of LLDPE in co rotating intermeshing twin-screw extruder. II. Effect of peroxide treatment on processability. *J Appl Polym Sci* 58:2433–2449
100. Rosales C, Perera R, Gonzalez J (1999) Grafting of polyethylene by reactive extrusion. II. Influence on rheological and thermal properties. *J Appl Polym Sci* 73:2549–2567
101. Narkis M, Raiter I, Shkolnik S, Eyerer P, Siegmann A (1987) Structure and tensile behavior of irradiation-crosslinked and peroxide-crosslinked polyethylene's. *J Macromol Sci* 26:37–58
102. Ribes-Greus A, Diaz-Calleja R Relationship between the mechanical relaxations in the zone and the calorimetric transitions in low density polyethylene. *J Appl Polym Sci* 34:2819–2828
103. Liu TM, Baker WE (1992) The effect of the length of the short chain branch on the impact properties of linear low density polyethylene. *Polym Eng Sci* 32:944–955
104. Tsui SW, Duckett RA, Ward IM (1992) Structure-property-processing relationships in chemically modified polyethylene. *J Mater Sci* 27:2799–2806
105. Krauss S, Metzger TH, Fratzl P, Harrington MJ (2013) Self-repair of a biological fiber guided by an ordered elastic framework. *Biomacromol* 14:1520–1528
106. Chen X, Dam MA, Ono K, Mal A, Shen H, Nutt SR, Sheran K, Wudl F (2002) A thermally re-mendable cross-linked polymeric material. *Science* 295:1698–1702
107. Liu Y, Hsieh C, Chen Y (2006) Thermally reversible cross-linked polyamides and thermo-responsive gels by means of Diels-Alder reaction. *Polymer* 47:2581–2586
108. Peterson AM, Jensen RE, Palmese GR (2010) Room-temperature healing of a thermosetting polymer using the Diels-Alder reaction. *ACS Appl Mater Interfaces* 2:1141–1149
109. Chen X, Wudl F, Mal AK, Shen H, Nutt SR (2003) New thermally remendable highly cross-linked polymeric materials. *Macromolecules* 36:1802–1807
110. Maeno Y, Hirai N, Ohki Y, Tanaka T, Okashita M, Maeno T (2005) Effects of crosslinking byproducts on space charge formation in crosslinked polyethylene. *IEEE Trans Dielectr Electr Insul* 12(1):90–97
111. Lau WS, Chen G (2006) Simultaneous space charge and conduction current measurements in solid dielectrics under high dc electric field. In: *Proceeding of 2008 international conference on condition monitoring and diagnosis*
112. Maeno T, Kushibe H, Takada T, Cooke CM (1985) Pulsed electro-acoustic method for the measurement of volume charges in E-beam irradiated PMMA. In: *Annual report, conference on electrical insulation and dielectric phenomena*
113. Malec D (2000) Technical problems encountered with the laser induced pressure pulse method in studies of high voltage cable insulators. *Meas Sci Technol* 11(5):N76–N80
114. Lee DC, Lee NH, Mizutani T, Ieda M (1988) Thermally stimulated current due to ionic carriers in polysulfone. In: *Proceeding of 2nd international conference on properties and applications of dielectric materials*, pp 363–366
115. Levy RA (1968) *Principles of solid state physics*, Academic Press. Lewiner J (1986) Evolution of experimental techniques for the study of the electrical properties of insulating materials. *IEEE Trans Dielectr Electr Insul* EI-21(3):351–360
116. Lewis TJ (1955) Some factors influencing field emission and fowler-nordheim law. *Proc Phys Soc Sect B* 68(11):938–943
117. Lewis TJ (2002) Polyethylene under electrical stress. *IEEE Trans Dielectr Electr Insul* 9(5):717–729
118. Li KC, Tang KC, Lee JS, Chao CL, Chang RK (1997) Thermal stimulated current study of core-shell impact modifier/PVC blends. *J Vinyl Add Tech* 3(1):17–20
119. Li Y, Takada T (1992) Experimental observation of charge transport and injection in XLPE at polarity reversal. *J Appl Phys D* 25:704–716
120. Li Y, Takada T (1994) Progress in space charge measurement of solid insulating materials in Japan. *IEEE Electr Insul Mag* 10(5):16–28
121. Li Y, Yasuda M, Takada T (1994) Pulsed electroacoustic method for measurement of charge accumulation in solid dielectrics. *IEEE Trans Dielectr Electr Insul* 1(2):188–195

122. Lim FN, Fleming RJ (1999) The temperature dependence of space charge accumulation and DC current in XLPE power cable insulation. In: Proceeding of annual report, conference on electrical insulation and dielectric phenomena, pp 66–69
123. Lim FN, Fleming RJ, Naybour RD (1999) Space charge accumulation in power cable XLPE insulation. *IEEE Trans Dielectr Electr Insul* 6(3):273–281
124. Molinié P (2005) Measuring and modeling transient insulator response to charging: the contribution of surface potential studies. *IEEE Trans Dielectr Electr Insul* 12(5):939–950
125. Montanari GC, Laurent C, Teyssedre G, Campus A, Nilsson UH (2005) From LDPE to XLPE: investigating the change of electrical properties. Part I: space charge, conduction and lifetime. *IEEE Trans Dielectr Electr Insul* 12(3):438–444
126. Long W, Nilsson S (2007) HVDC transmission: yesterday and today. *IEEE Power Energ Mag* 5(2):22–31
127. Liu R, Takada T, Takasu N (1993) Pulsed electroacoustic method for measurement of space charge distribution in power cables under both Dc and Ac electric field. *J Phys D Appl Phys* 26:986–993
128. Liu Z, Liu R, Wang H, Liu W (1989) Space charges and initiation of electrical trees. *IEEE Trans Dielectr Electr Insul* 24(1):83–90
129. Maeno T, Futami T, Kushibe H, Takada T, Cooke CM (1988) Measurement of spatial charge distribution in thick dielectrics using the pulsed electroacoustic method. *IEEE Trans Dielectr Electr Insul* 23(3):433–439
130. Many A, Rakavy G (1962) Theory of transient space-charge-limited currents in solids in the presence of trapping. *Phys Rev* 126(6):1980–1988
131. Maruyama S, Ishii N, Shimada M, Kojima S, Tanaka H, Asano M, Yamanaka T, Kawakami S (2004) Development of a 500 kV DC XLPE cable system. *Furukawa Rev* 25:47–52
132. Mellinger A, Singh R, Gerhard-Multhaupt R (2005) Fast thermal-pulse measurements of space charge distributions in electret polymers. *Rev Sci Instrum* 76:013903
133. Meunier M, Quirke N, Aslanides A (2001) Molecular modelling of electron traps in polymer insulators: Chemical defects and impurities. *J Chem Phys* 115(6):2876–2881
134. Migliori A, Hofler T (1982) Use of laser-generated acoustic pulses to measure the electric field inside a solid dielectric. *Rev Sci Instrum* 53(5):662–666
135. Mizutani T (1994) Space charge measurement techniques and space charge in polyethylene. *IEEE Trans Dielectr Electr Insul* 1(5):923–933
136. Montanari GC, Mazzanti G, Palmieri F, Motori A, Perego G, Serra S (2001) Space-charge trapping and conduction in LDPE, HDPE and XLPE. *J Appl Phys D* 34:2902–2911
137. Murooka Y, Takada T, Hidaka K (2001) Nanosecond surface discharge and charge density evaluation Part I: review and experiments. *IEEE Electr Insul Mag* 17(2):6–16
138. Neagu ER, Dias CJ (2009) Charge injection/extraction at a metal-dielectric interface: experimental validation. *IEEE Electr Insul Mag* 25(1):15–22
139. Montanari GC, Mazzanti G, Palmieri F, Perego G, Serra S (2001) Dependence of space-charge trapping threshold on temperature in polymeric DC cables. In: Proceeding of the international conference on solid dielectrics, pp 81–84
140. Morse PM, Ingrad KU (1968) *Theoretical acoustic*. McGraw-Hill Book Company, New York.
141. Morshuis PHF, Jeroense M (1997) Space charge measurements on impregnated paper: a review of the PEA method and a discussion of the results. *IEEE Electr Insul Mag* 13(3):26–35
142. Muronaka T, Tanaka Y, Takada T, Maruyama S, Mutou H (1996) Measurement of space charge distribution in XLPE using PEA system with flat electrode. In: Proceeding of annual report, conference on electrical insulation and dielectric phenomena, pp 266–269
143. Notingher Jr P, Agnel S, Toureille A (2001) Thermal step method for space 188 charge measurements under applied dc field. *IEEE Trans Dielectr Electr Insul* 8(6):985–994
144. Orton HE, Hartlein R (2006) *Long-life XLPE-insulated power cables*. Pascoe KJ (1973) *Properties of materials for electrical engineers*. Wiley. Pollock DD (1993) *Physical properties of materials for engineers*. CRC Press
144. Precopio F, Gilbert A (1999) The invention of chemically crosslinked polyethylene. *IEEE Electr Insul Mag* 15(1):23–25. Roland C (1979) *Physics of dielectrics for the engineer*. Elsevier Scientific Publishing Company

145. Serra S, Tosatti E, Iarlari S, Scandolo S, Santoro G, Albertini M (1998) Interchain states and the negative electron affinity of polyethylene. In: Annual report, conference on electrical insulation and dielectric phenomena, pp 19–22
146. Sessler GM (1982) Nondestructive laser method for measuring charge profiles in irradiated polymer films. *IEEE Trans Nucl Sci NS-29*:1644–1649
147. Sessler GM (1997) Charge distribution and transport in polymers. *IEEE Trans Dielectr Electr Insul* 4(5):614–628
148. Roy S Le, Segur P, Teyssedre G, Laurent C (2003) Description of bipolar charge transport in polyethylene using a fluid model with a constant mobility: model prediction. *J Appl Phys D* 37:298–305
149. Rudervall R, Charpentier J, Sharma R (2000) High voltage direct current (HVDC) transmission systems technology review paper. In *Energy Week*, Washington, D.C., USA
150. Sanden B, Ildstad E, Hegergerg R (1996) Space charge accumulation and conduction current in XLPE insulation. In: Conference on dielectric materials, measurements and applications, pp 368–373
151. See A, Dissado LA, Fothergill JC (2001) Electric field criteria for charge packet formation and movement in XLPE. *IEEE Trans Dielectr Electr Insul* 8(6):859–866
152. Carstensen P, Farkas AA, Campus A, Nilsson UH (2005) The effect of the thermal history on the space charge accumulation in HVDC crosslinked polyethylene cables. In: Annual report, conference on electrical insulation and dielectric phenomena, pp 381–388
153. Sekii Y, Ohbayashi T, Uchimura T, Mochizuki K, Maeno T (2002) The effects of material properties and inclusions on the space charge profiles of LDPE and XLPE. In: Annual report, conference on electrical insulation and dielectric phenomena, pp 635–639
154. Boggs S, Damon D, Hjerrild J, Holbol J, Henriksen M (2001) Effect of insulation properties on the field grading of solid dielectric DC cable. *IEEE Trans Power Deliv* 16(4):456–461
155. Sessler GM, West JE, Gerhard R (1982) High-resolution laser-pulse method for measuring charge distribution in dielectrics. *Phys Rev Lett* 48:563–566
156. Chen G, Chong YL, Fu M (2006) Calibration of the pulsed electroacoustic technique in the presence of trapped charge. *Meas Sci Technol* 17:1974–1980
157. Sessler GM, West JE, Gerhard R (1981) Measurement of charge distribution in polymer electrets by a new pressure-pulse method. *Polym Bull* 6(1–2):109–111
158. Chen G, Fu M, Liu XZ, Zhong LS (2005) AC aging and space-charge characteristics in low-density polyethylene polymeric insulation. *J Appl Phys* 97:083713
159. Solymar L, Walsh D (1999) Electrical properties of materials. Oxford University Press
160. Suh KS, Hwang SJ, Noh JS, Takada T (1994) Effects of constituents of XLPE on the formation of space charge. *IEEE Trans Dielectr Electr Insul* 1(6):1077–1083
161. Chen G, Tanaka Y, Takada T, Zhong L (2004) Effect of polyethylene interface on space charge formation. *IEEE Trans Dielectr Electr Insul* 11(1):113–121
162. Sze SM (1981) Physics of semiconductor devices. Wiley
163. Takada T (1999) Acoustic and optical methods for measuring electric charge distributions in dielectrics. *IEEE Trans Dielectr Electr Insul* 6(5):519–547
164. Abou-Dakka M, Bulinski AT, Bamji SS (2006) Space charge evolution in XLPE with long-term aging under DC Voltage—the effect of temperature and polarity reversals. In: Annual report, conference on electrical insulation and dielectric phenomena
165. Boukezzi L, Boubakeur A, Lallouani M (2007) Effect of artificial thermal aging on the crystallinity of XLPE insulation cables: X-ray study. In: Annual report, conference on electrical insulation and dielectric phenomena
166. Choo W, Chen G (2008) Electric field determination in DC polymeric power cable in the presence of space charge and temperature gradient under dc conditions. In: Proceeding of 2008 international conference on condition monitoring and diagnosis, pp 321–324
167. Burns N, Eichhorn R, Reid C (1992) Stress controlling semiconductive shields in medium voltage power distribution cables. *IEEE Electr Insul Mag* 8(5):8–24
168. Chong YL, Chen G, Hosier IL, Vaughan AS, Ho YFF (2005) Heat treatment of cross-linked polyethylene and its effect on morphology and space charge evolution. *IEEE Trans Dielectr Electr Insul* 12(6):1209–1221

169. Dissado LA, Fothergill JH (1992) Electrical degradation and breakdown in polymers. Peter Peregrinus Ltd, London, United Kingdom
170. Christen T (2004) A simple model for DC-conduction and space-charge formation in insulation material. In: Proceeding of the international conference on solid dielectrics, pp 513–516
171. Delpino S, Fabiani D, Montanari GC, Dissado LA, Laurent C, Teyssedre G (2007) Fast charge packet dynamics in XLPE insulated cable models. In: Annual report, conference on electrical insulation and dielectric phenomena, pp 421–424
172. Donald B et al (1978) Standard handbook for electrical engineers, 11th ed. McGraw Hill
173. Fabiani F, Montanari GC, Bodega R, Morshuis PHF, Laurent C, Dissado LA (2006) The effect of temperature gradient on space charge and electric field distribution of HVDC cable models. In: Proceeding of 8th international conference on properties and applications of dielectric materials, pp 65–68
174. Agnel S, Toureille A (1997) Two complementary techniques: the thermal step technique and the thermally stimulated currents technique. Study of polycrystalline Al_2O_3 . In: Annual report, conference on electrical insulation and dielectric phenomena
175. Ahmed NH, Srinivas NN (1997) Review of space charge measurements in dielectrics. *IEEE Trans Dielectr Electr Insul* 4(5):644–656
176. Bambery KR, Fleming RJ (1998) Space charge accumulation in two power cable grades of XLPE. *IEEE Trans Dielectr Electr Insul* 5(1):103–109
177. Bambery KR, Fleming RJ, Holböhl JT (2001) Space charge profiles in low density polyethylene samples containing permittivity/conductivity gradient. *J Appl Phys D* 34(20):3071–3077
178. Ando N, Numajiri F (1979) Experimental investigation of space charge in XLPE cable using dust figures. *IEEE Trans Dielectr Electr Insul* 14(1):36–42
179. Andrews T, Hampton RN, Smedberg A, Wald D, Waschk V, Weissenberg W (2006) The role of degassing in XLPE cable manufacture. *IEEE Electr Insul Mag* 22(6):5–16
180. Bahrman MP, Johnson BK (2007) The ABC of HVDC transmission technologies. *IEEE Power Energ Mag* 5(2):32–44
181. Bamji SS, Bulinski AT (1995) An optical technique for in situ measurement of the concentration of the crosslinking by products in XLPE cables. *JICABLE* 95:158–161
182. Bartnkias R, Eichhorn RM (1983) Engineering dielectrics, volume IIA electrical properties of solid insulating materials: molecular structure and electrical behavior. American Society for Testing and Materials
183. Beltzer AI (1988) Acoustic of solids. Springer, Berlin Heidelberg
184. Blaise G (1995) Space-charge physics and the breakdown process. *J Appl Phys* 77:2916–2927
185. Blythe AR, Bloor D (2005) Electrical properties of polymers, 2nd ed. Cambridge University Press
186. Fabiani F, Montanari GC, Laurent C, Teyssedre G, Morshuis PHF, Bodega R, Dissado LA, Campus A, Nilsson UH (2007) Polymeric HVDC cable design and space charge accumulation. Part 1: Insulation/semicon interface. *IEEE Electr Insul Mag* 23(6):11–19
187. Fleming RJ (2005) Space charge profiles measurement techniques: recent advances and future directions. *IEEE Trans Dielectr Electr Insul* 12(5):967–978
188. Fothergill JC, Montanari GC, Stevens GC, Laurent C, Teyssedre G, Dissado LA, Nilsson UH, Platbrood G (2003) Electrical, microstructural, physical and chemical characterization of HV XLPE cable peelings for an electrical aging diagnostic data base. *IEEE Trans Dielectr Electr Insul* 10(3):514–527
189. Frutos F, Acedo M, Mudarra M, Belana J, Òrrit J, Diego JA, Cañadas JC, Sellarès J (2007) Effect of annealing on conductivity in XLPE mid-voltage cable insulation. *J Electrostat* 65(2):122–131
190. Fu M, Chen G, Davies AE, Head JG (2000) Space charge measurements in power cables using a modified PEA system. In: Proceeding of 8th international conference on dielectric materials, measurements and applications, pp 74–79
191. Fukunaga K, Miyata H, Takahaashi T, Yoshida S, Niwa T (1991) Measurement of space charge distribution in cable insulation using the pulsed electroacoustic method. In: Proceeding of 3rd international conference on polymeric insulated power cables (JICABLE 1991), pp 520–525

192. Gallot-lavallee O, Teysedre G (2004) Space charge measurement in solid dielectrics by pulsed electro-acoustic technique. In: Proceeding of 2004 IEEE international conference solid dielectrics, pp 268–271
193. Hanley TL, Burford RP, Fleming RJ, Barber KW (2003) A general review of polymeric insulation for use in HVDC cables. *IEEE Electr Insul Mag* 19(1):13–24
194. Garton A, Groeger JH, Henry JL (1990) Ionic impurities in crosslinked polyethylene cable insulation. *IEEE Trans Electr Insul* 25(2):427–434
195. Goshowaki M, Endoh I, Noguchi K, Kawabe U, Sekii Y (2007) Influence of antioxidants on electrical conduction in LDPE and XLPE. *J Electrostat* 65(9):551–554
196. Kao KC, Hwang W (1981) *Electrical transport in solids*. Pergamon Press
197. Hampton N (1995) Insulations for polymeric supertension cables. In: Proceeding of IEE two day colloquium supertension, pp 511–515
198. Kawasaki K, Arai Y, Takada T (1991) Two-dimensional measurement of electrical surface charge distribution on insulating material by electrooptic pockels effect. *Jpn J Appl Phys* 30(6):1262–1265
199. Kon H, Mizutani T, Suzuoki Y, Shigetsugu H (1994) High-field conduction and space charge in polyethylene. In: Proceeding of annual report, conference on electrical insulation and dielectric phenomena, pp 268–273
200. Ho YFF, Chen G, Davies AE, Swingler SG, Sutton SJ, Hampton RN (2003) Effect of semi-conducting screen on the space charge dynamic in XLPE and Polyolefin Insulation under dc and 50 Hz AC electric stresses conditions. *IEEE Trans Dielectr Electr Insul* 10(3):393–403
201. Salah Khalil M (1997) International research and development trends and problems of HVDC cables with polymeric insulation. *IEEE Electr Insul Mag* 13(6):35–47
202. Khalil MS, Jevase JA (2000) Development of polymeric insulating materials for HVDC using additives: evidence from a multitude of experiments using different techniques. In: IEEE international symposium on electrical insulation, pp 485–488
203. Holbøll JT, Henriksen M, Hjerrild J (2000) Space charge build-up in XLPE cable with temperature gradient. In: Annual report, conference on electrical insulation and dielectric phenomena, pp 157–160
204. Holé S, Ditchi T, Lewiner J (2003) Non-destructive methods for space charge distribution measurements: what are the differences? *IEEE Trans Dielectr Electr Insul* 10(4):670–677
205. Jones JP, Llewellyn JP, Lewis TJ (2005) The contribution of field-induced morphological change to the electrical aging and breakdown of polyethylene. *IEEE Trans Dielectr Electr Insul* 12(5):951–966
206. Khalil MS, Hansen BS (1988) Investigation of space charge in low-density polyethylene using a field probe technique. *IEEE Trans Dielectr Electr Insul* 23(3):441–445
207. Lalam F, Hoang (2000) Pressure effect on the electrical ageing of polyethylene. *J Appl Phys D* 33:L133–L136
208. Lang SB, Das-Gupta DK (1981) A technique for determination the 186 polarization distribution in thin polymer electrets using periodic heating. *Ferroelectrics* 39(1):1249–1252
209. Hozumi N, Takeda T, Suzuki H, Okamoto T (1998) Space charge behavior in XLPE under 0.2–1.2 MV/cm DC fields. *IEEE Trans Dielectr Electr Insul* 5(1):82–90
210. Takada T, Hozumi N (2000) Space charge measurements as a diagnostic tool 189 for power cables. *IEEE Power Eng Soc Winter Meet* 3:1609–1614
211. Hozumi N, Okamoto T, Imajo T (1992) Space charge distribution measurement in a long size XLPE cable using the pulse electroacoustic method. In: IEEE international symposium on electrical insulation, pp 294–297
212. Ishikawa I, Nakamura S, Utsunomiya S, Yamamoto S, Niwa T (1994) The research of peroxide decomposition in XLPE cables. In: Annual report, conference on electrical insulation and dielectric phenomena
213. Takada T, Sakai T (1983) Measurement of electric fields at a dielectric/electrode interface using an acoustic transducer technique. *IEEE Trans Dielectr Electr Insul* EI-18(6):619–628
214. Takeda T, Hozumi N, Suzuki H, Fujii K, Terashima K, Hara M, Murata Y, Watanabe K, Yoshida M (1998) Space charge behavior in full-size 250 kV DC XLPE cables. *IEEE Trans Power Deliv* 13(1):28–39

215. Fu M, Chen G, Dissado LA, Fothergill JC (2007) Influence of thermal treatment and residues on space charge accumulation in XLPE for DC power cable application. *IEEE Trans Dielectr Electr Insul* 14(1):53–64
216. Tanaka T, Greenwood A (1983) *Advanced power cable technology*, vol I. CRC Press Inc, USA
217. Fu M, Dissado LA, Chen G, Fothergill JC (2008) Space charge formation and its modified electric field under applied voltage reversal and temperature gradient in XLPE cable. *IEEE Trans Dielectr Electr Insul* 15(3):851–860
218. Wang X, Tu D, Tanaka Y, Muronaka T, Takada T, Shinoda C, Hashizumi T (1995) Space charge in XLPE power cable under dc electrical stress and heat treatment. *IEEE Trans Dielectr Electr Insul* 2(3):467–474
219. Tanaka T, Greenwood A (1983) *Advanced power cable technology*, vol II. CRC Press Inc, USA
220. Fukunaga K, Miyata H, Sugimori M, Takada T (1990) Measurement of charge distribution in the insulation of cables using pulsed electroacoustic method. *IEE Trans Japan* 110-A(9):647–648
221. Yamanaka T, Maruyama S, Tanaka T (2003) The development of DC ± 500 kV XLPE cable in consideration of the space charge accumulation. In: *Proceeding of 7th international conference on properties and applications of dielectric materials*, pp 689–694
222. Zhang Y, Lewiner J, Alquie C, Hampton N (1996) Evidence of strong correlation between space-charge buildup and breakdown in cable insulation. *IEEE Trans Dielectr Electr Insul* 3(6):778–783
223. Tanaka Y, Chen G, Zhao Y, Davies AE, Vaughan AS, Takada T (2003) Effect of additives on morphology and space charge accumulation in low density polyethylene. *IEEE Trans Dielectr Electr Insul* 10(1):148–154
224. Fu M, Chen G, Davies AE, Head J (2001) Space charge measurements in cables using the PEA method: signal data processing considerations. In: *Proceedings of the international conference on solid dielectrics*, pp 219–222
225. Weedy BM (1980) *Underground transmission of electric power*. Wiley
226. Fukuda F, Irie S, Asada Y, Maeda M, Nakagawa H, Yamada N (2002) The effect of morphology on the impulse voltage breakdown in XLPE cable insulation. *IEEE Trans Dielectr Electr Insul* 17(5):386–391
227. Weedy BM, Chu D (1984) HVDC extruded cables, parameters for determination of stresses. *IEEE Trans Power Apparatus Syst Insul PAS-103*(3):662–667
228. Tanaka Y, Takada T, Shinoda C, Hashizume T (1994) Temperature dependence of space charge distribution in XLPE cable. In: *Annual report, conference on electrical insulation and dielectric phenomena*
229. Wu X, Chen G, Davies AE, Hampton RN, Sutton SJ, Swingler SG (2001) Space charge measurements in polymeric HV insulation materials. *IEEE Trans Dielectr Electr Insul* 8(4):725–730
230. Xu Z, Choo W, Chen G (2007) DC electric field distribution in planar dielectric in the presence of space charge. In: *Proceedings of the international conference on solid dielectrics*, pp 514–517
231. <https://www.forencisresearch.com/pex-xlpe-market/>. Accessed on 9th October 2020
232. <https://www.wfmj.com/story/42550981/cross-linked-polyethylene-foam-xlpe-market-size-2020-to-2026-share-emerging-trends-demand-revenue-and-forecasts-research>. Accessed on 9th October 2020
233. <https://www.grandviewresearch.com/industry-analysis/cross-linked-polyethylene-pex-market>. Accessed on 9th October 2020
234. <https://www.mordorintelligence.com/industry-reports/cross-linked-polyethylene-xlpe-market>. Accessed on 9th October 2020
235. Han J, Garrett R (2008) Overview of polymer nanocomposites as dielectrics and electrical insulation materials for large high voltage rotating machines. *NSTI-Nanotech* 2:727–732

236. Matthews FL, Rawlings RD (1999) *Composite materials: engineering and science*, 2nd ed. CRC Press, Woodhead Publishing Limited, Cambridge, UK, Overview, pp 1–28
237. Camargo PHC, Satyanarayana KG, Wypych F (2009) Nanocomposites: Synthesis, structure, properties and new application opportunities. *Mater Res* 12:1–39
238. Nelson JK (2007) Overview of nanodielectrics: insulating materials of the future. In: *Proceedings of the electrical insulation conference and electrical manufacturing expo*, Nashville, TN, USA, 22–24 October 2007, pp 229–235
239. Sheer ML (1991) Advanced composites: the leading edge in high performance motor and transformer insulation. In: *Proceedings of the 20th electrical electronics insulation conference*, Boston, MA, USA, 7–10 October 1991, pp 181–185
240. Stone GC, Boulter EA, Culbert I, Dhirani H (2004) Historical development of insulation materials and systems. In: Kartalopoulos SV (ed) *Electrical insulation for rotating machines—design, evaluation, aging, testing, and repair*, 1st edn. Wiley-IEEE Press, Piscataway, NJ, USA, pp 73–94
241. Pyrhönen J, Jokinen T, Hrabovcová V (2014) *Design of rotating electrical machines*, 2nd ed. Wiley, West Sussex, UK. Insulation of electrical machines, pp 429–455
242. Park JJ (2012) AC electrical breakdown characteristics of an epoxy/mica composite. *Trans Electr Electron Mater* 13:200–203
243. Lenko D, Schlögl S, Bichler S, Lemesch G, Ramsauer F, Ladstätter W, Kern W (2015) Flexible epoxy-silicone rubber laminates for high voltage insulations with enhanced delamination resistance. *Polym Compos* 36:2238–2247
244. Schlögl S, Lenko D (2015) High voltage insulations with enhanced delamination resistance. *Rubber Fibres Plast Int* 10:260–261
245. Kojima Y, Usuki A, Kawasumi M, Okada A, Kurauchi T, Kagimoto O (1993) One-pot synthesis of nylon 6-clay hybrid. *J Polym Sci Pt A* 31:1755–1758. <https://doi.org/10.1002/pola.1993.080310714>
246. Lewis TJ (1994) Nanometric dielectrics. *IEEE Trans Dielectr Electr Insul* 1:812–825. <https://doi.org/10.1109/94.326653>
247. Frechette MF, Trudeau M, Alamdari HD, Boily S (2001) Introductory remarks on nanodielectrics. In: *Conference on electrical insulation and dielectric phenomena, 2001 annual report*, Kitchener, ON, Canada, 14–17 October 2001, pp 92–99
248. Cao Y, Irwin PC, Younsi K (2004) The future of nanodielectrics in the electrical power industry. *IEEE Trans Dielectr Electr Insul* 11:797–807
249. Johnston DR, Markovitz M (1998) Corona-resistant insulation, electrical conductors covered therewith and dynamoelectric machines and transformers incorporating components of such insulated conductors. 4760296 A. US Patent, 26 July 1998
250. Henk PO, Kortsen TW, Kvarts T (1999) Increasing the electrical discharge endurance of acid anhydride cured DGEBA epoxy resin by dispersion of nanoparticle silica. *High Perform Polym* 11:281–296. <https://doi.org/10.1088/0954-0083/11/3/304>
251. Fothergill JC, Dissado LA, Nelson JK (2002) Nanocomposite materials for dielectric structures. EPSRC, Swindon, UK, pp 1–6
252. Nelson JK, Fothergill JC (2004) Internal charge behaviour in nanocomposites. *Nanotechnology* 15:586–595. <https://doi.org/10.1088/0957-4484/15/5/032>
253. Pallon LKH, Hoang AT, Pourrahimi AM, Hedenqvist MS, Nilsson F, Gubanski S, Gedde UW, Olsson RT (2016) The impact of MgO nanoparticle interface in ultra-insulating polyethylene nanocomposites for high voltage DC cables. *J Mater Chem A* 4:8590–8601
254. Kango S, Kalia S, Celli A, Njuguna J, Habibi Y, Kumar R (2013) Surface modification of inorganic nanoparticles for development of organic–inorganic nanocomposites—a review. *Prog Polym Sci* 38:1232–1261
255. Shokoohi S, Arefazar A, Khosrokhavar R (2008) Silane coupling agents in polymer-based reinforced composites: a review. *J Reinf Plast Compos* 27:473–485
256. Rong MZ, Zhang MQ, Ruan WH (2006) Surface modification of nanoscale fillers for improving properties of polymer nanocomposites: a review. *Mater Sci Technol* 22:787–796

257. Tasdelen MA (2011) Diels-Alder “click” reactions: recent applications in polymer and material science. *Polym Chem* 2:2133–2145
258. Neouze MA, Schubert U (2008) Surface modification and functionalization of metal and metal oxide nanoparticles by organic ligands. *Chem Monthly* 139:183–195
259. Roy M, Nelson JK, Schadler LS, Zou C, Fothergill JC (2005) The influence of physical and chemical linkage on the properties of nanocomposites. In: Proceedings of the annual report conference on electrical insulation and dielectric phenomena (CEIDP), Nashville, TN, USA, 16–19 October 2005, pp 183–186
260. Reed CW (2007) Self-assembly of polymer nanocomposites for dielectrics and HV insulation. In: Proceedings of the IEEE international conference on solid dielectrics (ICSD), Winchester, UK, 8–13 July 2007, pp 397–400
261. Manias E, Touny A, Wu L, Strawhecker K, Lu B, Chung TC (2001) Polypropylene/montmorillonite nanocomposites. Review of the synthetic routes and materials properties. *Chem Mater* 13:3516–3523. <https://doi.org/10.1021/cm0110627>
262. Tronto J, Bordonal AC, Naal Z, Valim JB (2013) Chapter 1—conducting polymers/layered double hydroxides intercalated nanocomposites. In: Mastai Y (ed) Materials science—advanced topics. InTechOpen, London, UK, pp 3–31
263. Lutz B, Kindersberger J (2010) Influence of absorbed water on volume resistivity of epoxy resin insulators. In: Proceedings of the 10th IEEE international conference on solid dielectrics (ICSD), Potsdam, Germany, 4–9 July 2010, pp 1–4
264. Smith RC, Liang C, Landry M, Nelson JK, Schadler LS (2007) Studies to unravel some underlying mechanisms in nanodielectrics. In: Proceedings of the annual report conference on electrical insulation and dielectric phenomena (CEIDP), Vancouver, BC, Canada, 14–17 October 2007, pp 286–289
265. Patel RR, Gupta N (2008) Volume resistivity of epoxy containing nano-sized Al_2O_3 fillers. In: Proceedings of the fifteenth national power systems conference (NPSC), Bombay, India, 16–18 December 2008, pp 361–365
266. Mera G, Gallei M, Bernard S, Ionescu E (2015) Ceramic nanocomposites from tailor-made preceramic polymers. *Nanomaterials* 5:468–540. <https://doi.org/10.3390/nano5020468>
267. Orton H (2015) Power cable technology review. *High Voltage Eng* 41:1057
268. Tan D, Irwin P (2011) Polymer based nanodielectric composites. In: Advances in ceramics—electric and magnetic ceramics, bioceramics, ceramics and environment. InTechOpen
269. Verweij J, Klootwijk J (1996) Dielectric breakdown I: a review of oxide breakdown. *Microelectron J* 27:611
270. Li S, Yin G, Chen G, Li J, Bai S, Zhong L, Zhang Y, Lei Q (2010) Short-term breakdown and long-term failure in nanodielectrics: a review. *IEEE Trans Dielectr Electr Insul* 17:1523
271. Roy M, Nelson JK, MacCrone R, Schadler L (2007) Candidate mechanisms controlling the electrical characteristics of silica/XLPE nanodielectrics. *J Mater Sci* 42:3789
272. Pitsa D, Danikas MG (2011) Interfaces features in polymer nanocomposites: a review of proposed models. *NANO* 6:497
273. Ashish Sharad P, Kumar KS (2017) Application of surface-modified XLPE nanocomposites for electrical insulation-partial discharge and morphological study. *Nanocomposites* 3:30
274. Worzyk T (2009) Submarine power cables: design, installation, repair, environmental aspects. Springer Science & Business Media
275. Chen G, Hao M, Xu Z, Vaughan A, Cao J, Wang H (2015) Review of high voltage direct current cables. *CSEE J Power Energy Syst* 1:9
276. Mazzanti G, Marzinotto M (2013) Extruded cables for high-voltage direct-current transmission: advances in research and development. Wiley
277. Bahrman MP, Johnson BK The ABCs of HVDC transmission technologies. IEEE
278. Badr Y, Ali ZI, Zahran AH, Khafagy RM (2000) Characterization of gamma irradiated polyethylene films by DSC and X-ray diffraction techniques. *Polym Int* 49:1555
279. Tanabe Y, Strobl G, Fischer E (1986) Surface melting in melt-crystallized linear polyethylene. *Polymer* 27:1147

280. Yamanouchi S, Inoue Y, Kondo M (1990) Cross-linked polyethylene-insulated cable. U.S. Patent US4894284A
281. Porto KMB, Napolitano CM, Borrelly SI (2018) Gamma radiation effects in packaging for sterilization of health products and their constituents paper and plastic film. *Radiat Phys Chem* 142:23
282. Takahashi Y, Masaoka T, Pezzotti G, Shishido T, Tateiwa T, Kubo K, Yamamoto K (2014) Highly cross-linked polyethylene in total hip and knee replacement: spatial distribution of molecular orientation and shape recovery behavior. *BioMed Res Int*
283. Kim B, White JL (1997) Simulation of thermal degradation, peroxide induced degradation, and maleation of polypropylene in a modular co-rotating twin screw extruder. *Polym Eng Sci* 37:576
284. Beltraán M, Mijangos C (2000) Silane grafting and moisture crosslinking of polypropylene. *Polym Eng Sci* 40:1534
285. Avila SM, Horvath DA (2000) Microscopic void detection as a prelude to predicting remaining life in electric cable insulation. In: International topical meeting on nuclear plant instrumentation, controls, and human-machine interface technologies, NPIC&HMIT 2000, Washington, DC
286. Busse G, Eyerer P (1983) Thermal wave remote and nondestructive inspection of polymers. *Appl Phys Lett* 43:355
287. Meola C, Carlomagno GM, Prisco U, Vitiello A (2004) Nondestructive control of polyethylene blanket insulation by means of lock-in thermography. *J Nondestruct Eval* 15:55
288. Abbassi Souraki F, Morshedian J (2001) On the improvement of physical and mechanical properties of PE by crosslinking. *Polym Sci Technol* 14:95
289. Morshedian J, Hoseinpour PM (2009) Polyethylene cross-linking by two-step silane method: a review. *Iran Polym J* 18:103
290. Rodríguez-Fernández O, Gilbert M (2011) Aminosilane grafting of plasticized poly (vinyl chloride) I. Extent and rate of crosslinking. *J Appl Polym Sci* 66:2111
291. Weedy B, Chu D (1984) HVDC extruded cables-parameters for determination of stress. *IEEE Power Eng Rev PER-4:43*
292. Terashima K, Sukuki H, Hara M, Watanabe K (1998) Research and development of/spl plusmn/250 kV DC XLPE cables. *IEEE Trans Power Deliv* 13:7
293. Nishikawa S, Sasaki K-I, Akita K, Sakamaki M, Kazama T, Suzuki K (2017) XLPE cable for DC link. *SEI Tech Rev* 84:59
294. (2000) Partial discharge measurement. In: International electrotechnical commission (IEC), Geneva, Switzerland
295. Densley J (2001) Ageing mechanisms and diagnostics for power cables—an overview. *IEEE Electr Insul Mag* 17:14
296. Raymond WJK, Illias HA, Bakar AHA, Mokhlis H (2015) Partial discharge classifications: review of recent progress. *Measurement* 68:164
297. Conlan S, Courtney J, Looby T (2015) Accelerated aging test on multiple XLPE MV cables simultaneously to induce water trees. In: 50th international universities power engineering conference (UPEC). IEEE, pp 1–4
298. Srinivas N, Allam S, Doepken H (1976) The effect of cross-linking and cross-linking agent by-products on tree growth in polyethylene. In: Conference on electrical insulation and dielectric phenomena, annual report 1976. IEEE, pp 380–385
299. Dissado LA, Fothergill JC (1992) Electrical degradation and breakdown in polymers. *IET* 9. <https://doi.org/10.1049/pbed009e>
300. Tanaka T, Fukuda T, Suzuki S, Nitta Y, Goto H, Kubota K (1974) Water trees in cross-linked polyethylene power cables. *IEEE Trans Power Appar Syst PAS-93:693*
301. Hui L, Smith R, Nelson J, Schadler L (2009) Electrochemical treeing in XLPE/Silica nanocomposites. In: Electrical Insulation and Dielectric Phenomena, CEIDP'09. IEEE, pp 511–514
302. Zhang L, Zhou Y, Cui X, Sha Y, Le TH, Ye Q, Tian J (2014) Effect of nanoparticle surface modification on breakdown and space charge behavior of XLPE/SiO₂ nanocomposites. *IEEE Trans Dielectr Electr Insul* 21:1554. <https://doi.org/10.1109/TDEI.2014.004361>

303. Crine J-P (2005) Influence of electro-mechanical stress on electrical properties of dielectric polymers. *IEEE Trans Dielectr Electr Insul* 12:791. <https://doi.org/10.1109/TDEI.2005.1511104>
304. Crine J-P (2005) On the interpretation of some electrical aging and relaxation phenomena in solid dielectrics. *IEEE Trans Dielectr Electr Insul* 12:1089. <https://doi.org/10.1109/TDEI.2005.1561789>
305. Han B, Wang X, Sun Z, Yang J, Lei Q (2013) Space charge suppression induced by deep traps in polyethylene/zeolite nanocomposite. *Appl Phys Lett* 102:012902. <https://doi.org/10.1063/1.4773918>
306. Tian F, Lei Q, Wang X, Wang Y (2011) Effect of deep trapping states on space charge suppression in polyethylene/ZnO nanocomposite. *Appl Phys Lett* 99:142903. <https://doi.org/10.1063/1.3646909>
307. Tanaka T, Kozako M, Fuse N, Ohki Y (2005) Proposal of a multi-core model for polymer nanocomposite dielectrics. *IEEE Trans Dielectr Electr Insul* 12:669. <https://doi.org/10.1109/TDEI.2005.1511092>
308. Wang Y, Li G, Yin Y (2015) The effect of Nano-MGO addition on grounded DC tree in cross-linked polyethylene. In: *IEEE 11th international conference on the properties and applications of dielectric materials (ICPADM)*. IEEE, pp 285–288
309. Murata Y, Goshowaki M, Reddy C, Sekiguchi Y, Hishinuma N, Hayase Y, Tanaka Y, Takada T (2008) Investigation of space charge distribution and volume resistivity of XLPE/MgO nanocomposite material under DC voltage application. In: *International symposium on electrical insulating materials (ISEIM 2008)*. IEEE, pp 502–505
310. Nagao M, Watanabe S, Murakami Y, Murata Y, Sekiguchi Y, Goshowaki M (2008) Water tree retardation of MgO/LDPE and MgO/XLPE nanocomposites. In: *2008 international symposium on electrical insulating materials (ISEIM 2008)*. IEEE, pp 483–486
311. Zhao H, Xu M, Yang J, Zhang W, Wang X, Lei Q (2012) Space charge and electric treeing resistance properties of MgO/LDPE nanocomposite. In: *Zhongguo Dianji Gongcheng Xuebao, Proceedings of the Chinese society of electrical engineering*. Chinese Society for Electrical Engineering, pp 196–202
312. Jarvid M, Johansson A, Kroon R, Bjuggren JM, Wutzel H, Englund V, Gubanski S, Andersson MR, Müller C (2015) A new application area for fullerenes: voltage stabilizers for power cable insulation. *Adv Mater* 27:897. <https://doi.org/10.1002/adma.201404306>
313. Mazzanti G, Montanari G, Palmieri F, Alison J (2003) Apparent trap-controlled mobility evaluation in insulating polymers through depolarization characteristics derived by space charge measurements. *J Appl Phys* 94:5997. <https://doi.org/10.1063/1.1616641>
314. Kaneko K, Mizutani T, Suzuoki Y (1999) Computer simulation on formation of space charge packets in XLPE films. *IEEE Trans Dielectr Electr Insul* 6:152. <https://doi.org/10.1109/94.765904>
315. Kassiba A, Tabellout M, Charpentier S, Herlin N, Emery J (2000) Conduction and dielectric behaviour of SiC nano-sized materials. *Solid State Commun* 115:389. [https://doi.org/10.1016/S0038-1098\(00\)00195-2](https://doi.org/10.1016/S0038-1098(00)00195-2)
316. Wang Y, Wang C, Xiao K (2016) Investigation of the electrical properties of XLPE/SiC nanocomposites. *Polym. Test.* 50:145. <https://doi.org/10.1016/j.polymertesting.2016.01.007>
317. Takada T, Hayase Y, Tanaka Y, Okamoto T (2008) Space charge trapping in electrical potential well caused by permanent and induced dipoles for LDPE/MgO nanocomposite. *IEEE Trans Dielectr Electr Insul* 15:152. <https://doi.org/10.1109/T-DEI.2008.4446746>
318. Li X, Xu M, Zhang K, Xie D, Cao X, Liu X (2014) Influence of organic intercalants on the morphology and dielectric properties of XLPE/montmorillonite nanocomposite dielectrics. *IEEE Trans Dielectr Electr Insul* 21:1705. <https://doi.org/10.1109/TDEI.2014.004317>
319. Zhang L, Khani MM, Krentz TM, Huang Y, Zhou Y, Benicewicz BC, Nelson JK, Schadler LS (2017) Suppression of space charge in crosslinked polyethylene filled with poly(stearyl methacrylate)-grafted SiO₂ nanoparticles. *Appl Phys Lett* 110:132903. <https://doi.org/10.1063/1.4979107>

320. Wang W, Takada T, Tanaka Y, Li S (2017) Trap-controlled charge decay and quantum chemical analysis of charge transfer and trapping in XLPE. *IEEE Trans Dielectr Electr Insul* 24:3144. <https://doi.org/10.1109/TDEI.2017.006637>
321. Blaško M, Mach P, Antušek A, Urban M (2018) Correction to DFT modeling of cross-linked polyethylene: role of gold atoms and dispersion interactions. *J Phys Chem A* 122:4591. <https://doi.org/10.1021/acs.jpca.8b03343>
322. Blaško M, Mach P, Antušek A, Urban M (2018) DFT modeling of cross-linked polyethylene: role of gold atoms and dispersion interactions. *J Phys Chem A* 122:1496. <https://doi.org/10.1021/acs.jpca.7b12232>
323. Zheng X, Liu Y, Wang Y (2018) Electrical tree inhibition by SiO₂/XLPE nanocomposites: insights from first-principles calculations. *J Mol Model* 24:200. <https://doi.org/10.1007/s00894-018-3742-4>
324. Song S, Zhao H, Zheng X, Zhang H, Liu Y, Wang Y, Han B (2018) A density functional theory study of the role of functionalized graphene particles as effective additives in power cable insulation. *R Soc Open Sci* 5:170772. <https://doi.org/10.1098/rsos.170772>
325. Liao R, Zhang F, Yuan Y, Yang L, Liu T, Tang C (2012) Preparation and electrical properties of insulation paper composed of SiO₂ hollow spheres. *Energies* 5:2943. <https://doi.org/10.3390/en5082943>
326. Paramane AS, Kumar KS (2016) A review on nanocomposite based electrical insulations. *Trans Electr Electron Mater* 17:239. <https://doi.org/10.4313/TEEM.2016.17.5.239>
327. Aigbodion V, Achiv F, Agunsoye O, Isah L (2016) Evaluation of the electrical porcelain properties of alumina-silicate nano-clay. *J Chin Adv Mater Soc* 4:99. <https://doi.org/10.1080/22243682.2015.1118356>
328. Contreras J, Rodriguez E, Taha-Tijerina J (2017) Nanotechnology applications for electrical transformers—a review. *Electr Power Syst Res* 143:573. <https://doi.org/10.1016/j.epsr.2016.10.058>
329. Li W, Yan H-D, Zhou Y, Zhang C, Chen X (2017) Supersmooth semiconductive shielding materials use for XLPE HVDC cables. In: 1st international conference on electrical materials and power equipment (ICEMPE). IEEE, pp 447–451
330. Hong G, Hong SM, Koo CM, Baek BK, Lee H-S, Lee Y-W (2015) A kinetic study on the De-crosslinking and decomposition of silane-cross-linked polyethylene in supercritical methanol. *Ind Eng Chem Res* 54:11961. <https://doi.org/10.1021/acs.iecr.5b00377>
331. Lee HS, Jeong JH, Hong G, Cho H-K, Baek BK, Koo CM, Hong SM, Kim J, Lee Y-W (2013) Effect of solvents on de-cross-linking of cross-linked polyethylene under subcritical and supercritical conditions. *Ind Eng Chem Res* 52:6633. <https://doi.org/10.1021/ie4006194>
332. Goto T, Ashihara S, Yamazaki T, Okajima I, Sako T, Iwamoto Y, Ishibashi M, Sugeta T (2011) Continuous process for recycling silane cross-linked polyethylene using supercritical alcohol and extruders. *Ind Eng Chem Res* 50:5661. <https://doi.org/10.1021/ie101772x>
333. Goto T, Ashihara S, Kato M, Okajima I, Sako T (2012) Use of single-screw extruder for continuous silane cross-linked polyethylene recycling process using supercritical alcohol. *Ind Eng Chem Res* 51:6967. <https://doi.org/10.1021/ie202303y>